Ministry of Industry and New Technologies

The Republican State Enterprise
"The National Nuclear Center of Kazakhstan"

Affiliated State Enterprise
"Institute of Radiation Safety and Ecology"

TOPICAL ISSUES IN RADIOECOLOGY OF KAZAKHSTAN

Issue 3
Volume 2

Proceedings of the National Nuclear Center of Kazakhstan for 2010

Pavlodar, 2011

УДК 621.039
ББК 31.4

А-43 Proceedings of the National Nuclear Center of Kazakhstan have been prepared by the Institute of Radiation Safety and Ecology NNC RK headed by the Deputy Director General for Radioecology of the RSE NNC RK Lukashenko S.N.

Reviewers:

1. **Panin M.S.** – Vice Rector for Research and International Relations, Head of the Department of Ecology and Geography of the Semipalatinsk State Pedagogical Institute, Doctor of Biological Sciences, Professor, Academician (Kazakhstan, City of Semey)

2. **Solodukhin V.P.** – Chief Scientific Officer, scientific supervisor for Radioecology of the Centre of Integrated Environmental Research of the Institute of Nuclear Physics NNC RK, Doctor of Physics and Math Sciences (Kazakhstan, City of Almaty)

Present proceedings have been made possible with the help of the printing house "Dom Pechati LLP" (Pavlodar) directed by Ye. A. Pisarevskaya in cooperation with G.V. Trubitskaya, Ye. Gorkin, A. Vus. The authors are thankful for generous assistance and fruitful cooperation.

Technical editors: Tonevitskaya O.V., Seraya O.V.
Translated by: Arman T. Kozhakhmetov
Artem N. Yermilov

А-43

Topical Issues in Radioecology of Kazakhstan [Proceedings of the National Nuclear Center of Kazakhstan for 2010] / supervised by Lukashenko S.N. – Issue 3. – Vol.2. – 390 p Pavlodar: Dom Pechati, 2010.

ISBN 978-601-7112-62-2

The book presents the activities of the National Nuclear Center of Kazakhstan for 2010. The articles reflect the issues of radioecology in the former Semipalatinsk Test Site (STS) and adjacent areas, other sites of nuclear testing in Kazakhstan (site "Azgir", "LIRA" facilities), assurance of safe works at STS, reports on special studies and research of "non-radiological" hazards at STS. The authors believe that the proposed issue will allow each reader to gain reliable information about current state of all major facilities in Kazakhstan where nuclear tests were conducted.

УДК 621.039
ББК 31.4

ISBN 978-601-7112-62-2 (Т.2)
ISBN 978-601-7112-60-8 (общ.)

TABLE OF CONTENTS

Volume 1

Dedicated
to the 20th Anniversary
of the Independence
of the Republic of Kazakhstan
and
to the 20th Anniversary
of the closure
of the Semipalatinsk
Nuclear Test Site

PART: ADVANCED STUDIES ON THE SEMIPALATINSK TEST SITE

УДК 631.4:577.4:504.75.05:539.16

STUDIES AND SYSTEMATIZATION OF HOT PARTICLES IN SOILS OF SEMIPALATINSK TEST SITE

[1]Gorlachev I.D., [1]Kvochkina T.N., [1]Knyazev B.B., [2]Lukashenko S.N.

1. Institute of Nuclear Physics NNC RK, Almaty, Kazakhstan
2. Institute of Radiation Safety and Ecology NNC RK, Kurchatov, Kazakhstan

Total 456 nuclear explosions were performed at Semipalatinsk Test Site (STS). The content and distribution of radionuclides for each type of soil contamination are different. One of the main sources of soil activity is the "hot" particles from tens of micron to millimetres in size. The ratio between the "hot" particle activity and general activity of specimen is determined by the nature of nuclear test. The knowledge of physical and chemical properties of "hot" particles is required in order to forecast the extent of radioactive product proliferation in the environment and to assess the hazard of external and internal exposure of human body.

The purpose of this study was to single out "hot" particles from soil samples taken from the places of various types of nuclear tests, to systemize them and study physical and chemical aspects of both soil fractions and separate "hot" particles. Total 20 soil samples were taken, of which 7 were taken from the "Experimental Field" site, 2 – from Atomic Lake, 3 – from Telkem1 Site, 3 – from P-2 Site and 5 samples from adits 177, 139, 503, and 609 on Degelen Site. All samples were studied for the presence of "hot" particles by means of visual identification and induced fission. In total, over 3,000 "hot" particles were separated from coarse particle-size fractions (with particle size being over 0.28 mm). Particles in small fractions were not separated, and only their content was estimated. For certain "hot" particles absolute and specific activity and density, ratio of $^{235}U/^{238}U$, $^{239+240}Pu/^{241}Pu$ and $^{240}Pu/^{239}Pu$ isotopes and average elemental composition were determined, and forms of plutonium presence therein were studied. Approach to identification of "hot" particle presence and assessment of their quantity and average activity was developed based on the analysis of standard deviation of gamma-ray and X-ray line counting rate. Both conventional analytical methods, such as gamma-, alfa- and mass spectrometry, and X-ray fluorescence analysis, and specially designed non-conventional approaches focused on the abilities of the Institute of Nuclear Physics were used in the studies.

INTRODUCTION

There were 456 nuclear explosions performed on the STS from 1949 to 1989. Studies undertaken by the Institute of Nuclear Physics (INP) over many years showed that the nature of radioactive contamination of soil on the STS is such that the sites with relatively low average activity have the areas where concentration of artificial radionuclides is hundreds and thousands times higher than the levels of global fallouts [1].

The studies have discovered that the sources of soil activity include, inter alia, the particles from tens of micron to millimetres in size. Scientific literature normally refers to such formations as to "hot" particles. Small, submicron formations usually determine the "matrix" activity of a sample. They are difficult to be identified unambiguously, therefore they are not considered as independent particles. So, one can say that "hot" particle is a mineral, unambiguously identifiable formation resistant to the environment that was produced during nuclear tests at high temperatures and that has high specific activity. Formation of

radionuclide composition of "hot" particles is conditioned by temperature changes and complex nuclear-and-physical and thermodynamic processes that occur in the fireball or cloud of a nuclear explosion. The knowledge of physical and chemical properties of "hot" particles is required for the forecast of the extent of radioactive product migration in the environment and for the assessment of the hazard of external and internal exposure of human body.

As a part of studies of physical and chemical properties and systematization of "hot" particles, gamma-spectrometric analysis of soil samples taken from the STS and separate "hot" particles was performed. "Hot" particles were recovered from coarse granulometric fractions of eleven soil samples by induced fission and visual identification methods developed in the INP NNC RK.

1. STUDY MATERIALS AND METHODS

1.1. Choice of STS areas for study

Main contaminated areas of the test site can be divided into four specific types according to the nature and scale of contamination and types of prevailing radionuclides:

- sites with areal contamination due to surface and air nuclear explosions;
- sites contaminated as a result of excavation and emergency underground explosions;
- sites contaminated as a result of hydronuclear explosions;
- areas near adit entrance with water effects.

Forms of radionuclide presence and distribution throughout the sites might be significantly different for each type of contamination. Therefore, the most typical sites were selected for each type of tests to find the specific features of radionuclide contamination. Such approach cannot produce comprehensive information about the places of nuclear explosions. However, it makes it possible to conduct comparative analysis, even though not based on much statistics, of the forms of radionuclide presence in different areas of test site, and thereby identify the features typical for certain types of nuclear test.

The objects selected for the study and their classification are set forth in Table 1. Location of the selected sites on the STS is shown in Figure 1.

Table 1.

Classification of the objects selected for the study

Site classification	Selected targets of study
Adits with water seepage (Degelen)	Adits 177, 503, 609
Excavation and emergency explosions	Telkem-1, Atomic Lake (Balapan), adit 139
Surface and air explosions	South-western trace, south-eastern trace
Hydronuclear explosions	P-2 and P-7 sites
"Clean" areas	Background areas on the "Experimental Field" site

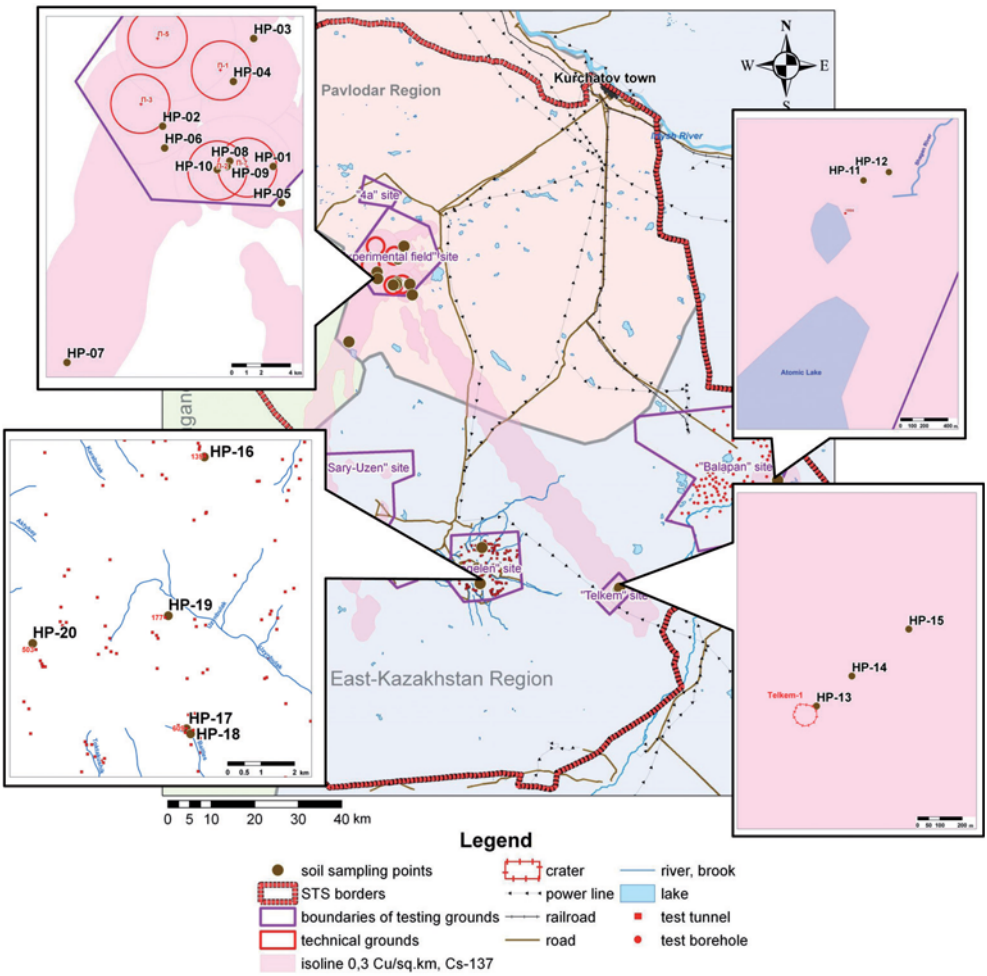

Figure 1. Layout of STS areas selected for the study

Background areas. Three sites of the "Experimental Field" site, which were further used as the background site based on their total activity, were defined in advance (samples HP-01, HP-02 and HP-03). Samples HP-04 - HP-07 were also taken from the "Experimental Field" site.

On P-2 site, three soil samples were taken: from nuclear explosion (sample HP-10), from hydroexplosion (sample HP-08) and from mixed explosion (sample HP-09). Samples were taken from the ridge of the crater pile and in such way that the explosions would have the least impact on each other.

Atomic Lake (Balapan). Samples were taken along the north-eastern ray (radioactive trace). The first sample was taken on the ridge of the lake crater pile (sample HP-11). The second one – 50m away (sample HP-12).

Telkem-1. Three samples were taken: the first sample was taken from the ridge of crater pile (sample HP-13), the second one – within 200m (sample HP-14), and the third one – within 500m (sample HP-15).

Degelen. Adit 139. The sample was taken at the adit entry on the hillside (sample HP-16).

Degelen. Adit 609. Two samples were taken from this adit. The first sample – at the entry (sample HP-17). The second one – within one hundred meters off the entry (sample HP-18).

Degelen. Adit 177 (sample HP-19). The sample was taken at the entry, in the streambed where the water was running.

Degelen. Adit 503 (sample HP-20). One sample was taken at the entry in the streambed where the water was running.

Field studies

Exposure dose rate (EDR) and density of surface contamination with α- and β-particles was measured in sampling points.

The soil samples were taken on the selected area from the depth of 3 - 5cm and 15x15 cm^2 area. The samples were weighed. The obtained soil mass was put into plastic bag and provided with a passport (explanatory note) and packed so that to prevent any mechanical damage. The passport specified the place and date of sampling, geographical coordinates, weight, code number, and name of the person who took the sample. At the same time, the relevant records were made in the sampling logbook.

Characteristic of soil samples is shown in Table 2.

The EDR was measured by the checked and calibrated DRG– 0.1T radiation detector with the measuring range 10 mcR/h- 9.999 R/h and maximum permissible error 15%. Measurements were conducted at the height of 1m and 3-4cm above ground. During measurements the instrument was located parallel to the surface.

Density of α- and β-particle surface contamination was measured by Harwel dose rate meter. The measuring range of the meter is from 0.3 to 5,000 particles/(min.·cm^2), the main measuring error does not exceed 20%. When measuring with α- and β-dose rate meters, there were selected such points where one could ensure the fullest contact of the meter with the contaminated surface without damaging the protective film of the meter.

GPS NAV 5000 DLX was used for determination of geographical coordinates. According to the technical specification this device is designed for determination of coordinates with the accuracy not less than 15 m.

Table 2.

Characteristics of the samples taken at STS

Sample No	Geographical coordinates		Sample weight, grams	Data on activity measurements		
	latitude	longitude		EDR, μR/h	β, pulse/sec	α, pulse/sec
HP-01	50⁰ 22' 39,5"	77⁰ 51 40,5"	1 950	18	14	<0.5
HP-02	50⁰ 24' 17"	77⁰ 45' 25,6"	1 500	30	20	<0.5
HP-03	50⁰ 27' 22,1"	77⁰ 50' 50,1"	1 410	18	15	<0.5
HP-04	50⁰ 25' 49,4"	77⁰ 49' 34,7"	1 490	26	40	<0.5
HP-05	50⁰ 21' 19"	77⁰ 51' 64"	1 330	15	12	<0.5
HP-06	50⁰ 23' 29"	77⁰ 45' 30"	1 450	22	17	<0.5
HP-07	50⁰ 15' 46"	77⁰ 39' 28"	1 550	25	17	<0.5
HP-08	50⁰ 22' 54,9"	77⁰ 49' 12,1"	1 530	30	600	450
HP-09	50⁰ 22' 43,4"	77⁰ 49 2,3"	1 570	380	190	2
HP-10	50⁰ 22' 37,3"	77⁰ 48' 27,6"	1 300	1,200	800	3
HP-11	49⁰ 56'14,7''	79⁰ 00' 40.8''	2 100	300	500	<0.5
HP-12	49⁰ 56' 16,6'	79⁰ 00' 51,7"	2 020	60	120	<0.5
HP-13	49⁰ 43' 43,7"	78⁰ 29' 10,4"	1 620	120	35	<0.5
HP-14	49⁰ 43' 47,8"	78⁰ 29' 18,6"	2 520	22	17	<0.5
HP-15	49⁰ 43' 54,2"	78⁰ 29' 31,8"	2 690	22	20	<0.5
HP-16	49⁰ 49' 39,6"	78⁰ 03' 34,4"	1 270	100	25	1.5
HP-17	49⁰ 45' 17,6"	78⁰ 2' 51,1"	1 260	2,500	2,000	<0.5
HP-18	49⁰ 45' 12,5"	78⁰ 2' 57"	1 240	2,000	5,000	<0.5
HP-19	49⁰ 47' 7,6"	78⁰ 2' 30,9"	1 170	150	600	<0.5
HP-20	49⁰ 46' 46"	77⁰ 59' 6,6"	1 170	30	70	<0.5

1.2 Devices and methods of study

Apart from the standard methods of studying radionuclide composition of soil fractions (γ-spectrometry¸ α-spectrometry, X-ray fluorescence analysis), a number of non-conventional methods and approaches was developed and used which allowed expanding the analytical abilities and obtaining additional information about properties of the distinguished "hot" particles.

1.2.1 Methods of soil fraction study

Instrumental Radionuclide Analysis

The analytical device used in radionuclide analysis was the planar detector of superpure Ge with high detection efficiency within the energy range from several keV to several hundreds of keV and with high resolution within the energy range of 13–22 keV for efficient decomposition of complex X-ray spectrums of plutonium and americium isotopes.

Instrumental radionuclide analysis was used for both the analysis of particle-size fractions and study of properties of separate "hot" particles.

Detection of the presence, assessment of quantity and average activity of "hot" particles in soil samples.

The principle ability to assess the presence of hot particles in soil samples is based on the radioecological studies of soil and bottom deposits of objects at STS, in particular gamma-spectrometric analysis of concentration of such radionuclides as ^{137}Cs and ^{241}Am. It was noticed that the error of repeated measurements of the same samples was often significantly higher than the instrumental error related to the counting statistics only [1]. Analysis of possible reasons for such variability of counting rate under fixed geometric conditions of measurements resulted in conclusion that certain samples had hot particles accumulating considerable portion of activity of the entire sample. Accidental presence of several highly active "hot" particles in one sample explained the sudden change of counting rate when sample material was mixed or when specimens produced after dividing samples into equal parts were measured.

The analytical parameter in the study of "hot" particle presence and integral characteristics was the counting rate registered by detector of gamma and X-ray radiation. Application of mathematical formalism described in studies [2 - 5], and use of method of direct instrumental detection of plutonium in soil [6] allowed developing an algorithm and methodical approach called Monte Carlo method in order to determine integral characteristics of soil specimens containing hot particles.

Given the geometrical dimensions of "hot" particles (from hundreds of micron to millimetres), the collocation of particle and sensitive surface of detector will have big effect on the analytical parameter applied in the developed mathematical model (detector response). In other words, the counting rate of selected gamma-ray or X-ray line of "hot" particle radiation will depend not only on its activity but also on the distance between the detector and "hot" particle, as well as on attenuation characteristics of the sample materials containing "hot" particle. The less the energy of detected radiation the stronger this effect will be.

If it is assumed that the specimen with *m* mass contain *n* "hot" particles with the average activity of certain nuclide $\bar{A}_{HP}$, and the matrix of specimen has the activity of the same nuclide A_M and such activity is homogenous throughout the entire sample volume, then, in case of accident evenly distributed location of all "hot" particles in the sample volume, the accounting rate will be [3]:

$$N_{total} = \varepsilon_{\text{int}} p \left\{ \overline{A}_{HP} \sum_{i=1}^{n} \varepsilon_p(x_i, r_i) + \varepsilon_v A_M \right\} \qquad (1)$$

where ε_{int} is the internal efficiency of detector registration, i.e. the ratio between high number of pulses and number of photons fallen on the sensitive surface of detector [4]; $\varepsilon_p(x_i r_i)$ is the geometrical efficiency of detection of "hot" particle (point source) and ε_v is the geometrical efficiency of specimen matrix (volume source); p is the transition probability of detected gamma-ray line.

If the measuring vessel is located coaxially to the detector, the efficiency $\varepsilon_p(x_i r_i)$ of a separate "hot" particle located inside the measuring vessel in arbitrary point can be calculated with the use of detector fictitious point concept. According to this approach, the efficiency of

point source is proportionate to $1/(HP \leftrightarrow P)^2$, where $HP \leftrightarrow P$ is the distance between the "hot" particle *HP* and fictitious point *P* located in detector's sensitive volume below the actual surface [4]. If we define the distance from this point *P* to the bottom of the measuring vessel as *d* and distance from the bottom of the vessel to the "hot" particle *HP* as *x*, then the distance $HP \leftrightarrow P$ will be equal to $\{r^2+(x+d)^2\}^{1/2}$. Description of the experimental determination of d can be found in [4] or [5]. And the distance that the photon has to cover inside the specimen before registered by the detector can be calculated as follows:

$$z = \frac{x\sqrt{r^2 + (x+d)^2}}{x+d} \tag{2}$$

Efficiency of radiation detection from one hot particle in the position *(x,r)* inside the measuring vessel will be, therefore, proportional to:

$$\varepsilon_p(x,r) = \propto \frac{Exp(-\mu \cdot \rho \cdot z)}{r^2 + (x+d)^2} \tag{3}$$

where μ is the mass attenuation coefficient of the specimen material, ρ is the density of the specimen material.

Geometrical efficiency of the bulk specimen is proportional to [3]:

$$\varepsilon_v \propto \frac{2}{R^2}\frac{1}{H}\int_0^R\int_0^H \frac{Exp(-\mu \cdot \rho \cdot z)}{r^2 + (x+d)^2} rdxdr \tag{4}$$

Double integral (4) can be calculated only numerically, employing for instance Monte Carlo method.

If the geometrical efficiency of bulk specimen ε_v is taken outside the parentheses in formula (1), then we will have the following:

$$N = \varepsilon_{\text{int}}\varepsilon_v p\left\{\overline{A}_{HP}\frac{\sum_{i=1}^{n}\varepsilon_p(x_i,r_i)}{\varepsilon_v} + A_M\right\} \tag{5}$$

The product of $\varepsilon_{int}\,\varepsilon_v$ in formula (5) represents the efficiency of the peak of full absorption detection. It can be experimentally determined for fixed geometrical conditions when measuring homogenous specimens with known activities. The ratio between the sum of separate efficiencies of "hot" particles evenly distributed in the specimen and efficiency of bulk specimen with high values of *n* will tend to *n*. Therefore, with rather high *n*, the left part in parentheses in formula (5) will tend to $\boldsymbol{n \cdot \bar{A}_{HP}}$. The value of $n \cdot \bar{A}_{HP}$ is the important integral index of "hot" particles in the studied specimen material. This value can serve as the key criterion in decision taking about the necessity of remediation or utilization of potentially hazardous areas of soil during radioecological survey of the nuclear test areas.

The number of *n* in the "hot" particles formula (5) determines the behaviour of a specimen in terms of independent measurements for arbitrarily selected positions of all "hot" particles in each measurement with coordinates (x_i, r_i). If to conduct *m* independent measurements of the specimen containing *n* "hot" particles each time ensuring strictly arbitrary distribution of "hot" particles throughout the specimen, the counting rate for k measurement will be described by the formula:

$$N_k = \varepsilon \cdot p \left\{ \overline{A}_{HP} \frac{\sum_{i=1}^{n} \varepsilon_p(x_{ki}, r_{ki})}{\varepsilon_v} + A_M \right\} \tag{6}$$

where ε is the full detection efficiency of the peak of full absorption; $\varepsilon_p(x_{ki}, r_{ki})$ is the geometrical efficiency of *i*-th "hot" particle in *k*-th measurement.

If the number of "hot" particles in the specimen is small, then different counting rate will be produced in each measurement. The extent of such difference will be determined by the number of hot particles, attenuation and geometrical characteristics of specimen and by the ratio between "hot" and "not hot" fractions of specimen activity. On the other hand, with very high values of *n* the entire specimen material, including "hot" and "not hot" fractions, will be practically homogenous (as elementary volumes of hot particles will practically evenly fill the entire volume of specimen) and, accordingly, changes in counting rate in the next statistical test will tend to nil. The extent of difference of each counting rate measurement from its average value can be expressed analytically by average standard deviation:

$$\sigma_N = \sqrt{\frac{\sum_{k=1}^{m} (N_k - \overline{N})^2}{m-1}} \tag{7}$$

By placing in formula (7) the formula (6) and instead of average value of counting rate – the formula (5), the following will be produced after certain transformations:

$$\sigma_N = \varepsilon \cdot p \cdot n \cdot \overline{A}_{HP} \cdot \sqrt{\frac{\sum_{k=1}^{m} \left\{ \frac{\sum_{i=1}^{n} \varepsilon_p(x_{ki}, r_{ki})}{n \cdot \varepsilon_V} - 1 \right\}^2}{m-1}} \tag{8}$$

In this formula, the ratio $\sum_{i=1}^{n} \varepsilon_p(x_{ki}, r_{ki}) \Big/ n$ is an arithmetic mean value ε_v of n arbitrary values. With $n \to \infty$, σ_N will tend to nil, i.e. the specimen material will be homogenous

from the point of view of analytical parameter detection. This is confirmed by the previously made conclusion of specimen homogeneity at very high values of *n*.

If we use estimated activity of the specimen for the fixed geometrical conditions of the measurements (specimen height, diameter, mass, and detector-specimen distance), rather than counting rate, as an analytical parameter for statistical tests, we can write down the following formula for the average standard deviation of estimated activity:

$$\sigma_A = n \cdot \bar{A}_{HP} \cdot \sqrt{\frac{\sum_{k=1}^{m} \left\{ \frac{\sum_{i=1}^{n} \varepsilon_p(x_{ki}, r_{ki})}{n \cdot \varepsilon_V} - 1 \right\}^2}{m-1}} \tag{9}$$

By defining

$$D(n,m) = \sqrt{\frac{\sum_{k=1}^{m} \left\{ \frac{\sum_{i=1}^{n} \varepsilon_p(x_{ki}, r_{ki})}{n \cdot \varepsilon_V} - 1 \right\}^2}{m-1}} \tag{10}$$

we will have

$$\sigma_A = n \cdot \bar{A}_{HP} \cdot D(n, m) \tag{11}$$

where *n* is the number of "hot" particles in a specimen and *m* is the number of statistical tests.

Function *D(n,m)* in the right side of the formula (11) must be proportional to the relative standard deviation of the number of "hot" particles in the specimen. Since the absolute value of standard deviation for the *n* number of discrete events is equal to $\sqrt{n}$, the relative value of this parameter will be equal to $\sqrt{n}/n = 1/\sqrt{n}$, i.e. *D(n,m)* will be the function $1/\sqrt{n}$. The formula

$$R(\mu) = D(n, m) \cdot \sqrt{n} \tag{12}$$

is the function of only geometrical conditions of measurements and attenuation characteristics of the specimen (mass attenuation coefficient).

In order to calculate *R(μ)*, a computational procedure was developed based on Monte Carlo method and mathematical formalism described by formulas (1-6) for calculation of standard deviation of counting rate for different values of *n* number of hot particles and for different energies of detected radiation. The selected geometric specimen parameters were close to the standard ones used in practical gamma-spectrometry: specimen diameter - 7.2 cm, height - 2.0 cm, specimen mass – 168g, distance from the upper surface of detector to the lower surface of specimen - 0.8 cm.

Figure 2 shows the dependence of standard deviation of counting rate of gamma-ray and X-ray lines on the their mass attenuation coefficient for the most active sample out of tested sample – specimen HP-08. This dependence can be well approximated by an exponent function.

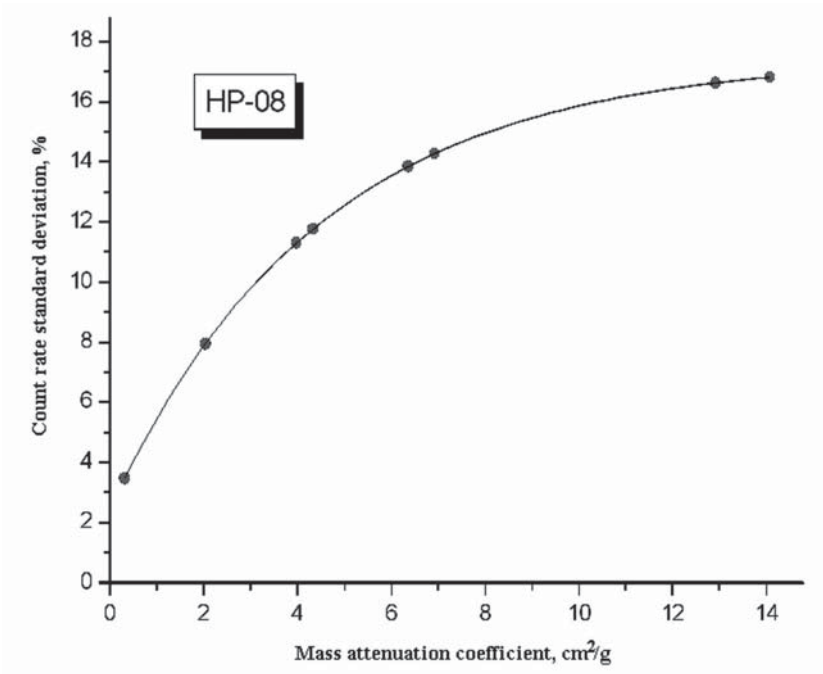

Figure 2. Counting rate standard deviation as a function of mass attenuation coefficient for the specimen HP-08

Approximation of ratio $R(\mu)$ was described by the least square method where the following function was used as an analytic expression:

$$R(\mu) = y_0 + A_1 \cdot Exp(-\mu/t) \qquad (13)$$

where y_0, A_1 and t are empirical coefficients established in the process of fitting.

By using formula (13) and dividing (12) by the total activity of sample we will produce the formula for the relative standard deviation of analytical parameter:

$$S = \frac{n \cdot \bar{A}_{HP}}{n \cdot \bar{A}_{HP} + A_M} \frac{R(\mu)}{\sqrt{n}} \qquad (14)$$

where $n \cdot \bar{A}_{HP}$ is the activity of "hot" fraction of sample; A_M – "matrix" activity of sample.

The ratio

$$R_{HP} = \frac{n \cdot \overline{A}_{HP}}{n \cdot \overline{A}_{HP} + A_M} \tag{15}$$

defines the "hot" fraction of total activity of a sample, i.e. when A_M tends to nil all activity of sample is conditioned by the presence of hot particles and visa versa.

Finally, we have the following formula for the number of "hot" particles in the sample:

$$\frac{n}{R_{HP}^2} = \frac{R^2(\mu)}{S^2} \tag{16}$$

With the known activity share of "hot" particles in the sample, formula (16) enables estimating their number through the standard deviation of measured counting rate. With $R_{HP} = 1$ (i.e. when all activity of the sample is associated with "hot" particles) the formula becomes more simplified

$$n = \frac{R^2(\mu)}{S^2} \tag{17}$$

Knowing the number of n "hot" particles, by using formula (11), one can calculate the average activity of one hot particle.

X-ray fluorescence analysis (XFA)

SLP10180 Si(Li) detector with the active area 80mm^2, active thickness 5.0 mm, resolution 175 keV to 5.9 keV and entry shielding window 25 micron thick was used in the XFA. ^{109}Cd and ^{241}Am isotopes were used as excitation source in XFA.

Radiochemical analysis of soil fraction samples for $^{239+240}$Pu and ^{90}Sr

The basis for radiochemical determination of plutonium and strontium isotope concentration in soil samples is the *Method for determination of concentration of artificial radionuclides of plutonium (239+240) and strontium-90 in environmental targets (soil, ground, bottom deposits and plants)* developed and certified in the Engineering Ecology Laboratory of the INP, State Registration No. KZ.07.00.00471-2005 dated November 21, 2005.

1.2.2 The method of "hot" particle separation

Two alternative approaches to identification and separation of "hot" particles from soil fractions were applied, because each of these methods has its own advantages and limitations. Their use in complex enables large compensation of such limitations by enhancing the efficiency of "hot" particle separation.

Induced fission method

Since not all "hot" particles have magnetic properties and not all particles sensitive to magnetic field are the "hot" particles, and due to ultimate sensitivity, the magnetic separation method has limited capacity to separate active particles from soil fractions. Therefore, the problem solution as to finding, separating "hot" particles and producing reliable results concerning qualitative characteristics of distribution of such "hot" particles in soil samples requires additional high-performance method of discovery of such particles with the detection efficiency close to 100%. For this purpose, the improved version of induced fission method was developed based on detection by solid-state detectors of ^{239}Pu fragments of fission by thermal neutrons. Previously such approach was used for determination of low concentrations of ^{235}U and ^{239}Pu in industrial and geological samples, as well as when assessing the consequences of accident at Chernobyl NPP.

Large fission cross section of ^{239}Pu (σ_f = 742.5 barn) and its high specific content in "hot" particles enables measurements under relatively small flows of thermal neutrons ~10^9-10^{10} n/(cm^{2}s). To produce such flow, it is enough to use the thermal neutron generator developed on the basis of INP UУ-150 isochronous cyclotron. In this case, neutrons are produced as a result of nuclear reactions of ^{9}Be (p, xn) or ^{9}Be (d, xn).

During irradiation of actual soil fraction samples, silica glass was used as a detector. At the same time, samples were attached to the object substrate by adhesive tape and covered by detector. After irradiation, detectors were treated in 35% fluoride acid to identify tracks of fission fragments.

Detectors were inspected throughout the entire area by MBI-9 microscope at 70-fold zooming.

Visual identification method

The induced fission method is not an ideal way for separation of "hot" particles. It has a number of disadvantages:

1. In this case, separation of "hot" particles is based on the detection of fission products of transuranium elements (α-particles and heavy nucleuses). Given small runs of fission products in the substance (several micron), identification of "hot" particles becomes possible only when there is activity in the near-surface area of the object.
2. The source of fission fragments registered by the detector can be not only ^{235}U and ^{239}Pu but also the natural stable isotope ^{238}U. Given that the natural occurrence of ^{238}U in the earth crust is $2.4 \cdot 10^{-4}$%, it will generate additional background reducing thereby the method's sensitivity.
3. According to the data from the previous studies [1], STS has "hot" particles with no transuranium elements in them. The sources of their activity are ^{137}Cs, ^{60}Co and ^{152}Eu. In this case the use of induced fission method becomes difficult.
4. Taking into account the labour intensity and duration of the analysis of fission fragment tracks, only small portion of soil sample material can be studied employing the induced fission method.

Limited capacity of the induced fission method resulted in the requirement to elaborate alternative approach for separation of "hot" particles to exclude the above-mentioned disadvantages. Visual identification method can be such an alternative approach.

The visual identification method is based on the assumption that the appearance of "hot" particles must be different from the appearance of typical soil particles which is conditioned by formation of "hot" particles under the conditions of high temperatures and pressures. Preliminary inspection of soil fractions did show the presence of particles that are not typical for soil in terms of appearance. Analysis of fraction activity before and after such separation of "hot" particles made it possible to conclude that the majority of fraction activity is concentrated in these particular particles – fraction activity after particle separation was several times less than before separation.

The obvious advantage of the developed method for "hot" particle visual identification is the simplicity and availability. This method does not require any additional equipment. Optical microscope might be used to study particle-size fractions of less than 0.5mm in size. The visual identification method is more express than the induced fission method, which makes it possible to study more material, and, consequently, to separate more particles professed to be the "hot" ones.

The method limitation is conditioned by the assumption that the "hot" particle form is unique. This is not always true, which results in forced loss of particles. The particles of samples taken from the Degelen site are the most inconvenient for separation by such method. This is because the "hot" soil fraction was formed here not as a result of nuclear explosions, but as a result of sorption or sedimentation of activity carried by the water flowing from the adit with show of water. Therefore, "hot" particles in this case will have the form of those natural objects (soil particles, plant stems, roots and etc.) on which the activity settles.

1.2.3 The methods to study properties of "hot" particles

The methods of electron and proton microscopy, mass-spectrometry of "hot" particles and X-ray crystal analysis were used to study structure, phase composition and distribution of elements in "hot" particles.

The methods of γ-spectrometry and α-spectrometry were used to analyse activity of separated "hot" particles.

Mass-spectrometry of "hot" particles

At present, the mass-spectrometry, thanks to its high sensitivity, is practically the only method of measuring isotope ratio between uranium and plutonium [7–10].

Measurement of small radionuclide concentrations normally requires creation of mass-spectral equipment with the maximum high sensitivity [10, 11] that is quite often unobtainable for devices in serial production. During analysis of isotope composition of the targets, mass-spectrometric unit developed in the Institute of Nuclear Physics of the National Nuclear Centre of the Republic of Kazakhstan was used [12, 13]. In this unit, high sensitivity is reached by improvement of the beam focusing quality based on the use of new deflecting and focusing elements of prismatic ion optics [14]. "Hot" particles were studied by thermoionizing mass-spectrometry with the use of developed and certified method of measuring isotopic ratio of plutonium. It was established that when using this method for isotopic analysis the activity of "hot" particles in terms of plutonium of about 10^{-2}-10^{-3} Bq is enough, which is at the level of limiting sensitivity for such types of measurements [7, 8].

The conducted studies showed that the applied mass-spectral equipment could be efficiently used in the studies of isotope composition of radionuclides in fine "hot" particles despite their small absolute activity (up to 10^{-3} Bq).

Electron and proton microscopy

Both methods are based on gaining information about elemental composition of sample areas of micron and submicron sizes. In the first case, JEOL electron microscope was used for this purpose, which microscope allowed producing electron beam of 40 keV at spatial resolution of up to 50 nm. Proton microscopy was developed on UKP-2-1 accelerator, and in this case the proton beam of 1.5 MeV and spatial resolution of ~10 μm was used. Scanning of electron and proton beam on the surface of the tested sample enables producing maps of element distribution.

Apart from the study of the surface of "hot" particles, depth distribution of elements was also analysed. For this purpose, technique of certain particle fixation and grinding was fine-tuned.

Hydrostatic weighing method

Hydrostatic weighing method was used to measure density of "hot" particles.

Density of the object of study is determined by the formula:

$$\rho_т = M_1/(M_1-M_2)_*(\rho-D)+D,$$

where – M_1-is the body weight in air,

M_2 is the body weight in water,

ρ is the density of liquid under certain temperature,

D is the average air density (0.0012 g/cm^3).

Mass of "hot" particles was measured with VLR-20 weigh-scales (scale spacing 0.005 mg).

Leaching of "hot" particles

The method of fractional leaching based on selective dissolution of compounds at successive treatment of solid phase with different reagents was used to study radionuclide Speciations and chemical elements' occurrence in aerosols, fallouts, "hot" particles and soils.

To reveal the composition of biogeochemical and radioecological forms, the leaching circuit is most often used when water soluble, exchangeable, movable, acid soluble and solidly fixed forms (including those connected with sesquioxides, organic material and amorphous silicic acid) are separated.

Radionuclides that are in solid phase in ion condition and incorporated in soluble complex compounds pass into aqueous extract. The number of radionuclides in exchange and mobile forms are separate by means of treatment with 1M acetate-ammonium buffer. Mobile forms of radionuclides, i.e. those that are predominantly in non-exchangeable condition and not passing into soil solutions in the natural environment under normal conditions but capable to be absorbed by plants when received through roots, pass into hydrochloric acid extract. Acid-soluble forms of strontium and plutonium radionuclides are produced by 6M hydrochloric acid and 7.5M nitric acid accordingly.

Strongly fixed radionuclide forms include the portion of radionuclides that was left after solid phase treatment with the above reagents. These radionuclides, which are permanently adsorbed by crystal lattice of soil minerals, are connected with the organic portion of soil by sesquioxides and amorphous silicic acid. Acid-soluble and solidly fixed forms under normal conditions are inaccessible for plants, but they are potentially mobile forms as with the time they can pass into mobile forms which is facilitated by the products of life and decay of vegetable remains and soil micro fauna which are strong complexing ligands (ethanedioic, lemon, lactic and other acids).

2 RESULTS AND DISCUSSION

2.1. Study of soil samples and their separate fractions

2.1.1. Sample preparation, quartering, and gamma-spectrometric analysis of the samples after quartering

20 soil samples selected during field works were dried in a drier for 4 hours at 110˚C and cleared of fine stones and rootstock remains. After that the samples packed in special polyethylene jars were thoroughly agitated during 3 hours for to ensure material homogenization. Agitation was manual in order to preserve the fractional composition of sample.

The entire volume of each soil sample was divided into sub-samples by quartering (7 sub-samples for each sample). Radionuclide composition was studied for each sub-sample by using instrumental radionuclide analysis.

The results of sample analysis are set out in Table 3. The error indicated in Table 3 is formed from statistical error and uncertainty conditioned by variations in sub-sample activity.

Table 3.

Radionuclide contents in STS samples

Sample	$^{239+240}$Pu, Bq/g	^{241}Am, Bq/kg	^{137}Cs, Bq/kg	^{60}Co, Bq/kg	^{152}Eu, Bq/kg	^{154}Eu, Bq/kg	^{155}Eu, Bq/kg
HP-01	3,69 ± 1,1	453 ± 136	79,6 ± 8,0	< 3	< 2	< 1,8	< 2
HP-02	1,63 ± 0,29	97,3 ± 17,2	707 ± 129	< 1,1	6,4 ± 1,2	< 1,2	3,7 ± 0,5
HP-03	2,94 ± 1,82	122 ± 38	260 ± 174	< 5	13 ± 3	< 3	8 ± 2
HP-04	11,1 ± 1,9	1190 ± 212	962 ± 60	< 5	158	7 ± 3	10 ± 2
HP-05	3,16 ± 1,39	136 ± 27	172 ± 42	< 2	14 ± 3	< 2	< 2
HP-06	1,32 ± 0,22	105 ± 12	443 ± 59	< 3	4 ± 2	< 2	2,6 ± 0,4
HP-07	0,54 ± 0,12	25,8 ± 2,3	507 ± 14	< 4	< 3	< 3	1,3 ± 0,8
HP-08	13067 ± 744	1748310 ± 99654	2300 ± 129	86 ± 9	1510 ± 70	< 13	< 9
HP-09	11,28 ± 1,23	839 ± 112	1130 ± 87	194 ± 13	4500 ± 45	181 ± 1,9	< 10
HP-10	46,9 ± 2,4	2400 ± 161	21000 ± 600	83 ± 8	2500 ± 80	92 ± 5	46 ± 9
HP-11	11,2 ± 1,4	1040 ± 130	12100 ± 460	4000 ± 400	7600 ± 700	3600 ± 360	67 ± 9
HP-12	< 0,39	20,9 ± 2,4	540 ± 20	91 ± 10	198 ± 15	83 ± 5	
HP-13	18,12 ± 1,20	2010 ± 120	1880 ± 96	10 ± 4	34 ± 5	6 ± 3	3,7 ± 1,0

Sample	$^{239+240}$Pu, Bq/g	^{241}Am, Bq/kg	^{137}Cs, Bq/kg	^{60}Co, Bq/kg	^{152}Eu, Bq/kg	^{154}Eu, Bq/kg	^{155}Eu, Bq/kg
HP-14	1,14 ± 0,45	143 ± 37	247 ± 76	< 3	8 ± 2	< 1,9	2 ± 1
HP-15	< 0,35	2,8 ± 1,6	106 ± 9	< 3	4 ± 2	< 1,4	< 3
HP-16	514 ± 99	42300 ± 8400	135 ± 3	< 3	4 ± 2	< 1,4	< 3
HP-17	< 3,6	128 ± 14	302000 ± 16300	< 16	< 44	< 32	< 42
HP-18	< 12	< 87	4490000 ± 67000	< 48	< 164	< 136	< 155
HP-19	16,0 ± 1,2	583 ± 53	4790 ± 90	< 21	< 16	< 13	< 16
HP-20	< 0,20	< 1,2	49 ± 5	< 3	< 3	< 2	1,8 ± 1,0

The most active in terms of $^{239+240}$Pu and ^{241}Am are the samples taken at the place of hydro-nuclear explosion (HP-08) and at the entry of the adit 139 at Degelen site (HP-16). The anomaly high concentrations of ^{137}Cs were found in samples HP-10 – nuclear explosion and HP-17, HP-18 – adit 609 on Degelen site. Record concentrations of ^{60}Co, ^{152}Eu and ^{154}Eu are noticed in sample HP-11 – Atomic Lake on Balapan site. Increased concentration of ^{152}Eu and ^{154}Eu isotopes is also observed in samples HP-10 and HP-09 (mixed explosion).

^{241}Am is the product of β-decay of ^{241}Pu with the half-life period of 14.35 years, which is, in its turn, accumulated through (n, γ) reaction from ^{240}Pu. Over the period that passed after tests on the STS, concentrations of ^{239}Pu and ^{240}Pu, which have long half-life periods (6564 and 24110 years accordingly), could not suffer any noticeable quantitative changes because of decay. Concentration of ^{241}Am, with the half-life period 432 years, also could not noticeably decrease over the same period of time. Therefore, the $^{239+240}$Pu/^{241}Am ratio is the indication of nuclear test age.

Based on Table 3, one can conclude that the "youngest" explosion is the nuclear test conducted in the adit 177 at Degelen site (sample HP-19). The $^{239+240}$Pu/^{241}Am ratio for this would be 26.8. The same ratio for sample HP-08 is 7.47, that is why the hydro-nuclear explosion on P-2 site is the "oldest" one of all nuclear tests under study. Such conclusions, however, can be made only with the assumption that isotope composition of nuclear charge used in different tests is identical, which is not always true.

The data in Table 3, in terms of sample activity, correlate well with the results of γ-, β- and α- background levels measured during sampling (Table 2).

2.1.2. Sample Separation According to Granulometric and Magnetic Fractions

Separation of soil samples into granulometric fractions was done by wet screening at the Analysette 3 vibratory sieve shaker produced by FRITSCH with dimensions 1.25, 0.50, 0.28, 0.112 and 0.040mm. After each test, the screens were washed in Laborette 17 ultra-sound bath made by FRITSCH.

The soil samples were divided into factions with the use of standard wet screening technique. To reduce the possible contamination of low-activity soil with the high-activity soil, the less active samples were screened first.

After the particle-size 9granulometric) separation, the produced sub-samples were divided into magnetic and non-magnetic components in accordance with the technique described above.

Table 4 in Appendix 1 shows the data on mass output for granulometric and magnetic soil fractions. Hereinafter the granulometric fraction f > 1.25 μm is referred to as fraction 1, fraction 1.25 > f > 0.5 μm – as fraction 2, fraction 0.5 > f > 0.28 μm – as fraction 3, fraction 0.28 > f > 0.112 μm – as fraction 4, fraction 0.112 > f > 0.04 μm – as fraction 5 and fraction 0.04 > f μm – as fraction 6.

Table 4.

Data on mass yields of STS soil sample fractions at an aqueous dissemination

Sample	Fraction weight, g											
	f > 1.25 μm		1.25 μm >f> 0.5 μm		0.5 μm >f> 0.28 μm		0.28 μm >f> 0.112 μm		0.112 μm >f> 0.04 μm		0.040 μm >f	Total sample mass
	Magnetic	Nonmagnetic	Magnetic	Nonmagnetic	Magnetic	Nonmagnetic	Magnetic	Nonmagnetic	Magnetic	Nonmagnetic		
HP 01	60	340	9	308	2	118	2	110	5	96	472	1522
HP 02	50	226	10	115	12	62	5	117	5	91	497	1190
HP 03	59	289	8	147	10	70	7,5	91	8,5	80	231	1001
HP-04	31	131	7	243	4	189	6	194	4	87	283	1179
HP 05	161	79	57	324	18	105	16	111	11	66	150	1098
HP 06	68	290	7	139	17	74	17	106	10	64	226	1018
HP 07	1	126	11	95	18	56	15	81	6	86	418	913
HP-08	44	186	7	230	2	113	4	109	5	82	296	1078
HP-09	46	185	7	235	25	133	13	131	6	61	213	1055
HP-10	30	108	4	189	1	134	5	155	4	89	172	891
HP-11	37	229	2	250	1	113	3	122	1	86	287	1131
HP 12	10	99	6	137	10	92	1	203	0	208	509	1275
HP-13	16	116	2	152	6	65	2	100	1	84	495	1039
HP 14	50	118	33	247	15	153	42	166	28	111	472	1435
HP 15	69	217	112	168	83	98	59	185	27	133	481	1632
HP-16	12	77	3	126	1	46	1	88	4	169	157	684
HP-17	44,5	41	4	70	2	38	1,5	54	4	56	67	385
HP-18	28	14,5	3	48	0,5	38	0	57	2	67	63	321
HP-19	7	95	2	118	3	27	0	40	0	91	397	780
HP 20	39	92	6	214	13,5	44	8,5	54	2	104	234	821

According to Table 4, non-magnetic fraction is the material basis for the majority of samples and fractions. Certain samples have no magnetic fractions at all. The exceptions are the first fractions of the samples HP-05, HP-17 and HP-18, where the major part of the sample material is concentrated in the magnetic fraction.

The sixth granulometric fraction was not divided into magnetic and non-magnetic components.

2.1.3. Gamma-spectrometric analysis of soil fractions

Gamma-spectrometric analysis of soil fractions was performed in accordance with the technique described above. Contents of ^{241}Am, $^{239+240}Pu$, ^{152}Eu, ^{154}Eu and ^{137}Cs isotopes were the analytical parameters. The produced values of absolute activities with the distribution throughout fractions are graphically shown in Figure 3. The sample H-12 was analysed without fraction division into magnetic and non-magnetic components, but only for ^{241}Am, $^{239+240}Pu$, and ^{152}Eu isotopes.

Depending on the sampling point, the following features of activity distribution within fractions are distinguished:

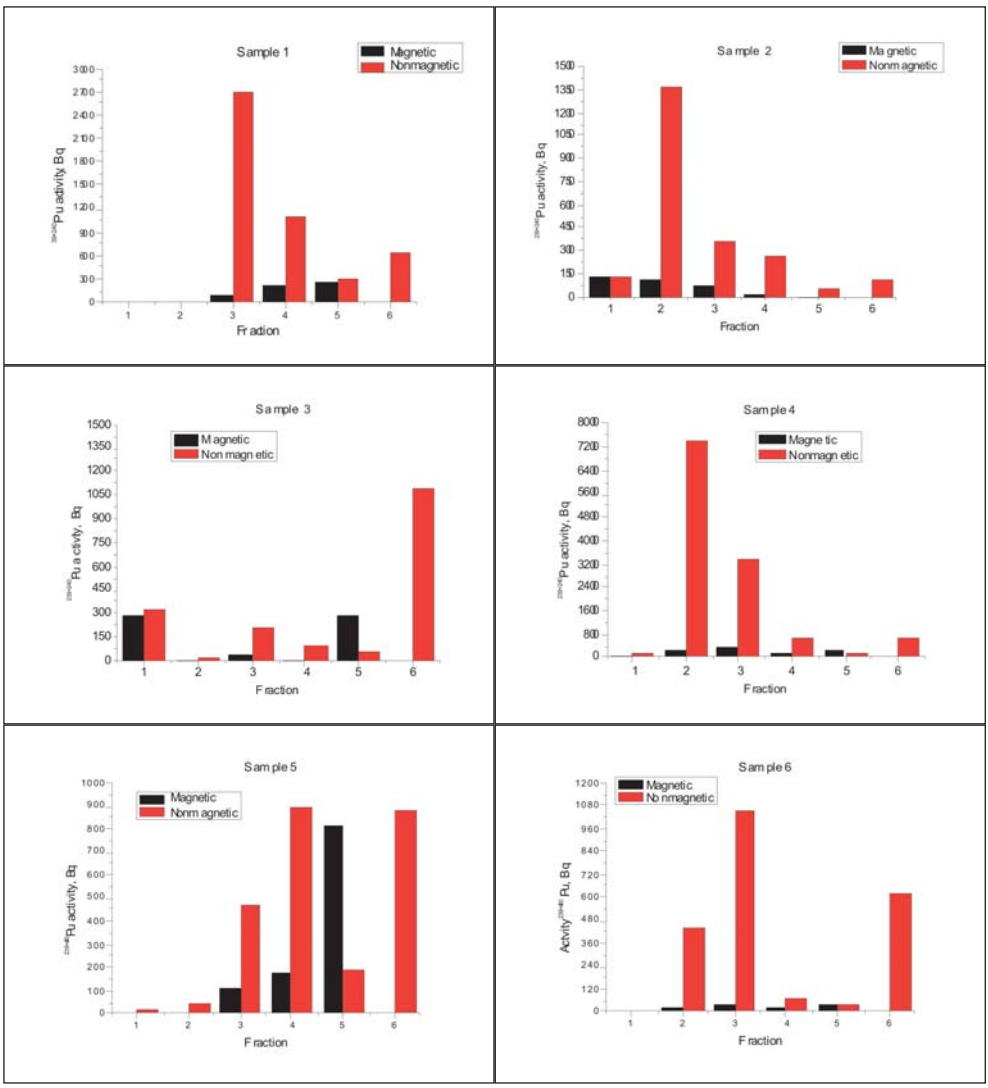

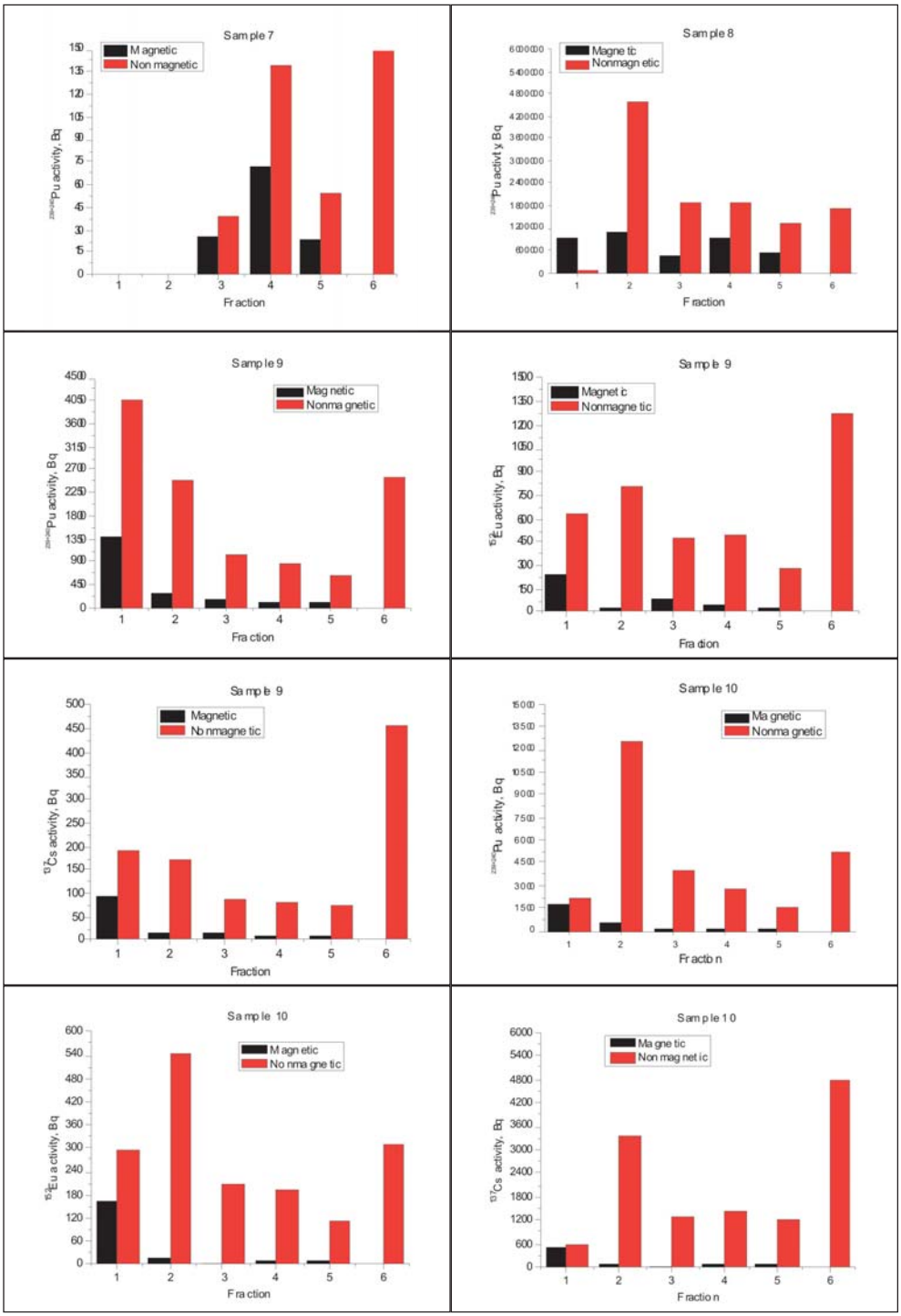
Sample 7
Magnetic
Non magnetic
Fraction
Sample 8
Magnetic
Nonmagnetic
Fraction
Sample 9
Magnetic
Nonmagnetic
Fraction
Sample 9
Magnetic
Nonmagnetic
Fraction
Sample 9
Magnetic
Nonmagnetic
Fraction
Sample 10
Magnetic
Nonmagnetic
Fraction
Sample 10
Magnetic
Nonmagnetic
Fraction
Sample 10
Magnetic
Nonmagnetic
Fraction

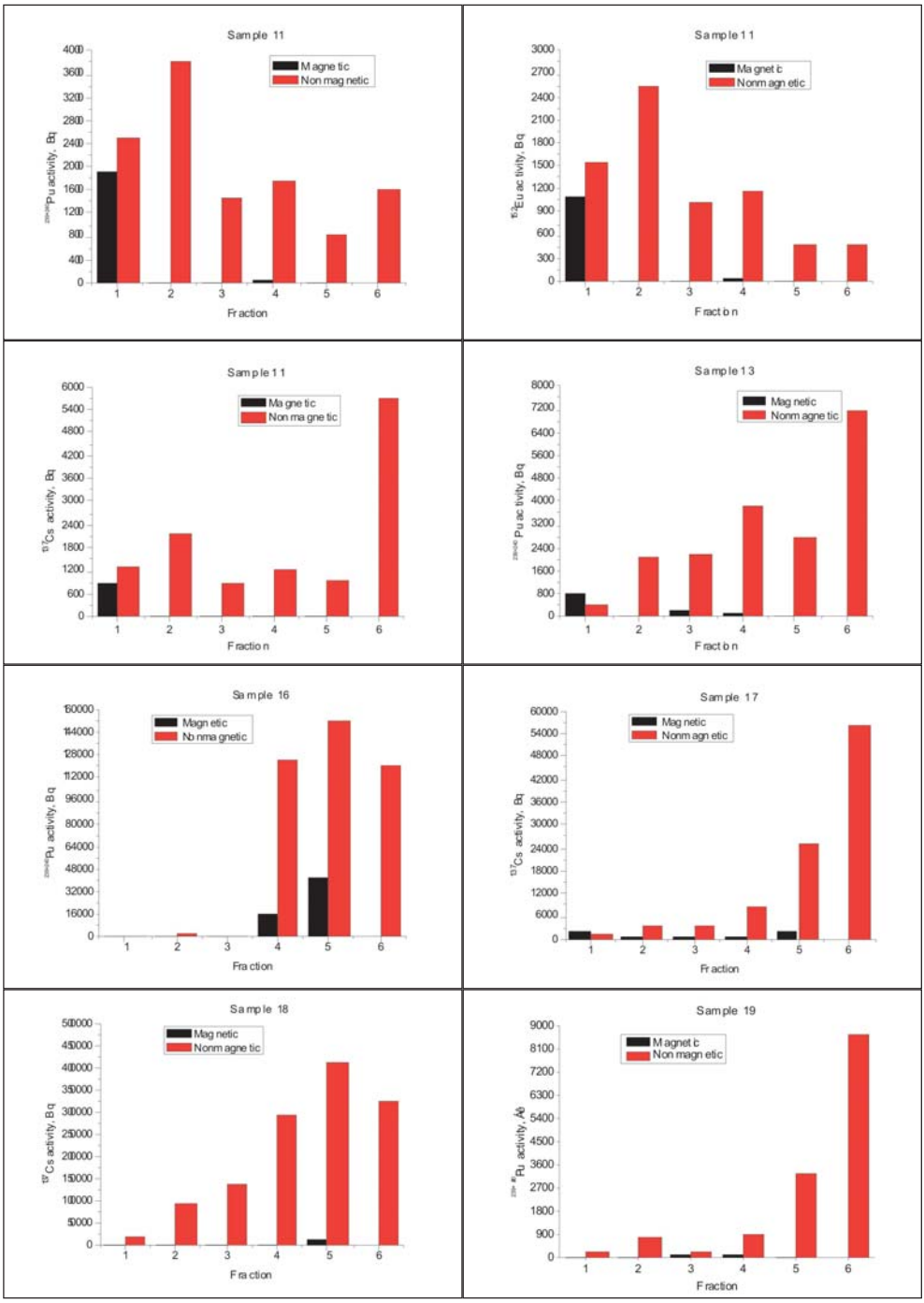

Figure 3. Sample activity distribution within the granulometric fractions

"Experimental Field" site, south-eastern and south-western traces (samples HP-01-HP-07)

The samples, including the reference ones (HP-01-HP-03), are similar in their radionuclide composition. Activity of $^{9+240}$Pu varies within the range from 540 Bq/kg (HP-07) to 11,100 Bq/kg (HP-04). Dependence of sample activity on the distance to the explosion epicentre is traced. As a rule, the majority of activity is concentrated in non-magnetic fractions, which is first of all determined by the ratio between the magnetic fraction mass and non-magnetic fraction mass.

For the most active sample HP-04 (south-eastern trace within 1.2 km of the epicentre), the peak of plutonium activity is concentrated in the second granulometric fraction (57% of the total sample activity). Moving away from the epicentre (sample HP-05 – 10 km from the explosion epicentre), the peak of activity shifts towards finer fractions 4, 5 and 6. Similar situation is observed with regard to the samples from the south-western trace. If the peak of activity for the sample HP-06 (8 km of the epicentre) falls on the 3rd fraction (47% of the total sample activity), then the 4th and 6th fractions become more active for the sample HP-07 (16 km of the epicentre). Since small fractions are mostly exposed to wind transport, one can assume that as you move away from the epicentre, the activity brought from the districts that are mostly close to the epicentre areas starts playing bigger role.

P-2 site (samples HP-08-HP-10)

The sample HP-08 (epicentre area of hydro-nuclear explosion) is the most active one of all selected samples in terms of $^{239+240}$Pu isotopes (average specific activity is 13067000 Bq/kg). The peak of activity falls on the second fraction (37% of the total sample activity). In other fractions, activity is distributed approximately evenly. The peak of sample absolute activity in terms of ^{137}Cs falls on the 6th (34%) and 2nd (32%) fractions, and in terms of ^{152}Eu – on the 2nd fraction – 41% of the total sample activity. Except for the 6th fraction, high correlation value in distribution of plutonium and caesium activities in fractions is observed (correlation factor is 0.987). ORIGIN software was used to compute correlation factors.

The same is observed in the sample HP-10 taken from the place of nuclear explosion. The peak of activity in terms of plutonium also falls on the second fraction (42% of the total sample activity), although specific activity of the sample HP-10 is 279 times lower than the activity of the sample HP-08. Out of all samples taken from P-2 site, the sample HP-10 has the highest specific activity in terms of cesium (21,000 Bq/kg) and high activity in terms of ^{152}Eu (2,500 Bq/kg). The peak of absolute activity in terms of cesium falls on the 6th (36%) and 2nd (26%) fractions, and in terms of europium – on the second (30%) and first (25%) fractions. The highest correlation degree is observed in distribution of plutonium and europium activities in fractions (correlation factor 0.929) and except for the 6th fraction for plutonium – cesium (correlation factor 0.953). It shows the common nature of origin of these isotopes.

Specific activity of the sample HP-09 taken from the place of mixed explosion is three orders less than the same parameter for the sample HP-08. For this sample, the most active particle-size fraction in terms of plutonium is the first one (40% of the total sample activity). At the same time, out of three samples the sample HP-09 is the most active in terms of ^{152}Eu with the peak of absolute activity falling on the sixth particle-size fraction (29%). However, the first and the second fractions also have comparable activities (20% and 19%, respectively). Same as in the samples HP-08 and HP-10, except for the 6th fraction, high cor-

relation degree is observed in distribution of plutonium and cesium activities in the fractions (correlation factor 0.948) and cesium and europium (correlation factor 0.947).

Therefore, despite different nature of explosions conducted in the places where samples HP-08, HP-09 and HP-10 were taken and big differences in activities, distribution of $^{239+240}$Pu, ^{152}Eu and ^{137}Cs activities in the granulometric fractions is practically identical with the peak falling on coarse fractions (1 and 2) for europium and plutonium. The most of activities of these samples in terms of cesium, except for coarse fractions, is concentrated in the smallest part of the sample - in the sixth fraction. In all three samples, high correlation degree is observed in distribution of plutonium and cesium activities in fractions which shows the common nature of origin of these isotopes. Apparently, some portion of activity of the sixth sample fractions in terms of cesium is introduced. The relation between ^{152}Eu, $^{239+240}$Pu and ^{137}Cs has not been revealed for all samples.

Atomic Lake (samples HP-11, HP-12)

The characteristic feature of the sample HP-11 is its high specific activity in terms of ^{152}Eu (7,600 Bq/kg) – the highest out of all collected samples. Concentrations of $^{239+240}$Pu and ^{137}Cs in the sample are not the record ones but are also rather high (11,200 Bq/kg and 12,100 Bq/kg, respectively). The peak of absolute activities in terms of plutonium and europium falls on the coarse granulometric fractions: the first fraction has 32% of sample activity in terms of plutonium and 32% in terms of europium, and the second fraction – 28% in terms of plutonium and 30% in terms of europium. The most active in terms of cesium is the sixth fraction (43% of the total sample activity). Very good correlation is observed in $^{239+240}$Pu, ^{137}Cs and ^{152}Eu distribution. Correlation factors for plutonium-cesium is 0.977 and cesium–europium is 0.967. Only the 6th cesium fraction falls out of the correlation.

The sample HP-11 was collected on the ridge of the lake, and the sample HP-12 – at 50m distance. The shift of sampling point for 50 meters entails reduction of sample specific activity in terms of plutonium for more than two orders of magnitude, and in terms of europium – in 38 times and cesium – in 22 times which shows that practically all activity in the Atomic Lake area is concentrated in the immediate proximity of the nuclear explosion area and quickly goes down away from the epicentre.

Telkem-1 (samples HP-13-HP-15)

The sample HP-13 taken from the ridge has the highest specific activity. As moving away from the ridge, the sample activity quickly goes down. Specific activity of the sample HP-14 (200m away from the collection point of the sample HP-13) in terms of plutonium is 16 times less than the activity of the sample HP-13, and the sample HP-15 – almost for two orders less.

The peak of absolute activities in terms of plutonium and cesium in the sample HP-13 is in the 6th fraction (37% and 82%, respectively). And if the activity of coarser fractions in terms of plutonium is also significant, almost the entire activity in terms of cesium is concentrated in the smallest fraction. Such activity distribution within the granulometric fractions apparently attests that the majority of active particles are introduced in the area of study due to different natural factors. Plutonium-europium correlation (correlation factor 0.94) is traced in the sample HP-13, where only 1 non-magnetic fraction falls out of the general regularity. Due to low fraction activity, such links are impossible to be identified for cesium.

Degelen Site (samples HP-16-HP-20)

Samples taken at same one site have different radionuclide composition. Out of all 20 samples, the sample HP-16 (adit 139) has the second after HP-08 specific activity in terms of plutonium (514,000 Bq/kg). The samples HP-17 and HP-18 (adit 609) are more active in terms of cesium (203,000 Bq/kg and 4,490,000 Bq/kg, respectively) and practically inactive in terms of plutonium and europium. The sample HP-19 (adit 177) has rather high, although not record, activities in terms of both plutonium (16,000 Bq/kg) and cesium (4,790 Bq/kg). Finally, the sample HP-20 (adit 503) is practically inactive in terms of all isotopes. Such wide variety of isotope compositions is apparently determined by both the nature of nuclear tests and conditions of activity transfer from inside cavity of the adit to its entry.

Despite the difference in radionuclide compositions, samples taken at the Degelen Site have similar distribution of activities within the granulometric fractions. The majority of absolute activities therein is concentrated in small particle-size fractions (5, 6, and sometimes, 4) which differs them from the rest samples taken on the test site.

Practically all activity in terms of plutonium in the sample HP-16 is concentrated in the 4^{th} (31% of the total sample activity), 5^{th} (42%) and 6^{th} (26%) granulometric fractions. The peak of activity in terms of cesium in the samples HP-17 and HP-19 is concentrated in the 6^{th} fraction (54% and 72%, respectively). Finally, the nature of cesium activity distribution in fractions in the sample HP-18 has smoother nature with the peak being in the 5^{th} fraction (33% of the total sample activity).

Prevalence of small fractions, which have the best sorption properties, in activity distributions is explained by the fact that radionuclides are accumulated here as a result of interaction of soil particles with ground waters running from adits. This fact also explains anomalously high concentrations of cesium that has the best migration capabilities out of all radionuclides under study.

Specific feature of the adit 609 (the samples HP-17, HP-18) is the increase of specific activity of samples in terms of cesium as moving away from the entry. This phenomenon is apparently explained by the relief specifics of the sampling area.

Conclusions:

Soil samples taken in different places of STS ("Experimental Field" site, P-2 Site, Atomic Lake, Telkem-1), where different types of nuclear tests were conducted (surface, air, and excavation), have common specifics of radionuclide activity distribution in the granulometric fractions. In the areas located in immediate proximity to the explosion epicentre, the most of the sample activities is concentrated in coarse particle-size fractions: normally in the 2^{nd} (particle size from 0.5 to 1.25 mm), less often – 1 (>1.25 mm) and 3 (0.28 – 0.5 mm). Activity of these samples was formed as a result of interaction of soil particles with the charge material at the time of nuclear explosion. Away from the epicentre, the peak of sample activities shifts towards smaller fractions – 6 (<0.04 mm) and less often 4 (0.112 – 0.28 mm) and 5 (0.04 – 0.112 mm). This process is accompanied by reduction of total sample activity. Wind transport of small soil particles plays the defining role in the activity accumulation.

Prevalence of small particle-size fractions in activity distribution is typical for the samples taken from Degelen site. Radionuclides are accumulated here as a result of interaction of soil particles with ground waters flowing from adits.

Magnetic soil factions have high specific activities. However, the mass of these fractions is normally significantly less than the mass of relevant non-magnetic fractions. That is why for the majority of samples the main portion of absolute activities is concentrated in non-magnetic factions.

For the samples HP-08-HP-11 and HP-13, correlation in distribution of separate isotopes in granulometric fractions is well traced which indicates the common nature of their origin. Normally, the exception is only the sixth granulometric fraction where the largest portion of activity is apparently introduced.

Magnetic separation for certain samples and fractions is present. However, the device used in the Project to divide samples into magnetic and non-magnetic components is inefficient for practical use. Probably, structural change of separator with the increase of magnetic field gradient might increase efficiency of its use.

2.1.3. X-ray fluorescence analysis of soil samples

In the study of STS soils, apart from radionuclide concentration and distribution, the presence of stable chemical elements accompanying radionuclides might be the important characteristics of nuclear test. Identification of such relations can help determine the conditions of explosion and type of the nuclear charge. XFA method described above was used as the analytical instrument for such types of studies during the Project. Average concentrations of chemical elements in samples taken from the STS are similar to such concentrations in usual non-disturbed soils. Therefore, in order to identify the relations, the distributions of chemical elements and radioactive isotopes within the granulometric fractions were studied.

Comparison of data on X-ray fluorescence analysis of fractions and specific activities of soils in terms of plutonium shows that correlation is traced for $^{239+240}$Pu isotopes and Fe (correction factor 0.87) and Sr (correlation factor 0.90) only in the most plutonium active sample HP-08. As for the other samples, even if there is contribution of the charge material it is considerably smaller than the average concentration of chemical elements in fractions.

One can therefore state that the assumption of possible genetic relation of certain chemical elements and plutonium in active samples in general and in "hot" particles in particular cannot be proved by the produced experimental data. The majority of the sample material and, as a result, chemical elements connected therewith have natural origin.

2.1.4. Identification of presence and assessment of quantity and average activity of "hot" particles in the samples

Based on the developed approach, tests were conducted to assess the presence of "hot" particles in soil material with the use of repeated agitation. To achieve maximum effect of sample material agitation, recommendations on selection of geometric conditions for measurements described in study [4] were taken into account.

Mass of each of five samples prepared for the test was 98 gram. The height of samples varied depending on the material density.

16 consecutive agitations and measurements were conducted for each sample. For the sample HP-16, 3 such series were conducted. After each measurement series, the counting rate for the lines with energies 13.5 keV ($^{238+239+240}$Pu), 13.9 keV ($^{238+239+240}$Pu), 17.2 keV ($^{238+239+240}$Pu), 17.7 keV ($^{238+239+240}$Pu), 20.2 keV ($^{238+239+240}$Pu), 20.8 keV ($^{238+239+240}$Pu), 26.4 keV (^{241}Am), 59.5 keV (^{241}Am) and 129.3 keV (^{239}Pu) was determined. Standard deviations

were calculated for 16 measured counting rates. For each gamma-ray or X-ray line full mass attenuation coefficients were calculated by reference tables [15] based on the assumption of silicon matrix as this element, according to its characteristics, is close to soils with average elemental composition.

The produced dependences of standard counting rates of gamma-ray and X-ray lines on their mass attenuation coefficient for the most active samples out of the studied ones – the samples HP-08 and HP-16 – have pronounced exponential nature (for the sample HP-08, the dependence is shown on Figure 2). According to mathematical formalism, in case of absence of "hot" particles in the sample (all activity is concentrated in fine matrix fraction) or in case of big number of "hot" particles, when they determine the total matrix activity of sample, the standard deviations in counting rates of gamma-ray and X-ray lines must be determined only by statistical measurement errors. As it is obvious from Table 3, for samples 8 and 16 and for all energy lines, the ratio between standard deviation and statistical error exceeds the order. Significant difference of the standard deviations from the statistical errors shows that the number of "hot" particles in these samples is ultimate. Exponential nature of the dependence of standard deviations in counting rate on mass attenuation coefficient proves the correctness of mathematical tool selection.

For the samples 9, 10 and 13, the ratio between standard deviations and statistical errors does not exceed 5, and in certain cases statistical error exceeds standard deviation. This is conditioned by minimum activity concentrated in "hot" fraction of samples.

In [4], conclusion was made with the help of mathematical modelling that the increase of attenuation properties of the environment results in the increase of width and frequency of counting rate distribution (increase of standard deviation) and skewness of distribution. Data produced in this test proves these assumptions and gives impression of the nature of standard deviation change at the increase of attenuation characteristics of the environment.

2.2 Structure and composition of the "hot" particles

2.2.1 Identification and separation of "hot" particles

As it was mentioned above, the works related to "hot" particle separation were conducted with the use of two methods: induced fission and visual identification. Quantity, average absolute and specific activities of the "hot" particles separated in the 1, 2 and 3 granulometric fractions are shown in Table 5. Separation from fraction 3, due to limitations of visual identification method, was performed by induced fission method. Table 5 shows separation methods in different colours (blue colour – induced fission method, red colour – visual identification method).

For the fractions 4 and 5, particles were not separated and only their number was calculated. In this case, the induced fission method was used for identification. Conditionally discovered particles of these fractions were divided into four colour groups depending on the number of tracks (particle activity) on detector (black colour – the number of particle fragments on detector from 5 to 10, blue – the number of fragments from 10 to 30, green colour – the number of fragments from 30 to 100 and red colour – the number of fragments over 100). The produced results are shown in Table 6. Particle activities of the 4^{th} and 5^{th} fractions were not measured.

The obtained data suggest that the number of "hot" particles, their form, and average activities depend on the overall activity of a sample and the type of nuclear test performed. Figure 4 shows typical "hot" particles sampled at different STS grounds.

"Experimental Field" site (samples HP-01 – HP-07)

The sampled particles appear to constitute sintered mineral formations. The fused form of particles indicates their formation at high temperatures and pressures. Particles of teardrop and spherical shape are present.

On the whole, in the seven samples taken at the "Experimental Field" site there were isolated 46 "hot" particles from the first fraction, 215 from the second fraction and 61 from the third fraction (table 5). 91 "hot" particles were found in the fourth fraction and 118 particles in the fifth fraction (table 6). The average number of particles found in 1 gram of sample is 0.1 for the fraction 1, 1.1 for the fraction 2, 5.2 for the fraction 3, 135 particles for the fraction 4, and 440 for the fraction 5. On the average 10,000 particles of soil contain 4 "hot" particles in the first fraction, 13 particles in the second fraction, and 16 particles in the 3rd fraction.

The largest number of particles in large granulometric fractions falls on the most active sample HP-04 (166 particles); most of them (121 particles) belong to the second granulometric fraction. The largest number of particles of the fractions 4 and 5 was found in the ample HP-05 (310 and 685, respectively).

The average absolute and specific activity of particles of the 1st granulometric fraction comprised 11 Bq and 2,000 kBq/kg, respectively. For the 2nd fraction, these numbers are 7 Bq and 3,430 kBq/kg and for the 3rd fraction - 0.59 Bq and 3,700 kBq/kg, respectively.

Particles of the first fraction in the sample HP-03 (3 particles) have the greatest average absolute (53 Bq) and specific (5,000 kBq/kg) activity.

Average efficiency for activity release from the first fraction is 37%, from the second -19%, and from the third -32%. "Hot" particles can therefore most efficiently be extracted from the first and the third fractions.

Site P-2 (samples HP-08 – HP-10)

Hydro-nuclear explosion, crest (sample HP-08)

The fused form of particles indicates their formation at high temperatures and pressures. Almost all of the particles have tear-drop or spherical shape.

The sample HP-08 is an absolute record-holder for the amount of "hot" particles. On the whole, 243 "hot" particles were separated from the first fraction, 652 from the second fraction, and 34 from the third fraction. 9,247 "hot" particles were found in the fourth fraction and 83,549 particles in the fifth fraction. The average number of particles in 1 gram of sample was 1.9 for the first fraction, 5.5 for the second fraction, 24 for the 3rd fraction, 21,020 particles for the 4th fraction, and 417,730 for the 5th fraction. On the average 10,000 particles of soil contain 80 "hot" particles of the first faction, 61 particles of the second fraction, and 72 particles of the 3rd fraction.

Table 5.

"Hot" particles separated from 1st, 2nd, and 3rd granulometric fractions

Fraction	Fraction mass, g	Absolute fraction activity for Pu, Bq	Average specific fraction activity for Pu, kBq/kg	Extraction method	Number of particles	Number of particles in 1 g of sample (for 1000 soil particles)	Average absolute particle activity for Pu, Bq	Average specific particle activity for Pu, kBq/kg	Activity of the fraction associated with "hot" particles
					Sample HP-01				
1	194	6.3	0.028	V.i.	2	0.01 (0.04)	0.45	41	14
					Sample HP-02				
1	150	139	0.93	V.i.	4	0.03 (0.12)	13	3200	37
2	75	890	12	V.i.	41	0.55 (0.61)	2.8	5500	13
	2.6	31		F.d.	2	0.77 (0.85)	0.51	1000	3.3
3	2.1	12	5.9	F.d.	5	2.4 (0.72)	0.35	~3500	15
					Sample HP-03				
1	190	336	1.8	V.i.	3	0.02 (0.08)	53	9000	47
3	1.7	5.3	3.1	F.d.	23	14 (4.2)	0.1	~330	43
					Sample HP-04				
1	110	96	0.87	V.i.	33	0.3 (1.3)	1.2	280	41
	8.9	7.7		F.d.	2	0.22 (0.92)	2.8	650	72
2	150	4620	31	V.i.	96	0.64 (0.70)	4.5	7500	9.4
	5.9	183		F.d.	25	4.2 (4.6)	1.8	3000	25
3	1.5	29	19	F.d.	10	6.7 (2.0)	1.9	~9000	67
					Sample HP-05				
1	120	8.6	0.072	V.i.	1	0.008 (0.03)	3.8	170	44
	9.5	0.68		F.d.	1	0.11 (0.46)	0.03	1.3	4.4
2	190	9.2	0.048	V.i.	9	0.05 (0.06)	0.23	140	23
3	2.2	10	4.6	F.d.	6	2.7 (0.81)	0.62	~3700	37
					Sample HP-06				
2	90	287	3.2	V.i.	34	0.38 (0.42)	1.6	4400	19
	5.6	18		F.d.	8	1.4 (1.5)	0.89	2450	40
3	2.0	24	12	F.d.	9	4.5 (1.4)	0.40	~4000	15
					Sample HP-07				
3	10	8.8	0.88	F.d.	8	0.8 (0.25)	0.17	~1700	16

Fraction	Fraction mass, g	Absolute fraction activity for Pu, Bq	Average specific fraction activity for Pu, kBq/kg	Extraction method	Number of particles	Number of particles in 1 g of sample (for 1000 soil particles)	Average absolute particle activity for Pu, Bq	Average specific particle activity for Pu, kBq/kg	Activity of the fraction associated with "hot" particles
					Sample HP-08				
1	124	518000	4180	V.i.	83	0.67 (2.8)	3600	770000	58
	3.6	15100		F.d.	160	44 (185)	28	6000	30
2	117	2790000	23900	V.i.	539	4.6 (5.1)	1300	1100000	25
	1.0	23900		F.d.	113	113 (124)	185	157000	88
3	1.4	28400	20300	F.d.	34	24 (7.2)	102	~1000000	12
					Sample HP-09				
1	123	2890	23.5	V.i.	142	1.2 (5.0)	8.5	1300	42
	10	235		F.d.	12	1.2 (5.0)	1.3	199	6.7
2	134	1530	11	V.i.	41	0.31 (0.34)	1.4	2800	3.8
	5.5	61		F.d.	66	12 (13)	0.52	1040	56
3	2.2	17	7.7	F.d.	64	29 (8.7)	<0.01	~100	<4
					Sample HP-10				
1	82	2350	29	V.i.	798	9.7 (41)			
	10	290		F.d.	129	13 (55)	2.2	320	98
2	104	7050	68	V.i.	377	3.6 (4.0)			
	3.5	238		F.d.	193	55 (61)	0.77	408	62
3	1.5	45	30	F.d.	99	66 (20)	0.23	~2300	51
					Sample HP-11				
1	120	2000	17	V.i.	17	0.14 (0.59)	0.58	140	0.5
2	127	1950	15	V.i.	33	0.26 (0.29)	0.11	12	0.2
					Sample HP-12				
3	10	<1.6	<0.16	F.d.	1	0.1 (0.03)	<0.01	~100	
					Sample HP-13				
1	10	89	8.9	F.d.	1	0.1 (0.42)	7.2	1700	8.1
3	1.9	64	34	F.d.	2	1.1 (0.33)	3.1	~31000	10
					Sample HP-14				
3	3.0	8.4	2.8	F.d.	10	3.3 (0.99)	0.08	~800	10
					Sample HP-15				
3	3.0	<0.18	<0.06	F.d.	4	1.3 (0.39)	0.16	1400	

Fraction	Fraction mass, g	Absolute fraction activity for Pu, Bq	Average specific fraction activity for Pu, kBq/kg	Extraction method	Number of particles	Number of particles in 1 g of sample (for 1000 soil particles)	Average absolute particle activity for Pu, Bq	Average specific particle activity for Pu, kBq/kg	Activity of the fraction associated with "hot" particles
					Sample HP-16				
1	3.2	10	3.2	F.d.	7	2.2 (9.2)	0.085	17	6
2	68	1220	18	V.i.	26	0.38 (0.42)			
	2.5	45		F.d.	5	2 (2.2)	0.46	290	5
3	1.0	15	15	F.d.	4	4 (1.2)	0.052	100	1.4
					Sample HP-17				
1	10	<4.6	<0.46	F.d.	64	6.4 (27)	<0.01	<2	
2	3.9	<1.9	<0.49	F.d.	Not counted				
3	0.6	1.6	2.6	F.d.	Not counted				
					Sample HP-18				
1	8.1	<9.0	<1.1	F.d.	268	33 (139)	0.022	15	
2	2.5	<1.9	<0.75	F.d.	Not counted				
3	0.34	<0.2	<0.61	F.d.	Not counted				
					Sample HP-19				
1	10	13	1.3	F.d.	97	9.7 (41)	0.05	34	35
2	3.5	24	6.7	F.d.	Not counted				
3	0.85	6.3	7.4	F.d.	Not counted				
					Sample HP-20				
1	6.8	<0.68	<0.1	F.d.	7	1.0 (4.2)	0.01	6.8	
2	4.5	<0.45	<0.1	F.d.	5	1.1 (1.2)	0.11	30	
3	3.1	<0.5	<0.16	F.d.	45	15 (4.5)	0.06	65	

Extraction method:
F.d. – forced decay
V.i. – visual identification

Table 6.

Number of "hot" particles found in the sample fractions 4 and 5

Sample	Group of "hot" particles	Fraction 4			Fraction 5		
		Sample weight, g	Number of particles	Number of particles in 1g of sample	Sample weight, g	Number of particles	Number of particles in 1g of sample
HP-02	Red	0.39	no	no	0.24	no	no
	Green		16	40		12	50
	Blue		12	30		32	134
	Black		20	50		56	235
	TOTAL		**48**	**120**		**100**	**419**
HP-03	Red	0.65	1	2	0.26	6	23
	Green		2	3		7	27
	Blue		14	21		22	85
	Black		53	81		64	245
	TOTAL		**70**	**107**		**99**	**380**
HP-04	Red	0.53	1	2	0.26	5	20
	Green		4	8		11	43
	Blue		15	29		32	125
	Black		42	80		55	215
	TOTAL		**62**	**119**		**103**	**403**
HP-05	Red	0.77	2	2.6	0.35	1	2.9
	Green		6	8		10	35
	Blue		87	113		60	171
	Black		144	187		170	485
	TOTAL		**239**	**311**		**241**	**694**
HP-06	Red	0.70	<1	<1	0.26	12	46
	Green		10	14		16	62
	Blue		29	42		46	177
	Black		88	126		81	312
	TOTAL		**128**	**182**		**155**	**597**
HP-07	Red	0.90	5	5.6	0.21	1	4.8
	Green		11	12.2		11	52
	Blue		36	40		31	148
	Black		41	46		82	392
	TOTAL		**93**	**104**		**125**	**597**
HP-08	Red	0.44	245	560	0.20	2508	12540
	Green		1699	3860		5319	26590
	Blue		3836	8720		40410	202040
	Black		3467	7880		35312	176560
	TOTAL		**9247**	**21020**		**83549**	**417730**
HP-09	Red	0.72	39	54	0.30	50	167
	Green		41	57		62	206
	Blue		54	75		123	410
	Black		43	59		114	380
	TOTAL		**177**	**245**		**349**	**1163**
HP-10	Red	0.72	7	10	0.36	4	10
	Green		54	75		20	55
	Blue		238	330		260	720
	Black		357	495		492	1365
	TOTAL		**656**	**910**		**776**	**215**
HP-11	Red	0.41	no	no	0.25	no	no
	Green		4	10		8	32
	Blue		48	117		20	80
	Black		188	459		212	848
	TOTAL		**240**	**586**		**240**	**960**

Sample	Group of "hot" particles	Fraction 4			Fraction 5		
		Sample weight, g	Number of particles	Number of particles in 1g of sample	Sample weight, g	Number of particles	Number of particles in 1g of sample
HP-12	Red	1.00	no	no	0.27	no	no
	Green		1	1		no	no
	Blue		64	64		34	125
	Black		88	88		78	289
	TOTAL		**153**	**153**		**112**	**414**
HP-13	Red	0.37	12	32	0.25	28	112
	Green		no	no		17	68
	Blue		no	no		29	116
	Black		no	no		39	156
	TOTAL		**12**	**32**		**113**	**452**
HP-14	Red	0.36	no	no	0.37	no	no
	Green		5	14		3	8
	Blue		42	117		9	24
	Black		147	408		140	380
	TOTAL		**194**	**539**		**152**	**412**
HP-15	Red	0.79	no	no	0.46	11	24
	Green		5	6		28	60
	Blue		78	99		121	263
	Black		269	340		265	576
	TOTAL		**352**	**445**		**425**	**923**
HP-16	Red	0.24	7	29	0.12	15	125
	Green		10	42		24	200
	Blue		64	266		102	850
	Black		54	225		78	650
	TOTAL		**135**	**562**		**219**	**1825**
HP-17	Red	0.39	126	320	0.27	11	41
	Green		262	670		35	130
	Blue		3230	8280		1276	4725
	Black		3898	9995		2105	7798
	TOTAL		**7516**	**19265**		**3427**	**12694**
HP-18	Red	0.10	450	4500	0.09	38	420
	Green		7405	74050		1912	21240
	Blue		18398	183980		33750	375000
	Black		4500	45000		37875	420830
	TOTAL		**30753**	**307530**		**73575**	**817490**
HP-19	Red	0.79	97	125	0.12	no	no
	Green		2092	2650		230	1920
	Blue		9292	11760		13790	114915
	Black		5425	6865		25565	213040
	TOTAL		**16906**	**21400**		**39585**	**329875**
HP-20	Red	0.31	16	50	0.09	15	165
	Green		202	650		15	165
	Blue		4469	14415		612	6800
	Black		2948	9510		2025	22500
	TOTAL		**7635**	**24625**		**2667**	**29630**

Note:

Red – number of fragment tracks in the HP mark **(> 100)**
Green – number of fragment tracks in the HP mark **(30-100)**
Blue – number of fragment tracks in the HP mark **(10-30)**
Black – number of fragment tracks in the HP mark **(5-10)**

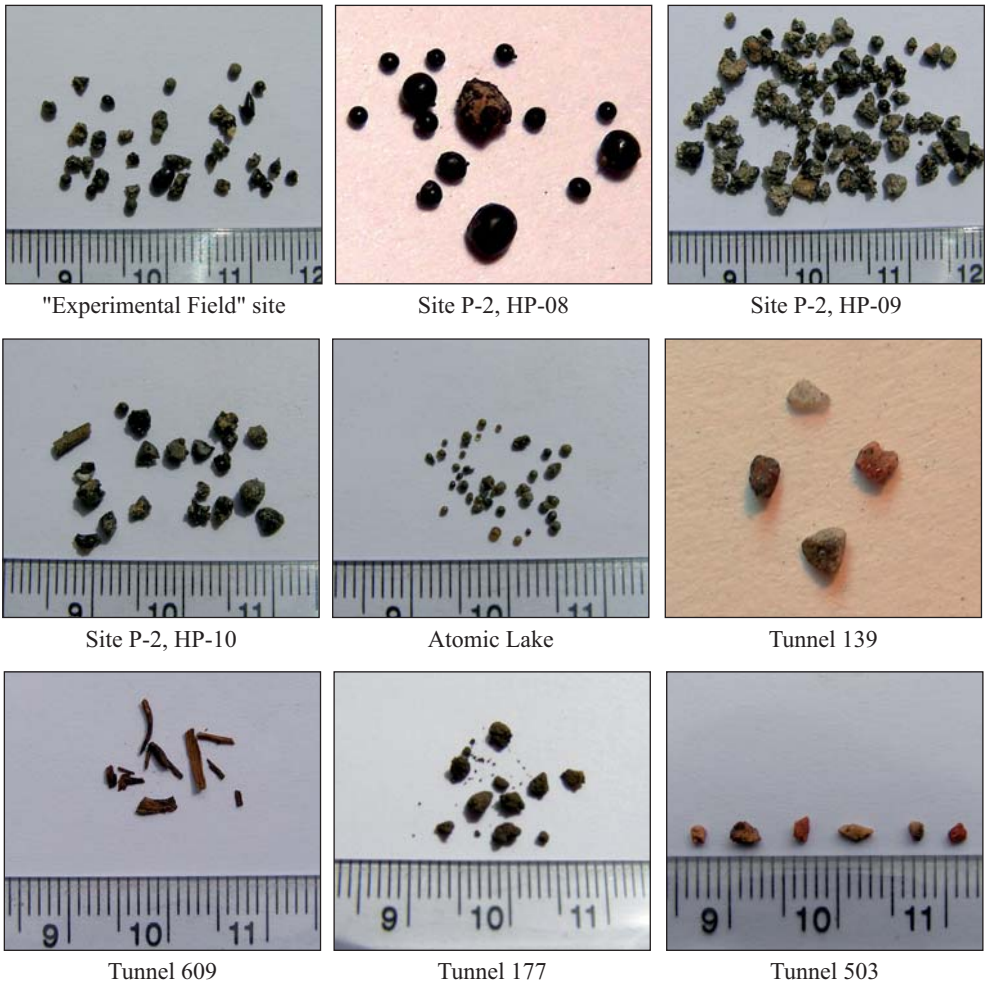

Figure 4. The typical "hot" particles sampled at the different areas of STS

The average absolute and specific activity of particles of the 1st granulometric fraction is 1,250 Bq and 267,000 kBq/kg, respectively. For the 2nd fraction, these characteristics are 1,110 q and 937,000 kBq/kg, respectively; and for the 3 fraction - 102 Bq and ~1,000,000 kBq/kg, respectively.

Average efficiency for activity release from the first fraction is 57%, from the second fraction - 26%, and from the third fraction -12%.

Combined explosion, crest (sample HP-09)

The sampled particles appear to constitute a sintered mineral formation. The fused form of particles indicates their formation at high temperatures and pressures.

On the whole for the sample, 154 "hot" particles were separated from the first fraction, 107 from the second fraction, and 64 from the third fraction. In the fourth fraction 177 "hot particles were found and in the fifth fraction -349 particles.

The average number of particles in 1 gram of sample is 1.2 for the 1st fraction, 7.5 for the 2nd fraction, 29 for the 3rd fraction, 245 particles for the 4th fraction, and 1,163 for the 5th fraction. On the average 10,000 particles of soil include 50 "hot" particles of the first faction, 8.4 particles of the second fraction, and 87 particles of the 3rd fraction.

The average absolute and specific activity of particles of the 1st granulometric fraction is 7.9 Bq and 1,214 kBq/kg, respectively. For the 2nd fraction, these numbers are 0.86 Bq and 1,714 kBq/kg, and for the 3rd fraction - <0.01 and ~ 100 kBq/kg, respectively.

Average efficiency for activity release from the first fraction is 39%, from the second - 5.8%, and from the third - <4%.

Nuclear explosion¸ crest (sample HP-10)

The sampled particles in appearance are similar to the "hot" particles sampled at the "Experimental Field" site (the samples HP-01 -HP-07), which seems to indicate the same nature of their origin.

By the number of detected "hot" particles the sample HP-10 is second after the sample HP-08. At the same time, in this case, the highest number of particles has been separated from major size fractions. On the whole for sample HP-10, 927 "hot" particles were separated from the first fraction, 570 from the second fraction, and 99 from the third fraction. In the fourth fraction there were found 656 "hot" particles, and in the fifth fraction – 776 particles. The average number of particles in 1 gram of sample is 10 for the 1st fraction, 21 for the 2nd fraction, 66 for the 3rd fraction, 910 particles for the 4th fraction, and 215 for the 5th fraction. On the average 10,000 particles of soil include 425 "hot" particles of the first fraction, 58 particles of the second fraction, and 200 particles of the 3rd fraction.

The average absolute and specific activities of particles were measured only for the "hot" particles identified by the method of induced fission. For the first granulometric fraction, these activities are 2.2 Bq and 320 kBq/kg, respectively. These numbers for the fraction 2 comprise 0.77 Bq and 408 kBq/kg, and for the 3rd fraction - 0.23 Bq and 2,300 kBq/kg, respectively.

Average efficiency for activity release by the method of induced fission comprised for the first fraction 98%, from the second - 62%, and from the third – 51%.

Thus, although more "hot" particles with high efficiency have been separated from the sample HP-10, their average activity is relatively low. Therefore, the total plutonium activity of the samples is not as high as one might expect.

Atomic Lake (samples HP-11 – HP-12)

Of the three samples taken at the site of excavation explosion (Atomic Lake), particles were identified from virtually the only sample HP-11 (Crest). As it was mentioned above, the activity of soil samples rapidly decreases with larger distance from the epicenter. Therefore, a small amount of "hot" particles separated from the sample HP-12 only confirms this fact.

The fused shape of separated particles similar to the particles in the sample HP-08 indicates their formation at high temperatures and pressures. Almost all of the particles are of spherical and tear-drop shape.

From the whole sample HP-11, by method of visual identification, 17 "hot" particles have been found, and from the second – 33. The method of induced fission revealed no "hot" particles in these fractions. 240 "hot" particles were found in the fourth and fifth fractions. The average number of particles in 1 gram of sample is 0.14 for the 1st fraction, 0.26 for the 2nd fraction, 586 particles for the 4th fraction, and 960 for the 5th fraction. On the average 10,000 particles of soil have 5.9 "hot" particles of the first fraction and 2.9 particles of the second fraction.

The average absolute and specific activity of particles for the 1st granulometric fraction is 0.58 Bq and 140 kBq/kg, respectively. These characteristics for the 2nd fraction are 0.11 Bq and 12 kBq/kg.

The average efficiency of activity release from the first fraction is 0.5%, and from the second – 0.2%. Apparently, the sample contains "hot" particles indistinguishable in appearance from regular soil particles, making it difficult to separate them by the method of visual identification.

Telkem-1 site (samples HP-13 – HP-15)

In samples taken at the Telkem-1 site, no "hot" particle was detected by the method of visual identification. By the method of induced fission only 17 particles left tracks on a glass detector. Of 17 particles, 16 belong to the third granulometric fraction and only one to the first one. Most of the particles are low-active. The only exception are three particles in the sample HP-13 with average absolute activity exceeding 3 Bq.

Degelen site (samples HP-16 – HP-20)

By their appearance, "hot" particles sampled at the Degelen site can be divided into 2 categories:

1. Particles of the sample HP-16 (adit 139) and HP-20 (adit 503) are natural mineral formations. Signs of fusion on the surface are absent what distinguishes them from most other particles sampled from the soil at STS.
2. The detected active formations of the samples HP-17, HP-18 (adit 609) and HP-19 (adit 177) are of pronounced organic origin. In the first case, this appears to be the remnants of wood, grass and leaves and in the second, easily destructible amorphous conglomerates similar to remains of peat.

Given the nature of the adits (water development), it can be assumed that the activity is due to contact with water particles flowing out from the interior of the adit. The appearance of particles, apparently, is determined by the conditions and place of sampling.

Except for the particles of the 1st fraction of the sample HP-16, all other "hot" particles were detected and isolated by the method of induced fission. Difficulties of the method of visual identification are due to the fact that the external features of separated active formations resemble little typical "hot" particles of STS.

At visual inspection of the detectors it was found that in the second and third fractions of the samples 17-HP - HP-19 the track marks of hot particles are very weak but cover almost the entire surface of the glass. The detailed examination with microscope shows that the marks of individual particles in them overlap. Using a microscope, it was impossible to determine the total number of hot particles in these fractions on the whole area of the detec-

tor. Therefore, in table 5 for these fractions it is indicated that particles are not accurately quantified. Activity distribution within the fraction falls more under the category of "matrix activity".

Average absolute activity of separated "hot" particles in plutonium is low (from 0.01 to 0.46 Bq) that determines their low specific activity (6.8 kBq/kg to 290 kBq/kg). At the same time, as it can be seen from tables 5 and 6, the number of detected "hot" particles is large enough, particularly in the samples HP-17 – HP-19.

2.2.2. Pu/Am ratio for isolated "hot" particles in the sample HP-08

As it was mentioned above, Pu/Am ratio in the samples is determined by the date and type of nuclear testing. However, the question remains whether all "hot" particles from the same samples have a common genesis or Pu/Am ratio remains constant for all particles. Measurement of plutonium and americium activities for individual particles is quite difficult, especially if the activity of small particles is low. It was therefore decided to try to answer the question about the common origin of "hot" particles at least for one most active sample, HP-08. For this purpose, activities of $^{239+240}$Pu and ^{241}Am isotopes were measured using gamma spectrometry for 249 of particles of three major granulometric fractions.

The average ratio Pu/Am for all investigated particles is 7.0, which fits well with the ratio of plutonium to americium obtained for the whole sample HP-08 (equal to 7.5). Despite the great variation in activities of individual particles (standard deviation is 2,863%), Pu/Am ratio varies within a small range and, as a result, the standard deviation for all fractions is less than 5.4%.

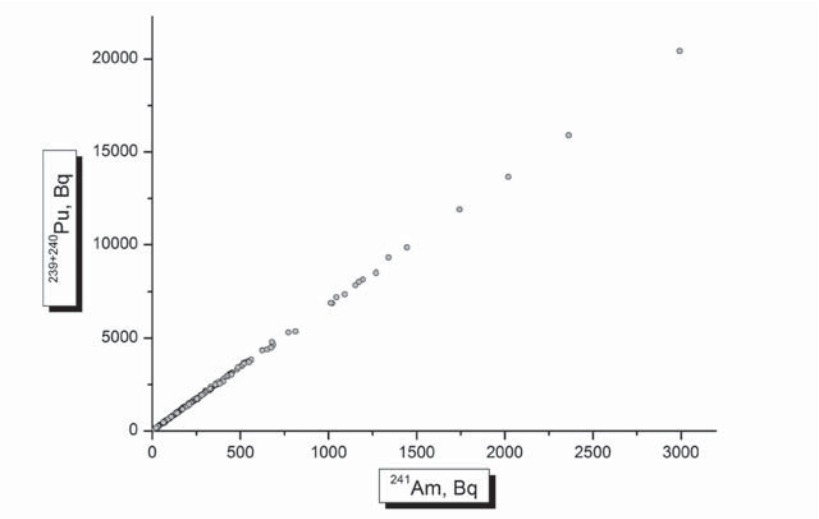

Figure 5. Plutonium activity vs americium activity for different "hot" particles in the sample HP-08

This finding is supported by the figure 5, which shows the relationship of plutonium and americium activities for different "hot" particles in the sample HP-08. As one can see in the Figure, almost all points perfectly lie on a line (the correlation coefficient is 0.9999), the slope angle of which conforms to Pu/Am = 7.0 ratio.

Thus, it can be stated that for the majority of "hot" particles in the sample HP-08 the Pu/Am ratio is to a good extent constant independent of the sizes of particles and their activities.

Figure 6 shows the distribution of the number of "hot" particles by plutonium activity. For that, the full range of activities was split in log scale into five subranges. As it can be seen from Figure 6, smaller particle size makes the maximum shifted to the range of lower activities. So, the first granulometric fraction has more particles with activity exceeding 1,000 Bq. The second fraction has more particles with the activities ranging from 100 up to 1,000 Bq. Finally, the third fraction has more particles with the activities ranging from 10 to 100 Bq.

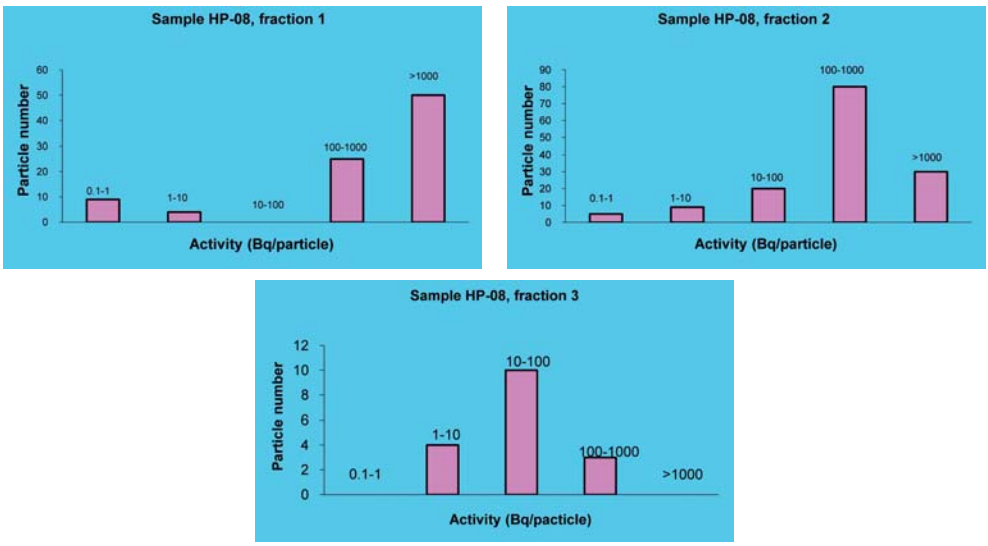

Figure 6. Distribution of "hot" particles by plutonium activity for the fractions 1, 2 and 3. Particles are extracted from the sample HP-08.

2.2.3. Mass-spectrometry of "hot" particles

Considering that "hot" particles are formed due to interaction of nuclear charge material with soil substance under high pressure and temperature, isotopic ratios of plutonium and uranium in "hot" particles carry information on the isotopic composition of the charge and represent therefore an important characteristic of a nuclear test. Therefore, as a part of the Project, there has been investigated the isotopic ($^{240}Pu/^{239}Pu$ and $^{235}U/^{238}U$) composition of 21 particles extracted from soil samples taken at the Site. For this purpose, the mass-spectrometry method described above was used.

The measurement results are presented in table 7. The last column of the table shows the ratios of total ion currents for uranium isotopic lines of to the total ion currents for the

plutonium isotopic lines. These relations, knowing the natural occurrence of uranium, make it possible to estimate plutonium content in "hot" particles.

Table 7.

Determination of isotopic ratios $^{235}U/^{238}U$ and $^{240}Pu/^{239}Pu$

Particle No	Mass, mg	Activity by $^{239+240}Pu$, Bq	$^{235}U/^{238}U$	$^{240}Pu/^{239}Pu$	I_{Pu}/I_U
HP-03, 1 fraction (>1.25 mm)					
1	5.1	not determined	0.22	0.07	0.17
HP-03, 2 fraction (from 0.5 to 1.25 mm)					
2	1.0	2.5	0.17	0.062	0.19
HP-03, 3 fraction (from 0.28 to 0.5 mm)					
3	not determined	0.17	0.44	0.071	0.83
4	not determined	0.09	0.33	0.06	0.48
HP-04, 2 fraction (from 0.5 to 1.25 mm)					
5	0.1	14.9	0.25	0.048	4
6	0.3	1.4	0.22	0.053	4
HP-04, 3 fraction (from 0.28 to 0.5 mm)					
7	not determined	6.2	0.69	0.052	0.48
HP-08, 1 fraction (>1.25 мм)					
8	5.2	4.71	0.14	<0.02	<0.1
9	not determined	not determined	8.2	0.048	0.21
HP-08, 2 fraction (from 0.5 to 1.25 mm)					
10	0.26	209	9.1	0.049	1.31
11	1.7	2530	10.6	0.048	1.15
12	not determined	280	10.5	0.038	0.36
13	not determined	not determined	7.4	0.048	0.21
14	not determined	not determined	0.77	0.049	0.41
HP-09, 1 fraction (>1.25 mm)					
15	5.45	8.71	<0.005	0.052	<0.1
16	6.32	7.90	0.20	0.065	0.67
HP-09, 2 fraction (from 0.5 to 1.25 mm)					
17	not determined	1.2	0.23	0.050	0.042
18	not determined	3.72	0.008	<0.02	<0.1
19	1.61	2.26	0.18	0.045	0.77
HP-10, 1 fraction (>1.25 mm)					
20	9.6	9.6	0.010	0.067	0.089
21	11.7	8.7	0.009	0.07	0.10

As it follows from table 7, the ratio of the isotopes $^{240}Pu/^{239}Pu$ for particles of different fractions sampled on different areas of STS varies within a small range (from <0.02 to 0.07).

A somewhat different situation exists for the ratio of the isotopes $^{235}U/^{238}U$. The natural balance of these isotopes is $^{235}U/^{238}U \approx 0.0072$. Close to this value are the ratios for only

four particles extracted from the first (^{235}U and ^{238}U) and the second ($^{235}U/^{238}U$ = 0.008) fractions of the sample HP-09 and from the first fraction of the sample HP-10 ($^{235}U/^{238}U$ = 0.01 and 0.009). For all other particles, this ratio varies in the range 0.14 ÷ 10.6. Maximum values for the $^{235}U/^{238}U$ ratio have been detected in the sample HP-08 (site P-2, hydronuclear explosion).

2.2.4. Electron and proton microscopy of "hot" particles

The presence of elevated concentrations of radioactive isotopes in the identified "hot" particles, especially isotopes of plutonium, is an extremely important fact as such. However, the nature of activity distribution within a volume remains unclear. The methods of gamma- and alpha-spectrometry used to measure $^{239+240}Pu$ contents do not give answer to this question. However, this information could help to understand the mechanism of formation of "hot" particles. So, if a particle is formed by sintering of nuclear charge activity with the soil substance, the distribution of radioisotopes in the volume must be quite uniform. At the same time, if the soil particles interact with the radioactive cloud under moderate temperatures and pressures, the deposition of activity must occur onto the particle surface. In this case, radioactive isotopes must be present only in the surface layers of "hot" particles.

Electron and proton microscopy were used to study the volume distribution of activity in "hot" particles. The methods used are described above. All measurements were made by consistent scanning of selected sample areas of 200 x 200 μm with ~ 20 μm increments. After analyzing the surface distribution of elements, metallographic section of particle was made, and the scanning of surface scanning was resumed. The section thickness was ~150 μm. For each particle 3 sections were made.

Analysis of three-dimensional distribution of chemical elements was made for "hot" particles of the first granulometric fraction (diameter more than 1.25 mm). This is due to the difficulties in fixing the particles on the surface of substrate and their sectioning in case of particles of smaller fractions.

Within the framework of the Project, three "hot" particles were analyzed by two of the methods used. As one of the main objectives of this work was to obtain distribution maps of radioactive elements, active particles (with activity in plutonium from 200 to 1,000 Bq) identified from the sample HP-08 were taken for the analysis.

Based on the obtained data the following conclusions can be made:

1. All studied particles have similar average element composition of both the natural surface and the sections. The average element composition is close to the element composition of the typical soils (SiO_2 base with the admixtures of Al_2O_3, NaO, and Fe_2O_3 oxides), which indicates that the matrix base of "hot" particles is the soil material.
2. No elements – products of nuclear explosions (particularly, Pu) was found in the "hot" particles. For the most active particles under study (plutonium absolute activity of about 1,000 Bq) at uniform distribution of elements in volume of a particle, the content of elemental plutonium must be ~ 25 μg/g. The sensitivity of the method used for plutonium in the case of 1,000 second measurement of spectra in a point comprises ~ 1,500 μg/g for electron microprobe and ~ 300 μg/g for proton microprobe. At uniform distribution of plutonium with the particle bulk, sensitivity of both methods is insufficient to analyze transuranic elements.

So both analytical methods are only capable to record plutonium in case of its localization in a small area compared to the volume of the whole particle.

3. There has been found no area with abnormally high content of transuranic elements. This either means that there is no plutonium localization and it is evenly distributed within the volume of a "hot" particle, or plutonium concentration is still insufficient to be registered.
4. The limitation of sensitivity in the area of transuranic elements is determined in the case of electron microprobe by high background levels of bremsstrahlung. When analyzing the proton beam (proton microprobe), the situation is different: the background radiation in the energy range of x-ray quanta corresponding to transuranic elements (from 13 to 18 keV) is determined by bremsstrahlung from the proton beam in the particle media the yield of which is approximately for two orders of magnitude lower than that of bremsstrahlung from electrons. Therefore, sensitivity of the method in the case of proton microprobe is conditioned, first of all, by the statistics, which can be increased by increasing the time of spectrum measurement at each point. In this way, in principle, it is possible to achieve the sensitivity sufficient for recording x-ray lines of elemental plutonium. However, this results in very long times of plutonium distribution measurements within the volume of "hot" particles.

2.2.5. Density measurements in "hot" particles

In accordance with the described above method, densities of 427 "hot" particles identified in the 1st and 2nd fractions of soil samples taken at STS were measured. Table 8 shows average values and variations intervals for density of studied particles. As it can be seen from table 8, the average densities of "hot" particles in different samples and fractions vary within quite a narrow range, from 1.5 to 3.2 g/cm^3, which is close to the density of ordinary soil particles. For individual particles, the density reaches 1.16 g/cm^3 (sample HP-16, fraction 2) and 4.5 g/cm^3 (sample HP-08, fraction 2).

Table 8.

Average densities of the "hot" particles and density variations

Sample	Fraction	Number of particles	Average mass, mg	Mass range, mg	Average density, g/cm^3	Density range, g/cm^3
HP-01	1	1			2,4	
HP-02	1	1			2,0	
HP-03	1	2			2,2	2.13–2.21
HP-04	1	1			1,7	
HP-04	2	2			1,5	1.35–1.61
HP-05	1	1			2,3	
HP-05	2	3			1,6	1.53–1.65
HP-08	1	102	5.1	1.2–23	2,6	1.81–3.9
HP-08	2	30	0.98	0.3–3.1	2,7	1.5–4.5
HP-09	1	144	8.0		2,1	
HP-09	2	42	3.1		2,0	

Sample	Fraction	Number of particles	Average mass, mg	Mass range, mg	Average density, g/cm^3	Density range, g/cm^3
HP-11	1	19	4.83		2.2	
HP-11	2	36	1.26		1.5	
HP-16	1	5	5.7	3.0–9.5	2.0	1.9–2.1
HP-16	2	24	1.2	0.3–3.2	1.8	1.16–4.07
HP-16	3	2	0.30	0.17–0.44	3.2	2.7–3.7
HP-17	1	3	22	18–25	2.6	2.4–2.9
HP-18	1	1	4.4		1.7	
HP-19	1	1	13.8		2.9	
HP-20	1	1	3.2		2.0	
HP-20	2	6	6.5	4.0–11	2.0	1.8–2.3

2.2.6. Leaching out of "hot" particles

Leaching out of plutonium is quite a labor consuming procedure requiring a large amount of tracer agent (^{236}Pu) what limits the number of objects to be studied. Therefore, methodologically, it was decided to explore more fully the array of particles identified from one sample, HP-08. This choice was stipulated by high content of plutonium in the original sample HP-08 (13,067 Bq/g) and a wide range of activities of obtained there "hot" particles (up to tens of thousands of Becquerel per particle).

On the whole, 11 "hot" particles of the 1st and 2nd granulometric fractions have been studied in the sample HP-08. Also two particles of the samples HP-09 and HP-10 have been studied for comparison. The activity of particles in the sample HP-08 ranges from 0.22 Bq to 1,740 Bq.

The obtained activities for different forms of plutonium are presented in table 9. In the table, the prevailing forms of each particle are shown in orange.

The results of leaching out of "hot" particles show that in the particles with the absolute activity of more than 100 Bq, most of the plutonium (about 99%) is present in a hard-soluble form, i.e. mainly in the crystal lattice of low-soluble mineral part.

The detection of plutonium in different geochemical forms (mobile, acid-soluble, strongly fixed) in particles with lower absolute activity (<100 Bq) indicates its non-uniform distribution in within the matrix and inclusion in different groups of compounds differing by the properties and solubility.

The results can be interpreted with an assumption that the inclusion of plutonium in the compounds took place under two different mechanisms: 1. distribution of plutonium in the volume of chemically resistant matrix as a result of iso- and hetero-valent substitution, or 2. sorptive distribution on the surface or in the near-surface layer of radioactive substance.

The formation of different types of radioactive particles, each with different properties, is, probably, due to a variety of physical and chemical processes that occur at condensation and coagulation of agents in the fire ball. In case of ground explosions there occurs interaction of condensable fission products, non-fissioned nuclear fuel, and construction materials. A significant amount of soil material also enters the fire ball, where only some of it evaporates and, at condensation, particles consisting of a mixture of oxides are formed. The other

part is present in the liquid state as small droplets on which condensation occurs. In addition, some amount of soil material is present in an external peripheral zone of a fire ball where the temperature is not high enough for melting and evaporation. At that, fusion of particles from the surface occurs and entrapped activity diffuses in the molten state into the particles.

Thus, significant variations in the plutonium content noted for various "hot" particles can, probably, be attributed to the influence of primary formation processes.

Table 9.

Plutonium Speciations in "hot" particles

Sample, fraction	Initial activity, Bq	Activities for different plutonium forms, Bq		
		Mobile (1 M HCl)	Acid-soluble (7.5M HNO_3)	Strongly-bound (reminder after leaching)
HP-08, 1	5.0	2.5	1.9	0.65
HP-08, 1	1740	0.0049	0.003	1740
HP-08, 2	0.22	0.12	0.074	0.027
HP-08, 2	15.5	14.8	0.56	0.14
HP-08, 2	206	0.015	0.450	206
HP-08, 2	640	0.150	0.30	640
HP-08, 2	795	0.050	0.190	795
HP-08, 2	902	0.36	2.7	899
HP-08, 2	925	0.037	0.066	925
HP-08, 2	1200	0.810	3.24	1195
HP-08, 2	1550	0.031	0.047	1550
HP-09, 1	2.0	0.022	0.02	1.96
HP-09, 2	1.2	< 0.01	0.026	1.16
HP-10, 1	6.0	0.61	0.006	5.38
HP-10, 1	13.8	0.004	0.006	13.8

CONCLUSIONS

The following was revealed as a result of our works:

1. Soil samples taken at different STS places ("Experimental Field" site, site P-2, Atomic Lake, site Telkem-1), where the different types of nuclear tests were performed (ground, air, excavational), have common peculiarities in distributions of radionuclide activities in terms of granulometric fractions. At the places that are in close proximity to the explosion epicenters, the majority of activity in the soil samples is associated with large granulometric fractions as follows: usually 2^{nd} (with particles from 0.5 to 1.25 mm), more seldom – 1^{st} (>1.25mm) and 3^{rd} (0.28– 0.5 mm). These activities were formed as a result of soil particles interactions with charge material at the moment of nuclear explosions. Away from the epicenters, the activity maximums are shifted to smaller fraction range: 6^{th} (<0.04

mm), more seldom 4th (0.112–0.28 mm) and 5th (0.04–0.112 mm). This process is accompanied by decreasing of the total sample activity. The main factor in activity accumulation is played in this case by wind transfer of smaller soil particles. For the samples taken at Degelen site, a dominance of the smaller granulometric fractions is typical. Radionuclides are accumulated here because of interactions of soil particles with subterranean waters from adits.

2. Magnetic soil fractions have high specific activities. However, mass of these fractions, as a rule, is much lower than that of the corresponding nonmagnetic fractions. That is why the majority of absolute activity is associated with nonmagnetic fractions for the most samples.
3. The total number of "hot" particles extracted by the method of visual identification and the method of forced decay is as follows: 1,734 for the 1st granulometric fraction; 1,613 for the fraction 2; and 324 for the fraction 3. 63% of all 1st fraction particles and 74% of 2nd fraction particles are identified by the method of visual identification. Thus, this extraction method is more effective for the large granulometric fractions what is explained by greater sample mass included in the analysis at this case. At the same time, when calculated per 1g of sample, more particles are extracted by the method of forced decay what can be explained by higher sensitivity. That is why one can conclude that in case of "hot" particle identification in small-mass samples (up to 10g) it is better to use the method of forced decay. For large samples (> 10g) it is more effective to use the method of visual identification.
4. For the majority of samples, the average absolute activities of separated "hot" particles are not higher than 60 Bq for the fraction 1, 4.5 Bq for the fraction 2, and 3.1 Bq for the fraction 3. The exception is the sample HP-08 for which similar parameters are 1,248 Bq, 1,107 Bq, and 102 Bq, respectively.
5. Specific activities of all extracted particles are several orders higher than those of the corresponding granulometric fractions. This supports the statement that the extracted active formations are really associated with "hot" particles as it follows from the conventional definition of "hot" particles.
6. Extracted particles are different in visual appearance. It can be explained by different conditions their ulk structure was formed at.
7. The average $^{(239+240)}Pu/^{(241)}Am$ ratio for the "hot" particles extracted from large granulometric fractions (7.0) is similar to the isotope ratio for the whole sample HP-08. The standard deviation of $^{(239+240)}Pu/^{(241)}Am$ isotope ratio for different particles of the sample HP-08 does not exceed 5.4 %; that could point out to the common genesis of the considered particles.
8. $^{240}Pu/^{239}Pu$ isotope ratio for particles of different fractions taken at different STS places varies within the small range (from <0.02 to 0.07). A slightly different situation is for the $^{235}U/^{238}U$ ratio. Natural ratio for these isotopes is $^{235}U/^{238}U \approx 0.0072$. The measured $^{235}U / ^{238}U$ ratios are close to this value only for four particles taken from the fraction 1 ($^{235}U/^{238}U$ <0.005) and fraction 2 ($^{235}U/^{238}U$ = 0.008) of the sample HP-09; and from the fraction 1 ($^{235}U/^{238}U$ = 0.01 and 0.009) of the sample HP-10. For all other particles this ratio varies within the range from 0.14 to 10.6.

Maximal values of the $^{235}U/^{238}U$ ratio were observed in the sample HP-08 (P-2 site, hydronuclear explosion).

9. All particles investigated employing electronic and proton microprobes have similar average elemental composition both for their natural surface and sections. The average elemental composition of the particles is similar to that of typical soils (SiO_2 basis with Al_2O_3, NaO, and Fe_2O_3 oxides) what means that soil matter was a matrix basis for the "hot" particles.
10. The average densities of "hot" particles for different samples and fractions vary in narrow range from 1.5 to 3.2 g/cm^3, what is similar to density of usual soil particles.
11. The data on leaching out of "hot" particles show that for particles with the absolute activity of >100 Bq the majority of plutonium (about 99 %) remains in the hardly soluble form, i.e. this element stays in crystalline lattice of heavily-soluble mineral part. Plutonium determination in diverse geo-chemical forms (mobile, acid-soluble, strongly-bound) in particles with lower absolute activity (< 100 Bq) testifies its irregular distribution within the matrix and its presence in different compound groups of different properties and solubility. Obtained results may be interpreted by the assumption that plutonium inclusions in various compounds took place under the following two mechanisms: 1. plutonium distribution in chemically-stable matrix as a result of iso- and hetero-valence substitution, or 2. sorption distribution on the surface or in a thin near-surface layer of radioactive substance.

REFERENCES

1. Characteristics of radiological and non-radiological contaminants in the place of Semipalatinsc Nuclear Test Site: final technical report on INTC Project K-053-96/ Project manager – Sirazhet Khazhekber, December 1999. – [in Russian].
   Характеристика радиологических и нерадиологических загрязнителей в месте расположения Семипалатинского полигона: заключительный технический отчет по проекту МНТЦ К-053-96 / менеджер проекта Сиражет Хажекбер. -1999, декабрь.
2. *Prokhorov V.M.* Migration of Radioactive Contamination in Soils / V.M. Prokhorov. – M.: Energoizdat, 1981. – pp. 10-58. – [in Russian].
   Прохоров В.М. Миграция радиоактивных загрязнений в почвах / В.М. Прохоров. - М.: Энергоиздат, 1981. – С. 10-58.
3. Bunzl K. Probability for detecting Hot Particles in Environmental Samples by Sample Splitting / K. Bunzl // Analyst. -1997. –V. 122. P. 653-656.
4. Bunzl K. Detection of Radioactive Hot Particles in Environmental Samples by Repeat Mixing / K. Bunzl // Appl. Radiat. Isot. -1998. - V. 49. - No. 12. – P. 1625-1631.
5. Debertin K. Gamma- and X-ray spectrometry with semiconductor detectors / K. Debertin, R.G. Helmer. - North-Holland: Amsterdam, 1988.

6. Knyazev B.B. The instrumental method of plutonium determination / B.B. Knyazev, I.V. Kazachevskiy, V.P. Solodukhin, S.N. Lukashenko, M.K. Knatova, V.V. Kashirsky // Czechoslovak Journal of Physics. – 2002. -Vol. 52. – P. A45-A5.
7. Beasley T. M. Isotopic Pu, U, and Np Signatures in Soils from Semipalatinsk-21, Kazakh Republic and the Southern Urals, Russia. J. Environ / T. M. Beasley, J.M. Kelley, K.A. Orlandini, L.A. Bond, A. Aarkrog, A.P. Trapeznikov, V.N. Pozolotina // Radioactivity. – 1998. - Vol.39. - No.2. –P. 215-230.
8. Belayev B.N. Atomnaya Energiya / B.N. Belayev, V.M. Gavrilov, V.D. Domkin [at all.]. - 1997. - V.83. - № 4. - C. 298-304.
9. Krey P.W. Transuranium Nuclides in the Environment: Proc. Symp.(San Francisco, 17-21 November, 1975) IAEA-SM-199/39. / P.W. Krey, E.P. Hardy, C. Pachucki [et al.]. – Vienna: IAEA, 1976. - P. 671-677.
10. McCormick A. Thermal-Ionization Mass Spectrometry for Small Sample Analysis of Uranium and Plutonium /A. McCormick //Appl. Radiat. Isot. - Vol.43. - No. ½. - P. 271-278.
11. Shihomatsu H.M. Trace Uranium Analysis by Isotope Dilution Alpha and Mass Spectrometry and Comparison with Other Techniques / H.M. Shihomatsu , S.S. Iyer. // Nucl. Instr. Meth. In Phys. Recearh, A280. – 1989. –C. 488-491.
12. Mit A.G. Modernization of the mass-spectrometer MI-1201 in conformity to the tasks of isotopic analysis of glazed stratum and solid particles. Sem. " The converse in the national collaboration" / A.G. Mit, L.M Nazarenko, E.M. Yakushev. - Almaty, 1996.
13. Kadyrzhanov K.K. Techniques used at the national nuclear centre's institute of nuclear physics for studying soil probes and soil fragments at the semipalatinsk nuclear test site / K.K. Kadyrzhanov, V.P. Solodukhin, I.V. Kazachevskiy, S. Khazhekber, S.N. Lukashenko, G.N. Chumikov, M.F. Verestchak, A. Eliseev, A.K. Zhetbaev, L.M. Nazarenko, S.P. Pivovarov, A. Platov, A.B. Rukhin, T.A. Seredavina, P.V.,Chakrov E.M. Yakushev // Nuclear Physical Methods in Radioecological Investigations of Nuclear Test Sites. - Printed in the Netherlands: Kluver Academic Publishers, 2000. – P. 17-42.
14. Kelman V.M. Electro-optical elements of prism mass-spectrometer / V.M. Kelman, S.P Karetzkaya, L.V. Fedulina, E.M. Yakushev //Pub. "Science". - Alma-Ata, 1979.
15. Tables of total mass coefficients for attenuation of characteristic x-ray radiation. – Methodical recommendations / Ed.by Komyak N.I.; Marenkov O.S., Komkov B.G. – LSPO "Burevestnik", 1978, 274 pp. – [in Russian].
Таблицы полных массовых коэффициентов ослабления характеристического рентгеновского излучения. – Методические рекомендации / под общей ред. Н.И. Комяка; сост: О.С. Маренков, Б.Г. Комков. – ЛНПО: "Буревестник", 1978. - 274 с.

СЕМЕЙ СЫНАҚ ПОЛИГОНЫНЫҢ ТОПЫРАҒЫНДАҒЫ "ЫСТЫҚ" БӨЛШЕКТЕРДІ ЗЕРТТЕУ ЖӘНЕ ЖҮЙЕЛЕНДІРУ

[1]Горлачев И.Д., [1]Квочкина Т.Н., [1]Князев Б.Б., [2]Лукашенко С.Н.

[1] ҚР ҰЯО Ядролық физика институты, Алматы, Қазақстан
[2] ҚР ҰЯО Радиациялық қауіпсіздік және экология институты, Курчатов, Қазақстан

Семей сынақ полигонының (ССП) аумағында 456 ядролық жарылыс өткізілді. Топырақтың түрлі типінде ластанған радионуклидтердің таралуы мен құрамы әртүрлі. Топырақтың белсенділігінің негізгі көздерінің бірі, ондаған микроннан миллиметрлік бірлікке дейінгі мөлшерде "ыстық" бөлшектер болып табылады. Үлгінің жалпы белсенділігіне "ыстық" бөлшектердің белсенділігінің арақатынасы ядролық сынақтың табиғатымен анықталады. Қоршаған ортадағы радиоактивті өнімдердің жылыстауының дәрежесін болжау үшін және адам ағзасының ішкі және сыртқы сәулеленуін бағалау үшін "ыстық" бөлшектердің физико-химиялық қасиеттерін білу қажет.

Ұсынылған жұмыстың мақсаты, түрлі типтегі ядролық сынақтар өткізілген жерлерден іріктеп алынған топырақ сынамаларынан "ыстық" бөлшектердің бөлінуі, оларды жүйелендіру және топырақ фракцияларының және белгілі бір "ыстық" бөлшектердің физико-химиялық ерекшеліктерін зерттеу жұмыстары болып табылады. Барлығы топырақтың 20 сынамасы іріктеп алынды, оның ішінде "Тәжірибе даласынан" - 7, "Атом" көлінен – 2, "Телькем-1" алаңынан – 3, П-2 телімінен – 3 және "Дегелең" алаңынан 177, 139, 503, 609 штольняларынан 5 сынама сәйкес келеді. Барлық сынамалар визуалды сәйкестендіру әдісімен "ыстық" бөлшектердің орын алуына және еріксіз бөлінуіне зерттелді. Жалпы алғанда ірі түйіршікметриялық фракциялардан 3000-нан аса "ыстық" бөлшектер бөлінді (бөлшектердің көлемі 0,28 мм аса). Ұсақ түйіршікметриялық фракцияларда бөлшектер айқындалған жоқ, тек қана олардың құрамы есептелді. Жеке бір "ыстық" бөлшектер абсолютті және тиесілі белсенділігі, тығыздығы, $^{235}U/^{238}U$, $^{239+240}Pu/^{241}Pu$ және $^{240}Pu/^{239}Pu$ изотоптарына арақатынасы, орташа элементтік құрамы анықталды және ондағы плутонийді анықтау формасы зерттелді. Гамма және рентген желілерінің есебінің жылдамдығының стандартты ауытқуларын талдамалауға негізделген "ыстық" бөлшектердің орташа белсенділігі мен мөлшерін бағалау, орын алуын анықтау тәсілі әзірленді. Зерттеулерді орындау барысында дәстүрлі аналитикалық әдістермен, гамма-, альфа- және масс-спектрометрия, рентгенофлуоресцентті талдамамен қатар, Ядролық физика институтына бейімделген арнайы әзірленген дәстүрлі емес тәсілдер де пайдаланылды.

ИССЛЕДОВАНИЯ И СИСТЕМАТИЗАЦИЯ "ГОРЯЧИХ" ЧАСТИЦ В ПОЧВАХ СЕМИПАЛАТИНСКОГО ИСПЫТАТЕЛЬНОГО ПОЛИГОНА

[1]Горлачев И.Д., [1]Квочкина Т.Н., [1]Князев Б.Б., [2]Лукашенко С.Н.

[1] Институт ядерной физики НЯЦ РК, Алматы, Казахстан
[2] Институт радиационной безопасности и экологии НЯЦ РК, Курчатов, Казахстан

На территории Семипалатинского испытательного полигона (СИП) было проведено 456 ядерных взрывов. Состав и распределение радионуклидов для каждого типа загрязнения почв различны. Одним из основных источников активности почв являются "горячие" частицы

с размерами от десятков микрон до единиц миллиметров. Отношение активности "горячих" частиц к общей активности образца определяется природой ядерного испытания. Знание физико-химических свойств "горячих" частиц необходимо для прогнозирования степени миграции радиоактивных продуктов в окружающей среде и для оценки опасности внешнего и внутреннего облучения человеческого организма.

Целью представленной работы было выделение "горячих" частиц из проб почв, отобранных в местах проведения разных типов ядерных испытаний, их систематизация и изучение физико-химических особенностей как почвенных фракций, так и отдельных "горячих" частиц. Всего было отобрано 20 проб почв, 7 из которых на "Опытном поле", 2 – на "Атомном" озере, 3 – на площадке "Телькем-1", 3 – на участке П-2 и 5 проб соответствуют штольням 177, 139, 503, 609 площадки "Дегелен". Все пробы были исследованы на наличие "горячих" частиц методами визуальной идентификации и вынужденного деления. В общей сложности было выделено более 3000 "горячих" частиц из крупных гранулометрических фракций (размер частиц более 0,28 мм). В мелких гранулометрических фракциях частицы не выделялись, а лишь подсчитывалось их содержание. Для отдельных "горячих" частиц определены абсолютные и удельные активности, плотности, отношение изотопов $^{235}U/^{238}U$, $^{239+240}Pu/^{241}Pu$ и $^{240}Pu/^{239}Pu$, средний элементный состав и исследованы формы нахождения в них плутония. Был разработан подход для выявления присутствия, оценки количества и средней активности "горячих" частиц, основанный на анализе стандартных отклонений скоростей счета гамма и рентгеновских линий. При выполнении исследований использовались как традиционные аналитические методы, такие как гамма-, альфа- и масс-спектрометрии, рентгенофлуоресцентный анализ, так и специально разработанные нетрадиционные походы, ориентированные на возможности Института ядерной физики.

УДК 577.391:504.064:539.16

PECULIARITIES OF ARTIFICIAL RADIONUCLIDES ACCUMULATION IN CROPS IN THE AREA OF ABOVE GROUND NUCLEAR TESTS ("EXPERIMENTAL FIELD" SITE)

Kozhakhanov T.Ye., Lukashenko S.N., Larionova N.V., Ivanova A.R., Keller S.A.

Institute of Radiation Safety and Ecology NNC RK, Kurchatov, Kazakhstan

The article describes the research outcomes on accumulation of artificial radionuclides by crops cultivated in the radioactively contaminated areas of "Experimental Field" site (also known as *Opytnoye Pole*) at the former Semipalatinsk Test Site (STS). As a result of study, peculiarities of accumulation and distribution of anthropogenic radionuclides in vegetative and generative organs of studied plants were determined. Accumulation factors for ^{137}Cs, ^{90}Sr, $^{239+240}$Pu and ^{241}Am were determined in crops, which factors are required to predict concentrations of these radionuclides when assessing the possibility to transfer the STS areas for the commercial farming. Relation between radionuclide accumulation factor and the type of planting was determined for studied crops. It was established that ^{90}Sr is the critical radionuclide at the "Experimental Field" site of STS.

Keywords: radioactive contamination, radionuclides, ^{241}Am, ^{137}Cs, ^{90}Sr, $^{239+240}$Pu, crop, specific activity (SA), accumulation factor (AF), principal agro (vegetation) products, permissible specific activity (PSA).

INTRODUCTION

Solution to the problem of farming in radioactively contaminated areas is one of the key steps amongst the measures designed to reduce radionuclide concentration in plantings [1, 2, 3, 4]. The studies conducted in the areas that were exposed to radioactive contamination as a result of accidents occurred at nuclear power cycle facilities showed that in many radiological situations the contribution from internal exposure of population via consumption of food containing radionuclides to the total radiation dose is equal to or even higher than the contribution from external exposure [1, 5].

Up to date, all studies conducted in the STS area were associated with the study of radionuclide redistribution and migration in the natural biogeocenosis and evaluation of the livestock output quality. No study of radionuclides uptake by crops in the STS areas has been previously conducted.

Most of the studies carried out in various soil and climate conditions are focused on the study of quantitative characteristics of anthropogenic radionuclide accumulation by crops [1,2,3,4,5]. Notwithstanding the above, the world practice has virtually no similar studies conducted in the environmental conditions that are typical to the areas of former STS. The first such studies of peculiarities of radionuclides accumulation by crops and their distribution in separate plant organs commenced in 2010 on the "Experimental Field" site, STS area. The requirement to study peculiarities of anthropogenic radionuclide uptake by crops in the STS area appeared during the large-scale works concerning transfer of some lands in that area to the farm use.

The key objective of the work was to study the specifics of anthropogenic radionuclide uptake by crops during their cultivation in the areas of above ground nuclear tests. The crops that are zoned for this region were of the most interest from the perspective of radionuclide accumulation study.

It is still quite important to study the nature of accumulation of $^{239+240}$Pu and ^{241}Am in agro products which topic is very rarely covered even in the world studies [6]. The study of peculiarities of transuranium radionuclide uptake by crops was one of the main objectives of our work as the affect of these radionuclides, given their half-life of hundreds and thousands years, on radiation situation in the STS area and its outskirts will grow with the time.

1. EXPERIMENT

The technical site P-2 characterised by high concentration of radionuclides, which are referred to transuranium radionuclides ($^{239+240}$Pu and ^{241}Am), was selected for conduction of a full-scale experiment to study the accumulation of radionuclides by crops. The level of radionuclide concentrations in topsoil (0-5 cm) is as follows: ^{241}Am – n*10^4 Bq/kg, ^{137}Cs – n*10^3 Bq/kg, ^{90}Sr – n*10^3 Bq/kg and $^{239+240}$Pu- n*10^5 Bq/kg [7].

Site P-2 characterised by high concentration of transuranium radionuclides ($^{239+240}$Pu and ^{241}Am) in soil was selected for conduction of studies based on the previous data on anthropogenic radionuclide distribution in soil profile [7] in the "Experimental Field" site area. The land cover of the area under study is represented by light chestnut soils and steppe herbs.

Subjects of the study were 12 types of agricultural plants that are referred to 5 vegetative groups depending on the part of the plant that is used in food: grain, fruit, leaf, bulbous vegetables and root crops.

The vegetables under study were planted in the periods recommended for the selected types of crop subject to natural environment of the region.

The cropping system included the following activities: land treatment (turning over the soil, levelling the topsoil, removal of weeds) and melioration (artificial irrigation). Agrochemical methods of farming (use of fertilizers and other chemicals) were not applied in order to obtain information about peculiarities of radionuclide uptake by crops without exposure to such factor.

Meteorological conditions of the site of interest were studied from May to September 2010 [8].

1.1. Experimental site

Based on the dosimeter measurements (β-articles flow density and exposure dose rate (EDR)) that were taken at the elevation of 0–5 cm from the soil level, the area of Site P-2 with homogenous relief and even soil contamination was selected as an experimental site. The selected site is characterised by the following readings of dosimeter measurements: β-articles flow density ranges within 90–120 particles /minute *cm^2, γ- exposure dose rate – 0.95–1.18 μSv/h. The area of the selected site is ~200 m^2. The map of the experimental site is presented at Figure 1 below.

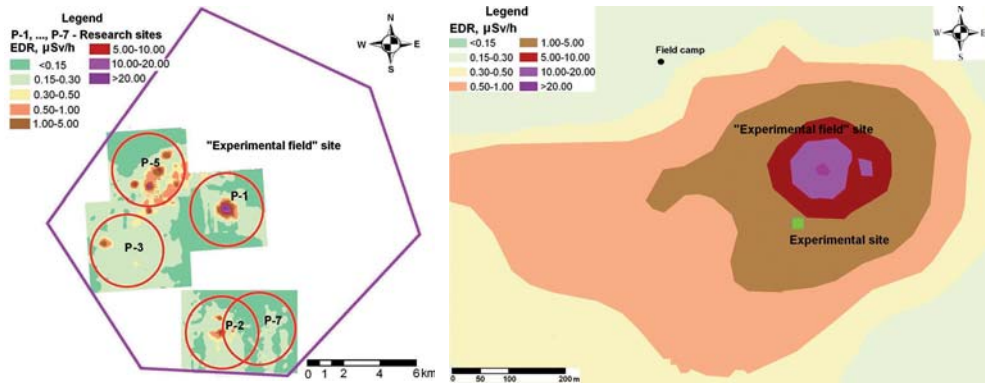

a) b)

Figure 1. Map of the technical sites on the STS (a) and experimental area on "Experimental Field" site (b)

1.2. Subjects of study

The species of crop that are normally grown by the community and private farms outside the STS area under the environmental conditions of arid climate of this region with artificial irrigation were selected as the test agricultural plants. The selected agricultural plants are described in the table (Table 1).

Table 1.

Agricultural plants under study

#	Types of agricultural plants	Kind
1	water melon (*Citrullus vulgaris*)	Ogonek and Sugar Baby
2	melon (*Cucumis melo*)	unknown
3	tomato (*Solanum lycopersicum*)	local
4	capsicum (*Capsicum annuum)*	local
5	egg-plant (*Solanum melongena*)	local
6	cabbage (*Brassica oleracea*)	local
7	parsley (*Petroselinum vulgare*)	"Ordinary"
8	carrot (*Daucus carota*)	"Shantane"
9	onion (*Allium cepa*)	"Kassatik"
10	wheat (*Triticum vulgare*)	"Beloozerka"
11	barley (*Hordeum vulgare*)	"Meschanski"
12	bean (*Phaseolus vulgaris*)	"Red"

1.3. Layout of the experimental area and crop planting

The experimental area was divided into three main sectors (melon, grain and vegetable crops), the layout of plots is shown in Figure 2.

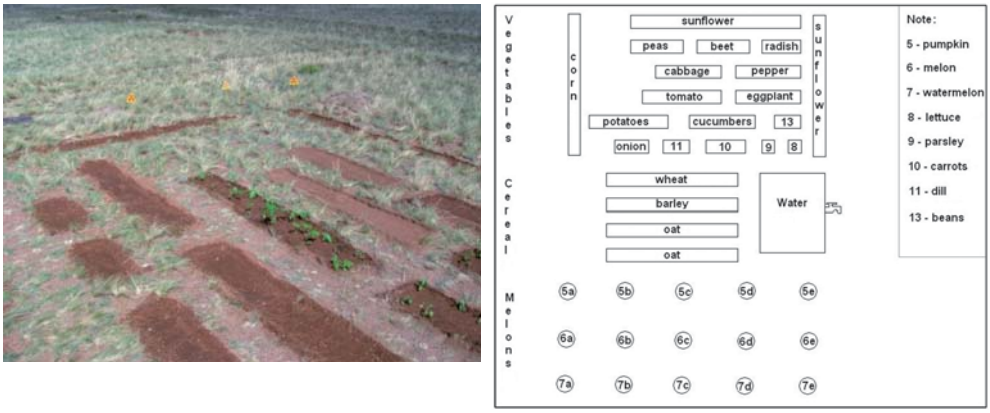

a) b)

Figure 2. General layout of the pilot site in spring (a), layout of plots (b).

The areas of plots are from 0.25 m^2 to 2 m^2 depending on the quantity of planting material and plant spacing density. Description of planting areas and planting methods are provided in the table (Table 2).

Table 2.

Area of plots and quantity of planting material

Crop	Type of planting material	Quantity of planting materials	Planting area, m^2	Planting method	Plant spacing density, piece/m^2
watermelon	seeds	25 pieces	1.25	checkrow	20
melon	seeds	25 pieces	1.25	checkrow	–
tomato	sprouts	15 pieces	1.5	wide–row	10
capsicum	sprouts	26 pieces	1.25	wide–row	20,8
egg-plant	sprouts	19 pieces	1.25	wide–row	15,2
cabbage	sprouts	15 pieces	1.25	wide–row	12
parsley	seeds	1–2 g	0.25	strip	–
carrot	seeds	1–2 g	0.75	strip	–
onion	bottom set*	42 pieces	0.35	dotted	120
	seeds	0.5–1 g	0.5	dotted	–
wheat	seeds	60 g	2	narrow–row	–
barley	seeds	50 g	2	narrow–row	–
bean	seeds	19 pieces	0.5	continuous row	38
Note: *– bulbil of up to 2cm in diameter					

Periods of crop planting versus periods recommended for our environmental conditions are shown in the table (Table 3) [9].

Table 3.

Periods of crop planting

Crop	Period of seed and sprout planting	
	test (2010)	recommended for Kazakhstan
watermelon	May 15	end of April – early May
melon	May 15	end of April – early May
tomato	May 18	May 1–15
capsicum	May 18	May 1–15
egg-plant	May 18	May 1–15
cabbage	May 29	May 1–10 *
parsley	May 15	April 1–20
carrot	May 16	April 1–20
onion	May 16	April 1–20
	May 15	May 10–20
wheat	May 15	May 15–25
barley	May 18	May 1–15

1.4. Land treatment and melioration activities

Seedbed preparation included the following land treatment: digging down to 20–25 cm, levelling of topsoil and removal of weed plants. No fertilizers were added since the objective was to study the radionuclide accumulation without affect of this factor.

Artificial irrigation (hereinafter the "watering") was used to grow the crop under the dry climate conditions. In view of no ability to use ground waters, clean imported water was used for watering by means of overhead irrigation (watering-can) and letting water flow to the plots. Watering was: continuous (4 times a week) for vegetable crop, and as required (2 times a week) for grain and melon crop. The average watering volume was 0.03m^3 (for vegetables) and 0.06m^3(for grain and melon crop) per 1m^2 at a time.

2. INVESTIGATION METHODS

2.1. Meteorological measurements

Meteorological conditions were surveyed in the period from May to September 2010. The ambient temperature was measured by the outside thermometer type TSN-13 (with admissible error ±1.0°C) and Vantage Pro 2 weather station (temperature range is from -40°C to 65°C) that determines the following parameters: temperature and relative weather humidity, precipitations, wind velocity and direction. Weather readings were taken in the morning, afternoon and evening hours 8^{00}– 9^{00}, 13^{00}–14^{00} and 19^{00}– 20^{00}, respectively.

2.2. Sampling of crops and soil

Crop samples were taken as the main products ripen with the subsequent sampling of aboveground and underground parts of the plants. Immediately after sampling, the plant samples were divided by vegetative organs and weighed in the raw state in field conditions. Plant samples were placed in plastic bags and assigned with the passport [15]. The exception was melon plantations the areas of which were accounted subject to those plots where there were grown plants. Total of 39 plant samples were taken (different plant organs).

Along with plant sampling the soil was also sampled. For sampling purposes the metal sampler of cylinder shape 3.5 cm in diameter and 20 cm long was used. Since the depth of rooting zone of the plants under study was maximum 10 cm, the samples were taken by the sampler at the depth of 10 cm. Soil samples from the square-shaped plots were taken by an envelope method and from rectangular-shaped plots by linear method at 0.7 m space (in average 5.3 samples from 1m^2). The example of soil sampling from certain crop plots is shown in the figure (Figure 3). After soil samples were taken they were combined, mixed and quartered for each plot.

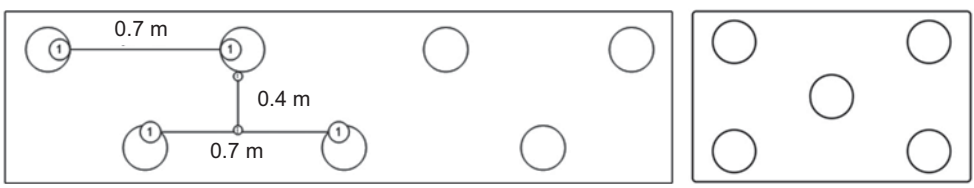

Figure 3. Layout of soil sampling on tomato and capsicum plots (a), onion, parsley and watermelon crops (b), ○ - sampling point

2.3. Determination of radionuclide composition

Plant and soil sample preparation

Plant samples were washed and rinsed by distilled water 2–3 times, dried in a dryer at 80–100°C till the sample constant weight and coarse grinded to 1–3cm long by pruning shears. Plant samples were additionally grinded to 1mm particles by the laboratory mill for gamma-ray spectrometry of ^{137}Cs and ^{241}Am. Dried, grinded and mixed plant samples of 5–50 g were weighed and transferred for the gamma-ray spectrometry.

To determine $^{239+240}$Pu and ^{90}Sr, a dried grinded sample was additionally treated which included thermal concentration: carbonization and ashing. Carbonization was conducted in muffle roaster or by means of calcination on hot plate in exhaust fume hood till stoppage of fume and appearance of black residue. Thereafter, samples were cooled down, grinded and placed in porcelain cups, bowls for further ashing. Samples were ashed in muffle roaster at 550°C to determine ^{90}Sr and 650°CC – $^{239+240}$Pu. After ash was produced, the cups with ash were cooled in exciccator. The ash residue produced was weighed and ashing factor was determined for each plant sample. Then, 1–10g samples were taken for radiochemical split off and further measurement of ^{90}Sr and $^{239+240}$Pu.

Soil samples were dried in drying cabinet at 60–70°C till air-dried condition. After removal of coarse stones and impurities (plant roots) they were weighed on counter balance. Further, the entire sample volume was thoroughly mixed, gradually (by portions) grinded in porcelain mortar with a pestle and screed through the 1mm slot screen. Then, after quartering, a 300–500g soil sub-sample was taken to determine ^{241}Am and ^{137}Cs, ^{90}Sr and $^{239+240}$Pu – 50g and 10g, respectively.

Radionuclide analysis

Analysis to determine specific activity of radionuclides in soil and plant samples were performed in compliance with the standardized methodical guidance by using certified laboratory equipment [10, 11]. Specific activity of ^{137}Cs and ^{241}Am for soils and plants was determined by Canberra GX-2020 gamma spectrometer, ^{90}Sr for soil by Progress beta spectrometer. $^{239+240}$Pu was determined by radiochemical split off followed by the measurements at Canberra Model 7401 alpha spectrometer. Concentration of ^{137}Cs in plants was determined in dry grinded samples, ^{241}Am, ^{90}Sr and $^{239+240}$Pu – in ash followed by subsequent recalculation for dry substance. Detection thresholds were as follows depending on type of a sample and a sub-sample: ^{137}Cs 1–10 Bq/kg (dry substance for plant and soil samples), ^{241}Am – 1–10 Bq/kg, $^{239+240}$Pu – 0,1 Bq/kg and 1 Bq/kg, ^{90}Sr – 1–10 Bq/kg, respectively. Inaccuracy of measurements for ^{137}Cs and ^{241}Am did not exceed 10–20 %, ^{90}Sr – 15-25 %, $^{239+240}$Pu – 30%.

2.4. Calculation of specific activity and accumulation factor of radionuclides in plant samples

Calculation of accumulation factors (AF), which are required to get quantitative parameters of radionuclides transferred from soil to the aboveground part of plants, consisted of determination of the ratio between radionuclide concentration in a plant unit mass and radionuclide concentration in a soil unit mass [12].

Radionuclide concentrations in crop products were determined for dry weight of plant products, therefore in order to convert them to wet weight the experimental data was used as shown in Table 6. Radionuclide concentration was calculated as follows:

$$C_{wet} = C_{dry} * K_i, \quad (1)$$

$C_{wet,\ dry}$ – radionuclide concentration in wet and dry weight of plants (Bq/kg);
K_i – coefficient of desiccation.
Coefficient of desiccation was calculated as follows

$$K_i = m_{dry} / = m_{wet}, \quad (2)$$

$m_{\ dry,\ wet}$ – dry and wet weight of plant product (kg).

3. RESULTS AND DISCUSSIONS

3.1. Environmental conditions

The weather data for the period from May to September 2010 on the "Experimental Field" site, P-2 Site, is shown in the table (Table 4).

Table 4.

Weather data of the surveyed area

Natural factor	Month									
	May		June		July		August		September	
	2010	2005–2009*	2010	2005–2009*	2010	2005–2009*	2010	2005–2009*	2010	2005–2009*
Average monthly temperature, °C min-max, °C	16.6 9-30	18.6	23.1 12-39	23.3	21.1 11-36	25.4	21.5 5.2-37.4	22.3	12.8 -3.4-36.2	14.5
Average monthly relative air humidity, %	-	-	-	-	-	-	42	-	45.9	-
Precipitation, mm	-	-	-	-	-	-	8.6	-	0	-
Average monthly wind velocity (max), m/c	-	3.3	-	2.8	-	2.5	2.9	2.8	2.7	2.5
Prevailing wind direction	-	n, n-e, n-w	-	n, w	-	n,w	s-w (27%), n (18%)	n, n-w	s-w (25%) n (20%) w and n-w (10%)	n, n-w, s-w

notes: * - average data of metrological service of Semipalatinsk city over the last 5 years;
"-" – not available

Data for May-July is based on measurements by household outside thermometer, and for August and September – by Vantage Pro 2 weather station.

Based on the temperature data, which is lower than average values for the period from 2005 to 2009, one might state that the spring-summer period in 2010 was colder than similar periods over the last 5 years. Maximum relative air humidity is observed in the morning hours before the dawn (from 00^{00} to 4^{00}) up to 91%, and minimum –at day time (from 12^{00} to 18^{00}) as low as 10%. The prevailing wind directions fixed for this period were typical to this region. Despite insignificant difference in average monthly temperatures in different years, given the extremely continental climate of the region, one might state that the spring-summer period was typical for this region.

3.2. Yield of crops under study

Arrangement of artificial irrigation system (watering) helped grow the planted crop and produce the harvest under such environmental conditions.

The yield of test plants was estimated subject to wet weight of plants and area of sampling (plot). Comparative data of the harvest of certain crops is shown in the table (Table 5) [13,14,15,16].

Table 5.

Crop yield

Crop		Main product		K_i	Sampling area, m^2	Yield, c/he	Average yield, c/he
		Wet weight, g	Dry weight g				
Watermelon		144.5	14.9	0.10	1.00	~15	101**
Melon		54.8	4.8	0.09	1.00	~6	101**
Tomato		674.9	100.2	0.15	1.50	~45	405**
Capsicum		586.9	40.9	0.07	1.25	~47	170*
Egg-plant		204.5	13.8	0.07	1.25	~16	300*
cabbage		652.8	184.8	0.28	1.25	~52	276**
Parsley		20.7	10.6	0.51	0.25	~8	200*
Carrot		1078.5	162.2	0.15	0.75	~144	188**
Onion	Seed onion	314.7	48.8	0.16	0,35	~90	150*
	seeds	125.4	16.4	0.13	0,50	~25	180*
Wheat		45.9	37.1	0.81	2	2,3	5**
Bean		181.4	91.1	0.50	0.50	~36	80*
Note: * - CIS data; ** - Kazakhstan data							

The potato harvest was higher than the average harvest most likely because of the use of virgin soil and permanent watering.

The resulting crop yield implies that potato, radish and carrot can be grown on the surveyed area only with the use of artificial irrigation and simple land treatment. Yield of bean, onion, capsicum, tomato, wheat and watermelon is 2-7 times lower than the average yield of these crops as indicated in reference literature. The other crops did not produce harvest under the farming conditions that we chose to use.

Therefore, one might state that without the use of a range of land treatment activities (technical treatment and soil preparation, choice of irrigation system and relevant watering volume, fertilizing, pest control and plant disease control and etc.) it will be difficult to produce harvest in the selected area.

3.3. Accumulation factors for artificial radionuclides in crop grown under the radioactive contamination conditions

Based on the determined specific activity (SA) of radionuclides in the surveyed plants and soil (Table 6), accumulation factor (AF) of ^{241}Am, ^{137}Cs, ^{90}Sr and $^{239-240}$Pu was determined for the surveyed plants. The range of ^{90}Sr AF (0.0019-8.65) for all plant samples is 4, $^{239-240}$Pu AF (0.0004–0.29) is 3, ^{241}Am AF (0.00023–0.035) and ^{137}Cs AF (0.0021–0.103) is 2. The distribution of radionuclide AF is represented in the form of frequency of occurrence AF Lg (Figure 4).

Table 6.

Specific activity of radionuclides in plants and soils

Crop	Type of sample	Specific activity, Bq/kg (in air-dry conditions)			
		^{241}Am	^{137}Cs	^{90}Sr*	$^{239-240}$Pu
Water melon	fruits	0.24 ± 0.12	5 ± 0.2	-	< 4
	overground part **	9.7 ± 0.4	89 ± 1	-	163±13
	roots	6.2 ± 1.4	53 ± 3		-
	soil	1000 ± 100	2200 ± 200	2000 ± 500	3480±210
Melon	fruits	0.8±0.4	4.9±0.7	-	-
	overground part	5.9±0.4	56±2	3050±16	136±11
	roots	2.8±0.7	26±2	-	-
	soil	1100±100	2400±200	2000±400	3100±200
Tomato	fruit	0.32 ± 0.11	6 ± 0.4	<1.5	< 3
	leaves	6.3 ± 0.3	55 ± 1	640±6	120±20
	stems	1.6 ± 0.3	15,3 ± 0,7	1020±8	18±3
	roots	34.3 ± 0.7	250 ± 2	700±8	880±40
	soil	1400 ± 100	2500 ± 300	2700 ± 500	3000±800
Capsicum	fruit	0.5 ± 0.2	2,5 ± 0,3	< 2,3	< 2,16
	leaves	2.4 ± 0.2	26,8 ± 0,5	650±5	61±9
	stems	1.7 ± 0.2	14,9 ± 0,6	1100±10	10±3
	roots	1.5 ± 0.4	22 ± 1	390±8	65±6
	soil	670 ± 70	1200 ± 100	1700 ± 400	5600±500
Egg-plant	fruit	-	-	< 5,1	130±20
	leaves	4.7±0.4	45,6±1,4	950±8	120±20
	stems	0.7±0.2	5±0,4	980±10	10±3
	roots	1.8±0.3	16,2±0,7	360±5	38±4
	soil	690±70	1100±100	1200±300	2350±220
Cabbage	leaves	0.85 ± 0.15	12,3 ±0,5	780±5	5,3±2,4
	stems*	3.2 ± 0.5	21,1 ± 1,1	60±2	105±5
	roots	13.3 ± 0.4	89,2 ± 1,1	107±3	270±10
	soil	1100 ± 100	1500 ± 200	1800±400	4800±300
Parsley	leaves	1.5 ± 0.3	12 ± 1	78±6	-
	stems	0.7 ± 0.1	6,7 ± 0,4	< 3,2	-
	roots	390 ± 40	540 ± 50	520 ± 230	13800±700
Carrot	leaves	0.9 ± 0.2	10,5 ± 0,4	97±3	4,8±2,2
	root-crop	0.83 ± 0.08	4,6 ± 0,2	380±5	108±15
	soil	530 ± 50	690 ± 70	990±270	3600±500
Bulb onion (seeds)*	leaves	20 ± 1	60 ± 2	550±16	35±10
	bulb	7 ± 1	46 ± 3	234±6	20±5
	soil	570 ± 60	1100 ± 100	770 ± 280	3000±200
Bulb onion (bottom set)	leaves	1.7 ± 0.2	14,9 ± 0,6	232±3	23,9±2,4
	bulb	2.2 ± 0.5	22 ± 1	1070±13	45±15
	soil	1100 ± 100	2000 ± 200	2300±400	4900±300
Wheat	grain	< 1.85	4±2	-	-
	grain film	3.2±1.3	6,8±2,3	< 1,8	-
	stems	<3.4	30,5±4,2	8300±35	-
	roots	8.1±2.8	109±10	46±3	-
	soil	560	1100	960±300	4600±600

Crop	Type of sample	Specific activity, Bq/kg (in air-dry conditions)			
		^{241}Am	^{137}Cs	^{90}Sr*	$^{239-240}$Pu
Barley	stems	2.5±0.6	15±1	89±4	-
	roots	15.3±2.2	93±7	95±3	-
	soil	890±90	900±90	870±290	5800±500
Been	pod	< 0.68	1,26±0,7	46±2	-
	leaves	< 2.2	17,6±3,4	470±7	-
	stems	< 1.4	< 3,1	370±6	-
	Roots	3.46±1.14	18,7±2,5	-	-
	soil	320±30	530±50	700±220	5700±100
note: * - cabbage stump, aboveground part ** – leaves + stems, "-" - samples are being analysed					

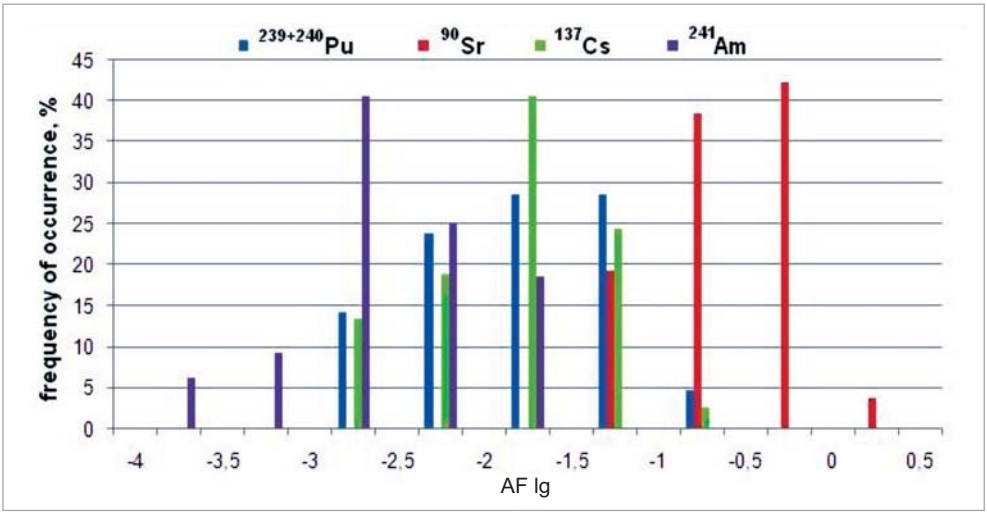

Figure 4. Distribution of Lg AF ^{241}Am, ^{137}Cs, ^{90}Sr и $^{239-240}$Pu for all analysed plant samples.

For the purpose of quantitative assessment of the difference in radionuclide accumulation by analysed plants the following ratios were determined: ^{90}Sr AF /^{137}Cs AF (23,6), ^{137}Cs AF / $^{239-240}$Pu AF (2,1), $^{239-240}$Pu AF / ^{241}Am AF (5,4). If ^{241}Am accumulation factor is assumed to be one (1), the following decreasing series can be made:

AF ^{90}Sr	>	**AF ^{137}Cs**	>	**AF $^{239+240}$Pu**	>	**AF ^{241}Am**
267.6±59,8		**11.3±2,7**		**5.4±1**		**1**

In our case one can notice significant excess of ^{90}Sr AF over the AF of other analysed radionuclides (up to two digits) and rather insignificant difference between AF of ^{137}Cs and $^{239-240}$Pu, however they exceed the ^{241}Am AF.

To evaluate the AF of ^{241}Am, ^{137}Cs, ^{90}Sr and $^{239-240}$Pu, these AFs were compared with the similar AF for crops indicated in summary data of world studies [6].

Since the world practice has insufficient data on radionuclide accumulation for certain organs of cultivated plants and such information is available for group of plants that are com-

bined by their biological feature and there is no data on certain separate types of plants, we used the AF values for such groups of plants that can be conditionally referred to the plants that are analysed (Table 7).

Table 7.

AF of radionuclides for agricultural plants

Groups of plants	Type of plants that are analysed	Organ	AF							
			^{241}Am		^{137}Cs		^{90}Sr		$^{239-240}$Pu	
			Experimental	[6]	Experimental	[6]	Experimental	[6]	Experimental	[6]
Vegetables with no leaves	water melon	Fruit, bulb	$2.5*10^{-4}$	$2.3*10^{-5}$ - $1.9*10^{-3}$ (8)**	$2.3*10^{-3}$	$6.3*10^{-3}$ – $3.0*10^{-1}$ (5)*	-	$9.0*10^{-1}$ – 2.3 (3)*	$1.1*10^{-3}$	$6.0*10^{-6}$- $2.0*10^{-4}$ (8)*
	melon		$7.3*10^{-4}$		$2.0*10^{-4}$		-		-	
	capsicum		$7.5*10^{-4}$		$2.1*10^{-3}$		$<1.4*10^{-3}$		$3.9*10^{-4}$	
	egg-plant		-		-		$<4.3*10^{-3}$		$5.5*10^{-2}$	
	tomato		$2.3*10^{-4}$		$2.4*10^{-3}$		$<5.6*10^{-4}$		$1.0*10^{-3}$	
	onion (seeds)		$1.2*10^{-2}$		$4.2*10^{-2}$		$3.0*10^{-1}$		$6.7*10^{-3}$	
	onion (bottom set)		$2.0*10^{-3}$		$1.1*10^{-2}$		$4.7*10^{-1}$		$9.2*10^{-3}$	
Leafy vegetables	cabbage	leaves	$7.7*10^{-4}$	$6.0*10^{-5}$ – $4.1*10^{-4}$ (2)*	$8.2*10^{-3}$	$3*10^{-4}$ – $7.3*10^{-1}$ (119)*	$4.3*10^{-1}$	$4.1*10^{-2}$ – 5.0 (84)*	$1.1*10^{-3}$	$2.8*10^{-4}$ (1)*
Root vegetables	carrot	root crop	$1.6*10^{-3}$	$7.3*10^{-4}$ – $1.7*10^{-3}$ (3)**	$6.7*10^{-3}$	$1.0*10^{-3}$ – $1.6*10^{-1}$ (21)*	$3.8*10^{-1}$	$4.4*10^{-2}$ – 4.5 (16)*	$3.0*10^{-2}$	$7.0*10^{-5}$- $5.8*10^{-3}$ (4)**
	parsley	leaves	$3.9*10^{-3}$	-	$2.2*10^{-2}$	$9.0*10^{-3}$- $4.3*10^{-2}$ (2)*	$1.5*10^{-1}$	-	-	$1.1*10^{-3}$- $4.9*10^{-3}$ (5)
Grain	wheat	grain	$<3.3*10^{-3}$	$1.0*10^{-6}$ – $3.4*10^{-2}$ (3)*	$3.6*10^{-3}$	$8.0*10^{-4}$ – $2.0*10^{-1}$ (158)*	-	$1.6*10^{-2}$ – $7.2*10^{-1}$ (71)*	-	$3.5*10^{-7}$- $3.1*10^{-4}$ (10)*
Legumes	bean	pod with seeds	$<2.1*10^{-3}$	$2.2*10^{-5}$- $7.9*10^{-4}$ (12)**	$2.4*10^{-3}$	$1.0*10^{-3}$- $4.2*10^{-1}$ (42)*	$7.0*10^{-2}$	$1.7*10^{-1}$- 4.6 (68)*	-	$3.7*10^{-5}$- $1.5*10^{-4}$ (18)**
Note: * - for loamy soil, ** - for sandy-loam; in brackets (n) – quantity of works; "-" - no data available .										

Experimental values of AF do not exceed or are equal to the values indicated in the summary data of world studies for the main agricultural products. The exception is ^{241}Am AF for bulb onion (planted by seeds) and beans (pod with seeds) that is one order of magnitude

higher than the worldwide values and $^{239-240}$Pu AF for tomatoes, egg-plants, water melons (fruits), onion (bulb) is one-two orders of magnitude higher.

For certain measures to be taken to produce agricultural product not contaminated with radionuclides, the summary world data on AF was applied to our environmental conditions incorrectly. These values will be unreliable as they vary within a large range (2-5 orders of magnitude) and were produced under the environmental conditions different from the typical conditions of Kazakhstan. Therefore, the AF values from world studies can be used only as a guide for the STS. AFs produced during experiment more accurately reflect the specifics of radionuclide accumulation with respect to the crops and radionuclide distribution in plant organs.

At the moment, there are AF values with regard to steppe wild plants which were produced on the "Experimental Field" site of STS. To have a general picture of peculiarities of radionuclide uptake by the plants in the STS area, the AF values produced for wild plants were compared with the values for the crop as the they were growing in similar soil and climate conditions ("Characteristics of transfer of artificial radionuclides from soil to plants in steppe ecosystems on the "Experimental Field" site of the former STS", N.V.Larionova et al.).

Comparative distribution of radionuclide AF for the aboveground part of one of the dominant type of steppe plants (feather grass -*Stipa capillata*) and experimental crops is shown on histograms of frequency AF Lg occurrence (Figure 5).

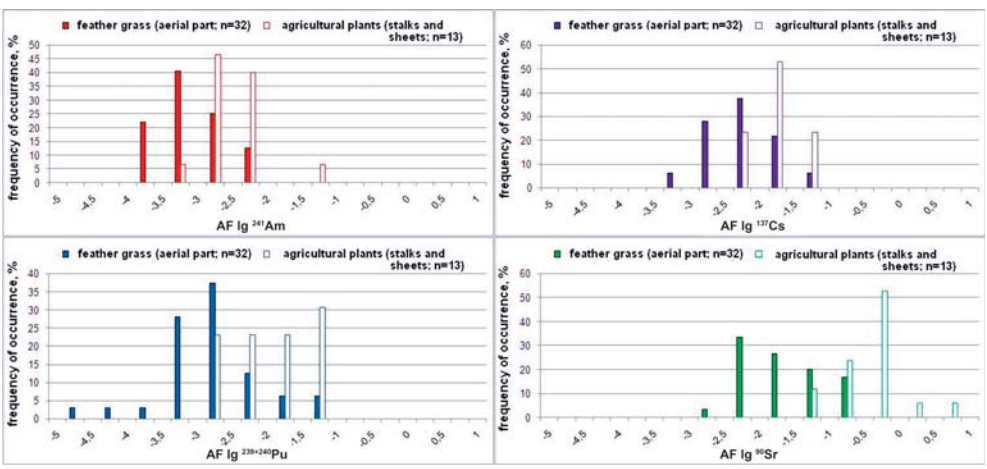

Figure 5. Distribution of AF Lg of ^{241}Am, ^{137}Cs, ^{90}Sr and $^{239-240}$Pu for the aboveground part of feather grass (*Stipa capillata*) and crops on the "Experimental Field" site of STS area

Based on the above histograms one can see the obvious shift of AF of all radionuclides towards higher values in the crops compared to the steppe plant – feather grass (*Stipa capillata*) on the "Experimental Field" site of STS area.

As mentioned in the reference literature [17], the plant ability to accumulate radionuclides is conditioned not only by their specific types but also depends on many factors and, first of all, on the growing conditions. The agricultural plants were grown with artificial (additional) irrigation unlike wild plants that are watered depending on atmospheric precipi-

tations. The reference literature contains assumptions that irrigation that changes the water conditions of soil affects the migration of radioactive substances and their entry in plants, and it explains the current situation with radionuclide accumulation in cultivated and wild plants. The work [1] indicates that the irrigation effect on radionuclide accumulation in plants is connected with the change of water conditions as a result of which there are changes in mobility of radioactive substances and their accessibility for root system of plants, as well as changes in physiological processes connected with volume of mineral elements entering the plants and their transfer by certain organs.

3.4. Radionuclide distribution pattern in vegetative and generative organs of agricultural plants

To assess radionuclide distribution in separate organs of the analysed plants of various families, the determined AFs were compared and results of comparison are set out in the tables (Tables 9-19). To have pictorial presentation and to compare the values of radionuclide AF in vegetative and generative organs of various agricultural plants, all values of AF determined for the plants of various kinds were standardized against values of ^{241}Am AF in main products (fruits, leaves, root crops, bulbs, grain).

Table 8.

AF of radionuclides in plant organs from gourd family

Crop	Type of sample	AF	$\frac{AF_1}{AF_2}$ **	AF	$\frac{AF_1}{AF_2}$	AF	$\frac{AF_1}{AF_2}$	AF	$\frac{AF_1}{AF_2}$
		^{241}Am		^{137}Cs		^{90}Sr		$^{239-240}$Pu	
water melon	fruits	0.00025	1	0.0023	9	-	-	0.0011	4.4
	o.p.*	0.01	40	0.040	160	-	-	0.047	187
	roots	0.0064	26	0.024	96	-	-	-	-
melon	fruits	0.00073	3	0.0020	8	-	-	-	-
	o.p.*	0.0054	22	0.023	93	1.5	6100	0.044	176
	roots	0.0026	10	0.011	43	-	-	-	-

Note: * - aboveground part of plants (stems + leaves),
** - ratio between accumulation factor of ^{241}Am in water melon fruit (AF_1) and accumulation factor of other radionuclides in various plant organs (AF_2),
"-" - no data available

In some cases when AFs of certain radionuclides in plants of various families are similar (within small range of values) and in other cases they differ a lot (up to 2 degrees) which made it difficult to calculate average values of radionuclide AF for separate organs of the plants of one family with high degree of probability. However, the average values of AF can be used for primary purposes, i.e. approximate assessment of radionuclide concentrations in plant samples. Table (Table 10) shows approximate values of radionuclide AF for the plants of gourd family in different organs in case the AF in fruits is equal to one (1).

Table 9.

Radionuclide distribution in organs of plants from gourd family

Gourd family	AF			
	^{241}Am (min-max) n	^{137}Cs (min-max) n	^{90}Sr (min-max) n	$^{239-240}$Pu (min-max) n
Fruits	2 (1-3) 2	8 (8-9) 2	-	4.4
o.p.	30 (22-40) 2	120 (93-160) 2	6100	180 (176-187) 2
Roots	20 (10-26) 2	70 (43-96) 2	-	-
Note: in brackets – minimum and maximum values of AF, n – number of samples, "-" - no data available				

As it may be seen from the table data on the plants of gourd family, the minimum accumulation of ^{241}Am and ^{137}Cs were found in fruits and maximum accumulations in the aboveground parts of the plants. The pattern of radionuclide distribution in organs of plants of gourd family is similar to the following descending series:

aboveground part >roots>fruits

Table 10.

Radionuclide AF in organs of the plants from gourd family

Crop	Type of samples	AF	$\frac{AF_1}{AF_2}$	AF	$\frac{AF_1}{AF_2}$	AF	$\frac{AF_1}{AF_2}$	AF	$\frac{AF_1}{AF_2}$
		^{241}Am		^{137}Cs		^{90}Sr		$^{239-240}$Pu	
tomato	fruits	0.00023	1	0.0024	10	< 0.00056	< 2.4	0.001	4
	leaves	0.0045	20	0.022	5	0.24	1000	0.04	170
	stems	0.0011	5	0.0061	5	0.38	1600	0.006	26
	roots	0.024	107	0.1	430	0.26	1100	0.29	1300
capsicum	fruits	0.00075	3	0.0021	9	< 0.0014	< 6.1	0.00039	2
	leaves	0.0036	16	0.022	97	0.38	1700	0.011	47
	stems	0.0025	11	0.012	54	0.65	2800	0.0018	8
	roots	0.0022	10	0.018	80	0.23	1000	0.012	50
egg-plant	fruits	-	-	-	-	< 0.0043	< 19	0.055	240
	leaves	0.0068	30	0.041	180	0.79	3400	0.051	220
	stems	0.0010	4	0.0045	20	0.82	3600	0.0043	19
	roots	0.0026	11	0.015	64	0.3	1300	0.016	70
Note: AF_1 – accumulation factor for ^{241}Am in tomato fruit; AF_2 – accumulation factor for remaining radionuclides in different organs of the plants, "-" - no data available									

There is practically no radionuclide accumulation in solanaceous fruits, the exception is AF of $^{239-240}$Pu for egg-plant fruits that is significantly higher than AF of $^{239-240}$Pu for other organs of egg-plant. ^{90}Sr is accumulated more intensively than other radionuclides in solanaceous plant organs, except for fruits.

Table 11.

Radionuclide distribution in solanaceous plant organs

Solanaceous	AF			
	^{241}Am (min-max) N	^{137}Cs (min-max) n	^{90}Sr (min-max) n	$^{239-240}$Pu (min-max) n
fruits	2 (1-3) 2	10 (9-10) 2	< 19	120 (2-240) 3
leaves	20 (16-30) 3	100 (5-180) 3	2000 (1000-3400) 3	150 (47-220) 3
stems	7 (4-11) 3	26 (5-54) 3	2600 (1600-3600) 3	18 (8-26) 3
roots	40 (10-107) 3	200 (64-430) 3	1100 (1000-1300) 3	500 (50-1300) 3
Note: in brackets – minimum and maximum values of AF, n – number of samples, "-" - no data available				

The determined values of AF for ^{241}Am and ^{137}Cs make it possible to built descending series of their accumulation in solanaceous plant organs, except for fruits:

leaves > stems ≥ roots > fruits

The exception was tomato where maximum radionuclides are found in roots.

Accumulation of ^{90}Sr in solanaceous plant organs is different and has the following descending series:

stems > leaves ≥ roots > fruits

Accumulation of $^{239+240}$Pu in solanaceous plant organs has the following descending series:

roots ≥ leaves > stems > fruits

The exceptions are fruits and leaves of egg-plant where maximum values are noticed. High values of SA and accordingly AF of $^{239+240}$Pu in egg-plant fruits might be connected, as literatures states, with purely mechanical uptake of radionuclide particles by flower elements and their subsequent inclusion in the fruit [18].

Table 12.

Radionuclide AF in plant organs of cabbage family

Crop	Type of sample	AF	$\frac{AF_1}{AF_2}$	AF	$\frac{AF_1}{AF_2}$	AF	$\frac{AF_1}{AF_2}$	AF	$\frac{AF_1}{AF_2}$
		^{241}Am		^{137}Cs		^{90}Sr		$^{239-240}$Pu	
Cabbage	leaves	0.00077	1	0.0082	11	0.43	560	0.0011	1.4
	stems	0.0029	4	0.014	18	0.033	43	0.022	28
	roots	0.012	16	0.059	77	0.059	77	0.056	73

Based on the determined values of radionuclide AF, distribution of ^{241}Am, ^{137}Cs and $^{239+240}$Pu in plant organs of cabbage family is as follows:

roots> stems> leaves

Distribution of ^{90}Sr in plant organs of cabbage family looks opposite:

leaves> roots> stems

Values of SA of certain radionuclides that were below the detection limits of measuring equipment were regarded as quantitative values to calculate their AF in separate organs (with the relevant sign "<"). In the same way was determined the ratio between radionuclide AF in various organs and AF of ^{241}Am in wheat grain (Table 13) and other crops.

Table 13.

Radionuclide AF in plant organs of Gramineae family

Crops	Type of sample	AF	$\frac{AF_1}{AF_2}$	AF	$\frac{AF_1}{AF_2}$	AF	$\frac{AF_1}{AF_2}$	AF	$\frac{AF_1}{AF_2}$
		^{241}Am		^{137}Cs		^{90}Sr		$^{239-240}$Pu	
wheat	grain	<0.0033	< 1	0.0036	1	-	-	-	-
	grain film	0.0057	2	0.0062	2	0.0019	0.6	-	-
	stems	< 0.0061	< 2	0.028	8	8.6	2600	-	-
	roots	0.014	4	0.099	30	0.048	15	-	-
barley	stems	0.0028	0.85	0.017	5	0.10	31	-	-
	roots	0.017	5	0.10	31	0.11	33	-	-
Note: "-" - no data available									

As it may be seen from the table, radionuclide accumulation in plant organs of Gramineae family goes down from roots to grains. The exception was ^{90}Sr that has maximum AF noticed in stems. AF of ^{241}Am and ^{137}Cs for grain are comparable, and accumulation of ^{137}Cs in stems and roots is in average 6 times higher than ^{241}Am. AF of ^{90}Sr relative to AF of ^{241}Am determined for stems and roots is one magnitude higher. The difference between accumulation of ^{137}Cs and ^{90}Sr ambiguous as ^{90}Sr is more actively accumulated in stems of wheat and barley. ^{137}Cs is accumulated more actively in wheat roots than ^{90}Sr, and their accumulation in barley roots is practically similar.

Table 14.

Radionuclide distribution in plant organs of Gramineae family

Gramineae	AF			
	^{241}Am (min-max)	^{137}Cs (min-max)	^{90}Sr (min-max)	$^{239-240}$Pu (min-max)
	n	n	n	n
grain	< 1	1	-	-
grain film	2	2	0.6	-
stems	< 2 (< 2-0,85)	7 (5-8)	1300 (33-2600)	-
	2	2	2	
roots	4 (4-5)	30 (30-31)	24 (15-33)	-
	2	2	2	
Note: in brackets – minimum and maximum values of AF, n – number of samples, "-" - no data available				

^{241}Am and ^{137}Cs distribution in plant organs of Gramineae family is as follows:

roots> stems> grain film> grain.

Distribution of ^{90}Sr in plant organs of Gramineae family is ambiguous (in stems and roots) and can be presented as follows:

stems > roots> grain film (wheat);
roots ≥ stems (barley).

Table 15.

Radionuclide AF in plant organs of pea family

Crop	Type of sample	AF	$\frac{AF_1}{AF_2}$	AF	$\frac{AF_1}{AF_2}$	AF	$\frac{AF_1}{AF_2}$	AF	$\frac{AF_1}{AF_2}$
		^{241}Am		^{137}Cs		^{90}Sr		$^{239-240}$Pu	
bean	pod	< 0.0021	< 1	0.0024	1	0.07	31	-	-
	leaves	< 0.0069	< 3	0.033	16	0.67	320	-	-
	stems	< 0.0044	< 2	<0.0058	< 3	0.53	250	-	-
	roots	0.011	5	0.035	17	-	-	-	-
Note: "-" - no data available									

The general regularity of distribution of ^{241}Am and ^{137}Cs in plant organs of pea family:

roots> leaves> stems> pod

Distribution of ^{90}Sr in over ground parts of plants of pea family:

leaves> stems> pod

AF of ^{90}Sr exceeds AF of ^{241}Am by 2 orders of magnitude, and ^{137}Cs – by one order of magnitude.

Table 16.

Radionuclide AF in plant organs of celery family

Crop	Type of sample	AF	$\frac{AF_1}{AF_2}$	AF	$\frac{AF_1}{AF_2}$	AF	$\frac{AF_1}{AF_2}$	AF	$\frac{AF_1}{AF_2}$
		^{241}Am		^{137}Cs		^{90}Sr		$^{239-240}$Pu	
Carrot	leaves	0.0017	1	0.015	9	0.098	61	0.0013	0.8
	root crop	0.0016	1	0.0067	4	0.38	240	0.03	19
Parsley	leaves	0.0038	2	0.022	14	0.15	94	-	-
	roots	0.0018	1	0.012	8	<0.0062	< 4	-	-
Notes: "-" - no data available									

According to the data in the above table, one can see that ^{90}Sr is more actively accumulated in the plants of celery family than other radionuclides: AF of ^{90}Sr exceeds AF of ^{241}Am by up to 2 orders of magnitude, and ^{137}Cs – by 1 order of magnitude. AF of $^{239-240}$Pu for carrot leaves is higher by 2 orders of magnitude and by 1 order of magnitude for root crops, respectively.

Table 17.

Radionuclide distribution in plant organs of celery family

Celery family	AF			
	^{241}Am (min-max) n	^{137}Cs (min-max) n	^{90}Sr (min-max) n	$^{239-240}$Pu (min-max) n
leaves	1.5 (1-2) 2	11 (9-14) 2	78 (61-94) 2	0.8
root crops, roots	1	6 (4-8) 2	120 (< 4-240) 2	19
Note: in brackets – minimum and maximum values of AF, n – number of samples				

Distribution of ^{241}Am and ^{137}Cs in the plant organs of celery family:

aboveground part (leaves) **> underground part** (roots, root crops)

Distribution pattern of ^{90}Sr and $^{239+240}$Pu (for carrot) in the plant organs of celery family is as follows:

aboveground part > underground part (parsley);
underground part> aboveground part (carrot)

Table 18.

Radionuclide AF in plant organs of lilaceous family

Crop	Type of sample	AF	$\frac{AF_1}{AF_2}$	AF	$\frac{AF_1}{AF_2}$	AF	$\frac{AF_1}{AF_2}$	AF	$\frac{AF_1}{AF_2}$
		^{241}Am		^{137}Cs		^{90}Sr		$^{239-240}$Pu	
Bulb onion (bottom set)	leaves	0.0015	1	0.0075	5	0.10	67	0.0049	3
	bulb	0.002	1	0.011	7	0.47	310	0.0092	6
Bulb onion (seeds)	leaves	0.035	23	0.054	36	0.71	480	0.0117	8
	bulb	0.012	8	0.042	28	0.30	200	0.0067	4

Distribution of ^{241}Am, ^{137}Cs, ^{90}Sr and $^{239+240}$Pu in plant organs of lilaceous family is different depending on the type of planting material:

leaves> bulbs (seeds); **bulbs> leaves** (bottom set)

The findings show significant dependence of AF of radionuclides in the plants of lilaceous family on the type of planting materials used: seeds or bottom set (bulb). Thus, for ^{241}Am, ^{137}Cs, such regularity is stronger than for ^{90}Sr and $^{239+240}$Pu, although their AF (^{241}Am and ^{137}Cs) is one order of magnitude lower than the AF (^{90}Sr and $^{239+240}$Pu).

It is therefore established that the most active accumulation of ^{241}Am and ^{137}Cs is in the underground part of the plants of Gramineae, cabbage, lilaceous (planted by bottom set) and solanaceous (tomato) families, and in the aboveground part of plants of celery, gourd, pea, solanaceous (egg-plant, capsicum)) and lilaceous (planted by seeds) families. Accumulation

of $^{239+240}$Pu is more intensive in the underground part of agricultural plants, except for lilaceous (seeds) and solanaceous (egg-plant). ^{90}Sr is mostly accumulated in leaves of plants of solanaceous (egg-plant), cabbage, pea, celery (parsley), lilaceous (planted by seeds) families, in stems of solanaceous (tomato, capsicum), Gramineae (wheat) families, and in the underground part of celery (carrot) and lilaceous (planted by seeds) families. The least accumulation of all analysed radionuclides is noticed in generative organs (fruits and grain).

All findings about peculiarities of radionuclide accumulation are heterogeneous for separate families, separate types and separate organs of agricultural plants. General regularity observed in radionuclide accumulation in separate plant organs, with some exceptions, is that there is least accumulation in generative organs.

3.5. Prospects for agricultural crop production under the conditions of radionuclide contamination on the STS lands

The determined values of specific activity of radionuclides make it possible to evaluate the ability to produce agro products in the radiation contaminated area and compare them with the permissible normative parameters (standards indicated in SanPiN 4.01.071.03 (Sanitary Regulations and Standards)). Since the standards of SA for agro products are indicated applicable to wet weight, experimental data was recalculated for wet weight and results are shown in Table 5. Comparative data on radionuclide concentration in crops and permissible concentrations in food products as per SanPiN 4.01.071.03 is shown in the table (Table 20) [18].

Concentration of $^{239+240}$Pu and ^{241}Am in food is not standardised, however, since the limit of their annual consumption with food by people, as stated in NRB-99 (radiation standards) (Appendix P-2) [19]), is one order of magnitude lower than similar value for ^{90}Sr, and considering their high radiotoxicity, once can assume that the permissible levels for them would be one order of magnitude lower than for ^{90}Sr.

Table 19.

Specific activity in agricultural plant products (for wet weight)

Type of plants	Type of samples	Specific activity, Bq/kg (PSA* as per SanPiN 4.01.071.03)			
		^{241}Am	^{137}Cs	^{90}Sr*	$^{239+240}$Pu
Water melon	fruits	0.025 (4)	0.5 (120)	-	< 0.4 (4)
Melon	fruits	0.07 (4)	0.44 (120)	-	-
Tomato	fruits	0.047 (4)	0.89 (120)	< 0.22 (40)	< 0.45 (4)
Capsicum	fruits	0.035 (4)	0.17 (120)	< 0.16 (40)	< 0.15 (4)
Egg-plant	fruits	-	-	< 0.36 (40)	9.1 (4)
Parsley	leaves	0.77 (4)	6.12 (120)	< 39.76 (40)	-
Cabbage	leaves	0.24 (4)	3.44 (120)	218.4 (40)	1.48 (4)
Carrot	root crops	0.125 (4)	0.69 (120)	57.0 (40)	16.2 (4)
Onion (seeds)	bulbs	0.91 (4)	5.98 (120)	30.42 (40)	2.6 (4)
Onion (bottom set)	bulbs	0.35 (4)	3.52 (120)	171.2 (40)	7.2 (4)
Wheat	grain	< 1.5 (4)	3.24 (70)	-	-
Bean	pod with seeds	< 0.34 (6)	0.63 (50)	23 (60)	-

Notes: PSA- permissible specific activity of radionuclides in plants,
"-" - no data available

Comparative assessment of findings on specific activity of ^{241}Am, ^{137}Cs with PSA of these radionuclides in plants (used by people in food) shows that specific activity in analysed plants does not exceed the standards of SanPiN. However, ^{90}Sr concentrations 1.4-5 times exceeding the permissible concentrations are observed in cabbage, carrot and onion (planted by bottom set), and 2-4 times exceeding of $^{239+240}$Pu in main products of egg-plant, carrot and onion (bottom set).

Therefore, by using the AF determined for the crops and permissible specific activity of radionuclides in the plants, one can calculate permissible radionuclide concentration in soil (under the analysed soil and climate conditions) that would allow producing "clean" agro products. The maximum allowable concentration of radionuclides in soil was calculated as follows:

$$MAC_{soil} = PSA/AF, \quad (3)$$

where MAC_{soil} – maximum allowable concentration of radionuclide in question,
PSA – permissible specific activity of radionuclides in plants,
AF – accumulation factor of radionuclide in question.

The maximum allowable concentration of certain analysed radionuclides in soil is shown in the table (Table 20).

Table 20.

Estimated maximum allowable concentration of radionuclides in soil

Crop	Products	Maximum allowable concentration of radionuclides in soil, Bq/kg			
		^{241}Am	^{137}Cs	^{90}Sr	$^{239+240}$Pu
Water melon	fruits	161700	528000	-	34800
Melon	fruits	61100	653000	-	-
Tomato	fruits	117000	333000	480000	26700
Capsicum	fruits	76600	823000	422000	148000
Egg-plant	fruits	-	-	134000	1000
Parsley	leaves	2000	10600	500	-
cabbage	leaves	18500	52300	300	12800
Carrot	root crop	17000	120000	700	900
Onion (seeds)	bulbs	2500	22100	1000	4600
Onion (bottom set)	bulbs	12500	68200	540	2700
Wheat	grain	1500	23800	-	-
bean	pod with seeds	5600	42100	1800	-
Note: "-" - no data available					

The studies were conducted on the most contaminate area of the "Experimental Field" site of STS with the highest concentration of ^{241}Am and $^{239+240}$Pu in soil. However, despite this fact the experimental findings indicate that there is ability to produce the agricultural products of acceptable quality on STS with high level of radionuclide contamination of soil with ^{241}Am and $^{239+240}$Pu. The exceptions are the main products of celery, cabbage and lilaceous plants in terms of MAC of ^{90}Sr in soil and $^{239+240}$Pu for carrots, which plants can be grown on condition of low radionuclide contamination with ^{90}Sr and $^{239+240}$Pu. Emphasis shall be placed

on ^{90}Sr contained in soil in lesser concentrations than ^{241}Am and $^{239+240}$Pu which, however, will define principal contamination of plant products on the "Experimental Field" site of STS.

CONCLUSIONS

- With regard to all analysed radionuclides in plant samples it has been established that average accumulation of ^{90}Sr is 23 times higher than that of ^{137}Cs, ^{137}Cs and twice higher than of $^{239+240}$Pu, and $^{239+240}$Pu, 5 times higher than that of ^{241}Am.
- It has been revealed that generative organs have the least radionuclide accumulations, expect for the egg-plant fruits.
- It is noticed that accumulation of ^{241}Am, ^{137}Cs and ^{90}Sr in lilaceous plants depends on the type of planting material. If the plants are planted with seeds there is more intensive accumulation of these radionuclides in lilaceous plants than when they are planted with bottom sets.
- The most "mobile" radionuclide is ^{90}Sr the AF of which is higher than AF of all other analysed isotopes for experimental plants; although concentration of ^{90}Sr in soil is one order of magnitude lower than concentrations of $^{239+240}$Pu. Therefore, with the ability to grow the crop in the STS area, it is ^{90}Sr that will first of all affect the quality of plant products.
- Findings on AF and MAC of radionuclides for all crops indicate the principle ability to grow agricultural products even on the "Experimental Field" site of STS and produce the plant product of acceptable quality.

The authors of this articles express their gratitude to the employees of Institute of Radiation Safety and Ecology Y.S. Shevchenko, A.M.Kozkeyeva, and L.A.Nemytova for preparation of plant samples, O.Yu.Korovina, N.V.Bryantseva, S.E.Salmenbayev et al for organization and high quality performance of spectrometric and radiochemical analysis, and Yu.Yu. Yakovenko for preparation of map materials. I extend special gratitude to all employees of OKIE for direct engagement in field works.

REFERENCES

1. Сельскохозяйственная радиоэкология / под ред. академика ВАСХНИЛ Р.М. Алексахина и академика ВАСХНИЛ Н.А. Корнеева. М.: Экология, 1992. - С. 3-11, 54-79, 196-217.
   Agricultural Radioecology / edited by academician VASKHNIL, Aleksakhin R.M., Korneyev N.A., M.: Ecology, 1992. - p. 3-11, 54-79, 196-217. – [in Russian].
2. *Корнеев Н.А.* Задачи и перспективы сельскохозяйственной радиологии / Корнеев Н.А., Поваляев А.П., Алексахин Р.М.//Вестник сельскохозяйственной науки. – 1978. - №1.- С. 108-114.
   Korneyev N.A. Objectives and prospects of agricultural radioecology / Korneyev N.A., Povalyayev A.P., Aleksakhin R.M.// Bulletin of Agricultural Science. – 1978. – No.1.- p. 108-114. – [in Russian].

3. *Лысенко Н.П.* Ведение животноводства в условиях радиоактивного загрязнения среды / Н.П. Лысенко, А.Д. Пастернак, Л.В. Рогожина, А.Г. Павлов. – Санкт-Петербург: Издательство "Лань", 2005. – С. 3-4, 29-34, 93-103.
Lysenko N.P. Animal breeding in the conditions of radioactive environmental contamination / Lysenko N.P., Pasternak A.D., Rogozhina L.V., Pavlov A.G. – St. Petersburg: "Lan" edition, 2005. – p. 3-4, 29-34, 93-103. – [in Russian].
4. *Агеец В.Ю.* Система радиоэкологических контрмер в агросфере Беларуси / В.Ю. Агеец. - Гомель:РНИУП "Институт радиологии", 2001. – С. 4-6, 157-189.
Ageyets V.Yu. System of radioecological counter-measures in agriculture of Belorussia / Ageyets V.Yu. – Gomel: Institute of Radiology Republican Research and Development Unitary Enterprise, 2001. – p. 4-6, 157-189.
5. *Фесенко С.В.* Динамика снижения коэффициентов перехода в сельскохозяйственные растения после аварии на Чернобыльской АЭС / С.В. Фесенко С.В., Н.И. Санжарова, К.Б. Лисянский, Р.М. Алексахин // Радиационная биология. Радиоэкология. - 1998. - Т. 38. вып. 2. - С. 256-265.
Fessenko S.V. Dynamics of decline of coefficient of transfer in agricultural plants after accident at Chernobyl NPP / Fessenko S.V., Sanzharova N.I., Lisyanskii K.B., Aleksakhin R.M.// Radiation Biology. Radioecology. - 1998. - V. 38. Issue. 2. - p. 256-265. – [in Russian].
6. INTERNATIONAL ATOMIC ENERGY AGENCY, Quantification of radionuclide transfer in terrestrial and freshwater environments for radiological assessments, IAEA -TECDOC-1616, Vienna: IAEA, 2009. С. 155-178.
7. Отчет о научно-технической деятельности Института радиационной безопасности и экологии НЯЦ РК, выполненного в составе мероприятия 1 "Реализация научно–технической программы развития атомной энергетики в республике Казахстан" за 2010 г. - г. Курчатов, 2010. - С. 13-14.
Report on scientific and technical activities of Institute of Radiation Safety and Ecology NNC of RK prepared as part of the 1st activity "Implementation of scientific and technical program of nuclear power development in the Republic of Kazakhstan" for 2010. – Kurchatov city, 2010. - p. 13-14.
8. *Найдин П. Г.* Полевой опыт / под ред. П. Г. Найдина, д-ра с.-х. наук. Изд. 2-е, испр. и доп. М.: Колос, 1967. – С. 120-130.
Naidin P.G. Field Test / edited by Naidin P.G., Doctor of Agricultural Science. 2nd Edition, as amended. M.: Kolos, 1967. – p. 120-130. – [in Russian].
9. *Рамазанов Б.Г.* Рекомендации по системе ведения сельского хозяйства. Павлодарская область / Б.Г. Рамазанов, А.П. Осняч, Н.М. Савенко, Г.И. Зубов, В.А. Леонов и др. – Алма-Ата: Кайнар, 1981. – С. 75-116.
Ramazanov B.G. Recommendations on Farming System. Pavlodar Region / Ramazanov B.G., Osnyach A.P., Savenko N.M., Zubov G.I., Leonov V.A.et al. – Alma-Ata: Kainar, 1981. – p. 75-116. – [in Russian].
10. МИ 5.06.001.98 РК "Активность радионуклидов в объемных образцах. Методика выполнения измерений на гамма-спектрометре МИ 2143-91" - 18 с.

MI 5.06.001.98 RK "Activity of Radionuclides in Bulk Samples. Methods of Measurements by Gamma-Spectrometer MI 2143-91" – p.18.

11. Методика измерения активности радионуклидов с использованием сцинтилляционного бета-спектрометра с программным обеспечением "Прогресс", Менделеево, - 20 с.
    Methods of measuring radionuclides with the use of scintillation beta-spectrometer with Progress software, Mendeleyevo, - p.20.
12. *Анненков Б.Н.* Основы сельскохозяйственной радиологии/ Б.Н. Анненков, Е.В. Юдинцева. – Москва, 1991. – С. 56-83.
    Annenkov B.N. Basics of Agricultural Radiology / Annenkov B.N., Yudintseva E.V.– Moscow, 1991. – p. 56-83.
13. Основные аспекты технологии возделывания овощных культур / Айтбаев Т.Е. к. с.-х. наук КазНИИ картофелеводства и овощеводства - www.agroinnovations.kz/files/lib/65/75/208.doc.
    Main aspects in technology of vegetable cultivation / Aitbayev T.E., candidate of agricultural science, Kazakhstan Research and Development Institute of potato and vegetable growing - www.agroinnovations.kz/files/lib/65/75/208.doc.
14. Казахстанский зерновой портал информационного агентства "Казах-Зерно" - www.kazakh-zerno.kz
    Kazakhstani grain portal of Kazakh-Zerno information agency - www.kazakh-zerno.kz
15. Региональная программа на 2008-2009 годы по насыщению регионов плодовоовощной продукцией. Утверждена решением сессии Восточно-Казахстанского областного маслихата от 19 декабря 2008 г. - Усть-Каменогорск, 2008 г., - №10/140-IV г.
    Regional Program for 2008-2009 on enriching regions with fruit and vegetable products. Approved by resolution of East-Kazakhstan Region Maslikhat session dated December 19 December 2008 – Ust-Kamenogorsk, 2008, - №10/140-IV.
16. *Эдельштейн В.И.* Овощеводство. 3-е, перераб. изд. - М.: Сельхозидат, 1962. - 440с.
    Edelshtein V.I. Vegetable Growing . 3rd revised edition. - M.: Selhozizdat, 1962. – 440p. – [in Russian].
17. *Гудков И.Н.* Основы общей и сельскохозяйственной радиобиологии: Учеб. для вузов. - Киев: Изд-во УСХА, 1991, С. 185-186, 223-228.
    Gudkov I.N. Basics of general and agricultural radiobiology: Textbook for high educational institutions. – Kiev: Edition USHA, 1991, p.185-186, 223-228. – [in Russian].
18. Санитарные правила и нормы N 4.01.071.03 "Гигиенические требования к безопасности и пищевой ценности пищевых продуктов". Утверждены приказом министра здравоохранения Республики Казахстан от 11 июня 2003 г. - С.53-56.
    Sanitary Rules and Standards N 4.01.071.03 "Sanitary requirements to safety and nutritional value of food products". Approved by the Order of the Minister of Health of the Republic of Kazakhstan dated June 11, 2003. - p.53-56. – [in Russian].

19. Нормы радиационной безопасности (НРБ-99). СП 2.6.1.758-99. Издание официальное. – Алматы, 2000.-80 с.
Radiation Safety Standards (NRB-99). SP 2.6.1.758-99. Official Edition. – Almaty, 2000.-80p. – [in Russian].

ЖЕРҮСТІ ЯДРОЛЫҚ СЫНАҚТАР ӨТКІЗІЛГЕН АУДАНДА ("ТӘЖІРИБЕ ДАЛАСЫ" АЛ.) АУЫЛ ШАРУАШЫЛЫҒЫ ДАҚЫЛДАРЫНЫҢ ТЕХНОГЕНДІ РАДИОНУКЛИДТЕРДІ ЖИНАҚТАУ ЕРЕКШЕЛІГІ

Кожаханов Т.Е., Лукашенко С.Н., Ларионова Н.В., Иванова А.Р., Келлер С.А.

ҚР ҰЯО Радиациялық қауіпсіздік және экология институты, Курчатов, Қазақстан

Бұл мақалада, бұрыңғы Семей сынақ полигонының (ССП) "Тәжірибе даласы" алаңының радиоактивті-ластанған аумағында өсірілген ауыл шаруашылығы дақылдарының техногенді радионуклидтерді жинақтау нәтижелері келтірілген. Жасалған жұмыстардың нәтижесінен, зерттеліп жатқан өсімдіктердің вегетативті және генеративті мүшелерінде техногенді радионуклидтердің таралуы мен жинақталуының ерекшеліктері анықталды. Өсімдік шаруашылығы өнімдерінде ^{137}Cs, ^{90}Sr, $^{239+240}$Pu және ^{241}Am жинақталу коэффициенті алынды, бұл нәтиже ССП аумағының бөліктерін халық шаруашылығына пайдалануға беру мүмкіндігін бағалау барысында аталған радионуклидтердің шоғырлануына болжау жасау үшін қажет. Зерттеліп жатқан өсімдіктердің өсіру типтеріне қатысты радионуклидтердің жинақталу коэффициентіне байланыстылығы анықталды. ССП аумағының "Тәжірибе даласы" алаңындағы қатерлі радионуклидтер ^{90}Sr болып табылады.

Түйінді сөздер: радиоактивті ластану, радионуклидтер, америций-241 (^{241}Am), цезий-137 (^{137}Cs), стронций-90 (^{90}Sr), плутоний-239+240 ($^{239+240}$Pu), ауыл шаруашылық (а/ш) дақылдары, тиесілі белсенділік (ТБ), жинақталу коэффициенті (Жк), негізгі ауылшаруашылық (өсімдік) өнімі, рауалы тиесілі белсенділік (РТБ).

ОСОБЕННОСТИ НАКОПЛЕНИЯ ТЕХНОГЕННЫХ РАДИОНУКЛИДОВ СЕЛЬСКОХОЗЯЙСТВЕННЫМИ КУЛЬТУРАМИ В РАЙОНЕ ПРОВЕДЕНИЯ НАЗЕМНЫХ ЯДЕРНЫХ ИСПЫТАНИЙ (ПЛ. "ОПЫТНОЕ ПОЛЕ")

Кожаханов Т.Е., Лукашенко С.Н., Ларионова Н.В., Иванова А.Р., Келлер С.А.

Институт радиационной безопасности и экологии НЯЦ РК, Курчатов, Казахстан

В статье представлены результаты исследования накопления техногенных радионуклидов сельскохозяйственными культурами, выращенными на радиоактивно-загрязненной территории площадки "Опытное поле" бывшего Семипалатинского испытательного полигона (СИП). В результате работы выявлены особенности накопления и распределения техногенных радионуклидов в вегетативных и генеративных органах исследуемых растений. Получены коэффициенты

накопления ^{137}Cs, ^{90}Sr, $^{239+240}$Pu и ^{241}Am для продукции растениеводства, необходимые для прогноза концентраций данных радионуклидов при оценке возможности передачи части территории СИП в хозяйственное пользование. Выявлена зависимость коэффициента накопления радионуклидов для исследуемых растений от типа посадки. Установлено, что критическим радионуклидом на площадке "Опытное поле" территории СИП является ^{90}Sr.

Ключевые слова: радиоактивное загрязнение, радионуклиды, ^{241}Am, ^{137}Cs, ^{90}Sr, $^{239+240}$Pu, сельскохозяйственные (с/х) культуры, удельная активность (УА), коэффициенты накопления (Кн), основная сельскохозяйственная (растительная) продукция, допустимая удельная активность (ДУА).

УДК 577.4:577.391: 504.73:539.16

TRANSITION FEATURES OF ARTIFICIAL RADIONUCLIDES FROM SOIL INTO PLANTS WITHIN STEPPE ECOSYSTEMS AT THE "EXPERIMENTAL FIELD" SITE OF FORMER STS

Larionova N.V., Lukashenko S.N., Kunduzbaeva A.E., Ivanova A.R., Keller S.A.

Institute of Radiation Safety and Ecology NNC RK, Kurchatov, Kazakhstan

The paper presents the quantitative parameters of radionuclides accumulation in steppe plants at "Experimental field" site. Value ranges were established for the coefficients of accumulation of ^{241}Am, ^{137}Cs, ^{90}Sr and $^{239+240}$Pu. There were specified some differences in the accumulation of radionuclides for certain plant species and for various ground zeros of nuclear tests. There were examined physicochemical properties of the light-chestnut soils and their influence on the accumulation of radionuclides in plants. A comparative analysis of radionuclides accumulation factors in steppe plants from the "Experimental field" with accumulation factors for plants from other parts of the former Semipalatinsk Test Site.

Keywords: Radioecology, radioactive contamination, radionuclides, ^{241}Am, ^{137}Cs, ^{90}Sr, $^{239+240}$Pu, radionuclides speciation, light chestnut soil, physical and chemical properties of soils, plants, accumulation factors (AF).

INTRODUCTION

Importance of the studies of artificial radionuclides accumulation by the steppe plants is called forth by initiation of the large-scale activities on transfer of the some territories within former Semipalatinsk Test Site (STS) for agricultural use. In this case the parameters of radionuclide redistribution in soil-plant system are essential for forecasting the levels of radioactive contamination of foodstuff. Afterwards, they can be used in calculating the dose loads on population living in STS territories.

Some separate studies of radionuclides' accumulation by the plants were previously carried out at the STS, but regular studies in this field were started only recently. In 2007, the works were begun to collect valid data on artificial radionuclides accumulation by some plants at "Degelen" site. Thus, redistribution and dynamics of accumulation of the radionuclides in aerial parts of the plants of meadow ecosystem was studied in adits # 176 and # 177 where the majority of the influencing factors were kept under control [1].

At present, accumulation of transuranium radionuclides $^{239+240}$Pu and ^{241}Am by the plants is a relatively poorly studied issue both at STS and worldwide. In this regard, reliable information about the parameters of their transfer from soil to the aerial parts of the plants can be only obtained for highly contaminated soils. Thus, "Experimental field" site was selected as a research area, which is characterized by a high content of transuranium radionuclides $^{239+240}$Pu and ^{241}Am in the soils.

The acquired data on radionuclides accumulation by specified plant species will be used in the calculation of the dose loads on population living at the STS. They also can be used as a basis for developing specific, practical recommendations addressing the problem of soil-vegetation radioactive contamination in the area, and for developing the measures

to reduce the radionuclide content in the products gathered under conditions of radioactive contamination.

1. MATERIALS AND METHODS

Field works

Areas under study were selected on the basis of square distribution of exposure dose rate (EDR) and measured during expeditionary works radiological parameters (β-particle flow density and EDR) [2]. Research areas (32 in total) were located at all twelve epicenters of various ground tests carried out at the "Experimental field" site; there were 2–4 areas for each epicenter. (Figure 1).

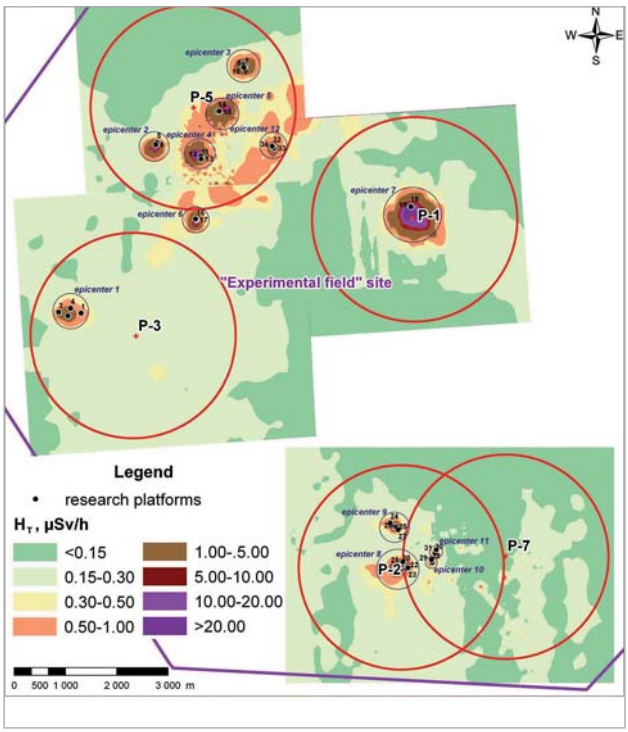

Figure 1. Location of research areas at "Experimental field" (# areas)

Study of the vegetation cover was carried out by the methods of geo-botanical description and identification of main vegetation types, determination of projective cover and vegetation species composition [3]. The samples of aerial part of one of the main arid steppe cenosis-formers – feather-grass (*Stipa capillata*) – were picked out in all the research areas. Additionally, the samples of the following plants were taken in several areas for comparative analysis of their radionuclide accumulation abilities: fescue (*Festuca alesiaca*) and wormwood (*Artemisia sublessingiana*).

Aboveground parts of the studied plants and mixed soil samples (envelop technique at the depth of 5 cm) were taken at each area (Figure 2).

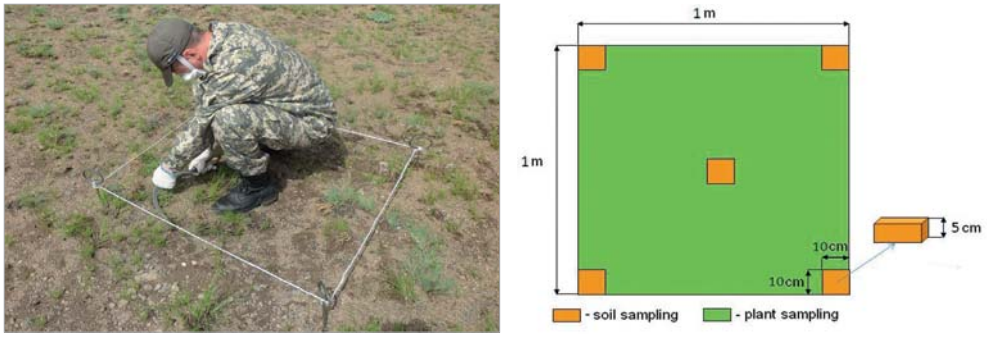

a) b)

Figure 2. Sampling of aboveground parts of the plants (a), soil and vegetation sampling layout (b)

Preparation of vegetation and soil samples

Vegetation samples were roughly chopped (1–3 cm in length) by using a secateur, washed and rinsed with distilled water 2–3 times. Then the samples were dried in a drying chamber at temperature of 80–100°C until constant mass of a sample. Laboratory mill was used for fine grinding. After that, the samples were thermally concentrated (charring, ashing). Dry remain was charred in a muffle furnace or was baked at an electric range in a dry box by preventing ignition of a sample until the smoke stopped and a black residue was obtained. Then the samples were cooled, grinded ant transferred into the porcelain cups, crucibles for following ashing. At first, temperature was increased up to 200°C during 50–60 min, then limiting temperature was established in the muffle furnace: ashing temperature for ^{137}Cs determination was 400°C, ^{90}Sr – 550°C, ^{241}Am and $^{239+240}$Pu – 650°C. After that, the cups with ashes were cooled in a desiccator. Prepared ashes were sifted through a sieve to remove the impurities; cooled ash residue was weighed, and ashing coefficient was determined.

Soil samples were dried to air-dry state in a drying chamber at temperature of 60–70°C. Upon removal of large rocks and inclusions (roots of plants), the samples were weighed on a technical balance. Then the entire volume of a sample was mixed thoroughly, gradually (by batches) grinded in a porcelain mortar with a pestle, and screened through a sieve with a hole diameter of 1 mm. Grinding and sieving was repeated until only the particles of soil skeleton were left in a sieve. The completeness of screening was checked by shaking each a sieve over a sheet of paper. Sieving was continued until no particles fell to the paper.

Physical-chemical analysis of soils

Mechanical composition of the soils was determined by the pipette-technique, which allows for determination of quantitative percentage ratio of soil fractions for any group of the particles of different sizes [4]. Humus content in the soils was measured by Tyurin's method, Nikitin's modification [4]. Measurement of soil acidity was carried out by the method based on measuring the pH in water extracts of rocks employing an electrode system consisting of an indicator glass electrode (its potential is determined by the activity of hydrogen ions in solution) and an auxiliary flow-through reference electrode with a known potential [5]. Carbonate content was determined by a Golubev's volumetric method, based on measurement of additional pressure in a calcimeter due to carbon dioxide released during exposure

of 18% HC1 solution onto the carbonates contained in the soils. The pressure was measured by a height of mercury column in a glass tube; a special scale was used for measurements [4]. Radionuclide forms, which are the most common in the plants, were determined by a technique of sequential leaching with various reagents (water for water soluble form and a solution of 1M ammonium acetate for an exchangeable form) and following measurement of their content in the extracts [6].

Radionuclide analysis

Measurements of specific activity of the radionuclides in the soil and plant samples were carried out in compliance with the standard methodical guides [7, 8, 9] by using the accepted laboratory equipment. The specific activity of radionuclides ^{137}Cs and ^{241}Am was measured by gamma-spectrometer Canberra GX-2020, ^{90}Sr – beta-spectrometer "Progress", and $^{239+240}$Pu was determined by radio-chemical separation followed by measurement at alpha-spectrometer Canberra, mod.7401. ^{137}Cs concentration in the plants was determined in the dry (pre-washed) chopped samples; concentrations of ^{241}Am, ^{90}Sr and $^{239+240}$Pu were measured in the ashes with following recalculation for dry substance. Detection limit for ^{137}Cs was 1 Bq/kg (for plant samples) and 4 Bq/kg (for soil samples), ^{241}Am – 0.3 Bq/kg and 1 Bq/kg, $^{239+240}$Pu – 0.1 Bq/kg and 1 Bq/kg, respectively; ^{90}Sr – 200 Bq/kg. Measurement errors for ^{137}Cs and ^{241}Am didn't exceed 10-20 %, for ^{90}Sr – 15-25 %, and error for $^{239+240}$Pu was 30%.

2. RESULTS AND DISCUSSION

2.1. Quantitative parameters of radionuclide accumulation by dominant species of steppe plants at the "Experimental Field" site

The most frequently used indicator, accumulation factor (AF), was used for quantitative assessment of the parameters of radionuclides accumulation in the aerial parts of the plants; accumulation factor (coefficient) is the ratio of radionuclide content per unit mass of vegetation to the radionuclide content per unit mass of soil [10]. Table 1 shows the results of the tests on determination of the specific activity and AF for the radionuclides ^{241}Am, ^{137}Cs, ^{90}Sr and $^{239+240}$Pu for the test plant – feather-grass (Stipa capillata), which was gathered at all the research areas.

Analyzing the obtained data, it can be noted that all the selected research areas have a high content of transuranium radionuclides $^{239+240}$Pu and ^{241}Am, and are relatively less contaminated with ^{137}Cs and ^{90}Sr.

Accumulation factor AF of ^{90}Sr is of particular interest, since its values do not exceed 1.0, which is not typical for this radionuclide.

AF for $^{239+240}$Pu (0.00001-0.04) varies for three orders of magnitude, AF for ^{241}Am (0.0001–0.01), ^{137}Cs and ^{90}Sr (0.001-0.1) – two orders of magnitude. Distribution of AF values is presented as a histogram of occurrence frequency ***Lg AF*** (Figure 3).

Table 1.

Activity and AF intervals for the radionuclides ^{241}Am, ^{137}Cs, ^{90}Sr and $^{239+240}$Pu (for feather-grass (Stipa capillata))

##	Sampling Point	Specific Activity, Bq/kg								AF			
		^{241}Am		^{137}Cs		^{90}Sr		$^{239+240}$Pu		^{241}Am	^{137}Cs	^{90}Sr	$^{239+240}$Pu
		grass	soil	grass	soil	grass	soil	grass	soil				
1	Э1-1	2.8±0.1	2100±200	6.1±0.2	1000±100	13±1	780±280	21±1	10000±2000	0.0013	0.0061	0.017	0.0021
2	Э1-2	1.2±0.1	2200±200	24±1	1500±200	9.4±1.1	1600±410	6.4±0.2	7000±700	0.00052	0.016	0.0059	0.00091
3	Э1-3	529±1	101600±10000	23±1	600±60	38±1	700±270	9500±300	1300000±80000	0.0052	0.038	0.055	0.0073
4	Э1-4	34.3±0.5	4600±500	4.5±0.3	700±70	11±1	800±290	180±10	4200±1100	0.0075	0.0064	0.014	0.043
5	Э2-1	1.4±0.1	1200±100	5.1±0.2	1300±100	19±3	1900±500	27±1	14200±800	0.0012	0.0039	0.010	0.0019
6	Э2-2	4.5±0.2	2300±200	103±1	7500±700	1970±10	12000±1800	69±2	25800±1300	0.0020	0.014	0.16	0.0027
7	Э3-1	4.1±0.1	2200±200	3.9±0.2	1800±200	21±1	2600±600	18±1	6600±1100	0.0019	0.0022	0.0080	0.0028
8	Э3-2	0.97±0.13	3800±400	3.5±0.3	340±30	23±1	<100	5.5±0.2	5000±1000	0.00026	0.010	-	0.0011
9	Э3-3	4.5±0.1	1400±100	10.4±0.3	600±60	17±1	1100±300	24±1	900±100	0.0032	0.017	0.015	0.026
10	Э3-4	8.1±0.2	3800±400	11.4±0.4	800±80	35±1	860±300	55±2	1300±400	0.0021	0.014	0.040	0.042
11	Э4-1	8.7±0.2	12700±1000	16.2±0.5	7300±700	79±2	8600±1400	40±1	38000±5000	0.00068	0.0022	0.0092	0.0011
12	Э4-2	3.9±0.2	15600±2000	6.1±0.3	9000±1000	134±3	11000±1700	21±1	54000±8000	0.00025	0.00068	0.012	0.00039
13	Э4-3	2.5±0.1	6200±600	3.8±0.2	2800±300	26±1	3300±600	11.7±0.4	23500±2600	0.00041	0.0014	0.0077	0.00050
14	Э5-1	0.85±0.13	2200±200	3.1±0.3	2100±200	53±2	2000±400	13.0±0.4	14200±1900	0.00039	0.0015	0.026	0.00091
15	Э5-2	2.6±0.2	6000±600	8.7±0.4	2300±200	70±1	2700±600	30±1	9400±2500	0.00043	0.0038	0.026	0.0032
16	Э6-1	0.26±0.07	1000±100	2.1±0.2	600±60	56±2	1010±250	1.8±0.1	30000±3000	0.00026	0.0035	0.055	0.000061

##	Sampling Point	Specific Activity, Bq/kg								AF			
		^{241}Am		^{137}Cs		^{90}Sr		$^{239+240}$Pu		^{241}Am	^{137}Cs	^{90}Sr	$^{239+240}$Pu
		grass	soil	grass	soil	grass	soil	grass	soil				
17	Э6-2	0.61±0.08	700±70	4.0±0.2	500±50	45±1	<100	6.2±0.2	4700±600	0.00087	0.0080	-	0.0013
18	Э7-1	0.71±0.12	1200±100	8.3±0.3	8500±900	57±1	29000±3800	11.6±0.3	13000±1000	0.00059	0.0010	0.0020	0.00089
19	Э7-2	1.1±0.2	1000±100	14.5±0.5	3000±300	59±2	7600±1200	24±1	10200±500	0.0011	0.0048	0.0077	0.0024
20	Э8-2	2.3±0.2	9000±1000	16.5±0.5	2400±200	480±10	2000±500	44±1	164000±8000	0.00025	0.0069	0.24	0.00027
21	Э8-3	8.9±0.3	1500±200	34±1	3300±300	190±4	2500±600	93±3	16100±600	0.0059	0.010	0.075	0.0058
22	Э9-1	10.4±0.3	18000±2000	4.3±0.4	1000±100	9.8±1.4	1400±400	44±1	22000±6000	0.00058	0.0043	0.0070	0.0020
23	Э9-2	7.7±0.2	19600±2000	3.2±0.2	1800±200	16±1	2000±500	43±1	84000±6000	0.00039	0.0018	0.0079	0.00051
24	Э9-3	0.36±0.11	2600±300	10.7±0.4	4200±400	94±2	3400±700	2.1±0.1	194000±5000	0.00014	0.0025	0.028	0.000011
25	Э9-4	9.9±0.2	12400±1000	5.9±0.3	700±70	11±1	560±240	48±2	2800±400	0.00080	0.0084	0.020	0.017
26	Э10-1	0.79±0.12	2200±200	49±1	700±70	150±2	580±250	5.5±0.2	6000±950	0.00036	0.070	0.25	0.00092
27	Э10-2	0.90±0.09	3100±300	6.3±0.2	600±60	170±3	860±290	8.6±0.3	12800±1400	0.00029	0.010	0.19	0.00067
28	Э11-1	3.8±0.2	4000±400	6.6±0.4	2500±300	130±3	2100±500	30±1	14700±1200	0.00095	0.0026	0.061	0.0020
29	Э11-2	12.0±0.3	9500±1000	36±1	7900±800	540±10	5100±900	118±4	31000±6000	0.0013	0.0045	0.11	0.0038
30	Э12-1	1.44±0.03	6000±600	4.2±0.1	3700±400	23±1	6200±1000	11.5±0.3	17200±600	0.00024	0.0011	0.0037	0.00067
31	Э12-2	2.03±0.15	1500±200	4.9±0.3	1200±100	25±2	1700±400	21.0±0.5	11400±1500	0.0014	0.0040	0.015	0.0018
32	Э12-3	6.8±0.2	18500±2000	10.8±0.4	9000±900	42±10	9200±1400	47±1	27200±600	0.00037	0.0012	0.0046	0.0017

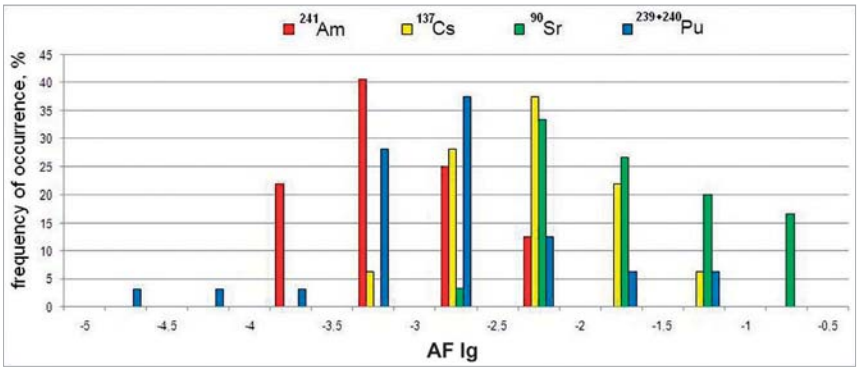

Figure 3. Distribution of *Lg AF* values for ^{241}Am, ^{137}Cs, ^{90}Sr and $^{239+240}$Pu for the studied areas (for feather-grass (*Stipa capillata*))

The histogram demonstrates well that accumulation rates of the studied radionuclides varies within wide intervals obeying the following sequence:

^{90}Sr AF > ^{137}Cs AF > $^{239+240}$Pu AF > ^{241}Am AF

To make qualitative assessment of differences in accumulation of radionuclides by the plants we calculated the ratios of ^{90}Sr AF / ^{137}Cs AF, ^{137}Cs AF / $^{239+240}$Pu AF, and $^{239+240}$Pu AF / ^{241}Am AF for each studied area. Upon elimination of irregularities, the average ratios comprised:

- ^{90}Sr AF / ^{137}Cs AF ~ 7,6;
- ^{137}Cs AF / $^{239+240}$Pu AF ~ 2,4;
- $^{239+240}$Pu AF / ^{241}Am AF ~ 2,7.

So, if we accept accumulation of ^{241}Am by plant as a unit, the sequence take the numerical form:

^{90}Sr AF	**>**	***^{137}Cs AF***	**>**	***$^{239+240}$Pu AF***	**>**	***^{241}Am AF***
49±8		***6.5±1***		***2.7±0,4***		***1***

The table below presents the ranges of AF values for the radionuclides ^{241}Am, ^{137}Cs, ^{90}Sr and $^{239+240}$Pu for all studied vegetation types (Table 2).

Table 2.

AF values for the radionuclides ^{241}Am, ^{137}Cs, ^{90}Sr and $^{239+240}$Pu for all studied plants

plant	AF			
	^{241}Am	^{137}Cs	^{90}Sr	$^{239+240}$Pu
feather-grass (*Stipa capillata*)	**0.001** (n=32) 0.0001 - 0.01	**0.01** (n=32) 0.001-0.1	**0.1** (n=30) 0.002-0.3	**0.01** (n=32) 0.00001-0.04
fescue (*Festuca alesiaca*)	**0.001** (n=13) 0.0003 - 0.01	**0.01** (n=13) 0.001-0.01	**<0.1** (n=13)	-*
wormwood (*Artemisia sublessingiana*)	**0.01** (n=9) 0.00003 - 0.1	**0.01** (n=10) 0.0002-0.1	**<0.1** (n=31)	-*
Note: numerator – arithmetic mean, in the brackets – number of cases; denominator – range of values, *- results are not available				

The Table shows that the values AF of ^{241}Am and ^{137}Cs for the feather-grass and fescue plants are similar. The rather different picture is for wormwood plant: range of AF values is rather wide. The more detailed comparison of the AF values for various plants is given as a histogram of occurrence frequency *Lg AF* of the radionuclides ^{241}Am and ^{137}Cs (See Figure 4).

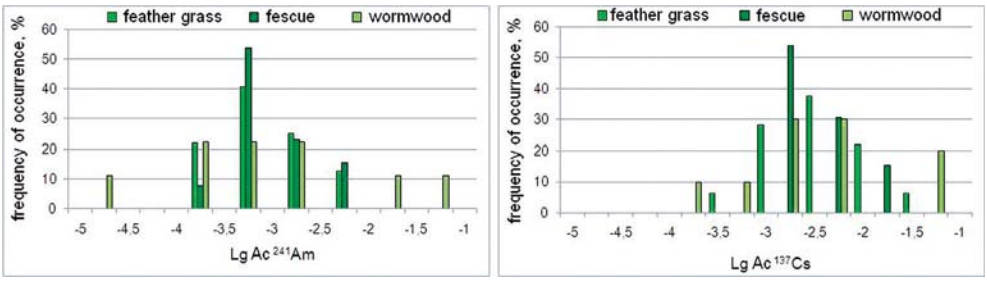

Figure 4. Distribution of Lg AF of ^{241}Am and ^{137}Cs for the plants under study

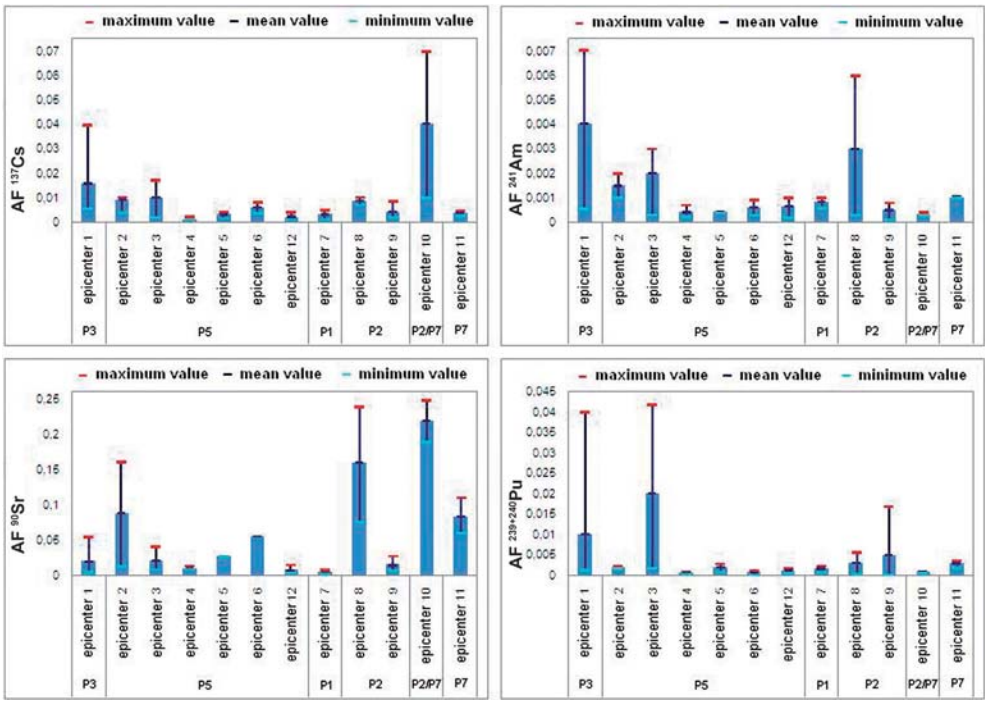

Figure 5. Average AF values for ^{137}Cs, ^{90}Sr, ^{241}Am and $^{239+240}$Pu at each of the epicenters (for the feather-grass *(Stipa capillata)*)

There is no apparent difference in radionuclide accumulation by the plants, but we cannot assert about identical accumulation either. For example, as mentioned above, the greatest range of AF values for ^{241}Am and ^{137}Cs was observed in wormwood (*Artemisia sub-*

lessingiana). In general, the AF values of ^{241}Am and ^{137}Cs are the same for feather-grass (*Stipa capillata*) and fescue (*Festuca alesiaca*), but AF value of ^{137}Cs for fescue (*Festuca alesiaca*) is characterized by a much smaller range of values than ones of the other two species.

Certain differences in the radionuclide accumulation by the plants are also revealed for the different epicenters. Figure 5 shows the average AF values for ^{137}Cs, ^{90}Sr, ^{241}Am and $^{239+240}$Pu in feather-grass (Stipa capillata) for each of the epicenters.

Based on the presented histograms we can say that the radionuclide accumulation by plants, in particular, feather-grass *(Stipa capillata)*, for the various epicenters is somewhat different. Thus, a clear shift of AF values towards high values was observed for the radionuclide ^{90}Sr in 8th, 10th and 11th epicenters and for ^{137}Cs – in 10th epicenter. Other cases can also be distinguished, but such shifts are mostly due to the relatively large range of AF values of the radionuclides (for instance, for ^{241}Am and $^{239+240}$Pu in 1st and 3rd epicenters).

2.2. Study and evaluation of the influence of soil physical-chemical properties on radionuclides accumulation by the plants at the "Experimental Field" site

The radionuclides accumulation by the plants can be influenced by both physical-chemical properties of the soils, and the forms of radionuclides in them [11]. Table 3 lists the ranges of the main physical-chemical properties of the soils (pH, humus, carbonates, amount of salts in the water extract, and texture (the content of physical clay)), as well as the radionuclides forms most available to the plants (water-soluble and exchangeable forms).

Table 3.

Physical-chemical properties and radionuclide forms in the soils

Physical-chemical properties of the soils					Content of the radionuclide forms in the soils, %							
pH	Humus	Salts total in water extract	Carbonates	Physical clay	^{241}Am		^{137}Cs		^{90}Sr		$^{239+240}$Pu	
	%				*w.	**ex.	w.	ex.	w.	ex.	w.	ex.
7.1-8.2	1.7-6.1	0.03-0.1	Up to 2	27.5- 67.6	<0.1	<0.1	<0.1	<0.7	<0.8	<0.1	<0.01	<0.01
Note: * - water-soluble form ** - exchangeable form												

The studied soils are light brown, normal (loose ground rate of more than 80 cm), loamy (the content of physical clay 27.5 - 67.6%), carbonate (up to 4-5%) and slightly saline (total salt 0.03-0.1%). As for the organic substance content, the soils under study are low-humus – total humus does not exceed 2-3.5%. The content of water-soluble and exchangeable forms of radionuclides in most cases is below the detection limit.

We considered acidity, humus and physical clay content in the soils for the plant feather-grass (*Stipa capillata*) as the factors in assessment of the influence of physical-chemical properties of the light chestnut soils on the accumulation of radionuclides ^{241}Am, ^{137}Cs, ^{90}Sr and $^{239+240}$Pu by the steppe plants (Figure 6).

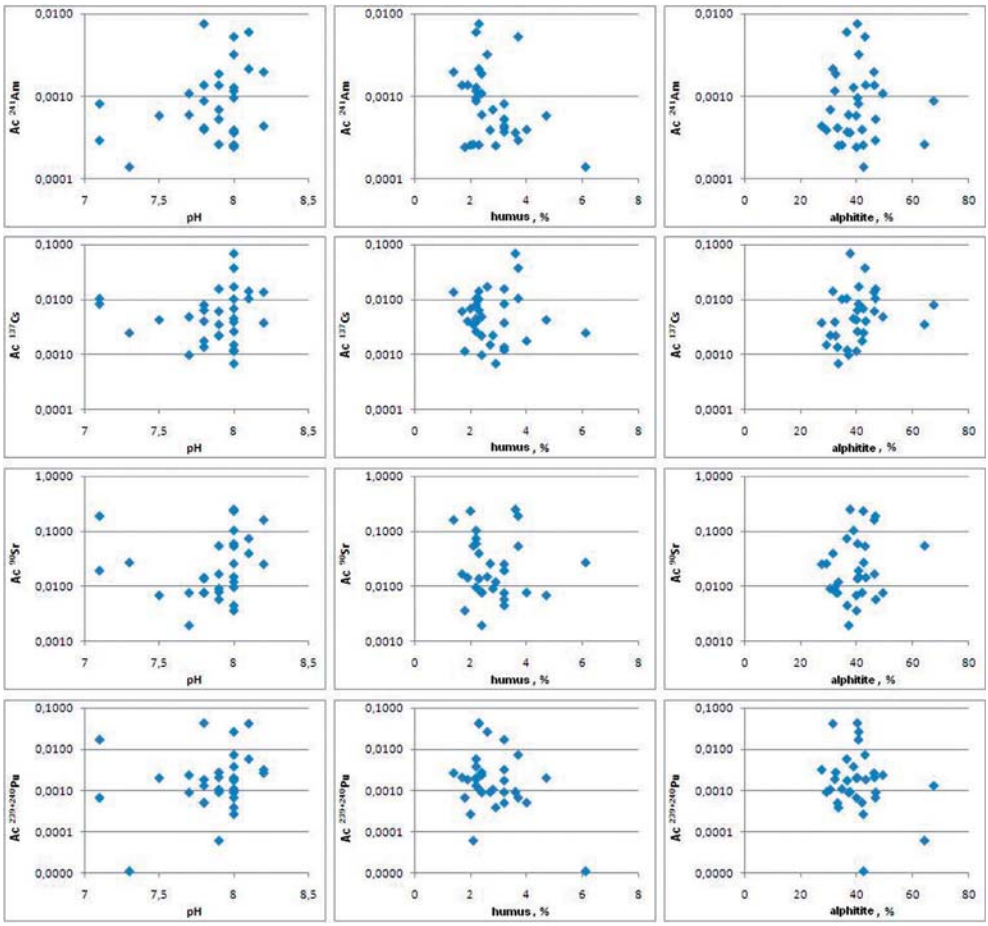

Figure 6. Dependence of radionuclides AF on some physical-chemical properties of light chestnut soils (for feather-grass (Stipa capillata))

As presented graphs show, there is no influence of the soil physical-chemical properties on accumulation of radionuclides ^{241}Am and ^{137}Cs by the plants. The reason for this may be both a low range of these factors within the study territory and absence of the most available radionuclides forms in the soils (Table 3).

2.3. Comparative analysis of factors of radionuclides accumulation by the steppe plants at the "Experimental Field" site with accumulation factors for the plants from other parts of the former Semipalatinsk Test Site

To assess the data obtained on the accumulation of ^{241}Am, ^{137}Cs, ^{90}Sr and $^{239+240}$Pu radionuclides by the steppe plants they were compared with the previously obtained data for different plants, selected from other STS areas. Additionally, we compared the data with

international summary materials [12] for two groups of the plants (miscellaneous herbs and pascual grasses) picked out on the loamy soils typical for the STS areas (Table 4).

Table 4.

Accumulation factors (AF) of the radionuclides for different plants at the STS lands

Plant	AF			
	^{241}Am	^{137}Cs	^{90}Sr	$^{239+240}$Pu
"Experimental Field" site ground				
feather grass (*Stipa capillata*)	0.001 (n=32) 0.00001 - 0.01	0.01 (n=32) 0.0001-0.1	<0.1 (n=32)	0.001 (n=12) 0.00001 - 0.002
Degelen site, vicinity of the adit № 176				
tansy (*Tanacetum vulgare*)	-	2.80 (n=10) 0.01 - 16.30	1.80 (n=10) 0.80 - 5.70	-
brier (*Rosa spinosissima*)	-	2.60 (n=10) 0.01 - 13.20	2.00 (n=10) 0.40 - 4.50	-
wild rye (*Leymus angustus*)	-	1.30 (n=10) 0.05 - 7.50	3.30 (n=10) 0.90 - 9.50	-
Degelen site, vicinity of the adit № 177				
tansy (*Tanacetum vulgare*)	<0.03 (n=10)	0.02 (n=10) 0.002 - 0.06	0.80 (n=11) 0.50 - 1.40	0.01 (n=5) 0.0003 - 0.02
willowweed (*Chamaenerium angustifolium*)	<0.13 (n=12)	0.20 (n=12) 0.001 - 1.00	1.30 (n=13) 0.50 - 4.00	0.004 (n=3) 0.001 - 0.003
thistle (*Cirsium arvense*)	<0.09 (n=9)	0.10 (n=11) 0.008 - 0.60	2.47 (n=11) 1.80 - 3.20	0.01 (n=2) 0.003 - 0.02
"reference" northern territories of STS				
Steppe miscellaneous herbs	0.06 (n=3) 0.02 - 0.11	0.02 (n=14) 0.003 - 0.06	<0.40 (n=4)	0.03 (n=9) 0.01 - 0.1
"reference" western territories of STS				
Steppe miscellaneous herbs	<0.20 (n=22)	0.05 (n=12) 0.01 - 0.1	0.8 (n=3) 0.1 - 1.7	0.04 (n=13) 0.002 - 0.2
Generalized international data (2009)				
miscellaneous herbs	-	0.1 (n=10) 0.01 - 0.2	0.9 (n=6) 0.3 - 2.0	-
Pascual herbs	0.003 (n=11) 0.005 - 0.02	0.4 (n=124) 0.01 - 2.6	1.2 (n=58) 0.4 - 2.6	0.0006 (n=10) 0.00006 - 0.003

Note: numerator – arithmetic mean, in the brackets – number of cases; denominator – range of values,
- results are not available

As the Table shows, statistically reliable quantitative ^{241}Am AF values for STS territories were obtained for the first time over the numerous studies carried out earlier. At that, number of the analyzed cases for the research area is five times greater than all currently available international results. The histograms show the distribution of values ***Lg AF*** for ^{241}Am and $^{239+240}$Pu at these STS territories and the ranges of AF values of international summary data (Figure 7).

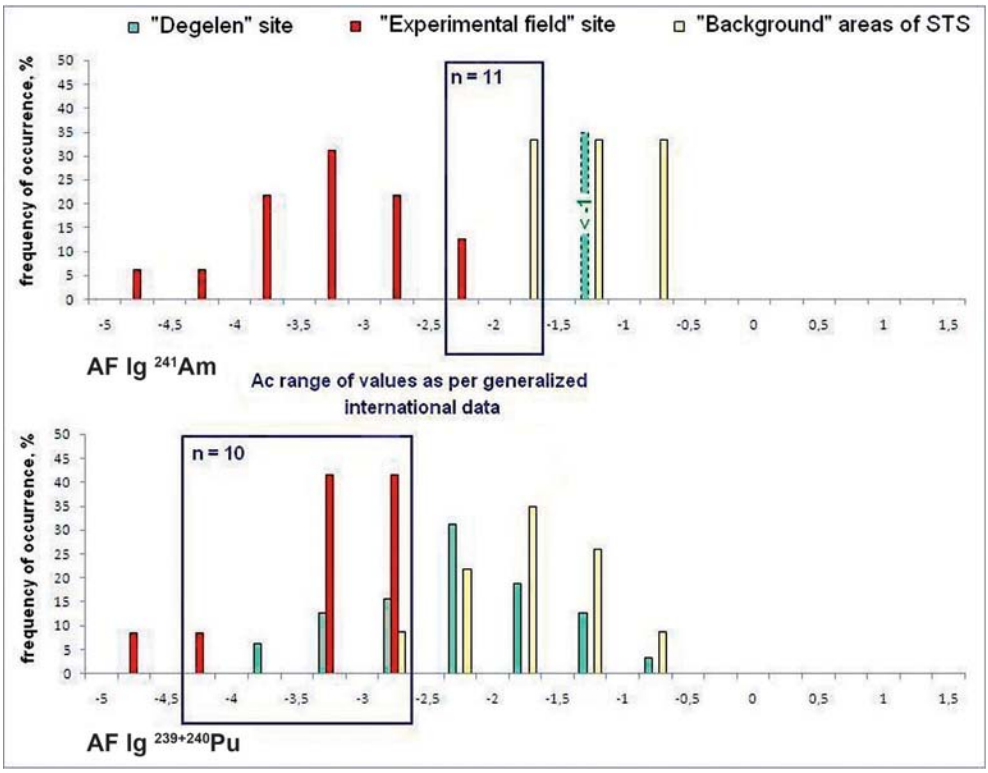

Figure 7. Distribution of Lg AF values for ^{241}Am and $^{239+240}$Pu at various STS territories

The presented histograms show that the values AF of the ^{241}Am radionuclide for the steppe plants on the "Experimental Field" site shifted toward lower AF values with regard to both the quantitative and estimated AF values of this radionuclide at other STS territories, and international generalized data for pascual herbs. AF values for $^{239+240}$Pu at the "Experimental Field" site are also lower than the ones in other areas of STS, but coincide in general with the range of the AF values of generalized international data.

Distribution of AF values for ^{137}Cs and ^{90}Sr at these STS territories is also presented as histograms of occurrence frequency Lg AF (see Figure 8).

Thus, the ^{137}Cs AF values for "Experimental Field" site plants are considerably lower than the values for miscellaneous herbs and pascual herbs given in the international sources, and for the plants picked out at the "Degelen" site (except of AF for tansy (*Tanacetum vulgare*) picked out in the adit # 177). But in general, the values coincide with AF of a certain radionuclide for the plants picked out at the "reference" STS territories.

A unique situation is observed for ^{90}Sr, which absolute AF value was clearly shifted toward lower values with respect to all previously received AF values for this radionuclide.

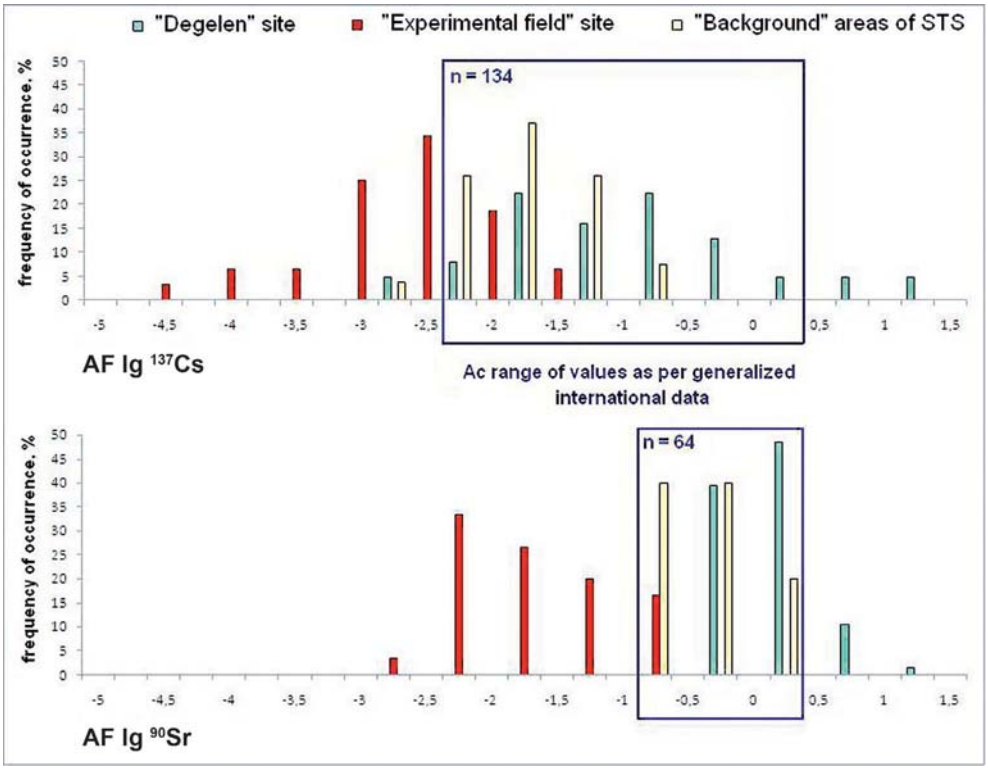

Figure 8. Distribution of AF values for ^{137}Cs and ^{90}Sr at various STS territories

CONCLUSIONS

The quantitative parameters of radionuclides accumulation by the steppe plants at the "Experimental field" site were determined. AF for $^{239+240}$Pu (0.00001-0.04) varies within the range of three orders of magnitude; AF for ^{241}Am (0.0001-0.01), ^{137}Cs and ^{90}Sr (0.001-0.1) – two orders of magnitude. Certain differences were observed for the radionuclides accumulation by some plant species and for different nuclear test epicenters.

Physical-chemical properties of the soils do not have significant influence on radionuclides accumulation by the plants.

The obtained results are statistically reliable; at that, the AF values are generally lower than the values for other STS territories and the international generalized data.

The authors acknowledge the staff of the Institute of Radiation Safety and Ecology: Yakovenko Y.Y., Yeremenko E.A., Yelizaryeva N.A, for the development of cartographic material, Shevchenko YA.., Kozkeeva A.M., Nemytova L.A., Subbotina L.F. for preparation of plant samples, Bayserkenova T.N., Bakirova G.A. for implementation of physical-chemical analysis of the soils, Korovina O.Y., Bryantseva N.V., Salmenbaev S.E., Cheredov O.I. and others, as well as members of the Institute of Nuclear Physics Glushchenko V.N., Koval A.P. and others for organization and high performance of the spectrometric and radiochemical analysis.

REFERENCES

1. Актуальные вопросы радиоэкологии Казахстана [Сборник трудов Института радиационной безопасности и экологии за 2007-2009 гг.] / под рук. Лукашенко С.Н. – Вып. 2. – Павлодар: Дом печати, 2010. – С. 301-320.: ил.- Библиогр.: с. 528. - ISBN 978-601-7112-28-8.
   Topical Issues in Radioecology of Kazakhstan [Proceedings of the Institute of Radiation Safety and Ecology for 2007-2009]/Sup. by Lukashenko S.N. – V.2. – Pavlodar: Printing House, 2010. – pp. 301-320.: illustration.- appendix.: p. 528. - ISBN 978-601-7112-28-8. – [in Russian]
2. Методика измерения гамма – фона территорий и помещений: утв. Зам. Главного государственного санитарного врача Республики Казахстан Спатаев М.Б. 25.08.1997: Зав. Отделом радиационной гигиены республиканской санэпидемстанции Вдавиченко Г.Д. - 1 с.
   The method for gamma-background measurements of territories and premises: est. by Satpayev M.B., vice State sanitary chief inspector of the Republic of Kazakhstan. 25.08.1997: Vdavichenko G.D., chief of the radiation hygiene department of State sanitary-and-epidemiologic institution. – 1 p.
3. Полевая геоботаника- т. 1.-1959.-444 с.; т. 2.-1960.-500 с.; т. 3.-1964.-530 с.; т.4.-1972.-336 с.; т.5.-1976.-320 с. М., Наука.
   Field geobotany – V.1. – 1959. – 444 pp.; V.2. – 1960. – 500 pp.; V.3. – 1964. – 530 pp.; V.4. – 1972. – 336 pp.; V.5. – 1976. – 320 pp. M.: "Nauka". – [in Russian]
4. Сборник методических указаний по лабораторным исследованиям почв и растительности Республики Казахстан / под рук. Дюсенбекова З.Д.; Государственный научно-производственный центр земельных ресурсов и землеустройства. – Алматы, 1998. – 222 с.
   Collection of methodological recommendations on laboratory research of soils and plants in the Republic of Kazakhstan/ Ed.by Dyusenbekov Z.D.; State scientific-production center for land resources and land management. – Almaty, 1998. – 222 pp. – [in Russian]
5. ГОСТ 17.5.4.01–84. Метод определения pH водной вытяжки вскрышных и вмещающих пород. Охрана природы. Рекультивация земель. – Введ. 01.07.85. – Изд. Стандартов. – М, 1985, - 3 с.
   State Standard GOST 17.5.4.01-84. Method of pH measurements for aqueous extract in overburden and bearing strata. Protection of nature. Reclamations. – Intr. 01.07.85. – Standards Publishing. – M, 1985, - 3 pp. – [in Russian]
6. Практикум по агрохимии / под ред. В.Г. Минеева. – М. : МГУ, 2001. – 268 с.
   Practice work in agricultural chemistry/ Ed. by Mineyev V.G. – Moscow: MSU, 2001. – 268 pp. – [in Russian]
7. МИ 5.06.001.98 РК "Активность радионуклидов в объемных образцах. Методика выполнения измерений на гамма-спектрометре МИ 2143-91" - 18 с.
   MI 5.06.001.98 RK "activity of radionuclides in bulk samples. Methods of measurement implementations using gamma-spectrometer. MI 2143-91" – 18 pp.

8. Методика измерения активности радионуклидов с использованием сцинтилляционного бета-спектрометра с программным обеспечением "Прогресс", Менделеево, - 20 с.
The method of radionuclide activity measurements using scintillation beta- spectrometer with "Progress" control software, Mendeleyevo, - 20 pp. – [in Russian]
9. Методика определения изотопов плутония-(239+240), стронция-90, америция-241 в объектах окружающей среды: МИ 06-7-98. – Алматы, 1998.
The Method of plutonium-(239+240), stroncium-90, and americium-241 isotope measurements in the environmental objects: MI 06-7-98. – Almaty, 1998. – [in Russian]
10. Анненков Б.Н. Основы сельскохозяйственной радиологии/ Б.Н. Анненков, Е.В. Юдинцева. – Москва, 1991. – С. 56-83.
Annenkov B.N. Fundamentals of agricultural radiology/ Annenkov B.N., Yudintseva Ye. V. – Moscow, 1991. – pp. 56-83. – [in Russian]
11. Лысенко Н. Ведение животноводства в условиях радиоактивного загрязнения среды/ Н.Лысенко, А.Пастернак, Л.Рогожина. - СПб: Лань, 2005. – С. 35-36.
Lysenko N. Animal-keeping in conditions of radioactive environmental pollution/ Lysenko N., Pasternak A., RogozhinaL. – Saint-Petersburg: "LAN", 2005. – pp.35-36. – [in Russian]
12. INTERNATIONAL ATOMIC ENERGY AGENCY, Quantification of radionuclide transfer in terrestrial and freshwater environments for radiological assessments, IAEA -TECDOC-1616, IAEA, Vienna (2009) – 163 p.

БҰРЫНҒЫ ССП "ТӘЖІРИБЕ ДАЛАСЫ" АЛАҢЫНЫҢ ДАЛА ЭКОЖҮЙЕЛЕРІНЕ ЖАСАНДЫ РАДИОНУКЛИДТЕРДІҢ ӨТУ ЕРЕКШЕЛІКТЕРІ

Ларионова Н.В., Лукашенко С.Н., Құндызбаева А.Е., Иванова А.Р., Келлер С.А.

ҚР ҰЯО Радиациялық қауіпсіздік және экология институты, Курчатов, Қазақстан

Бұл мақалада, "Тәжірибе даласы" алаңындағы дала өсімдіктерінде радионуклидтердің жинақталуының мөлшерлік параметрлері ұсынылған. ^{241}Am, ^{137}Cs, ^{90}Sr және $^{239+240}$Pu радионуклидтерінің жинақталу коэффициенті мәнінің диапазоны анықталды. Ядролық сынақтар өткізілген түрлі эпиорталықтардағы және өсімдіктердің жеке бір түрлеріне арналған радионуклидтердің жинақталуының анықталған айырмашылықтары анықталды. Ашық-сарғылт топырақтың физико-химиялық қасиеті және олардың өсімдіктерде радионуклидтердің жинақталуына әсері қарастырылды. Бұрынғы Семей сынақ полигонының басқа да телімдеріндегі өсімдіктердің радионуклидтерді жинақтау коэфициентімен "Тәжірибе даласындағы" далалық өсімдіктердің жинақтау коэфициентіне салыстырмалы түрде талдама жасалды.

Түйін сөздер: радиоэкология, радиоактивті ластану, радионуклидтер, ^{241}Am, ^{137}Cs, ^{90}Sr, $^{239+240}$Pu, радионуклидтерді анықтау формалары, ашық-сарғылт топырақ, топырақтың физико-химиялық қасиеті, өсімдіктер, жинақталу коэффициенті (Жк).

ОСОБЕННОСТИ ПЕРЕХОДА ИСКУССТВЕННЫХ РАДИОНУКЛИДОВ ИЗ ПОЧВЫ В РАСТЕНИЯ СТЕПНЫХ ЭКОСИСТЕМ НА ПЛОЩАДКЕ "ОПЫТНОЕ ПОЛЕ" БЫВШЕГО СИП

Ларионова Н.В., Лукашенко С.Н., Кундузбаева А.Е., Иванова А.Р., Келлер С.А.

Институт радиационной безопасности и экологии НЯЦ РК, Курчатов, Казахстан

В статье представлены количественные параметры накопления радионуклидов степными растениями на площадке "Опытное поле". Установлены диапазоны значений коэффициентов накопления радионуклидов ^{241}Am, ^{137}Cs, ^{90}Sr и $^{239+240}$Pu. Отмечены определенные различия в накоплении радионуклидов для отдельных видов растений и для разных эпицентров проведения ядерных испытаний. Рассмотрены физико-химические свойства светло-каштановых почв и их влияние на накопление радионуклидов растениями. Приведен сравнительный анализ коэффициентов накопления радионуклидов для степных растений с "Опытного поля" с коэффициентами накопления для растений с других участков бывшего Семипалатинского испытательного полигона.

Ключевые слова: радиоэкология, радиоактивное загрязнение, радионуклиды, ^{241}Am, ^{137}Cs, ^{90}Sr, $^{239+240}$Pu, формы нахождения радионуклидов, светло-каштановые почвы, физико-химические свойства почв, растения, коэффициенты накопления (Кн).

УДК 577.391:577.4:504.53:539.16

COMPARATIVE ASSESSMENT OF RADIONUCLIDES SPECIATION IN SOILS OF SOME AREAS AT STS

Kunduzbaeva A.E., Kabdyrakova A.M., Lukashenko S.N., Magasheva R.Yu.

Institute of Radiation Safety and Ecology NNC RK, Kurchatov, Kazakhstan

This paper presents the results of studies of the speciation of artificial radionuclides ^{137}Cs and ^{90}Sr, ^{241}Am and $^{239+240}$Pu in soils of different parts of the former Semipalatinsk Test Site being characterized by various levels and nature of contamination, soil type, topography and climatic conditions. Comparative analysis of the data revealed the behavior of radionuclides in soils of different parts of the STS territory. The "Experimental filed" site ("Experimental Field" site) is characterized by a low migration capacity of all the studied radionuclides ^{137}Cs, ^{241}Am, $^{239+240}$Pu, ^{90}Sr. Their main content is inaccessible form for plants. The "Degelen" site is characterized by somewhat different picture. In meadow soils with higher moisture, characteristic relief and soil conditions, radionuclides are characterized by the distinct migratory properties. A radionuclide ^{90}Sr has strong migratory abilities in soils of Degelen site, on average, more than half of the radionuclide content is in exchangeable form. Radionuclides ^{241}Am and ^{137}Cs are less mobile in the meadow soils. The behavior of radionuclides in the soils of "background" sections of the STS territory is intermediate between the behavior of soils at "Experimental filed" site and "Degelen" site. An exception is the radionuclide ^{90}Sr, characterized by greatest mobility in soils of the "northern" territories, on average, 77% of the total content of all species is accounted for easily accessible species.

Keywords: radioactivecontamination, STS, radionuclides speciation, sequential extraction, Experimental field site, Degelen site, "northern" and "western" territories.

INTRODUCTION

In order to assess a real hazard of radioactive contamination for people, it is very important to identify the mechanisms of biological accessibility of radionuclides in the environment. Soil is a primary link in the radionuclide migration along food chains, which specifies the necessity of detailed investigation of quantitative characteristics defining radionuclide mobility in soils and soil-vegetation system.

An analysis of numerous data on radionuclide behaviour in global fallouts, in soils of radioactively contaminated areas due to emissions from the Chernobyl NPP, in the Middle and South Ural – in the areas of influence of normally operating Beloyarskaya NPP and a complex of nuclear enterprises "Mayak" shows that different radionuclides have different behaviour in different soils.

Physico-chemical characteristics of radionuclides in the soil-vegetation cover change with time depending on their own properties, properties of absorbing complex, genetic structure of the soil profile and some ecological factors [1, 7, 9, 11]. The unique ecological, natural and climatic conditions of the territory of the former Semipalatinsk Test Site enable to use it as a natural laboratory for studying radionuclide behaviour in the environment. Such investigations become especially actual in the conditions of possible transfer of the studied STS territory to economic use with account for its specific features [5].

This research is a generalization of studying parameters of ^{137}Cs, ^{241}Am, ^{90}Sr and $^{239+240}Pu$ biological mobility in soils in different parts of the STS territory – soils of meadow ecosystems subjected to the impact of radioactively contaminated flows from adits, soils of steppe ecosystems subjected to the ground radioactive contamination of different types and soils with "background" radionuclide concentration.

The obtained data enable to reveal peculiarities of the behaviour of artificial radionuclides in soils in different parts of the STS territory. The results of studying forms of artificial radionuclides in soil may be used in future as a base for the development of practical recommendations on remediation, improvement of the radioecological state of the STS lands and to forecast the levels of radionuclide concentration in plants growing on different areas of the STS territory.

1. MATERIALS AND METHODS

1.1. Objects of investigations

The results presented in this paper were obtained in the long-term investigations (2008-2011) into radionuclide speciation in soils of various ecosystems on the STS territory. The studied areas were united into three groups depending on the character and level of radioactive contamination and soil-climatic conditions.

Sector I. Degelen site

The Degelen site is geographically a low mountain range called Degelen, a part of the south-east of the Kazakh folded country. The total area of the territory is 220 sq. km. At the time of nuclear tests on the STS it was used as a place for nuclear tests in horizontal excavations – adits (or tunnels). Though the main mass of the nuclear explosion products was concentrated in explosion cavities in adits, radionuclides were brought to the day surface with waters getting into the explosion cavities [2]. As the areas for investigations on the Degelen site we chose ecosystems of the near-portal areas of tunnels No.176 and No.177 with constant water flow [3–8]. It has been established that now the main sources contaminating the test grounds are water flows from the adits.

Sector II. "Experimental filed" site

The "Experimental filed" site is a plain of about 20 km in diameter surrounded by low mountains [9]. This test site is the place where ground, atmospheric and high-altitude nuclear explosions including model experiments were carried out. All in all, over 100 explosions were made. As a result of tests large areas were contaminated, both on the test ground and beyond it. The areas studied on the "Experimental filed" site are the places of nuclear tests – test sites P-1, P-2, P-3, P-5 and P-7 where ground and atmospheric tests were made. On the test site P-2G (P-7), in field conditions, the so-called model tests – hydrodynamic and hydro-nuclear experiments were made.

Sector III. Background sectors –"northern" and "western" sectors of the STS territory

The radionuclide speciation in the steppe soils of "northern" and "western" sectors of the STS territory were studied in the framework of complex radioecological investigations [10, 11]. As a result of investigations a conclusion was made that it is possible to use the territories without any limitations. Based on the accepted recommendations these areas were classified as "background" areas on the STS territory.

The radiation situation in "northern" and "western" territories is mainly formed by the following tests:

- atmospheric nuclear and model tests on "Experimental filed" site;
- tests of combat radioactive substances on the "4a" site;
- underground nuclear tests on the "Sary-Uzen" site in borehole No.1003 (also in boreholes No. 101, No, 125 for "western" areas).

1.2. Sampling

In all studied areas soil samples were taken in the places with the highest levels of radioactive contamination. The points of soil sampling were adjusted to the points of vegetation sampling taken to determine factors of radionuclides accumulation by vegetation.

On the Degelen site, the soil samples were taken in the near-portal areas of adits No. 176 and 177 along the riverbeds in the direction away from the adit portals. In 30 out of 36 research sites the soil samples were taken to a depth of 20 cm, the areas of sites were not less than 100 cm^2.

32 research sites were made on the "Experimental filed" site. The samples were taken at a depth 0-5 cm, on the area 100 cm^2, in the lots adjacent to the epicenters of tests. The total number of research lots was 12, they were located on the main five test grounds – P-1, P-2, P-3, P-5 and P-7.

In the so-called background sectors – "northern" and "western" STS territories 10 and 8 research sites were made. Sampling was made at the depth 0–3 cm on the area of 600 cm^2.

The figure (Figure 1) shows general layout of the studied areas.

1.3. Determination of speciation of radionuclides

To estimate biological accessibility of radionuclides reflecting their distribution among the elements of absorbing soil complex, the two main factors are used – aggregate of radionuclide speciation in soil and factors of radionuclide transfer (accumulation) into vegetation [12].

Among a variety of radionuclides states in the natural environments in terms of forecasting their distribution and behaviour in the environment, it is first expedient to identify water-soluble, exchangeable and non-exchangeable forms [13, 14]. Such identification is, to a considerable degree, conventional as fixation of radionuclides in soils is a consequence of different processes, and the accessibility of formed compounds for root absorption depends on physical-chemical properties of radionuclides themselves [15].

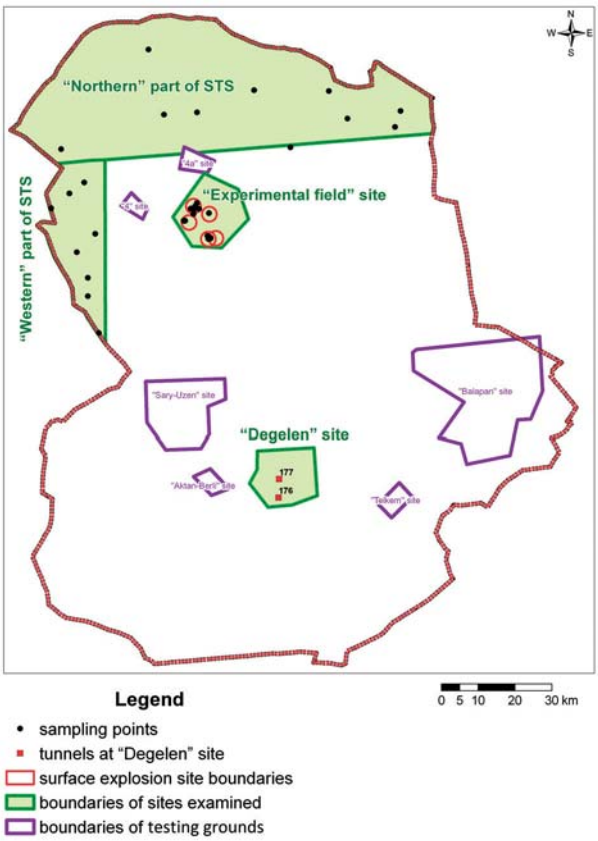

Figure 1. Layout chart of the STS studied areas

The water extract contains radionuclide cations, desorbed from soil by the mechanism of ion exchange, and complex soluble compounds of radionuclides with soil components (in neutral or active form). The concentration of radionuclide cations in the water extract is determined by the position of the ion-exchange equilibrium determined by the value of the soil volume capacity and concentration of exchange ions in solution. The main exchange ions in soil are Ca^{2+}, Mg^{2+}, Na^{+}, K^{+} и H^{+} [16].

Radionuclides sorbed in soil by the ion-exchange mechanism transfer to the ammonium acetate extract [8, 9].

The organic forms extracted by 0.1n NaOH solution contain radionuclides connected with soil organic substance. In particular, fraction I contains humic acid, fulfoacids and their salts, free or loosely bound with the soil mineral part soluble in 0.1n NaOH solution (by Tyurin) [17]. Soluble humus substances can interact with cations of heavy metals and artificial radionuclides forming humates and filvates. These reactions obey the laws of formation and behaviour of simple and complex heteropolar salts and influence migration, accumulation and inflow of toxic elements into vegetation.

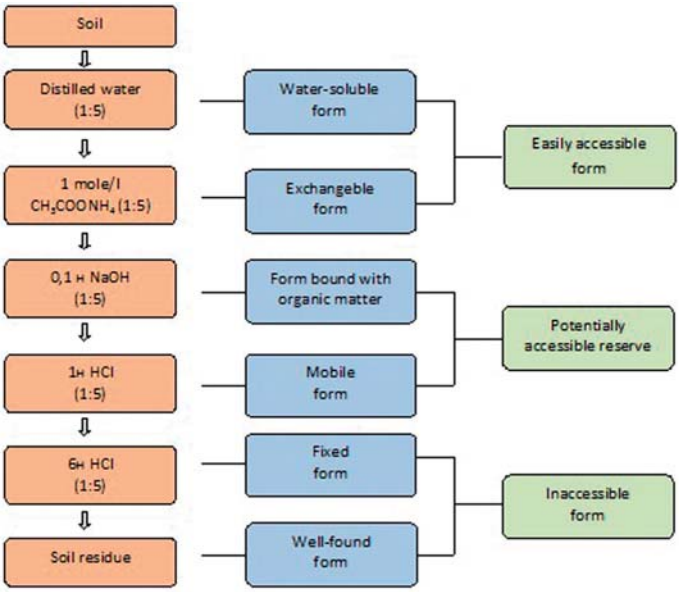

Figure 2. General scheme of step-by-step extraction

Soluble in acids compounds extracted by 0.1n NaOH solution mainly include radionuclides in the non-exchange state, i.e. forms of radionuclides which do not transfer into soil solutions in nature under normal conditions but can be absorbed by plants through roots forming so-called potentially-accessible reserve [11, 18]. Acid 6n HCl extracts contain radionuclides in the non-exchange, so-called irreversibly sorbed state inaccessible for plants.

Tightly bound forms contain radionuclides dissoluble in the above-listed reagents and inaccessible for plants.

In this research radionuclide speciation in soils were studied using step-by-step extraction, the scheme of which is shown in the figure (Figure 2).

In some cases, a reduced form of the step-by-step extraction was used. The shortest scheme was used to determine radionuclide speciation in background soils and to determine ^{241}Am and $^{239+240}$Pu in the soils of the ecosystem in the vicinity of the adit No. 177.

The water-soluble forms were extracted by distilled water (the ratio of soil to the leaching solution 1:5), the exchange forms were extracted by 1M CH_3COONH_4 (pH=6.8) (1:5). The organic forms were extracted by 0.1n NaOH. Non-exchangeable (acid-soluble) mobile and fixed forms were extracted by 1n HCl and 6n HCl, respectively. Tightly-bound forms were determined directly in the soil residues after extraction.

The time of soil contact with the leaching solution at all stages of the experiment was 12 ± 2 hours.

^{137}Cs and ^{241}Am concentration in soil samples and extracts was determined by the gamma-spectrometric analysis. The ^{90}Sr specific activity in soil samples was determined by the nondestructive method – a direct instrumental measurement of the ^{90}Sr effective specific activity on the beta-spectrometer with "Progress" software. The ^{90}Sr activity per unit of volume in the extract samples was determined by the radiochemical technique [19–23].

1.4. Characteristic of soil cover and studying of physico-chemical properties of the soils

A general characteristic of the soil cover in studied areas is given according to the published literature data [24–26]. To obtain a more detailed description soil profiles were used, and to determine the main physico-chemical characteristics of soil properties samples were taken along genetic horizons.

Physico-chemical parameters of soil samples were determined by the methods commonly accepted in soil science. The concentration of organic substance was determined using Tyurin's method modified in the Central Research Institute of Agrochemical Services of Agriculture; pH of the water extract was determined by the potentiometric method, the sum of absorbed base – by trilonometric method, concentration of water-soluble salts and carbonates – by the volumetric method, the granulometric composition – by the pipette method [27–31].

2. RESULTS AND DISCUSSION

2.1. Characteristic of the soils of studied ecosystem

2.1.1. Meadow soils of the Degelen site (adits Nos.176, 177)

In the soil-geographical context the territory of the low-mountain range Degelen is situated in the subzone of desertified steppes with zonal subtype of light-chestnut soils.

General description of the soil cover and obtained soil characteristics (Table 1) shows that soils of the two studied ecosystems of the adits No. 176 and 177 refer to meadow soils. The soils are mainly undeveloped or insufficiently developed. The soil thickness in the riverbed is not more than 40–60 cm, in the riverbank area – 20–40 cm. The soils have a rather high content of humus, especially, in the center of the riverbed, and are well washed from freely soluble salts and carbonates. pH of the water suspension on the water surface is rarely neutral, pH in the layers below the surface is often low-alkaline, more rarely – alkaline. Ca is the prevailing cation in the soil-absorbing complex. By the mechanical composition the soils in the detailed studied area of the 176-adit water-flow ecosystem are mainly light loamy and loamy sand, more rarely, middle loamy, whereas in the water-flow of the adit No. 177 middle-size and heavy clay loams prevail among loose sediments. It is caused by smaller slope of the surface and, as a rule, worse degree of drainage. All studied meadow valley soils contain a lot of fragmental material throughout the soil profile: gravel, large-sized sand and large-sized dust. It should be noted that in meadow soils of the adit-176 ecosystem the concentration of iliginous particles is within 0.1–11%, and in the soils of the ecosystem of the adit No. 177 with worse drainage, the silt content is as high as 19–31%. Therefore, the decrease in the area slope and, hence, the decrease in the flow rate causes natural changes in the degree of drainage – the number of thin particles increases, freely soluble salts accumulate in the surface aquifers and the amount of thin humus increases [32].

2.1.2. Soils of the "Experimental Field" site

Based on the field and laboratory investigations (Table 1) one can state that the soil cover is practically the same in the area. Studied soils refer to light loamy and loam clay soils. All soils are carbonate, boiling is registered both on the surface and in the lower part of the humus horizon. At a depth of about 100 cm all studied areas have crumbly, loamy-sand dust horizon. At the moment of investigations the soil was fresh, but at big depths and in spring it may be water-saturated. If the surface has a slope to the north, it may serve as a drainage system for the area, but probably the system is poor, otherwise, soils at a distance of 1m from the surface would not be carbonate.

Soils of the studied area are low-alkaline or alkaline on the surface with pH ranging from 7.0 to 8.4. Below the surface the soil alkalinity increases to 7.9–8.8. Humus content is usually within 2–3%, but in some places the values increase up to 5%. In surface horizons the sum of freely-soluble salts is less than 0.1%, which enables to refer them to not saline soils. However, with depth salinity increases, and the sum of salts goes up to 0.5%. Among absorbed bases, the absolute dominance of Ca over Mg is observed.

2.1.3. Soils of "northern" and "western" territories

The studied "western" territory is a rather narrow stripe (about 80 km) stretching to a distance of about 230 km along the meridian. The "northern" STS territory occupies north-eastern part of Kazakh hilly system and part of the pre-hill valley formed by the delluvial-alluvial tail. Zonal soils of background territories are chestnut soils under different types of dry steppes. Most part of the territory is covered by zonal poorly-developed and undeveloped chestnut soils. They are located on the slopes of hills formed by dense basement rocks. Soil-forming structures are thin alluvial-delluvial rubbly loamy clays with underlying marl or poorly weathered rocks. The thickness of the melkozem layer gradually increases from hill tops to the bottom accompanied by the increase in the degree of fracturing of the fractured material in soils.

The area also has meadow-chestnut and meadow soils in combination with solonetzic and brackish soils, solonetzs and solonchaks developed in the centers of depressions.

As a whole, the soil cover of the studied areas is characterized by low thickness of loose sediments and small content of organic substance.

The main morphological characteristics of poorly-developed and undeveloped soils, widely spread on the studied areas, are low thickness of humus horizon (15–25 cm) and loose layer (up to 40–60 cm), whereas thickness of humus horizon in ordinary chestnut soils is 15–40 cm. The ordinary soils, i.e. soils with fully developed profile, are rarely registered in the studied area, mainly in the delluvial-alluvial tail surrounding the hilly system in the north and northeast and in the low parts of hill slopes. The absence of carbonate horizon with close underlying of dense rocks and rubbly soils is registered throughout the profile. According to the mechanical composition the prevailing soils are freely-loamy and middle-loamy soils. The most widely spread soils are soils with middle humus content (2.5-3.5 % of humus). The chestnut soils have an average content of mobile forms of nitrogen and potassium and very low content of mobile phosphorous. The reaction of soil solution is close to neutral. As a rule, soils are not saline, occupy hypsometrically high position, are well drained and, therefore, are washed from freely-soluble salts and often from carbonates.

Table 1.

Physical-chemical properties of the studied soils

Soil characteristics	adit № 176	adit № 177	"Experimental Field" site	"North"	"West"
Concentration of organics, C, %	14.0 7.1 ÷ 23.0	16 11 ÷ 21	1.7	Not determ.	Not determ.
pH of water suspension (actual acidity)	7.5 6.8 ÷ 7.9	7.5 7.1 ÷ 7.9	7.9 7.0 ÷ 8.8	Not determ.	Not determ.
Total salts, %	0.045 0.02 ÷ 0.27	0.2 0.05 ÷ 0.6	0.13 0.04 ÷ 0.62	Not determ.	Not determ.
Total of exchange bases, mg-eqv/100g	27 17.0 ÷ 40.4	41 28 ÷ 52	14.7 6.0 ÷ 79.2	Not determ.	Not determ.
carbonates, %	-	-	1.3 0.1 ÷ 5.0	Not determ.	Not determ.
Granulometric composition					
Physical clay content (soil particles of <0.01 mm), % including:	23.0 15.0 ÷ 37.1	42.0 32 ÷ 59.0	27.5 67.6 ÷ 40.4	Not determ.	Not determ.
oozy particles (<0.001 mm), %	5.3 0.13 ÷ 10.8	24 19 ÷ 31.1	17.7 40.9 ÷ 23.8	Not determ.	Not determ.
fine dust (0.001-0.005 mm), %	9.1 0.2 ÷ 17.1	9.4 3.4 ÷ 25.0	9.2 0.53 ÷ 23.9	Not determ.	Not determ.
medium dust (0.005-0.01 mm), %	8.6 3.3 ÷ 13.8	9.4 3.2 ÷ 15.4	8.2 0.29 ÷ 17.3	Not determ.	Not determ.
large dust (0.01-0.05 mm), %	29 12.6 ÷ 41.0	35.0 3.2 ÷ 48.4	12.1 2.9 ÷ 22.4	Not determ.	Not determ.
^{137}Cs specific activity in soil, Bq/kg	27 371 26.0 ÷ 452 020	1 900 16 ÷ 8700	2 851 340 ÷ 9 000	26.1 13.5 ÷ 50.2	33.7 8.3 ÷ 52.1
^{90}Sr specific activity in soil, Bq/kg	11 874 610 ÷ 33050	72 000 1700 ÷ 117000	4 200 560 ÷ 29000	13.8 4.9 ÷ 76.5	7.0 1.0 ÷16.0
^{241}Am specific activity in soil, Bq/kg	Not determ.	400 200 ÷ 700	8 740 700-101 600	15.0 0.9 ÷ 2.5	3.7 0.3 ÷ 11.6
$^{239+240}$Pu specific activity in soil, Bq/kg	Not determ.	6 300 3 000 ÷ 12 000	67980 900 ÷ 1 300 000	7.4 1.1 ÷ 20.2	26.9 1.2 ÷ 101.0
(Average values are given over the line and the range of values is given below the line)					

Therefore, the soils most widely spread on the STS territory are zonal chestnut soils with subtype of poorly-developed and undeveloped chestnut and light-chestnut soils. They have many inclusions / chips. According to the mechanical composition, the prevailing soils are freely-loamy and middle-sized loamy differences. The soils are mainly well washed from freely-soluble salts and carbonates. pH of soil extracts of the arid zone ("northern" and "western" areas, "Experimental Field" site) are neutral on the surface and low-alkaline and alkaline below the surface. In meadow soils with additional moistening (Degelen site) pH increases to

low-alkaline and alkaline. According to the concentration of organic substances the soils of the "Experimental Field" site, "northern" and "western" areas have middle content of humus (on average, 2–3%), the meadow soils have rather high humus content, up to 21–23%.

2.2. Speciation of radionuclides in the STS soils

2.1.1. Speciation of radionuclides in the soils of the "Experimental Field" site

A special attention must be paid to the results of studying radionuclide speciation in the soils of the "Experimental Field" site, characterized by a unique structure of the radioactive contamination formed by atmospheric, ground and model tests on the territory.

The table (Table 2) shows the results of studying forms of radionuclides in the soils of the "Experimental Field" site.

Table 2.

Radionuclide speciation in the soils of the "Experimental Field" site, in percentage of the total concentration

Speciation	^{137}Cs, % (n=18)	^{241}Am, % (n=17)	^{90}Sr, % (n=24)	$^{239+240}$Pu, % (n=9)
water-soluble	< 0.4	< 1.3	< 0.07	< 0.02
exchange	< 0.7	< 1.2	< 1.4	< 0.02
organic	< 0.4	< 1.6	< 0.06	0.4
mobile	< 0.6	14.0	3.1	3.2
fixed	97.9	81.9	95.4	96.3
tightly bound				

As in most cases quantitative results were not obtained (values below the detection limit of the method of investigations), the table gives estimations of speciation for the studied radionuclides in percentage of the total concentration.

For ^{137}Cs, a typical picture for this radionuclide picture is observed – the main part of the radionuclide (97.9%) is in the tightly-bound form. The concentration of water-soluble, exchange, organic and mobile forms is usually below the detection limit of the applied technique. The prevailing amount of ^{241}Am (81.9%) is presented by the inaccessible forms (fixed and tightly-bound). Almost 14% of all forms of ^{241}Am refer to mobile forms presenting a potentially accessible reserve for vegetation. The easily-accessible forms of the radionuclide make not more than 1.2-1.3%. The lowest migration properties in the soils of the "Experimental Field" site have isotopes of $^{239+240}$Pu. The concentration of easily-accessible forms (water-soluble and exchange) of the radionuclide does not exceed 0.02% of the total concentration. The total concentration of fixed and tightly-bound forms of the radionuclide is, on average, 96.3%. The radionuclide ^{90}Sr, having the best mobile properties, is in the inaccessible form (95.4%) in the soils of the "Experimental Field" site like radionuclides ^{137}Cs, ^{241}Am and $^{239+240}$Pu. A small amount of the radionuclide, on average 3.1%, was registered in the mobile form. The concentration of water-soluble, exchange and organic forms is below the detection limit of the applied technique.

2.2.2. A comparative estimation of the radionuclide forms in the STS soils

To understand the general picture of studied radionuclides forms in soils in different parts of the STS we carried out a comparative analysis of the parameters of biological accessibility of radionuclides in the soils of the studied areas. The generalized data are presented in the tables (Table 3 – Table 6).

Table 3.

Contents of the ^{137}Cs radionuclide forms in soils of all studied areas, % of the total content

Area	Speciation					
	water-soluble	exchange	organic	mobile	fixed	tightly bound
adit № 176 (n=36)	< 0.5	6.8	-	4.5	26,0	62,2
adit № 177 (n=12)	< 0.2	<0.4	1.2	4.0	3,4	90,8
"Exp.Field" (n=18)	< 0.4	< 0.7	< 0.4	< 0.6	97,9	
"N" (n=10)	< 18.0		-	< 13.0	68.0	
"W" (n=8)	< 16.4		-	< 13.9	69.7	

The behaviour of ^{137}Cs radionuclide is different for different types of soils. The highest biological stability of ^{137}Cs was registered in the soils of the "Experimental Field" site where the concentration of non-exchangeable forms was, on average, 97.9%. In the soils of ecosystems around the adits No.176 and 177 the concentration of inaccessible forms was lower, about 86% - 91%. Here, higher values of radionuclide exchange (up to 6.8%) and organic (4.0-4.5%) forms were registered. A different behaviour of ^{137}Cs in the soils of the "background" areas is clearly seen – the concentration of accessible forms (water-soluble, exchange, mobile) increases with the corresponding decrease in the tightly-bound forms to, on average, 68-70%. It is known that the radionuclide ^{137}Cs is mainly concentrated in the mineral part of the soil-absorbing complex, which plays an important role in its mobility in soil and transfer into vegetation [33]. An important role in this difference may be played by the difference in the mineralogical composition of soils of the "background" areas, which are not studied yet. It is also necessary to note possible influence of soil moistening around waterways from adits No. 176 and 177 on the ^{137}Cs behaviour. It is difficult to make an unambiguous conclusion about the character of ^{137}Cs behaviour in soils with background levels as they require additional investigations with usage of more sensitive techniques.

Contents of ^{241}Am speciation are given in the table (Table 4).

Table 4.

Contents of the radionuclide ^{241}Am speciation in soils of all studied areas, % of the total content

Area	Speciation					
	water-soluble	exchange	organic	mobile	fixed	tightly bound
adit № 176 (n=36)	-	-	-	-	-	-
adit № 177 (n=12)	3.0		2.0	76.0	19.0	
"Exp.Field" (n=17)	< 1.3	< 1.2	< 1.6	14.0	81,9	
"N" (n=10)	< 17.6		-	58.2	< 24.2	
"W" (n=8)	≤ 30.8%		-	≤ 57.7%	≤ 11.5%	

Comparing contents of different forms of the radionuclide ^{241}Am in soils of different studied areas, one can make a conclusion that in the soils of the "Experimental Field" site the radionuclide has the lowest biological accessibility. The content of forms inaccessible to plants (fixed and tightly-bound) is as high as 81.9%. As it is mentioned before, in the soils of the "Experimental Field" site radionuclide ^{241}Am has the highest migration ability of all studied radionuclides. The ratios of ^{241}Am forms in the soils of the Degelen site and "background" areas confirm its migration properties. The highest mobility of radionuclide ^{241}Am was registered in meadow soils of the ecosystem around the adit No.177, where the content of easily-accessible forms went up to 5% and content of mobile forms was as high as 76%. Only 19% of the total amount of the radionuclide refers to the tightly-bound form. It may be a result of soil moistening in the studied area, the factor that has the strongest influence on the migration properties of radionuclides. Content of mobile forms of radionuclide ^{241}Am in the soils of "background" areas do not differ considerably from those for the soils of adit No.177 going up to 58%. Contents of radionuclide exchange forms in the soils of "northern" and "western" territories is rather high, reaching by estimations 18% and 31%, respectively. The fraction of tightly-bound and fixed forms does not exceed, 24% and 12%, respectively. It is necessary to carry out more detailed investigations of ^{241}Am forms in the soils of "background" areas, though the available data correctly show migration properties of the radionuclide.

Table 5.

Contents of the radionuclide ^{90}Sr speciation in soils of all studied areas, % of the total content

Area	Speciation					
	water-soluble	exchange	organic	mobile	fixed	tightly bound
adit № 176 (n=36)	1.1	53.4	-	35.2	6,4	3,9
adit № 177 (n=12)	53.00		1.8	33.1	8.2	3,9
"Exp.Field" (n=24)	< 0.07	< 1.4	< 0.06	3.1	95,4	
"N" (n=10)	77.1		-	≤ 20.0	≤ 2.9	
"W" (n=8)	48.8		-	38.9	12.3	

The prevailing Speciation of the radionuclide ^{90}Sr in the soils of all studied areas is the exchange form. The only exception is the soils of the "Experimental Field" site where ^{90}Sr is, mainly, in the inaccessible form making 95.4% of the total amount of all forms. A considerably less populated is a mobile form which is, on average, not higher than 3.1%. The content of water-soluble, exchange and organic forms is in most cases below the detection limit of the applied technique. The content of ^{90}Sr radionuclide in meadow soils of the mountain range Degelen does not show any peculiarities. In the soils of adits No. 176 and 177, on average, 53% of the ^{90}Sr total content is in the freely-soluble form (water-soluble and exchange). 33%–35% of ^{90}Sr radionuclide is in the mobile form, which makes a potential reserve for vegetation. Only 10%–12% of the total content of all radionuclide forms refers to forms inaccessible for vegetation. The earlier published data show a weak correlation between the properties of the Degelen site soils and radionuclide mobility. In particular, they detected a little influence of the soil mechanical composition (content of silt particles and physical clay) and reverse influence of the concentration of exchange bases on the content of fixed and tightly-bound radionuclide forms.

The ratios of ^{90}Sr forms in the soils of "western" territories practically do not differ from those for meadow soils.

The highest content of easily-accessible forms of the radionuclide ^{90}Sr registered in the soils of "northern" territories may be caused by the fallout of tests of combat radioactive substances on the "4a" site, which made a considerable contribution to the radioactive contamination of the area.

Table 6.

Content of the radionuclide $^{239+240}$Pu speciation in soils of all studied areas, % of the total content

Area	Speciation					
	water-soluble	**exchange**	organic	**mobile**	**fixed**	**tightly bound**
adit № 176 (n=36)	-	-	-	-	-	-
adit № 177 (n=12)	1.0		4.0	2.0	93.0	
"Exp.Field" (n=9)	< 0.01	< 0.01	0.3	1.0	98,7	
"N" (n=10)	< 1.3		-	≤ 3.8	94.9	
"W" (n=8)	≤ 3.0		-	≤ 2.6	94.3	

The highest degree of similarity in the behaviour of soils of studied areas has been registered for the radionuclide $^{239+240}$Pu. The ratios of the radionuclide speciation in the soils of the ecosystems in vicinity of the adit No.177, the "Experimental Field" site and "background" territories show that the main amount of the radionuclide is in the forms inaccessible for vegetation (fixed and tightly-bound). Maximal content of inaccessible forms is registered in the soils of the "Experimental Field" site, where it, on average, is as high as 98.7%. The content of inaccessible $^{239+240}$Pu forms in the soils of the Degelen site and background areas is practically the same, 93–95%, with observed increase in the number of radionuclide mobile forms. In the soils adjacent to the adit No.177 the content of easily-accessible forms is as high as 5%, organic forms – 2%.

A comparative analysis of the complex data enables to reveal specific features of radionuclides behaviour in different parts of the STS territory. For the "Experimental Field" site we obtained the results which enable to make a conclusion that in the soils of this test ground all studied radionuclides ^{137}Cs, ^{241}Am, $^{239+240}$Pu and ^{90}Sr are in relatively stable forms, which provide their little migration. The test ground Degelen has a somewhat different picture. In meadow soils with higher moistening, typical relief and soil conditions, the radionuclides have the highest, as compared with other areas, migration rate. The highest mobility in the soils of the Degelen site has ^{90}Sr as, on average, more than 50% of the radionuclide is in the exchange form. Radionuclides ^{241}Am and ^{137}Cs are less mobile in meadow soils. The behaviour of radionuclides in the soils of "background" areas of the STS territory can be classified as ‘intermediate" between the behaviour in the soils of the "Experimental Field" and "Degelen" sites. The only exception is radionuclide ^{90}Sr having the highest mobility in the soils of "northern" territories – on average, 77% of the total content of all forms refer to easily-accessible forms.

It should be noted that $^{239+240}$Pu has the same behaviour in all types of soils. The percentage of inaccessible to vegetation forms of this radionuclide in the meadow soils with high moistening, in the soils of "background" territories and in the soils of the "Experimental Field" site is not lower than 93%. The radionuclide ^{137}Cs in the soils of the studied STS areas prevails in the tightly-bound form. On the contrary, radionuclide ^{90}Sr has the highest mobility except for the soils of the "Experimental Field" site. The radionuclide ^{241}Am has lower mobility, mobile forms of the radionuclide present in soil are inaccessible for vegetation, though form a potentially accessible reserve except for the "Experimental Field" site.

CONCLUSION

The results of our investigations show that different parts of the STS territory have different ratios of radionuclide speciation depending on the types of tests, soil and climatic conditions and physical-chemical properties of the radionuclides.

Minimal radionuclide mobility was registered in the soils of the "Experimental Field" site, which is mainly caused by the type of nuclear explosions made on this test ground.

On the contrary, maximal radionuclide mobility was registered in the soils of the near-portal areas of the adits of the Degelen mountain ridge.

Soils with background levels of radionuclide concentrations require additional investigations with more sensitive techniques and methods.

$^{239+240}$Pu radionuclides have the same behaviour and the least biological accessibility in soils of all studied areas. The percentage of inaccessible to vegetation forms of this radionuclide in the meadow soils with high moistening, in the soils of "background" territories and in the places where ground and atmospheric tests were made is not less than 93%.

A relatively high mobility of the transuranic radionuclide ^{241}Am was detected, even in soils of the "Experimental Field" site, where this radionuclide had minimal mobility, the percentage of mobile forms was not less than 18%.

The radionuclide ^{90}Sr demonstrates clearly pronounced migration properties in all soils except for the soils of the "Experimental Field" site.

By the present time we have revealed the speciation of the radionuclides in the soils of the main STS sites – "Degelen" and "Experimental Field" sites, background "northern" and "western" territories. Investigations of the other STS sites (sites for tests of combat radioactive substances, excavation explosions, underground explosions in boreholes, etc.) planned for future will contribute to our understanding of the radionuclide behaviour in the soils of the STS territory.

The authors express gratitude to the specialists of the Institute of Radiation Safety A.V. Panitskiy, N.V. Larionova, S.A. Keller for their help in organizing and carrying out of field works, O.I. Cheredov, M.V. Sidorova, P.V. Govenko for making spectromentic analyses, S.E. Salmenbayev, G.I. Dosmambetova, N.A. Mikhailova, A.E. Zhienbekova, D.E. Iminova, G.D. Kubenov and Zh.E. Zhapasheva for making radiochemical analyses. The authors are especially grateful to G.A. Bakirova and T.N. Bayserkenova for their invaluable contribution to scientific research.

REFERENCES

1. Михайловская Л.Н. Физико-химическое состояние радионуклидов в почвах зон влияния предприятий ядерного топливного цикла. / Л.Н. Михайловская, И.В. Молчанова, Е.Н. Караваева // Агрохимия. – 2004. – вып. №7. – С. 67-71.
   Mikhailovskaya L.N. Physico-chemical conditions of the radionuclides in soils of the nuclear fuel cycle facilities influence zones. /Mikhailovskaya L.N., Molchanova I.V., Karavayeva Ye.N. // Agrochemistry. – 2004. Issue #7. – pp.67-71.
2. Особенности состава, форм нахождения и распределения радионуклидов на различных участках СИП / К.К. Кадыржанов [и др.] // Вестник НЯЦ РК. – 2000. – вып. 3. – С. 15-21.
   Peculiarities of composition, speciation and distribution of the radionuclides at various sites of STS / Kadyrzhanov K.K. et.al.// INP NNC RK Bulletin. – 2000. Issue #3.- pp.15-21.
3. Кабдыракова А.М. Формы нахождения радионуклидов в луговых почвах штольни № 176 площадки "Дегелен". / А.М. Кабдыракова [и др.] // Вестник НЯЦ РК – вып. № 2. – С. 136-142.
   Kabdyrakova A.M. Radionuclide speciation in meadow soils at the adit #176 of Degelen TEST SITE./ Kabdyrakova A.M. et.al. // INP NNC RK Bulletin. Issue #2.- pp.136-142.
4. Кабдыракова А.М. Формы нахождения техногенных радионуклидов в луговых почвах площадки " Дегелен". / А.М. Кабдыракова, С.Н. Лукашенко, Н.В. Ларионова // Материалы III Международной конференции "Семипалатинский испытательный полигон. Радиационное наследие и проблемы нераспространения" 6-8октября 2008 г. – Курчатов – 2008г. – С. 39-39.
   Kabdyrakova A.M. Artificial radionuclides speciation in meadow soils at Degelen TEST SITE./ Kabdyrakova A.M., Lukashenko S.N., Larionova N.V. // Proc. of III International Conf. "Semipalatinsk Test Site. Radiation Heritage and Nonproliferation Issues". Kurchatov 2008. – p.39.
5. Кабдыракова А.М. Формы нахождения техногенных радионуклидов в луговых почвах экосистемы штольни с водотоком на площадке "Дегелен". / А.М. Кабдыракова [и др.] // Материалы 7-й Международной конференции "Ядерная и радиационная физика" 8-11 сентября 2009 г. – Алматы – 2009г. – С. 203.
   Kabdyrakova A.M. Artificial radionuclides speciation in meadow soils of the adit #176 watercourse ecosystem at Degelen TEST SITE./ Kabdyrakova A.M. et.al. // Proc. of VII International Conf. "Nuclear and Radiation Physics". Almaty 2009. – p.203.
6. Кабдыракова А.М.Формы нахождения радионуклидов в почвах экосистем водотоков горного массива Дегелен. / А.М Кабдыракова, А.Е. Кундузбаева., С.Н.Лукашенко // Сборник трудов Института радиационной безопасности и экологии за 2007-2009 гг / под рук. Лукашенко С.Н.- вып. 2. - Павлодар : Дом печати, 2010. –527 с.

7. *Kabdyrakova A.M.* Radionuclides speciation in soils of the adit #176 watercourse ecosystem at Degelen mountain range./ Kabdyrakova A.M., Kunduzbaeva A.Ye., Lukashenko S.N. // Proc. of IRSE for 2007-2009. /ed.by Lukashenko S.N. – Issue #2. Pavlodar: Dom Pechati, 2010. – 527 pp.
Kabdyrakova A.M. / Radionuclides species in soils of the watercourse ecosystem at Degelen mountain of former Semipalatinsk Test Site/ / A.M. Kabdyrakova, A.E. Kunduzbaeva, S.N. Lukashenko // Book of abstracts "Environmental radioactivity", Rome 25th – 27th October, 2010y. – Rome – 2010 y.
8. Кабдыракова А.М.. Формы нахождения радионуклидов в почвах экосистем водотоков горного массива Дегелен. / А.М Кабдыракова, А.Е. Кундузбаева., С.Н.Лукашенко // Тезисы докладов IV Международной научно-практической конференции "Семипалатинский испытательный полигон. Радиационное наследие и перспективы развития" 25-27 августа, 2010г. – Курчатов – 2010г. – С. 67-69.
Kabdyrakova A.M. Radionuclides speciation in soils of the watercourse ecosystem at Degelen mountain range./ Kabdyrakova A.M., Kunduzbaeva A/Ye., Lukashenko S.N. // Abstracts of IV International Conf. "Semipalatinsk Test Site. Radiation Heritage and Nonproliferation Issues". Kurchatov 2010. – p.67-69.
9. Артемьев О.И. Радионуклидное загрязнение территории бывшего Семипалатинского испытательного ядерного полигона / О.И. Артемьев, М.А. Ахметов, Л.Д. Птицкая // Вестник НЯЦ РК. – 2001. – вып. № 3. – С. 12–18.
Artemiev O.I. Radionuclide contamination of territory of former Semipalatinsk Nuclear Test Site. / Artemiev O.I., Akhmetov M.A., Ptitskaya L.D. // INP NNC RK Bulletin – 2001. Issue 3. – pp.12-18.
10. Актуальные вопросы радиоэкологии Казахстана [Радиоэкологическое состояние "северной" части территории Семипалатинского испытательного полигона] / под рук. Лукашенко С.Н.- вып. 1. - Павлодар: Дом печати, 2010. – 234 с.
Topical Issues in Radioecology of Kazakhstan [Radioecological conditions of "northern" part of the Semipalatinsk Test Site] // ed.by. Lukashenko S.N. Issue 1. Pavlodar: Dom Pechati, 2010. – 234pp.
11. Материалы комплексного радиоэкологического обследования "западной" части территории СИП, выполненного в рамках мероприятия / ИРБЭ НЯЦ РК; отв. исп. Лукашенко С.Н. – Курчатов, 2011. – 197 с.
Materials of complex radioecological surveying of the "western" part of STS territory. / IRSE NNC RK; resp.executor Lukashenko S.N. – Kurchatov, 2011. – 197 pp.
12. Санжарова Н.И. Формы нахождения в почвах и динамика накопления ^{137}Cs в сельскохозяйственных культурах после аварии на чернобыльской АЭС. / Н.И. Санжарова [и др.] // Почвоведение – 1997. – вып.№ 2. – С. 159-164.
Sanzharova N.I. Speciation in soils and accumulation dynamics of ^{137}Cs in agricultural products after the Chernobyl NPP accident. / Sanzharova N.I. et.al.// Pochvovedeniye – 1997. – issue 2. – pp.159-164.

13. Коноплев А.В. Динамика вымывания долгоживущих радионуклидов, выпавших в результате аварии на ЧАЭС, из почвы поверхностным стоком / А.В. Коноплев [и др.] // Метеорология и гидрогеология – 1990. – вып. №; 12. – С. 63-74.
Konoplev A.V. Dynamics of washing-out of long-living radionuclides fallouted due to Chernobyl NPP accident (soils with surface drainage). / Konoplev A.V. et.al.//Meteorologiya I gydrogeologiya – 1990. Issue 12. – pp.63-74.
14. Павлоцкая Ф.И. Миграция радиоактивных продуктов глобальных выпадений в почвах. / Ф.И. Павлоцкая. – М. : Атомиздат, 1974. – 215 с.
Pavlotskaya F.I. Migration of radioactive products of global fallouts in soils. / Pavlotskaya F.I. – M.:Atomizdat, 1974. – 215 pp.
15. Котова А.Ю., Санжарова Н.И. Поведение некоторых радионуклидов в различных почвах. / А.Ю. Котова, Н.И. Санжарова // Почвоведение – 2002. – вып. № 1. – С. 108-120.
Kotova A.Yu., Sanzharova N.I. Behaviour of various radionuclides in various soils. // Pochvovedeniye – 2002. Issue 1.- pp.108-120.
16. Бобовникова Ц.И. Химические формы нахождения долгоживущих радионуклидов и их трансформация в почвах зоны аварии на ЧАЭС. / Ц.И. Бобовникова [и др.] // Почвоведение – 1990. – вып. № 10. – С. 20-26.
Bobrovlnikova C.I. Chemical speciation of long-living radionuclides and their transformation in soils subjected to the accident at ChNPP.// Pochvovedeniye – 1990. – Issue 10. – pp.20-26.
17. Орлов Д.С. Практикум по биохимии гумуса / Д.С. Орлов, Л.А.Гришина, Н.Л. Ерошинева. - М.: Изд-во Московского Университета, 1969. - 160с.
Orlov D.S. Practice works on humus biochemistry / Orlov D.S., Grishina L.A., Yeroshineva N.L. – M.: Moscow University, 1969. – 160pp.
18. Мартюшов В.В. Состояние радионуклидов в почвах Восточно-Уральского радиоактивного следа. / В.В. Мартюшов [и др.] // Экология – 1995. – вып. № 2. – С. 110-113.
Martiushov V.V. State of radionuclides in soils of East-Urals radioactive trace.// Ecology – 1995. Issue 2. – pp.110-113.
19. МИ 5.06.001.98 РК "Активность радионуклидов в объемных образцах. Методика выполнения измерений на гамма-спектрометре МИ 2143-91". – 18 с.
MI 5.06.001.98 RK "Activity of radionuclides in volumetric samples. The method for measurements at the gamma-spectrometer MI 2143-91. – 18pp.
20. Методика измерения активности радионуклидов с использованием сцинтилляционного бета-спектрометра с программным обеспечением "Прогресс",Менделеево. – 20 с.
The method for radionuclides activity measurements with scintillation beta-spectrometer with *Progress* software. Mendeleevo. – 20 pp.
21. Методика определения изотопов плутония-(239+240), стронция-90, америция-241 в объектах окружающей среды: МИ 06-7-98. – Алматы, 1998.
The method for determination of isotopes Pu-(239+240), Sr-90, Am-241 in environmental samples: MI 06-7-98. – Almaty, 1998.

22. Инструкция и методические указания по оценке радиационной обстановки на загрязненной территории. Госкомгидромет СССР. – М., 1989.
The Instruction and methodic aid for assessment of radiation conditions at contaminated lands. Goskomhydromet USSR. – M., 1989.
23. Методика выполнения измерений активности радионуклидов плутоний-238, плутоний-239+плутоний-240 в счетных образцах, приготовленных из проб объектов окружающей среды. Разработана ФГУП НПО Радиевый Институт им. В.Г.Хлопина.
The method for activity measurements for the radionuclides Pu-238, Pu-239+240 in environmental samples. Develped by FSUE SPC V.G. Khlopin Radievyi Institute.
24. Почвы Казахской ССР. Павлодарская область. – Вып.3. – Алма-Ата: Наук, 1960. – 265 с.
Soils of Kazakh SSR. Karaganda oblast. – issue 3. – Alma-Ata: Nauka, 1960. – 265pp.
25. Почвы Казахской ССР. Карагандинская область. – Вып.8. – Алма-Ата: Наук, 1967. – 330 с.
Soils of Kazakh SSR. Karaganda oblast. – issue 8. – Alma-Ata: Nauka, 1967. – 330pp.
26. Почвы Казахской ССР. Семипалатинская область. – Вып.10. – Алма-Ата: Наук, 1968. –474 с.
Soils of Kazakh SSR. Karaganda oblast. – issue 10. – Alma-Ata: Nauka, 1968. – 474pp.
27. ГОСТ 12536-79. Грунты. Методы лабораторного определения гранулометрического (зернового) состава и микроагрегатного состава. - Взамен ГОСТ 12536-67; введен 1980-07-01. - М.: Изд-во стандартов, 1979. -13 с.
State Standard GOST 12536-79. Soils. The methods for laboratory determination of granulometric (grain) composition and microcomposition. Replacement of the GOST 12536-67; from 1980-07-01. – M.:Standards, 1979. – 13 pp.
28. ГОСТ 17.5.4.01-84. Методы определения pH водной вытяжки вскрышных и вмешающих пород. –Введ. 1985-07-01. - М.: Изд-во стандартов, 1985. – 3 с.
State Standard GOST 17.5.4.01-84. The methods for determination of pH in water extracts of stripping and bulk rocks. from 1985-07-01. – M.:Standards, 1985. – 3 pp.
29. ГОСТ 26213-91. Почвы. Методы определения органического вещества. - Взамен ГОСТ 26213-84; введен 1991-12-29. - М.: Изд-во стандартов, 1992. – 6 с.
State Standard GOST 26213-91. Soils. The methods for determination of organic substance. Replacement of the GOST 26213-84; from 1991-12-29. – M.:Standards, 1992. – 6 pp.
30. ГОСТ 26423-85. – ГОСТ 26428-85. Почвы. Методы определения катионно - анионного состава водной вытяжки. –Введ. 1985-02-18. - М.: Изд-во стандартов, 1985. – 10 с.

State Standard GOST 26423-85. Soils. The methods for determination of cation-anion composition of water extracts; from 1985-02-18. – M.:Standards, 1985. – 10 pp.

31. Сборник методических указаний по лабораторным исследованиям почв и растительности Республики Казахстан / под рук. ДюсенбековаЗ.Д.; Государственный научно-производственный центр земельных ресурсов и землеустройства. - Алматы, 1998. – 226 с.
A set of methodical aids for laboratory investigation of soils and vegetation of the Republic of Kazakhstan / ed.by Dysenbekov Z.D.; State Scientific and production Center for Land Resources and Land Management. – Almaty, 1998. – 226 pp.
32. Паницкий А.В. Характерные особенности радиоактивного загрязнения компонентов природной среды экосистем водотоков штолен горного массива Дегелен / А.В. Паницкий [и др.] // Сборник трудов Института радиационной безопасности и экологии за 2007-2009 гг / под рук. Лукашенко С.Н.- вып. 2. - Павлодар : Дом печати, 2010. –527 с.
Panitskiy A.V. Peculiarities of radioactive contamination of the components of natural environment in the ecosystems of waterflows from adits in the mountain range Degelen / Panitskiy A.V. et.al.// Proc. of IRSE for 2007-2009 /Ed.by Lukashenko S.N. – Issue #2. Pavlodar: Dom Pechati printing house, 2010. -527 pp.
33. Тихомиров Ф.А. Долгоживущие радионуклиды иода, цезия и углерода в системе атмосфера-почва-растения. / Ф.А. Тихомиров, И.Т. Моисеев // Агрохимия – 1987. – вып. № 2. – С. 79-85.
Tihomirov F.A. Long-living radionuclides of iodine, cesium, and carbonin the system atmosphere-soil-plants.// Tihomirov F.A., Moiseyev I.T. //Agrochemistry – 1987. Issue #2, pp.79-85. - [in Russian]

ССП АУМАҒЫНДАҒЫ КЕЙБІР ТЕЛІМДЕРДІҢ ТОПЫРАҒЫНАН РАДИОНУКЛИДТЕРДІ АНЫҚТАУ ФОРМАСЫН САЛЫСТЫРМАЛЫ ТҮРДЕ БАҒАЛАУ

Құндызбаева А.Е., Қабдырақова А.М., Лукашенко С.Н., Магашева Р.Ю.

ҚР ҰЯО Радиациялық қауіпсіздік және экология институты, Қазақстан, Курчатов қ.

Бұл мақалада, радиоактивті ластанудың түрлі сипатымен және деңгейлерімен, топырақтың түрлерімен, рельефімен және климаттық жағдайларымен сипатталатын, бұрыңғы Семей сынақ полигоны аумағының түрлі телімдеріндегі топырақтан ^{137}Cs және ^{90}Sr, ^{241}Am және $^{239+240}$Pu техногенді радионуклидтерін анықтау формасына жасалған зерттеулердің нәтижелері келтірілген. Алынған деректерге салыстырмалы түрде талдамалау жасауда ССП аумағының түрлі телімдеріндегі топырақта радионуклидтердің қозғалысының ерекшеліктерін анықтауға мүмкіндік берді. "Тәжірибе даласы" алаңы үшін ^{137}Cs, ^{241}Am, $^{239+240}$Pu, ^{90}Sr зерттелген барлық радионуклидтерінің жылыстауының ерекшелігі төмен болуы тән. Олардың негізгі құрамы өсімдіктерге жетпейтін түрде орын алған. "Дегелең" алаңындағы көрініс басқа сипатта. Рельефтік және топырақтық жағдайлар тән, жоғары деңгейде ылғалданған жайылымдық топырақта радионуклидтердің

жылыстау қасиеті едәуір айқындалған сипатта. "Дегелең" алаңының топырағында жылыстау қасиетінің деңгейі жоғарылау деген радионуклид ^{90}Sr болып табылады, орташа шамамен алғанда аталған радионуклидтің жартысынан астам құрамы алмаспалы түрде орын алған. Жайылымдық топырақта қозғалысы аздау ^{241}Am және^{137}Cspадионуклидтері болып табылады. ССП аумағының "аялық" телімдеріндегі радионуклидтердің қозғалысы "Тәжірибе даласы" мен "Дегелең" алаңдарының топырақтарындағы қозғалысының аралық орналасуына ие. Ерекше түрде ^{90}Srрадионуклиді алынған, оның "солтүстік" аумақтың топырағындағы қозғалысы, жеңіл қол жетімді формалардың үлесіне барлық формалардың жиынтық құрамынан орташа алғанда 77% болып табылады.

Түйін сөздер: радиоактивтіластану, ССП, радионуклидтерді анықтау формасы, бірізді экстрагирлеу, "Тәжірибе даласы" алаңы, "Дегелен" алаңы, "солтүстік" және "батыс"аумақтар.

СРАВНИТЕЛЬНАЯ ОЦЕНКА ФОРМ НАХОЖДЕНИЯ РАДИОНУКЛИДОВ В ПОЧВАХ НЕКОТОРЫХ УЧАСТКОВ ТЕРРИТОРИИ СИП

Кундузбаева А.Е., Кабдыракова А.М., Лукашенко С.Н., Магашева Р.Ю.

Институт радиационной безопасности и экологии НЯЦ РК, Курчатов, Казахстан

В настоящей работе представлены результаты исследований форм нахождения техногенных радионуклидов ^{137}Cs и ^{90}Sr, ^{241}Am и $^{239+240}$Pu в почвах различных участков территории бывшего Семипалатинского испытательного полигона, характеризующихся различными уровнями и характером радиоактивного загрязнения, типом почв, рельефом и климатическими условиями. Сравнительный анализ полученных данных позволил выявить особенности поведения радионуклидов в почвах различных участков территории СИП. Для площадки "Опытное поле" характерным является низкая миграционная способность всех изученных радионуклидов ^{137}Cs, ^{241}Am,$^{239+240}$Pu, ^{90}Sr. Основное их содержание находится в недоступных растениям форме. Для площадки "Дегелен" характерна несколько иная картина. В луговых почвах с более высоким уровнем увлажнения, характерными рельефными и почвенными условиями радионуклиды характеризуются наиболее выраженными миграционными свойствами. В наибольшей степени миграционноспособным в почвах площадки "Дегелен" является радионуклид ^{90}Sr, в среднем, более половины содержания данного радионуклида находится в обменной форме. Менее подвижны в луговых почвах радионуклиды ^{241}Am и ^{137}Cs. Поведение радионуклидов в почвах "фоновых" участков территории СИП занимает промежуточное положение между поведением их в почвах площадок "Опытное поле" и "Дегелен". Исключением является радионуклид ^{90}Sr, характеризующийся в почвах "северных" территорий наибольшей подвижностью, в среднем, 77 % от суммарного содержания всех форм приходится на долю легкодоступных форм.

Ключевые слова: радиоактивное загрязнение, СИП, формы нахождения радионуклидов, последовательное экстрагирование, площадка "Опытное поле", площадка "Дегелен", "северные" и "западные" территории.

УДК 546.11.02.3:504.3.054:577.4

TRITIUM AS AN INDICATOR OF NUCLEAR TESTS LOCATIONS

[1]Lyakhova O. N., [1]Lukashenko S. N., [1]Larionova N. V., [1]Subbotin S. B., [2]Mulgin S. I., [2]Zhadanov S. V.

[1]Institute of Radiation Safety and Ecology NNC RK, Kurchatov, Kazakhstan
[2]Institute of Nuclear Physics NNC RK, Almaty, Kazakhstan

The Treaty on the Non-proliferation of Nuclear Weapons makes it to be a highly topical issue the accurate verification of nuclear explosion locations.

This paper proposes to consider a radically new method for verification of underground nuclear explosion sites employing tritium as an indicator. Detailed studies of tritium content in air were performed in the locations of underground nuclear tests - "Balapan" and "Degelen" testing sites at STS.

The paper presents data on the levels and distribution of tritium in the air where adits and wells are located – explosion epicentres, wellheads and adit portals, as well as in estuarine areas of the UNE locations. The possibility to use tritium in identification of the locations and in verifications of underground nuclear explosions is shown.

Keywords: nuclear tests, verification, Degelen site, Balapan site, tritium, atmospheric air, soil air, tritium contamination, distribution of tritium.

INTRODUCTION

The Treaty on the Non-Proliferation of Nuclear Weapons came into force on March 5, 1970, which is a convention to limit the nuclear weapons proliferation. The control system of the Treaty is a global monitoring to identify the characteristics of a nuclear explosion. There is a network of international monitoring stations – seismic, hydroacoustic, radionuclide and ultrasound to achieve this goal. The States Signatories may require on-site inspection which aims to clarify whether or not a nuclear explosion was conducted in violation of the Treaty. This paper proposes to consider a new method to verify locations of underground nuclear explosions by using tritium as an indicator, particularly for on-site inspections.

The long-term studies of radionuclide contamination at STS have revealed tritium in many objects of the environment – in plants, in surface and ground waters, soil and atmospheric air, in animal products [1], [2]. It is important to note that tritium has a long half-life equal to 12.4 years.

Given the aforesaid, as well as the fact that the tritium detection points geographically are confined to the nuclear test sites, it was decided to assess the feasibility of using tritium as an evidence for underground nuclear explosion location (UNE) by examining its contents in the air.

The two testing sites were thoroughly studied, where the nuclear testing formed local tritium contamination spots. These are the sites "Balapan" and "Degelen," where more than 300 underground nuclear tests were carried out.

The level and distribution of tritium in the selected sites were studied by field and laboratory works that involved sampling of water vapours from the atmospheric and soil air by cryogenic freezing, and studying the samples taken by liquid scintillation spectrometry

[3], [4]. The methods applied for sampling and measurements were previously used and are described in detail in [5].

1 TRITIUM RECOVERY CAUSED BY NUCLEAR EXPLOSIONS AND ITS DISTRIBUTION IN THE EXPLOSION CAVITY

The baseline values for long-term prognosis of tritium egress (T) from a cavity formed by underground nuclear explosions is the initial amount of *residual* and *accumulated* tritium in the tritium nuclear reactions – $N_T(t = 0)$. The value N_T $(t = 0)$ depends on the type of explosion (one, two and three-phase), its capacity, design features of the device and the chemical composition of rocks where an explosion was carried out. For the single-typed charges and the same chemical composition of the rock the tritium recovery is approximately directly proportional to the power of the explosion. Therefore, in numerical calculations of tritium, normally a value of recovery in the blast with power of 1 kiloton (kT) of TNT equivalent is used.

1.1 Tritium recovery at nuclear fission explosions

The initial phase of any nuclear explosion is a chain reaction of nuclear fission of ^{235}U or ^{239}Pu by neutrons from the fission fragments. Thus, let us first of all consider the recovery in a "pure" fission explosion. In this explosion tritium is generated as follows:

1. 1. in the decay of the fissionable nucleus into 3 fragments (ternary fission), one of which (the lightest) is tritium.
2. 2. tritium formation due to interaction of excess neutrons from the fission fragments with nuclei of light elements of the environment, i.e. nuclear reactions such as ^{6}Li (n, T).
3. 3. tritium recovery in the interaction of high-energy γ- quanta from the fragments with the nuclei of light elements of the environment, i.e. photonuclear reactions such as ^{7}Li (γ, T).

1kT explosion is achieved by a number of fission events of N_f, which is $\approx 1.42*10^{23}$ for ^{235}U or $N_f \approx 1.38*10^{23}$ for ^{239}Pu [6]. Since these values are almost similar, for further assessments we assume that the 1 kT explosion corresponds to $1.4*10^{23}$ of fission events.

Tritium recovery in the ternary fission. In the ternary fission the tritium atoms escape from the neck of the fissionable nucleus. The probability of such fission events is very small and is about 1/6000 nuclei of ^{3}H per fission event [6]. Thus, for the 1 kT explosion, we have:

$N_T = N_f*(1/6000) \approx 2.3*10^{19}$ - number of tritons

or

$A_T = N_T *[\ln 2/T_{1/2}\,(c)] = 2.3*10^{19}*1.7813*10^{-9} = 4.1*10^{10}$ Bq - tritium activity.

Tritium recovery from neutron activation. To assess the tritium recovery by neutrons from the fission fragments during the underground explosions it is necessary to know the total number of neutrons absorbed by the rock and relative probability of absorption of a neutron with tritium recovery.

During the explosions, ~2.6 neutrons are formed when nuclei of ^{235}U or ^{239}Pu are being fissionable, with an average energy En ≈ 2 MeV [6]. Of these, 1 neutron is spent for fission initiation of another nucleus, about 0.6 neutron is absorbed in the construction materials of

a nuclear device, and ~1 neutron remains "free". Thus, the 1 kt explosion emits ~$1.4*10^{23}$ neutrons into the environment.

When these neutrons come through the environmental matter they undergo elastic and inelastic scattering losing their kinetic energy (moderation). At the same time, there are nuclear reaction processes with neutron absorption, the probability of which increases rapidly with decreasing of neutron energy (E_n). These processes rapidly lead to the equilibrium energy spectrum of neutrons, which eventually are completely absorbed by the nuclei of the medium, forming new stable and radioactive isotopes. Some of these neutrons, by interacting with light elements contained in the rock, may recover tritium. Tritium can recover in small quantities in all nuclei with mass number A <20. Only a few reactions can however significantly contribute to tritium yield. Let us consider them in more detail.

The main channels for tritium recovery are through the reactions:

$$^{6}_{3}Li + n \rightarrow ^{4}_{2}He + T$$

$$^{10}B_5 + n \rightarrow 2^4He_2 + T$$

$$^{14}N + n \rightarrow ^{12}C + T$$

The reaction cross section at thermal neutrons for ^{6}Li is about 940 barns or 70.7 barns for natural lithium [7], ^{10}B – about $5*10^{-3}$ barns [8]. The reaction ^{14}N (n, T) is threshold ($Q_r \approx$ 4 4 MeV) and when E_n = 5-7 MeV, its cross section is ~ $2*10^{-2}$ barns [8]. This shows that (at comparable concentrations) the main channel for tritium recovery is the reaction ^{6}Li (n, T).

To assess the T recovery in this reaction for the 1 kt explosion, one can use the approximate relation:

$$N_T = N_F * \eta_{Li} * \sigma_{oLi} / \Sigma_i \eta_i * \sigma_{oi} ,$$

where: η_I - atomic percentage, %,

σ_{oi} - thermal neutron absorption section of i – chemical elements in the rocks.

The typical granite composition (SiO_2 = 70.18; TiO_2 = 0.34; Al_2O_3 = 14.98; MgO = 1.08; Fe_2O_3 = 1.62; FeO = 1.66; CaO = 2.20; Na_2O = 3.28; K_2O = 3.95; H_2O = 0.78; P_2O_5 = 0.27) can be found in [9], and σ_{oi} section in [7]. Based on these data (at relatively low lithium concentrations η_{Li} < 0.1%) the tritium recovery will equal to $N_T = N_F * 5.15 * \eta_{Li}$%.

The Li content in the granitic rocks of Degelen Mountains, according to the analysis for the microelement composition, is about 20 g/t or $\eta_{Li}\% \approx 0.006$ of atomic percent. The maximal possible amount of tritium recovered in this reaction is about 1/30 of the tritium nuclei per fission event. Thus, the amount of tritium recovered and tritium activity in the Li activation by neutrons will be about:

$N_T = 4.3*10^{21}$ - number of nuclei

or

$A_T \approx 7.6*10^{12}$ Bq - tritium activity per 1kT explosion

Tritium recovery by high-energy γ-quanta. A third possible mechanism for tritium recovery in a fission explosion is tritium recovery by high energy fission γ-quanta on nuclei of light elements. This reaction has a high energy threshold which on average is about Eγ >10 MeV. For reactions such as 7Li (γ, T), which is the most advantageous in this aspect, in

terms of tritium recovery, at an energy threshold Eγ> 6 MeV the section is ~ 10^{-4} barn [8]. The probability of tritium formation in these gamma-quanta is about 1/100 000.

Since, in the fission spectrum the γ – quanta fraction with Eγ> 6 MeV is only ~ 10^{-2} γ – quanta per fission event [6] and the lithium content of the rock is no more than ~ 20 g/t, then the tritium recovery in such reactions would be less than 1/1 000 000 per fission event, i.e. considerably less than the above two cases:

$N_T = 1.4*10^{17}$- number of triton

or

$A_T \approx 2.5*10^8$ Bq - tritium activity per 1kT explosion.

Table 1 presents information on each considered tritium recovery reactions during the fission explosions.

Table 1.

Reaction of tritium recovery during the fission explosion

##	Tritium recovery reactions	Probability of reaction	Number of nuclei	Tritium activity, Bq/kT
1	Ternary fission	1/6 000	$2.3*10^{19}$	$4.1*10^{10}$
2	Neutron activation (Li)	1/30	$4.3*10^{21}$	$7.6*10^{12}$
3	High energy γ-quanta	1/1 000 000	$1.4*10^{17}$	$2.5*10^8$

The results in Table 1 showed that in the underground "pure" fission explosion the main contribution to tritium recovery is made by the reaction ^{6}Li (n, T), which gives the maximal activity of tritium for the 1kT explosion.

1.2 Assessment of residual tritium during the nuclear fission explosions with use of additional sources of high-energy neutrons

For accurate assessment of the initial tritium amounts in the explosion cavity it is needed to consider not only the above processes, but also the amounts of so-called residual tritium, which recovers during the explosions with the use of structures that act as additional powerful high-energy neutron source. These sources were used to ensure high efficiency of the blast in the design of most types of nuclear (*not thermonuclear*) charges, and were based on the thermonuclear fusion T + D → α + n. These sources are:

a) a neutron tube (compact, pulsed accelerator of tritium ions and deuterium target) that provides intensive launch of the fission chain reaction;

b) a booster (a container with a mixture of deuterium and tritium in the centre of the nuclear charge), in which during the development of the explosion a thermonuclear reaction begins and there is an additional stream of neutrons, which provides more intensive burn-out of ^{235}U or ^{239}Pu and increases the explosion power [10].

Calculation of residual tritium. The amount of deuterium and tritium in these devices during the combustion must provide the number of excess neutrons that is comparable to the number of neutrons from the fission reaction, i.e. ~ 10^{23} neutron per 1kT explosion.

This means that, even at very high efficiency of the mixture burnout (T+D) - about 90%, after 1kT explosion the explosion cavity has:

$N_T = 1*10^{22}$- unused tritium atoms

or

$A_T \approx 1.8*10^{13}$ Bq - tritium activity per 1kT explosion.

The resulting activity of the residual tritium is 3 times more than tritium recovery in "pure" fission explosion.

Tritium recovery from neutron activation. Like at "pure" fission explosion, about 50% of neutrons from a thermonuclear reaction activate surrounding rocks with tritium recovery from the reaction ^{6}Li (n, T). The amount of tritium accumulated on the thermonuclear neutrons can be estimated by analogy with the fission neutrons, which gives:

$N_T = 4*10^{21}$- tritium atoms

or

$A_T \approx 7*10^{12}$ Bq - tritium activity per 1kT explosion.

The total amount of tritium recovered due to fission explosions with additional sources of high-energy neutrons can be measured as the amount of tritium recovered by fusion reactions during the explosion, and tritium produced from neutron activation.

Recovery of tritium in the tests with neutron bombs. From the viewpoint of tritium recovery, of particular interest are underground tests of neutron bombs. In these devices, a multiple increase in the neutron yield is achieved by adding excessive amounts of the mixture to the nuclear charge (T + D) and this can result in:

$N_T = 1*10^{23}$- tritium atoms

or

$A_T \approx 1*10^{15}$ Bq - tritium activity per 1kT explosion

The obtained activity is comparable to the tritium activity at a *two-phase thermonuclear explosion.*

Table 2.

Tritium recovery during the explosion by using additional sources of high-energy neutrons

##	Tritium recovery reaction type	Probability of reaction	Number of nuclei	Tritium activity, Bq/кТ
1	Residual tritium	-	$1*10^{22}$	$1.8*10^{13}$
2	Neutron activation (Li)	-	$4*10^{21}$	$7*10^{12}$
3	Use of neutron bombs	-	$1*10^{24}$	$1*10^{15}$

The above takes us to the conclusion – in order for tritium to recover in large quantities during the explosion it is necessary either tritium to be introduced in a nuclear device, in advance, to enhance the effectiveness of an explosion (pseudo thermonuclear explosion), or tritium to be used in the charge as the main component of fuel. In this case we are talking not about the fission explosion but about a thermonuclear explosion.

1.3 Tritium distribution in the explosion cavities

At the final stage of the explosion, tritium activity is concentrated in a relatively thin surface layer of the nuclear cavity. The distribution of tritium in the depth of the layer (h) can be described as:

$$N_T(h) = N_T(h=0)*\exp[-(\rho*h)/\lambda],$$

where: $N_T(h=0)$ – number of tritium atoms per 1cm^2 at h=0.
ρ - rock density, g/cm^3.
λ - relaxation length of neutrons in rock, g/cm^2.

For granites one can use the values $\rho = 2.6$ (g/cm^3) and $\lambda \approx 30$ (g/cm^2), according to [11]. Based on the calculations, it appears that, immediately after the explosion, 95% of the tritium activity is concentrated in the 35 cm surface layer of the cavity.

Further, considering the effects of melting and dripping of walls, this activity is concentrated in the influx at the bottom of the nuclear cavity. Further behaviour of tritium is defined by geochemical processes in the explosion cavity and the tritium speciation after its recovery.

It can be assumed that there were two tritium species in the explosion cavities. Part of tritium being condensed, penetrated the crystal lattice of the solidifying melt. Another part of tritium that remained in the gaseous form is likely to evaporate. We also should not exclude the existence of tritium in the undisturbed crystal structures, in the case of its recovery from Li activation as per the above reactions.

Most likely, during the explosions carried out in the adits, gaseous tritium evaporated in a relatively short period of time through rock fractures and tritium contained in the crystal structure remained. During the explosions carried out in wells a somewhat different situation may have been. Given the depth of the charge, tritium can remain much longer in the explosion cavity in the gaseous phase [12].

The fact that for many years concentration of tritium in the adit streams has been remaining relatively constant [13] make us assume that the inside of the sprung hole of the adit tritium is gradually washed out, accumulated during the explosions, from the crystal structure of melted surface of the walls, as well there is emanation of tritium into the atmosphere from the inner surface of an underground nuclear explosion cavity.

2. CONTENTS AND DISTRIBUTION PATTERN OF TRITIUM IN THE AIR AT UNE LOCATIONS OF THE "DEGELEN" SITE

2.1 Characteristics of objects and study methodology

Brief description of the research objects. At "Degelen" site the underground tests were carried in horizontal mine workings – the adits. Total 181 adits were built with a cross section of 9 up to 25 square meters each from 150 to 1,500 m deep. A nuclear charge was planted at the end of the adit in a specially designed box. To prevent release of fission products to the surface a special sealing complex was made in the adit: combination of cement plugs and gravel backfill. At elimination of the entire test site infrastructure the adits were closed by the

man-made collapse of the rock to prevent free access to the adits. The figure shows schematically the adit in a horizontal cross-sectional diagram and sampling points (Figure 1).

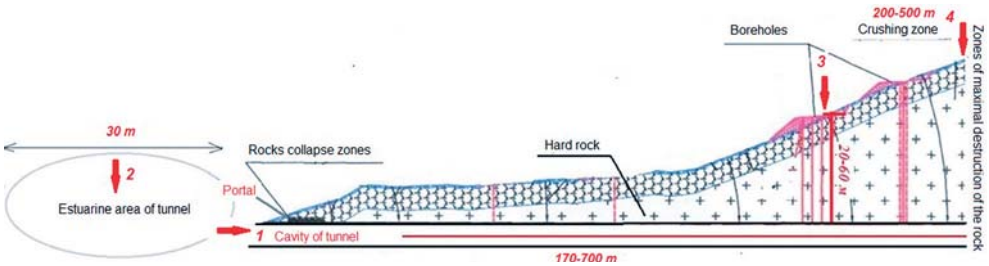

Figure 1. Horizontal section of an adit

Tritium concentrations were studied in air over 22 adits. The main characteristics of the explosions carried out in them are shown in Table (Table 3) [14].

Table 3.

Adits and the tests carried out

##	Adit #	Date of test	Purpose of test	Capacity, kT	Type of explosion [1]	Q-ty of tests
1	707	29.03.77	Nuclear weapons development	25	PCE	1
2	150	19.02.82	Nuclear weapons development	24	FCE	2
3	901	28.12.88	Nuclear weapons development	0.2	PCE	2
4	603	30.04.74	A study of factors affecting	24	FCE	3
5	103	20.11.81	Nuclear weapons development	8	PCE	1
6	A7	20.08.68	Nuclear weapons development	4.6	PCE	2
7	185	23.07.76	Nuclear weapons development	7	FCE	1
8	505	24.04.68	Nuclear weapons development	6.2	PCE	1
9	208	03.04.87	Nuclear weapons development	1	FCE	3
10	129	26.12.83	Fundamental research	30	FCE	1
11	107	29.06.78	Nuclear weapons development	14	FCE	2
12	132	09.09.84	A study of factors affecting	6	FCE	4
13	136	29.10.77	Nuclear weapons development; Fundamental research	42	FCE	2
14	501	30.10.67	Nuclear weapons development	25	FCE	1
15	169	23.11.88	Fundamental research	19	FCE	2
16	175	30.07.77	Nuclear weapons development	11	FCE	1
21	Ж-3	03.03.65	Nuclear weapons development	27	PCE	1
22	110	07.06.72	Nuclear weapons development	0.001-20	FCE	1

Note: FCE – Full camouflet explosion. Underground explosion of complete internal action accompanied by the formation of underground cavity. No gaseous fission products release into the atmosphere is observed.

PCE – Partial camouflet explosion. Underground explosion of total internal actions followed, as a rule, by insignificant emissions of short-lived radionuclides into the atmosphere (RNG)

Some adits located at Degelen site have water seepage. In all waters flowing from the adits the content of tritium is in tens and hundreds of kBq/kg. In our study we took waterless adits in order to avoid release of tritium into the atmosphere from the aquatic environment.

Research methodology. To study levels and distribution of tritium in the atmosphere over the sites of UNEs within Degelen site, given the specificity of the blasts, the following steps were identified:

- study of the level and distribution of tritium in the air inside the cavity of the adit;
- study the levels of tritium in the atmospheric air at the location of vertical wells;
- study of the levels of tritium in the atmospheric air in the zone of maximal destruction of the rock above the UNE cavity (zone of fragmentation);
- study of the tritium levels in the air medium in the adits near-mouth areas.

Level and distribution of tritium in the air medium inside the cavity of the adit. Inside the cavity of the adits the atmospheric air water vapor was sampled from the portal into the depths, until the box end. The sampler was placed in the center of the adit cavity at a distance of 50 cm from the surface. The distance between sampling points varied from 10 to 100 m, depending on the conditions of work. The depth of the adits ranged from 170 to 700 m (Figure 1. point 1).

Tritium contents in the location of vertical wells. During the research in a number of adits vertical wells were drilled into the body of the adit, sometimes with penetration into the end box (Figure 1. point 2). The depth of wells depended on the magnitude of the slope of rock and ranged from 20 m to 60 m.

The atmospheric water vapour were sampled twice at the location of each well – before drilling (a sampler was installed at the point defined for drilling) and then immediately after drilling (sampling was carried out in close proximity to the well at a distance of not more than 50 cm).

Tritium concentrations in the area of maximal destruction of the rock

Since there is no reliable information about the location of the adit end boxes, in addition the maximal destruction of the rock (*shattering zone*) were investigated for the content of tritium in the atmosphere over the adits. The research location was defined as by documented information about the design of the adits, as well as visually.

The atmospheric air water vapour was sampled at a height of the alleged explosion cavity – 200 m -500 m (Figure 1. point 3).

Tritium in the air medium at adits near-mouth areas. The adits near-mouth area is an area in front of the portal. The atmospheric air water vapour was sampled at a distance of 30 m from the adit portal on the same axis as its central one (Figure 1. point 4).

To better understand the results presented, it should be noted that according to the previous studies of contents and distribution pattern of tritium in the air, perofrmed at Degelen site, the background concentration of tritium in air is 0.2 Bq/m^3 [13]. The background level is marked with red horizontal line on all charts.

2.2 RESULTS AND DISCUSSION

2.2.1 Contents and distribution of tritium in the air inside the adit cavity

The concentrations of tritium in the air inside the cavity of the adits are shown in the figure (Figure 2). The horizontal axis shows the distance from the portal of each adit to the end box, a fraction of the maximum, taken as a unit. The point "0" corresponds to the adit portal. The vertical axis shows the volumetric activity of tritium inside the cavity of the adit on a logarithmic scale.

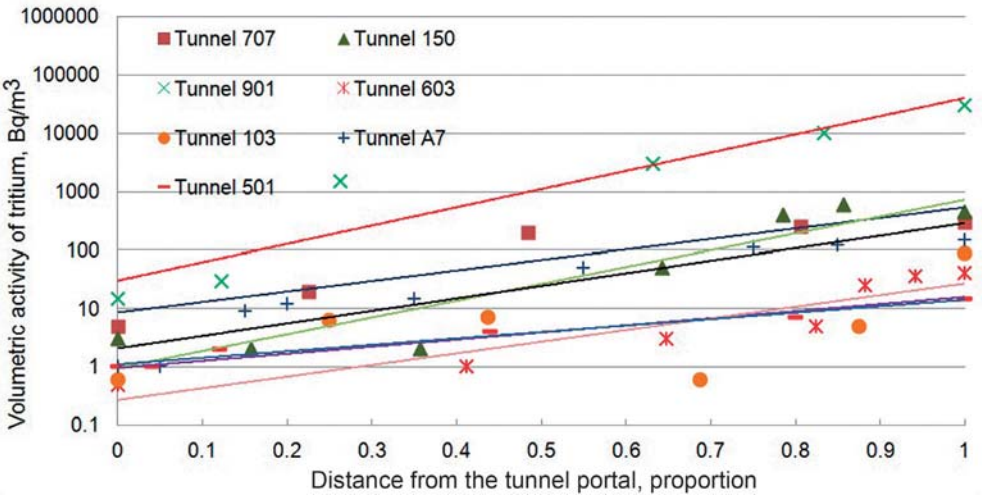

Figure 2. Tritium distribution with air flows inside the cavity of the adit

The concentration of tritium inside the cavity of the adits varies from 1 to 30,000 Bq/m^3. The maximal concentration of tritium corresponds to the point that is closest to the end box. The resulting distributions showed that the concentration of tritium inside the cavity of the adit has an exponential dependence on distance. Tritium concentration drops down with approaching the exit of the adit. The cause of the resulting distribution may be two mechanisms – the convective mixing of air layers inside the adit cavity and escape through cracks of the shattered rock.

Thus, the results showed that, despite the time passed since the explosions, tritium in the cavities of the adits is contained in detectable amounts that are much higher than the background level. The content of tritium in the air from the inner side of the portal is dozens of Bq/m^3.

2.2.2 Tritium contents in the near-mouth areas of the adits

Results are presented in the following figure (Figure 3).

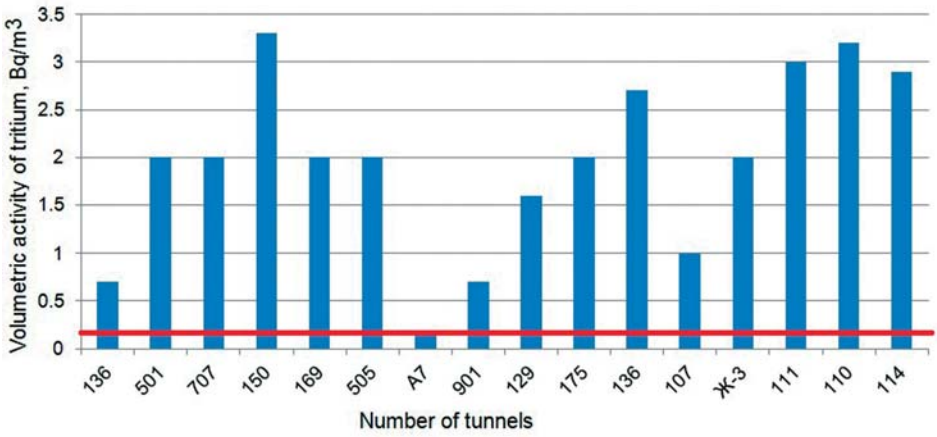

Figure 3. Content of tritium in the atmosphere at near-mouth areas of the adits

The results showed the presence of tritium in the atmospheric air, even at a distance of 30 m from the portal. In all cases except for the adit A7, tritium concentration is higher than the background levels for up to 15 times.

2.2.3 Tritium contents at locations of the vertical wells

Results are presented in the following figure (Figure 4).

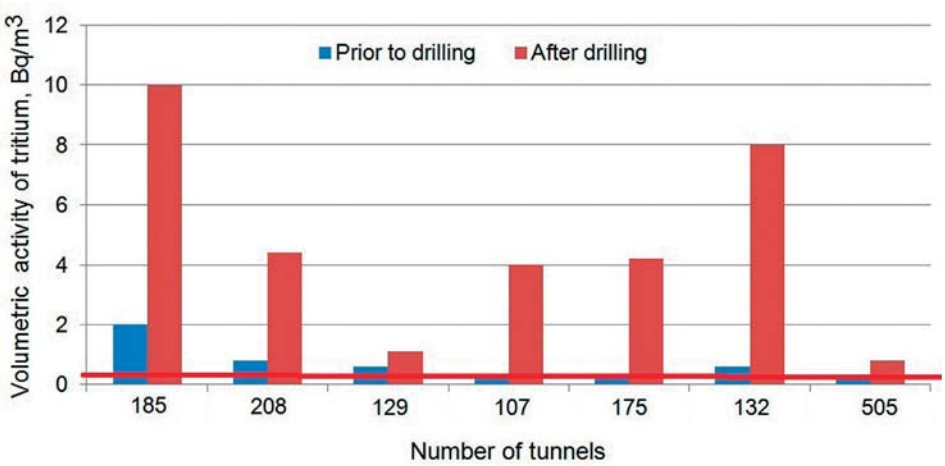

Figure 4. Content of tritium in the atmosphere at the well locations

Tritium outflow from the adit to the surface of the cavity has been found. As for the adits 185 and 13, the content of tritium in the atmosphere exceeded the background concentration and comprised 10 Bq/m^3 and 8 Bq/m^3, respectively.

The yield of tritium with air currents into the atmosphere after drilling was expected, but no one expected tritium in the air before the drilling. Probably this can be explained by good migration properties of tritium: it can pass easily with air through the decompactification zone of hard-rock.

Tritium in the atmosphere before drilling was recorded not in all cases. This may depend on many factors - the power of the explosion, type of test and date of test, etc. Unfortunately, at present, these parameters are rather difficult to assess due to the lack of accurate information on the test conditions.

2.2.4 Tritium contents in the area of maximal shattering over the UNE cavities

Results are presented in the following figure (Figure 5).

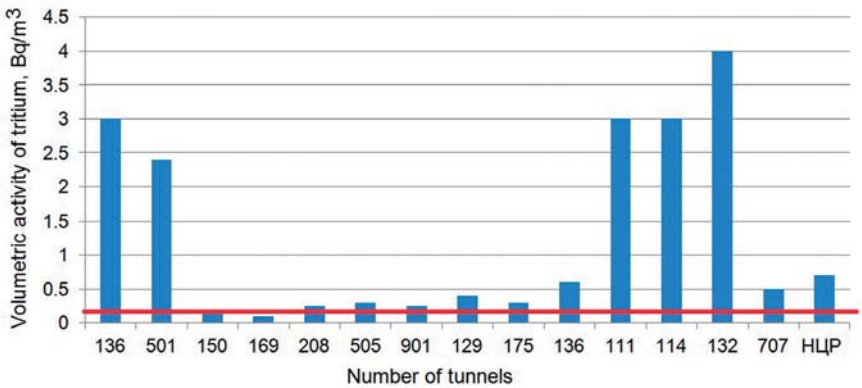

Figure 5. Content of tritium in the atmosphere in the zone of maximal shattering over the UNE cavity

In the area of maximal destruction almost at all the adits we recorded tritium in the concentrations higher than the background levels - from 1.5 to 15 times. Since the research was done on top of the rock formations, the presence of tritium can be caused only by its outflow from the adit cavity.

It is important to note that the tritium concentrations in the atmosphere were recorded at an altitude of 500 m from the UNE cavity.

Information about the presence of tritium in the air says the fundamental possibility of tritium release from the cavity of the adit. After more than 20 years since the last nuclear test at "Degelen" site, tritium was identified in detectable quantities not only inside the adit, but also in the mouth area, on the slope of the mountain massif, and also in the area of maximal rock destruction, which is located at an altitude of 500 meters from the explosion cavity.

Summarizing this section one can say that tritium, namely, information about its presence and levels in the air can be successfully used to verify the locations of UNEs conducted in underground workings based on the type of adits.

3. CONTENTS AND DISTRIBUTION PATTERN OF TRITIUM IN THE AIR OVER UNDERGROUND NUCLEAR EXPLOSION VENUES WITHIN "BALAPAN" SITE

3.1 Characteristics of the objects and research methodology

Brief description of research objects. Nuclear tests at "Balapan" site were carried out in wells - vertical openings, partly with casing pipes of different diameters, below is the open shaft with a diameter of 900 mm. The depth of the wells varied from 100 to 600 m. After planting the charge the well was tamped to full depth. The tamping complex is a combination of power and technological elements: cement plugs and gravel backfill areas [15]. The overall view of the well (by the example of well 1010), as well as the vertical section diagram of the well are shown in the figure (Figure 6).

In the course of this work the levels of tritium in the air around 8 wells were investigated (Table 4) [14]. At the near-mouth areas of 3 of them we studied in detail the level and distribution of tritium in the air – the wells 1010, 1355, and Glubokaya.

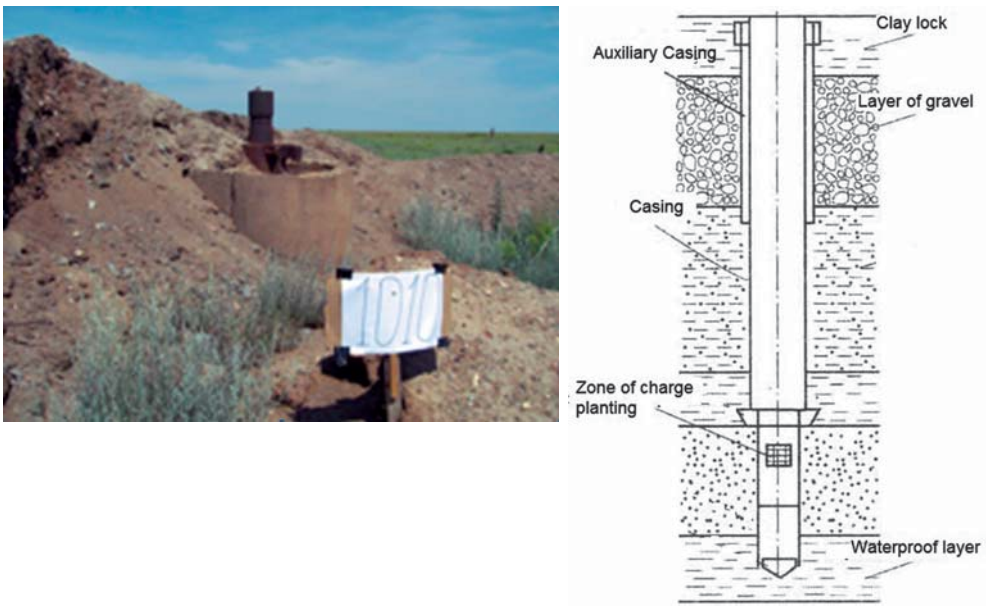

a) b)

Figure 6. Overall view of the well (a), vertical section diagram of the well (b).

Table 4.

List of the studied wells and characterization of the nuclear tests

##	Well #	Date of test	Purpose of test	Capacity, kT	Type of explosion [1]	Q-ty of tests	Charge planting depth, m
1	1010	11.06.78	nuclear weapons development	58	PCE	1	556
2	1236	18.10.81	nuclear weapons development	107	FCE	1	525
3	1361	13.02.88	nuclear weapons development	125 0.001-20	FCE	2	125
4	1355	13.12.87	nuclear weapons development	137 0.001-20	PCE	2	530
5	1317	31.02.88	nuclear weapons development	8	FCE	2	532
6	1053	19.06.68	Fundamental research	18	FCE	1	316
7	1315	12.03.87	nuclear weapons development	11	PCE	2	529
8	Glubokaya	30.11.77	nuclear weapons development	70 0.001-20	PCE	2	535

Virtually all the wells were constructed for nuclear weapons development, depth of the charge ranged from 125 to 556 m. Depending on the problem, the power of explosions varied from 0.001 kT to 150 kT. 23 years passed since the last test. Near the wells there are no visible sources of tritium release into the environment.

Research methodology. We selected eight "warfare" boreholes that were considered "critical" based on the previous studies. This term was assigned to them in view of identifying the effects of geothermal activity in the areas of their location, presence of un-collapsed "sprung" cavities, a gas content occurrences (high gas content in the soil air), as well as various mechanical effects of UNEs (changes in ground features, formation of subsidence craters etc.) [16].

Initially, in order to be able to compare the tritium contents in the near-mouth areas of 8 wells a conjugative sampling of the atmospheric and "soil" air water vapor was carried out. To accomplish this, at each near-mouth section we selected a point located as close to the well head at a distance of 50 cm.

Further, based on the results we selected three wells for more detailed areal studies in the near-mouth areas which had the highest contents of tritium in the air.

It was suggested that a tritium release spot to the surface does not always correspond to the location of the wellhead. Thus, for sampling during the areal survey we selected a scheme which covers the entire well near-mouth area (Figure 7a). Sampling was conducted on three profiles – two diagonal and one cross-sectional. All three profiles had a central point of intersection at the location of the wellhead mouth. The distance between points in the diagonal profiles was about 70 m, between the points in the cross profile - about 50 m.

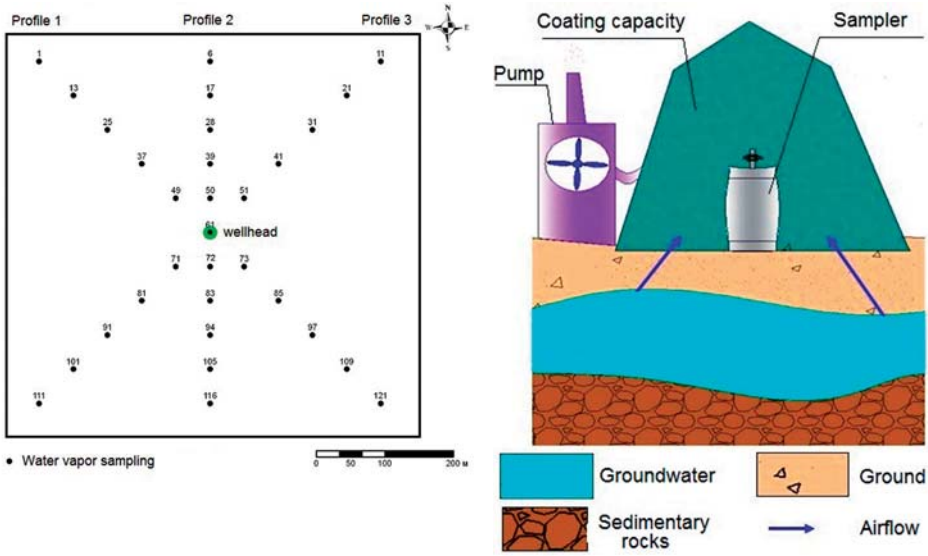

a) b)

Figure 7. Arrangement of "soil" air sampling points in the near-mouth areas of wells (a), sampling "soil" air by cryogenic freezing (b)

Since the explosions were carried out in the deep wells, it is possible that the main mechanism for tritium inflow into the atmosphere may be an emanation of tritium from the soil surface. Thus, a detailed study of the levels of tritium was decided to carry through sampling the "soil" air. The "soil" air was sampled in accordance with the scheme shown in the figure (Figure 7b). The sampling point during the sampling was maximally isolated from the atmospheric air. It was provided by having a special 100-litre isolating vessel, which covers the place of sampling together with the sampler installed. To isolate from the atmosphere, the edge of the vessel was buried in the soil, which then was well compacted on the top. A vacuum pump inside the vessel made a rarefaction controlled by a liquid manometer.

The sampling time with the vessel was about 120 min. During the air sampling a temperature and relative humidity were measured with an electronic hygrometer. These parameters were used to convert the specific activity of tritium in water vapor (Bq/kg) to volumetric activity (Bq/m^3).

3.2 Results and discussion

3.2.1 Tritium content in the air at the near-mouth areas of 8 "critical" wells

The results are presented in Figure (Figure 8).

The results showed that at the near-mouth sections of the wells along with the presence of tritium in the atmospheric air water vapor there is also an emanation of tritium from the soil surface. The concentration of tritium in water vapour of the "soil" air varies from 15 to 82 000 Bq/kg, in all cases it is significantly higher than background levels of tritium in the

atmospheric air water vapour: a minimal detectable activity of tritium, equal to 14 Bq/kg, was taken as a background.

The data obtained showed us the presence of tritium in water vapor of the soil air, as well as the possibility of its release to the surface where "emplacement" wells are located, so it was decided to carry out further more detailed studies.

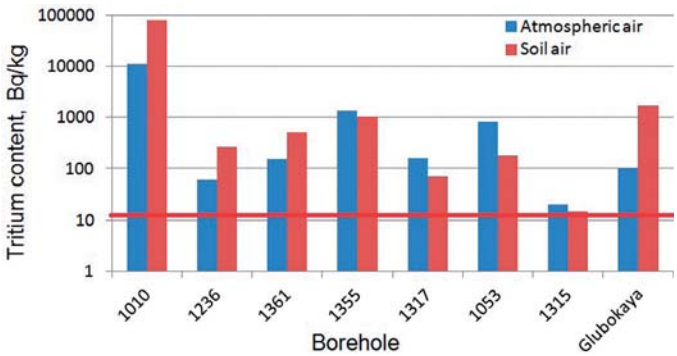

Figure 8. Content of tritium in water vapor of the atmospheric and "soil" air at the well near-mouth

3.2.2 A detailed study of contents and distribution pattern of tritium in the near-mouth sections of the wells

Graphs were constructed based on the tritium content in the near-mouth areas of the three wells – 1355, 1010 and Glubokaya. They show the distribution of tritium profiles passed, according to the above methodology of the study.

In the construction a mark "0" was assumed a location of the well head, the horizontal axis represents the distance in meters from the well to the left and right from the well mouth, along a vertical axis - volumetric activity of tritium, Bq/m^3.

The red line on the charts shows the level of background concentrations of tritium in the "soil" air in the study area for which it was decided to take minimal detectable activity concentration of tritium equal to 0.03 Bq/m^3.

Well 1355. The results showed that there is tritium emanation from the soil surface to the atmosphere at the mouth area of the well 1355. The concentration of tritium in the "soil" air at the mouth area of the well ranges from 0.04 to 20 Bq/m^3 (Figure 9).

Concentration of tritium in the location of the wells was 0.5 Bq/m^3. The analysed results showed that the greatest content of tritium is typical for the profile 2 that passes from the north-east to south-west of the investigated area.

It should be particularly noted that the maximal concentration of tritium was recorded at a point 70 meters from the wellhead, and is 20 Bq/m^3 (Figure 9b).

Well 1010. The studies showed that the main input of tritium from the soil surface to the atmosphere occurs near the location of the wellhead, where we recorded maximal concentration of tritium - 70 Bq/m^3 (Figure 10).

Also, at two points in the northern part of the studied area we recorded elevated, with respect to others, concentration of ^{3}H which is 4 Bq/m^3 (Figure 10c).

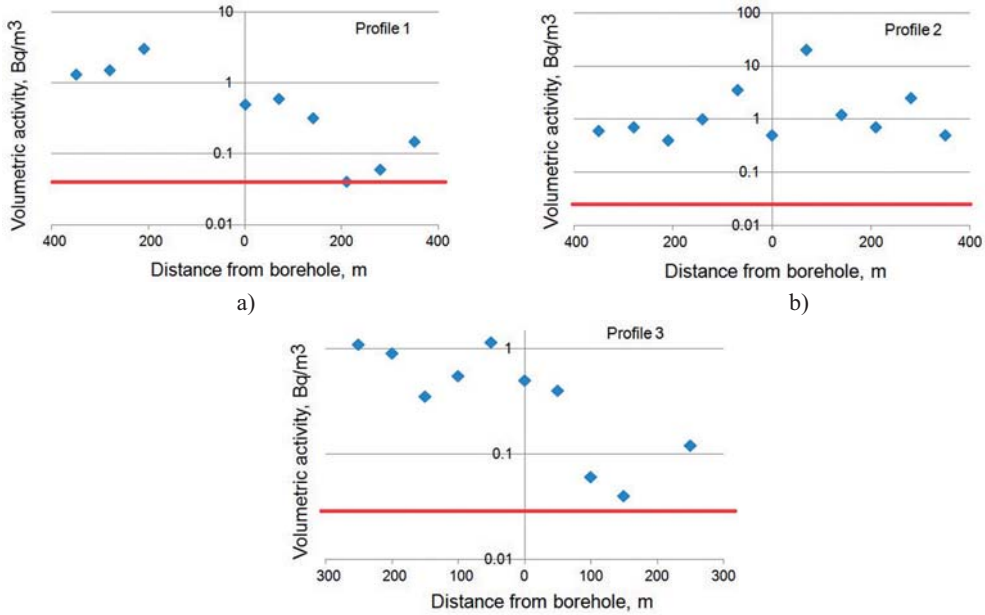

Figure 9. Distribution of ^{3}H at the near-mouth area of the well 1355 with respect to the mouth on the diagonal profiles (a, b) and transverse profile (c)

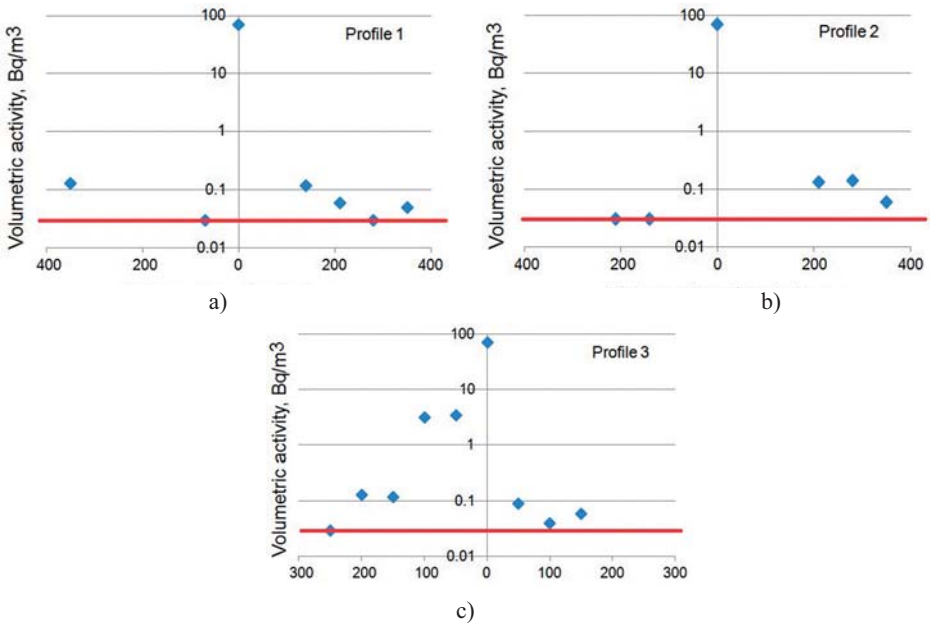

Figure 10. Distribution of ^{3}H at the near-mouth area of Well 1010 with respect to the mouth on the diagonal profiles (a, b) and the transverse profile (c)

Glubokaya well. The investigation of the near-moth area of Glubokaya well also detected presence of tritium in the "soil" air, and as a consequence, the input of tritium into the atmosphere.

50 m way from well crater in the northern part of the near-mouth area tritium concentration was 5 Bq/m^3. The concentration of tritium in the location of the wellhead was 0.6 Bq/m^3 (Figure 11).

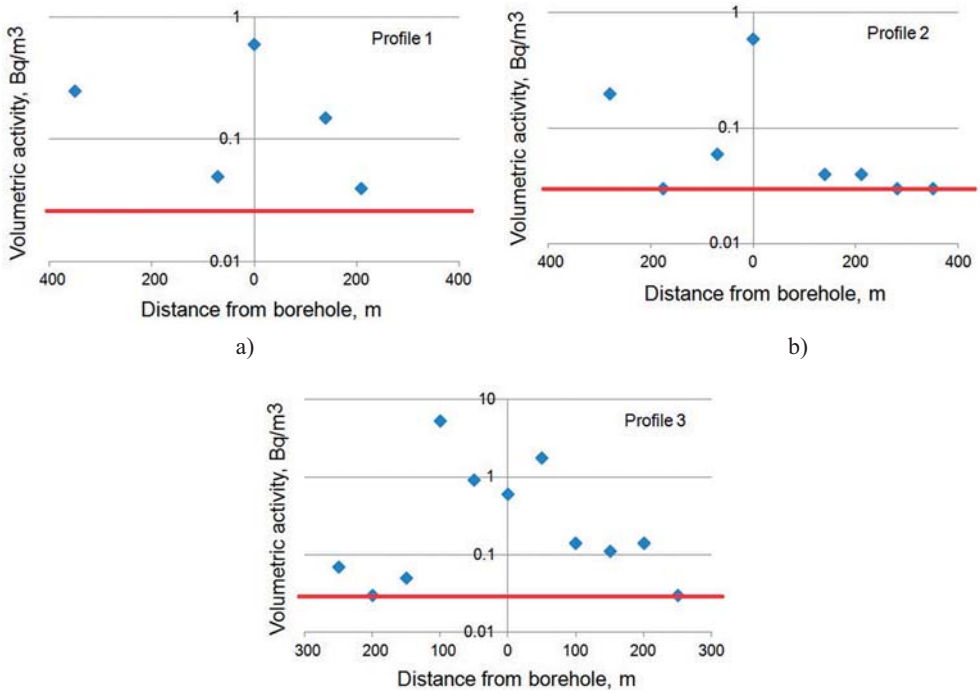

Figure 11. Distribution of ^{3}H at the near-mouth area of Well Glubokaya with respect to the mouth on the diagonal profiles (a, b) and the transverse profile (c)

According to the result analysis the largest tritium content is typical for the profile 3 that passes from north to south of the investigated area.

The results of the study as a whole showed that there is an active process of tritium emanation from the soil surface to the atmosphere near the wells near-mouth areas. However, the maximal concentration of tritium in air is not always confined geographically to the location of the wellhead. In a number of cases, significant concentrations of tritium in the "soil" air were recorded at a considerable distance from the well, up to 200 m.

CONCLUSION

The study of tritium content at Degelen site, where explosions were carried out in horizontal adits, recorded large amounts of tritium in the air inside the adits of the cavities, at their near-mouth areas, at a distance of 30 m from the portal, as well as in the zone of maximal rock destruction over the UNE cavity, at an altitude of 500 m. The studies conducted at "Balapan" site showed that the emanation of tritium from the soil surface is ongoing at present as well. Tritium was detected in the atmospheric air near the location of the wellhead, and "soil" air at various distances from it.

The study showed the presence of tritium where UNEs were carried out and its possibility to release into the air. The detectable tritium concentrations can be recorded 20 years after the nuclear tests. Thus, the studies in the former STS showed the possibility of using tritium as an indicator of venues for underground nuclear tests, both tests in the adits and in the wells.

The Comprehensive Nuclear Test Ban Treaty remains one of the most important elements for strengthening the nuclear non-proliferation regime. The results obtained in the present study are of particular importance when considering the issues concerning the verification of nuclear test sites in terms of on-site inspections.

According to the information obtained, the method of using tritium as an indicator of UNE places may help not only identify the location of testing, but also to prove the fact of testing, if necessary.

REFERENCES

1. N. V. Larionova et al. "Development and application of the method for assessment of contamination with tritium in groundwater by its content in vegetation" // N.V. Larionova, S.N. Lukashenko, O.N. Lyakhova, S.B. Subbotin, A.O. Aidarkhanov [Proceedings of the Institute of Radiation Safety and Ecology for 2007-2009] / Ed. by Sergey N. Lukashenko. – Issue 2 / – Pavlodar: Dom Pechati LLP" printing house, 2010. [in Russian]
   Ларионова Н.В. Разработка и применение метода оценки загрязнения тритием грунтовых вод по его содержанию в растительном покрове / Н.В. Ларионова, О.Н. Ляхова, С.Н. Лукашенко, А.О. Айдарханов, С.Б. Субботин // [Сборник трудов Института радиационной безопасности и экологии за 2007 – 2009гг.] / под рук. Лукашенко С.Н. – Вып. 2. – Павлодар: Дом печати, 2010. – С. 321-331.: ил.- Библиогр.: с. 224-231. - ISBN 978-601-7112-28-8.
2. Zh.A. Baigazinov et al. "Experimental studies of artificial radionuclides transfer in organs and tissues of sheep at STS" / Zh.A. Baigazinov, A.V. Panitskiy, S.N. Lukashenko et al. // [Proceedings of the Institute of Radiation Safety and Ecology for 2007-2009] / Ed. by Sergey N. Lukashenko. – Issue 2 / – Pavlodar: Dom Pechati LLP" printing house, 2010. [in Russian]
   Байгазинов Ж.А. Экспериментальное исследование особенностей перехода искусственных радионуклидов в органы и ткани овец в условиях СИП / Ж.А.Байгазинов, А.В.Паницкий, С.Н.Лукашенко [и др.]. //[Сборник трудов Института радиационной безопасности и экологии за 2007 – 2009гг.] / под

рук. Лукашенко С.Н. – Вып. 2. – Павлодар: Дом печати, 2010. – С. 355-386.: ил.- Библиогр.: с. 224-231. - ISBN 978-601-7112-28-8.

3. ISO 9698:1989 Water quality -- Determination of tritium activity concentration - Liquid scintillation counting method
   Methods for measuring tritium. Recommendations of NCRP, the U.S. [transl. from English.]. - Moscow: Atomizdat, 1978
4. Методы измерения трития. Рекомендации НКРЗ, США: [пер. с англ.]. - М.: Атомиздат, 1978.
5. O.N. Lyakhova et l. "Mechanisms for formation of air basin contamination with tritium within the "Degelen" massif" / O.N. Lyakhova, S.N. Lukashenko, N.V. Larionova // [Proceedings of the Institute of Radiation Safety and Ecology for 2007-2009] / Ed. by Sergey N. Lukashenko. – Issue 2 / – Pavlodar: Dom Pechati LLP" printing house, 2010. [in Russian]
   Ляхова О.Н. Механизмы формирования тритиевого загрязнения воздушного бассейна в пределах горного массива Дегелен / О.Н. Ляхова, С.Н. Лукашенко, Н.В Ларионова // //[Сборник трудов Института радиационной безопасности и экологии за 2007 – 2009гг.] / под рук. Лукашенко С.Н. – Вып. 2. – Павлодар: Дом печати, 2010. – С. 331-354.: ил.- Библиогр.: с. 224-231. - ISBN 978-601-7112-28-8.
6. Yu. Yegorov. Tritium in nature - man-made environment of NPP - Regional Environment N1-2. 2002 / Yu. Yegorov. [in Russian]
   Егоров Ю.А. Тритий в природно - техногенной среде АЭС - окружающая среда, Региональная экология N1-2.2002 / Ю.А. Егоров. – С. 13.
7. V. M. Gorbachev. The interaction of radiation with the nuclei of heavy elements and fission: a handbook / V.M. Gorbachev, Yu. S. Zamyatin, A. A. Lbov. - Moscow: Atomizdat, 1976. [in Russian]
   Горбачев В.М. Взаимодействие излучений с ядрами тяжелых элементов и деление ядер: справочник / В.М. Горбачев, Ю.С. Замятин, А.А. Лбов. – Москва: Атомиздат, 1976.
8. "NuclidKarte" Kernforschugszentrum Karlsruhe. – Nov, 1981.
9. IAEA-NDS-CD-05 EXFOR CD-ROM. – Version: 2000. January.
10. L.L. Perchuk, // Soros Educational Journal. - 1997. [in Russian]
    Перчук Л.Л. // Соросовский образовательный журнал. – 1997. - №6. – С. 56-63.
11. L.R. Kimel. Protection against Ionizing Radiation: A handbook / L.R. Kimel, V. P. Mashkovich. - Moscow: Atomizdat, 1972. [in Russian]
    Кимель Л.Р. Защита от ионизирующих излучений: справочник / Л.Р. Кимель, В.П. Машкович . – Москва: Атомиздат, 1972.
12. G.N. Romanov, The behavior of tritium in the environment and biological effects. Radioecology problems / G.N. Romanov. - Moscow: VINITI, 1983. [in Russian]
    Романов Г.Н. Поведение в окружающей среде и биологическое действие трития Проблемы радиоэкологии / Г.Н. Романов. – М.: ВИНИТИ, 1983.
13. O. N. Lyakhova. "Investigation of tritium of in the environment within Degelen site" / O. N. Lyakhova, S. N. Lukashenko, M.A. Umarov, A.O. Aidarkhanov // Bulletin of NNC. - 2007. - Issue 4. [in Russian]

Ляхова О.Н. "Исследование содержания трития в объектах окружающей среды на территории испытательной площадки Дегелен" / О.Н. Ляхова, С.Н. Лукашенко, М.А. Умаров, А.О. Айдарханов // Вестник НЯЦ РК. – 2007. – Вып.4. – С.80 – 86.

14. Database of nuclear tests. USSR 1949-1990 [e. resource] / PHP- Nuke Copyright by Francisco Burzi, 2005 - . –http//www.sonicbomb.com
15. Soviet Nuclear Testing / ed. by V.N. Mikhailov. - M., 1997. [in Russian] Ядерные испытания СССР / под ред. В.Н. Михайлова. - М., 1997. - 467с.
16. S.B. Subbotin. "Assessment of possibilities for catastrophic events at "Balapan" site" / S.B. Subbotin, S.N. Lukashenko et al. // [Proceedings of the Institute of Radiation Safety and Ecology for 2007-2009] / Ed. by Sergey N. Lukashenko. – Issue 2 / – Pavlodar: Dom Pechati LLP" printing house, 2010. [in Russian] Субботин С.Б. Оценка возможности последствий катастрофического характера на территории площадки "Балапан" / С.Б. Субботин, С.Н. Лукашенко [и др.]. // [Сборник трудов Института радиационной безопасности и экологии за 2007 – 2009гг.] / под рук. Лукашенко С.Н. – Вып. 2. – Павлодар: Дом печати, 2010. – С. 401-450.: ил.- Библиогр.: с. 224-231. - ISBN 978-601-7112-28-8.

ТРИТИЙ ЯДРОЛЫҚ СЫНАҚТАР ӨТКІЗІЛГЕН ЖЕРЛЕРДІҢ ИНДИКАТОРЫ РЕТІНДЕ

Ляхова О.Н., Лукашенко С.Н., Ларионова Н.В., Субботин С.Б.*, Мульгин С.И., Жданов С.В.**

**** ҚР ҰЯО Радиациялық қауіпсіздік және экология институты, Курчатов, Қазақстан***
***** ҚР ҰЯО Ядролық физика институты, Алматы, Қазақстан***

Қазіргі уақытта, Ядролық қаруды таратпау жөніндегі келісім-шартқа қол қойылғалы бері, ядролық жарылыстар өткізілген жерлерді шынайы верификациялау жайлы мәселе өзекті болып тұр.

Бұл жұмыста, жерасты ядролық жарылыстары өткізілген жерлерді верификациялаудың жаңа әдісін қарастыруда, тритийді индикатор ретінде пайдалану ұсынылады. Ауа ортасындағы тритийдің құрамын толық зерттеу – ССП аумағында орналасқан, "Дегелең" алаңы мен "Балапан" сынақ алаңдарындағы жерасты ядролық сынақтар өткізілген жерлерде жасалды.

Жұмыс барысында, ұңғымалардың сағалары орналасқан жерлерде және штольняның порталында, сонымен қатар ЖЯЖ өткізілген жерлердің сағалық телімдерінде, жарылыстардың эпиорталығы орналасқан аймақтарда – ұңғымалар мен штольнялар орналасқан жеріндегі ауа ортасында тритийдің таралу сипаты мен құрамының деңгейі бойынша деректер келтірілген. Жерасты ядролық жарылыстарының өткізілгендігін нақтылайтын деректі және орнын анықтау мақсатында тритийді пайдалану мүмкіндігі көрсетілді.

Түйін сөздер: ядролық жарылыстар, верификация, "Дегелең" алаңы, "Балапан" алаңы, тритий, атмосфералық ауа, топырақ ауасы, тритиймен ластану, тритийдің таралу сипаты.

ТРИТИЙ КАК ИНДИКАТОР МЕСТ ПРОВЕДЕНИЯ ЯДЕРНЫХ ИСПЫТНИЙ

Ляхова О.Н., Лукашенко С.Н., Ларионова Н.В., Субботин С.Б.*, Мульгин С.И., Жданов С.В.**

****Институт Радиационной Безопасности и Экологии НЯЦ РК, Курчатов, Казахстан***
*****Институт ядерной физики НЯЦ РК, Алматы, Казахстан***

В настоящее время в связи с существованием Договора о нераспространении ядерного оружия, весьма актуальным является вопрос о достоверной верификации мест проведения ядерных взрывов.

В данной работе предлагается рассмотреть новый метод верификации мест проведения подземных ядерных взрывов с использованием трития в качестве индикатора. Подробные исследования содержания трития в воздушной среде проведены в местах проведения подземных ядерных испытаний – это испытательная площадка "Балапан" и площадка Дегелен, расположенных на территории бывшего Семипалатинского Испытательного полигона (СИП).

В работе представлены данные по уровню содержания и характеру распространения трития в воздушной среде в месте расположения штолен и скважин - в зонах эпицентра взрывов, в местах расположения устья скважин и портала штолен, а так же на приустьевых участках мест проведения подземных ядерных взрывов (ПЯВ). Показана возможность использования трития с целью определения мест и подтверждения факта проведения ПЯВ.

Ключевые слова: ядерные испытания, верификация, площадка Дегелен, площадка "Балапан", тритий, атмосферный воздух, почвенный воздух, тритиевое загрязнение, характер распределения трития.

УДК 577.391:577.4:504.74:636.32/.38:539.16

TRANSURANIC ELEMENTS IN THE BODIES OF FARM ANIMALS AT BREEDING THEM IN CONDITIONS OF "DEGELEN" SITE

Panitskiy A.V., Baigazinov Zh. A., Lukashenko S. N., Koval A. V.

[1]Institute of Radiation Safety and Ecology NNC RK, Kurchatov, Kazakhstan
[2]Institute of Nuclear Physics NNC RK, Almaty, Kazakhstan

The article presents the results of field experiments on sheep performed on the radioactively contaminated territory of "Degelen" testing site of the former Semipalatinsk Test Site (STS). The research determined the nature of distribution of transuranic radionuclides in the bodies of experimental animals. There were obtained transfer factors of ^{241}Am and $^{239+240}$Pu into animal products (mutton), needed to predict concentrations of these radionuclides when assessing the feasibility of releasing the STS territory for economic use.

Keywords: transfer factor (Tf), sheep, farm products, koumiss, the Semipalatinsk Test Site (STS), transuranic elements, plutonium -239+240 ($^{239+240}$Pu), and americium-241 (^{241}Am).

INTRODUCTION

These investigations were carried out in the framework of the stage 01.01.01. "*Investigations of ecosystems subjected to impact of radioactively-contaminated waterways*", task 01.01. "*Studying of the current state and consequences of operation of the nuclear power industry objects on the Semipalatinsk Test Site on the environment"* of the scientific-technical program 004 "Applied scientific- technical investigations of the fuel-and-energy complex, petrochemistry and mineral resources", action 1, "Implementation of the scientific-technical program of the nuclear power industry development in the Republic of Kazakhstan" in 2009-2011.

Complex investigations of the possibility of transfer of some STS territories into economic usage are currently under way. However, to obtain a comprehensive assessment of the safety of potential territory transfer it is necessary to get additional experimental data to forecast possible radionuclide concentrations in agricultural products in case they are produced on the studied area. The quantities in the IAEA database were obtained by the results of investigations on the territories located in the natural conditions different from those on the STS territory with an absolutely different type of radionuclide contamination caused, as a rule, by radiation accidents. Literature sources practically have no information about the transfer factors into agricultural products typical for the region such as horse-flesh and koumiss, which occupy an important place in the food basket of the local population. There is no information on the transfer factors for transuranic radionuclides $^{239+240}$Pu and ^{241}Am into vegetal and animal agricultural products. Investigations in the "experimental farms" aimed at getting prognostic values of radionuclide transfer into animal products are of high practical importance for assessing dose rates of the population living on the STS and adjacent territories.

Taking into account ^{241}Am activity caused by decay of ^{241}Pu as well as half-life values of transuranic elements in the long-term future (hundreds of years), the importance of radionuclides in formation of radiation environment on the STS and adjacent territories will increase.

The problems of quantitative transfer of transuranic elements into animal products depending on duration and forms of their intake by animals have not been solved yet. The scientific world still has very few investigations devoted to plutonium and americium transfer, their main results are included in the IAEA database [1], and some of them are presented in the table (*Table 1*).

Table 1.

Coefficients of radionuclide transfer into sheep's muscular tissue

Radionuclide	min	Max	Total works
Pu	2.0×10^{-5}	8.5×10^{-5}	2
Am	4.8×10^{-4}		1

1. METHODS AND MATERIALS

Place of investigations. The investigations were carried out on the experimental Degelen si*te* located in the southern part of the former STS. For the purposes of investigations we chose the tunnel #177 with a water flow formed by the ground waters flowing from the former explosion cavity in the tunnel [2], bringing radioactive contamination to the environment, soil, water, vegetation and air. The area was chosen as one of the areas most contaminated with transuranic radionuclides $^{239+240}$Pu and ^{241}Am.

Objects of investigations. As tested animals we used sheep of Kazakh fat-tail coarse-haired breed (*Edilbayevskaya*). All animals had similar clinical state and exterior type.

The choice of objects and the place of investigations are caused by the fact that sheep breeding is the main form of agricultural works in the region and most sheep-breeding farms on the STS territory are located near *Degelen* testing site [3] (Figure 1).

Procedure of investigations. The investigations were carried out in the conditions of sheep stabling in the vicinity of tunnel # 177. The animals were kept in the sheep-pens (4×4 m) with the exercise yard (10×10 m) to provide motion to animals. The animals were divided into two groups (group 1 and group 2) according to the conditions of radinuclide intake by the organism. The animals of groups 1 and 2 were fed by radioactively contaminated fodder (2 kg/day) and were watered by radioactively contaminated water (0.9-1.0 l/day). The animals in the second group in addition had radioactively contaminated soil in amount of 50 g/day in the ration. The duration of the experiment was determined by the scheme and was equal to 7, 14, 28, 56 and 112 days. When the time of pasturing was over, the animals were slaughtered, and tissue (muscle, bone, skin) and organs (heart, liver, lungs, kidney) samples were taken for radionuclide analyses.

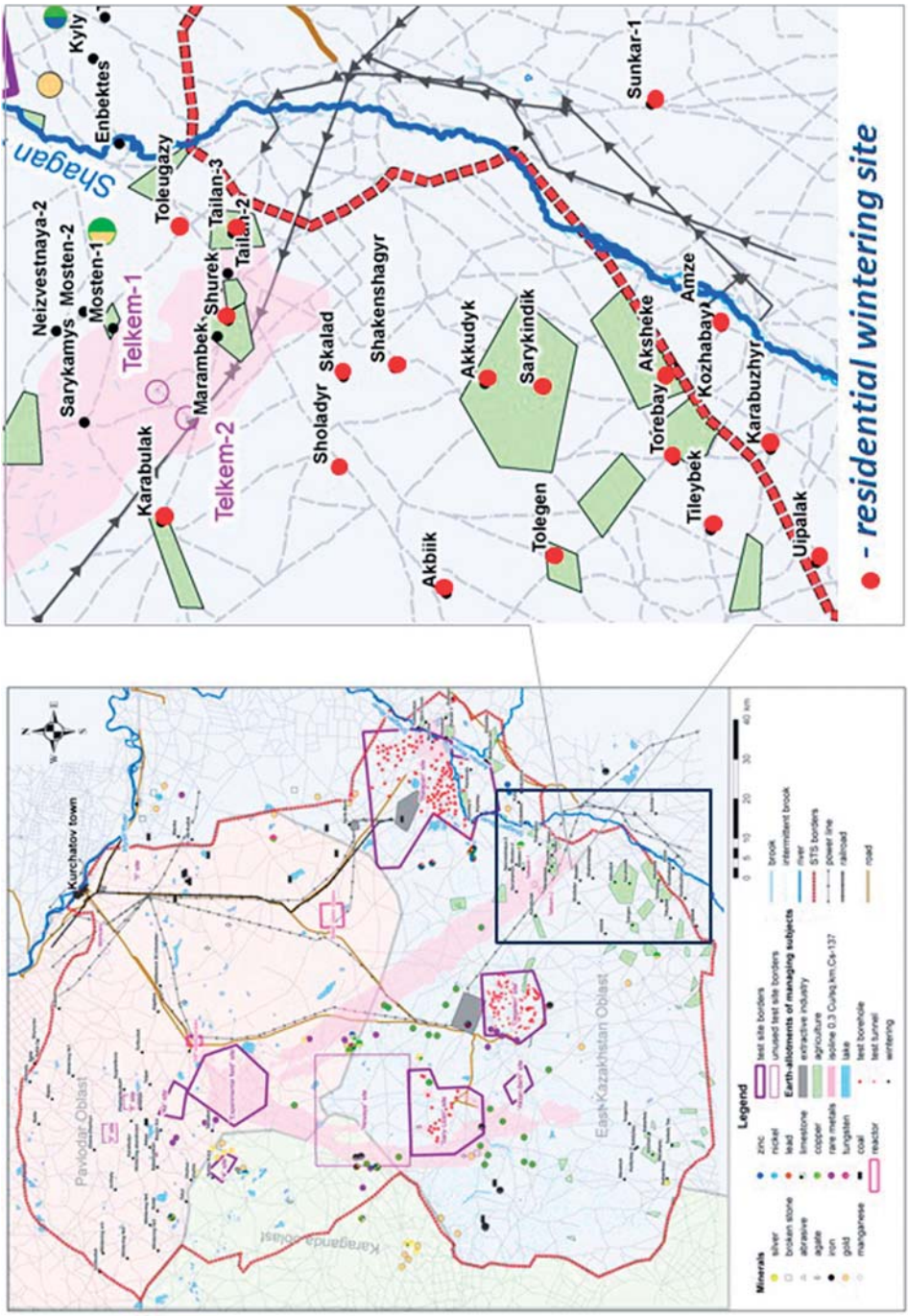

Figure 1. Inhabited winter-houses located in the STS southwestern part

In the experimental investigations with animals we used the scheme of scientific experiments based on the principles of groups-periods and pairs-analogues [4]. To estimate general physical state of animals, every day they passed clinical examination. The animals were not given additional feeding in the form of concentrated fodder or other types of fodder.

The vegetation was mowed along the banks of the radioactively contaminated stream (at a distance of up to 180–200 m from the beginning of the stream flowing from tunnel #177, at a distance of 2m from the waterway riverbed). The water for watering was taken from the beginning of the stream riverbed flowing from under the pile in tunnel #177. The soil added to the animal fodder was also taken from the stream bank in the range 0-15 cm, cleaned from sod, sieved through a 1mm sieve and carefully homogenized.

Radionuclide analyses. Laboratory analyses determining radionuclide concentrations in the environmental samples were made according to the methodological instructions on tested laboratory equipment. ^{241}Am concentration was determined by the method used in [5], $^{239+240}$Pu concentration was determined by the radiochemical method [6, 7].

Analysis of water samples. 500 ml of the sample aliquot was taken and it was marked by ^{242}Pu isotope mark of certified activity. Then $^{239+240}$Pu was extracted using radiochemical methods, and its concentration in water was determined.

Analysis of vegetation and soil samples. Specific activities of radionuclides in soil and vegetation (unwashed) samples were measured according to the methodological instructions on tested laboratory equipment. The specific activities of radionuclide ^{241}Am were measured on gamma-spectrometer Canberra GX-2020, the specific activity of $^{239+240}$Pu was determined by radiochemical extraction with further measurements on Canberra alpha-spectrometer. The detection limit for ^{241}Am was 0.3 Bq/kg (for vegetation samples) and 1 Bq/kg (for soil samples) for $^{239+240}$Pu – 0.1 Bq/kg and 1 Bq/kg, respectively. The measurement error for ^{241}Am did not exceed 10–20 %, for $^{239+240}$Pu – 30%.

Skin tissue preparation. Skins were kept at room temperature in the laboratory premises for 7–8 days for souring (formation of putrefactive bacteria). Then the hair side, wool, was removed from skin. Cleaned skins were washed by water of room temperature from dirt, blood and lymph glueing fiber derma structure. The washed skin was cleaned from the hypodermic fatty layer, muscle layer and hypodermic cellular tissue with scalpel. After cleaning the skin was 3 times washed by distilled water and wrapped into clean dry gauze for drying. Then the skin was dried at a temperature of 250 °C for 96 hours, milled on the mill and placed in the weighted glass for measurement in the γ-spectrometer.

Preparation of hair cover (wool). The wool from the sheepskin was soaked in the washing powder solution for 2-4 hours, then washed 3 times for 20 minutes in the running water, after which rinsed 2 times in the distilled water. Then the wool was dried in the drying box at a temperature of 85°C. After drying the wool, if necessary, was cleaned from foreign particles. Further the wool was dissolved in the concentrated nitric acid to the state of complete decomposition, and the obtained solution was subjected to the γ-spectrometric analysis.

Preparation of soft tissues and organs. The internal organs and muscle tissue were carefully grinded to paste, placed into a preliminary weighted plastic glass, weighted on scales, after which their sample mass and geometrical parameters (height, diameter) were determined, and the sample was measured on the γ-spectrometer. In order to determine the concentration of plutonium isotopes the biological samples were subjected to radiochemical decomposition by placing in the nitric acid, combusting in the muffle furnace, and dissolving

the ash. According to the method described in [3] plutonium isotopes were precipitated from the obtained solution on the membrane filters, and the obtained sources of alpha-radiation were analyzed according to the technique presented in [7].

Gamma-spectrometric analysis of bioassays. To determine concentration of gamma-radiating radionuclide ^{241}Am in the samples of biological objects we used gamma-spectrometric facilities with planar (BE 2020) germanium detector "Canberra". The detection limits were calculated based on the preparation geometry and measurement time and were estimated as < 0.2 Bq/kg.

For energy calibration of spectrometers we used a set of standard γ-sources, for geometry calibration we used a special measure of activity concentration per unit of volume containing the following radionuclides: ^{40}K, ^{137}Cs, ^{152}Eu, ^{232}Th, ^{241}Am.

The measurements were made according to the instructions for making measurements on gamma-spectrometer No.5.06.001.98 RK [5].

Alpha-spectrometric analysis of bioassays. $^{239+240}$Pu concentration in biological samples (sheep's organs and tissues) was determined on the alpha-spectrometer "Alpha Analyst" manufactured by "Canberra". In the 20-gram samples prepared from sheep's organs the detection limit for $^{239+240}$Pu was < 0.1 Bq/kg.

Assessment of radionuclide concentration in fodder, water and soil

To estimate radionuclide concentration in the vegetation fodder, for a week, daily, 300 g of vegetation were taken from the daily mass of the radioactively contaminated fodder, and a vegetation sample of 2.1 kg in mass (300 g×7 days) was formed and further used for determining radionuclide composition. The plants were given for radiochemical analyses and analyzed without washing. The results of measuring radionuclide concentration in the vegetation fodder for each week-period (16 weeks) of the experiment are presented in the table (Table 2).

Table 2.

Radionuclide concentration in vegetation used to feed experimental animals

№	Radionuclide specific activity, Bq/kg	
	^{241}Am	$^{239+240}$Pu
1	<1.4	20±2
2	11±4	26±2
3	<1.4	25±3
4	<1.2	7±2
5	<1.3	0.5±0.2
6	<1.2	0.8±0.2
7	<1.2	5±1
8	<1.2	30±10
9	5±2.5	8±1
10	<1.2	5±1
11	<1.4	6±1
12	<1.3	40±8
13	<1.3	4±1
14	<1.2	10±1
15	12±2	0.9±0.4
16	<1.2	20±2
average	2.8	13

The values of $^{239+240}$Pu specific activity in the vegetation fodder varied within 0.5–30 Bq/kg (Table 2).

Based on the vegetation samples characterizing weekly stages of the experiment we calculated daily average intake for every animal taking into account weekly dynamics (*Table 4*).

^{241}Am activity in all samples was lower than 1.4 Bq/kg, only in three samples it was 5, 11 and 12 Bq/kg. In calculating the mean arithmetic value the lower detection limit was taken as a significant value. Thus, the mean arithmetic value was 2.8 Bq/kg.

^{241}Am specific activity in all samples of water effluent from tunnel #177 is below 1.5 Bq/kg, $^{239+240}$Pu – within <0.001-2.14 Bq/kg. The mean arithmetic value is 0.8 Bq/kg (Table 3).

Table 3.

Radionuclide concentration in water and soil used in the ration of experimental animals

№	Radionuclide specific activity, Bq/kg			
	^{241}Am	$^{239+240}$Pu	^{241}Am	$^{239+240}$Pu
	water		soil	
1	<1.5	2.14±0.26	900±30	11650±185
2	<1.5	0.08±0.03	1080±30	10000±150
3	<1.5	0.14±0.001	870±30	16200±90
average	**<1.5**	**0.8**	**950**	**12550**

The results of γ–spectrometric and radiochemical analyses of soil samples showed that specific activity of radionuclides ^{241}Am and $^{239+240}$Pu was, on average, 950 Bq/kg and 12600 Bq/kg, respectively (Table 3).

Assessment of the average daily radionuclide intake by experimental animals

Based on the data on radionuclide concentration in vegetation, water and soil we calculated the average daily radionuclide intake by animals. The table (Table 4) shows average daily radionuclide intake by animals in groups 1 and 2.

Table 4.

Daily radionuclide intake in group No. 1 and group No. 2

Intake $^{239+240}$Pu. Bq	Duration of the experiment. days									
	Group 1					Group 2				
	7	14	28	56	112	7	14	28	56	112
Daily intake with water	0.8	0.8	0.8	0.8	0.8	0.8	0.8	0.8	0.8	0.8
Daily intake with fodder	60.0	69.0	58.5	42.9	39.0	60.0	69.0	58.5	42.9	39.0
Daily intake due to soil	-	-	-	-	-	627.5	627.5	627.5	627.5	627.5
Daily average intake	60.8	69.8	59.3	43.7	39.8	688.3	697.3	686.8	671.2	667.3
Intake ^{241}Am. Bq	**Duration of the experiment. days**									
	Group 1					Group 2				
	7	14	28	56	112	7	14	28	56	112
Daily intake with water	<1.5	<1.5	<1.5	<1.5	<1.5	<1.5	<1.5	<1.5	<1.5	<1.5
Daily intake with fodder	8.4	8.4	8.4	8.4	8.4	8.4	8.4	8.4	8.4	8.4
Daily intake due to soil	-	-	-	-	-	50	50	50	50	50
Daily average intake	8.4					58.4				

Therefore, based on the calculation of daily radionuclide intake by sheep of group No.1 one can state that the main faction of $^{239+240}$Pu is taken with vegetation fodder. The water fraction does not exceed 3 % (Figure 2).

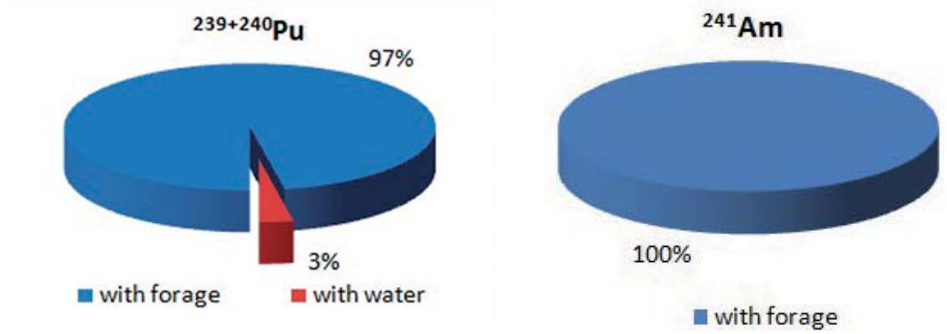

Figure 2. Water, fodder and soil contributions to the daily radionuclide intake in group No. 1

Based on the calculation of daily radionuclide intake by sheep of group No.2 it was determined that the main fraction of $^{239+240}$Pu and ^{241}Am intake came with soil, whereas fodder and water contribution to daily radionuclide intake did not exceed 13% (Figure 3).

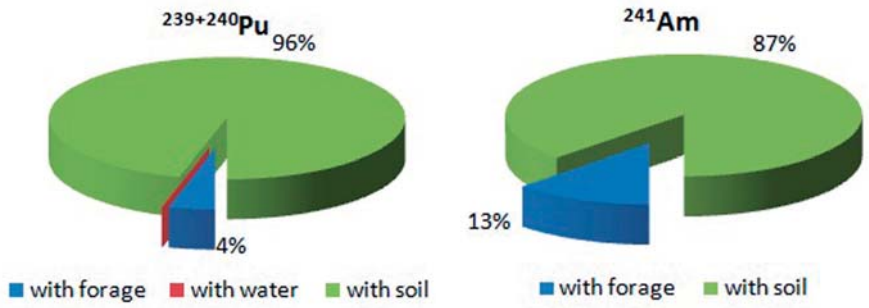

Figure 3. Water, fodder and soil contribution to daily radionuclide intake in group No.2

3. RESULTS AND DISCUSSION

3.1. Specific features of $^{239+240}$Pu transfer into sheep body

$^{239+240}$Pu contents in the organisms of experimental animals. The table (Table 5 below) shows the data of $^{239+240}$Pu specific activity in sheep's organs and tissue for different periods of its intake with different components of the environment.

Table 5.

$^{239+240}$Pu specific activity in sheep's organs and tissue for different periods of its intake with different components of the environment

Organs and tissues	*At daily average intake with fodder and water (Group 1)*					*At daily average intake with fodder and water (Group 2)*				
	Days of observation					Days of observation				
	7	14	28	56	112	7	14	28	56	112
	Specific activity $^{239+240}$Pu in organs, Bq/kg									
heart	< 0.019	< 0.013	< 0.015	< 0.024	0.0220	< 0.014	0.0380	< 0.015	0.0140	0.0120
liver	< 0.007	0.0130	0.1120	-	0.1390	0.0900	0.3670	0.4600	0.9090	-
kidney	< 0.028	< 0.023	< 0.024	0.0580	0.0740	0.0490	0.1330	0.0910	0.1380	0.1210
lungs	0.0170	< 0.007	-	0.0260	0.0110	0.0230	-	0.0230	0.0300	0.0430
spleen	< 0.022	< 0.096	< 0.065	< 0.071	0.0650	< 0.033	0.0790	< 0.035	0.0720	0.2570
muscles	< 0.0048	0.0051	0.0069	0.0070	0.0031	0.0049	0.0125	0.0084	0.0162	0.0025
skin	0.1560	0.0550	0.0440	0.0500	0.0850	0.2390	0.1860	0.2590	0.0650	0.2220
wool	0.6000	0.6900	0.1100	0.2700	0.4900	1.3600	2.1900	2.0	1.99	2.20
Note: measurement error of less than 30%										

The maximal $^{239+240}$Pu specific activity was registered in wool independent of the feeding period and ration components. As it could be expected the highest concentrations of $^{239+240}$Pu in "soft" organs were registered in liver. The activities of other organs were 2-3 times less than that of liver.

$^{239+240}$Pu distribution in sheep's organisms. Maximal radionuclide concentrations were registered in wool. Little difference between values of $^{239+240}$Pu specific activity within each group excludes possibility of bad wool washing. Maximal $^{239+240}$Pu concentrations in wool registered for all experimental animals in each group show a possibility of making rough forecasts of $^{239+240}$Pu presence in other tissues by its presence or absence in wool. In this case there is no ned to kill animals to take samples. The ratio of specific activity in wool to specific activities in tissues and organs clearly demonstrates such possibility. The table gives the average values of ratios of specific activity in wool to specific activities in tissues and organs of experimental animals.

Table 6.

Ratio of specific activity in wool to specific activities in tissues and organs

Organ or tissue	Spec.activity in wool/spec.activity of organs and tissues
heart	75.0
liver	11.3
kidney	10.2
lungs	41.3
spleen	14.4
muscles	187.8
skin	9.1

The table (Table 7) presents $^{239+240}$Pu distribution in sheep's organs and tissues after 112 days of its intake with fodder and water expressed as a relative concentration in tissues and organs in percentage of daily intake.

Table 7.

$^{239+240}$Pu distribution in sheep's organs and tissues after 112 days of its intake as percentage of daily intake

Organs and tissues	$^{239+240}$Pu relative concentration in organs and tissues, %		$^{239+240}$Pu relative concentration on Group 1. / $^{239+240}$Pu relative concentration on Group 2.
	With fodder and water (Group 1.)	At intake with fodder, water and soil (Group 2.)	
heart	0.055	0.002	27.5
liver	0.349	-	-
kidney	0.186	0.018	10.3
lungs	0.028	0.006	4.7
spleen	0.163	0.039	4.2
muscles	0.008	0.0004	20
skin	0.214	0.033	6.5
wool	1.231	0.330	3.7
average	0.25	0.053	**11**

The table data (Table 7) and the ratios of relative concentrations of $^{239+240}$Pu intake with fodder and water to relative concentrations of $^{239+240}$Pu intake with fodder, water and soil show that $^{239+240}$Pu taken with fodder and water is, on average, 10 times better assimilated than $^{239+240}$Pu taken with soil. It can be explained by the fact that plants contain $^{239+240}$Pu in mobile or exchange state, i.e. easily accessible state and, hence, easily assimilated, whereas in soil most of fixed $^{239+240}$Pu taken into account in calculating the average daily intake may be in the tightly-bound state, i.e. the state inaccessible for plants. It may explain the low percentage of $^{239+240}$Pu transfer taken with soil.

Specific features of $^{239+240}$Pu transfer in different conditions and intake periods. The figure (Figure 4) shows factors of $^{239+240}$Pu transfer into skin, wool, muscle tissues, liver, lungs, heat, spleen of sheep in groups 1 and 2 fed by different components from the ecosystems of waterways from Degelen tunnels. The results of the experiment shows that in the conditions of long-term daily inflow of $^{239+240}$Pu to sheep's organisms with various components of the environment, the $^{239+240}$Pu concentration in organs does not increase and the accumulation process does not depend on the intake time. A positive dynamics of accumulation is registered only in liver, where at first stages $^{239+240}$Pu transfer is more intensive and with further decrease in the rate of accumulation decreases to the equilibrium state (Figure 4).

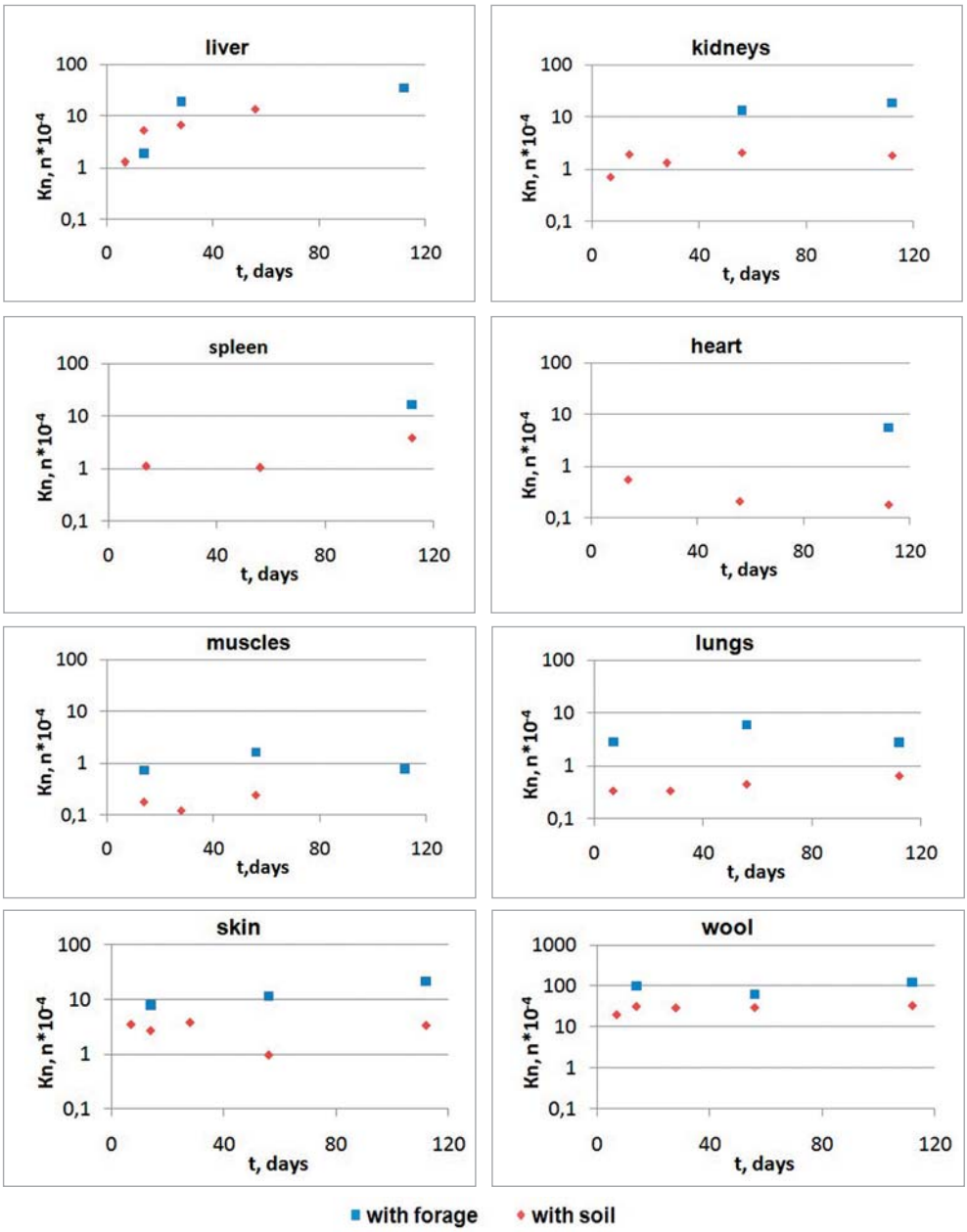

Figure 4. Dynamics of $^{239+240}$Pu transfer into sheep's organs and tissues (groups 1 and 2)

The range of factors of $^{239+240}$Pu transfer obtained in the investigations and their average values are presented in the table (Table 8).

Table 8.

Coefficients of $^{239+240}$Pu transfer into tissues and organs of experimental animals

Organs and tissues	Intake with fodder and water, ×10^{-3}				Intake with fodder, water and soil, ×10^{-3}			
	max	min	total samples	average	max	min	total samples	average
heart	0.55		1	0.55	0.05	0.02	3	0.03
liver	3.49	0.19	3	1.85	1.35	0.13	4	0.67
kidney	1.86	1.33	2	1.59	0.21	0.07	5	0.16
lungs	0.59	0.28	3	0.38	0.06	0.03	4	0.04
spleen	1.63		1	1.63	0.39	0.11	3	0.20
muscles	0.16	0.07	4	0.11	0.02	0.004	5	0.01
skin	2.57	0.74	5	1.48	0.38	0.10	5	0.28
wool	12.3	1.86	5	8.02	3.30	1.98	5	2.86

It is seen that the critical organ for estimation of possible $^{239+240}$Pu intake with sheep-breeding products is liver, and it must be taken in account in regulation of this radionuclide concentration in the daily sheep ration.

In our investigations the summarized activity of tissues and organs of animals of group 2 can be calculated as follows:

$$A_{organ} = C_{fodder} \quad Ct_{fodder} + C_{soil} \quad Ct_{soil} \tag{1}$$

where A_{organ} is activity of an organ or tissue; C_{fodder} is a daily average intake with ration, Ct_{fodder} is a transfer factor from fodder, C_{soil} is a daily average intake with soil, Ct_{soil} is a transfer factor from soil.

Based on the equation (1) and using the data obtained in the investigation, one can calculate Ct from soil into animal tissue and organs by the following relation:

$$Ctsoil = \frac{A_{organ} - C_{org.} \; Ctn_{fodder}}{C_{soil}} \tag{2}$$

Based on the above considerations we obtained the following values of radionuclide transfer factors from soil Ct (Table 9).

Table 9 .

Factors of $^{239+240}$Pu transfer from soil into tissues and organs of the experimental animals in group 2.

Organs and tissues	Average Ki at intake with fodder and water, ×10^{-3}	Assessed Ki at soil intake, ×10^{-3}
heart	0.55	-
liver	1.85	0.54

Organs and tissues	Average Ki at intake with fodder and water, $\times 10^{-3}$	Assessed Ki at soil intake, $\times 10^{-3}$
kidney	1.59	0.059
lungs	0.38	0.02
spleen	1.63	0.10
muscles	0.11	0.005
skin	1.48	0.17
wool	8.02	2.22

The obtained estimations of the factors of radionuclide transfer from soil into tissues and organs of animals in group 2 are 1-2 orders of magnitude lower than the average Ct for radionuclides intake with fodder and water, which must be taken into account in estimating possible radionuclide concentrations in the agricultural products in case they are produced on the radioactively contaminated area.

3.2. Studying of specific features of ^{241}Am transfer to sheep organisms

^{241}Am concentration in organisms of experimental animals. The table (Table 10) contains the data on specific activity of sheep's organs for different durations of ^{241}Am intake with different environmental components.

Table 10.

^{241}Am specific activity in sheep's organs and tissues for different durations of its intake with various components of the environment

Organs and tissues	Daily average intake with fodder and water 8,4 Bq/kg					Daily average intake with fodder, water and soil 58,4 Bq/kg				
	Duration, days					Duration, days				
	7	14	28	56	112	7	14	28	56	112
	Activity of organs, Bq/kg									
heart	< 0.36	< 0.19	0.46	< 0.23	< 0.21	0.42	0.34	0.54	0.32	< 0.27
liver	< 0.38	no	< 0.28	0.58	< 0.28	< 0.21	< 0.34	0.56	< 0.26	0.42
kidney	< 0.43	< 0.21	< 0.23	< 0.25	< 0.27	0.56	0.57	< 0.24	< 0.25	< 0.32
lungs	< 0.39	no	0.32	< 0.27	0.30	no	0.45	0.29	< 0.28	< 0.30
spleen	0.48	< 0.56	0.74	< 0.41	< 0.46	< 0.30	0.68	0.32	0.29	< 0.51
muscles	< 0.42	no	< 0.26	< 0.26	0.32	0.33	< 0.25	< 0.23	< 0.27	< 0.24
skin	< 0.10	< 0.10	< 0.10	< 0.10	< 0.10	< 0.10	< 0.10	< 0.10	< 0.10	< 0.10
wool	no	no	no	no	no	no	no	no	no	no

In the majority of cases, ^{241}Am specific activity in organs and muscle tissues was below the detection limit. The investigations did not detect any organ depositing ^{241}Am, which can be explained by low radionuclide concentrations taken by the organism. An analysis of the results shows that registered quantitative values are specified by the errors of the measuring equipment. Therefore, the available data only enable to give an estimation of maximal possible factors of ^{241}Am transfer into sheep's organs and tissues. The table (Table 11) shows the results of estimations of the factors of ^{241}Am transfer into sheep's organs and tissues.

Table 11.

Factors of ^{241}Am transfer into sheep's organs and tissues

Organs and tissues	Intake with fodder and water, $\times10^{-3}$		Intake with fodder, water and soil, $\times10^{-3}$	
	Ki	Total samples	Ki	Total samples
heart	<54.8	5	<9.3	5
liver	<69.1	4	<9.6	5
kidney	-*	-	<9.8	4
lungs	<38.1	5	<7.7	5
spleen	<88.1	4	<11.6	5
muscles	<38.1	5	<5.7	5
Note: "–" no data				

3.3. Assessment of permissible concentration of transuranic elements in sheep ration

Based on the obtained quantities characterizing transfer of $^{239+240}$Pu and ^{241}Am radionuclides, one can calculate the permissible daily intake of these radionuclides with ration. However, the permissible levels of radionuclides concentrations in food stuffs are not regulated by any documents. Though concentrations of $^{239+240}$Pu and ^{241}Am in food stuffs are not regulated, taking into account that in NRB-99 (Appendix P-2) the limit of yearly intake of $^{239+240}$Pu and ^{241}Am with food for people is an order of magnitude lower than that for ^{90}Sr ($^{239+240}$Pu –2.4*10^3 Bq/year, ^{241}Am – 2.7*10^3 Bq/year, ^{90}Sr – 1.3*10^4 Bq/year) and taking account of their high radiotoxicity, one can suppose that their permissible levels must be an order of magnitude lower than those for ^{90}Sr [1]. According to SanPiN 4.01.071.03 [2] the permissible ^{90}Sr concentration in meat of domestic animals is 50 Bq/kg. Hence, the permissible concentration of $^{239+240}$Pu and ^{241}Am in meat of domestic animals can be taken as 5 Bq/kg. This value can be used for the internal organs (liver, kidney, etc.).

The limit of radionuclide concentration in sheep ration (maximal permissible concentration) can be estimated from the relation:

$$MPC = PSA/Ct, \quad (3)$$

where PSA is a permissible specific activity (PSA) of radionuclides in agricultural products, Ct is the factor of radionuclide transfer.

As liver is a critical organ with respect to other tissues and organs eaten by people, the calculation uses maximal radionuclide Ct from ration to liver. For $^{239+240}$Pu the factor of radionuclide transfer into liver is 3.5*10^3, for ^{241}Am – <6.9*10^{-2}.

Based on the above data, the permissible concentrations of transuranic radionuclides in the daily ration for durable feeding must be: 1430 Bq/day for $^{239+240}$Pu and <72 Bq/day for ^{241}Am. It means that for standard intake of the vegetation fodder on this type of pasture, 3 kg, the specific activity in vegetation must not exceed 476.6 Bq/kg for $^{239+240}$Pu and 24 Bq/kg for ^{241}Am.

As a whole, if liver is not taken as a critical organ, the radionuclide concentration in the daily ration for each type of animal products can be estimated according to the standards

presented in the table (Table 12). Based on the calculated permissible specific activities of vegetation and radionuclide transfer factors calculated before for the mixed-grass area Degelen [3], it is not difficult to calculate permissible specific activity of soil for meadow pastures, the excess of which will cause the excess of standards for sheep-breeding products (Table 12).

Table 12.

Permissible values for radionuclide concentration in the sheep's ration for different types of products

	Permissible values					
	Activity of radionuclides in sheep ration, Bq/day		Specific activity of vegetation, Bq/kg		Specific activity of soil at pasture, Bq/kg	
Organ	**$^{239+240}$Pu**	**^{241}Am**	**$^{239+240}$Pu**	**^{241}Am**	**$^{239+240}$Pu**	**^{241}Am**
heart	9050	<91	3020	30	$5.46*10^6$	$<5.56*10^2$
liver	**1430**	**<72**	**480**	**25**	**$1.37*10^5$**	**$<3.50*10^2$**
kidney	2690	<520	896	170	$4.82*10^5$	$<1.78*10^4$
lungs	8400	<130	2800	43	$4.71*10^6$	$<1.15*10^3$
spleen	3060	<60	1020	20	$6.25*10^5$	$<2.15*10^2$
muscle tissue	31200	<130	10400	43	$6.49*10^7$	$<1.15*10^3$

The table presents the results for all organs used as food, however, as it is stated above, the critical element is liver, we must use the results obtained for liver.

The values of specific activity in soil given in the table (Table 12) are localized in places of direct tests of nuclear weapons. These are the test grounds *"Experimental Field"* P-2, P-7, near-portal areas of tunnels with water flows on the Degelen si*te*. Therefore, pasturing around the territory of Degelen site and even inside the territory (with forbidden access to radioactively contaminated water ways) is possible without control of concentration of transuranic elements $^{239+240}$Pu and ^{241}Am.

CONCLUSION

- It has been established that woolen cloth is the main cloth depositing $^{239+240}$Pu. Among the internal organs the highest concentrations were registered in liver. The activities of other organs were 2-3 times lower than that of liver.
- It has been shown that in the conditions of prolonged daily $^{239+240}$Pu intake by sheep with different components of the environment, $^{239+240}$Pu concentration in skin, wool, heart, kidneys, lungs, spleen and muscle tissue does not increase, and the accumulation process does not depend on the intake period. $^{239+240}$Pu is accumulated only in liver.
- The obtained estimations of the factors of radionuclide transfer from soil into tissues and organs of animals in group 2 are 1-2 orders of magnitude lower than the average Ct for radionuclides intake with fodder and water, which must be taken into account in estimating possible radionuclide concentrations in the agricultural products in case they are produced on the radioactively contaminated areas.

- Transuranic radionuclides taken with soil are assimilated worse than those taken with fodder.
- The authors detected a possibility of controlling $^{239+240}$Pu presence in sheep-breeding products by its presence in wool without killing animals.
- The authors calculated permissible $^{239+240}$Pu and ^{241}Am content in the sheep's daily ration and permissible specific activity of radionuclides in vegetation and soil of potential pasturing areas. The obtained values show possibility of sheep pasturing on territories adjacent to the Degelen site not controlling $^{239+240}$Pu and ^{241}Am content in the sheep-breeding products.

REFERENCES

1. INTERNATIONAL ATOMIC ENERGY AGENCY, Quantification of radionuclide transfer in terrestrial and freshwater environments for radiological assessments, IAEA –TECDOC–1616. - Vienna: IAEA, 2009.
2. Ахметов М.А. Радиационный мониторинг водотоков и проблемы реабилитации на горном массиве Дегелен Семипалатинского испытательного полигона / М.А. Ахметов, О.И. Артемьев, Л.Д. Птицкая // Вестник НЯЦ РК Радиоэкология. Охрана окружающей среды. – 2000. - Вып.3 (9). - С.23-28.
   Akhmetov M.A. Radiation monitoring of streams and rehabilitation problems on Degelen massif of the Semipalatinsk Test Site / M.A. Akhmetov, O. Artemyev, L.D. Ptitskaya // Bulletin of NNC Radioecology. Protection of the Environment. - 2000. – Issue 3 (9). - P.23-28.
3. Отчет о научно-технической деятельности Института радиационной безопасности и экологии НЯЦ РК, выполненного по республиканской бюджетной программе 011 "Обеспечение радиационной безопасности на территории РК" Задание 1, Задача 1.2. "Мониторинг хозяйственной деятельности на территории СИП и прилегающих территориях" 2009 г.: отчет о НИР /рук. Лукашенко С.Н. –Курчатов: ИРБЭ, 2009. – 12 с.
   Report on the scientific and technical activities of the Institute of Radiation Safety and Ecology NNC carried out under the Republican Budgetary Program 011 "Radiation Safety in the territory of the RK" Objective 1, Task 1.2. "Monitoring of economic activity in the STS and adjacent areas" 2009: Report on R&D /headed by Lukashenko S.N. -Kurchatov: IRSE, 2009. – p.12.
4. Овсянников А.И. Основы опытного дела в животноводстве // А.И. Овсянников – М.: Колос, 1976. – 304 с.
   Ovsyannikov A.I. Fundamentals of experimental work in livestock farming / / A.I. Ovsyannikov - M.: Kolos, 1976. – p.304.
5. Активность радионуклидов в объемных образцах. Методика выполнения измерений на гамма - спектрометре: МИ 2143-91. - Введ. 1998-06-02. - Рег. № 5.06.001.98. – М.: НПО ВНИИФТРИ, 1991. - 17 с.

Activity of radionuclides in bulk samples. Methods of measurement on the gamma - spectrometer: MI 2143-91. – Introduc. 06/02/1998. - Reg. № 5.06.001.98. - M.: NPO VNIIFTRI, 1991. - 17 p.

6. Методические рекомендации по санитарному контролю за содержанием радиоактивных веществ в объектах внешней среды. - Введ. 1999. - Рег. №5.05.008.99.
   Guidelines for the sanitary control over the content of radioactive substances in the environment. – Introduc. 1999. - Reg. № 5.05.008.99.
7. СТП 17.66-92. Плутоний-238,239,240. Радиохимическая методика выделения из проб почвы и приготовления препаратов для альфа - спектрометрических измерений. Стандарт предприятия. Комплексная система управления качеством разработок.- Введ. 1993-01-02. – Санкт-Петербург: НПО "Радиевый институт им. В.Г. Хлопина", 1993. – 10 с.
   STP 17.66-92. Plutonium-238, 239.240. The radiochemical method of separation of soil samples and preparation of specimen for alpha - spectrometric measurements. Standard of the enterprise. A comprehensive quality management system of designs. - Introd. 02/01/1993. - St. Petersburg NGO "V.G. Khlopin Radium Institute", 1993. – p. 10.
8. Государственные санитарно-эпидемиологические правила и нормативы. Нормы радиационной безопасности (НРБ-99): СП 2.6.1. 758-99; ввод. в действие 01.01.2000. – Алматы: Агентство по делам Здравоохранения РК, 1999. - 80с. – ISBN 9965-501-42-4.
   The state sanitary and epidemiological rules and regulations. Radiation Safety Standards (NRB-99): SP 2.6.1. 758-99; put. into force 01.01.2000. - Almaty: RK Agency for Healthcare, 1999. – 80p. - ISBN 9965-501-42-4.
9. Санитарные правила и нормы №4.01.071.03 "Гигиенические требования к безопасности и пищевой ценности пищевых продуктов". Утверждены приказом министра здравоохранения Республики Казахстан от 11 июня 2003 г. № 447.
   Sanitary rules and norms № 4.01.071.03 "Hygienic requirements for safety and nutritional value of food". Approved by the Minister of Health of the Republic of Kazakhstan from June 11, 2003 № 447.
10. Ларионова Н.В. Особенности накопления техногенных радионуклидов растениями в районе штольневых водотоков площадки «Дегелен» / Н.В. Ларионова, С.Н. Лукашенко, А.М. Кабдракова [и др.]. // Актуальные вопросы радиоэкологии Казахстана [Сборник трудов Института радиационной безопасности и экологии за 2007 – 2009гг.] / под рук. Лукашенко С.Н. – Вып. 2. – Павлодар: Дом печати, 2010. – С. 301-320.: ил.- Библиогр.: с. 224-231. - ISBN 978-601-7112-28-8.
    Larionova N.V. Peculiarities of artificial radionuclides accumulation in at the area of tunnel watercourses of "Degelen" site / N.V. Larionova, S.N. Lukashenko, A.M. Kabydrakova [et al]. // Topical Issues in Radioecology of Kazakhstan [Proceedings of the Institute of Radiation Safety and Ecology for 2007 - 2009.] / ed. by Lukashenko SN - Issue 2. - Pavlodar: Printing House, 2010. - P. 301-320. Ill. - Ref.: P. 224-231. - ISBN 978-601-7112-28-8.

"ДЕГЕЛЕҢ" СЫНАҚ АЛАҢЫНЫҢ ЖАҒДАЙЫНДА АУЫЛ ШАРУАШЫЛЫҒЫ ЖАНУАРЛАРЫН ӨСІРУ БАРЫСЫНДА ОЛАРДЫҢ АҒЗАСЫНДАҒЫ ТРАНСУРАНДЫ ЭЛЕМЕНТТЕР

[1]Паницкий А.В., [1]Байғазинов Ж.А., [1]Лукашенко С.Н., [2]Коваль А.В.

[1]ҚР ҰЯО Радиациялық қауіпсіздік және экология институты, Қазақстан, Курчатов қ.
[2]ҚР ҰЯО Ядролық физика институты, Қазақстан, Алматы қ.

Мақалада, бұрынғы Семей сынақ полигонының (ССП) "Дегелең" алаңының радиоактивті-ластанған аумағында қойларға жүргізілген табиғи зерттеулердің нәтижелері келтірілген. Жұмыстардың нәтижесінде зерттеліп жатқан жануарлардың ағзасында трансуранды радионуклидтердің таралу сипаты анықталды. ССП аумағын шаруашылыққа пайдалануға беру мүмкіндігін бағалау барысында ^{241}Am және $^{239+240}$Pu шоғырлануын болжау үшін қажетті, ауыл шаруашылығы өнімдеріне (қой етіне) аталған радионуклидтердің өту коэфициенті алынды.

Түйін сөздер: өту коэффициенті (Өк), қойлар, ауылшаруашылық өнімі, қымыз, Семей сынақ полигоны (ССП), трансуранды элементтер, плутоний – 239+240 ($^{239+240}$Pu), америций-241 (^{241}Am).

ТРАНСУРАНОВЫЕ ЭЛЕМЕНТЫ В ОРГАНИЗМЕ СЕЛЬСКОХОЗЯЙСТВЕННЫХ ЖИВОТНЫХ ПРИ ИХ РАЗВЕДЕНИИ В УСЛОВИЯХ ИСПЫТАТЕЛЬНОЙ ПЛОЩАДКИ "ДЕГЕЛЕН"

[1]Паницкий А.В., [1]Байгазинов Ж.А., [1]Лукашенко С.Н., [2]Коваль А.П.

[1]Институт радиационной безопасности и экологии НЯЦ РК, Курчатов, Казахстан
[2]Институт ядерной физики НЯЦ РК, Алматы, Казахстан

В статье представлены результаты натурных исследований с овцами, проведенных на радиоактивно-загрязненной территории площадки "Дегелен" бывшего Семипалатинского испытательного полигона (СИП). В результате работ определен характер распределения трансурановых радионуклидов в организме исследуемых животных. Получены коэффициенты перехода ^{241}Am и $^{239+240}$Pu в продукцию животноводства (баранину), необходимые для прогноза концентраций этих радионуклидов при оценке возможности передачи территорий СИП в хозяйственное пользование.

Ключевые слова: коэффициент перехода (Кп), овцы, сельскохозяйственная продукция, кумыс, Семипалатинский испытательный полигон (СИП), трансурановые элементы, плутоний – 239+240 ($^{239+240}$Pu), америций-241 (^{241}Am).

УДК 577.4:504.064:551.49:539.16

IDENTIFICATION OF MIGRATION PATHS OF ARTIFICIAL RADIONUCLIDES BEYOND "BALAPAN" TEST SITE BOUNDARIES

[1]Subbotin S.B., [1]Lukashenko S.N., [1]Romanenko V.V., [1]Kashirsky V.V., [2]Pestov E.Yu., [3]Gorbunova E.M., and [4]Kuzevanov K.I.

[1] Institute of Radiation Safety and Ecology NNC RK., Kurchatov, Kazakhstan
[2] Institute of Geophysical Research NNC RK, Kurchatov, Kazakhstan
[3] Institute of Geosphere Dynamics, RAS, Moscow, Russia
[4] Institute of Geology and Oil and Gas Industry, Tomsk, Russia

The paper reports on the investigation of the nature of artificial radionuclide transport with groundwater from nuclear test locations at the Balapan test site. Based on the executed radioecological works, monitoring wells were arranged for long-term monitoring of groundwater condition. New data on levels of the radioactive contamination in groundwater both within the Balapan site and beyond its boundaries have been obtained. Conclusions have been drawn as to the migration pattern of artificial radionuclides with groundwater in the directions studied.

Keywords: groundwater, nuclear test, radionuclide migration, cesium-137, strontium-90, tritium, plutonium, geological structure and hydrogeological conditions at the Balapan site, regional faults, Shagan River, Karazhyra coal deposit.

INTRODUCTION

The migration of radioactive products of underground nuclear explosions (UNE) with groundwater beyond the Balapan test site boundaries is one of the key issues of radiation safety on the territory of the former Semipalatinsk Test Site (STS). The nature of radioactive contamination in groundwater and the conditions for further migration of artificial radionuclides with underground streams is governed by the geological structure and hydrogeological conditions of Balapan.

After the cessation of nuclear tests at STS, the NNC RK divisions in different years performed field and laboratory research to define the hydrogeological conditions and nature of radioactive contamination of groundwater at the Balapan site [1, 2]. One of the basic tasks was to identify possible migration paths of groundwater contaminated with artificial radionuclides. Meanwhile, most attention was directed to the identification of locations of groundwater discharge to the Shagan River water and investigation of the nature of migration of UNE radioactive products with groundwater by regional fault zones.

Integrated exploration to determine the concentration of artificial radionuclides in groundwater propagating within the test sites has become of paramount importance and timely owing to the intended commercialization of a part of STS. Prediction estimates on the radionuclide migration outside the UNE sites are necessary to properly evaluate safety of the territories to be involved in commercial activities. This paper presents the data of the various research within this field carried out by NNC RK in different years.

1. GENERAL INFORMATION ABOUT THE BALAPAN TEST SITE

1.1. Physiographic description of the area

Administratively, Balapan is a part of East Kazakhstan Region with an administrative center in the city of Ust-Kamenogorsk. The territory of interest is connected with the city of Semipalatinsk by a highway of 90 km length changing into an earth road of 40 km length. Balapan settlement is located in the north of the site, and 10–15 km to the west there is a railroad going from Kurchatov. The operations area is located in the eastern part of STS and occupies about 780 km^2 territory.

Geomorphologically, the Balapan site is confined to the north-eastern edge of Kazakh Upland or Central Kazakh low hills with generally weakly-dissected relief formed mainly during Quaternary period. The surveyed territory includes two morphogenetic types typical for the low hills: denudation-erosion and accumulative reliefs. In addition, artificial forms of relief are widely spread here due to the underground and above-surface nuclear tests, and construction of various-application facilities.

In the north and east of the area, a hillocky plain prevails with up to 12-20 m elevations. South-westward, the relief changes to the hummocky topography with 200-300 m absolute heights and 30–80 m local difference in elevation. The hillocky area contains uplifts and ridges divided by wide valleys and basins. Shallow salty lakes and solonchaks are confined to depressions. Sor-deflation declines and depressions are developed within the plain area. In the areas where clay of Neocene and Paleocene outcrops to surface there prevail heaving hummocks of 1m height and 2-3m in diameter.

The lakes are saline and biter, non-perennial. The biggest of them are Karazhireksor, Kishkeneksor and Kayaksu forming a typical deep isometric hollow in the midst of the plain surface of alluvial-proluvial terrace. The hydrographic network is developed poorly. The area contains several dry sais with temporary watercourses in spring and rainy periods falling into the local lakes. The Shagan River is the only water artery in the area and on some of its sections has permanent current.

1.2. Geological structure

The territory of STS makes a part of the eastern sector of broad Paleozoic Ural-Mongolian Belt. The well known fold structures within the study area belong to two main tectonic structures: Caledonian Chingiz-Tarbagataisky meganticlinorium and Herzinian Zaisansky fold structures. The border between the structures passes along the steeply-dipping deep Kalba-Chingizsky fault. The fold structures differ by not only the history of their development but also the age and structure of folded base complex. Brief description of them is given below.

Geological structure of the Balapan site (Figure 1) is stupulated by its location at the south-west slope of Zharminsky synclinorium formed into the Herzinian cycle of tectogenesis. In the south of the area, behind the Kalba-Chingizsky fault, caledonides of Chingiz-Tarbagataisky meganticlinorium outcrop as Middle Cambrian rocks broken by a big granite intrusion of Middle-Upper Carboniferous.

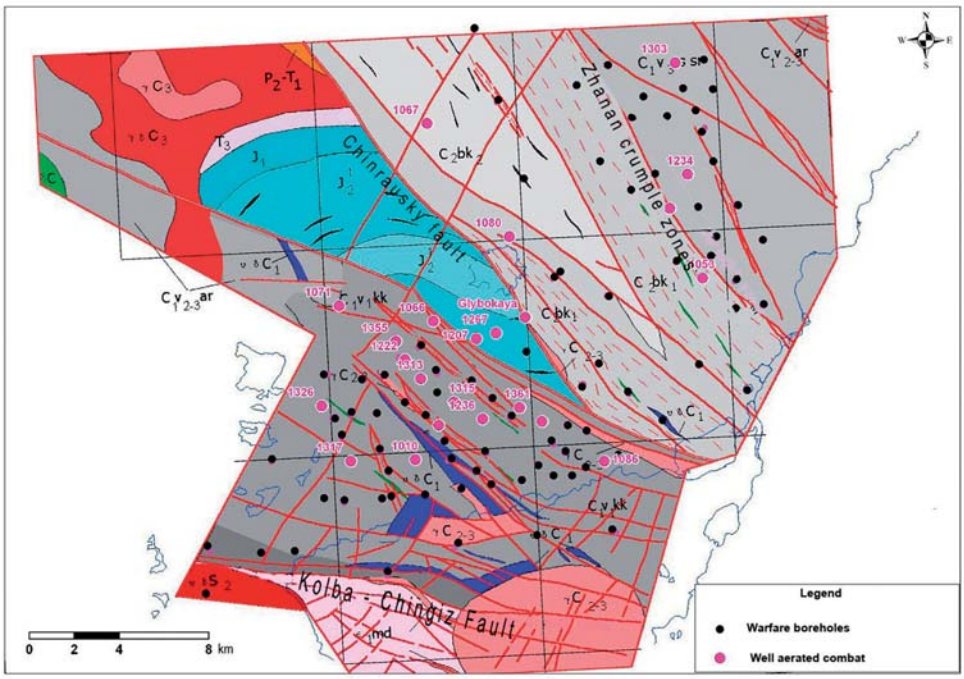

J_2^2 Middle	Upper stratum. Conglomerates, sandstones, siltstones	$\epsilon_2$md — Middle Cambrian, Maidan suite. Tuff- sandstones and tuffs of intermediate composition. siliceous schist and siltstones
J_2^1 Jurassic	Lower stratum. Conglomerates, sandstones, siltstones with interlayers and coal lentils	γC_3 — Upper Carboniferous granites
J_1	Lower Jurassic. Conglomerates, sandstones, siltstones	$\gamma, \gamma\delta C_{2-3}$ — Middel- Upper Carboniferous granites
T_3	Upper Triassic. Conglomerates, sandstones, siltstones	$\omega\delta C_1$ — Lower Carboniferous gabbrodiorite
P_2-T_1	Upper Permian - Lower Triassic, sandstones, siltstones	$\gamma\delta C_1$ — Lower Carboniferous granodiorite
C_2bk_2 Middle	Middle subsuite of Bukon suite. Conglomerates, sandstones, clay and carbonaceous siltstones with interlayers and coal lentils	δC_1 — Lower Carboniferous diorite
C_2bk_1 Carbon	Lower subsuite of Bukon suite. Conglomerates, sandstones, siltstones, tuffs of intermediate composition	$\gamma\delta S_2$ — Upper Silurian granodiorite
C_1 Lower	Serpukhovian Stage, Kokpekti suite. Conglomerates, sandstones, siltstones, tuffs of basic and intermediate composition	Lentils and coal seam
$C_1V_{2-3}ar$	Middle and Upper substage of the Visean stage, Arkalyk suite. Conglomerates, sandstones, siltstones, and limestones	Dykes of intermediate composition of Late Carboniferous age
C_1v_1kk Carbon	Middle substage of Tournaisian Stage and lower substage of Visean Stage, kokon suite. Conglomerates, sandstones, siltstones, limestones, tuff- sandstones, tuffs of basic and intermediate composition	

	Regional faults
	Minor faults
	Schistosity zone

Figure 1. Geological map of the Balapan site

Cambrian system. Middle division. The deposits of this age are combined into the Maidansky suite ($Є_2$md) divided into two strata: lower – volcanic-terrigenous and upper – siliceous-terrigenous. The thickness of sediments is up to 1120 m.

Carbonic system. Lower division.

Tournaissian stage. Koyandinsky suite (C_1tkn). The sediments are dislocated and crushed into linear folds subordinate to the general northwest direction with the dip angles of 30° to 70° on the wings. The rock is marked by the facies instability of section; due to the contact and dislocation metamorphism, the sediments are hornfelsed to various degree, silicified, quartzy and boudinaged, and have numerous white quartz and quart-carbonate interbeds and pyrite impregnations. The suite contains tuff, tuffite, tuff sandstone, tuff aleurites, sandstone, aleurite and schist intensively cracked and, sometimes, sheeted.

Viseian stage.

Lower Viseian substage. Kokonsky suite (C_1v_1kk). The rocks of Kokonsky suite spread in the southwest of the area, within the Chinrausky geoblock located between the Kalba-Chingizsky and Chinrausky faults. The contacts with the overlying strata are tectonic. The sediments form lengthy linear folds of mostly northwest direction broken by felsic intrusions and numerous interbedding porphyrites of basic and intermediate composition. Under the effect of intrusions and tectonic processes the sedimentary rocks of the suite are hornfelsed, sheeted and quartzy.

The composition of suite is carbonate-silicon-sand-shiest with rare intercalations of lava and tuff of andesitic and andesitic-basalt porphyrites. The interior structure of suite is complicated by the facial changes of sections and wide development of contact and dislocation metamorphism. The total thickness of sediments is up to 2,300 m.

Middle – Upper substages. Arkalyk suite ($C_1v_{2\text{-}3}$ar). Within the Balapan site, the Arkalyksky suite sediments spread as a belt of northwest direction in the Zharminsky zone in the northeast of the area behind the Baiguzin-Bulaksky fault. In the northwest they are disconformably overlaid (with basal conglomerates in the base) by Sirektasky suite sediments, and in the southwest – by the conglomerates of Middle and Upper Carboniferous. The sediments contain conglomerates, gravellite, sandstones and siltstones with interlayers of basalt porphyrites and their tuffs and calc-siliceous silt sandstones. The Arkalyksky suite sediments form thicker strata the total thickness of which is about 4,000 m.

Serpukhovian stage. Sirektasky suite (C_1v_3-ssr). The sediments of this suite have wide lateral extension in the northeast of the area between the Baiguzin-Bulaksky and North-Zhanansky faults. Contacts with the underlying strata are tectonic.

In the formation section, mostly basic and intermediate tuffs spread. Andesitic porphyrite tuffs are of green-gray, sometimes light-grey color and have chaotic structure. The sediments of the suite are crumpled into folds of northwest direction and broken into separated blocks by numerous, differently directed ruptures.

The total thickness of suite is 1,500–3,700 m.

Upper Visean substage- Namurian stage. Kokpektinsky suite (C_1v_3-nkp). Represented by volcanic-sedimentary rocks. The sediments spread in the northeast part of the territory. In the section, there prevail tuffs of basic and intermediate composition, in the lower part of the stratum alternating with tuff sandstones and rarely carbonaceous-siliceous siltstones.

Middle division. Bukonsky suite (C_2bk). The sediments of this suite are confined to the Zhanansky zone of crush bounded by ruptures. According to the lithological composition, the sediments of Middle Carboniferous are divided into two sub-suites: continental and subcontinental represented by sandstones, conglomerates, siltstones and carbonaceous shale

interstratifying with coal beds and lenses. The total thickness of Bukonsky suite sediments is 2,500–3,000 m.

Middle-upper divisions (poorly defined). Maityubinsky suite (C_{2-3}mt). The sediments of this suite spread in the center of the territory as a northwestward-extending belt confined to the South-Zharminsky and Chinrausky faults. In the lower part of section, there are encountered mostly conglomerates with lenses and interlayers of sandstone and siltstone and in the upper part - sandstone, siltstone and often carbonized carbonaceous-argillaceous shale with lenses and interlayers of conglomerates.

Permian system, upper division – Triassic system, lower division. Akbotinsky suite (P_2-T_1 ab). Sediments of this age are encountered in the northern part of the section. They compose the southern part of Akbotinsky fault-line depression of 1.5-2 km width visible at the southwestern side of Chinrausky fault at 30 km length. The Chinrausky fault cuts off the north-eastern wing of depression; along the same fault the coal formation is thrust on the edge of depression.

Basal conglomerates are present in the base of the section of Permian-Triassic sediments. They are overlaid by fine sandstones and siltstones with lenses and intercalations of coal. Basalt and andesite horizons of low thickness are also encountered. The thickness of sediments is up to 350 m.

Triassic system. Upper division (T_3). The Upper Triassic sediments occur in the base of Mesozoic Yubileynaya basin and outcrop at its northern side. Here, sandstones and siltstones represented by intercalations of conglomerate of 1-3 m thickness and coal lenses of 0.1–0.4 m thickness are predominant. The thickness of sediments ranges from 90 to120 m.

Jurassic system. Lower division (J_1). The Lower Jurassic sediments occur conformably in the Upper Triassic rock directly or on a granite base and are divided into two formations.

The lower part of section is singled out as a *below-coal formation (J_1^1)* composed by conglomerates, sandstone and gravelstone. The thickness is 95 m.

The conglomerate stratum is overlaid by the rock of Lower *carbon-bearing formation (J_1^2)* represented by siltstone, argillite and coal beds. The thickness of formation is 135 m.

Middle division (J_2). The Upper coal-bearing formation is represented by mostly siltstone and sandstone with coal beds. Gravelstone, conclomerates and pyroshale are encountered rarely. The thickness of Middle Jurassic rocks is up to 100 m.

Upper division (J_3). Above-coal formation. It is composed by speckled conglomerates, gravelstone and alternating sandstone. Siltstone and argillite are not so often encountered. The thickness of formation is 180 m.

Neocene system (N). Virtually the entire territory of Balapan is overlaid by a sedimentary mantle of Neocene except for the northwestern and southern parts and erosion areas.

The sediments of Neocene are represented by two suites: Kalkamansky (N_1kl) dated to Lower-Middle Miocene and Pavlodarsky (N_{1-2} pv) of Upper Miocene – Middle Pliocene. The Kalkamansky suite is composed by green-grey and green-brownish clay, mostly montmorillonite, containing lenses of sand and siltstone. The clays include psilomelan favas, fine druses of gypsum and calcareous bundles. Sediments of Kalkamansky suite within the Balapan site are overlaid by Pavlodarsky suite without visible signs of erosion.

The Pavlodarsky suite is represented by brown-grey and brown-red clays with lenses and intercalations of sand. The mantle thickness ranges from 10 to 70–80 m.

Quaternary system (Q). The sediments are developed on the entire territory of Balapan from surface. On flat-plain areas there prevail loams and sandy loam with detritus and debris, in valleys and lake basins – sand, sandy loam, loam and slimy clay, and on hill slopes – debris and detritus with sandy loam filler. The thickness of quaternary sediments on hill tops is from 0.5 to 3 m, on flat slopes 5 to 10 m, and on the plains and in the river valley 15 to 25 m..

Intrusive magmatism within the area described here spreads widely. Intrusions accompany mainly the faults (Kalba-Chingizsky and Chinrausky) bounding the structural and formational zones and are represented by the massifs and veins of various composition, shape and size, sometimes underlying directly Cenozoic sediments. In the northern part of the territory, sub-volcanic small intrusions of Permian are encountered.

The territory of Balapan is marked by the complicated plicative and fault tectonics. Fold structures are mapped out among the sediments of Maidansky suite of Middle Cambrian and Kokonsky suite of Lower Carboniferous. The Maidansky suite sediments compose the northeastern wing of Arkalyksky anticlinorium with 40–60°dip angles. The Kokonsky suite sediments form a big Karabassky anticlinal complicated by a sequence of folds of mostly northwest trend. The spread of fold wings is 1.5 to 2.5 km and the dip angles 30 to 50°.

The biggest fracture is the Kalba-Chingizsky fault dividing the Chingiz-Tarbagataisky and Zharma-Saursky structural and formational zones (SFZ). The general fault strike is northwestward and within the Balapan site has sub-latitude direction. The plane of dislocation moves down south-west at 70–85°angles. The width of the fault influence zone is 2 km. Quite often the Kalba-Chingizsky fault is divided into to a series of echelon-like faults.

The Chinrausky fault mapped in the central part of Balapan site has northwest strike and represents an abyssal long-living structure. According to the geophysical data, the northern and southern branches of Chinrausky fault bound the Mesozoic graben.

In the north-west of the Balapan site and outside its territory, there is the Baiguzin-Bulaksky fault dividing the Zharminsky SFZ to subzones. The fault is accompanied by a thick zone of crush within which the rocks are strongly dislocated, schistose, sometimes silicified and broken by small intrusions. The fault displacement amplitude is 1 to 3 km.

The Zhanansky zone of crush is a peculiar structure that complicates the northeastern wing of geosynclinal fold composed by Bukonsky suite sediments. The zone width ranges from 3 to 4 km. Along with the reviewed deep faults, numerous multidirectional faults feathering and intersecting the basic structures have been mapped at the Balapan site [3, 4].

1.3. Hydrogeology of the Balapan site

Two hydrogeological complexes, quite often relating to each other, of 100 to 150 m thickness, are distinguished on the territory described here (Figure 2). The first complex includes water occurring in the local hydrogeological basins. The bearing strata are loose formations of Neocene to Contemporary age. The second complex is a part of regional hydrogeological system. It includes fissure water of Paleozoic basement, water of Mesozoic weathering crust, and water of Paleocene sediments. The local hydrogeological basins in which water occurs at low depths (up to 50 m) are confined to:

a) diluvial-proluvial sediments of valleys and fragments of alluvial piedmont plains of Middle Quaternary- Contemporary age (Q II-IV);

b) alluvial-proluvial sediments of Late Quaternary-Contemporary age (Q III-IV) forming the above-floodplain terraces of Shagan River.

Groundwater of diluvial-proluvial sediments of Middle Quaternary-Contemporary age (Q_{II-IV}), unconfined, occur at more than 1.5 m depth, developing mostly in sand-gravel sediments. The composition of water is sulfate-chloride, less frequently chloride, with elevated hardness. The total mineralization widely ranges from 0.4 to 4 g/dm^3. Highly mineralized waters are most frequently encountered in closed catchment basins.

Groundwater of Upper Quaternary-Contemporary (Q III-IV) alluvial-proluvial sediments are represented by sand and gravel and prevails in the left bank area of Shagan River. The water is unconfined and occurs at 1 to 5 m depth, rarely, deeper. The total mineralization is up to 9.7 g/dm^3.

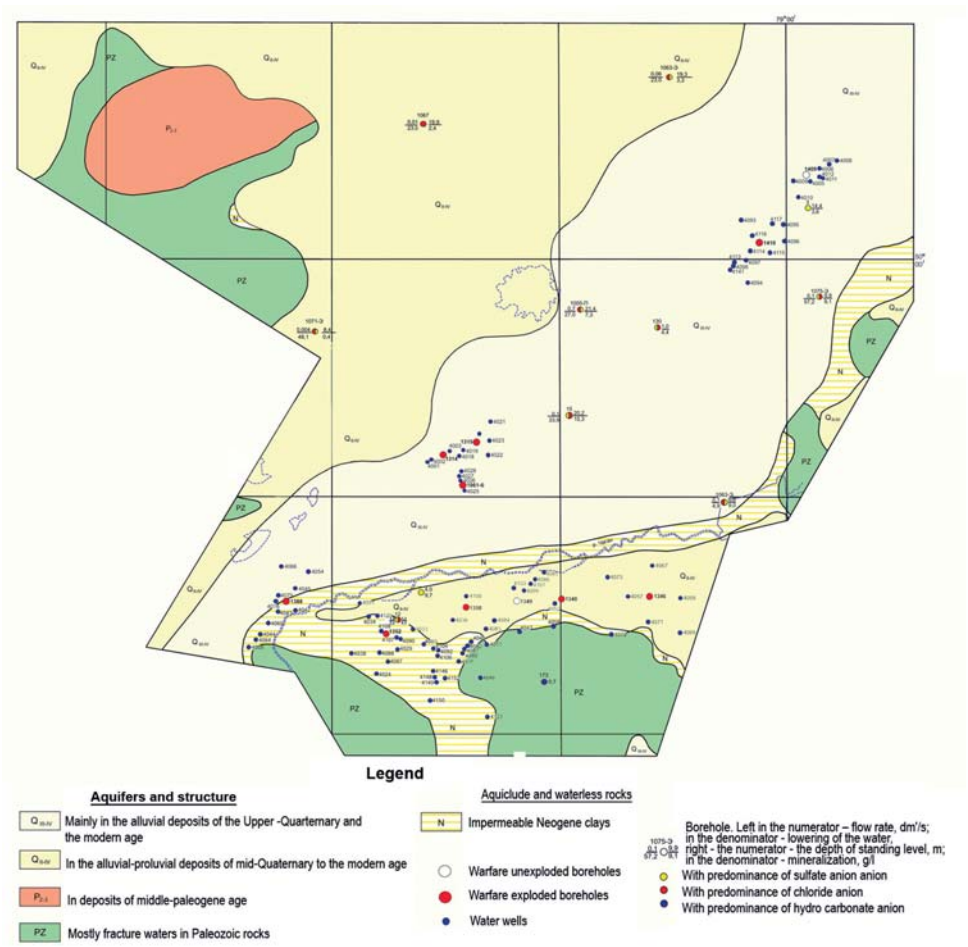

Figure 2. Hydrogeological map of the Balapan site

Perched water relates to the pore and capillary water of aeration zone and occurs primarily in the upper parts of loose sediments. The water is highly mineral because it dissolves salts contained in the loose sediments during strong evaporation. Perched water occurs at low depths (the first meters) and is of quite unstable nature, directly dependent on the amount of precipitation.

Groundwater and perched water occurring at low depths are more affected by hydrometeorological factors. In droughty periods the groundwater level can considerably go down and perched water can disappear completely. A reverse picture is observed in rainy periods and during snow melting. Accordingly, the total water mineralization increases or decreases. Near the mountain structures, additional recharge of water-bearing formations of local basins occurs through springs, i.e. directly from the regional groundwater basin.

Groundwater confined to the regional basin is subdivided into three types: water of Paleocene sediments, water of Mesozoic weathering crust and fissure water of Paleozoic basement. They are usually interrelated and form a single hydrosystem.

Fissure water is concentrated in the exogenous fracture zone and, depending on the geological and structural conditions, occurs at different depths ranging from 150 to 170 m. The aquifer thickness depends on the depth of exogenous weathering zone and increases on the sections adjacent to faults. The recharge area is confined to the Kazakh Upland and "erosion" windows developed on the areas of pinching out of relative confining beds. Fissure water is subdivided into the water occurring in intrusive formations, terrigenous sedimentary rocks and effusive-sedimentary complexes.

Water in effusive-sedimentary rocks of Maidansky suite of Middle Cambrian ($Є_2$md) has sulfate-chloride composition, low (1.5 g/dm^3) mineralization, and occurs at low depths.

Fissure water in effusive-sedimentary formations of Kokonsky suite (C_1v_1kk) is mostly sulfate-chloride and has low mineralization of 15.3 g/dm^3.

Fissure water of Middle-Upper Viseian sediments of Arkalyksky suite (C_1v_{2-3}ar) has sulfate-chloride composition. The mineralization is higher than 4 g/dm^3.

Fissure water related to tuffaceous-sedimentary stratum of Kokpetinsky suite (C_1skp) occurs at low depths. It is hard and has sulfate-chloride, rarely, chloride composition.

Fissure water of Bukonsky suite (C_2bk) sediments occurs at 1.0 m to 21.4 m depths. The water is sulfate-chloride. The total mineralization varies from 2.4 g/dm^3 to 9.1 g/dm^3.

The composition and mineralization of fissure water prevalent in Triassic and Jurassic sediments and occurring in the Yubileynaya basin does not virtually differ from that of the water described above.

Fissure water in granitoids, irrespective of the age, has hydrocarbonate, sulfate-carbonate or sulfate composition. The total mineralization is low, 0.7 g/dm^3.

Hydrochemical characteristic of the Balapan site. The geological and structural features of the territory described here have preconditioned the preferential development of artesian fissure water circulating in exogenous and tectonic cracking zones. Under the conditions of extreme climate with severe evaporation and low amount of precipitation the diversity of lithologic and petrographic composition of water-bearing rocks affects the formation of the chemical composition of groundwater.

Groundwater with prevalence of chloride anion occupies about 70% of this area. Water with prevalence of sulfate anion occurs in the southern and eastern parts of the site. The concentration of sulfate anion in groundwater does not exceed 10%. The cationic composition is marked by and elevated content (more than 60%) of alkali ions of potassium and sodium.

Water prevailing on the territory described here is salty (the dry residue content varies within 1-20 g/dm^3), occupying more than 80% of the area. Salt water lenses with more than 20 g/dm^3 mineralization are confined to drainless basins. (Figure 3) [3, 4].

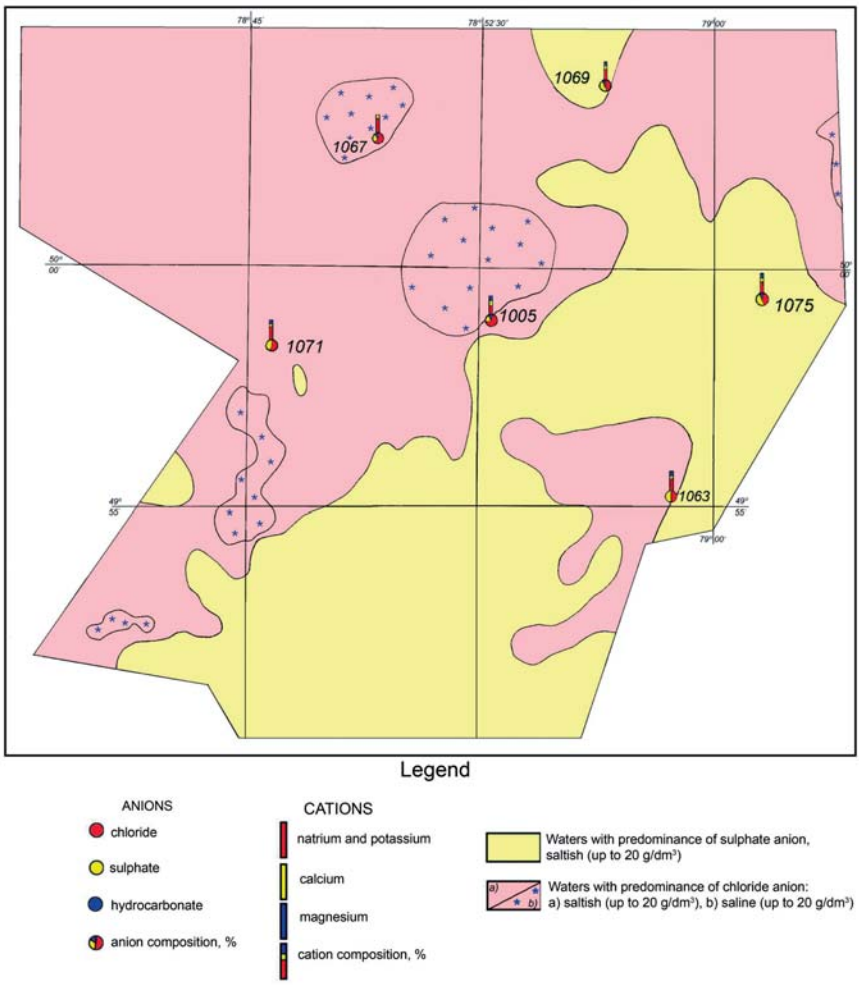

Figure 3. Hydrochemical map of the Balapan site

1.4. NUCLEAR TESTS AT THE BALAPAN SITE

1.4.1. Information on accumulated activity in the rocks

The contamination of central UNE zones by artificial radionuclides is due to:

- remains of fissile material;
- fission fragments; and
- induced activity radionuclides.

In order to assess possible contribution of UNE to the radioactive contamination of rocks, we assume that all nuclear explosives are based on ^{239}Pu. First, such assumption is due to absence of precise data on conducting thermonuclear tests on the site. Second, in thermonuclear explosives ^{239}Pu functions only as a fuse, and the remains of fissile material would be much less compared to the classical nuclear explosion.

Remaining fissile materials. The amount of fissile material remaining by the time of nuclear device destruction is determined by the efficiency of nuclear explosion, η, which, depending on the type and design of nuclear device and time of conducting of tests, can vary from 1 to 30 %. Due to absence of official data on each explosion, for further calculations we took to be 20 %.

Total, 106 underground tests have been conducted at the Balapan site [5]. The full range of explosive equivalent yields is divided into two parts: 0.001 to 20 kt and 20 to 150 kt. The calculation of absolute activities has been carried out for the lower and upper limits. Then the respective limits have been added to obtain minimum and maximum possible values of total activity for a given moment. The ratio of isotope activity to $^{239+240}$Pu activity has also been calculated. The obtained data are listed in the Table 1 below.

Table 1

Maximum and minimum possible total activity of plutonium and daughter ^{241}Am isotopes at the site by 2011 and their ratio to $^{239+240}$Pu activity

Isotope	Half-life, years	Lower limit of activity, Bq	Ratio to $^{239+240}$Pu	Upper limit of activity, Bq	Ratio to $^{239+240}$Pu
^{238}Pu	87.7	6.9×10^{13}	0.28	1.2×10^{15}	0.27
^{239}Pu	2.4×10^{4}	1.9×10^{14}	1	3.4×10^{15}	1
^{240}Pu	6.5×10^{3}	6.0×10^{13}		1.1×10^{15}	
^{241}Pu	14.4	6.9×10^{14}	2.76	1.4×10^{16}	3.11
^{242}Pu	3.7×10^{5}	7.3×10^{10}	2.9×10^{-4}	1.3×10^{12}	2.9×10^{-4}
^{241}Am	432	1.3×10^{14}	0.52	2.2×10^{15}	0.49

As one can see, major contribution to the total activity of remaining fissile material is made by ^{241}Pu. In fact, its activity can be somewhat higher due to the activation of ^{240}Pu by instantaneous neutrons; however, the reaction cross-section is very small to make significant contribution. With time, the contribution of its daughter decay product, ^{241}Am will be increasing due to the decay of ^{241}Pu.

Fission fragments. Similar to the calculation of fissile material remains, the calculation of fission fragments has been carried out for two ranges of explosion yields: 0.001 kt to

20 kt and 20 kt to 150 kt, with the formation of upper and lower total activity values by 2011. Ratios of the activity of fissile fragments to the activity of ^{137}Cs have been calculated. Table 2 presents the obtained data.

Table 2

Theoretically calculated minimum and maximum possible activity of fission fragments by 2011 and their ratio to the activity of ^{137}Cs

Radionuclide	Half-life, year	Lower limit of activity, Bq	Ratio to ^{137}Cs	Upper limit of activity, Bq	Ratio to ^{137}Cs
^{79}Se	65000 years	6.8×10^{9}	6.2×10^{-6}	1.2×10^{11}	6.3×10^{-6}
^{90}Sr	28.5 years	8.1×10^{14}	0.74	1.5×10^{16}	0.79
^{90}Y	64.1 h	$8.\times10^{14}$	0.74	1.5×10^{16}	0.79
^{107}Pd	6.5×10^{6} years	5.4×10^{8}	4.9×10^{-7}	9.2×10^{9}	4.8×10^{-7}
^{121}Sn-m	50 years	4.2×10^{11}	3.8×10^{-4}	7.5×10^{12}	3.9×10^{-4}
^{125}Sb	2.77 years	5.9×10^{10}	5.4×10^{-5}	3.0×10^{12}	5.4×10^{-4}
^{129}I	1.57×10^{7} years	6.3×10^{8}	5.7×10^{-7}	1.1×10^{10}	5.8×10^{-7}
^{137}Cs	30.17 years	1.1×10^{15}	1	1.9×10^{16}	1
^{137}Ba-m	2.55 min	1.1×10^{15}	1	1.9×10^{16}	1
^{151}Sm	93 years	4.2×10^{11}	3.8×10^{-4}	7.5×10^{12}	3.9×10^{-4}
^{154}Eu	8.8 years	2.1×10^{8}	1.9×10^{-7}	4.8×10^{9}	2.5×10^{-7}
^{99}Tc	213 000 years	1.7×10^{13}	1.6×10^{-2}	3.0×10^{14}	1.6×10^{-2}

The data in Table 2 show that currently the activity of ^{90}Sr and ^{137}Cs is predominant. On the longer term however, the radiological situation will be formed by ^{99}Tc and ^{151}Sm.

Induced activity radionuclides. Due to the effect of neutron current on the rocks, the elements contained in them undergo activation processes. Due to a relatively long lifetime, the samples taken from nuclear explosion locations contain radionuclides, such as ^{152}Eu,^{154}Eu, ^{155}Eu, ^{60}Co, ^{36}Cl.

Such activation product as ^{3}H is also worth mentioning. During explosions, the fusion reaction yields ~7×10^{14} Bq/kt and fission reaction yields ~4×10^{10} Bq/kt. Underground explosions increase these figures due to the nuclear reactions proceeding on boron and lithium present in primary rocks.

Similar to the remains of fissile material and fission fragments, the lower and upper limits of total activity of tritium have been calculated to be 1.9×10^{12} Bq and 5.0×10^{13} Bq, respectively.

Most likely, the artificial tritium forming as a result of explosion can be present as three basic compounds: tritiated water (HTO), tririated hydrogen (HT) and tritiated methane [6].

Thus, the basic radionuclides which now determine the radioactive contamination of groundwater are the "long-living" radionuclides: ^{3}H, ^{90}Sr, ^{137}Cs and $^{239+240}$Pu the yield of which is the highest. Presence of such radionuclides as ^{241}Am, ^{238}Pu, ^{241}Pu, ^{36}Cl, ^{99}Tc, etc. in groundwater is also quite possible.

1.4.2. Mechanisms of groundwater contamination

The borehole explosion cavities are located much below the groundwater level unlike the case of UNE in adits. High temperatures in the cavity last for a long time due to the presence of overlying rock stratum of more than 400 m thickness. Accordingly, the nuclear explosion cavity can act as a long-term "vapor generator" similar to natural thermal springs. On reaching the cavity, water is heated, dissolves chemical elements and radionuclides and returns together with them to the upper horizons where various processes of radionuclide migration and their discharge can occur. Other ways of groundwater contamination are also possible, for example, ingress of radioactive products by the zones adjacent to artificial fissures and faults.

The mechanical effect of UNE causes irreversible strain of rock mass manifested in the formation of cavity, crushed zones, rock fracturing, induced cracking cleavage, and rubble chimney. As an example, Figure 4 illustrates the structure of central UNE zone investigated in the borehole 102 [7, 8]. The radiation and gas-dynamic situation depends on the time of rubble chimney formation [9].

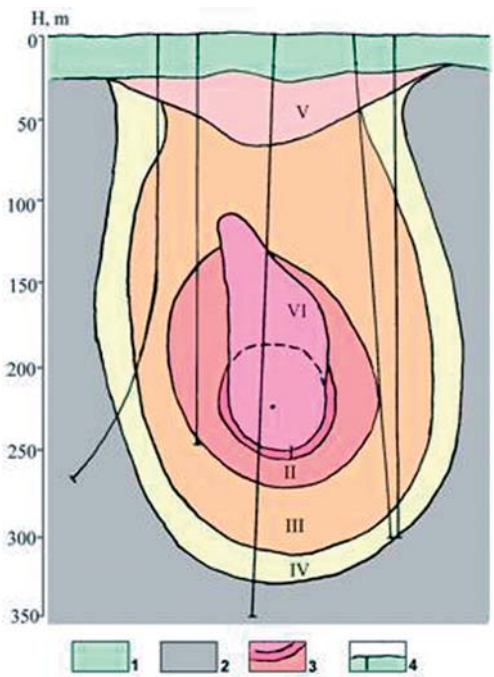

(1 – Mesozoic -Cenozoic sediments; 2 – Paleozoic rocks;
3 – irreversible strain zones of: I – crush, II – fracturing,III – intensive cracking,
IV – block cracking, V – cleavage, VI – rubble chimney; 4 – borehole.

Figure 4. Diagram of central explosion zone in the borehole 102

The rock in the crushed zone has transformed into loose powdery material. In the fractured zone the rock has disintegrated to granules and cobbles. The intensive cracking zone is characterized by renewal of natural cracking and formation of new cracks – cleavages in radial direction from the explosion epicenter and ruptures in concentric directions. The block cracking zone has asymmetric shape, the highest thickness on the strike and on the rise of rock and the lowest thickness below the cavity and on-dip. The cleavage zone has formed on the interface of the media of different acoustic stiffness. The configuration of formed artificial zones depends considerably on geological and structural conditions (for instance, presence of disjunctive structures, geological boundaries and lithologic composition of host rocks).

As a consequence of UNE, two basic radionuclide sources have formed in the central zone. The first source is the radioactive zone of aerosol-dust component allocated on the fractured rock and in massif fissures. The second source is the radioactive slag glass rock containing a major proportion of ^{90}Sr, ^{137}Cs and almost all $^{239+240}$Pu. Moreover, a considerable proportion of radioactive isotopes (fission products) exist as inert gases or volatile elements for a period of time comparable to the time during which the cavity can collapse. Isotopes as inert gases do not condense until a decay to other elements, and those of more volatile materials do not condense until a decrease in the temperature or decay to less volatile elements. As the radioactive decay process continues after the explosion, the relative abundance of gaseous and nonvolatile isotopes changes. A greater proportion of ^{90}Sr forms on fission of inert ^{90}Kr (about 80%) except for the small amounts of directly forming ^{90}Sr or ^{90}Rb. Hence, when the hole cavity collapses during a period comparable to the lifetime of ^{90}Kr (33 s), most of the final ^{90}Sr is not entrapped by the molten material and releases from the cavity with other gases. It is found that even on explosion of the whole camouflet and formation of insoluble vitreous mass containing most of the decay products, a greater part of ^{90}Sr and ^{137}Cs existing during the cavity collapse as inert gases (^{90}Kr and ^{137}Xe) is not contained in the vitreous mass but rather propagates with other gases [9, 15-17]. Thus quite a significant amount of ^{90}Sr and other isotopes, the precursors of which are the gaseous and volatile elements, deposit at a considerable distance from the high activity area and propagate in the destroyed environment.

At temperatures 1,000–1,500 °C, some products of radionuclide decay formed in the explosion cavity become volatile that results in their leak from the vitreous material, this being typical, for instance, for cesium.

Upon attenuation of radionuclides migration with gas, a basic migration agent and carrier of UNE radionuclides from the central UNE zone is the groundwater. The long-term observations at STS indicate that the concentration of radionuclides in groundwater grows during the first several years after the explosion, and then gradually decreases due to both the depletion of aerosol-dust source and decay of radionuclides. The migration of radionuclides from the stiffened radioactive rock melt, compared to the migration of radionuclides from the first source, is virtually insignificant during the first years and, possibly, decades because leaching of radionuclides from this source proceeds at 10^{-3} – 10^{-7} g/cm^2×day rates, with the specific surface of this source being also a few orders lower than that of the first source (rocks in fractured zones) [18].

Thus at present, as regards the migration of UNE radioactive products, the material present in a aerosol-dust source is of fundamental interest. Presumably, the area of elevated concentration of radioactive material has a form schematically presented in Figure 5.

The area of conventional intersection of groundwater reservoir with the elevated concentration area is a source of radioactive material transported with water [7].

Figure 5 presents an "ideal" case of $R_c > R_*$, where R_* is the radius of elevated radioactive concentration in the explosion depth. However, other variants are not excluded also, for instance, $R_c < R_*$ occurring when radioactive material comes in the reservoir through the faults regenerated by explosion or induced cracking areas affecting the aquifer bottom.

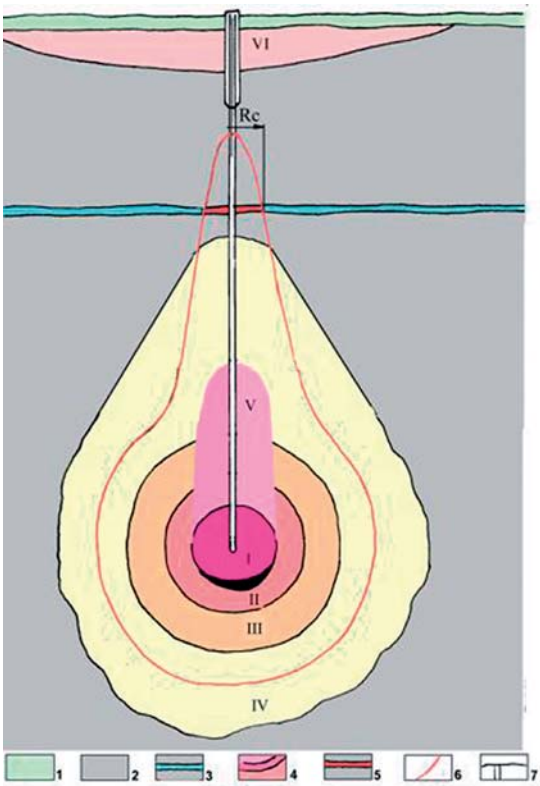

(1 – Mesozoic-Cenozoic sediments; 2 – Paleozoic rocks; 3 – groundwater reservoir;
4 – irreversible strain zones of: I – melt cavity, II – fractures, III – intensive cracking,
IV – block cracking, V – rubble chimney; VI – cleavage; 5 – source of radionuclides;
6 – boundary of increased radionuclide concentration area; 7 –hole.

Figure 5. Schematic map of increased concentration area and radioactive material source

1.4.3. Hydrodynamic effects due to UNE

A considerably non-uniform strain of complicated-structure real geological structure does not make it possible to analyze in detail the behavior of groundwater under the impact of explosions. However, the basic features of hydrodynamic processes caused by underground explosions can be followed by the following schematization of the phenomenon (Figure 6) [8].

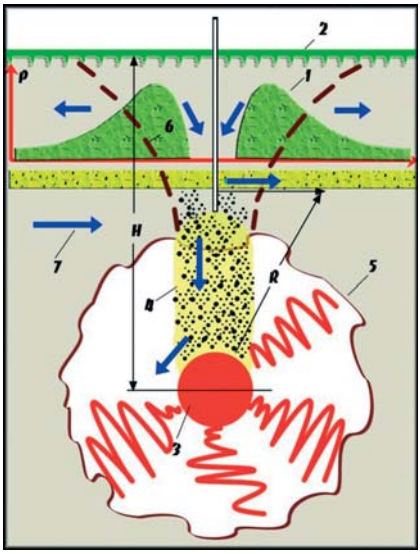

(1 – distribution of groundwater pressure on rubble chimney formation;
2 – day surface; 3 – camouflet cavity, 4 – ruble chimney,
5 – induced cracking zone, 6 – area of near-surface decompaction;
7 – direction of groundwater proliferation)

Figure 6. Change of pressure in the rock strata due to UNE execution

In a continuous low-impermeable medium containing subhorizontal water-saturated bed, on some depth H, explosion of yield q is conducted. The wave processes corresponding to the explosion cause strain of the medium, the condition of reservoir bed changing to a greater extent than that of host, relatively solid rocks. The dynamic compression of reservoir causes an increase in the fluid pressure on some area – formation of dome-shaped, effective or real rise of groundwater table formally made to conform to the fluid pressure P using the Dupuit approximation:

$$\text{grad}\,(P) = \rho g \cdot \text{grad}\,(h)$$

where: h is the absolute level of groundwater;
ρ is the fluid density.

The process is accompanied by water injection into the pore-crack space of the rock mass under study, into earlier existing and new, explosion-formed cracks. The time of completion of camouflet cavity formation determines the time of disturbance of water-saturated reservoir bed. The subsequent formation of rubble chimney (area of increased decompaction of medium up to the free surface) causes central depression in the groundwater dome formed.

A general scheme of groundwater level change under the impact of explosions is shown in Figure 7 [8]. Presence of high pressure zone (dome) of groundwater above the explosion epicenter causes naturally rise of piezometric surface (segment I). The next stage (segment II) is caused by groundwater run-off to explosion-formed zones of induced cracking. For example, high cracking of rock located in the rubble chimney (permeability coef-

ficient is up to 10^{-9} m2) causes quick relief and drop of excessive pressure much below the natural level in the area of explosion epicenter. The general tendency towards a decrease in the groundwater table causes formation of cone of depression. The final stage (segment III), restoration of piezometric surface, begins from the time the induced cracking zones are filled.

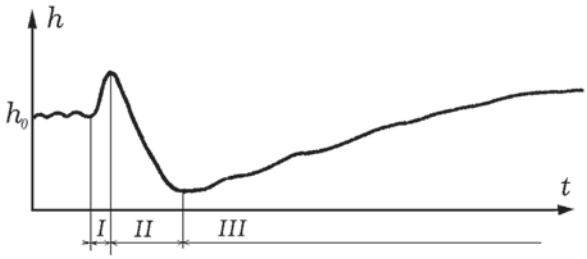

(Stages: I – formation of "dome"; II –induced cracking filling; III – restoration of level)

Figure 7. Scheme of groundwater level change on conducting UNE

To give an idea of the groundwater level dynamics, Figure 8 illustrates the results of observations in hydrogeological wells after UNE in the "warfare" borehole 1315.

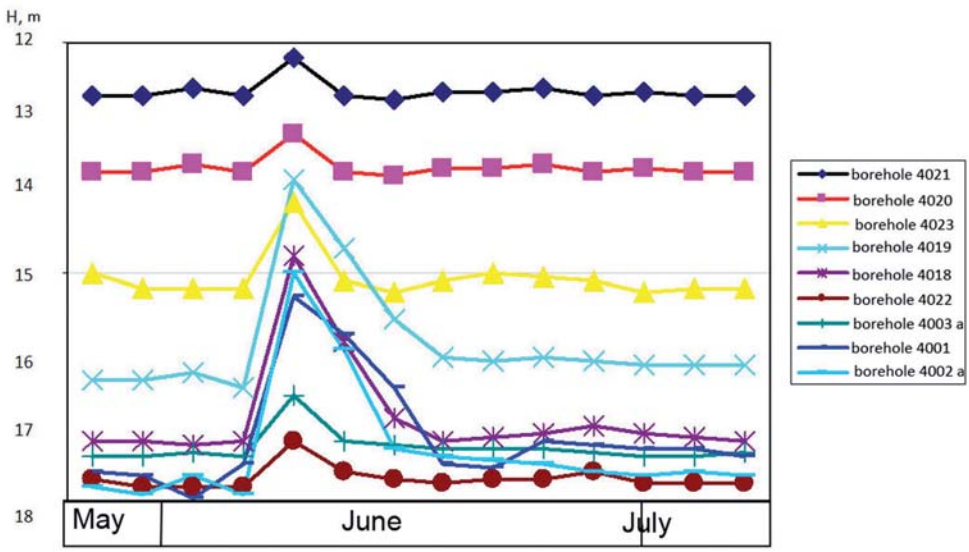

Figure 8. Graph of water level behavior in observational wells located in the zone of influence of the test (emplacement) well 1315

The groundwater level rises immediately after execution of UNE, during passage of surface waves. Sometimes, groundwater appears to spout from observational wells. Afterwards, for a long time (the first hours – the first days) the groundwater level decreases due to filling of newly formed cracks with water. Some time (0.5 months - 1 year) after the explosion the groundwater level is restored to static position [10].

2. CURRENT STATE OF GROUNDWATER AT THE BALAPAN SITE

2.1. Preliminary assessment of the hydrogeological conditions

On the STS territory, more than 100 wells have been drilled to study the effect of UNE on the geological environment and groundwater (Figure 9).

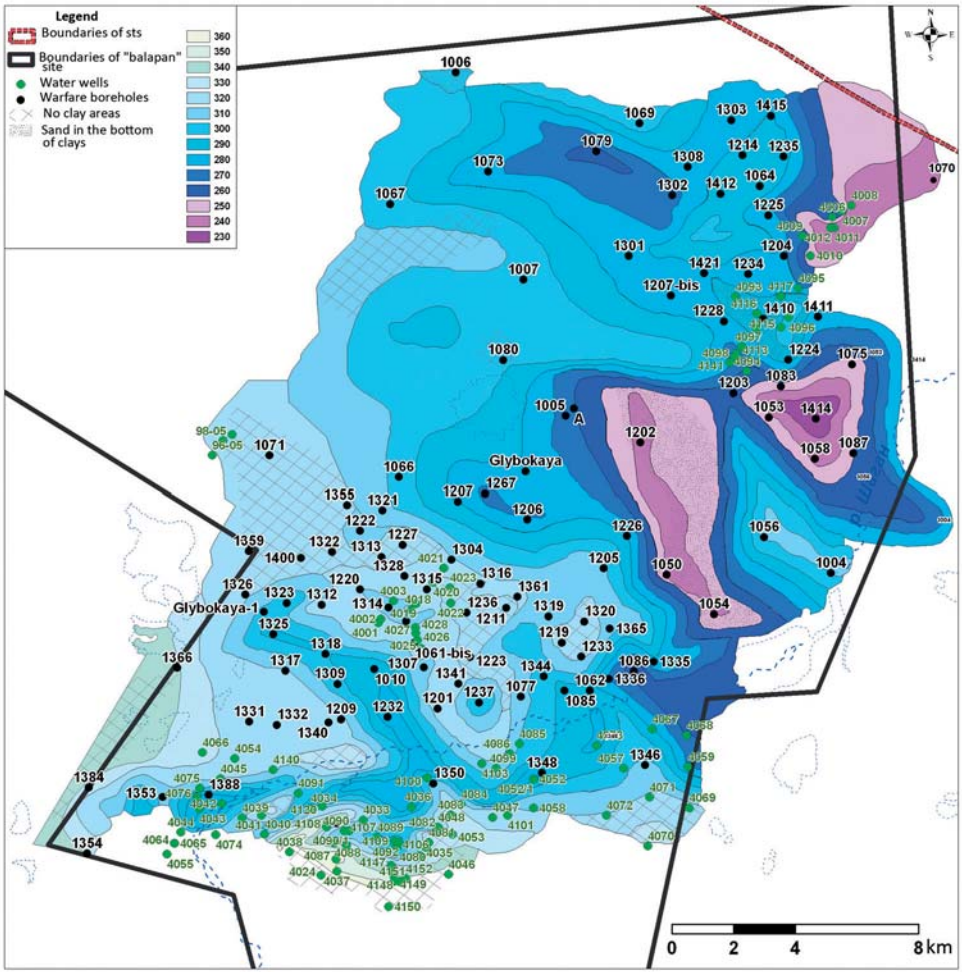

Figure 9. Map of bedding of water-bearing rock roof at the Balapan site (absolute height, m.)

Subsequently, in 1996–2003, part of these wells was used for the implementation of projects after closing down the nuclear infrastructure, and some of them were destroyed by unauthorized interference of the local people. Accordingly, in order to provide hydrogeo-

logical monitoring it was necessary to inspect the observational wells including the following measures:

- collection and analysis of archival data on the location and characteristic of the observational wells on the territory of the Balapan site;
- field visits to survey the technical condition of the wells and possibility of their restoration and use for observations.

According to literature sources, 140 observational wells have been drilled to follow the nuclear tests conducted in the wells on the territory of the Balapan site. However, field surveys have identified 104 wells relating to 11 locations of underground nuclear tests. The inspection has shown that a great number of the wells is either fully clogged up with extraneous material or destroyed. Of 104 wells, 22 cannot be restored and 22 are fully lost. Among the remaining 82 wells, 35 have been assessed as subject to restoration and cleaning.

In order to assess the hydrogeological conditions at the Balapan site, an additional data analysis has been performed for the core-wells drilled to choose the sites for conducting UNE to 600 m depth to define. Based on the processed and systematized data, a map of confining overlying bed has been drawn at a scale of 1:50 000 (Figure 9).

Analysing source data on the boreholes, it was possible to determine the key features of groundwater flow. Irregularities of rock foundation are filled with clays of Neocene of up to 80 m thickness. The aquifer occurrence conditions vary on the strike and in section. Throughout the entire territory, groundwater is mostly of pressure type with the pressure head of up to 73 meters; unconfined water occurs less frequently, in the areas of regional aquifer (clays of Neocene) wedging out or scouring.

Balapan is an area of groundwater transit. The basic direction of groundwater propagation is northeast, at up to 0.002 grade. The absolute marks of piezometric surface decrease from 330 to 270 m (Figure 10). Hence, the general groundwater proliferation is directed to the natural discharge area on STS territory in the direction of River Irtysh located 100km north of the Balapan site. The groundwater proliferation proceeds at quite low hydraulic gradient values and low filtration rates. It is facilitated by the low values of filtration factor which are not higher than 1m/day on most of the territory [1, 2].

2.2. Assessment of ground waters contamination with radionuclides at the Balapan site

Sampling in drilled hydrogeological wells has been done to assess the nature of contamination with artificial radionuclides. On some areas, additional research has been carried out. It includes drilling and geophysical works and testing for underground water flow, drawing groundwater samples for chemical and radionuclide analyses. The chosen reference wells on the territory of Balapan site are located irregularly. Accordingly, the assessment of artificial radionuclides proliferation with groundwater was performed only on some sites identified as: "Northern", "North-Eastern", "Central", "Zarechie", "South-Western", "Karazhyra", sites No 1, No 2, No 3 and No 4 (Figure 10).

In some wells on these areas, annual radionuclide monitoring was performed. The data show tritium to be a basic groundwater contaminant at Balapan. A basic characteristic feature of this radionuclide is that tritium is a part of water and is not sorbed by rocks. It is,

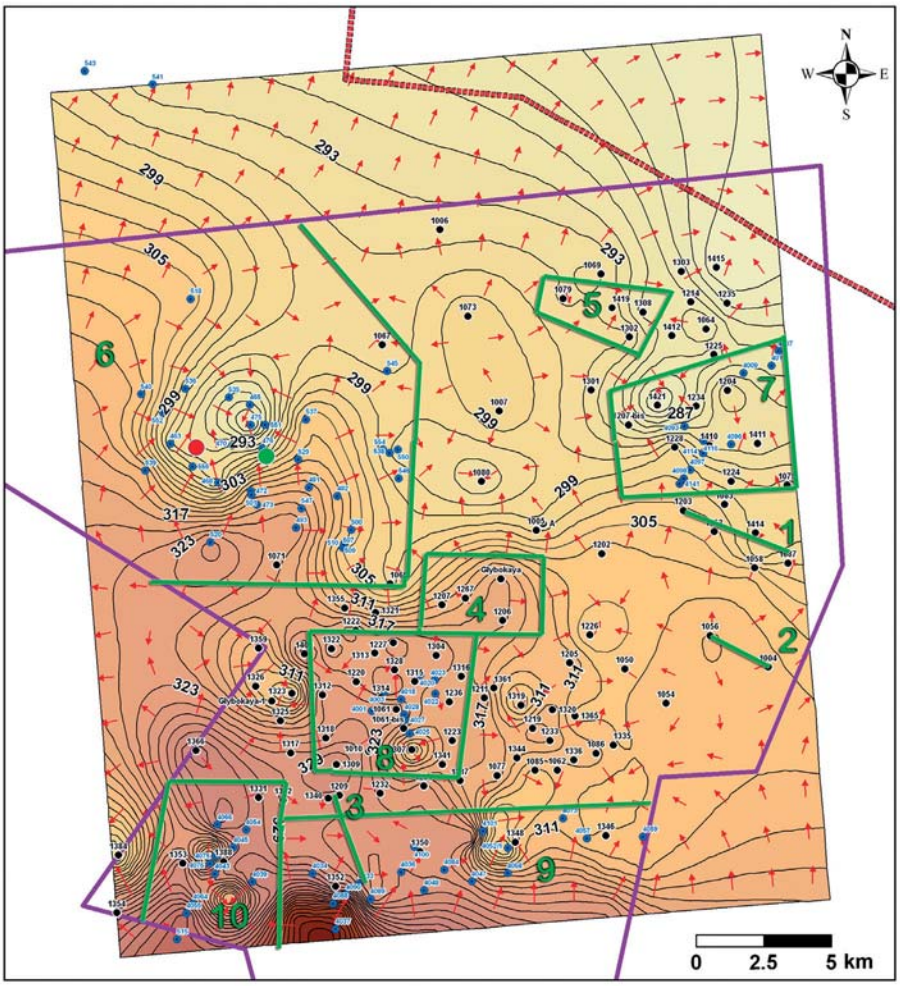

Figure 10. Hydro-geological layout of the Balapan site (hydroisobaths in abs. marks, m)

therefore, an ideal indicator of migration processes. Hence, while monitoring the nature of radioactive product proliferation beyond the boundary of central UNE zones, basic attention was focused on the assessment of tritium concentration in groundwater samples.

2.2.1. The "northern" site

"Northern" site is located in the northern part of Balapan (Figure10). Based on the results of preliminary groundwater survey at the Balapan site in the well 1419 drilled for UNE but not used because of liquidation of nuclear testing facilities, the concentration of ^{3}H and ^{90}Sr artificial radionuclides appears to be the highest. The well is located in the downfold zone of Paleozoic foundation relief. In 2005, integrated exploration was carried out around the well 1419 including geophysical and drilling works and testing for underground water flow to identify the nature of radioactive groundwater contamination at this site and possible pathways of contaminated flows.

2.2.1.1. Hydrogeological conditions at the northern site

Geophysical research at this site has been conducted to choose locations for drilling hydrogeological wells. Seismic prospecting by curved-path refraction method (CPR) and electrical prospecting by VES method have been conducted in the "warfare" boreholes 1079–1302 of 9 km lateral length. CPR seismic prospecting has been performed with 10m step, the distance between vibro-poins (VP) being 110 m, and the maximum length of produced TD curve – 1,190 m. The obtained velocity profile is shown in Figure 11.

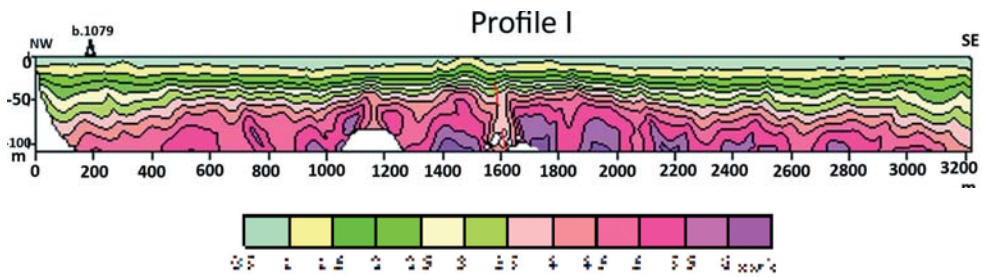

Figure 11. "Northern" site. Velocity profile across the well 1079

Based on the results of integrated interpretation, a geologic-geophysical section of profile through the wells 1079–1302 has been drawn (Figure 12) making it possible to delineate the geological boundaries of roof and base of clay horizon.

Taking into consideration the geologic-geophysical section, three geological wells have been drilled: 15a (71 m depth) – in the range of the wells 1419–1302, 250 m from the well 1302; 16p (60 m depth) – in the range of the wells 1419–1079, 1,500 m from the well 1079; and 17a (114 m depth) – in the range of the wells 1419–1308, 950 m from the well 1308 (Figure 12,b).

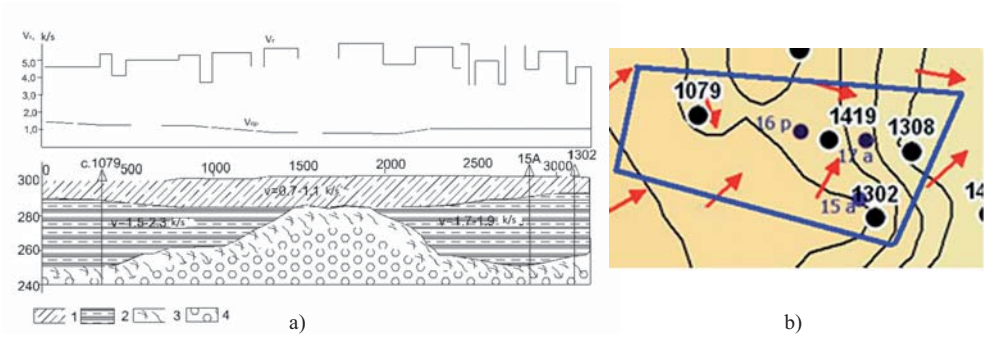

1 – sandy loam, loam, 2 – clay, 3 – exogenous cracking zone, 4 – host rock (tuff)

Figure 12. "Northern" site: a) geologic-geophysical section of profile on 1079 – 1302; b) layout of the wells

Pumping tests have been carried out in the drilled wells (Table 3).

Table 3.

"Northern" site. Test data on the wells 15a – 17a and concentration of radionuclides in groundwater

Well No.	Depression, m	Discharge, m^3/day	Transmis-sibility, m^2/day	Thickness of water-bearing horizon, m	Permeability, m/day	^{3}H, kBq/kg	^{90}Sr, Bq/kg	^{137}Cs, Bq/kg	Nearest "warfare" borehole, km
15a	25.65	86.40	2.64	50	0.06	1215.33±6.07	1.98±0.10	0.27±0.07	1302 / 0.25
16p	3.60	43.20	3.60	40	0.08	-	-	-	-
17a	7.15	3.12	4.30	40	0.05	4764.62±23.72	0.47±0.14	0.011±0.003	1308 / 0.95
1419						1194	225		1302 / 1.3

The results of drilling and geophysical works have made it possible to define more exactly the geological structure of the study area. In the center of the site, there has been identified a rise of the rock foundation with up to 40 m local difference in elevation. Thus the closed downfold zone of Paleozoic foundation of interest is partitioned to two local downfolds. By filtration characteristics, water-bearing rocks can be classified as rather low-permeable (K<0.1 m/day).

2.2.1.2. Radionuclide contamination of groundwater at the northern site

Table 3 lists the data of laboratory analyses on the assessment of artificial radionuclide concentrations in groundwater samples [2].

Based on the results of hydrogeological sampling, the well 17a appears to have high concentrations of tritium (4764.62 kBq/kg). At the same time, the concentration of ^{90}Sr remains at the level of marginal values (0.47 Bq/kg) compared to its concentration in the well 1419 (225 Bq/kg). In the well 15a, high concentration of tritium is also found like in the well 1419 (1215.33 Bq/kg), however, the concentration of strontium (1.98 Bq/kg) is slightly lower than in the well 1419.

Judging by the structure of seepage flow illustrated in Figure 10, contaminated water comes in the well 1419, most likely, from the "warfare" boreholes 1069, 1079 and 1302. However, the presence of high concentrations of ^{90}Sr in water of the well 1419 cannot be so far explained.

The following conclusions can be drawn from testing the groundwater occurring within the Northern site:

- A basic aquifer bound by the zones of exogenous and tectonic rock cracking of Paleozoic occurs everywhere and is mostly of pressure type;
- A basic direction of groundwater proliferation is northeast;
- Water abundance of the complex is not high; specific yields vary from 0.001 to 0.44 l/s, and in the areas of fault influence increase to 0.42–2.2 l/s. By filtration characteristics, water-bearing rocks can be classified as low-permeable (K<0.1 m/day);
- Concentrations of ^{137}Cs in groundwater are insignificant and do not exceed the values established by NRB-99 IL_{pop} (Interference Level for general population) for drinking water [19];
- Basic radioactive contaminants of groundwater are tritium and ^{90}Sr; their concentrations exceed the values established by NRB-99 IL_{pop} for drinking water 619 and 45 times respectively;
- At a distance from contamination source ("warfare" boreholes) the concentration of tritium appreciably decreases;
- Presence of high concentration of ^{90}Sr in the well 1419 cannot be so far explained.

2.2.2. The "north-eastern" site

The site is located in the northeastern part of Balapan. The radioactive contamination of groundwater within the site is due to the aftereffects of UNE conducted in the "warfare" boreholes 1204, 1228, 1203, 1410 and 1411. The nature of radionuclide contamination at the site has been investigated using the sampling data on 9 hydrogeological wells drilled earlier (Figure 10).

2.2.2.1. Geological structure of the north-eastern site

In the northeast of the study area, vocanogenic-sedimentary rocks of Kokpektinsky suite of Upper-Visean – Namurian stage of Lower Carboniferous (C_1v_3-n·kp) prevail. In the southwest, there develop sediments of Bukonsky suite of Middle Carboniferous (C_2bk) broken by intrusive formations of Permian (αβμP) – andesite and diabase porphyrites. (Figure 13).

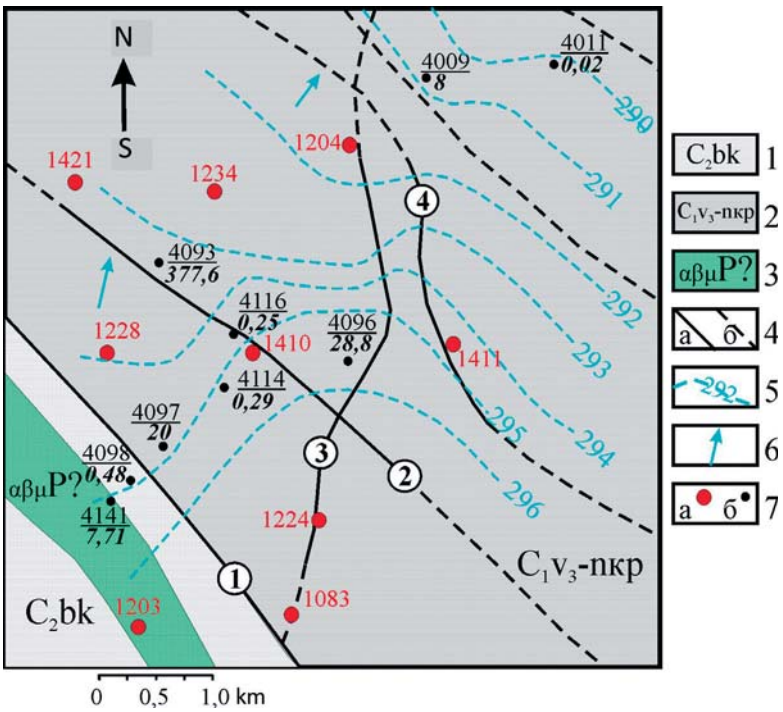

(1-3 – fissure and fissure-vein groundwater in: 1 – sediments of Bukonsky suite of Middle Carboniferous, 2 – volcanogenic-sedimentary rocks of Kokpektinsky suite of Lower Carboniferous, 3 – Intrusive formations of Permian; 4 – faults: a – establihed, б – predicted; 5 – piezometric contours by the year of 1989, abs. mark, m; 6 – basic direction of groundwater propagation; 7 – well and its number: a – test, b – observational, a figure in the denominator denotes the concentration of tritium in groundwater, kBq/kg)

Figure 13. Geological and hydrogeological conditions at the "North-Eastern" site

The rock is marked by lithologic variation and is complicated by folds and fractures. In section, by the degree and type of rock fracture, zones of exogenous weathering, tectonic cracking and relatively intact rock have been distinguished.

The rock is overlaid by clays of Miocene (N_1) filling the irregularities of paleorelief and bedding horizontally. On surface, there prevail Middle Quaternary sediments of alluvial genesis represented by sandy loam and sand of up to 15 m thickness with the tributary clay and loam intercalations. The thickness of sedimentary stratum is up to 20–80 m.

In the study area, by the character of massif discontinuity and length [SNiP 2.02.85], the ruptures are subdivided to:

- II order faults 1 of northwest direction (hereinafter, the numbering is used conventionally for the study area);
- III order faults 2, 3, 4 of northwest and submeridional strike;
- Higher-order faults and big cracks of mostly northwest, submeridional and northeast strike.

The Fault 1 – Baiguzin-Bulaksky, shown as a zone of rock schistosity and brecciation (the wells 4094 and 4098), a tectonic boundary between the vocanogenic-sedimentary rock of Kokpektinsy suite of Lower Carboniferous and sediments of Bukonsky suite of Middle Carboniferous [2].

2.2.2.2. Hydrogeological conditions at the north-eastern site

A basic aquifer confined to the zones of exogenous and tectonic rock cracking of Paleozoic occurs everywhere and is mainly of pressure type. A basic direction of ground water propagation is northward; elevations decrease from 296 to 292 m. The gradient is 0.002–0.003.

The groundwater level regime is plain-like. The water abundance in the aquifer is not high; debits vary from 0.001 to 0.44 l/s, and in ruptured influence zones increase to 0.42–2.2 l/s. The groundwater is moderately subsaline with 3.7 to 6.3 g/l mineralization, commonly chloride-sulfate and, less frequently, sulfate-chloride, calcium- and magnesium-sodium, very hard and neutral.

By the conditions of formation and circulation, the groundwater is referred to fissure and fissure-vein and hydraulically interrelated. The aquifer develops in the areas of exogenous and tectonic cracking of:

- Sediments of Bukonsky suite of Lower Carboniferous;
- Volcanogenic-sedimentary rock of Kokpektinsky suite of Lower Carboniferous;
- Intrusive formations of Permian.

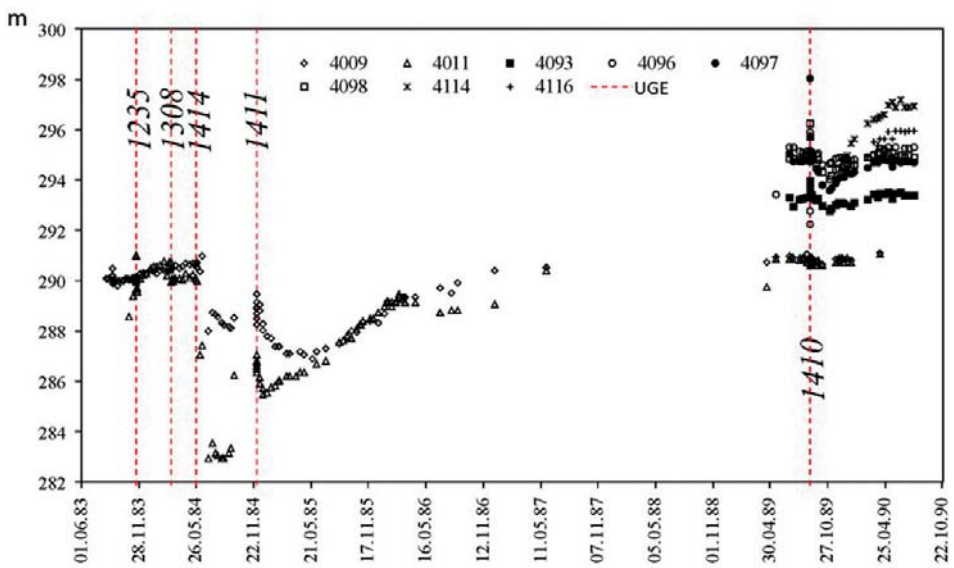

Figure 14. North-Eastern site. Diagrams of groundwater level

Execution of UNE in the wells 1414 and 1411 located 6 km upstream has resulted in a decrease in the piezometric surface of groundwater with up to 9 m amplitude for half a year. The level discontinuity in the range of the wells 4009 - 4011, for instance, indirectly

testifies to the redistribution of underground flow due to the regional drain of aquifer caused by formation of artificial cracking zones adjacent to UNE locations. Execution of UNE in the well 1410 has caused temporary violation of groundwater regime traced in up to 1 km radius (Figure 14) [10].

2.2.2.3. Radionuclide contamination of groundwater at the north-eastern site

Based on the sampling data on 9 observational wells, 4 halos of radioactive contamination of groundwater due to UNE in the wells 1204, 1228, 1203 and 1411 can be identified (Figure 13, Table 4) [1, 2].

Table 4.

"North-Eastern" site. Radionuclide concentration in groundwater

UNE Date	*Distance, km	Well No	Date of sampling	^{3}H, kBq/kg	^{90}Sr, Bq/kg	^{137}Cs, Bq/kg	$^{239+240}$Pu, Bq/kg
Fissure and fissure-vein water in volcanogenic-sedimentary rock of Lower Carboniferous							
1204 1972	0.9	4009	2004	7.12	0.07	0.003	-
			2005	7.90	0.08	0.03	-
			2007	8.23	0.01	0.03	-
			2010	5.00	0.01	< 0.2	< 0.006
	2.1	4011	2004	0.02	0.12	< 0.02	-
1228 1978	0.9	4093	2004	321.22	6.50	0.002	-
			2005	-	5.45	1.17	-
			2007	390.41	0.25	1.17	-
			2010	300.00	-	<0.03	< 0.002
	1.0	4097	2004	20.00	1.30	0.20	-
			2005	-	0.33	0.20	-
			2007	10.45	1.30	0.01	-
			2010	10.00	-	-	-
1410 1989	1.1	4114	2004	0.29	-	-	< 0.002
	1.12 (0,3)	4116	2004	0.25	0.03	0.02	-
			2005	0.21	0.81	0.26	-
1411 1984	0.95	4096	2004	28.80	0.20	0.03	-
			2005	-	0.30	0.03	-
			2010	5.00	<0.01	<0.03	< 0.002
Fissure and fissure-vein water in sediments of Middle Carboniferous (well 4098) and intrusive formations of Permian (4141)							
1203 1981	0.8	4141	2004	7.71	0.24	<0.005	-
			2007	1.74	0.24	0.01	-
			2008	0.30	0.01	0.01	< 0.002
	1.0	4098	2004	0.48	-	-	-
			2007	0.46	-	-	-
			2008	0.10	0.07	0.10	< 0.002

Note: * The distance from hydrogeological to the nearest "warfare" borehole located downstream the groundwater propagation
"-" – no measurements were performed

In all water samples analyzed, the concentrations of ^{90}Sr and ^{137}Cs are insignificant and do not exceed the levels established by NRB-99 IL_{pop} for drinking water. At the same time, the concentration of tritium varies over a wide range of values. A maximum concentration of lithium (378 kBq/kg) has been measured in the observational well 4093, and is almost 50 times higher than the level established by NRB-99 IL_{pop} for drinking water (7.7 kBq/kg.) The contaminated groundwater flows to this well from the well 1228 located 0.9 km southwest. It should be noted that now at the well 228 there has been detected the release of gas with prevalence of carbon monoxide and methane, indirectly testifying to significant deformation of rock massif at this site [20].

In the observational wells 4009 and 4011 located northeast of the well 1204 downstream the groundwater flow the concentration of tritium is not high and regularly decreases. Most probably, it is due to the fact that the main stream of contaminated groundwater from the well 1204 is drained by tectonic faults in the northeast direction (Figure 13).

In the well 4096, an elevated concentration of tritium is caused by the groundwater contamination from UNE in the well 1411. It is confirmed by the file records of groundwater regime (Figure 14). On the presented diagram it can be seen that the well 4096 is located in the influence zone of drain and subsequent restoration of piezometric surface after execution of UNE in the well 1411.

Observational wells 4114, 4098 and the test well 1203 are located within the Zhanansky zone of crush, south of Baiguzin-Bulaksky fault. The highest concentration of tritium has been measured in the well 4141 compared to the well 4098 because the well 4141, like the well 1203, penetrates the same aquifer of fissure and fissure-vein water of intrusive formations. Higher concentrations of tritium in the well 4097 compared to the well 4098, are probably due to the contaminated water coming from the "warfare" boreholes 1083 and 1224 along the influence zone of Baiguzin-Bulaksky-fault.

The results of multiple water sampling from the wells 4093, 4096, 4097 performed in 2010 indicate a gradual decrease in the concentration of tritium in groundwater (Table 4).

From the results of research on the groundwater occurring within the North-Eastern site, the following conclusions can be drawn:

- A basic aquifer confined to the areas of exogenous and tectonic cracking of Paleozoic rocks spreads everywhere and is mostly of pressure type.
- A basic direction of groundwater proliferation is northward.
- Water inflow to the aquifer is not high; debits vary from 0.001 to 0.44 l/s, and in the influence zones of rupture increase to 0.42–2.2 l/s. The groundwater is moderately saltish and saltish, with 3.7 to 6.3 g/l mineralization.
- Concentrations of ^{90}Sr and ^{137}Cs in all water samples are not significant and do not exceed the levels established by NRB-99 IL_{pop} for drinking water. The concentration of $^{239+240}Pu$ in groundwater at the site does not exceed the MDA level, and is 0.002 Bq/kg.
- Tritium is a basic radioactive contaminant of the groundwater. Maximum concentration of tritium has been measured in the well 4093 (377.6 kBq/kg), which is almost 50 times higher that the level established by NRB-99 IL_{pop} for drinking water.
- High concentrations of tritium in groundwater are typical for linearly elongated zones stretching in the direction of groundwater propagation from the "warfare"

boreholes for 1.5–2.0 km. The concentration of tritium markedly decreases with distance from the "warfare" boreholes;

- The elevated concentrations of tritium at this site are typical for the tectonic fault zones, sections undergoing more severe disintegration and for the aquifer system of fissure and fissure-vein water of intrusive formations.

2.2.3. The "south-western" site

The study area is located in the outermost southwest of the Balapan site and occupies an area of 14 km^2. On 27th December, 1987, group UNE of two NT of 20–150 kt and 0.001–20 kt yield were conducted in the "warfare" borehole 1388 aimed for the purpose of nuclear weapons development.

The research at this site was given special attention in connection with a possible carry-over of UNE radioactive products with groundwater outside the territory of Balapan. The case is that this site is located within the bounds of the southwest boundary of Balapan, and UNE were conducted near the northern zone of influence of Kalba-Chingizsky regional fault.

2.2.3.1. Geological structure of the south-western site

The territory of the site is divided by the regional Kalba-Chingizsky deep fault into two different structural and formational zones of unequal area (Figure 15).

The northern portion of the site is a part of Irtysh-Zaisansky megasinclinorium and is composed by terrigenous siliceous and volcanogenic sediments of Lower Carboniferous (C_1tkn). The southern portion is confined to Chingiz-Tarbagataisky meganticlinorium and is formed by the rock of Middle Cambrian ($Є_2$md).

The study area is located in the zone of influence of regional Kalba-Chingizsky fault of I order distinguished in accordance with SNiP 1.02.07-87 and represented by a sequence of contiguous faults of I/1 – I/6 sub-latitude direction. In the northern part of the area, there has been identified a branch of higher-order (7-9) ruptured dislocations subparallel to the regional fault. The ruptured zones of northwest and northeast strike are represented by zones of elevated cracking and crush.

2.2.3.2. Hydrogeological conditions at the south-western site

The hydrogeological conditions at the area are governed by the geological structure features and presence of ruptured zones. The groundwater of fissure and fissure-vein type is confined to the area of exogenous weathering and ruptured zones of Paleozoic base respectively.

Groundwater assumes sporadic development in the loose stratum of Mesozic-Cenosoic formations. The formation of single aquifer complex of interstitial-fissure water (well 4041 and well 4040, respectively) has been recorded in the areas of relative aquifer (clays of Neocene) wedging-out or partial sanding of sedimentary mantle.

Groundwater has been tapped at the depth of 2.1 m to 78.5 m. Piezometric levels range from 4.1 to 23 m creating up to 61.7 m head. In the southeast portion of central block, a closed hydrogeological structure with elevated head values bound by the piezometric contour 50 has been identified. In the intersection nodes of ruptured zones of north-west and north-east strike, a decrease in the head values to 20-40 m has been measured. The most appreciable

crosshead has been recorded for the eastern block in the center of which artesian groundwater prevails due to the relative aquifer wedging out.

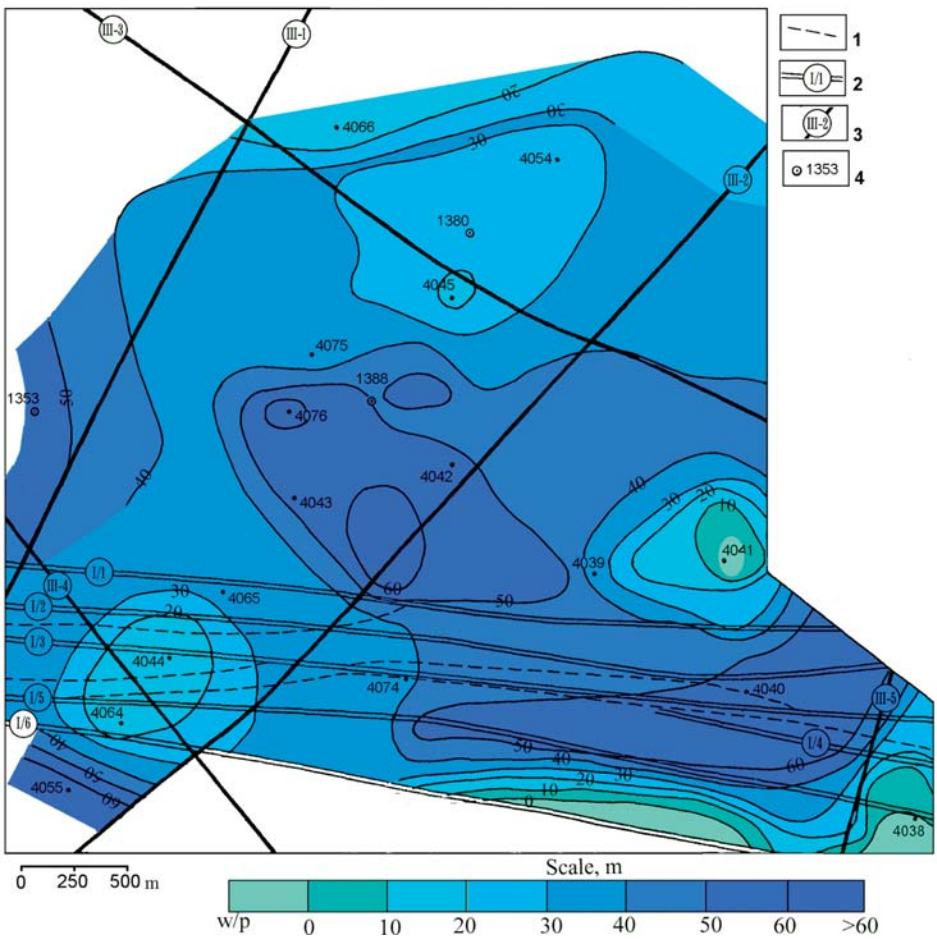

(1 – geological boundary; 2,3 – faults, their class and number: 2 – I order, 3 – III order; 4 – well and its number)

Figure 15. Diagram of distribution of groundwater pressure at the well 1388 before UNE

The groundwater proceeds mostly in the northwest direction with 0.003 average grade (Figure 15). Absolute elevations of piezometric surface are non-uniform throughout the area. Within the central block they are 334–334.2 m, in the northeastern block – 334.4 m, in the

eastern block increase to 336–336.2 m and in the southeastern block reach 343.9. In the zone of influence of regional fault the piezometric surface is inclined to the east, and the absolute elevations decrease below 334–360.4 m (wells 4038, 4040) in the southeast and to 332.8 m in the northeast.

Data on hydrogeological sampling in the wells before UNE are listed in Table 5.

Table 5.

Data on hydrogeological sampling in the wells

Well No	Level of water, м		Head, m	Debit Q, l/s	Depression S, m	Specific yield q, l/s	Water transmissibility of rock km, m^2/day
	emerging	established					
4039	36	4.1	31.9	0.40	32.2	0.01	1.3
4040	61	18	43	0.03	34.0	0.001	0.1
4041	2.1	2.1	-	0.08	43.2	0.002	0.2
4042	66	9.2	56.8	2.08	19.6	0.11	14.3
4043	69.9	16.6	53.2	0.21	30.2	0.01	0.9
4045	39	15.9	23.1	0.91	11.7	0.08	10
4054	37.5	13.2	24.3	0.36	12.1	0.03	3.9
4038	36	4.1	31.9	0.40	32.2	0.01	1.3
4044	39.5	23	16.5	0.40	14.8	0.03	3.5
4055	71	9.3	61.7	0.23	17.3	0.01	1.3

The groundwater tapped by the wells located within the blocks has low water inflow, up to 1.3 m^2/day. The presence of various-order ruptured zones predetermines the non-uniformity of filtration characteristics of hydrophilic medium. In the zone of influence of Kalba-Chingizsky fault, the rock transmissibility ranges from 0.05 m^2/day (the well 4040) to 3.5 m^2/day (the well 4044), and near higher-order ruptured zones increases to 14.3 m^2/day.

Based on the down-well flow meter data, a regular decrease in the fractured rock water content with the depth has been ascertained. The permeability is 1–1.6 m/day, increasing in tectonic cracking areas to 5 m/day.

Thus the hydraulic relation between the identified blocks can vary from perfect to difficult according in accordance with the generated piezometric surface charts within which a difference between the blocks amounts to dozens of meters [11].

2.2.3.3. Radionuclide contamination of groundwater at the south-western site

The data of laboratory analysis of groundwater samples taken from hydrogeological wells are listed in Table 6 [1, 2].

Table 6.

"South-Western" site. Radionuclide concentration in groundwater

UNE Date	*Distance, km	Well No	Sampling date	^{3}H, kBq/kg	^{137}Cs, Bq/kg	^{90}Sr, Bq/kg	$^{239+240}$Pu, Bq/kg
Aquifer system of Lower Carboniferous							
Central block							
1388 1987	0.4	**4075**	2003	437.35	1.30	37	-
			2004	561.70	0.28	37	<0.002
	0.4	**4076**	2003	55.28	<1.30	0.40	-
			2004	51.44	0.01	1.32	-
			2007	42.26			-
			2008	50	0.05	<0.01	-
	0.6	**4045**	2003	13.15	<0.60	1.20	-
			2004	21.54	0.002	0.03	-
	0.6	**4043**	2003	0.28	0.90	0.10	-
			2004	<0.16	0.01	2.01	-
			2005	0.13	0.90	0.30	-
			2007	0,10			-
Northeastern block							
1388 1987	1.2	**4066**	2002	<0.16	-	-	-
			2003	<0.16	-	-	-
			2004	<0.16	0.004	0.07	-
			2005	<0.6	-	-	-
			2007	0.03	0.0	0.20	-
	1.4	**4054**	2002	<0.16	-	-	-
			2003	<0.16	-	-	-
			2004	<0.16	0.003	0.03	-
			2007	<0.01	-	-	-
			2008	0.10	<0.01	0.14	<0.002
Southeastern block							
1388 1987	1.3	**4039**	2004	0.16	1.50	0.25	-
Aquifer system of Middle Cambrian							
In the southern zone of influence of Kalba-Chingizsky fault							
1354 1985	3.6	**4064**	2002	<0.16	-	-	-
			2003	<0.16	-	-	-
			2004	<0.16	0.01	0.03	-
			2007	0.02	1.20	0.50	-
			2008	<0.01	0.02	<0.01	<0.002
Outside the zone of influence of Kalba-Chingizsky fault							
1354 1985	3.5	**4055**	2002	<0.16	-	-	-
			2003	<0.16	-	-	-
			2004	<0.16	0.002	0.09	-
			2007	<0.01	-	-	-
			2008	0.04	-	-	<0.002

Note: * Distance from a hydrogeological to the nearest "warfare" borehole located downstream the ground water proliferation

"-" – no measurements were made

According to the tabular figures, the concentration of ^{137}Cs in all water samples is at the level of MDA. In most of the samples the concentration of ^{90}Sr ranges from 0.1 to 2.0 Bq/kg. Maximum concentration of ^{90}Sr has been measured in the water of the well 4075 where it is 37 Bq/kg, which is 7 times higher than the level established by NRB-99 IL_{pop} for drinking water at 5 Bq/kg. The concentration of tritium in groundwater widely ranges from 0.1 to 55.3 Bq/kg. Maximum concentration of tritium has been measured in the well 4075 (437.35 kBq/kg), which is almost 57 times higher than the level specified by NRB-99 IL_{pop} for drinking water (7.7 kBq/kg.)

The character of lateral extension of radionuclides is accounted for by the following peculiarities of hydrogeological conditions. Non-uniformity of rock impermeability is significant and different throughout the area due to presence of various-order ruptured zones. As mentioned above, the basic direction of groundwater propagation is northwest. Additional groundwater discharge can occur in the northwest and south directions [12]. The above-noted peculiarities account for the high concentrations of tritium in the wells 4075 and 4076 (437.4 and 55.3 kBq/kg, respectively). At the same time, these wells are located nearer to the "warfare" borehole 1388 compared to others. The presence of rather high concentrations of tritium in the well 4045 is due to the fact this well is located also on one of the paths of ground water propagation from the well 1388. The concentration of tritium in water from the well 4043 is much lower than in the well 4045, although this well is located at approximately the same distance southwest of the well 1388. This explains the fact that the groundwater proliferation from the well 1388 in the southwest direction is much slower than in other directions. The presence of low concentrations of tritium in the wells 4064, 4055, 4054 and 4066 is, in the first place, due to their remoteness from the well 1388.

Annual monitoring of tritium concentration in groundwater at this site was performed from 2002 to 2008. The analysis of tabular data shows that the dynamics of tritium concentration in groundwater has a complicated and ambiguous character. The concentration of tritium in the wells 4064 and 4076 has not virtually changed and in the well 4075, compared to the year of 2003, it has markedly decreased.

From the research data on the groundwater present within the South-Western site, the following conclusions can be drawn:

- The basic aquifer system is confined to the exogenous and tectonic cracking areas of Paleozoic rock, propagates everywhere and is of mostly pressure type.
- The groundwater proceeds mostly in the northwest direction with 0.003 average grade.
- The presence of various-order ruptured zones preconditions the heterogeneity of filtration characteristics of hydrophilic medium. The water transmissibility ranges from 0.05 m^2/day to 3.5 m^2/day and increases to 14.3 m^2/day near ruptured zones of higher order. The permeability is 1–1.6 m/day, increasing in tectonic cracking zones to 5 m/day.
- ^{137}Cs concentration is at MDA level, ranging from 0.002 to 1.3 Bq/kg. For most of the samples, the concentration of ^{90}Sr ranges from 0.1 to 2.0 Bq/kg. Maximum concentration of ^{90}Sr has been measured in water of the well 4075 where it is 37 Bq/kg, exceeding 7 times the level established by NRB- 99 IL_{pop} for drinking water. The concentration of $^{239+240}Pu$ in the groundwater of this site does not exceed MDA, being 0.002 Bq/kg.

- Tritium concentration in the groundwater ranges from 0.1 to 55.3 kBq/kg. Maximum concentration of tritium has been detected in the well 4075 where it is up to 437.4 kBq/kg, exceeding 57 times the level established by NRB -99 IL_{pop} for drinking water at 7.7kBq/kg.
- Proliferation of contaminated water front generally coincides with the direction of groundwater transport and has northwest direction.
- The distribution of radionuclides in groundwater depends on the geologic-structural conditions of the site.
- The groundwater of Lower Carbonaceous occurring within the central block is most exposed to radioactive contamination. A relatively high concentration of radionuclides in the groundwater of southeastern block compared to the northeastern one testifies to the predominant groundwater transit in the direction of Kalba-Chingizsky fault;
- Presence of radionuclides in the aquifer system of Middle Cambrian is due to UNE conducted in the well 1354 in 1985, which has resulted in the disturbance of groundwater dynamics and long-time restoration of piezometric surface. Elevated radioactive contamination of Middle Cambrian aquifer has been recorded in the southern zone of influence of Kalba-Chingizsky fault.

2.2.4. The "central" site

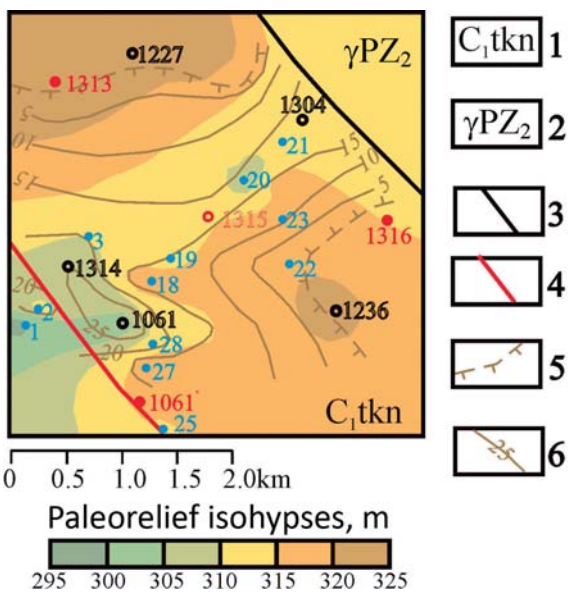

(Hereinafter: 1 – effusive-sedimentary deposits of Lower Carbonaceous;
2 – Upper Paleozoic intrusive formations; 3 – geological boundary; 4 – ruptured zones;
5, 6 – sediments of Neocene (seat clay): 5 – distribution limit with hachures; 6 – thickness isolines, m)

Figure 16. Schematic map of site paleorelif

This area of interest is located in the central part of the Balapan site. Basic sources of groundwater contamination with radionuclides at the site are the central zones of UNE conducted in the "warfare" boreholes 1061-bis, 1061, 1314, 1315 and 1236. Assessment of the nature of groundwater contamination with radionuclides has been made on the basis of sampling data on 8 hydrogeological wells drilled earlier (Figure 16).

2.2.4.1. Geological structure of the central site

The *Central* site is located within the bounds of alluvial-prolluvial plain. The geological structure of the site contains sedimentary-effusive sediments of Koyandinsky suite of Tournaissian stage of Lower Carboniferous (C_1t·kn) represented by mostly sandstones, shale, and tuff sandstones, interbedded, with a pronounced dip of rock to the northeast (Figure 16).

A ruptured zone of northwest strike conforming to the regional structure direction has been identified along the south-west boundary. The rupture is hydrogeologiclly active because it is traced beyond the boundaries of study area at the outermost southeast, more than 10 km away, within the Kazakh Upland area, serving as an area for groundwater recharge.

The change of lithologic composition and physicochemical characteristics of host rock has preconditioned considerable ruggedness of the surface of host rock roof. The paleorelief altitude difference is up to 30 m (Figure 16). A palaeovalley with the bottom gently dipped to the southwest stretches in the northeast direction. The paleorelif is filled with clays of Neocene, with a regular increase in the thickness downstream the paleovalley from 5 to 20 m and more.

In the northwest and east, the elevated areas show wedging out of clays of Neocene and represent "erosion windows" serving as local zones of infiltration recharge of groundwater.

2.2.4.2 Hydrogeological conditions at the central site

Groundwater within the *Central* site is confined to the upper zone of exogenous weathering of host rock and is tapped at a depth of 15.2 to 37 m. The pressure distribution conforms to the site paleorelief. Within the U-shaped areas of paleovalley the heads increase to 10 m and higher and decrease on the edges (Figure17). Unconfined groundwater prevails in the east of the site. Along the ruptured zone of northwest strike the head increases from 3.6 to 7.5 m.

The site is located in the area of groundwater transit with mostly northwest direction of proliferation. The local deviation of groundwater flow to the north and southwest is, probably, due to the presence of hydrogeologically active ruptured zone and execution of UNE in the wells located along the ruptured zone [13].

In the geological section, vertical zonality is maintained. On increasing the bedding depth, the seepage characteristics of water-absorbing rock decrease. The non-uniform spread of water transmissibility values in different periods of hydrogeological sampling is due to conducting of UNE.

Groundwater is moderately saltish and saltish, with 3.7–6.2 g/l mineralization; in the central part the mineralization increases to 7.4–7.6 g/l. By composition, groundwater is sulfate-chloride, and in the center - chloride-sulfate magnesium-sodium and hard; the water reaction is subacid.

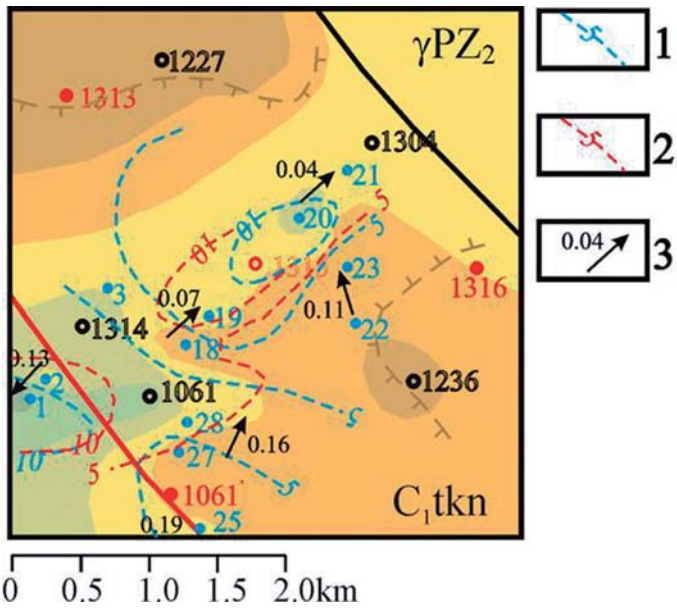

(1, 2 –isolines of groundwater head: 1 – under natural conditions, 2 – artificial disturbance from UNE in the well 1318; 3 – major direction of groundwater propagation and rate of level decrease under natural conditions)

Figure 17. Diagram of head distribution

2.2.4.3. Groundwater contamination with radionuclides at the central site

The results of laboratory analysis of groundwater are summarized in Table 7 [1, 2].

Table 7.

"Central" site. Radionuclide concentrations in the groundwater

UNE date	*Distance, km	Well No	Date of sampling	^{3}H, kBq/kg	^{137}Cs, Bq/kg	$^{239+240}$Pu, Bq/kg	^{90}Sr, Bq/kg
1061 1972	0.5	**4018**	2004	3.22	0.01	-	0.09
			2005	5.39	0.02	-	0.07
			2007	1.44	0.02	-	0.56
			2010	0.05	<0.01	<0.002	<0.01
1236 1981	0.6	**4022**	2004	0.22	0.003	-	0.10
			2005	0.03	1.16	-	0.78
			2007	0.01	1.16	-	0.08
			2008	0.10	<0.02	<0.002	0.03
	1.0	**4023**	2004	0.06	0.01	-	0.07
			2005	.02	0.18	-	0.14
			2007	<0.01	0.18	-	0.01
			2008	0.10	<0.01	<0.002	<0.01

UNE date	*Distance, km	Well No	Date of sampling	^{3}H, kBq/kg	^{137}Cs, Bq/kg	$^{239+240}$Pu, Bq/kg	^{90}Sr, Bq/kg
1314 1982	0.4	**4003**	2004	0.04	0.04	-	0.04
			2005	0.21	0.01	-	0.04
			2007	0.01	0.01	-	0.01
			2008	0.04	<0.01	-	<0.01
			2010	-	0.12	<0.002	0.20
	0.6	**4001**	2004	2.68	0.01	-	.07
			2005	0.02	0.02	-	0.04
			2007	<0.01	0.02	-	<0.01
			2008	0.02	<0.03	<0.002	<0.01
1061-bis 1985	0.3	**4027**	2004	0.45	0.01	-	0.04
			2005	-	0.06	-	0.17
			2007	1.24	0.02	-	0.70
			2008	0.50	<0.01	-	0.02
			2010	1.80	<0.01	<0.002	<0.01
	0.4	**4025**	2004	0.04	0.01	-	0.11
			2005	0.06	0.01	<0.002	6.42
	0.5	**4028**	2004	-	0.13	-	0.72
			2007	0.32	-	-	0.01
			2008	0.30	<0.01	<0.002	<0.01
1315 1987	0.4	**4020**	2004	0.12	0.02	-	0.18
			2005	-	0.08	-	0.07
			2007	1.24	0.08	-	0.02
			2008	0.10	<0.02	<0.002	0.02
			2010	0.24	<0.01	-	<0.02

Note: * Distance from a hydrogeological to the nearest "warfare" borehole located downstream the groundwater flow
"-" – no measurements were made

The research has shown that the concentration of ^{137}Cs in all water samples is within low values and ranges from 0.012 to 0.18 Bq/kg, with the maximum concentration of 1.16 Bq/kg in the well 4022. ^{90}Sr has also very low concentrations ranging from <0.01 to 0.7 Bq/kg. The concentration of tritium in the groundwater ranges from <0.007 to 1.44 kBq/kg. Maximum concentration of tritium was measured in 2010 in the well 4027 to be 1.8 kBq/kg. The obtained values constitute no radiological danger and do not exceed the levels specified by NRB-99 IL_{pop} for drinking water.

Thus, a characteristic feature of this site is the presence of marginal concentrations of artificial radionuclides despite the fact that hydrogeological wells are located close to 5 "warfare" boreholes. One of the explanations of this peculiarity is the prevalence of non-artesian groundwater at this site. Hence, wash-out of radionuclides from central zones occurs less intensively than at other sites. On the other hand, as noted above, this site is marked by a

zone of increased values of filtration flow discharge against its average values that is indicative of the presence of local groundwater recharge. In this case, there are grounds to state that the low radionuclide concentrations are due to their dilution by permanently received atmospheric precipitation.

In spite of the low radionuclide concentrations, during analysis of the obtained data it could be observed that the radioactive contamination of groundwater decreases on increasing the distance from 5 UNE.

Relatively high concentrations of tritium have been detected in the nearest zone of UNE conducted in the well 1061. Elevated concentrations of cesium have been measured in the east of the site, in the area of artesian water occurrence in the wells 4022 and 4023.

The following conclusions can be drawn from the survey data on the groundwater occurring within the Central site:

- The basic aquifer system confined to the areas of exogenous and tectonic cracking of Paleozoic rock occurs everywhere and it is both artesian and non-artesian.
- The major direction of groundwater proliferation is northeast.
- A characteristic feature of this site is the presence of low concentrations of artificial radionuclides in spite of the fact that hydrogeological wells are located close to the "warfare" boreholes (the concentrations do not exceed the values specified by NRB-99 IL_{pop} for drinking water). The concentration of $^{39+240}Pu$ in groundwater of the site does not exceed MDA, amounting to 0.002 Bq/kg.
- In spite of the low radionuclide concentration in groundwater, in general, this site revealed a decrease in the radioactive contamination of groundwater at larger distances from the central zones of UNE.

2.2.5. The "Zarechie" site

The formation of artificial-disturbed hydrogeodynamic situation at the Zarechie site in 1987–1990 period is due to 5 UNE conducted in the wells 1348, 1388, 1350, 1346 and 1352 [14]. 16 earlier drilled hydrogeological wells have been sampled to study the nature of radionuclide contamination at the site (Figure 18).

2.2.5.1. Geological structure of the Zarechie site

"Zarechie" site is located within the alluvial-proluvial plain, flatly dipping to the northeast at 0.001–0.002 grade. The study area is located in the northeast of Kazakh Shield in a zone of joining of two folded systems. The southern portion is confined to caledonides of Tarbagataisky meganticlinorium and the northern one – to the south-western wing of Zaisansky megasinclinorium of Herzinian age. The Caledonian and Herzinian structures collectively form a folded Paleozoic base marked by plicated and ruptured dislocation of sediments, fractured and crushed rocks (Figure 18).

Within the site, quite a number of various-order ruptured dislocations and big cracks bounding the blocks of relevant rank have been identified [SNiP 2.02.85]. The major ruptured dislocations of I–III order govern the position of the zone of influence of regional Kalba-Chingizsky fault of northwestward strike.

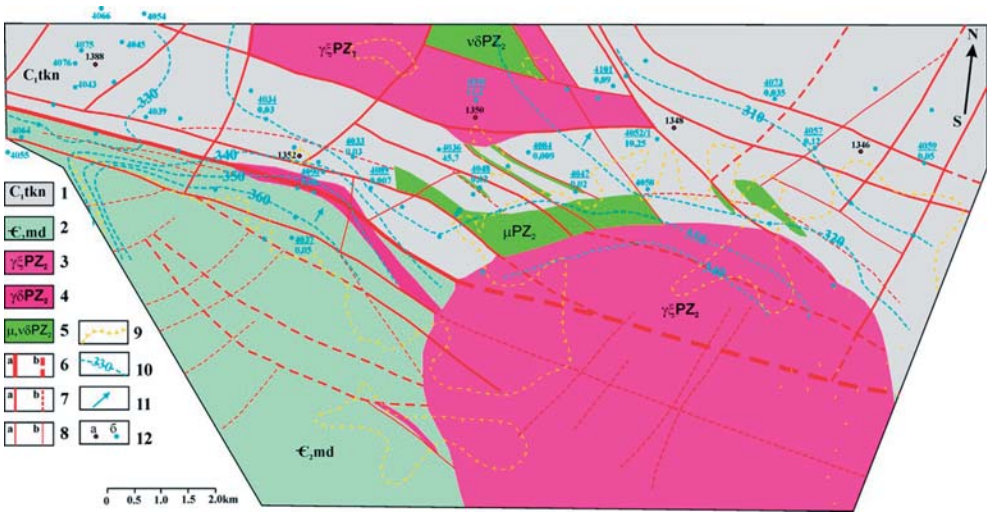

(1-5 – fissure and fissure-vein water : 1 – volcanogenic-sedimentary and metamorphized sediments of Lower Carbonaceous, 2 – volcanogenic and sedimentary deposits of Middle Cambrian, 3-5 – intrusive formations of Upper Paleozoic: 3 – granite, syenite, granite porphyrite; 4 – granodiorite; 5 – diorite, gabbrodiorite, porphyrite; 6-8 – ruptured dislocations (a – established, b – predicted): 6 – I order, 7 – III order, 8 – V and higher order; 9 – limits of propagation sediments of Miocene, bergstrichs are directed towards the development of sediments; 10 – hydroisobaths as of 1989.; 11 – major direction of groundwater propagation; 12 – well and its number: a – test, b - observational, figure in the denominator denotes the concentration of tritium in groundwater, kBq/kg)

Figure 18. Diagram of geological and hydrogeological conditions at the "Zarechie" site

2.2.5.2. Hydrogeological conditions at the Zarechie site

By the conditions of formation, propagation and age of water-bearing rock, at the site three complexes of fissure and fissure-vein pressure-non-artesian water are distinguished, hydraulically interconnected with each other:

- water-bearing complex of volcanogenic-sedimentary and metamorphized sediments of Lower Carbonaceous (C_1),
- water-bearing complex of volcanogenic-metamorphized and sedimentary deposits of Middle Cambrian ($Є_2$), and
- water-bearing complex of intrusive formations of Upper Paleozoic (PZ_2).

Groundwater is mainly artesian and is tapped at the depth of 2.1 to 70 m. The piezometric level ranges from 2 to 26.8 m creating up to 60–66 m head in the zone of regional fault influence.

Absolute elevations of piezometric surface along the horizontal decrease from 360m in the southwest to 310 m in the northeast. The major direction of groundwater proliferation is northeast with inclination ranging between 0.001 and 0.003. The local deviations of underground flow are due to the presence of ruptured dislocations and a concealed zone of discharge within the structural-erosion sections. In the zone of influence of Kalba-Chingizsky fault the groundwater gradient increases to 0.02–0.05.

Groundwater tapped by the wells located within the blocks has low water inflow coefficient, and the water-transmitting capacity of rock ranges from 0.01 to 1 m^2/day. The presence of various-order ruptured dislocations has preconditioned the heterogeneity of permeability characteristics of water-bearing medium. Thus in the northern zone of influence of Kalba-Chingizsky fault the water-transmitting capacity of rock is 0.01–1 m^2/day, and in the southern zone – up to 3–18m^2/day, increasing to 30 m^2/day near higher-order ruptured dislocations. The permeability ranges from 0.01 to 1 m/day and in tectonic cracking zones increases to 7 m/day and more.

Groundwater in the aquifer system of volcanogenic-sedimentary and metamorphized deposits of Lower Carbonaceous is mostly highly saltish with 3.2 to 8.9 g/l mineralization, and in the outermost northeast of the site –saline, with up to 10.9 g/l mineralization. By composition, the water is sulfate-chloride near ruptured dislocations, and on sections of local aquifer wedging out – chloride-sulfate-sodium-potassium, rarely, sodium-potassium-calcium, hard and very hard. The water reaction varies from weak acid to slightly alkaline.

Groundwater in the aquifer system of volcanogenic-metamorphized and sedimentary deposits of Middle Cambrian is mostly fresh, with 0.5–1.0 g/l mineralization, and in the zone of influence of Kalba-Chingizsky fault - low saltish to highly saltish in the outermost northwest of the site, sulfate-chloride and sodium-potassium-calcium. The gypsometrical postion of aquifer system has preconditioned the water hardness. On the absolute elevations of 360–365 m, the water is soft, moderately hard, and lower – hard and very hard. The water reaction varies from weak acid to slightly alkaline.

2.2.5.3. Groundwater contamination with radionuclides at the Zarechie site

The data of laboratory testing of groundwater samples are summarized in Table [1, 2].

Table 8.

"Zarechie" site. Radionuclide concentrations in groundwater

UNE date	*Distance, km	Well No	Date of sampling	^{3}H, kBq/kg	^{90}Sr, Bq/kg	^{137}Cs, Bq/kg	$^{239+240}$Pu, Bq/kg
1348 1987	0.4	4052/1	2004	10.25	0.23	0.05	-
			2007	54.70	0.34	0.01	-
	1.5	4101	2004	0.09	0.06	0.14	-
			2007	<0.01	-	-	-
1350 1988	0.4	4100	2005	-	0.11	0.04	-
			2007	12.20	0.38	0.01	-
	1.0	4036	2004		0.06	0.03	-
			2005	45.67	0.51	0.02	-
1346 1988	0.9	4057	2004	0.12	1.49	0.08	-
			2005	0.03	0.79	0.04	-
			2007	0.02	-	-	-
			2010	<0.01	<0.01	<0.01	<0.002
	1.3	4059	2004	0.05	0.04	0.004	-
			2005	-	0.09	0.02	-
			2007	<0.01	-	-	-
	2.0	4073	2004	0.04	0.65	0.09	-
			2005	-	0.25	0.05	
			2007	0.01	-	-	

UNE date	*Distance, km	Well No	Date of sampling	^{3}H, kBq/kg	^{90}Sr, Bq/kg	^{137}Cs, Bq/kg	$^{239+240}$Pu, Bq/kg
1352 1989	0.5	4090	2004	0.08	0.07	0.23	-
			2005	0.03	-	-	-
			2007	<0.01	-	-	-
	0.5	4088	2004	0.05	0.03	0.02	-
			2005	0.04	0.09	0.01	-
	1.0	4033	2004	0.03	0.42	0.40	-
			2005	-	0.09	0.06	-
			2007	0.01	-	-	-
	1.1	4034	2004	0.03	0.06	0.04	-
			2005	0.03	-	-	-
			2007	<0.01	-	-	-
Aquifer system C_1							
Groundwater recharge – Kazakh Upland	0.1	4058	2005	-	0.21	0.09	-
			2007	<0.01	-	-	-
	0.9	4084	2004	-	0.11	0.02	-
			2005	-	1.48	0.62	-
			2007	0.01	-	-	-
	1.8	4089	2004	-	0.27	0.18	-
			2005	-	0.10	0.32	-
			2007	<001		-	-
	Aquifer system C_2						
	0,3	4037	2004	0,05	0,05	0,03	-
			2007	<0,01	-	-	-
	Aquifer system PZ_2						
	0,2	4047	2004	0,07	0,34	0,03	-
			2005	0,03	0,28	0,03	-
			2007	<0,01	-	-	-
	0,5	4048	2004	0,02	0,05	0,04	-
			2005	0,02	0,17	0,26	-
			2007	0,02	-	-	-

Note: * Distance from a hydrogeological to the nearest "warfare" borehole located downstream the groundwater flow
"-" – No measurements have been made

The data in the Table show that the concentration of ^{137}Cs in groundwater varies from 0.02 to 0.62 Bq/kg. Maximum concentration of ^{137}Cs (1.9 Bq/kg) has been measured in water sampled in the well 4058. The concentration of ^{90}Sr ranges from 0.01 to 0.38 Bq/kg. Such values constitute no radiological hazard and do not exceed the levels specified by NRB-99 IL_{pop} for drinking water. The concentration of tritium in the groundwater varies within a wide range of values from <0.01 to 54.7 kBq/kg, which is almost 8 times higher that the level specified by NRB-99 IL_{pop} for drinking water.

In 2007, at 0.4 km distance from the test well 1348, 54.7 kBq/kg concentration of tritium was measured in the aquifer system of Lower Carbonaceous. At 1 km distance from the test well 1350, the concentration of tritium in the well 4036 is up to 45.67 kBq/kg. In the well 4100 drilled into granites showing high cracking, permeability and water inflow, located 2.5 times closer to the test well 1350, the concentration of tritium is 12.2 kBq/kg. Hence it

follows that the radioactively contaminated water is localized in the depressions of water-bearing rock roof of Lower Carbonaceous and Upper Paleozoic bedding at the elevations of 270 m and lower.

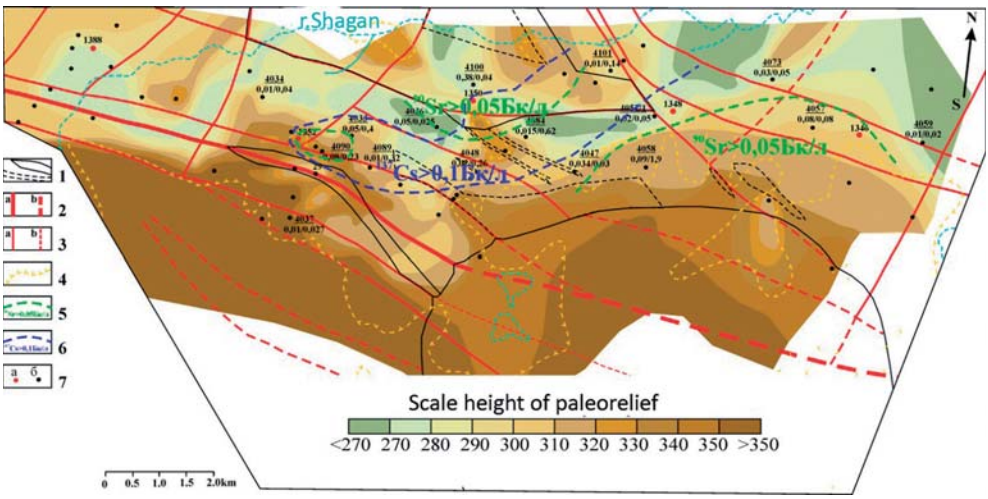

(1 – geologic boundary; 2-3 – ruptured dislocations (a – established, b – predicted): 2 – I order, 3 – III order, 4 – limit of propagation of Miocene sediments, bergstrichs are directed to the sediments development; 6, 7 – contours of relatively high radionuclide concentration: 6 – strontium, 7 – cesium; 8 – well and its number: a – test, b – observational, figures in the denominator correspond to the concentration of strontium and cesium in groundwater, Bq/kg)

Figure 19. Schematic map of palaeotopography of the Zarechie site with data on radionuclides concentration in the aquifer systems

Within 2 km from UNE epicenters, the concentration of tritium decreases with distance from UNE epicenter (Figure 18). Of note is a regular decrease in the concentration of basic radionuclides in different-age aquifer systems with distance from the basic recharge area, Kazakh Upland due to an increase in the groundwater run-off component.

The elevated concentrations of strontium (more than 0.05 Bq/kg) in groundwater, compared to the background concentration, are associated with the intrusive massif slopes, central - partly exposed in "erosion" windows, and south-eastern - outcropping on surface (Figure 19). The "plume" of increased concentration of cesium (more than 0.1 Bq/kg) extends along the steeper right edge of palaeovalley and is drawn towards the sites of UNE execution in the wells 1350 and 1352. Rather high concentrations of cesium (up to 1.9 Bq/kg) have been measured for the well 4058.

From 2002 to 2008, the wells available at the site were subject to annual radionuclide monitoring of groundwater. In the wells 4064 and 4076 the concentration of tritium has not practically changed, in the wells 4043, 4066 and 4054 slight decrease has been recorded, and in the well 4075 the concentration of tritium, compared to the year of 2003, has decreased markedly.

The following conclusions can be drawn from the results of groundwater monitoring within the Zarechie site:

- By the conditions of formation, spreading and age of water-bearing rock, at the site, three complexes of fissure and fissure-vein pressure-non-artesian water have been distinguished, hydraulically interrelated with each other.
- Ground water is mainly artesian. The piezometric level ranges from 2 to 26.8 m creating 60–66 m head in the zone of regional fault influence.
- The basic direction of groundwater proliferation is northeast.
- This site is notable for considerable heterogeneity of filtration characteristics of water-bearing medium ranging within 0.01–1m^2/day range and increases to 30 m^2/ day in zones of ruptured dislocations. The transmission coefficient ranges from 0.01 to 1 m/day, and in the tectonic cracking zones it increases to 7 m/day and more.
- Concentrations of ^{137}Cs and ^{90}Sr in groundwater do not exceed the level specified by NRB -99 IL_{pop} for drinking water.
- Concentrations of tritium in groundwater widely range from <0.007 to 45.7 kBq/ kg what is almost 6 times higher than the level specified by NRB -99 IL_{pop} for drinking water. The direction of tritium migration from the central zone of UNE coincides with the basic direction of groundwater proliferation.
- According to the sampling data on the well 4057, concentration of $^{239+240}Pu$ in the groundwater of the site does not exceed MDA, amounting to 0.002 Bq/kg.
- The site shows a decrease in the concentration of major radionuclides in different-age aquifer systems at a distance from the basic area of recharge due to an increase in the underground runoff.

2.2.6. The "Karazhyra" site

The "Karazhyra" site is located in the southwestern part of Balapan (Figure 10). At the present time, Karazhyra coal deposit is developed at the study area. The geological structure and hydrogeological conditions of the site are described in detail in paper [21]. Monitoring of radionuclide contamination of groundwater has been performed since 2003 based on the data of sampling 42 hydrogeological wells and drainage water of the operating open pit and evaporator pond (Figure 10) [21].

The following conclusions can be made based on studying of Karazhyra site groundwater:

- Lower Jurassic aquifer system spreads within the Karazhyra deposit. The aquifer system provides the major volume of water inflow to the open pit. The general flow of groundwater is directed from the southwest to the north and northwest, to the River Irtysh valley.
- At the area of deposit, the aquifer system of Lower Jurassic contains mainly water with mineralization 9.4-55.5 g/dm^3. By chemical composition, the water is chloride and sulfate-chloride-magnesium-sodium.
- Concentrations of artificial radionuclides ^{137}Cs, ^{90}Sr, $^{239+240}Pu$ and tritium in groundwater do not exceed the level specified by -99 IL_{pop} for drinking water;

- The results of groundwater monitoring show relative stability of migration processes. A tendency to overall reduction of concentrations of artificial radionuclides in groundwater has been noted.

2.2.7. The site No.1 (Profile of the wells 1203, 1414 to Shagan River)

The site is located in the eastern part of Balapan (Figure 20). By analysis of the data on the hydrogeological conditions, this site has been identified as one of the areas governing the most critical direction of possible discharge of contaminated water to the Shagan River water. The site has a depression in the bottom relief of about 8 km^2 composed by clays of Miocene. 7 UNE have been performed at the site. The experience of work at STS shows that such depressions have generally higher concentrations of artificial radionuclides than the surrounding rock blocks. In relation to this, the main objective for our works at this site was to obtain data on the radioactive contamination of fissure groundwater and identify possible relation of fissure groundwater to the Shagan River water.

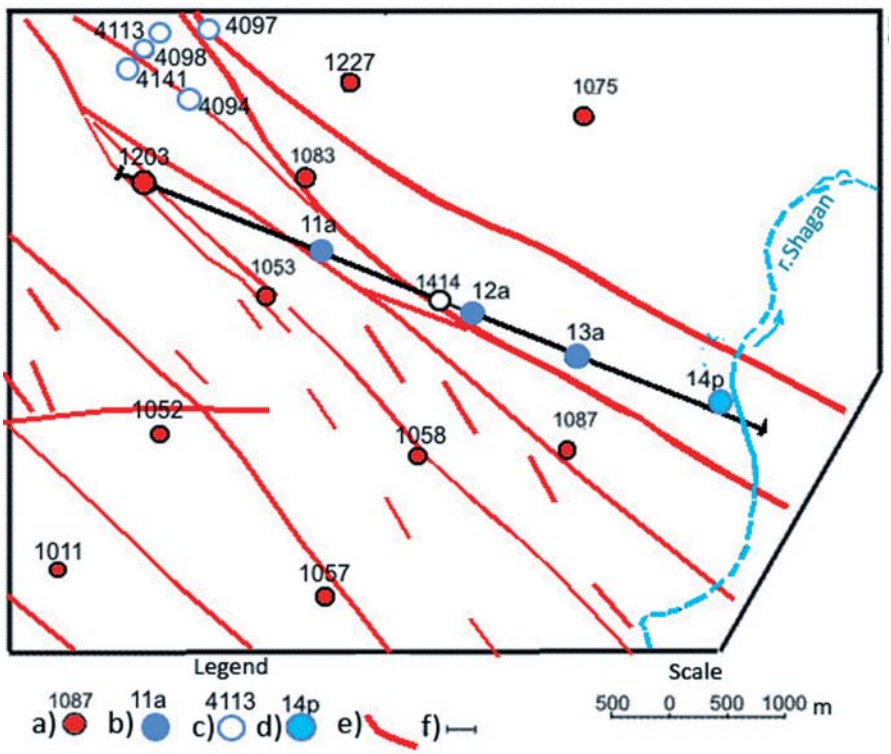

Wells: a - emplacement; b – hydrogeological, 2006.; c – hydrogeological, drilled earlier; d – observational; e – tectonic dislocations; e –geologic-geophysical section line

Figure 20. Site No1. Layout of the wells drilled on profile near the Shagan River

2.2.7.1. Geological and hydrogeological conditions at the site No 1

Based on the geophysical data, locations have been chosen for drilling three hydrogeological wells: 11a, 12a and 13a of 114, 92 and 60 m deep, respectively (Figure 21). In the wells, a complex of geologic-geophysical and hydrogeological studies has been performed, including the 24-hour pumping tests. Based on drilling of new wells and taking into account the earlier-drilled neighboring wells, a geologic-geophysical section has been constructed, making it possible to detail the geological situation in the area surveyed (Figure 21).

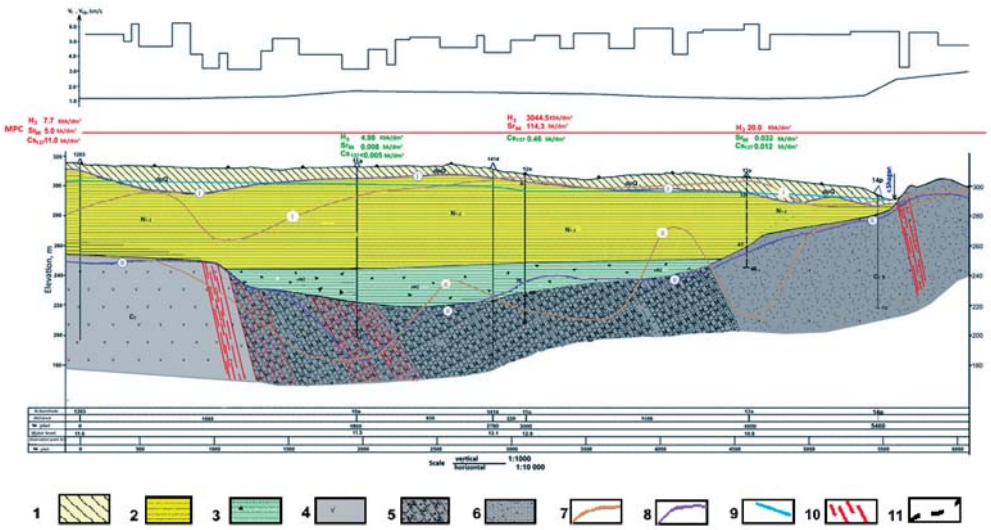

1 –sandy loam, loam of Quaternary; 2 –clay of Neocene; 3 –weathering crust, alluvial rubble-clay soil of Mesozoic; 4–6 – Carbonaceous: 4 – andesite 5 –sandstones and siltstones, 6 – tuff sandstones; 7 – interface of layers having different resistance: I – bottom of Quaternary sediments with 30–600 Ohm·m resistance; II – between argilliferous formations (2–12 Ohm·m resistance) and bottom rocks (more than 1,000 Ohm·m resistance); 8 – interface of layers with different rate characteristics; I – boundary of Quaternary formations with less than 1 km/s velocity; II – upper boundary of rock bottom with more than 2.5 km/c speed; 9 – groundwater level; 10 – tectonically fractured zones; 11 – conjectural base of exogenous cracking zone. At the top: plots of boundary speed and average speed (km/s)

Figure 21. The Site No.1 Geologic section based on the results of geophysical surveying

Sedimentary rocks of Viseian stage of Lower Carbonaceous (C_1v), represented by carbon-bearing siltstones and sandstones have been penetrated by the wells 11a and 12a at a depth of 95 and 80 m respectively. The wells 13a and 14p have penetrated tuff sandstone of Serpukhovian stage of Lower Carbonaceous (C_1s) at a depth of 47 and 14 m, respectively. In all wells, a zone of exogenous cracking is visible to 30–40 m depth. The thickness of clays of Neocene (N_{1-2}) ranges within 0–60 m in the west and in the center.

At the right bank of Shagan River, clays of Neocene wedge out. The wells 11a and 12a have penetrated alluvial rubble-clay formations of Mesozoic (*eMZ*) developed on siltstones and sandstones of Lower Carbonaceous (C_1v) at 65–67 m depth. Assessment of debits, transmissibility, permeability, and aquifer thickness in the wells 11a, 12a, 13a, 14p is summarized in Table 9.

Table 9.

Testing for underground water inflow and radionuclide concentration in groundwater

Well No	Depression, m	Debit, m^3/day	Transmissibility, m^2/day	Aquifer thickness, m	permeability m/day	^{3}H, kBq/kg	^{90}Sr, Bq/kg	^{137}Cs, Bq/kg^3	Nearest "warfare" borehole, km
11a	6.95	86.40	3.00	50	0.060	4.98 ±0.04	0.008±0.003	<0.005	1053 / 0.6
12a	9.40	43.20	3.40	40	0.085	3044.5 ±0.9	114.0 ± 5.7	0.46 ± 0,11	1414 / 0.3
13a	2.5	3.12	1.96	40	0.049	20.0 ±0.1	32 ± 13	0.012 ±0.004	1087 / 0.8
14p	10.10	9.20	0.25	40	0.006				

According to the data listed in the Table, the rock penetrated by the wells 11a, 12a and 13a has rather high (1.96–3.4 m^2/day) water transmissibility, as distinct from the rock penetrated by the well 14p (km=0.25 m^2/day). The highest transmissibility is exhibited by the rock composing the area of the well 11a that, judging by the low boundary velocity values, can be attributed to zones of elevated cracking and, accordingly, elevated permeability. The water table gradient in the direction of the Shagan River is 0.002.

2.2.7.2. Groundwater contamination with radionuclides at the site No. 1

The results of assessment of artificial radionuclides in groundwater samples from the wells 11a, 12a, 13a, 14p are presented in Table 9 [2].

Analysis of water samples taken from the drilled wells showed high concentrations of tritium and strontium-90 in the well 12a (3,045 kBq/kg and 114.0 Bq/kg, respectively) and tritium in the well 13a (20 kBq/kg).

Based on the results of geologic-geophysical survey at the site, the existence of enclosed depression of Paleozoic foundation composed by waterproof clays of Neocene of up to 60 m thickness has been confirmed. Moreover, hidden groundwater discharge to the Shagan River according to the grade is possible. According to the hydrological survey data, the Shagan River bed at the Site No 1 is composed by hard rock overlaid by a low-thickness cover of loose sediments. Within the erosion "window" of interest there has been traced steady hydraulic relation between different-age aquifers developed in seamy rock and alluvial sediments and surface water. Thus the areas of hidden groundwater discharge present potentially active zones of radioactive contamination of the Shagan River surface water with tritium, in particular.

2.2.8. The site No. 2 (Profiles of the wells 1056 – "Atomic" lake)

The site is located in the eastern part of Balapan (Figure 10). A basic task of works at this site was to identify possible relation between fissure groundwater and surface water of the artificial reservoir, the "Atomic" lake. The nearest "warfare" borehole 1056 is located 2.5 km away from the "Atomic" lake, to the north-west. At the time of well drilling, the

piezometric level was 12.46 m and the current water level in the "Atomic" lake is 306.3 m. It gives grounds to state that the groundwater discharge proceeds from the well 1056 in the direction of the "Atomic" lake.

2.2.8.1. Geologic-hydrogeological conditions at the site No 2

Geophysical study, drilling of three hydrogeological wells (1A, 2A and 3A), and testing for underground water inflow with the subsequent groundwater sampling for chemical and radionuclides analyses have been performed to study the hydrogeological conditions of the Site No 2. The obtained data are presented in Table 10 for each well.

Table 10.

Groundwater levels in the monitoring wells

Monitoring well No	Well depth, m	Distance from C-1056, m	Absolute elevation of wellhead, m	Water level, m	Absolute water mark, m	Water level difference, m
C-1A	43.0	50	317.72	5.7	312.02	
C-2A	50.0	250	314.89	4.6	310.29	1.73
C-3A	62.0	750	320.72	13.0	307.72	2.57
Funnel					306.31	1.41

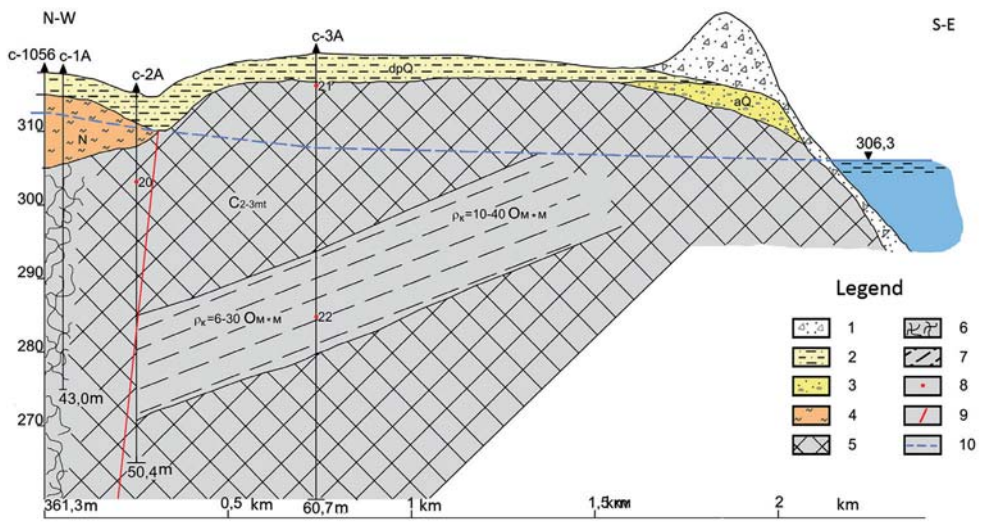

1– rock fragments ejected by explosion; 2 – deluvial-proluvial sandy loam and sand (dpQ);
3 – alluvial sand and pebble (aQ); 4 – waterproof clay of Neocene (N);
5 – terrigenous coarse sediments of Maityubinsky suite of Middle-Upper Carbonaceous (C_{2-3}mt);
6 – rock breakage zone on blasting in the well 1056; 7– rock horizon with low specific electrical resistance;
8 – elevated gamma-ray activity according to the log data (μR/hour); 10 – groundwater level.

Figure 22. Profile section: well 1056 – well 1004 ("Atomic" lake)

In the wells (Figure 22), there develops mainly the terrigenous stratum of Middle-Upper Carbonaceous represented by sandstones, conglomerates, carbonaceous clay shale and siltstones with carbonaceous shale intercalations. In the upper part of drill core the rock is subject to exogenous weathering.

At the Site No. 2, groundwater is artesian. The aquifer level penetrated by the wells C-1A – C-3A, decreases from 321 m absolute marks to 307.7 m in the direction of the "Atomic" lake. The chemical composition of fissure water is identical (Figure 23); water is chloride-sulfite-sodium.

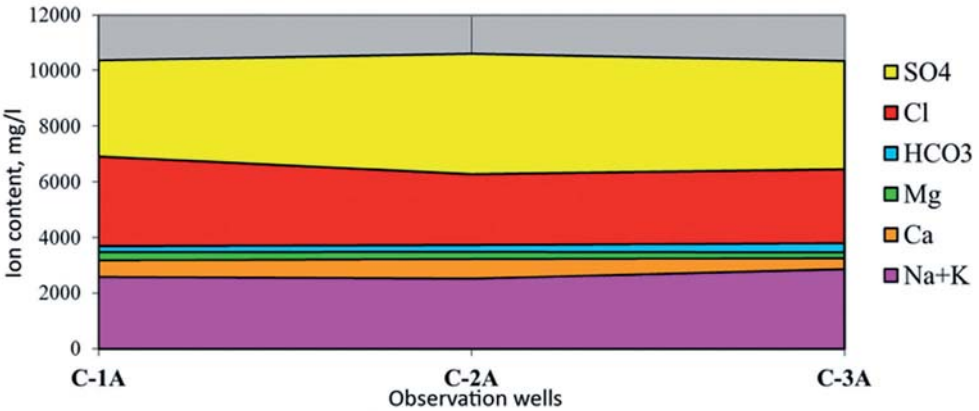

Figure 23. Chemical composition of groundwater along the profile of the wells C-1A – C-3A

Test pumping in the wells C-2A and C-3A on two depression levels has been performed, making it possible to determine the dependence of debit on the depression value necessary for reduction of the debit to a single depression value (for instance, 40 m) and obtaining comparable results (Table 11).

Table 11.

Characteristics of aquifer penetrated by the wells C-1A – C-3A

Well No	Pumping	Debit, Q, m^3/hour	Depression S, m	Sampling interval, m	Transmis-sibility km, m^2/day	Perme-ability k, m/day	Coefficients of formula of Q on s dependence		Debit re-duced to 40 m depression
							A	β	
C-1A		3.6	0	-	-	-	-	-	-
C-2A	1	0.756	16.1	4.4-20.5	0.36	3.86	-81.6	136.1	0.95
	2	0.864	31.1	4.4-35.5	0.18	2.28			
C-3A	1	0.43	4.6	13.4-18.0	1.0	8.0	-94.35	244.3	0.64
	2	0.50	13.9	13.4-27.3	0.26	3.08			

The reduction of debit value to a single depression at 40 m level has shown the debit in the well C-3A to be much lower (by 33 %). Rather high permeability (k=8.0 m/day) has been measured in the upper portion of the well C-3A. The permeability coefficient for the same aquifer thickness in the well C-2A appears to be more than 11 m/day. The obtained high coefficients indicate that the groundwater seepage is more intensive in the upper part of aquifer confined to the exogenous weathering zone [2].

2.2.8.2. Groundwater contamination with radionuclides at the site No. 2

As shown by the data of laboratory testing of water samples taken from the wells 1A, 2A, 3A, fissure groundwater in the profile under consideration is contaminated with radionuclides; the highest contamination level was observed near the well 1056 (Table 12) [2].

Table 12.

Site No. 2. Concentration of radionuclides in groundwater

No	Sampling location	Sampling date, Month, year	^{3}H, kBq/kg	^{90}Sr, Bq/kg	^{137}Cs, Bq/kg	Nearest "warfare" borehole, km
1	C-1A	06.2005	281.6	1240.0	4.0	1056 0,06
2	C-2A, 20 m depth	06.2005	152.7	49.0	<0.1	1056 0.2
3	C-2A, 35 m depth	06.2005	150.8	40.0	<0.1	
4	C-3A	07.2005	0.161	0.02	<0.1	1056 0.8
5	"Atomic" lake	05.2005	3.1	0.2	2.0	

The character of radionuclide propagation along the well profile shows the rock block penetrated by the well 3A to be a boundary between the contamination caused by tests in the "warfare" boreholes 1056 and 1004. It can be seen from the Table that minimum concentrations of tritium have been measured in water from the well C-3A located in the central part of the profile and penetrated within the partly drained water of exogenous weathering zone. The high concentration of tritium in the artesian aquifer penetrated by the well C-2A indirectly testifies to limited migration of tritium with groundwater in the direction of the "Atomic" lake. Propagation of contaminated water halo can proceed mainly along the paleovalley identified in the rock roof of Paleozoic, from the east of the well C-2A, in conformity with the pressure type of aquifer under study (Figure 22).

2.2.9. The site No.3 (Profile of the wells 1209 and 4033)

The study area is located on the profile between the "warfare" borehole 1209 and the hydrogeological well 4033 (Figure 24).

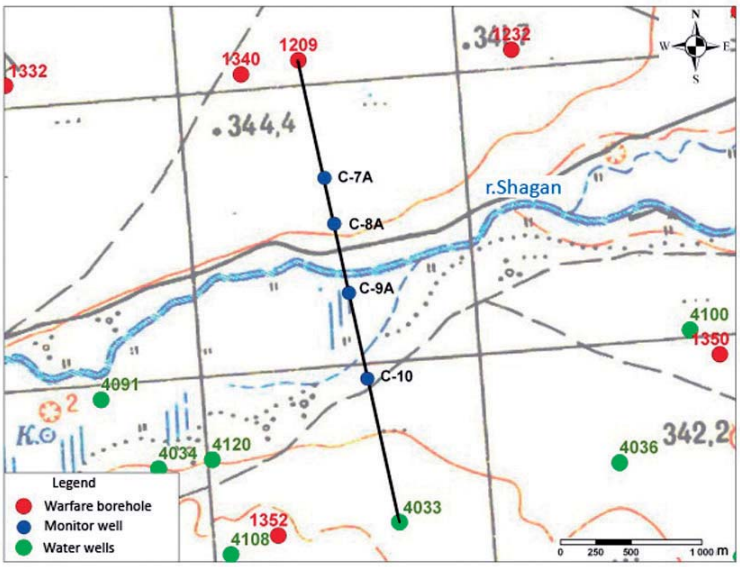

Figure 24. Site No. 3. Layout of the wells drilled by profiles 1209–4033

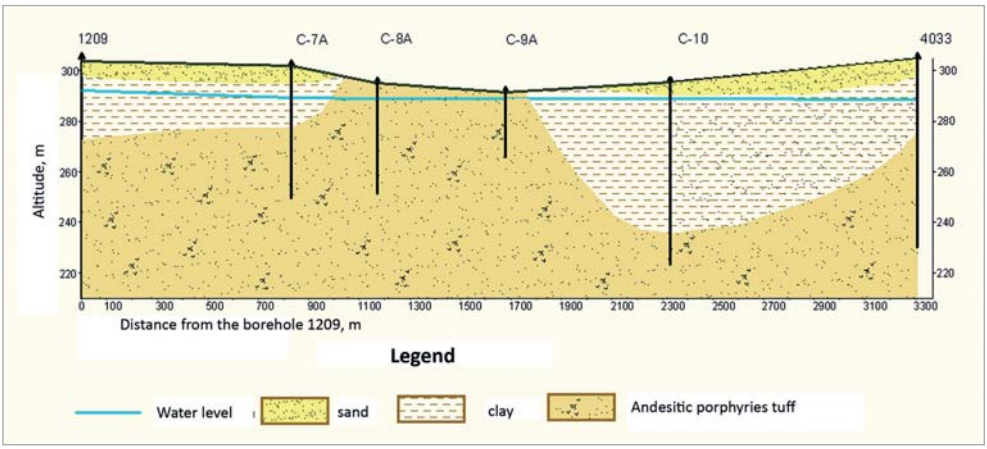

Figure 25. Geological section of the well profiles

The analysis of data on the structure of filtration flow at this site (Figure 10) shows that contaminated groundwater can enter the Shagan River water both from the right bank of UNE execution in the well 1352 and from the left bank – "warfare" boreholes 1209, 1340, 1332. Along the profile of the wells 1209 – 4033, clay sediments of the Shagan River wedge out. Quaternary alluvial sediments as a low-thickness mantle overlie the rock of Lower Carbonaceous (Figure 25). Within the "erosion window" under consideration, aquifers prevailing in the alluvial sediments and fissure rock are hydraulically interrelated with the Shagan River surface water.

2.2.9.1. Geologic-hydrogeological conditions at the site No. 3

4 monitoring wells (C-7A – C-10A) (Figures 24, 25) have been drilled between the well 1209 and the hydrogeological well 4033 on the profile of 3.3 km length intersecting the Shagan River bed in the direction from north to south.
Groundwater survey has been accomplished for all wells. The data on the wells are summarized in Table 13.

Table 13.

Results of groundwater level survey along the profile of the wells 1209 – 4033

Well No	Well depth, m	Distance from "warfare" borehole 1209, m	Water level,	Absolute mark of water, m	Relative decrease of level, m	Underground flow gradient
1209	601.0	0	11.6	331.9		
C-7A	52.8	830	12.8	329.17	2.73	0.003↓
C-8A	44.1	1170	6.4	328.67	0.5	0.001↓
C-9A	25.6	1680	2.15	329.01	+0.34	0.001↑
C-10	72.0	2330	6.35	328.97	0.04	0.001↓
4033	74.7	3310	16.6	328.3	0.67	0.001↓

It can be seen, that from the "warfare" borehole 1209 the groundwater table has a grade in the direction of the Shagan River. According to the survey data, the Shagan River floodplain has a local difference in elevation of 34 cm in the well C9-A indicative of additional infiltration recharge of groundwater within the identified "erosion" window [2].

2.2.9.2. Groundwater contamination with radionuclides at the site No. 3

The radionuclide analysis of water samples taken from the wells C-7A, C-8A, C-9A and C-10A drilled between the well 1209 and the hydrogeological well 4033 along the profile of 3.3 km length intersecting the Shagan River bed in the direction from north south shows the concentration of artificial radionuclides to be low and not in excess of the allowable values for drinking water (Table 14) [2].

Table 14.

Site No 3. Radionuclide concentrations in groundwater

No	Sampling location	Sampling date, Month, year	^{3}H, kBq/kg	^{90}Sr, Bq/kg	^{137}Cs, Bq/kg	Nearest "warfare" borehole, UNE yield is 20 - 150 kt
1	C-7A	08.05	n/a	0.25	0.31	1340 / 0.8
2	C-8A	08.05	0.1	0.03	<0.005	1340 / 1.2
3	C-9A	06.05	0.02	0.02	0.01	-
4	C-10A	08.05	n/a	0.19	0.17	1350 / 2.3
5	4033	05.05	0.03	<0.01	0.06	1350 / 2.4

According to the monitoring data in the wells 1209 – 4033, the underground flow gradient in the south direction decreases from 0.003 to 0.001 except for the area of the well C-9A. Within the identified "erosion: window, groundwater receives additional infiltration recharge. The same is indicated also by the radionuclide analysis data. In water samples taken from the well C-9A the concentration of tritium is minimum, 0.02 kBq/kg. On the contrary, in the wells C-7A and C-10A falling within the hydrodynamic influence zone of UNE conducted in the wells 1340 and 1350, relatively high concentrations of strontium and cesium have been measured.

Thus, the water stream from the upper valley is rather high and blocks the penetration of fissure water from the northern side of the site. It can be assumed that in extremely drought seasons, when the seepage in alluvial sediments decreases, the contaminated fissure water from the "warfare" boreholes can penetrate into the river water.

2.2.10. The site No.4

The site is located in the central part of Balapan in the zone of joint of Chinrausky and Karazhyra faults. At this site, 5 UNE have been conducted in the "warfare" boreholes: "Glubokaya", 1206, 1267, 1207 and 1287. 12 coring wells have been drilled to study the nature of radionuclide contamination in the groundwater (Figure 26).

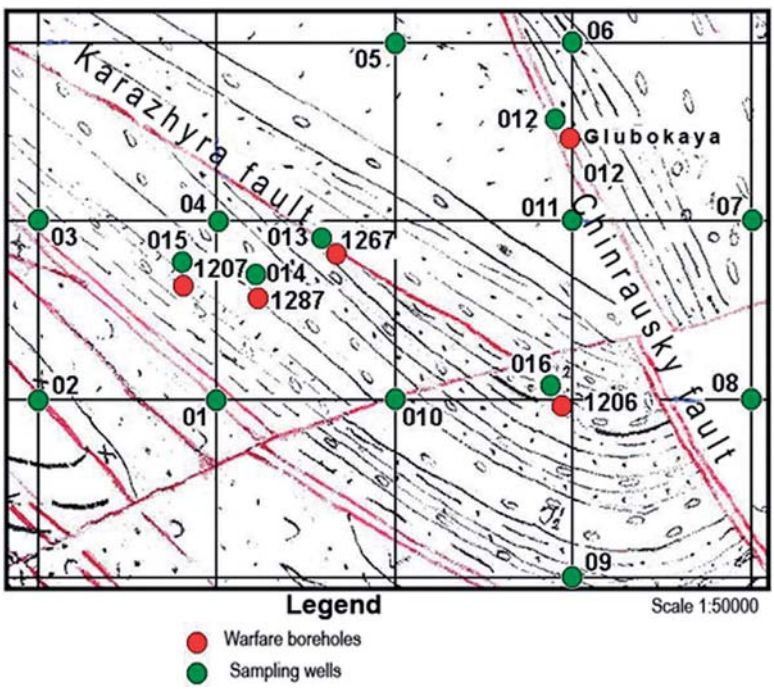

Figure 26. Balapan site. Layout of the wells drilled for radiation monitoring of groundwater

2.2.10.1. Geological structure of the site No.4

According to the drilling data, the upper portion of well section is composed by a low-thickness (5 m) cover of loose alluvial-deluvial sediments of Quaternary. Clays of Neocene of up to 55m thickness underlie below. The rock sediments are represented by conglomerates, sandstones, siltstones and argillite of Early-Middle Jurassic.

According to the results of reduced chemical analysis, the water mineralization is 8 to 21 mg/dm^3. The water is alkaline, with pH<7. The basic anions are Cl^- and SO_4^{2-}. Chloride water is developed in the basic suture zone of Chinrausky fault in the northeast and east parts of the site. Sulfate water prevails in the western portion of the site. In the south and east of the site, water is mainly chloride. With regard to cations, Na^+ prevails (>60%) in all samples. It is noteworthy that in water with the prevalent sulfate anion the content of hydrocarbonate component and calcium cation is 2–3 times higher than in water with the prevalent chloride anion. The main flow of groundwater in the surveyed area of the site is northward, eastward and northeastward [2].

2.2.10.2. Groundwater contamination with radionuclides at the site No.4

The results of analyses on the assessment of tritium concentration in water samples are presented in Table 15. Of the artificial radionuclides contained in the water samples, concentrations have been determined for ^{137}Cs, ^{90}Sr and tritium. Concentration of ^{90}Sr in all samples is not higher than 0.19 Bq/kg, and concentration of ^{137}Cs is not higher than 0.82 Bq/kg. These values are much below the IL_{pop} specified by NRB-99 [2].

Table 15.

Site No 4. Radionuclide concentrations in groundwater

No	Well No	Activity of tritium, kBq/kg	Nearest "warfare" borehole, km
1	01	0.024	1206 1.9
2	06	150	Glubokaya 0.5
3	07	140	Glubokaya 1.2
4	08	160	1206 1.0
5	09	0.02	1206 1.1
6	010	0.02	1206 1.0
7	011	130	Glubokaya 0.6
8	012	160	Glubokaya
9	013	0.03	1267 0.1
10	014	0.04	1267 0.5

No	Well No	Activity of tritium, kBq/kg	Nearest "warfare" borehole, km
11	015	0.03	1207 0.1
12	016	0.04	1206 0.1

The character of lateral propagation of tritium in groundwater is governed by the geological structure features and hydrogeological conditions at the site. The research has shown that the concentration of ^{3}H in groundwater in the zone of influence of Chinrausky fault is considerably higher and ranges from 140 to 160 kBq/kg, and in Karazhira fault zone from 0.02 to 0.04 Bq/kg. Thus, the northwestern boundary of elevated concentrations of tritium in groundwater has been confirmed according to the results of works.

It should be noted that ruptured dislocations at the Balapan site have different time of embedding. The Chinrausky fault represents a structure of later embedding compared to the Kalba-Chingizsky and Baiguzin-Bulaksky ruptured zones and Zhanasky zone of crush because they bound the Mesozoic graben. According to the results of accomplished hydrogeological sampling, the water-bearing rock in the zone of Chinrausky fault influence has elevated vales of water transmissibility and hydraulic permeability affecting the migration of tritium with groundwater from the UNE locations.

3. MIGRATION OF THE RADIONUCLIDES WITH GROUNDWATER BEYOND THE BOUNDARIES OF THE BALAPAN SITE

Earlier, the problem of possible migration of artificial radionuclides with groundwater streams beyond the boundaries of the Balapan site has not been attended properly. Recently, this problem has been studied as a part of integrated exploration aimed at using some of STS territories for economic purposes.

In order to get a general idea of possible pathways of contaminated water, one should remember that the test site is a part of regional hydrogeological system of the left bank of River Irtysh. The basic direction of groundwater proliferation is north – northeast. The groundwater discharge area is the well valley of River Irtysh. Within the area of interest, there prevails fissure water confined to the zones of exogenous weathering of bottom rock and ruptured dislocations.

It is known from the international geological survey practice that groundwater in zones of influence of ruptured dislocations have rather high seepage characteristics. Hence, the regional faults at the Balapan site such as Chinrausky, Kalba-Chingizsky and Baiguzin-Bulaksky may be considered as one of the major migration pathways of radionuclides with groundwater. The Zhanansky zone of crush is special in this regard.

Based on the geological structure features and quantitative distribution of underground nuclear explosions at the Balapan site, two basic blocks of radionuclide concentrations divided by a wedge-shaped graben filled with mainly Jurassic sediments, have been distinguished (Figure 27, 1).

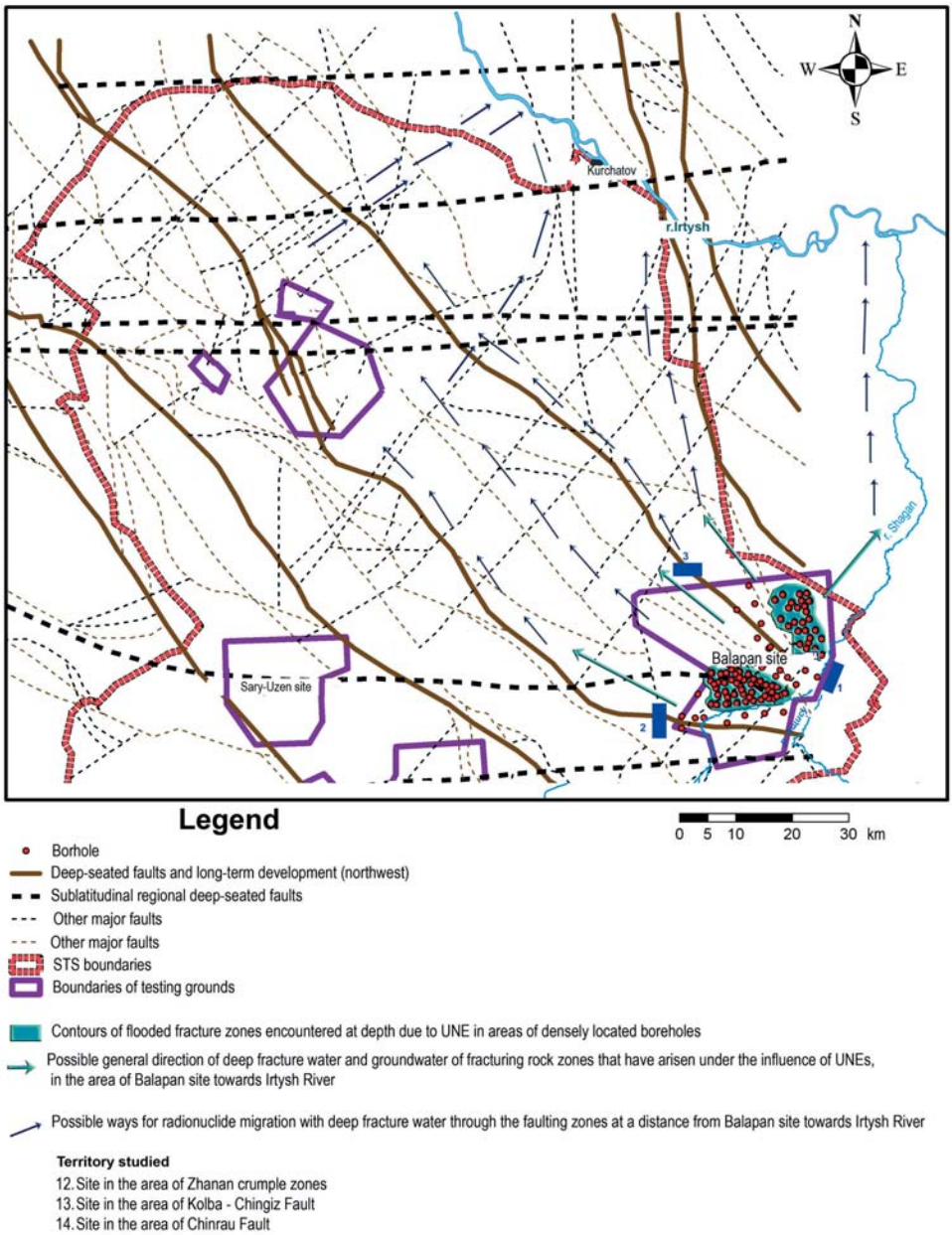

Figure 27. Diagram of possible regional migration pathways for artificial radionuclides with fissure-vein water

Central zone. The zone contains 64 "warfare" boreholes, most of which (56) are allocated at 80 km^2 site between Shagan River and the southern branch of Chinrausky fault, Karazhirsky fault. Execution of such a number of UNE has resulted in irreversible deformation of rock at a hypocenter level, formation of conjugate artificial cracking zones and rejuvenation of existing cracks. For some explosions, the observational wells have shown change of hydrogeological situation and strongly pronounced regional downward trend in the piezometric surface [13]. The study area has a position favorable for flooding and active groundwater dynamics owing to the development of a great number of ruptured dislocations of north-westward direction. Thus, the most probable groundwater pathway from the central zone would be north-westward with the discharge of fissure water in the direction of River Irtysh.

Northeast zone. In this zone, 42 subsurface nuclear tests have been conducted, the highest density of "warfare" boreholes (27) being recorded for 80 km^2 area in the northeastern part of Balapan. The direction of groundwater proliferation from the north-eastern zone is governed by the direction of ruptured structures, and it is north-westward, northward and north-eastward.

Thus, at present, the studies on the migration of radioactive products with groundwater outside the Balapan test site are focused on the analysis of the condition of regional fault zones of influence. The results of works on this subject obtained recently are presented below.

3.1. Conditions of groundwater in the Kalba-Chingizsky fault zone

3.1.1. Geologic-hydrogeological conditions

The biggest tectonic structure at the Balapan site is the Kalba-Chingizsky fault dividing the Chingiz-Tarbagataisky and Zharma-Saursky structural-formational zones (SFZ). The general fault strike is north-westward, and within the Balapan site – sublatitude. The fault plane dips to the southwest at an angle of 70–85°. The width of zone of influence of fault is up to 10 km. The Kalba-Chingizsky fault is quite often partitioned to a sequence of echelon-like faults.

The study area is located in the southwest of Balapan site, and in Figure 28 is designated by number 2. The scope of works includes geophysical surveys, drilling and testing for underground water inflow, and groundwater sampling for radionuclide analysis.

Geophysical surveys. Seismic study was carried out at the Kalba-Chingizsky fault by method of refracted waves (RWM) to choose most suitable points for drilling wells. The length of profiles on each section was chosen with due account for the topographical relief features and geological-and-structural conditions. The geophysical profile in the zone of Kalba-Chingizsky fault influence has 1840 m length. This method was used to confirm the structure of the upper part of geological section to 150 m depth. Each profile was traversed by a set of reversed time-distance and catching-up time-distance curves; the station interval was 10 m, and the distance between the points of seismic energy excitation - 100 m. The obtained velocity section in shown on Figure 28.

Based on the analysis of seismic velocity profile, rock decompaction zones of low seismic velocity have been identified within 180–260 m, 1130–1180 m and 1520–1580 m station distances, informative for the well location.

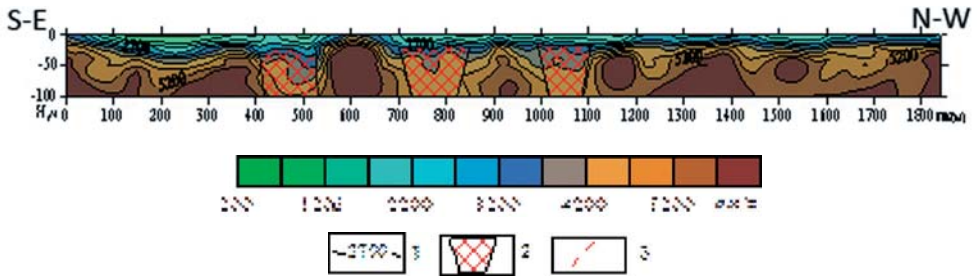

1 – isovelocity contour, m/s; 2 – tectonic zone; 3 – tectonic fault

Figure 28. Velocity profile

Drilling of wells. Taking into account the results of geophysical works, well locations have been chosen, and 2 wells have been drilled. The well 30/1 has been drilled for studying interstitial water and the well 30P for studying fissure water. The data on the wells are summarized in Table 16.

Table 16.

Summary data on the wells

Well No	Well depth, m	GWL, m	Fault pathway	^{137}Cs, Bq/kg	$^{239+240}$Pu, Bq/kg	^{3}H, kBq/kg
30/1	4.5	3.30	Kalba-Chingizsky	<0.01	<0.004	<0.011
30P	49	4.7	Kalba-Chingizsky	<0.01	<0.0016	0.05

According to the data on testing for underground water inflow for the well 30/1, K_f = 0.72 m/day; q=0.09 m^3/hour.

3.1.2. Groundwater contamination with radionuclides

The results of radionuclide analysis of groundwater samples taken from the drilled wells are presented in Table 16 [2]. The contents of artificial radionuclides ^{137}Cs and $^{239+240}$Pu in groundwater of Kalba-Chingizsky fault is below MDA, and the contents of ^{3}H in the well 30P is 0.05 kBq/kg. The measured radionuclide contents are not dangerous and are considerably below the intervention level specified by NRB for the general population to be received with water and food. At the same time, the fact of detecting tritium in fissure-vein water is indicative of the migration of artificial radionuclides along the Kalba-Chingisky fault zone in the northwest direction.

3.2. Groundwater conditions in the Chinrausky fault zone

3.2.1. Geologic-hydrogeolocal conditions

The study area is located in the northwest part of Balapan site and on Figure 28 is designated by number 3.

Geophysical study. Seismic works by RWM method and electric exploration by the transient electromagnetic technique in the near-field zone were carried out to map the faults

and choose suitable locations for the observational wells on the Chinrausky fault pathway. The profile has 920 m length and is confined to the pronounced depression in the relief. *Method of refracted waves* (RWM). The obtained velocity profile is shown on Figure 29.

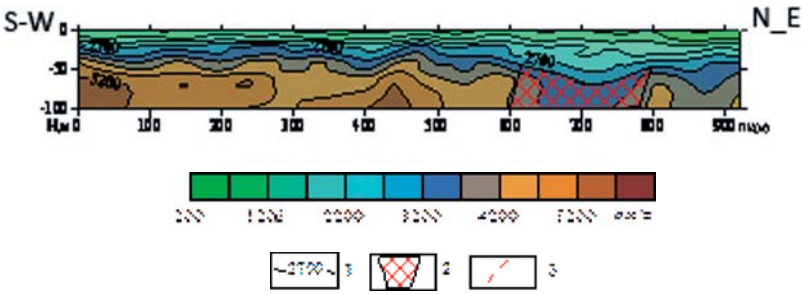

1 – isovelocity contour, m/s; 2 – tectonic zone; 3 – tectonic fault

Figure 29. Section of velocity profile

Based on the analysis of the section of velocity profile, a zone of rock decompaction has been identified within the 450–580 m station distances; it is characterized by low seismic wave velocity and informative for the well location.

Well drilling. Taking into account the results of geophysical works, well locations have been chosen, and 2 wells have been drilled (Table 17). The well 31/1 has been drilled to study interstitial water, and the well 31P – to study fissure water. The data on the wells are summarized in Table 17.

Table 17.

Summary data on the wells

No.	Well No.	Well depth, m	GWL, m	Note
3	31/1	15	–	Weathering crust has been drilled by auger
4	31P	35	5.3	Artesian aquifer has been exposed

The data in Table 17 show that the groundwater level in the well 31/1 is below the target well depth intended for the water analysis control. The well 31P has been drilled aside of the well 31/1 taking into consideration possible presence of a mantle of loose sediments of high thickness there. An aquifer has been exposed at 5.3 m depth.

3.2.2. Groundwater contamination with radionuclides

The well 31/1 appeared to be waterless. According to the results of laboratory analysis of water samples from the well 31P, the concentration of tritium was 0.750 kBq/kg, which was considerably lower than the interference level specified by NRB -99 (7.7 kBq/kg) for the general population to be received with water and food [2]. At the same time, the fact of detecting tritium in fissure-vein water is indicative of the migration of artificial radionuclides along the Chinrausky fault in the northwest direction.

3.3. Groundwater condition in the Zhanansky zone of crush

The site is located downstream the Shagan River bed at 12 km distance, north of the external reservoir the "Atomic" lake, and on Figure 28 is designated by number of 1. Based on the results of executed geologic-geophysical works, a mechanism of tritium-contaminated groundwater inflow to surface water has been ascertained. The concentration of tritium in the Shagan River water is 700 kBq/kg, which is almost 100 higher than the intervention level specified in NRB-99 (7.7 kBq/kg) for the general population to be received with water and food.

The study of pathways and nature of artificial radionuclides migration to surface water is one of the basic tasks to evaluate radioecological situation within the area of radioactively contaminated groundwater discharge into the Shagan River. As a part of the study carried out at the eastern end of Balapan site, it is necessary to determine the basic features of hydraulic interrelation between the river and different-age aquifers and give a qualitative assessment of migration of artificial radionuclides from groundwater to surface water.

3.3.1. Preliminary study

3.3.1.1. Geologic-hydrogeological conditions

The area for preliminary studying the structure of the discharge zone of radioactively contaminated groundwater has been chosen at the river length having maximum concentrations of tritium in the underflow water. The study included geophysical survey, drilling, and testing for underground waters inflow to determine the chemical and radionuclide composition.

Geophysical survey. Measurements by RWCM-RWM (to 50-100 m depths) and VES (to 70 m depth) methods were made on two profiles – I (along the left bank) and II (along the right bank), each of 3 km length (Figure 30).

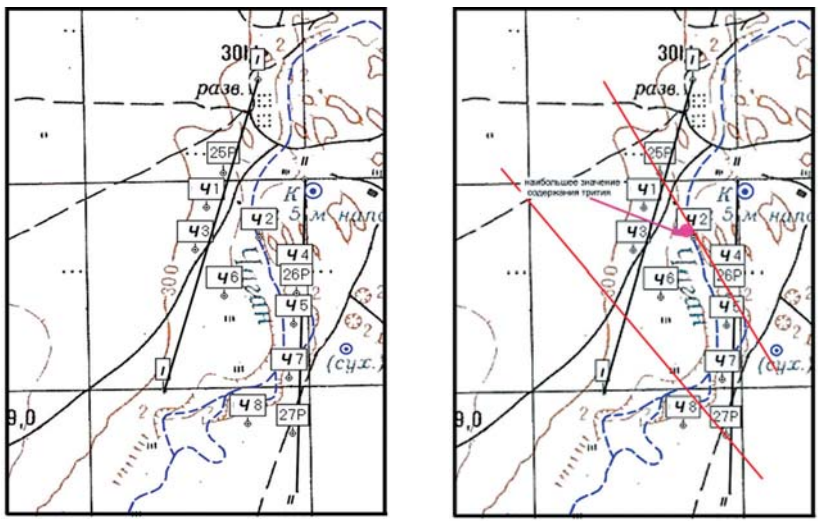

a) b)

Figure 30. Balapan site. Area of Shagan River :
a) schematic map of profiles (I, II) with the wells drilled in 2009; b) schematic map of tectonic dislocation according to the seismic study data (red lines)

Figure 31 shows the velocity sections constructed according to the seismic study results obtained by RWCM-RWM methods. The upper part of the sections is represented by low-velocity Quaternary sediments. Based on the standard velocity section constructed earlier for the Balapan site, the bottom of loose sediments, according to RWM data, can be delineated by a contour with up to 1.4 km/s longitudinal wave velocity (the layer velocities are 0.5–0.8 km/s). In this case, as seen on Figure 31, the thickness of Quaternary sediments is not more than 10–15 m (southwestern part of profiles). In the northern part of the profiles (Ch 350 – Ch 550) the thickness of Quaternary deposits decreases and it is 1-2 m, as confirmed by the TD curve.

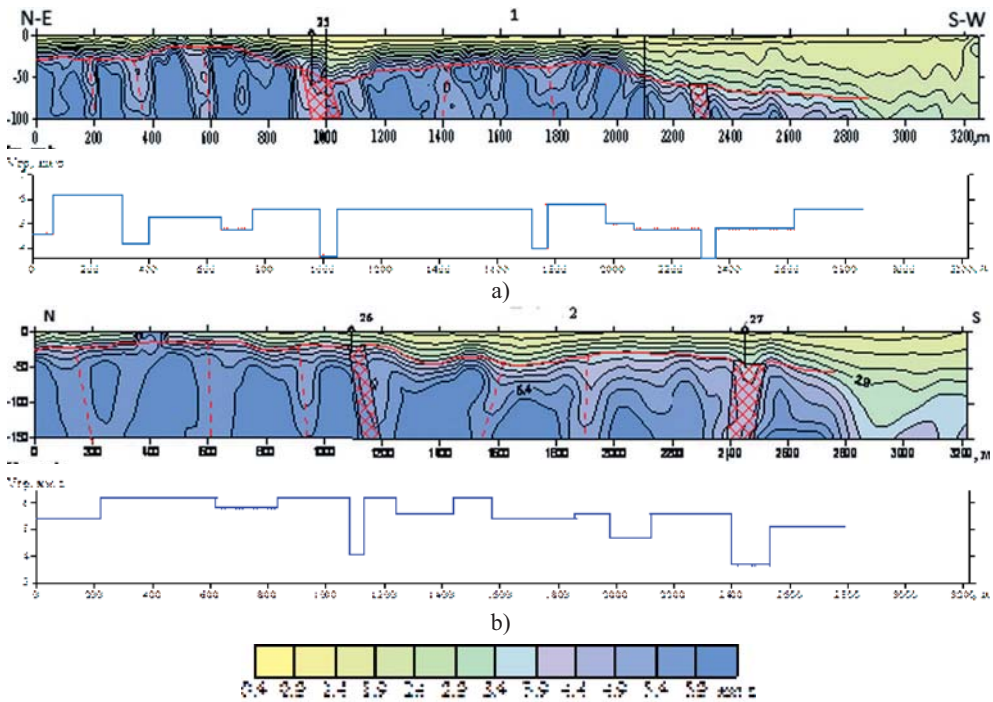

Figure 31. Balapan site. Area of Shagan River. Velocity profiles (with partial interpretation): a) I (left bank); b) II (right bank)

Downstream the section, there occur clays of Neocene the layer velocities of which range from 1.4–1.8 km/s (south of profiles) to 2.0–2.3 km/s (north of profiles). The Neocene clays thickness on profiles in the southwest and south directions increases to 60 m. In the region of profiles I and II, between Ch 350 and Ch 550, the clays wedge out. The weathering crust developed on the bottom rocks is characterized by a contour with the velocity values of about 2.5–4.5 km/s. The refractor passes along the bottom rock roof not affected by weathering. The cover thickness of this boundary varies from 12 to 80 m on profiles. The boundary velocities in the undisturbed massif are 4.2–6.2 km/s. The reduced zones in the undisturbed massif show low boundary velocities within 34 – 4.0 km/s range and are confined to the cracking zones accompanied by ruptured zones.

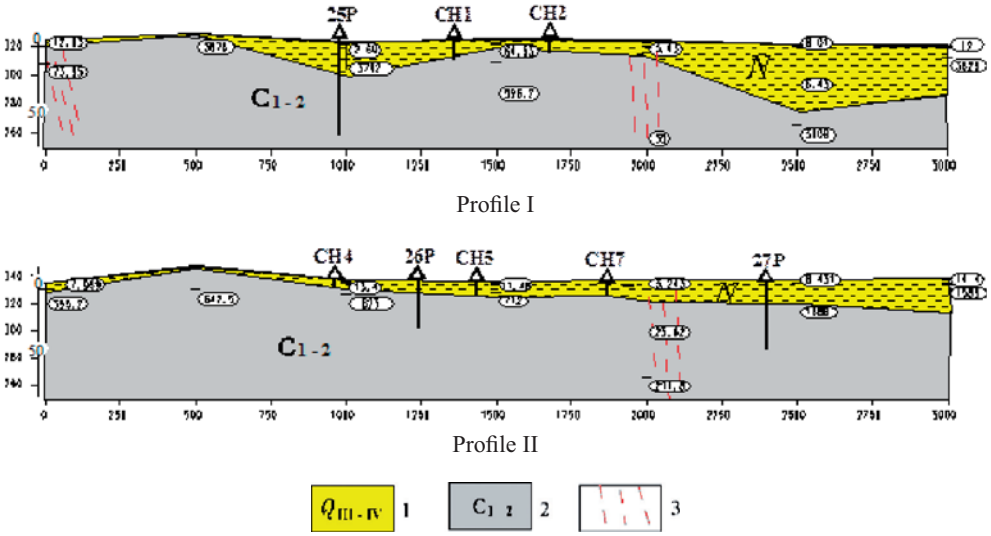

1 – upper part of section (loam, sandy loam, clay); 2 – host rocks of Carbonaceous;
3 – tectonically reduced zones

Figure 32. Balapan site. Shagan River area.
Geoelectric sections according to VES data ВЭЗ (with 500 m spacing)

In the northern part of the profile (Ch 350 – Ch 550), an uplift of bottom can be seen, and the upper edge depth is 12–20 m. The uplifted block, from the south and north, is bound by tectonic faults (PR I – Ch 370 and Ch 570, PRII – Ch 610 and Ch 920). Along the profiles I and II, measurements have been made by VES method with 500 m spacing to confirm the thickness of loose sediments in the upper part of section (Figure 32).

According to the electrical sounding data, the thickness of loose Quaternary sediments and clays of Neocene along Profile I ranges from units of meters (Ch 500) to 50 m (Ch 2500), and along Profile II – from units of meters (Ch 500) to 18 m (Ch 2500). A zone of relatively low electrical resistance of about 30 Ohm*m has been recorded on Ch 2000 to a depth of about 75 m. Ruptured zones in individual VEZ points show relatively low electrical resistance values.

Drilling works. Based on the data on the velocity and geo-electrical sections, the locations for core and auger wells confined to the tectonic fault influence zones have been established (Figures 31, 32). 3 core observational and 8 auger wells have been drilled, in which the testing for underground waters inflow has been performed. Based on the drilling data, geologic-geophysical sections have been plotted (Figure 33).

The obtained data have made it possible to confirm the relief of rocks of Paleozoic base within a three-kilometer length of the Shagan River bed. Water-bearing rocks on the study area are represented by tuff sandstones. In the wells 25P, 26P, 27P exposing the fissure water horizon, groundwater occurs at a depth of 0.8 to 7.5 m. The permeability ranges from 0.04 m²/day to 0.13 m²/day, and the debit varies from 3.24 m³/day to 6.4 m³/day. Hence the rocks penetrated by the wells 25P – 27P can be considered as low-permeable ones.

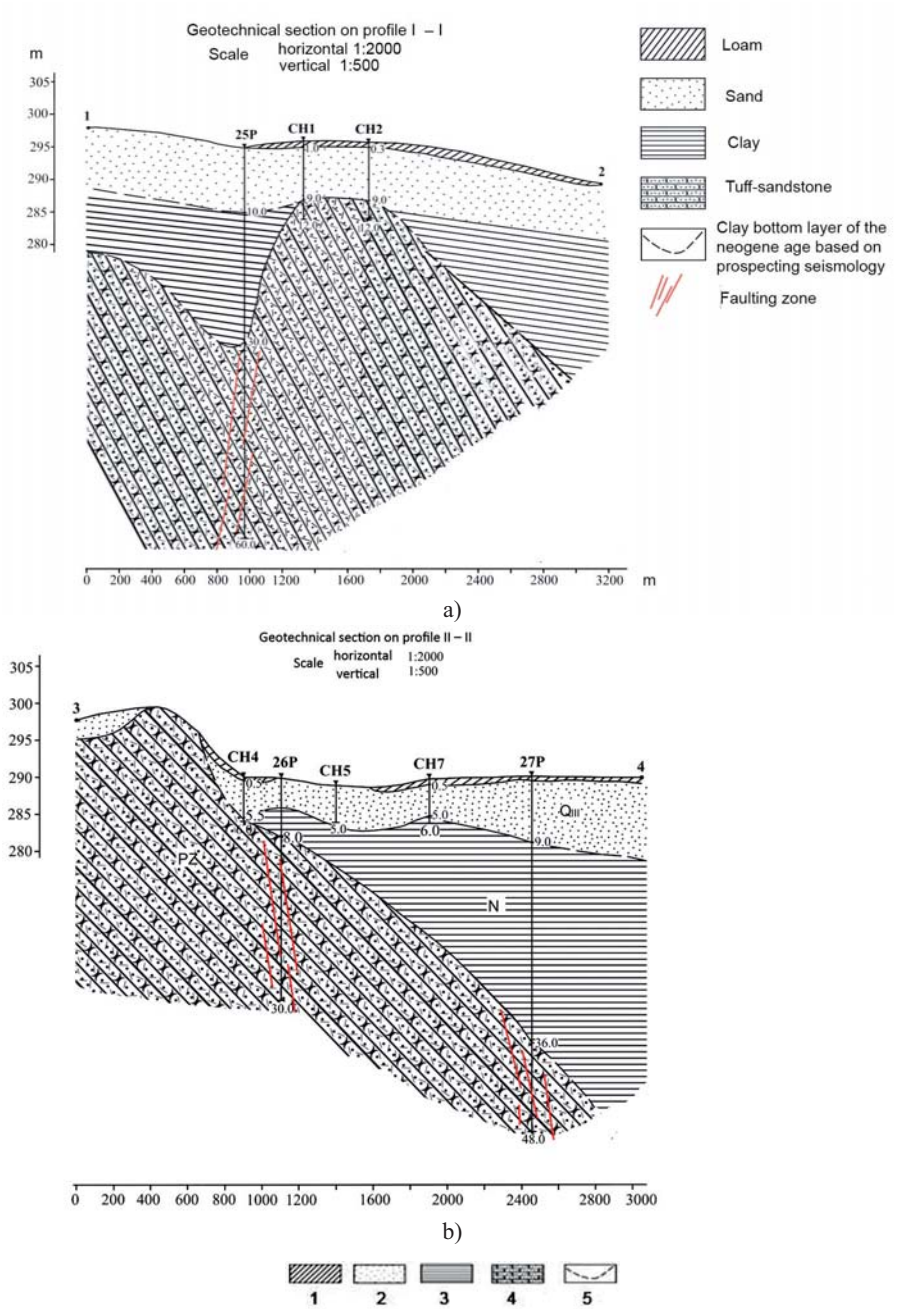

Figure 33. Balapan site. Area of the Shagan River. Geologic-geophysical sections of profiles: a) I - I (left bank); b) II - II (right bank)

3.3.1.2. Groundwater contamination radionuclides

Profile 1. On the first profile, the observational well 25P has been drilled within the range of northern tectonic fault propagation. According to the laboratory analysis data, the concentration of tritium in the water from the well 25P is only 0.8 kBq/kg. Considering that maximum concentration of tritium in the Shagan River is at the level of 700 kBq/kg, a conclusion can be made that the major channel of contaminated water inflow is located elsewhere.

Profile 2. 3 auger wells (CH4, CH5 and CH7) have been drilled to study interstitial water on Profile 2. Of them, only the well CH7 has appeared to contain water. The concentration of tritium is 3.2 kBq/kg. In order to study fissure water, the well 26P has been drilled in the zone of northern ruptured zone influence, and the well 27P – within the southern zone. According to the laboratory analysis data, the concentration of tritium in groundwater confined to the ruptured zones is different: 2.5 kBq/kg in the well 26P and 140 kBq/kg in the well 27P. It should be noted that the ruptured zones of interest are subparallel to the northern boundary of Zhanansky zone of crush and are remote at 0.1 km (southern branch) and 1.5 km (northern branch) distances respectively. Hence, a considerable concentration of tritium in the groundwater developed in the southern ruptured zone influence (20 times higher than specified by NRB-99) can be due to the migration of artificial radionuclides along the northern boundary of Zhanansky zone of crush from the UNE locations It should be noted that, according to the data of experimental investigations carried out within the Northern site located at 13.2 km distance north-west of the study area, there have been measured maximum high concentrations of tritium at the Balapan site, up to 1194–4765 kBq/kg.

The halo of radiation-contaminated groundwater identified according to the data of radiological testing of the well 27P, is safely isolated from the overlying aquifer developed in the alluvial sediments of Shagan River by a clay stratum of Neocene of more than 20 m thickness. It is also indirectly confirmed by a relatively low concentration of tritium in the underflow water (1.3 kBq/kg) compared to its concentration in groundwater.

3.3.2. Detailed study at the area of Shagan River

3.3.2.1. Confirmation of geologic-hydrogeological conditions

Integrated geophysical studies, drilling, and testing for underground waters inflow have been additionally carried out to confirm the geological structure and hydrogeological conditions at the area of propagation of tritium-contaminated groundwater.

Areal Studies by MG-IP method. Areal studies by the method of median gradient of induced polarization (MG-IP) have been carried out at the area of propagation of radiation-contaminated groundwater of 3x3 km size. The obtained data are shown on Figure 34.

The ruptured zones sub-parallel to the northern boundary of Zhanasky zone of crush have also been plotted on the electrical resistance map according to the file materials. In the northeast of the area, there has been identified a region of high electrical resistance values indicative of the low water saturation of sediments. In the center and southeast of the area, low values of electrical resistance have been measured, indicative of possible rock watering.

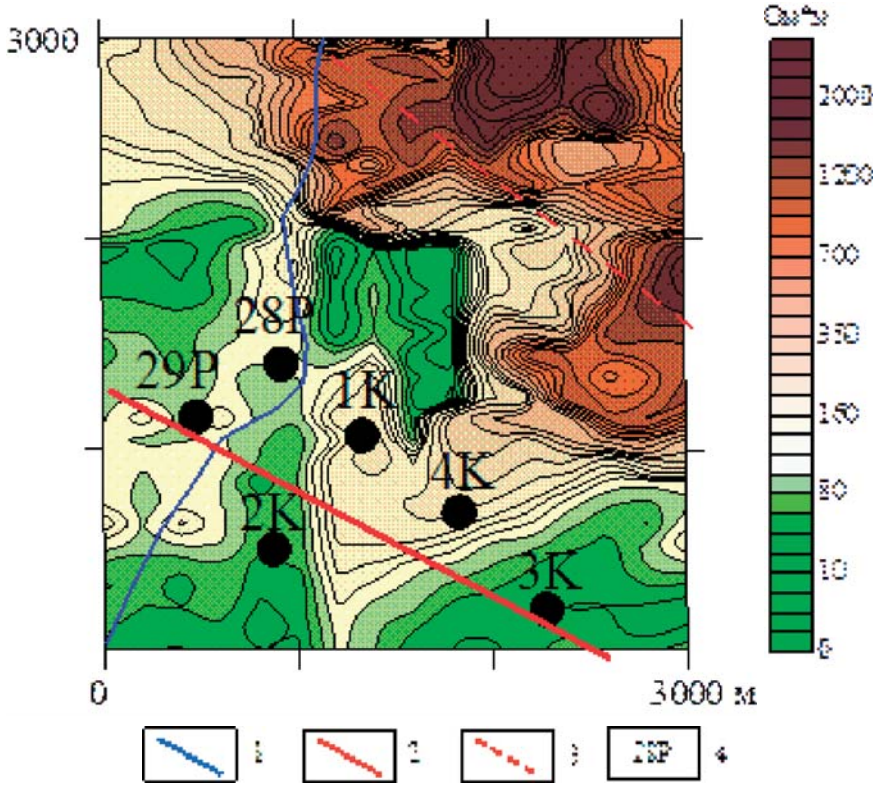

1 – Shagan River ; 2, 3 – ruptured zones sub-parallel to Zhanansky zone of crush; 4 – well

Figure 34. Shagan River area. Map of distribution
of geo-electrical resistance compiled according to MG-IP data

Well drilling. 5 wells, 28P, 29P, 1K, 2K and 3K have been staked and drilled in the Shagan River bed in conformity with the geologic-geophysical data. The layout of the wells is shown at Figure 35.

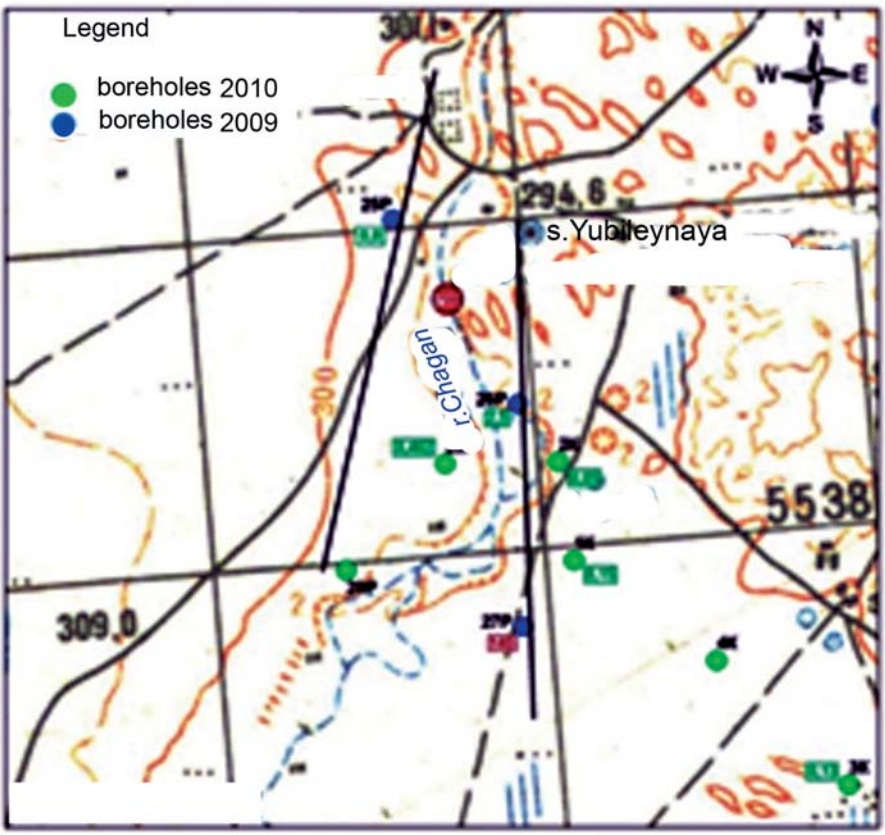

Figure 35. The Shagan River area. Layout of the observational and core drill wells.

The data on the drilled wells are summarized in Table 18.

Table 18.

Shagan area. Summary data on the wells

No.	Well No.	Well depth, m.	GWL, m.	^{137}Cs, Bq/kg	^{90}Sr, Bq/kg	$^{239+240}$Pu, Bq/kg	^{3}H, kBq/kg
1	28P	35	2.1	<0.01	<0.01	<0.00251	0.45
2	29P	81	6.3	<0.01	<0.005	<0.004	1.5
3	1K	65	2.9	<0.01	<0.01		0.15
4	2к	30	3.7	<0.01	<0.01		0.05
5	3K	31	1	<0.02	<0.01		0.13
6	4K			<0.01	<0.004	<0.0019	0.025

3.3.2.2 Radionuclide contamination of groundwater within the Shagan River area

The results of laboratory analyses to determine tritium concentration in groundwater samples taken from the drilled wells are listed in Table 18 [2]. The low concentrations of artificial radionuclides in groundwater in the study area are indicative of local discharge of radiation-contaminated water into the Shagan River. The most favorable conditions exist within the erosion "window" at the section of wedging out of waterproof clays of Neocene, between the observational wells 25P and 26P (Figure 33). Judging by a considerable difference between the tritium concentration values in the surface watercourse (700 kBq/kg) and the concentration values in the water samples taken from the wells (0.8 to 2.5 kBq/kg), the aquiferous system has low thickness and, probably, strongly pronounced fissure-vein type.

CONCLUSION

The results of groundwater survey at the Balapan site allow one to make the following conclusions:

1. Groundwater contamination with artificial radionuclides at the Balapan site

The basic propagators of UNE radioactive products at the Balapan site are fissure and fissure-vein waters.

Due to absence of adequate network of hydrogeological wells, it is not possible to make unambiguous conclusions about the nature of artificial radionuclide propagation at the Balapan site. According to the results of studies carried out at 10 sites, the nature of areal radioactive contamination of groundwater can be presented as follows.

Cesium-137. In water samples under study, concentration of ^{137}Cs does not exceed the allowable values for drinking water. Maximum values (4 Bq/kg) of ^{137}Cs concentration have been measured in the hydrogeological well 1A located at a distance of 50 m from the "warfare" borehole 1056.

Strontium-90. At a greater part of the territory, ^{90}Sr concentrations in groundwater are not higher than 1.0 Bq/kg, which is not higher than the allowable values for drinking water. Maximum ^{90}Sr concentration of 1240 Bq/kg has been measured for the well 1A. At a distance from the "warfare" boreholes of the first hundreds of meters, the concentration of this radionuclide decreases to mBq/kg.

Hence, any peculiarities in the nature of areal propagation of ^{137}Cs and ^{90}Sr have not been revealed due to the low concentration values. At the same time, elevated concentrations of ^{90}Sr in groundwater at Zarechie site have been measured in the areas confined to the intrusive massif slopes, and a zone of elevated concentration of ^{137}Cs stretches along the steeper edge of paleovalley, being confined to the UNE locations in the wells 1350 and 1352.

Plutonium-(239+240). Concentration of $^{239+240}$Pu in groundwater on the surveyed areas does not exceed MDA, being 0.002 Bq/kg.

Tritium. It is a basic contaminator of the groundwater. Concentration of ^{3}H in groundwater widely ranges from the minimum detectable activity of 0.007 to 4,760 kBq/kg. A main distinctive feature of this radionuclide is that tritium enters into the composition of water and is not sorbed by rocks. In this connection, owing to the hydrogeological peculiarities of the Balapan site, the areal propagation of this radionuclide at different sites has its own distinctive features. Maximum concentration of tritium, 4,760 kBq/kg has been measured at

the Northern site in the well 17A located 950 m away from the "warfare" borehole 1308. It is found that at distance 1.3 km from the contamination source, tritium concentration decreases considerably to 1,200 kBq/kg.

At "North-Eastern", "South-Western" and "Zarechie" sites, a noticeable decrease in the concentration of tritium at larger distances from the "warfare" boreholes has also been measured (at up to 2 km distances the concentration of tritium decreases to the allowable level for drinking water).

The "Central" site is worth mentioning. A basic feature of this site is the presence of low concentrations, within the allowable values for potable water, not only of ^{137}Cs and ^{90}Sr but also tritium, in spite of the fact that the hydrogeological wells are located close to 5 "warfare" boreholes. Analyzing the data, it was found that despite the low concentrations of tritium at this site, its concentration in groundwater also decreases at larger distances from the central UNE zones.

Thus, the nature of tritium proliferation with groundwater at the Balapan site mostly depends on the geologic-hydrogeological conditions at UNE sites and presence of regional faults. On the whole, it can be observed that any significant radioactive and widespread contamination of groundwater at the Balapan site has not occurred in the past years after the cessation of nuclear weapon tests.

2. Migration of artificial radionuclides with groundwater beyond the boundaries of the Balapan site

The following data have been obtained by studying the migration of artificial radionuclides with groundwater through the ruptured zones beyond the boundaries of the Balapan site:

- Basic discharge of groundwater contaminated with radioactive materials from the Balapan site into surface and interstitial waters occurs mainly in the areas of wedging out of a relative aquifer – Neocene clays (in erosion "windows").
- A local zone of radioactively contaminated groundwater discharge into the surface waters of the Shagan River has been identified within the eastern boundary of the Balapan site. The discharge zone is confined to the Zhanansky zone of crush. Tritium concentration in the Shagan River in this area comprises 700 kBq/kg (^{137}Cs and ^{90}Sr contents do not exceed MDA). Tritium contents in water samples taken from the hydrogeological wells drilled at the right bank of the Shagan River are up to 140 kBq/kg. Thus, in addition to the contaminated water coming into the Shagan River within the local zone of discharge, migration of tritium with groundwater takes place in the southeast direction beyond the boundaries of the Balapan site. This fact must be considered more particularly as there is a probability of contaminated groundwater propagation outside the territory of STS.
- Within the northeast boundary of the Balapan site, in the groundwater occurring in the zone of influence of Chinrausky fault, tritium content is at the level of 0.75 Bq/kg (^{137}Cs and ^{90}Sr contents do not exceed MDA).
- Within the southwest boundary of the Balapan site, in the groundwater confined to the zone of influence of Kalba-Chingizsky regional fault, tritium content is at the level of 0.05 Bq/kg (^{137}Cs and ^{90}Sr contents do not exceed MDA).

Thus, the obtained data allow stating that migration of UNE radioactive products outside the Balapan site takes place with groundwater along the regional fault zones. It is necessary to continue the studies of the radioactively contaminated water proliferation beyond the boundaries of the Balapan site; this is also stipulated by the on-going comprehensive research aimed at substantiation of transfer of a part of STS lands into commercial use.

The authors would like to acknowledge the staff of NNC INP RK for the elaboration of procedures and carrying out of laboratory analyses to study the radionuclide composition of groundwater; the workers of the Institute of Radiation Safety Uliankin V.A., Korovin V.A. for the execution of field works, Yakovenko Yu.Yu., Kuzevanova O.V., Yelizarieva N.A., Yeremenko Y.A., Barsukova S.A., Novikova E.A. for the processing and systematization of data on the subject.

REFERENCES

1. Субботин С.Б., Пестов Е.Ю. Годовые отчеты по проекту МНТЦ К-893 "Организация системы мониторинга состояния подземных вод на территории бывшего Семипалатинского испытательного полигона". Курчатов, 2003 - 2007.
   Subbotin S.B., Pestov E.Yu. Annual Reports on the ISTC Project K-893 "Provision of the System of Groundwater Condition Monitoring on the Territory of Former Semipalatinsk Test Site", Kurchatov, 2003 - 2007.
2. Отчеты по программе 011 "Обеспечение безопасности бывшего Семипалатинского испытательного полигона". Курчатов, 2005 - 2010.
   Reports on the State Program 011 "Provision of Safety of Former Semipalatinsk Test Site". Kurchatov, 2005 - 2010.
3. Инженерно-геологические условия объекта 905 МО СССР: отчет о результатах инженерно-геологической съемки масштаба 1:200000 /коллектив авторов Бардина И.Ю., Ветрова С.И. и др. Москва, 1976.
   Engineering-Geological Conditions of Facility 905 of MD of the USSR: Report on results of engineering-geological survey at a scale of 1:200000 /a team of authors Bardin I.Yu., Vetrov S.I.. et al., Moscow, 1976. - [in Russian].
4. Геологическая карта Казахской ССР. Восточно-Казахстанская серия. Масштаб 1:500 000: объяснительная записка. Алма-Ата, 1979.
   Geological map of the Kazakh SSR. East Kazakhstan series. Scale 1:500 000: Explanatory Note. Alma-Ata, 1979.
5. Семипалатинский испытательный полигон. Создание, деятельность, конверсия /коллектив авторов под рук. В.С. Школьника. Алма-Ата: Казахстан, 2003.
   Semipalatisk Test Site. Establishment, Activities, Conversion /a team of authors under the direction of V.S. Shkolnik. Alma-Ata: Kazakhstan, 2003.
6. Ляхова О.Н., Лукашенко С.Н., Ларионова Н.В., Субботин С.Б., Мульгин С.И., Жданов С.В. Тритий как индикатор мест проведения ядерных испытаний

//Актуальные вопросы радиоэкологии Казахстана /под руководством Лукашенко С.Н. Казахстан, выпуск 3, 2011.
Lyakhova O.N., Lukashenko O.N., Larionova N.V., Subbotin S.B., Mulgin S.I. and Zhdanov S.V. Tritium as an Indicator of Nuclear Test Execution Locations //Topical Issues of Radioecology of Kazakhstan /under the direction of Lukashenko S.N. Kazakhstan, Issue 3, 2011. - [in Russian].

7. Проект МНТЦ К-810 "Исследование миграции радионуклидов с подземными водами на территории Семипалатинского полигона с целью прогноза возможных последствий радиоактивного загрязнения питьевой воды и геологической среды". Москва, 2002 - 2004.
ISTC Project K-810 "Investigation of Migration of radionuclides with groundwater on the territory of Semipalatinsk Test Site to forecast possible aftereffects of radioactive contamination of drinking water and geological environment". Moscow, 2002 - 2004.
8. Адушкин В.В., Спивак А.А., Горбунова Э.М., Каазик П.Б., Недбаев И.Н. Гидрогеологические эффекты при крупномасштабных подземных взрывах (препринт). М.: ИФЗ АН СССР, 1990, 40с.
Aduskin V.V., Spivak A.A., Gorbunova E.M., Kaazik P.B. and Nedbayev I.N. Hydrogeological effects of large-scale underground detonations (preprint). M.: IFE AS USSR, 1990, 40pp. - [in Russian].
9. Израэль Ю.А., Стукин Е.Д. Феноменология загрязнения подземных вод после подземного ядерного взрыва //Радиоактивность при ядерных взрывах и авариях. Труды международной конференции. Москва 24-26 апреля 2000г. С.-Пб.: Гидрометеоиздат, 2000. Т.1, с.616-623.
Izrael Yu.A., Stukin E.D. Phenomenology of groundwater contamination due to underground nuclesr detonations //Radioactivity due to nuclear explosions and accidents. Proceedings of International Conference. Moscow 24-26 April 2000. S.-Pb.: Gidrometeoizdat, 2000. V.1, pp.616-623. - [in Russian].
10. Горбунова Э.М., Спивак А.А. Изменение режима подземных вод при подземных ядерных взрывах //Геоэкология, 1997, № 6, с.29-37.
Gorbunova E.V., Spivak A.A. Change of Groundwater Regime due to underground nuclear detonations // Geoekologiya, 1997, No. 6, p.29-37. - [in Russian].
11. Горбунова Э.М., Иванов А.И. Изменение гидрогеологических параметров в техногенно-нарушенных условиях //Ядерная энергетика Республики Казахстан. Международная конференция, 3-5 сентября 2007, г.Курчатов, Казахстан (доклады). Курчатов, Вестник НЯЦ РК, вып.2 (33). 2008, с.27-32.
Gorbunova E.M., Ivanov A.I. Change of Hydrogeological Parameters under Artificially Disturbed Conditions // Nuclear Power Engineering in the Republic of Kazakhstan. International Conference, 3-5 September 2007, Kurchatov, Kazakhstan (reports). Kurchatov, Vestnik NNC RK, Issue 2 (33). 2008, p.27-32.
12. Volkova E.V., Gorbunova E.M., Rastorguev I.A. Evaluation of fractured aquifer bottom position according to groundwater level observation data in the region of underground nuclear explosion execution //International Conference "Finite-Elements Models, Modflow and More 2004. Solving Groundwater Problems". Carlsbad, 13-16 September 2004. Carlovy Vary, Czech Republic, 2004, p.159-162.

13. Горбунова Э.М., Свинцов И.С. Ретроспективный анализ режима подземных вод при проведении крупномасштабных экспериментов //Мониторинг ядерных испытаний и их последствий. Тезисы докладов. VI Международная конференция. 09-13 августа 2010 г. Курчатов, Казахстан: НЯЦ РК. 2010, с.72-75.
Gorbunova E.M., Svintsov I.C. Retrospective Analysis of groundwater regime during large-scale experiments //Monitoring of nuclear tests and their aftermaths. Abstracts of reports. VI International Conference. 09-13 August, 2010. Kurchatov, Kazakhstan: NNC RK. 2010, pp.72-75. - [in Russian].
14. Горбунова Э.М. Особенности деформирования массива горных пород при воздействии взрывом (на примере участка Заречье Семипалатинского испытательного полигона) //Геофизика и проблемы нераспространения. Вестник НЯЦ РК. Вып.2. Курчатов: НЯЦ РК, 2003, с.113-122.
Gorbunova E.M. Peculiarities of rock massif strain under the impact of explosion (with Zarechie site of Semipalatinsk Test Site as an example) //Geophysics and Problems of Non-Proliferation. Vestnik NNC RK. Issue.2. Kurchatov: NNC RK, 2003, pp.113-122. - [in Russian].
15. Violet C.E. Mining Congress. Journal. #3, 1960, p.79-83.
16. Johnson G.W. Mining Congress. Journal. #11, 1958, p.78.
17. Johnson G.W., Higgins G.H., Violet C.E. Underground Nuclear Detonations // Geophysical Research, –1959, vol.64, #10, p.1457.
18. Дубасов Ю.В. и др. Заключительный отчет "Радиологическое исследование 30 штольневых порталов в горном массиве Дегелен Республики Казахстан". С.-Пб., 1996.
Dubasov Yu.V. et al. Final Report "Radiological Survey of 30 tunnel portals in Delegen rock massif of the Republic of Kazakhstan ". S.-Pb., 1996. - [in Russian].
19. Нормы радиационной безопасности (НРБ-99). Издание официальное. Агентство по делам Здравоохранения Республики Казахстан. Алма-Ата, 1999.
20. Radiation Safety Standards (NRB-99). Official publication. Health Protection Agency of the Republic of Kazakhstan . Alma-Ata, 1999. - [in Russian].
Актуальные вопросы радиоэкологии Казахстана /под руководством Лукашенко С.Н. Павлодар: Дом печати, выпуск 2, 2010.
Current issues in Radioecology of Kazakhstan /under the direction of Lukashenko S.N. Pavlodar: Printing House, Issue 2, 2010.
21. Субботин С.Б., Лукашенко С.Н., Айдарханов А.О., Романенко В.В. Радиоэкологическое состояние территории угольного месторождения "Каражыра" //Актуальные вопросы радиоэкологии Казахстана. /под руководством Лукашенко С.Н. Павлодар: Дом печати, выпуск 3, 2011.
Subbotin S.B., Lukashenko S.N., Aidarkhanov A.O., Romanenko V.V. Radioecological situation on the territory of Karazhyra coal deposit" //Topical Issues in Radioecology of Kazakhstan / under the direction of Lukashenko S.N. Pavlodar: Printing House, Issue 3, 2011.

"БАЛАПАН" СЫНАҚ АЛАҢЫНЫҢ ШЕГІНЕН ТЫС ЖЕРЛЕРГЕ ТЕХНОГЕНДІ РАДИОНУКЛИДТЕРДІҢ ЖЫЛЫСТАУ ЖОЛДАРЫН АНЫҚТАУ

[1]Субботин С.Б., [1]Лукашенко С.Н., [1]Романенко В.В., [1]Каширский В.В., [2]Пестов Е.Ю., [2]Бахтин Л.В., [3]Горбунова Э.М., [4]Кузеванов К.И.

[1]ҚР ҰЯО Геофизикалық зерттеулер институты, Курчатов қ., Қазақстан
[2]РҒА Геосфера динамикасы институты, Мәскеу қ., Ресей
[3]Геология және мұнайгаз ісі институты, Томск, Ресей

Бұл мақалада "Балапан" алаңындағы ядролық сынақ өткізілген телімдерден жерасты суларымен техногенді радионуклидтердің шығу сипатын зерттеу нәтижелеріне шолу жасалды. Істелінген радиоэкологиялық жұмыстардың негізінде жерасты суларының жай-күйін ұзақмерзімді мониторингілеу үшін тіректі бақылау ұңғымалары жабдықталды.

"Балапан" алаңының шегінде, сонымен қатар оның шекарасынан тыс жерлерде де жерасты суларының радиоактивті ластану деңгейі жайлы жаңа деректер алынды. Зерттелген бағыттар бойынша техногенді радионуклидтердің жерасты суларымен жылыстау сипаты жайлы қорытынды жасалды.

Түйінді сөздер: жерасты сулары, ядролық сынақ, радионуклидтердің жылыстауы, цезий-137, стронций-90, тритий, плутоний, "Балапан" алаңының геологиялық құрылымы және гидрогеологиялық жағдайы, аймақтық омырулар, Шаған өзені, Қаражыра көмір кенорны.

ВЫЯВЛЕНИЕ ПУТЕЙ МИГРАЦИИ ТЕХНОГЕННЫХ РАДИОНУКЛИДОВ ЗА ПРЕДЕЛЫ ИСПЫТАТЕЛЬНОЙ ПЛОЩАДКИ "БАЛАПАН"

[1]Субботин С.Б., [1]Лукашенко С.Н., [1]Романенко В.В., [1]Каширский В.В., [2]Пестов Е.Ю., [2]Бахтин Л.В., [3]Горбунова Э.М., [4]Кузеванов К.И.

[1]Институт радиационной безопасности и экологии НЯЦ РК, Курчатов, Казахстан
[2]Институт геофизических исследований НЯЦ РК, Курчатов, Казахстан
[3]Институт динамики геосфер РАН, Москва, Россия
[4]Институт геологии и нефтегазового дела, Томск, Россия

В статье представлен обзор результатов исследований характера выноса техногенных радионуклидов с подземными водами с участков проведения ядерных испытаний на площадке "Балапан". На основе выполненных радиоэкологических работ оборудованы опорные наблюдательные скважины для долгосрочного мониторинга состояния подземных вод. Получены новые данные об уровнях радиоактивного загрязнения подземных вод как в пределах площадки "Балапан", так и за ее границами. Сделаны выводы о характере миграции техногенных радионуклидов с подземными водами на изученных направлениях.

Ключевые слова: подземные воды, ядерное испытание, миграция радионуклидов, цезий-137, стронций-90, тритий, плутоний, геологическое строение и гидрогеологические условия площадки "Балапан", региональные разломы, река Шаган, угольное месторождение Каражыра.

УДК 546.11.02.3:577.4:504.064:539.16

TRITIUM CONTENT IN SNOW COVER OF DEGELEN MOUNTAIN RANGE

Turchenko D.V., Lukashenko S.N., Aidarkhanov A.O., Lyakhova O.N.

Institute of Radiation Safety and Ecology NNC RK

The paper presents the results of investigation of tritium content in the layers of snow located in the stream beds of the "Degelen" massif contaminated with tritium. The objects of investigation were creek watercourses Karabulak, Uzynbulak, Aktybai located beyond the "Degelen" site. We studied the spatial distribution of tritium relative to the bed of watercourses and defined the borders of the snow cover contamination. In the center of the creek watercourses the snow contamination in the surface layer is as high as 40 kBq/kg. The values of the background tritium level in the areas not related to the streambed were calculated; they ranged from 40 to 50 Bq/kg. The results of snow cover measurements in different seasonal periods were compared. The main mechanisms causing tritium transfer in snow were examined and identified. The most important mechanism of tritium transfer in the streams is tritium emanation from ice or soil surface.

Keywords: groundwater, tritium, snow cover, Uzynbulak, Karabulak, Aktybai, STS, migration of radionuclides, surface snow layer, near-the-ground snow layer, an emanation of tritium from soil.

INTRODUCTION

Many investigations devoted to studying of artificial radionuclides migration to the environment both on the territory of the experimental site "Degelen" and beyond it have been carried out. Among the most hazardous artificial radionuclides, such as ^{137}Cs, ^{90}Sr, $^{239+240}Pu$, and ^{3}H (tritium) present in the ecosystem, the tritium has the highest migration rate. In [1, 2] high tritium concentrations in surface and ground waters as well as in the components of the ecosystem (animals, plants, atmospheric air) were registered. The tritium concentration in the surface waters of the streams on the site "Degelen" goes up from tens to hundreds of kBq/kg, the lengths of streambeds of some streams exceed ten kilometers, therefore they go beyond the territory of the "Degelen" massif.

A comparative analysis of the tritium concentration in the ecosystem components showed that the main contribution to the ecosystem contamination is made by the streams located on the territory of the "Degelen" massif. No information on tritium concentration in the snow cover on the contaminated areas was obtained before this study.

In different climatic periods of snow accumulation, the tritium inflow may be caused by the two main transfer mechanisms:

- Tritium inflow from the atmosphere as a result of transfer of snow particles or condensation of water vapor on snow particles during precipitations.
- Tritium emanation from soil or ice cover.
- This research is devoted to studying of the degree of influence of transfer mechanisms on tritium spatial distribution in the snow cover and estimation of the tritium background concentration on the test ground "Degelen".

1. OBJECTS AND METHODS OF INVESTIGATIONS

The snow cover was studied in the spring-winter period. The areas to be studied were chosen based on the results of studying of the ecosystem components (atmospheric air, plants, water vapors of atmospheric and soil air). The objects of investigations were streams Karabulak, Uzynbulak, and Aktybai, the watercourses of which go beyond the "Degelen" massif (Figure 1). Figure 1 shows the scheme of location of studied profiles in the streambeds.

The examination of the snow cover consisted of the three main stages:

- reconnaissance on the territory, choice of slots to be studied;
- studying of tritium distribution in-depth of the snow cover in the centers of streambeds;
- studying of spatial tritium distribution relative to the streambeds;
- studying of tritium concentration dynamics in the snow cover

To estimate the spatial distribution of tritium, the research profiles perpendicular to the water flow were made on the streams. The points of the research profile were located on the right and left sides of the stream. The center of the profile was located in the center of the streambed, the distance between the examined points was 50 m, and the depth of sampling was 0–10, 10–20 and 20–30cm.

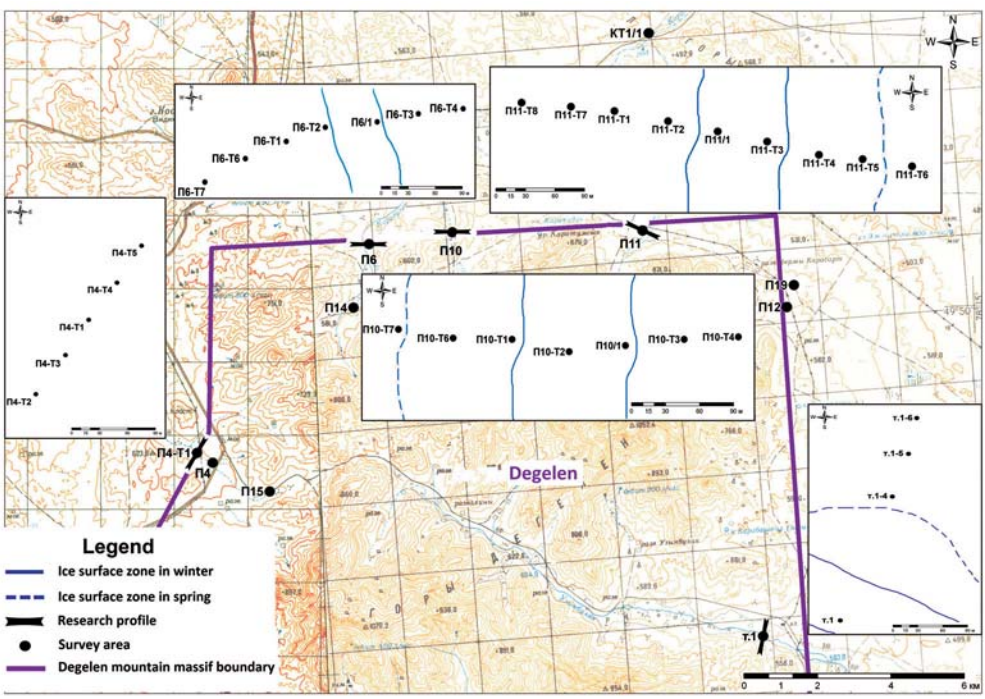

Figure 1. A scheme of location of studied areas

The dynamics of tritium concentration in the snow cover was studied based on the periodic snow examination on the same research slots in various climatic periods.

The snow cover thickness was measured with a measuring bar.

To determine tritium concentration the snow samples were placed in the polyethylene bag and frozen to a liquid state. The obtained samples were placed in a 20 ml plastic vessel. In order to remove mechanical admixtures the snow samples were filtered by the filters "Blue Ribbon". The obtained filtered sample was placed in a 20 ml metallic cavity, and a scintillation cocktail in proportion 3:12 ml was added.

To determine the specific activity of tritium in the snow samples we used a liquid scintillation spectrometer TriCarb 2900 TR and the standard technique of measurements [3].

Background tritium concentrations were measured on conventionally clean areas, not related to tritium contamination. For this purpose the areas in Kurchatov-city and beyond the perimeter of the "Degelen" massif in points P-12, P-14, P-15 and P-19 were chosen (Figure 1).

2. RESULTS

Visual examination of the studied objects showed that in the winter period the streambed surface is covered by ice, the thickness of which varies from 5 to 15 cm. As a rule, the snow cover on the ice surface was either absent or was not thicker than 3-5 cm on the surface of the ice cover. Beyond the streambed the depth of the snow cover usually did not exceed 20-30 cm.

2.1. Spatial distribution of tritium in the streams

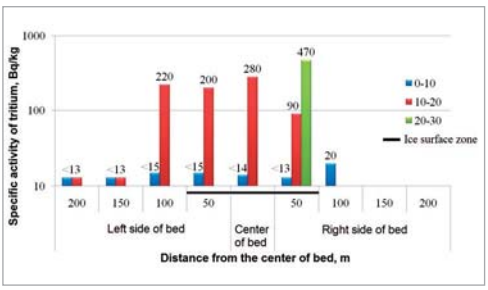

a – Karabulak, profile П6

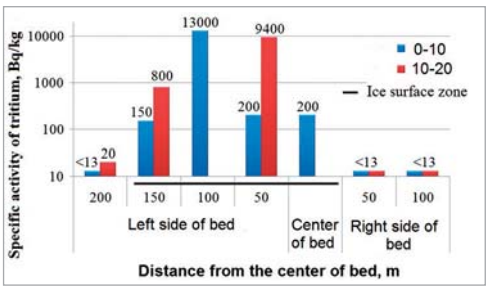

b – Karabulak, profile П10

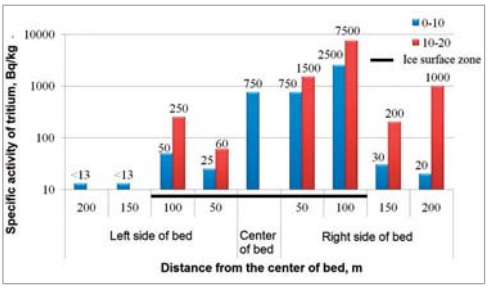

c – Karabulak, profile П11

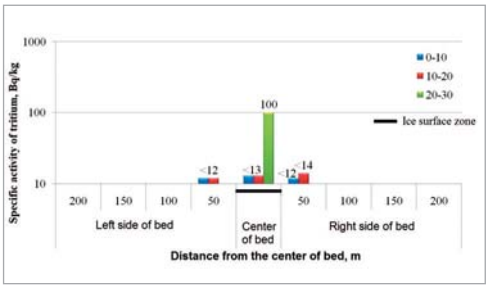

d – Karabulak, tributary confluence area

Figure 2. Spatial distribution of tritium in the snow cover in the tributaries of the Karabulak stream

2.1.1. Karabulak stream

The bed of the Karabulak stream consists of three water-bearing tributaries flowing beyond the "Degelen" massif. Research profiles were made in each tributary of the Karabulak stream in points P6, P10 and P11.

Figure 2 shows the dependence of the spatial tritium distribution in the snow cover on the distance from the streambeds. In the lower part of each histogram in Figure 2 the blue line shows the boundary of the snow cover surface in the studied area.

Profile in point P6 *(Figure 2,a).* The visible thickness of the water flow in the stream did not exceed 5m. The width of the ice cover reached 100m in the center of the riverbed. The tritium concentration in the surface layer (0-10 cm) ranged from <13 to 20 Bq/kg. The tritium concentration in the near-ground level varied from 90 to 280 Bq/kg.

Profile in point P10 *(figure 2,b).* The ice cover of the stream was located on the left side of the streambed, its width was 150 m from the center of the bed. In the surface layer of the snow cover maximal tritium concentration was registered in the reed bushes, it was 13 kBq/kg with the average concentration not exceeding 200 Bq/kg. In the end points of the profile, not related to the stream flow, the tritium concentration in all layers of the snow cover did not exceed 13 Bq/kg.

Profile in point P11 *(figure 2,c).* The width of the ice cover on the stream was about 100m from the center of the streambed. Maximal tritium concentrations in the surface and near-ground layers were registered in the center and in the right side of the streambed. Their values ranged from 0.75 to 2.5 kBq/kg and from 0.1 to 7.5 kBq/kg, respectively.

Profile in the place of confluence of the Karabulak tributaries *(figure 2, d).* Tritium concentrations in the surface and near-ground layers of the snow cover did not exceed 14 Bq/kg. In the near-ground layer of the snow cover the tritium concentration in the center of the streambed was 100 Bq/kg.

2.1.2. Uzynbulak stream

In the winter period the streambed of the Uzynbulak stream was covered with a 3-10 cm layer of ice. The width of the ice cover did not exceed 50m. In spring, during spring floods, the surface of the ice cover increased towards the left side of the stream to a distance of 200 m from the center of the stream.

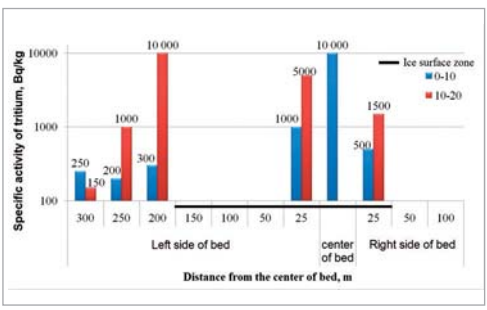

Uzynbulak brook, profile at point 1

a)

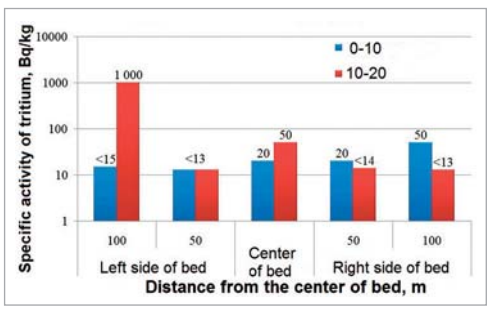

Aktybay brook, profile P4-1

b)

Figure 3. Spatial distribution of tritium in the snow cover of the streams Uzynbulak and Aktybay

Figure 3(a) shows spatial tritium distribution relative to the streambed of the Uzynbulak stream.

Maximal tritium concentrations of 10 kBq/kg were registered in the center of the streambeds (on the ice surface) and in the near-ground layer of the snow cover beyond the ice cover.

2.1.3. Aktybay stream

In point P4 no visible signs of water were detected. The research profile was located at a distance of 500m from point P4. Figure 3(b) shows the spatial tritium distribution relative to the streambed of the Aktybay stream.

Maximal tritium concentration of 1 kBq/kg was registered in the near-ground layer of the snow cover; in the surface layer of the snow cover the tritium concentration varied from <13 to 50 Bq/kg.

Thus, the results of investigations show that the snow cover of the streams Karabulak, Uzynbulak, and Aktybay can contain quite high tritium concentrations. The tritium is not distributed uniformly among the layers: in most cases in the near-ground layer its concentration is higher than that in the surface layer.

In order to estimate tritium distribution in depth of snow cover, the ratio of tritium concentrations in the near-ground layer to that in the surface snow layer was calculated. In calculations, if the numerical values of tritium concentration were absent, the value of minimal detected activity was taken as the numerical value. An analysis of the results of tritium concentration in the near-ground and surface snow layer showed that the ratio of tritium concentrations varied from 0.70 to 0.66 with the average value equal to 11. The obtained average ratio of tritium concentration can be used for rough estimation of tritium concentration in the near-ground and surface snow layer if its concentration in the other layer of the snow cover is known. As the distance from the center of the streambed in the perpendicular direction increases, at a distance of 300m tritium concentration in the near-ground and surface snow layer decreases to its background values.

The results of our investigations showed that maximal tritium concentrations in the snow cover are registered in the zones having ice cover in the near-ground soil cover. However, in some cases high tritium concentrations were registered in the absence of snow in the underlying surface. One can suppose that there are at least 2 mechanisms of tritium penetration to the snow cover:

- Tritium redistribution in the system ice – snow cover (the tritium present in the ice cover partially evaporates and penetrates to the snow cover);
- Tritium emanation from soil with subsequent condensation of tritium-containing water vapors on the particles of the snow cover.

2.2. Snow cover on the background areas

Table 1 presents the results of tritium concentration in the samples of the snow cover taken at the background areas.

Table 1.

Tritium concentration in the snow cover at the background areas in Kurchatov-city and in "Degelen" massif

Layer, cm	Tritium specific activity, Bq/kg							
	Outskirts of Kurchatov-city				Perimeter of the "Degelen" massif			
	North	East	South	West	P12	P14	P15	P19
0-10	<13	<13	<13	<14	55±7	35±7	<14	35±7
10-20	<15	-	<13	-	50±7	<14	20±7	-
20-30	-	-	-	-	45±7	-	-	25±7

On the studied areas of the mountain range "Degelen" in points P12, P14, P15 and P19, the tritium concentration in the near-ground and surface snow layers is rather low and does not exceed 55 Bq/kg. The character of tritium distribution in the snow cover layers in the background points is principally different from the character of tritium distribution in the streambeds. The difference is that in the background points the tritium concentration in all layers of the snow cover has almost the same values. Such character of distribution of the tritium concentration in the snow cover layers can be explained by the fact that in the time of snow accumulation, tritium-containing water vapors, present in the atmospheric air, are condensed on snow particles and are uniformly distributed throughout the snow cover thickness.

No tritium was discovered in the snow cover in the outskirts of Kurchatov-city, with the detection limit equal to 14 Bq/kg. Therefore, the tritium contained in the air of the "Degelen" mountains does not reach Kurchatov-city, which can be caused by tritium dilution in the atmosphere.

2.3. Tritium concentration dynamics in the snow cover

Table 2 presents the results of studying of tritium concentration in the snow cover layers in the same sampling points, at various moments of time.

Table 2.

Dynamics of tritium concentration in the snow cover, tritium concentration in the streambed waters in the examined areas

Examined area	Layer, cm	Snow cover, Bq/kg			Streambed waters, Bq/kg
		November 2010	January 2011	February 2011	
Karabulak, P6	0-10	-	200÷20	14÷7	11 000÷1 000
	10-20	-	3 500÷300	280÷200	
Karabulak, P10	0-10	<8	2 500÷200	200÷20	66 000÷6 000
	10-20	200÷20	40 000÷4 000	-	
Karabulak, P11	0-10	1 000÷100	4 000÷400	750÷70	44 000÷4 000
	10-20	4 000÷400	30 000÷3 000	-	

It should be noted that maximal tritium concentration in the near-ground layer of the snow cover does not exceed tritium concentrations in the stream water. The percentage of tritium transfer from the stream water to the snow cover does not exceed 30%-70% of its concentration in the stream water.

A comparative analysis of the results of study of the snow cover in various periods shows that the falling snow does not contain high tritium concentrations. The tritium concentration in the surface layer of the snow cover changes with time. At the moment of snow precipitation the tritium concentration in the surface layer of the snow cover does not exceed the background values, after snow precipitation the tritium concentration increases due to tritium emanation from the ice or soil cover. The obtained results confirm the earlier assumption about the mechanisms of tritium contamination of the snow cover, namely, tritium penetration to the snow cover from the soil or ice cover.

3. DISCUSSION OF THE RESULTS

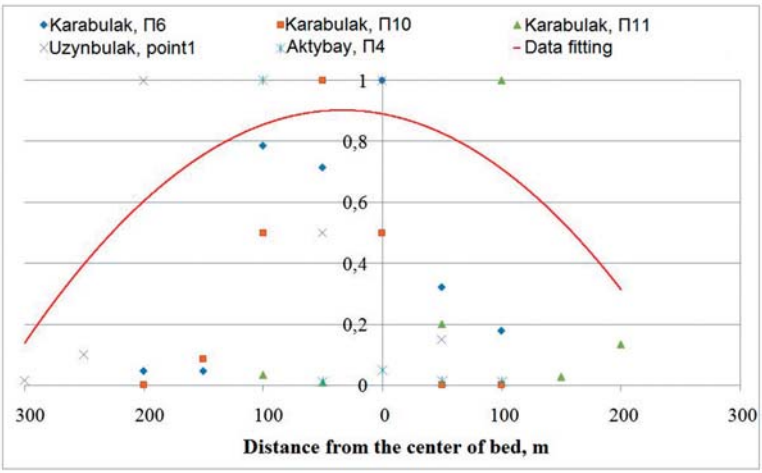

Figure 4. Spatial distribution of tritium as a function of distance from the studied streams, the distribution is normalized to the maximal value of tritium contamination.

Figure 4 shows spatial distribution of tritium as a function of distance from all studied streams. For each case (stream) the tritium concentration is normalized to the maximal value. The approximation curve in figure 4 shows the dependence of tritium contamination on the distance from the streambeds.

Maximal levels of contamination with tritium (up to 20-40 kBq/kg) are, on average, located at a distance not more than 100-200m from the streambed center and are limited by the streambed. As the distance from the streambed in the perpendicular direction increases, the tritium concentration in the snow cover falls to the background values.

A comparison of the results in the surface and near-ground layers of the snow cover on the streambeds shows that in all cases maximal tritium concentrations were registered in the near-ground layer of the snow cover, and could reach 40 kBq/kg. This fact shows that the

main source of tritium contamination is the stream; the mechanism of tritium transfer to the snow cover depends on the underlying surface, namely, tritium emanation from the surface of the soil or ice cover.

Study of the background areas of the Degelen mountains showed uniform tritium distribution in the snow cover layers. The tritium concentration in the surface layer of the snow cover reaches 55 Bq/kg, whereas in the near-ground layer it is 45 Bq/kg. Such tritium distribution is caused by the mechanism of tritium inflow from the atmosphere as a result of precipitations and condensation of water vapors on snow particles. It is possible to suppose that in the air above the territory of the Degelen massif a microregional basin, whose ecosystem constantly contains tritium in concentrations not exceeding 60 Bq/kg, was formed.

Therefore, we can state that the mechanisms of tritium penetration to the snow cover have been determined, the character of spatial tritium distribution in the snow cover relative to the streambeds has been studied, background tritium concentrations have been determined, however, the questions of dynamics of tritium concentration in time and tritium distribution in the system water-ice-snow cover still remains unanswered.

CONCLUSION

The results of investigations enable us to make a conclusion that the snow cover of the Degelen mountain range may have quite high tritium concentrations both in the near-ground and surface snow cover. Highest levels of contamination with tritium are, on average, located at a distance of 100-200m from the streambed center and are limited by the streambed, reaching the values comparable to tritium concentrations in the stream water. As the distance from the streambed increases, the tritium concentration in the snow cover falls to the background values.

The obtained complex data show that in the Degelen massif there are 2 main mechanisms of tritium penetration to the snow cover:

- Condensation of tritium-containing water vapors on snow particles in the moment of snowfall, which gives tritium concentrations in the snow cover layers not more than 60 Bq/kg;
- Tritium emanation from the underlying surface of the soil or ice cover, and tritium redistribution from the near-ground to the surface layer of the snow cover.

No tritium was registered in the snow cover at the outskirts of Kurchatov-city; the detection limit was 14 Bq/kg. Therefore the tritium contained in the air of the Degelen massif does not reach Kurchatov-city, which may be caused by tritium dilution in the atmosphere.

The authors are thankful to the specialists of the Institute of Radiation Safety and Ecology V.A. Ul'yankin and V.A. Korovin for their help in equipping and carrying out of field works, N.A. Elizar'yeva for mapping, S.V. Genova and the group of general chemistry for preparation of snow samples.

REFERENCES

1. Суботин С.Б. Подземная миграция искусственных радионуклидов за пределы горного массива Дегелен / С.Б. Субботин, С.Н. Лукашенко, В.М. Каширский, Ю.Ю. Яковенко, Л.В. Бахтин // Актуальные вопросы радиоэкологии Казахстана [Сборник трудов Института радиационной безопасности и экологии за 2007 – 2009 гг.] / под рук. Лукашенко С.Н. – Вып. 2. – Павлодар: Дом печати, 2010. – 527с.: ил.- Библиогр.: С.518. - ISBN 978-601-7112-32-5.
   Subbotin S.B. Subterranean migration of artificial radionuclides beyond Degelen massif / Subbotin S.B., Lukashenko S.N., Kashirskii V.M., Yakovenko Yu.Yu., Bakhtin L.V. // Current Issues in radiology of Kazakhstan [Proceedings of the Institute of Radiation Safety and Ecology for 2007-2009] / Sup. by Lukashenko S.N. – V.2. – Pavlodar: Printing House, 2010. – 527 pp.: illustration.- appendix.: p. 518. - ISBN 978-601-7112-32-5. – [in Russian]
2. Ляхова О.Н. Исследование содержания трития в объектах окружающей среды на территории испытательной площадки Дегелен / О.Н. Ляхова, С.Н. Лукашенко, М.А. Умаров, А.О. Айдарханов // Вестник НЯЦ РК. – 2007. – Вып.4. – С.80 – 86.
   Lyakhova O.N. Research on tritium concentration in environmental objects on the territory of Degelen site/ Lyakhova O.N., Lukashenko S.N., Umarov M.A., Aidarkhanov A.O.// NNC RK Bulletin. – 2007. Vol.4. – pp.80-86. – [in Russian]
3. Качество воды – определение активности трития, соответствующей данной концентрации – жидкостной метод сцинтилляционного счета: ISO 9698-1989 /E/.
   Water quality – determination of tritium activity concentration – liquid scintillation counting method: ISO 9698-1989.

ДЕГЕЛЕҢ ТАУЛЫ МАССИВІНІҢ ҚАР ЖАМЫЛҒЫСЫНДАҒЫ ТРИТИЙДІҢ ҚҰРАМЫН ЗЕРТТЕУ

Турченко Д.В., Лукашенко С.Н., Айдарханов А.О., Ляхова О.Н.

ҚР ҰЯО Радиациялық қауіпсіздік және экология институты

Бұл мақалада, "Дегелең" таулы массивіндегі тритиймен ластанған ағын сулары арнасында жатқан қар жамылғысының қабатындағы тритийдің құрамын зерттеу нәтижелері келтірілген. Зерттеу нысандары ретінде "Дегелең" тәжірибелік-сынақ алаңынан тыс жерге ағып жатқан, Қарабұлақ, Ұзынбұлақ және Ақтыбай бұлақтарының ағын сулары таңдап алынды. Бұл жұмыста ағын суларының арналарына қатысты тритийдің кеңістікте таралуы зерттелді және қар жамылғысының ластану шекаралары анықталды. Бұлақтың ағын суларының ортасында, жербеті қабатының мәні 40 кБк/кг-ға жететін қар жамылғысының ластануы байқалды. Ағын судың арнасымен байланыспайтын телімдердегі тритийдің аялық мәні анықталды, ол 40-тан 50 Бк/кг-ға дейінгі мәнді құрайды. Түрлі маусымдық кезеңдегі қар жамылғысына жасалған зерттеулердің нәтижелеріне салыстырмалы талдама өткізілді. Қар жамылғысына тритийдің өтуінің негізгі механизмдері қарастырылды және анықталды. Бұлақтардағы тритийдің өтуінің негізгі механизмі ретінде мұздың немесе топырақтың беткі қабатындағы тритийдің эманациясы болып табылады.

Түйін сөздер: жерасты сулары, тритий, қар жамылғысы, Ұзынбұлақ, Қарабұлақ, Ақтыбай, ССП, радионуклидтердің жылыстауы, қар жамылғысының беткі қабаты, қар жамылғысының жербеті қабаты, топырақтан тритийдің эманациясы.

ИЗУЧЕНИЕ СОДЕРЖАНИЯ ТРИТИЯ В СНЕЖНОМ ПОКРОВЕ ГОРНОГО МАССИВА ДЕГЕЛЕН

Турченко Д.В., Лукашенко С.Н., Айдарханов А.О., Ляхова О.Н.

Институт радиационной безопасности и экологии НЯЦ РК, Курчатов, Казахстан

В статье представлены результаты исследования содержания трития в слоях снежного покрова, расположенного на загрязненных тритием руслах водотоков массива "Дегелен". Объектами исследования были выбраны водотоки ручьев Карабулак, Узынбулак и Актыбай, выходящие за пределы опытно-экспериментальной площадки "Дегелен". В работе изучено пространственное распределение трития относительно русла водотоков, определены границы загрязнения снежного покрова. В центре водотока ручьев прослеживается загрязнение снежного покрова, достигающее в приземном слое значений 40 кБк/кг. Определены значения фоновых уровней трития на участках, не связанных с руслом водотока, которые составляют от 40 до 50 Бк/кг. Проведен сравнительный анализ полученных результатов снежного покрова в различные сезонные периоды. Рассмотрены и определены основные механизмы перехода трития в снежный покров. Наиболее значимым механизмом перехода трития на ручьях является эманации трития с поверхности льда или почвы.

Ключевые слова: подземные воды, тритий, снежный покров, Узынбулак, Карабулак, Актыбай, СИП, миграция радионуклидов, поверхностный слой снежного покрова, приземный слой снежного покрова, эманация трития из почвы.

УДК 591.146:577.391:577.4:539.16

ON THE QUALITY OF KOUMISS MADE AT THE PRODUCTION SITE IN SARZHAL VILLAGE

Panitskiy A.V., Lukashenko S.N., Bitenova M.M.

Institute of Radiation Safety and Ecology NNC, Kurchatov, Kazakhstan

This paper reports on the studies of ^{3}H content in koumiss produced at the koumiss shop located in Sarzhal village, as well as in koumiss produced at farms located in the south-eastern part of the STS grazing areas of which are in close proximity to the radiation-hazardous sites *Degelen*, *Balapan*, and *Telkem*.

Keywords: tritium (^{3}H), radioactive contamination, agricultural products, koumiss, Semipalatinsk Test Site (STS).

INTRODUCTION

In the territory adjacent to the south-eastern part of the STS there is Sarzhal locality with a population of more than 2,000 people. The main activity in Sarzhal village is livestock farming. In particular, there is a shop in Sarzhal for production of the traditional Kazakh beverage - koumiss which is one of the main agricultural products in the area studied. The scope of koumiss production in 2010 exceeded 900 litres per day in summer and early autumn. Koumiss is sold then in settlements in surrounding areas and cities of Semey, Ust-Kamenogorsk, Almaty and Karaganda.

Koumiss is produced by processing mare's milk; therefore, the shop makes purchase of mare's milk from the farmers of the region, most of the farms of which are located in the territory of STS (Figure 1).

Animals from these farms are grazed around "Degelen" testing site where underground nuclear tests were carried out in adits. Also, there is haymaking for animal feed during the winter period in the territory adjacent to "Degelen" site.

The earlier studies [1] found that the main long-lived artificial hazardous radionuclides accumulate in soils within "Degelen" testing site and do not overstep its boundaries. However, it is also revealed [1] that the radiation situation has been and will be greatly affected in the future by ^{3}H radionuclide which proliferates far beyond "Degelen" testing site with groundwater. In this regard, studies were carried out on the possible content of ^{3}H in koumiss produced in the shop in Sarzhal village and in farms located in south-eastern part of the STS.

1. EXPERIMENT

Inflow of ^{3}H radionuclide into mare's milk can occur both during grazing of animals in the area adjacent to "Degelen" testing site and at stall feeding with hay harvested in the area. Therefore, an assessment of ^{3}H content in the mare's milk was carried out during the period of pasture feeding in the area, and during stall feeding with hay harvested in the studied area.

Samples were collected from the wintering sites, located in STS territory. In some cases, samples were taken monthly in 3–4-fold replication. Koumiss was also sampled from the shop in Sarzhal village from a 60 l wood vessel in which the koumiss is brought to readiness. In total, 52 samples of koumiss were taken.

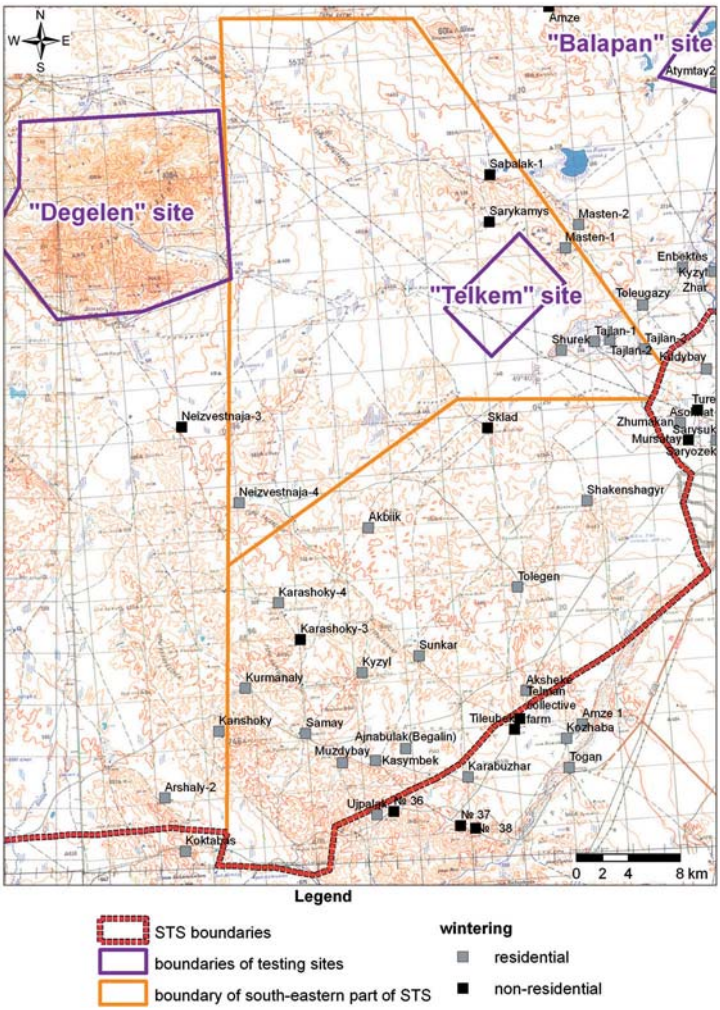

Figure 1. Wintering sites in the studied territory

1.1. Preparation and analysis of samples

A sample for determination of ^{3}H was obtained by distillation of koumiss at 100˚C. The first obtained condensate in amounts of 10 ml was removed, and the following 5-6 ml of free water from koumiss was taken for analyses. Tritium activity was measured in this

free water at the beta-spectrometer TRI CARB 2900 TR with liquid scintillation method in compliance with ISO 9698 [2]. The analytical measurement error was less than 30%. So, the results below do not consider organically-bound tritium.

2. RESULTS

In most of the cases no ^{3}H was recorded in koumiss obtained during the grazing of animals in the studied area. There were several values that are close to the lower detection limits of the equipment (Table 1).

Table 1.

Determination of ^{3}H in the mare's milk (koumiss) produced on farms in south-eastern part of the STS

Sampling point	Sampling date	Specific activity of ^{3}H, Bq/l	Sampling point	Sampling date	Specific activity of ^{3}H, Bq/l
Tailan wintering site	14.07.2010	20±10	Kudabay wintering site	24.08.2010	<18
	10.08.2010	<13		30.09.2010	< 14
	10.09.2010	40 ± 20	Toleugazy wintering site	14.08.2010	<11
Shurek wintering site	14.07.2010	20±10		17.10.2010	<14
	27.08.2010	<19	Tailan 2 wintering site	15.08.2010	<12
	25.09.2010	< 13		29.08.2010	<19
Nysan wintering site	19.08.2010	<19	Atymay wintering site	17.09.2010	<12
	29.09.2010	30 ± 3		11.10.2010	<15
	18.10.2010	<12	Togalak wintering site	14.08.2010	<12
Zhumakan wintering site	14.07.2010	30±15	Kara-Koryk wintering site	10.08.2010	<13
	14.08.2010	<12	Kudabay wintering site	15.08.2010	<12
	28.09.2010	< 15	Sary-Arka wintering site	24.08.2010	<20
	19.10.2010	<12	Tauysty	25.08.2010	25 ± 12
Tasbaskan wintering site	29.08.2010	< 18	Mosten 2 wintering site	18.08.2010	25 ± 12
	12.09.2010	20 ± 10	Mosten wintering site	13.10.2010	<12
	17.10.2010	<11	Zholdatay wintering site	19.08.2010	<20
Sary-Ozek wintering site	10.08.2010	<14	Bakizhan wintering site	10.09.2010	30 ± 15
	18.08.2010	25 ± 12	Kamys-Sheky wintering site	05.10.2010	<14
Karakan wintering site	15.09.2010	< 14	Sabalak wintering site	13.10.2010	<12
	16.10.2010	<11	Elubay wintering site	17.10.2010	<12

These recorded values that are close to the limits of detection may be due to the fact that plots of grazing farms, where numerical values of the radionuclide ^{3}H in mare's milk were recorded, are located in the territory where there is shallow groundwater occurrence (up to 2 m) containing ^{3}H up to 23 kBq/l [1]. Accordingly, the radionuclide ^{3}H from groundwater through the root system can penetrate the plants growing in the area, and be absorbed by the animals during grazing.

No ^{3}H was found in the samples of koumiss, taken from the koumiss production shop in Sarzhal (from total 60 l mixed mare's milk, Table 2).

In koumiss, produced during stall feeding of animals with hay harvested from areas adjacent to "Degelen" testing site in all cases the ^{3}H specific activity was below the determination threshold (Table 2).

Table 2.

^{3}H determination in the mare's milk (koumiss) produced in the koumiss shop in Sarzhal village

Sampling point	Sampling date	Specific activity of ^{3}H, Bq/l	Sampling point	Sampling date	Specific activity of ^{3}H, Bq/l
During pasture feeding			*During stall feeding*		
Shop for production of koumiss, Sarzhal village	04.09.2010	<19	Sarzhal village, small-scale family farms	21.03.2011	<12
	07.09.2010	<20		21.03.2011	<15
	07.09.2010	<20		21.03.2011	<12
	02.09.2010	<19		21.03.2011	<12
	20.09.2010	<12		21.03.2011	<13
	19.10.2010	<12		21.03.2011	<13

CONCLUSION

In general, the study have shown that the content of ^{3}H in most cases remains below the determination threshold of the measurement instruments, while the recorded in some cases quantitative values are thousands of times below the intervention levels of 7,700 Bq/kg (NRB-99) [3]. Thus, the koumiss, obtained both in farms located in the south-eastern part of the STS, and in the koumiss shop in Sarzhal village is safe in terms of radiological factors.

REFERENCES

1. Topical Issues in Radioecology of Kazakhstan [Proceedings of the Institute of Radiation Safety and Ecology for 2007 - 2009] / headed by S. N. Lukashenko [in Russian]
   Актуальные вопросы радиоэкологии Казахстана [Сборник трудов Института радиационной безопасности и экологии за 2007 – 2009гг.] / под рук. Лукашенко С.Н. – Вып. 2. – Павлодар: Дом печати, 2010. – С. 57-103.: ил.- Библиогр.: с. 224-231. - ISBN 978-601-7112-28-8.
2. The international standard ISO 9698. Water quality - determination of tritium activity, corresponding to a given concentration - liquid method of scintillation counting
3. State sanitary-epidemiological rules and standards. Radiation Safety Standards (NRB-99) [in Russian]
   Государственные санитарно-эпидемиологические правила и нормативы. Нормы радиационной безопасности (НРБ-99): СП 2.6.1. 758-99; ввод. в действие 01.01.2000. – Алматы: Агентство по делам Здравоохранения РК, 1999. - 80с. – ISBN 9965-501-42-4.

САРЖАЛ АУЫЛЫНДАҒЫ ӨНДІРІСТІК ТЕЛІМДЕ ӨНДІРІЛЕТІН ҚЫМЫЗДЫҢ САПАСЫ ЖАЙЛЫ МӘСЕЛЕГЕ

Паницкий А.В., Лукашенко С.Н., Битенова М.М.

ҚР ҰЯО Радиациялық қауіпсіздік және экология институты, Қазақстан, Курчатов қ.

Аталған жұмыста, Саржал а. орналасқан қымыз өндіру цехында өндірілетін қымыздың құрамындағы, сонымен қатар "Дегелең", "Балапан", "Телкем" алаңдарындағы – радиациялық-қауіпті нысандарға тікелей жақын орналасқан жайылым телімдерінде, ССП оңтүстік-шығыс бөлігінде орналасқан фермерлік шаруашылықтарда өндірілетін қымыздың құрамынан ^{3}H радионуклидінің анықтаудағы зерттеу нәтижелері келтірілген.

Түйін сөздер: тритий (^{3}H), радиоактивті ластану, ауылшаруашылық өнімі, қымыз, Семей сынақ полигоны (ССП).

К ВОПРОСУ О КАЧЕСТВЕ КУМЫСА, ПРОИЗВОДИМОГО НА ПРОИЗВОДСТВЕННОМ УЧАСТКЕ В ПОСЁЛКЕ САРЖАЛ

Паницкий А.В., Лукашенко С.Н., Битенова М.М.

Институт радиационной безопасности и экологии НЯЦ РК, Курчатов, Казахстан

В данной работе приведены результаты исследований содержания радионуклида ^{3}H в кумысе, производимом в цехе по производству кумыса, расположенном в с. Саржал, а также в кумысе, производимом на фермерских хозяйствах, расположенных на территории юго-восточной части СИП, участки выпаса которых находятся в непосредственной близости от радиационно-опасных объектов – площадок "Дегелең", "Балапан", "Телькем".

Ключевые слова: тритий (^{3}H), радиоактивное загрязнение, сельскохозяйственная продукция, кумыс, Семипалатинский испытательный полигон (СИП).

PART: "NON-RADIATIVE" RISK FACTORS ON THE STS

УДК 622.278: 577.4:504.064

RECONNAISSANCE RESEARCH OF GAS EMISSIONS AT "SARY-UZEN" SITE

[1] Romanenko V.V., [1] Lukashenko S.N., [1] Subbotin S.B., [2] Chernova L.V.

[1]Institute of Radiation Safety and Ecology NNC RK, Kurchatov, Kazakhstan
[2]Institute of Atomic Energy NNC RK, Kurchatov, Kazakhstan

The paper reports on the studies of the effects from underground nuclear explosions (UNE) manifested as underground gasification of rocks and subsidence events at "Sary-Uzen" TEST SITE of the STS. The reconnaissance allowed specifying the positions of "warfare" boreholes and identifying five sites with evidence of testing. The works made it possible to describe current status of the wells and presence of post-explosion phenomena in form of swelling, gaps and other deformations of the surface. At "Sary-Uzen" site all the wells have elevated concentrations of carbon dioxide and 14 wells have elevated concentrations of methane. In some wells concentrations of methane is much greater than at "Balapan" site, which is possible due to the depth of charges for the UNEs. No UNEs were carried out in the well 103, but elevated concentrations of methane and carbon dioxide were recorded in the soil air in the mouth area of the well. Recommendations for further study of the gasification processes at "Sary-Uzen" site are also made in the paper.

Keywords: Semipalatinsk Test Site, nuclear testing, "Sary-Uzen" site, soil air, subsidence, topographical works, geomorphological monitoring, methane, underground gasification, gas emission.

INTRODUCTION

Earlier studies at "Balapan" site [1, 2] show that the UNEs have caused not only radioactive contamination of the environment, but there is a great potential for impacts associated with activation of underground combustion of carbonaceous rock [3]. "Sary-Uzen" and "Balapan" sites were used for underground nuclear tests (Table 1). According to archive data [4], 24 underground tests were carried out in "warfare" boreholes from 1965 to 1980. Depth of the charges planted was about 250 meters in average. Archive data [5, 6] provide coordinates of positions of "warfare" boreholes, which in some cases differ. In this regard to examine the "warfare" boreholes, it was necessary to specify the coordinates of their location.

One of the UNEs features is that for many years blocks of rocks surrounding the central zone of UNE have had high temperature, slowly decreasing with time [7, 8], i.e. sprung cavities of UNEs are long-term holder and sources of thermal energy. The available data on the geological structure of "Sary-Uzen" site indicate the presence of carbonaceous rock. It is likely that within UNE area, groundwater penetrate through conjugated fractures where there are both high temperatures and carbonaceous rock, which is the impetus for gasification and pyrolysis. So, emergence of underground combustion processes caused by UNEs at "Sary-Uzen" site is quite possible.

1. PRECONDITIONS FOR CATASTROPHIC EVENTS AT "SARY-UZEN" SITE

1.1. Geological structure and hydrogeological conditions at "Sary-Uzen" site

"Sary-Uzen" site is located within the eastern edge of Central Kazakhstan, in Altybay intermountain valley, bordered on the west with Murzhik mountain range, in the east with mountains Maylykara and Degelen. Geomorphologically, the entire site territory is within the Kazakh Upland. The geological structure of the territory has faulted metamorphic, volcanogenic and sedimentary deposits of the Proterozoic, Devonian and Lower Carboniferous and horizontally lying loose sandy-clay sediments of Neogene and Quaternary systems.

1.1.1. Stratigraphy

Proterozoic group. The Upper Proterozoic sediments within the site represent a narrow 250 m band over 2.5-3 km at the foothills of Murzhik mountains in the extreme southwestern part. They are represented by gray-green, yellow-green and greenish-gray metamorphosed slates of different composition: quartz-chlorite, epidote-chlorite, siliceous -chlorite, siliceous. Their thickness in the territory adjacent to the west is approximately 2 km.

The Devonian System. The sediments of the Devonian system distinguish volcanic formations of Eifelian *(D_2ef)* and Givetian *(D_2gv)* stages in the middle series, undifferentiated volcanic and sedimentary deposits of the Givetian-Frasnian of the middle and upper series and carbonate sediments of the Famennian *(D_2gv-D_3f)* of the upper series. The composition of the strata is mainly andesite and andesite-basalt porphyry and tuffs, where, especially in the upper part of the section, occasionally there are layers of acid lava, sandstone and limestone lentils. Thickness of the sediments within the area site does not exceed 0.25–0.7 km. The entire thickness is highly metamorphosed and deformed into large folds.

Carboniferous system. The lower series. Visean stage, Lower substage (C_1v_1) are characterized by grey-colored, consertal, polymictic sandstones and dark gray and black carbonaceous slates. The carbonaceousness of the deposits is their characteristic feature. The deposit thickness is 0.15–0.2 km.

Neogene system. Neogene sediments cover folded Paleozoic basal complex for almost the entire area of the site except for small bare areas in the south, north, and northwest, northeast. Neogene sediments are represented by reddish-brown and green-coloured clays. The sediment thickness varies widely from 5 m to 86 m. The thickest clays (70–80m) are in the south-west of this territory.

Quaternary system. Quaternary sediments superpose with a solid cover all older formations throughout the area except for the chain of secondary quartzites in the southwest of the site. The sediments are represented by alluvial-proluvial, diluvial-proluvial, diluvial, eluvial-diluvial, alluvial, lacustrine sediments. The thickness of the sediments varies from tens of centimeters to 26 meters.

Intrusive rocks. Intrusive formations have been uncovered by drilled wells over a large area in the southwestern part of the site. Besides, some massifs were opened in the cen-

tral part of it. Intrusive rocks are represented by two different ages and different composition of the complexes: a complex of Lower Carboniferous subvolcanic intrusions of diorite and early Upper Paleozoic granitoid complex.

Tectonics. In regional terms, the territory is a part of the Genghis Tarbagatai Caledonian fold system, being within the Chu synclinorium. Here are two structural stages: Paleozoic and Cenozoic. Faults in the area are quite intensive. Their orientations are divided into the north-west faults and northeast strike.

1.1.2. Hydrogeological conditions

The main natural factors influencing the formation of the hydrogeological conditions of the site are the structural-tectonic features of the area, climate, topography and lithologic and petrographic composition of geological formations. The main recharge areas are off the site. They are Murzhik Mountains in the west and south-west, in the south – Degelen Mountains.

The main direction of groundwater flow us in the north-east towards Irtysh river valley, where they are recharged.

The following types of water are singled out at the site:

- fissure water, confined to the upper fractured zone of weathering of Paleozoic rocks;
- fracture-vein waters, enclosed in areas adjacent to tectonic faults in the areas of rock shattering;
- pore water of the sporadic distribution in alluvial-proluvial and alluvial deposits of quaternary age.

Adverse conditions for recharge related to deficiency of rainfall and the predominance of evaporation over the infiltration in summer and hindered water exchange cause salinity of groundwater and formation of specific chloride-sulphate, less sulphate-chloride-sodium types of mineralization, typical for arid and droughty zones.

Intensive water exchange in the zones of tectonic faults may cause accumulation of fresh and slightly brackish groundwater, which can be used for local water supply.

The aquifers are:

- waters of fractured zone of Upper Devonian Lower Carboniferous sediments (D_3fm-C_1t, C_1v_1);
- waters of fractured zone of medium-and Upper Devonian effusive-sedimentation (D_2gv- D_3f);
- waters of fractured zone of Middle Devonian effusive-sedimentation (D_2ef, D_2gv);
- waters of fractured zones of Upper Proterozoic metamorphic rocks (PR_3);
- waters of fractured zones of different intrusive formations (PZ_3);
- waters of sporadic distribution of alluvial and proluvial lacustrine sedimentation (apQ).

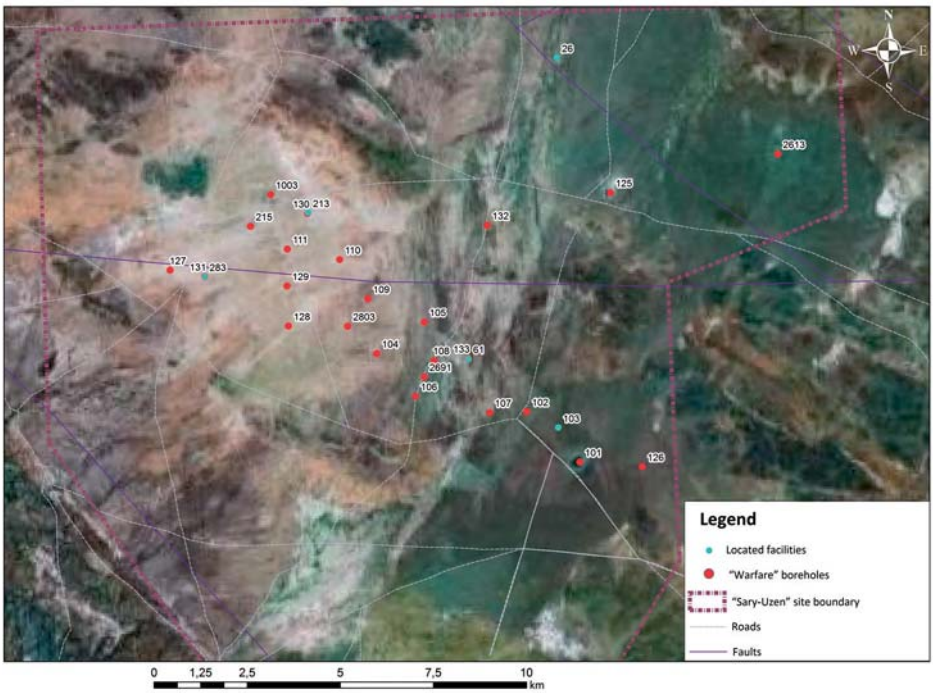

Figure 1. Wells at "Sary-Uzen" site

The lack of explicit foci of groundwater discharge and regional aquitard within the area give reason to consider ground water of fractured zones as a single hydrogeological basin. In general, groundwater in the fractured zones has the following parameters. Aquiferous rocks are: fractured limestones, sandstones, conglomerates, gravelite, siltstone, carbonaceous-argillaceous slate, porphyries, tuffs, and various effusions, granodiorites, granites, diorite-porphyry, and gabbro-diorite. The aquifer thickness is 50-110 m. Groundwater depth is 14-130 m. Waters are pressure-free, but in places where water-bearing sediments are covered with Neogene clays the waters get pressure up to 40 meters. Water, mostly, is fresh and brackish with mineralization up to 14.7 g/l, but basically it is 3-5 g/l. The filtration coefficient is defined by the degree of fracturing and varies widely from 0.001 to 4.4 m/day, increasing in zones of tectonic faults.

Sporadic distributed waters are in the alluvial-proluvial, alluvial and lacustrine sediments (apQ). The aquiferous rocks are common in inter-upland depressions, ancient hollows of runoff, and lake basins and are gravel-pebble sedimentations, less clay sand and loam. Thickness of the water-bearing rocks varies from 1.3 m to 20 m. Depth to groundwater is 7-15 m. Water is pressure-free, it gets about 3-15m where clay spread. The water is fresh and brackish with a salinity of 0.7-5.7 g/l. Flow rate is a few hundredths up to 0.1 l/s.

The available data on the geological structure and hydrogeological conditions of "Sary-Uzen" site suggest that UNE damaging factors may cause pyrolysis and underground gasification. To a greater extent, this process involves rocks containing carbonaceous materials (carbonaceous siltstones, slates, sandstones) [9].

1.2. Nuclear tests at "Sary-Uzen" site and their consequences

1.2.1. Background information about the nuclear tests at "Sary-Uzen"

At "Sary-Uzen" TEST SITE, 24 underground nuclear explosions at wells were carried out in 1965-1980. [4]. According to available data, in the majority of the tests the explosion power did not exceed 20 kt. The greatest development pressure caused by underground nuclear explosions happened in the center and north-western part of the site. The following table (Table 1) provides an overview of UNEs at "Say-Uzen" site, site outline is shown in Figure 1.

Table 1.

Underground nuclear explosions at "Say-Uzen" site

##	Well #	Nuclear test date	According to [10]				According to [11]			
			Nuclear test capacity	Radiation effects	Nuclear tests goal	Depth of charge	Magnitude of nuclear tests	Nuclear test capacity	Calculated capacity	Magnitude of nuclear tests
1	101	18.12.1966	20-150	PCE (ARS)	TIC	427	5.8	38	100	5.92
2	102	16.09.1967	0.001-20	PCE (RIG)	INW	230	5.3	11	16	5.25
3	104	21.07.1970	0.001-20	FCE	INW	225	5.4	14	23	5.38
4	105	22.09.1967	10	FCE	INW	229	5.2	9.2	10	5.16
5	106	22.11.1967	0.001-20	FCE	INW	227	4.8	3.6	1.6	4.41
6	107	28.12.1969	46	FCE	INW	388	5.7	30	40	5.79
7	108	31.05.1969	0.001-20	PCE	INW	258	n/d.	11	18	5.29
8	109	16.02.1979	0.001-20	PCE (RIG)	INW	n/d.	5.4	15	23	5.39
9	110	06.06.1971	16	PCE (RIG)	INW	299	5.5	17	16	5.53
10	111	09.10.1971	12	PCE (ARS)	INW	237	5.3	12	12	5.37
11	125	04.11.1970	0.001-20	PCE (RIG)	TIC	249	5.4	14	27	5.44
12	126	04.04.1980	0.001-20	FCE	INW	n/d.	4.9	6	6	4.9
13	127	21.10.1971	23	PCE (RIG)	INW	324	5.5	19	23	5.58
14	128	02.09.1972	2	PCE (RIG)	INW	185	4.9	4.3	2	5.1
15	129	19.06.1971	0.001-20	PCE (RIG)	INW	290	5.4	15	35	5.54
16	130	29.03.1977	20-150	PCE (RIG)	INW	n/d.	5.4	n/d.	n/d.	n/d.
17	131	19.04.1973	0.001-20	PCE (RIG)	INW	n/d.	5.4	12	21	5.36
18	132	26.08.1972	0.001-20	PCE (RIG)	INW	285	5.3	13	21	5.36
19	133	04.08.1976	0.001-20	PCE	INW	n/d.	4.1	0.06	0.9	4.2
20	215	28.11.1974	0.001-20	PCE(ARS)	INW	n/d.	n/d.	n/d.	0.01	2.7

##	Well #	Nuclear test date	According to [10]				According to [11]			
			Nuclear test capacity	Radiation effects	Nuclear tests goal	Depth of charge	Magnitude of nuclear tests	Nuclear test capacity	Calculated capacity	Magnitude of nuclear tests
21	1003	14.10.1965	1.1	ESO	IE	48	n/d.	n/d.	1.1	4.28
22	2613	18.07.1979	0.001-20	n/d.	n/d.	n/d.	n/d.	n/d.	12	5.16
23	2691	19.03.1978	0.001-20	FCE	INW	n/d.	5.2	9.4	13	5.19
24	2803	16.02.1989	0.001-20	FCE	INW	n/d.	5.2	n/d.	n/d.	n/d.

Abbreviations:

n/d.	no data
b/d	below detectable (for concentration of gas)
PCE	partial camouflet explosion (rapid and dynamic outflow of radioactive gaseous and vaporous products, followed by ignition of the mixture)
PCE - ARS	partial camouflet explosion with abnormal radiological situation (explosion of total internal actions with abnormal radiological situation (ARS), accompanied by an early and dynamic pressurized getting of explosion products in the gas and vapour phase into atmosphere, due to accidental abnormalities in the normal process of testing or its consequences not predicted in the project: it could cause or lead to over-exposure of people or material damage)
FCE	full camouflet explosion (with explosion no inert gases went into the atmosphere)
ESO	explosion with soil outburst (blasting cone)
PIE(RIG)	partial internal explosion with a joining of fracture zones and spallation destruction of the surface in the epicentral area of the explosion and the vent, usually negligible, outflow of short-lived radionuclides into the atmosphere - inert gases)
INW	improvement of nuclear weapons / nuclear weapons development
TIC	test of industrial charges (to perform nuclear explosions for peaceful purposes)
IE	industrial nuclear explosions for peaceful purposes and development of technology

2. BASIC METHODOLOGY AND INSTRUMENTAL METHODICAL WARE

2.1. Instrumental and methodical ware

2.1.1. Reconnaissance survey

In the initial stage of the works at all "warfare" boreholes of "Sary-Uzen" site, a condition survey of the territory in vicinity of the wells was performed. The initial data were: a coordinates and layout of the "warfare" boreholes drawn from the earlier works. When identifying the "warfare" boreholes in the area, coordinates of the mouth were determined

using GPS GARMIN 12 in the WGS 84 coordinate system, wellheads and visually the most prominent topographic features in the vicinity of the wells were photographed, sizes (diameter and depth) of the craters and depressions/uplands of the relief were described and assessed. In order to classify the wells as emplacement ones, we used attributes of underground tests, in particular – a wellhead as Ш1120 mm pipe, elevator, a dynamic clutch, nipping fork and discharge facility (Figure 2). According to [4], the diameter of an "warfare" borehole, as a rule, was ~1 m.

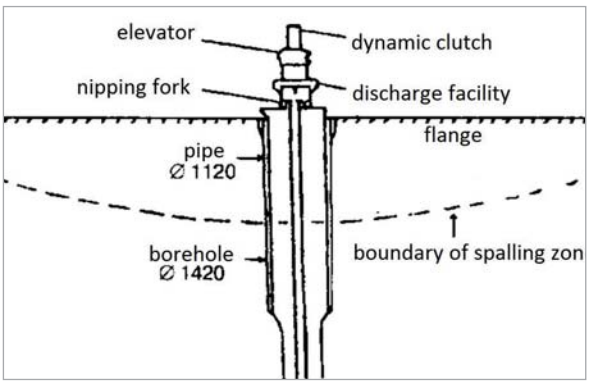

Figure 2. Well design [4]

2.1.2. Geomorphological monitoring

To create a topographic base for subsequent geomorphological monitoring, a tacheometric survey was carried out within the mouth area of the Well 104. A geomorphological monitoring to track the ongoing processes of the surface deformation by comparing the tacheometric data from different years has been initiated.

At the mouth area of the Well 104 the survey covered 1x1 km^2 on a scale of 1:2000 with a 0.5 m vertical interval [3]. The stations SOKKIA SET 510 ET 510 #33746 and SOKKIA SET 230 R3 #170094 were used.

The points of the geodetic network in the locality have been assigned with temporary signs in the form of 40 cm high metal rods. The systematic geodetic survey network was developed by a polar manner with an electronic total station, and the length of the polar direction not exceeding 1,000 m. The elevational geodetic network was developed by technical levelling.

The data processing results made it possible to built topographic maps using the software package GeoniCS Topoplan v. 09.09.

Precision of the engineering and topographic plan has been assessed based on the mean difference of the positions of objects and paths, as well as the heights of the points calculated by the contour lines, with the data from control field measurements. Average errors of topography's contour features with clear outline relative to nearest geodetic control points in plan view did not exceed 0.5 mm in plan scales. The average error of the relief survey and its image on the plan relative to the nearest point surveyor' pickup, did not exceed the adopted vertical interval – 1/3 (at angles of surface slope up to 10°).

Along with tacheometry, within the mouth area of the Well 104, long-term surveying bench marks were installed for subsequent real-time monitoring of the subsidence dynamics (Figure 3). Layout of the bench marks is shown in Figure 4. The distance between the bench marks set at the edges of the crater is about 250 meters; the central bench mark was at the bottom of the crater at a depth of 6 m.

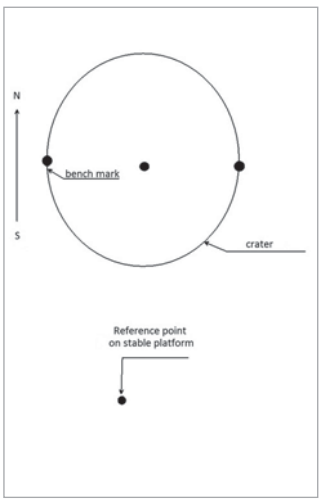

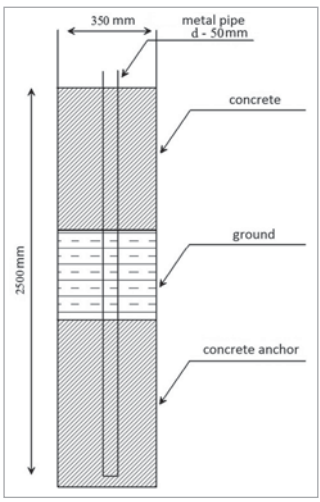

a b

Figure 3. Well 104. Topographic monitoring at failures: a - bench marks configuration, b - bench mark design

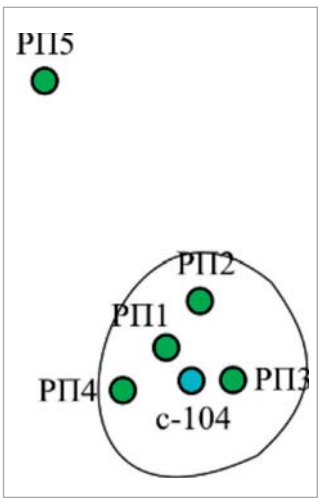

Figure 4. Bench marks at the well 104

The following table (Table 2) gives the coordinates of the five embedded bench marks. In 2011, a year after the installation of the bench marks, in accordance with the requirements of SNiP for surveying works, a high-precision levelling will be carried out by electronic digital levelling instrument. In 2012, the first data will be obtained to quantify the displacement of the ground surface at the well 104 where the bench marks were laid.

Table 2.

Well 104. Coordinates of 5 bench marks installed

Bench mark #	WGS 84 coordinates	
	north latitude	west longitude
104-I	49°57'10".6	77°40'19".5
104-II	49°57'11".8	77°40'20".9
104-III	49°57'09".9	77°40'22".1
104-IV	49°57'09".7	77°40'17".7
104-V	49°57'17".1	77°40'14".8

Figure 5 shows the bench mark installed.

Figure 5. Bench mark installed

2.1.3. Instrumental and methodological assurance to determine the gas composition

Methods and instrumentation employed

The gases in the soil and atmosphere were determined with the analyzers Sensis-200 and ANKAT-7664M.

The principle of Sensis-200 analyzer [12] is based on continuous transformation of signals from measuring transducers to digital ones, with subsequent processing by a built-in microprocessor. The gas analyzer is an instrument of continuous operation: it simultaneously measures the concentration in air of up to eight gases.

The gas analyzer uses electrochemical, optical, semiconductor, thermocatalytic, chemiluminescent, combined sensors as measuring transducers.

The gas analyzer ANKAT-7664M is designed for automatic continuous measurement of the volume fraction of oxygen, carbon monoxide (II), hydrogen sulphide, concentrations of the sum of saturated hydrocarbons (Ex). Some characteristics of the used gas analyzers are shown in Table 3 [13].

Table 3.

Ranges and units of measurement of the equipment

##	Name	Chemical formula	Measurement range	Precision	Gas analyzer
1	Hydrogen	H_2	0.001 - 1 %; 0.002 - 4%	$\pm 0.2C_{\text{inlet concentration}}$	Sensis-200
2	Methane	CH_4	0.02 - 5 % 0.2 – 100 %	$\pm 0.2C_{\text{inlet concentration}}$	Sensis-200
3	Sulphur dioxide	SO_2	0.1 – 20 mg/m^3 0.5 - 100 mg/m^3 1 - 2000 mg/m^3	$\pm 0.2C_{\text{inlet concentration}}$	Sensis-200
4	Carbon dioxide	CO_2	0.002 - 5 %; 0.001 - 2%	$\pm 0.2C_{\text{inlet concentration}}$	Sensis-200
5	Carbon oxide	CO	0 - 200 mg/m^3	± 5 mg/m^3	ANKAT-7664M
6	Hydrogen sulphide	H_2S	0 - 40 mg/m^3	$\pm (2.5+0.25(C_{BX}-10))$ mg/m^3	ANKAT -7664M

Complementary error limits – 5 %.

Sampling of air

Soil air was sampled with storage vessels (10 litre plastic cans equipped with nozzles for air sampling). Airtightness of the storage vessels was assured by submerging them 5-7 cm deep in soil and soil compaction around the vessel walls. The duration of gas accumulation was not less than one day. At the end of the day the gas mixture was sampled from the storage vessels.

When choosing points to install the storage vessels, the priority was given to the sites with anthropogenic origin deformed landforms (cracks, subsidences, etc.).

Parallel measurements were made for concentrations of gases in the air at the locations of the "warfare" boreholes. Concentrations of gases were measured by gas analyzer at ~ 1 meter above the surface.

For reference, soil air was sampled at points far away from the mouth areas (at a distance of 500 meters).

Sampling was performed with a device for collection and storage of gas samples PPG.

For transportation and storage of soil air samples we used a glass aspirator. The operating principle of the device is displacement of gas with water by using a levelling bottle [15].

3. RESULTS AND DISCUSSION

3.1. Findings of reconnaissance survey

State of the "warfare" boreholes mouths at "Sary-Uzen" site was identified and updated. The surface near the wells was photo-documented in the same perspective in the southern direction.

The total reconnaissance operations in 2007 [10] found 29 objects (see table below). According to the catalogue of "warfare" boreholes published in the "Soviet Nuclear Testing" [4], there are 24 emplacement objects. From this list we found 21 objects. Three objects – 105, 131 and 133 – were not found, later by 2009 their position was identified and their gridding was carried out [15].

In addition to the "warfare" boreholes specified in the catalogue [4], other five objects were found where most likely tests were performed. These objects were numbered 103, 283, 213, 61 and 26. Four wells with large diameter heads were found at the object 103.

Table 4.

Reconnaissance survey to identify coordinates of "warfare" boreholes

##	Well #	Explosion number accord. to [4]	Geographic coordinates, in degrees, minutes, seconds					
			Topographic precise positioning data		Accord. to [15]		Accord. to [16]	
			north latitude	east longitude	north latitude	east longitude	north latitude	east longitude
1	**101**	262	49 55 28,5	77 44 50.0	49 55 28,5	77 44 50.0	49 55 24,4	77 44 43,6
2	**102**	272	49 56 13,9	77 43 41,2	49 56 13,9	77 43 41,2	49 56 05,5	77 43 25,5
3	**104**	323	49 57 08,7	77 40 22,4	49 57 08,7	77 40 22,4	49 57 10.6	77 40 20.7
4	**105**	273	49 57 34,7	77 41 27,8	49 57 34,7	77 41 27,8		

##	Well #	Explosion number accord. to [4]	Geographic coordinates, in degrees, minutes, seconds					
			Topographic precise positioning data		Accord. to [15]		Accord. to [16]	
			north latitude	east longitude	north latitude	east longitude	north latitude	east longitude
5	**106**	278	49 56 31,0	77 41 12,36	49 56 31,0	77 41 12,36	49 56 32,6	77 41 10.6
6	**107**	314	49 56 14,4	77 42 51,2	49 56 14,4	77 42 51,2	49 56 16,0	77 42 49,0
7	**108**	301	49 57 01,1	77 41 39,2	49 57 01,1	77 41 39,2	49 57 03,0	77 41 37,0
8	**109**	515	49 57 56,5	77 40 13,0	-	-	49 57 56,5	77 40 13,0
9	**110**	339	49 58 31,5	77 39 37,0	49 58 31,5	77 39 37,0	49 58 33,4	77 39 34,7
10	**111**	347	49 58 42,3	77 38 27,0	49 58 40.4	77 38 29,2	49 58 42,1	77 38 26,9
11	**125**	328	49 59 21,2	77 45 44,8	49 59 21,2	77 45 44,8	49 59 26,2	77 45 41,2
12	**126**	544	49 55 22,4	77 46 13,8	-	-	49 59 30.2	77 38 06,9
13	**127**	348	49 58 27,5	77 35 48,1	49 58 25,7	77 35 50.4	49 58 27,5	77 35 48,1
14	**128**	369	49 57 35,3	77 38 24,8	49 57 33,9	77 38 27,2	49 57 35,3	77 38 24,8
15	**129**	340	49 58 10.2	77 38 24,7	49 58 08,5	77 38 26,9	49 58 10.2	77 38 24,7
16	**130**	458	49 59 12,7	77 38 55,9	-	-	49 56 47,5	77 41 25,0
17	**131**	380	49 58 20.9	77 36 34,5	-	-	-	-
18	**132**	367	49 58 56,8	77 42 57,1	49 58 55,1	77 42 59,8	49 58 56,7	77 42 27,2
19	**133**	447	49 57 1,5	77 42 25,3	-	-	-	-
20	**215**	412	49 59 03,3	77 37 38,5	49 59 03,3	77 37 38,5	49 59 03,3	77 37 38,5
21	**1003**	242	49 59 30.2	77 38 06,9	49 59 26,3	77 38 08,6	49 59 30.2	77 38 06,9
22	**2613**	524	49 59 49,4	77 49 32,0	-	-	49 59 49,4	77 49 32,0
23	**2691**	481	49 56 47,5	77 41 25,0	-	-	49 57 33,3	77 39 44,6
24	**2803**	515	49 57 33,3	77 39 44,6	-	-	49 55 22,4	77 46 13,8
Wells not included in catalogue [4]								
1	**26**	-	50 01 20.4	77 44 39,3	-	-	-	-
2	**283**	-	49 58 20.9	77 36 34,4	-	-	-	-
3	**213**	-	49 59 13,4	77 38 56,6	-	-	-	-
4	**61**	-	49 57 01,4	77 42 25,2	-	-	-	-
5	**103**	-	49 55 59,2	77 44 23,0	-	-	-	-
Note - Gray colour indicates the wells with the same coordinates								

Thus, the data on the actual location of the "warfare" boreholes at "Sary-Uzen" site were obtained. It should be noted that there are discrepancies between obtained coordinates of the "warfare" boreholes and published data [5 and 6]. The coordinates of the "warfare" boreholes obtained from gridding and updating were used to survey for gas emissions.

Today it has not yet been revealed whether chemical or nuclear tests were carried out at those found five objects. Advanced studies will establish their origin.

Gridding of the "warfare" boreholes' mouths, as well as objects with indications for UNEs and photo-documenting of discovered wells was accompanied by a brief description of the current state (Table).

Table 5.

Information about well mouth areas

##	# of well/ facility	Description
1	**101**	"Warfare" borehole, ø 350-400 m crater, coordinates were taken on the south side of the crater, γ = 120 μR/h, pile altitude ~10-15 m. The area around the crater formed is flat, poorly deformed after explosion.
2	**102**	"Warfare" borehole, mouth demolished, casing removed to a depth of 4 - 5 m.
3	**103**/1	"Warfare" borehole, is 15 m north-eastward to 103B3, mouth demolished, casing removed to a depth of 7 m
4	103/2	"Warfare" boreholes, 3 pcs locate nearby, head destroyed, casing removed to a depth of 3-4 m
5	**104**	"Warfare" borehole, large crater, on the south side of the crater is a small relief swelling up relief, head in the center of the crater, around a small lake.
6	104S	"Warfare" borehole, large crater, coordinates were taken on the crater southern side
7	104N	"Warfare" borehole, large crater, coordinates were taken on the crater northern side
8	**106**	"Warfare" borehole, mouth demolished, casing cut to a depth of 6 m
9	**107**/1	"Warfare" borehole, artificially created subsidence of about 40 meters from the wellhead, mouth demolished, casing cut at a depth of 4 m
10	107/2	Most likely, "warfare" borehole, large-diameter casing, filled with rock, concentric circles shaped surface bulging are moving away 70 m SE from well 107V1
11	**108**	"Warfare" borehole, there is raising of the soil in the wellhead area, mouth demolished, casing cut at a depth of 4-5 m
12	**109**	"Warfare" borehole, mouth demolished, casing removed to a depth of 7 m. The central pipe of "warfare" borehole has inscription *1226*. Low surface elevation ~ 2.0 m ø100-150 m. Around the well is a slight swelling of the relief and shallow dips.
13	**110**/1	"Warfare" borehole, mouth demolished, casing removed to a depth of 6 m. Swelling and lifting of the relief to the wellhead.
14	110/2	"Warfare" borehole, mouth demolished, casing removed to a depth of 6 meters, no head is visible, at the bottom of the hole is water near well 110V1
15	110/3	"Warfare" borehole, mouth demolished, casing removed to a depth of 5 m, is located 170 m to SW of well 110V1
16	**111**/1	"Warfare" borehole, mouth demolished, casing cut at a depth of 3-4 m. There is a raising of the soil in the wellhead area.
17	111/2	"Warfare" borehole, mouth demolished, casing cut at a depth of 3-4 m, located 5 m from the well 111V
18	111/3	"Warfare" borehole, mouth demolished, casing cut at a depth of 3-4 m, located 10 m from the well 111V
19	**125**	"Warfare" borehole, a big crater, a small lake in it, the coordinates taken on the northern side of the crater, in its upper part, see well 125G4 for a more precise location
20	**126**	"Warfare" borehole, mouth demolished, casing removed to a depth of 4 meters. Relief deformed: swelling and failures.

##	# of well/ facility	Description
21	**127** (235)	"Warfare" borehole, mouth demolished, casing pulled out
22	**128**	"Warfare" borehole, bordered and backfilled, no head, out of the ground barely seen the edge of the hole with a concreted metal casing
23	**129** (214)	"Warfare" borehole, the scheme doesn't have such an object, there is well 214, but still labelled as 129. Mouth demolished, casing cut to a depth of 6 m
24	**130**	"Warfare" borehole, mouth demolished, casing cut at a depth of 5 m
25	**131**	Well site is elevated as a hill in a radius of 100-150 m, elevation - 1.5-2.5 m. In south is a dip 40 meters from the wellhead.
26	**132**	"Warfare" borehole, mouth demolished, casing removed to a depth of 6 m
27	**133**	Slight wavelike terrain around the wellhead. On the west side is a depression of about 0.5 meters deep and 80 meters long.
28	**215**	"Warfare" borehole, mouth demolished, the inner casing pulled out. Swelling and minor gaps. The well site is elevated as a hill within 100 m, 1.5-2.0 m up
29	**1003**	Emplacement object, 150 m ø crater, pile height - about 10 m, coordinates were taken in the northern part of the crater on the edge.
30	**2613**	"Warfare" borehole, mouth demolished, casing removed to a depth of 5 meters. In north are wavy swelling of relief
31	**2691**	"Warfare" borehole, mouth demolished, casing cut to a depth
32	**2803**	"Warfare" borehole, mouth demolished, casing removed to a depth of 8 m. Low rise - 2.5 m in radius of 100-120 m. Around the wellhead are swelling and gaps in the earth's surface within 150 meter radius.
Wells not specified in catalogue [5]		
33	26/1	2 m diameter crater, H~1.5 m, 30 m east of well 26
34	26/2	1.5–2 m diameter crater, 20 m east of well 26
35	61	"Warfare" borehole, mouth demolished, casing cut at a depth of 5-6 m
36	283	"Warfare" borehole, mouth demolished, casing cut
37	213	Next to well 130V is a crater with a diameter of 20 m and H ~ 5 m, most likely a blasted well

Analysis of the data in Tables 1 and 5 showed that there is no apparent effect the explosions' magnitude on the post-explosion phenomena (wells 125, 105, 133 and 106), and the same can be said about the radiation effects (wells 104, 106, 102, 109) and charge capacity (102, 105, 106). Thus, it follows that the post-explosion phenomena in the mouth areas of the wells at "Sary-Uzen" site depend on the characteristics of the geological and tectonic structure of the explosions site epicentres.

The visual inspection revealed that almost at all the wells the mouths had been excavated (excavations depth is up to 3–6 m), only mouth of the well 128 was banked up and partially excavated (Figure 6). It has been established that subsidence craters were formed at 4 wells of "Sary-Uzen" site: 1003, 101, 104 and 125. At some objects we found series of wells with large diameters (111, 107, 103, 110 and 104).

a) b) c)

Figure 6. Examples of current status of the wells: a – well 128 (bordered, partial excavation); b – well 106 (excavation to a depth of 5-6 m); c – well 283 (not in the published catalogues)

Figure 7 shows pictures of craters at the wells' mouth areas caused by the UNE.

a) well 104

b) well 1003

c) well 101

d) well 125

Figure 7. Photographs of the well mouth areas, a) well 104; b) well 1003; c) well 101; d) well 125

As to the post-explosion phenomena, it can be noted (see Table 1) that after testing a nuclear device, the man-triggered phenomena are displayed as ground distending (wells 108, 110, 2613, as failures (105, 131, 133), subsidence craters (104, 125), with both distending and failures (104, 109, 126, 215, 2803).

At some wells the absolute elevations remained unchanged or insignificant (102, 106, 127, 128, 129, 130 and 132).

After unauthorized collections of scrap metal at STS only concrete seals of the wells and 10 meter deep pits were left from the majority of the wells: this fact greatly complicates the identification of "warfare" boreholes.

3.2. Findings of topographic operations

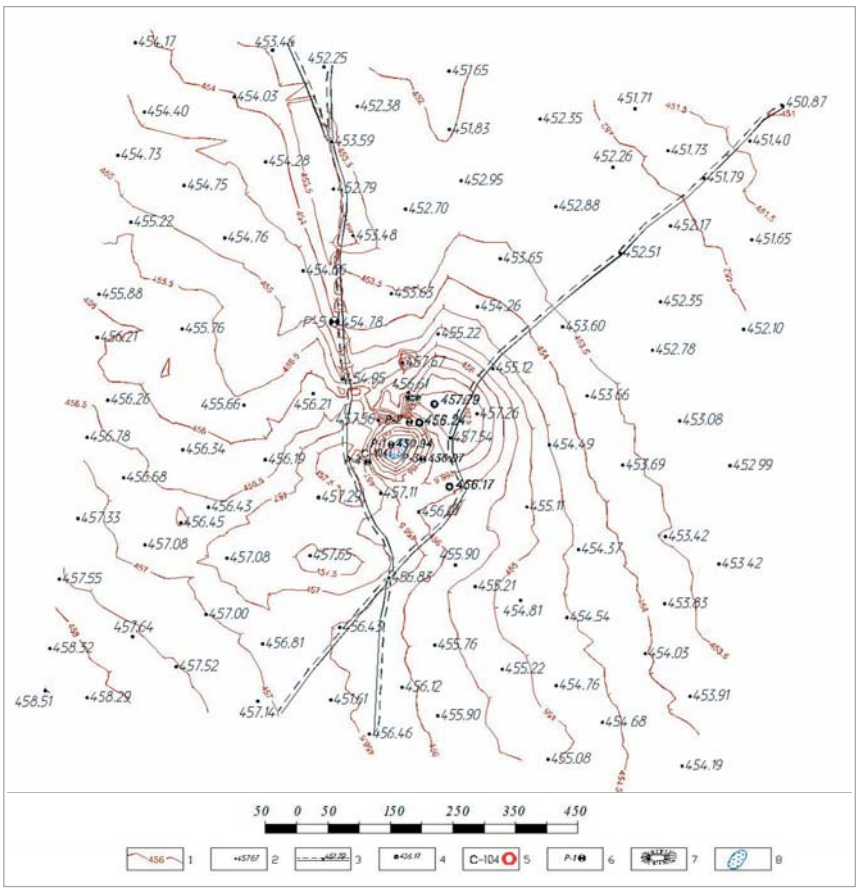

1 – terrain contour, m; 2 – elevation figure and its value, m; 3 – road;
4 – well with unknown number (digit – actual elevation); 5 – "warfare" borehole and its number;
6 – bench mark and its number; 7 – embankment; 8 – water level in crater

Figure 8. Well 104. Tacheometry survey in mouth area
(conventional map copy with a scale of 1:2000)

The topographic operations on the wellhead site of the well 104 have shown (Figure 8) that the relief there is flat terrain with a gently sloping relief from the southwest to the northeast. Absolute elevations vary from 458.5 meters in the south-west up to 450.9 m in the north-east. The area has a slight elevations and gentle degradations. Fluctuations in absolute elevations range within 1-7.6 m. In the center is an elliptical crater 103 m in diameter, 5.3 m deep. The major axis of the crater is from southwest to northeast. At 85 meters north of the crater's center is a mound caused by technological activities: its size is 12x23.5 m and 1.4 m high and filled with water.

The field operations at the well 104 identified relief deformations which then were attributed to the effects of anthropogenic impacts.

3.3. Findings of gas surveys in "warfare" boreholes

The primary survey of the gaseous mixture (Table 6) at the mouth areas of the wells determined the gas concentrations in atmospheric and soil air.

Table 6.

Findings of gases surveys in the "warfare" boreholes

Well #	Sam-pling object	Carbon dioxide, %	Carbon oxide (II), %	Hydrogen sulphide, %	Methane, %	Sulphur dioxide, %
101	atm. air	0.005±0.001	below detection	below detection	below detection	below detection
	soil air	0.0060±0.0012	below detection	below detection	below detection	below detection
102	atm. air	0.010±0.002	below detection	below detection	below detection	below detection
	soil air	0.160±0.032	below detection	below detection	0.20±0.04	below detection
103	atm. air	0.005±0.001	below detection	below detection	below detection	below detection
	soil air	0.0170±0.0034	below detection	below detection	0.20±0.04	below detection
104	atm. air	0.005±0.001	below detection	below detection	below detection	below detection
	soil air	0.0480±0.0096	below detection	below detection	0.15±0.03	below detection
105	atm. air	0.0030±0.0006	below detection	below detection	below detection	below detection
	soil air	0.0030±0.0006	below detection	below detection	below detection	below detection
106	atm. air	0.0020±0.0004	below detection	below detection	below detection	below detection
	soil air	0.0030±0.0006	below detection	below detection	below detection	below detection
107	atm. air	0.0030±0.0006	below detection	below detection	below detection	below detection
	soil air	0.005±0.001	below detection	below detection	0.10±0.02	below detection
108	atm. air	0.0030±0.0006	below detection	below detection	below detection	below detection
	soil air	0.005±0.001	below detection	below detection	below detection	below detection
109	atm. air	0.005±0.001	below detection	below detection	below detection	below detection
	soil air	0.0060±0.0012	below detection	below detection	0.20±0.04	below detection
110	atm. air	0.0070±0.0014	below detection	below detection	below detection	below detection
	soil air	0.180±0.036	below detection	below detection	0.15±0.03	below detection
111	atm. air	0.0020±0.0004	below detection	below detection	below detection	below detection
	soil air	0.0130±0.0026	below detection	below detection	0.10±0.02	below detection
125	atm. air	0.0060±0.0012	below detection	below detection	below detection	below detection
	soil air	0.170±0.034	below detection	below detection	below detection	$1{,}0*10^{-4}\pm2*10^{-5}$

Well #	Sampling object	Carbon dioxide, %	Carbon oxide (II), %	Hydrogen sulphide, %	Methane, %	Sulphur dioxide, %
126	atm. air	0.010±0.002	below detection	below detection	below detection	below detection
	soil air	0.0480±0.0096	below detection	below detection	0.20±0.04	below detection
127	atm. air	0.0030±0.0006	below detection	below detection	below detection	below detection
	soil air	0.0060±0.0012	below detection	below detection	0.10±0.02	below detection
128	atm. air	0.005±0.001	below detection	below detection	below detection	below detection
	soil air	0.0060±0.0012	below detection	below detection	0.10±0.02	below detection
129	atm. air	0.0040±0.0008	below detection	below detection	below detection	below detection
	soil air	0.0060±0.0012	below detection	below detection	0.20±0.04	below detection
130	atm. air	0.0040±0.0008	below detection	below detection	below detection	below detection
	soil air	0.0140±0.0028	below detection	below detection	below detection	below detection
131	atm. air	0.0060±0.0012	below detection	below detection	below detection	below detection
	soil air	0.160±0.032	below detection	below detection	below detection	below detection
132	atm. air	0.0040±0.0008	below detection	below detection	below detection	below detection
	soil air	0.0060±0.0012	below detection	below detection	below detection	below detection
133	atm. air	0.10±0.02	below detection	below detection	below detection	below detection
	soil air	0.10±0.02	below detection	below detection	0.30±0.06	below detection
215	atm. air	0.0030±0.0006	below detection	below detection	below detection	below detection
	soil air	0.0060±0.0012	below detection	below detection	0.20±0.04	below detection
1003	atm. air	0.0030±0.0006	below detection	below detection	below detection	below detection
	soil air	0.0030±0.0006	below detection	below detection	0.10±0.02	below detection
2613	atm. air	0.0020±0.0004	below detection	below detection	below detection	below detection
	soil air	0.0360±0.0072	below detection	below detection	below detection	below detection
2691	atm. air	0.0030±0.0006	below detection	below detection	below detection	below detection
	soil air	0.005±0.001	below detection	below detection	below detection	below detection
2803	atm. air	0.005±0.001	below detection	below detection	below detection	below detection
	soil air	0.0460±0.0092	below detection	below detection	0.15±0.03	below detection
"Novaya" site	atm. air	0.0020±0.0004	below detection	below detection	below detection	below detection
	soil air	0.0020±0.0004	below detection	below detection	below detection	below detection
Control points	soil air	0.0035±0.0015	below detection	below detection	below detection	below detection
Background	atm. air	0.03 [16]	10^{-5} [16]	10^{-5} [16]	10^{-5} [16]	10^{-5} [16]
	soil air	0.03-0.883 [17]	$(1 \div 8) \cdot 10^{-6}$ [16]	$2 \cdot 10^{-7}$ [16]	$(1 \div 8) \cdot 10^{-7}$ [16]	$3 \cdot 10^{-7}$ [16]

According to the data given in the table, the concentration of carbon dioxide in soil air at the well mouth areas exceeds those at the control points. In the air near the well 133 the concentration of carbon dioxide was 0.1%, which is significantly higher than at other wells. The average background concentration of carbon dioxide in the atmosphere is 0.03%.

The soil air of the wells 102, 103, 104, 107, 109, 110, 111, 127, 128, 129, 133, 215, 1003, 2613 and 2803 had methane with concentrations from 0.1 up to 0.3%. No methane was in the soil air of the control sites. The average background is $(1 \div 8) \cdot 10^{-7}$ % [12].

Also, the well 125 needs to be noted: there we revealed sulphur dioxide with a concentration of $1.0 \cdot 10^{-4}$ % in the soil air. In the control points, the sulphur dioxide concentration is below the detection limit. The average background values are 1000 less than at the well 125.

In the soil air of "Sary-Uzen" site we identified methane, sulphur dioxide and high concentrations of carbon dioxide in soil air of the wells 102, 104, 107, 109, 110. 111, 125, 126, 127, 128, 129, 130, 131, 133, 215, 1003, 2613 and 2803; it indicates the presence of underground sources of gas, and probably a combustion of carbonaceous rocks.

Another interest is the well 103. Elevated concentrations of methane and carbon dioxide were identified in the soil air at the mouth area. There is no evidence about underground nuclear tests were carried out in this well. Nevertheless, it might be chemical tests which caused destruction of rocks and high temperature. The geological structure and hydrogeological conditions at "Sary-Uzen" site, as mentioned above, contribute to underground combustion processes to emerge, not depending on whether it was a high power nuclear or chemical explosion.

The reconnaissance surveys of soil air at "Sary-Uzen" site can be compared with similar studies conducted in 2008 at "Balapan" site. At "Sary-Uzen" site no hydrocarbons, carbon monoxide (II), hydrogen and hydrogen sulphide in the soil air were detected. While at "Balapan" site there are 14 wells with elevated concentrations of carbon monoxide (II), in the range of concentrations from 0.01 to 0.003%. On the whole, the number of types of gases detected in the soil air at "Balapan" site is more. However, at "Sary-Uzen" site methane concentration is significantly higher than at "Balapan" site. The average depth of the charge at "Sary-Uzen" site is 250 m, and at "Balapan" site – about 500 m. It is quite possible that the regions with gasification are located closer to the surface at "Sary-Uzen" site that can affect the magnitude of the concentrations and amount of gas types coming to the surface.

Table 7.

Comparison of gas surveying results.
Table shows quantity of wells with concentrations in a given range

Concentration, %	"Balapan" site					"Sary-Uzen" site				
	H_2	CH_4	CO	SO_2	H_2S	H_2	CH_4	CO	SO_2	H_2S
0.2-0.4							6			
0.1-0.2							8			
0.02-0.1					1					
0.01-0.02	1		1							
0.003-0.01			2	1						
0.0001-0.003	10	7	11	8	1				1	
below detectable level	95	99	92	97	104	24	10	0	23	0
Wells with elevated reference value	**11**	**7**	**14**	**9**	**2**	**0**	**14**	**0**	**1**	**0**

It should also be noted that the dynamics of gases in soil air depends on the type of soil, its physical and biological properties, chemical composition, season, weather condi-

tions, as well as land use. The dynamics of gases in the soil is greatly subject to seasonal fluctuations, since the change of seasons is accompanied by sharp changes in temperature and humidity [17].

Thus, the concentrations of gases in soil air may vary significantly being influenced by environmental factors. This is reinforced by the gas monitoring carried out at "Balapan" site. In 2010 at "Balapan" site methane concentrations were recorded within the range from 0.07 to 1.97% [3]. This implies that repeated measurements for each well are needed to enumerate the wells with gas emissions, as well as obtain data on the extent of gas release.

CONCLUSION

The reconnaissance surveys provided more accurate positions and coordinates of the "warfare" boreholes at "Sary-Uzen" site as well as identified a number of other sites with evidence of testing. A brief description was done for the wells, and the facts of subsidence were detected at the wells 101, 104, 108, 109, 110, 111, 125, 126, 131, 133, 215, 1003, 2613 and 2803.

The survey of gases at "Sary-Uzen" site [3] shows that in the soil air of the wells 102, 104, 110, 111, 125, 126, 130. 131, 133 and 2803 concentrations of carbon dioxide is higher than at the control points, there is methane in soil air of 14 wells (102, 104, 107, 109, 110, 111, 127, 128, 129, 133, 215, 1003, 2613 and 2803), and well 125 – sulphur dioxide. These wells should be classified as "gas emitting". However, according to previous studies [2] at certain times no emissions are observed at "gas emitting" wells, or it is very weak, and this event might coincide with period of sampling of soil air; so, it is necessary to re-survey all "warfare" boreholes at "Sary-Uzen" site to reveal, perhaps, more "gas emitting" wells and, possibly, high concentrations in all the wells.

No nuclear test was performed in the well 103, but here in the soil air there are elevated concentrations of methane and carbon dioxide. Presumably there were chemical explosions carried out, or there took place gas proliferation due to underground gasification processes from the "warfare" borehole 102 located 950 meters to the northwest, where high concentrations of methane and carbon dioxide were recorded.

The primary survey findings showed higher levels of gas emissions at the site as a whole, compared to the "warfare" boreholes at "Balapan" site; it can be directly related to the depth of the charge, which is on average 250 meters less at "Sary-Uzen" site than at "Balapan" site. But the previous studies [2] showed that concentration of gases in soil air can considerably vary. Thus, the available data are not sufficient to make a final conclusion.

Since the gasification is accompanied by heat release [2], to evaluate the thermal parameters of this process, it is advisable to study the temperature gradient in the flow of groundwater in areas of potential gasification sources.

Thus, it has been established that at "Sary-Uzen" site catastrophic events may happen in the epicentral zones of the "warfare" boreholes, since the burning of rock in the underground destructions results in formation of weakened zones and underground cavities. Such phenomena are the main danger for businesses engaged in economic activities in the vicinity of "Sary-Uzen" site. It should also be borne in mind that there are comprehensive studies in the vicinity of "Sary-Uzen" site in order to transfer a part of the STS territory for economic

use. Under these conditions, to fully assess the safety of the areas to be transferred, it is needed to carry out a detailed study to forecast the possible consequences associated with the gasification of underground rock. Modelling of gasification processes and forecasting possible scenarios for geological destructions of environment need reliable data about presence and dynamics of post-explosion geodynamic phenomena in the blocks of rock surrounding the central zone of UNE. These data will form the basis for development of measures to restrict access of vehicles and people into dangerous areas, as well as recommendations for the management of economic activities in the vicinity of "Sary-Uzen" site.

REFERENCES

1. Safety assurance at former Semipalatinsk Nuclear Test Site. Republican budgetary program 011 "Ensuring Radiation Safety": A Report on R&D (informational) under the contract #17-2009 of 26.06.2009. / IRSE NNC RK; headed by S. N. Lukashenko – Kurchatov: IRSE NNC, 2009. – P. 164. [in Russian]
   Обеспечение Безопасности Бывшего Семипалатинского Испытательного Полигона Республиканская Бюджетная программа 011 "Обеспечение радиационной безопасности" : отчет о НИР (информационный) по договору № 17-2009 от 26.06.2009г. /ИРБЭ НЯЦ РК; рук. Лукашенко С.Н. – Курчатов: ИРБЭ НЯЦ РК, 2009. -164 с.
2. S. B. Subbotin. Assessment of possibilities for catastrophic events at Balapan site / S. B. Subbotin, S. N. Lukashenko // Topical Issues in Radioecology of Kazakhstan [Proceedings of the Institute of Radiation Safety and Ecology for 2007-2009]. – Issue 2. – Pavlodar: "Dom Pechati LLP" printing house, 2010 – P.401-448]. [in Russian]
   Субботин С.Б. Оценка возможностей протекания процессов катастрофического характера на площадке "Балапан"/ Субботин С.Б., Лукашенко С.Н. // Актуальные вопросы радиоэкологии Казахстана [Сборник трудов Института радиационной безопасности и экологии за 2007 – 2009гг.]. – Вып. 2. – Павлодар: Дом печати, 2010. – С. 401-448. : ил. - Библиогр.: с. 54. - ISBN 978-601-7112-32-5.
3. Safety assurance at the former Semipalatinsk Nuclear Test Site. Republican Budgetary Program 038 "Radiation Safety Assurance": R&D Report (informational) under the contract #4-20103 of 19.02.2010./IRSE NNC RK; headed by S. N. Lukashenko – Kurchatov: IRSE NNC, 2010. – P. 128. [in Russian]
   Обеспечение Безопасности Бывшего Семипалатинского Испытательного Полигона Республиканская Бюджетная программа 038 "Обеспечение радиационной безопасности" : отчет о НИР (информационный) по договору № 4-20103 от 19.02.2010 /ИРБЭ НЯЦ РК; рук. Лукашенко С.Н. – Курчатов: ИРБЭ НЯЦ РК, 2010. -128с.
4. Nuclear testing in the USSR [Objectives. Characteristics. Organization of nuclear testing. The first nuclear tests] / I.A. Andryushin, V. V. Bogdan, S. A. Zelentsov. - Vol.1. - Sarov: RFNC-VNIIEF. [in Russian]

Ядерные испытания в СССР [Цели. Общие характеристики. Организация ядерных испытаний. Первые ядерные исытания] / состав ред. И.А. Андрюшин, В.В. Богдан, С.А. Зеленцев. - Т.1. – Саров: РФЯЦ – ВНИИЭФ.

5. V.S. Bocharov Characteristics of 96 underground nuclear explosions at the Semipalatinsk Test Site / V.S. Bocharov, S.A. Zelentsov, V.N. Mikhailov // Atomic Energy. - 1989. - V. 67. – Iss. 3. - pp. 210 - 214. [in Russian]
   Бочаров В.С. Характеристики 96 подземных ядерных взрывов на Семипалатинском испытательном полигоне / В.С. Бочаров, С.А. Зеленцов, В.Н. Михайлов // Атомная энергии. – 1989. - Т. 67. - Вып. 3. - С. 210 – 214.
6. Semipalatinsk Test Site / V.A. Logachev. - Moscow, 1997. - p. 344. [in Russian]
   Семипалатинский полигон / под ред. В.А. Логачёва. – Москва, 1997. – 344 с.
7. Yu. A. Izrael. Peaceful nuclear explosions and the environment / Yuriy Izrael. - Leningrad: Gidrometeoizdat, 1974. - P. 136. [in Russian]
   Израэль Ю. А. Мирные ядерные взрывы и окружающая среда / Ю. А. Израэль. - Л.: Гидрометеоиздат, 1974. – С. 136 с.
8. B.I. Nifontov. Underground nuclear explosions / B.I. Nifontov [et al]. - Moscow: Atomizdat, 1965. [in Russian]
   Нифонтов Б. И. Подземные ядерные взрывы / Б. И. Нифонтов [и др.]. - М.: Атомиздат, 1965.
9. Химические вещества из угля /под ред. И.В. Калечица. – М.: Химия, 1980. [Chemicals from coal / I.V. Kalechitsa. - Moscow: Khimiya, 1980.] – in Russian
10. Safety assurance at former Semipalatinsk Nuclear Test Site. Republican budgetary program 011 "Radiation Safety Assurance at former Semipalatinsk Nuclear Test Site": R&D Report (informational) / IGR NNC RK; headed by N. N. Belyashova – Kurchatov: IRSE NNC, 2007. [in Russian]
    Обеспечение Безопасности Бывшего Семипалатинского Испытательного Полигона Республиканская Бюджетная программа 011 "Обеспечение радиационной безопасности бывшего Семипалатинского испытательного полигона " : отчет о НИР (информационный) /ИГИ НЯЦ РК; рук. Н.Н. Беляшова. – Курчатов: ИГИ НЯЦ РК, 2007.
11. http://www.sonicbomb.com/.
12. Sensis-200 gas analyzer. Owner's Manual. TU 4215-001-73819788-07. - Moscow, 2008. –p. 15. [in Russian]
13. Газоанализатор Сенсис-200. Руководство по эксплуатации. ТУ 4215-001-73819788-07. - Москва, 2008. -15с.
    Analyzers ANKAT-7664M Manual IBYAL.413411.043 RE. - Smolensk "Analitpribor", 2009. – p. 58. [in Russian]
    Газоанализаторы АНКАТ-7664М Руководство по эксплуатации ИБЯЛ.413411.043 РЭ. – Смоленск: "Аналитприбор", 2009. - 58с.
14. A device for sampling and storage of gas samples: Technical description. - V/O: Mashpribor, 1979. - 4. [in Russian]
    Прибор для отбора и хранения проб газа: Техническое описание. - В/О: Машприбор, 1979. - 4.
15. Safety Assurance at former Semipalatinsk Nuclear Test Site. Republican Budgetary Program 011 "Radiation Safety Assurance at former Semipalatinsk Nuclear

Test Site": R&D Report (informational) / IGR NNC RK; headed by N. N. Belyashova – Kurchatov: IRSE NNC, 2009. – p. 75. [in Russian]
Обеспечение Безопасности Бывшего Семипалатинского Испытательного Полигона Республиканская Бюджетная программа 011 "Обеспечение радиационной безопасности бывшего Семипалатинского испытательного полигона " : отчет о НИР (информационный) /ИГИ НЯЦ РК; рук. Н.Н. Беляшова. – Курчатов: ИГИ НЯЦ РК, 2009. -75с.

16. Handbook of Geochemistry / G.V. Voytkevich, A. V. Kokin, A.E. Miroshnikov, V.G. Prokhorov. - Moscow: Nedra, 1990.- p. 480 p. [in Russian]
Справочник по геохимии /Г.В.Войткевич, А.В. Кокин, А.Е. Мирошников, В.Г. Прохоров. – М.: Недра, 1990.-480 с.: ил.
17. http: //www.zoodrug.ru/topic3531.html

"САРЫ-ӨЗЕН" АЛАҢЫНДАҒЫ ГАЗ ШЫҒУЛАРДЫ РЕКОГНОСЦИРОВОЧНОГО ЗЕРТТЕУ НӘТИЖЕЛЕРІ

[1]Романенко В.В., [1]Лукашенко С.Н., [1]Субботин С.Б., [2]Чернова Л.В.

[1]ҚР ҰЯО Радиациялық қауіпсіздік және экология институты, Курчатов, Қазақстан
[2]ҚР ҰЯО Атом энергиясы институты, Курчатов, Қазақстан

Мақалада тау жыныстарының жерасты газ шығару процестері түрінде байқалған жерасты ядролық жарылыстар (ЖЯЖ), сондай-ақ бұрынғы ССП "Сары-Өзен" сынақ алаңында отырған жағдайлардың зардаптарын зерттеу нәтижелері ұсынылған. Рекогносцировочных жұмыстар "әскери" ұңғымалардың орныннақтылауға сондай-ақ сынақтар тәрітібінің белгілері бар 5 нысанды анықтауға мүмкіндік берді. Жұмыстар барысында ұңғымалардың ағымдағы жағдайлары, сондай-ақ дөмпейіп шығу, ойылу және күндізгі беттің басқа да деформацияланyы түрінде байқалған жарылыстан кейінгі жағдайлардың бар болуы суреттелді. "Сары-Өзен" алаңында барлық ұңғымаларда көмірқышқыл газының диоксидының жоғары шоғырлануы мен 14 ұңғымада метанның жоғары шоғырлануы анықталды. Кейбір ұңғымалардағы метанның шоғырлануы "Балапан" алаңындағыға қарағанда өте жоғары, бұл ЖЯЖ жүргізу кезінде зарядтарды салу тереңдігіне байланысты болуы мүмкін. 103 ұңғымасында ЖЯЖ ПЯВ жүргізілген жоқ, алайда ұңғыманың сағаалды алаңындағы топырақ ауасында метан мен көмірқышқыл газы диоксидының жоғары шоғырлануы тіркелген. Мақалада "Сары-Өзен" алаңыдағы газдану газификация процестерін ары қарай зерттеуге қатысты ұсыныстар келтірледі.

Түйін сөздер: Семей сынақ полигоны, ядролық жарылыстар, "Сары-Өзен", топырақ ауасы, ойылу жағдайлары, топографиялық жұмыстар, геоморфологиялық мониторинг, метан, жерасты газдану, газ шығу.

РЕЗУЛЬТАТЫ РЕКОГНОСЦИРОВОЧНОГО ИССЛЕДОВАНИЯ ГАЗОВЫДЕЛЕНИЙ У ПЛОЩАДКИ "САРЫ-УЗЕНЬ"

[1]Романенко В.В., [1]Лукашенко С.Н., [1]Субботин С.Б., [2]Чернова Л.В.

[1]Институт Радиационной Безопасности и Экологии НЯЦ РК, Курчатов, Казахстан
[2]Институт Атомной Энергии НЯЦ РК, Курчатов, Казахстан

В статье представлены результаты исследования последствий подземных ядерных взрывов (ПЯВ), проявленных в виде процессов подземной газификации горных пород, а также просадочных явлений на испытательной площадке "Сары-Узень" бывшего СИП. Рекогносцировочные работы позволили уточнить местонахождение "боевых" скважин, а также выявить 5 объектов с признаками проведения испытаний. В ходе работ проведено описание текущего состояния скважин, а также наличия поствзрывных явлений, которые проявлены в виде вспучиваний, провалов и других деформаций дневной поверхности. На площадке "Сары-Узень" на всех скважинах выявлены повышенные концентрации диоксида углерода и на 14 скважинах повышенные концентрации метана. Установлено, что на некоторых скважинах концентрация метана существенно больше, чем на площадке "Балапан", что возможно связано с глубиной заложения зарядов при проведении ПЯВ. На скважине 103 ПЯВ не проводились, однако в почвенном воздухе на приустьевой площадке скважины зафиксированы повышенные концентрации метана и диоксида углерода. В статье приводятся рекомендации относительно дальнейшего изучения процессов газификации на площадке "Сары-Узень".

Ключевые слова: Семипалатинский испытательный полигон, ядерные испытания, "Сары-Узень", почвенный воздух, провальные явления, топографические работы, геоморфологический мониторинг, метан, подземная газификация, газовыделение.

УДК 622.278: 577.4:504.064

INVESTIGATION OF THE GAS PRESENCE AT "BALAPAN" SITE

[1] Romanenko V.V., [1] Subbotin S.B., [1] Lukashenko S.N., [2] Chernova L.V.

[1]Institute of Radiation Safety and Ecology NNC RK;
[2]Institute of Atomic Energy NNC RK

The paper presents the 2010 investigation results on gas-bearing processes in the epicentral zones of the underground nuclear explosions (UNEs) at "Balapan" testing site. Gas monitoring results showed that in most cases the nature of the gassing process at the "critical" wells is individual. Concentration of gases at the same point during the observation period can range up to 4 orders of magnitude. It has been found that monitoring the concentration of hydrogen and methane is the most appropriate way for monitoring the wells with gas emissions. It has also been revealed that the monitoring of gases emerging from the annular space impartially reflects the actual processes of gasification – a set of "primary" factors. Areal gas survey found that the boundaries of gas anomalies in the mouth areas for a number of the wells can be revealed at distances over 350 meters. Recommendations are given for further study of gasification processes at UNE venues.

Keywords: Semipalatinsk Test Site, carbon dioxide, methane, hydrogen sulfide, background concentration, underground gasification, gas emission, areal gas surveying, gas-release monitoring, correlation.

INTRODUCTION

Detailed studies of the gasification processes in rocks in the vicinity of "warfare" boreholes were commenced in 2007. The previous studies showed that the gasification processes of mountain rocks where we revealed "critical" wells at Balapan site continue and are relatively stable.

Because the gasification processes of mountain rocks at UNE venues in the STS is related to potential catastrophic events, it was necessary to continue research on organization of effective monitoring, as well as forward-looking solutions of the problems related to the assessment of space-time character of their development, depending on the characteristics of structural-tectonic constitution of the array and composition of mountain rocks [1].

The main purpose of monitoring the composition and concentration of gases in the air coming to the surface in areas of "critical" wells in 2010 was to study the dynamics of the concentration of several gases in the soil air.

Another part of the research was aimed at improving the efficiency of gas monitoring. It should be noted that the dynamics of gas release is affected by many factors, but they can be conditionally divided into two groups. First, the gases are generated at depths as a result of chemical processes that determine the gas composition and its concentration. Such processes are conventionally attributed to the "primary" factor that originally shapes the character of gassing. The resulting flows of gases through the gas permeable zones pass through the rock layer, and then penetrate into the soil air. Physico-chemical properties of the mountain rocks, one way or another, affect the rate and composition of gas flows, and climatic factors have an impact on the gases that have already penetrated into the soil air. This complex effect can

be named "secondary" factor. This implies that improving the efficiency of gas monitoring involves design, using gas monitoring methods, at which the effect of the "secondary" factors distorting the dynamics of gassing is maximally low.

The previous works revealed that the well 1010 still has a head through which gas flows out. The gases, being generated in deep, pass through the annulus, virtually bypassing the cover of rock, including unconsolidated deposits. Thus, this flow of gas almost is not affected by the "secondary" factor described above, and the parameters of the flow more closely reflect the processes occurring at depth. Monitoring of the concentration and composition of gases being released from the well head provides data on the dynamics of gas emission with a much smaller influence of the "secondary" factor.

In the course of the research, it was decided to take samples of soil air at each site near the well in two points at once for getting information about the efficiency of gas monitoring. In the event of detection of a similar nature between such gas release points for same well, we my judge about insignificant impact of the "secondary" factor on the release of gases and, consequently, reduce the number of sampling points for monitoring up to one on each well.

As mentioned above, the gases are generated at depth. Gas generation centres is the "primary" factor which generates gas flows within a certain area. The rock mass (through which the gases pass) cannot be uniform and has a different permeability. Consequently, the passage of gases to the surface is accompanied by scattering of and changes in the original flow area. In order to determine the location of gassing zones in the estuarine areas of critical wells it is needed to carry out an areal gas survey. The research results provide data on the prevalence of gassing areas and find out the location features of the gas emanation zones.

1. EXPERIMENT

To assess the dynamics of gases in soil air, as well as to assess the impact from "secondary" factors on the gassing process, studies were carried out on samples of soil air at estuarine areas of the "critical" wells 1010, 1355, 1053, 1317, 1236, 1315, "Glubokaya" and 1361. At each well, the sampling of soil air was carried out monthly between May and September at two points. A well head was used as the second sampling point at the well 1010.

To study the nature of areal distribution of the gas concentrations a one-time sampling of soil air on a grid 500 by 500 meters was carried out in the estuarine areas of the "warfare" boreholes 1317, 1315, 1053, "Glubokaya", 1236, 1361 and 1355. The samples taken were analyzed for the methane and carbon dioxide. These gases were chosen as the most common based on the monitoring data [1].

1.1. Gas monitoring

Storage vessels (10 litre plastic cans equipped with nozzles for air sampling) are used for sampling the soil air, installed at two points (at the well 1010 one of the points is directly in the well head). The distance between the points is about 3 meters. When choosing a point for installation of a sampling vessel, the priorities were the places not more 6 m from the wellhead with faulting of relief of the technogenic origin (cracks, collapsed craters, etc.). Initially, the set location of sampling points did not change during the monitoring. Tightness is achieved by embedding the vessel 5-7 cm deep and compaction of soil adjacent to its walls. Duration of the sampling with a vessel was not less than one day. At the end of the day the

gas mixture was sampled from the vessel using a tool for sampling and storage of gas samples. Duration of storage vessel installation is chosen according to the method described in [1]. We used glass aspirators for transportation and storage of soil air samples. The operation principle of this device is based on the gas displacement by water using levelling bottle [3]. The taken samples were analyzed to determine the concentrations of the following gases: hydrogen, methane, carbon monoxide, sulphur dioxide, hydrogen sulphide, carbon dioxide, amount of hydrocarbons [4].

To obtain background values of gas concentrations in the soil air, similar sampling was performed at reference points far away from the estuarine areas (at least 500 meters). The sampling and analysis was carried out analogously to the method described above.

To assess the gas situation we measured gas concentrations in atmospheric air at the locations of "warfare" boreholes by a gas analyzer at about 2 meters above the surface.

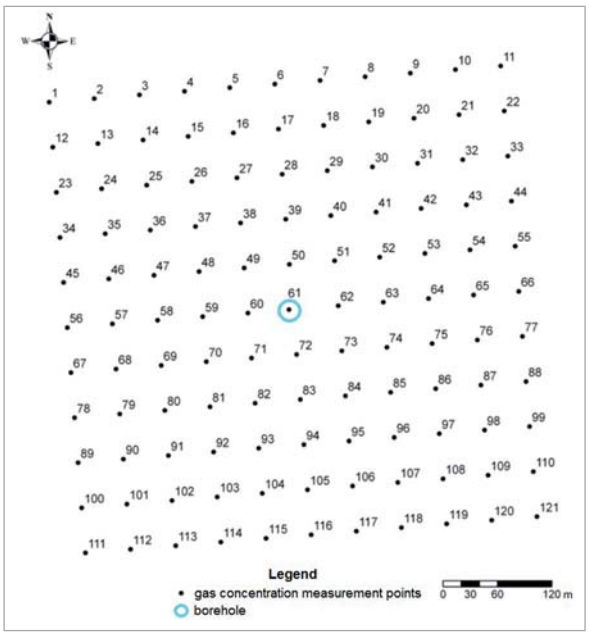

Figure 1. Gas sampling layout

The monitoring was carried out from May 11 to September 8. Total, sampling 5 stages were completed, with each lasting about 2 weeks. Key dates for counting the time between the sampling stages were the date in the middle of each stage. For example, the duration of monitoring is defined by counting the days between the date in the middle of the first stage of monitoring and the date in the middle of the last stage. Thus, the monitoring lasted 114 days.

1.2. Areal gas surveying

To clarify the characteristics of gas ingress from the rock slabs to the surface, soil air was sampled at the estuarine areas of the wells in a grid with increments of 50 meters. The area covered by the gas surveying at each well was 500*500 m (Figure 1). Sampling

of soil gas was also performed using the 10 l storage vessels; accumulation lasted for at least a day. The samples were measured for concentration of methane (CH_4) and carbon dioxide (CO_2). Total, sampling at each well lasted from 6 to 10 days (20-12 points per day).

2. RESULTS

2.1. Gas monitoring

We got data on the dynamics of gas release at the "critical" wells, as well as background levels of gas concentrations in the reference points for data assessment.

2.1.1. Background level

Based on the results of gas measurements at the reference points there were obtained background levels of gas concentrations (Table 1). The control points were located at distances ranging from 0.5 to 37.5 km from the "warfare" boreholes. In the range of 0.5 to 0.24 km the carbon dioxide concentration in the soil air is independent of the distance and is 0.0033 mol/m^3. The concentrations of hydrogen, methane, carbon monoxide, hydrogen sulphide and sulphur dioxide at these points are below the detectable levels.

At points located at a distance of 37.5 km from the "warfare" boreholes the concentration of carbon dioxide was below 0.0012 mol/m^3; average hydrogen concentration comprised 0.018 mol/m^3. The concentrations of methane, carbon monoxide, hydrogen sulphide and sulphur dioxide at these points are below the detectable values. Since at a distance of about 40 km from the nearest warfare well, the gasification of rocks cannot occur caused by the UNEs, as the background concentration of carbon dioxide in soil air we chose 0.0012 mol/m^3 and for hydrogen - 0.018 mol/m^3.

Table 1.

Background gas concentration obtained at the reference points, mol/m^3

Ref. point #	Background gas concentrations						# of the nearest "warfare" borehole	Distance to the nearest "warfare" borehole, km
	CO_2	H_2	CH_4	CO	H_2S	SO_2		
1	0.0020	b/d	b/d	b/d	b/d	b/d	1312	0.5
2	0.0036	b/d	b/d	b/d	b/d	b/d	1222	0.6
3	0.0032	b/d	b/d	b/d	b/d	b/d	1222	0.6
4	0.0036	b/d	b/d	b/d	b/d	b/d	1066	0.7
5	0.0036	b/d	b/d	b/d	b/d	b/d	1066	0.7
6	0.0040	b/d	b/d	b/d	b/d	b/d	1061	0.8
7	0.0040	b/d	b/d	b/d	b/d	b/d	1061	0.8
8	0.0020	b/d	b/d	b/d	b/d	b/d	1053	0.8
9	0.0044	b/d	b/d	b/d	b/d	b/d	1206	0.9
10	0.0036	b/d	b/d	b/d	b/d	b/d	1205	0.9

Ref. point #	Background gas concentrations						# of the nearest "warfare" borehole	Distance to the nearest "warfare" borehole, km
	CO_2	H_2	CH_4	CO	H_2S	SO_2		
11	0.0040	b/d	b/d	b/d	b/d	b/d	1206	0.9
12	0.0032	b/d	b/d	b/d	b/d	b/d	1206	0.9
13	0.0036	b/d	b/d	b/d	b/d	b/d	1314	1.0
14	0.0024	b/d	b/d	b/d	b/d	b/d	1355	1.2
15	0.0020	b/d	b/d	b/d	b/d	b/d	1054	2.4
16	0.0036	b/d	b/d	b/d	b/d	b/d	1054	2.4
17	<0.0012	0.013	b/d	b/d	b/d	b/d	1006	37.5
18	<0.0012	b/d	b/d	b/d	b/d	b/d	1006	37.5
19	<0.0012	0.018	b/d	b/d	b/d	b/d	1006	37.5
20	<0.0012	0.019	b/d	b/d	b/d	b/d	1006	37.5
21	<0.0012	b/d	b/d	b/d	b/d	b/d	1006	37.5
22	<0.0012	b/d	b/d	b/d	b/d	b/d	1006	37.5
23	<0.0012	0.016	b/d	b/d	b/d	b/d	1006	37.5
24	<0.0012	0.023	b/d	b/d	b/d	b/d	1006	37.5
MDC	0.0012	0.00039	0.0079	0.000073	0.0000014	0.0000016		

Note: b/d – below the detectable level
MDC – minimal detectable concentration

2.1.2. Dynamics of the gas concentrations in the soil and atmospheric air

The results of gas monitoring are presented in Figures (Figure 2 a-h, Figure 3). If the gas concentration did not exceed the detectable level, then to display such data in the graphs, the value of the minimal detectable concentration of the instrument was used.

All the wells showed carbon dioxide, hydrogen and methane in the samples of soil air. In the atmospheric air there are detectable concentrations of carbon dioxide and hydrogen.

Carbon dioxide

The carbon dioxide content in the soil air ranged from <0.0012 to 0.4 mol/m^3. The maximal concentration of carbon dioxide in the soil air was found in the well 1236 in June and comprised 0.4 mol/m^3. The dynamics of carbon dioxide concentration in each well varies and no common nature is visible.

In the atmospheric air the carbon dioxide concentration varied in the range from <0.0012 to 0.018 mol/m^3. The maximal value was recorded at the well "Glubokaya" in June. At the wells 1355, 1317, 1236, "Glubokaya", 1361 and 1053 the concentration curve of carbon dioxide in the atmosphere overlaps with its concentration curve in the soil air. The contents of carbon dioxide in the atmospheric air are maximal in May for the majority of the wells. From May to June the concentration drops, with further slight changes. There are no changes from August to September; the concentration of carbon dioxide remains below 0.0012 mol/m^3.

Hydrogen

Concentrations of hydrogen in the soil air were in the range from <0.0004 (detection limit) to 0.58 mol/m^3. The maximal concentration of hydrogen in the soil air was found at the mouth area of the well 1317 in June. From August to September all the wells are characterized by an increase in hydrogen concentration.

Hydrogen concentration in the atmospheric air of the wells under study varies from <0.0004 to 0.045 mol/m^3 during the study period. The maximal value is observed at the well 1355. The concentration of hydrogen in the atmospheric air at the observed wells from May to July was <0.0004 mol/m^3. From July to September, the hydrogen concentration increases to the values from 0.021 to 0.045 mol/m^3.

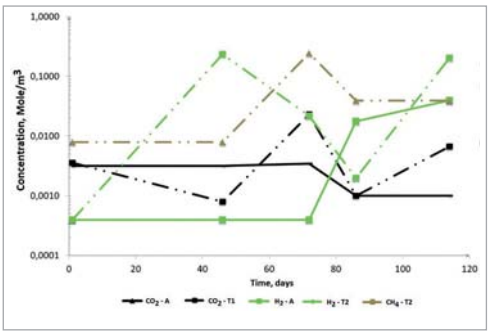

a) 1010

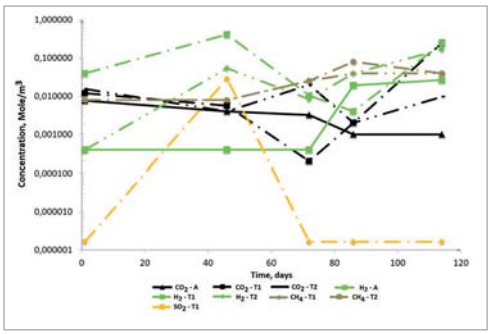

b) 1315

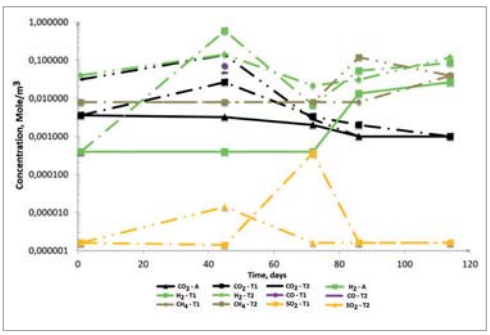

c) 1317

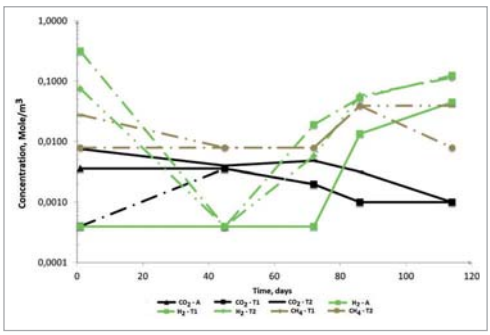

d) 1355

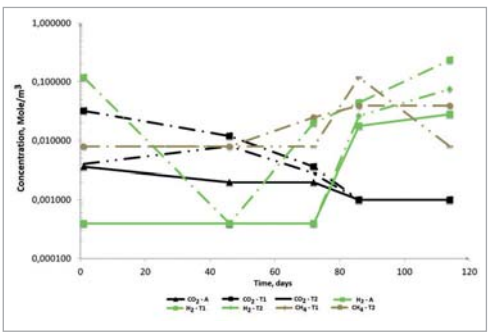

e) 1053

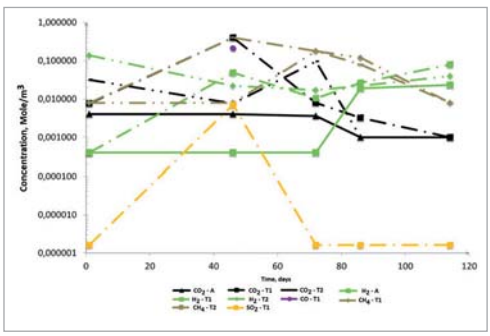

f) 1236

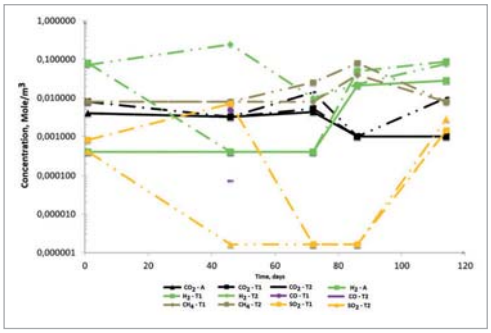

g) 1361

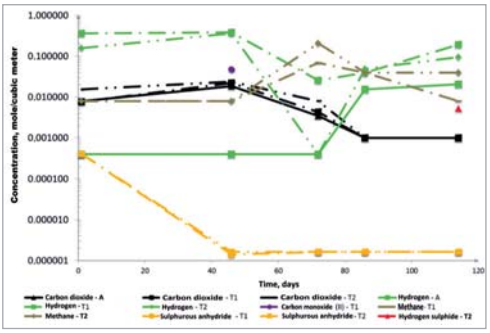

h) "Glubokaya"

Figure 2. Results of gas monitoring (solid line - atmospheric air; dotted with a single point - T1; dotted with two points - T2) a) well 1010; and b) well 1315; c) well 1317; d) well 1355; e) well 1053; e) well 1236;. g) well 1361; and h) well "Glubokaya"

Methane

Methane concentration in the soil air at the observed wells was recorded in the range from <0.0079 (detection limit) to 0.39 mol/m^3. The maximal concentration is observed at the well 1236 in June. In July and August there is an increase in methane concentration in soil air of the wells. For most of the wells the methane concentration in the soil air increases in the second half of the summer in July and August. No significant concentrations of methane in the atmosphere were found.

Carbon monoxide

The carbon monoxide (II) in the soil air is observed in June at the wells "Glubokaya", 1361, 1236 and 1317 in the range from 0.0047 to 0.21 mol/m^3. The maximal concentration of carbon dioxide in the soil air was recorded at the well 1236. No significant concentrations of carbon dioxide in the atmospheric air were detected.

Sulphur dioxide

The sulphur dioxide was recorded in soil air of the wells 1315, 1317, 1236, 1361 and "Glubokaya" in the range from <0.0000016 (detection limit) to 0.028 mol/m^3. Sulphur dioxide appears in the soil air of the wells tested occasionally. From May to June, the concentration increases at the well 1361 and reduces at the well "Glubokaya".

Hydrogen sulphide

Hydrogen sulphide was detected only in rare cases – at the well "Glubokaya" and in the annulus of the well 1010. The concentration of hydrogen sulphide at the well "Glubokaya" was 0.0052 mol/m^3. No significant concentrations of hydrogen sulphide in the atmospheric air were detected.

Hydrocarbons

In general, at each well in the samples of soil gas the hydrocarbons were recorded from time to time (Figure 3). The maximal value was recorded at the well 1315 in June. In May no hydrocarbons were detected. The hydrocarbons appear in June, the maximal release was recorded in August with a concentration of up to 3 mg/m^3. At the wells 1317 and "Glubokaya" the amount of hydrocarbons increases from July to August and decreases from August to September.

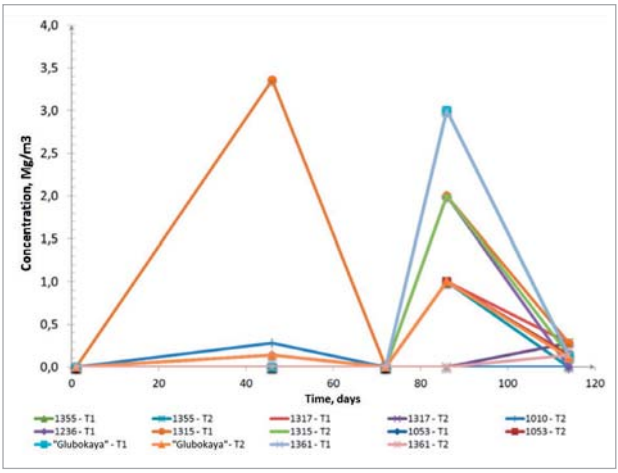

Figure 3. Changes in the concentration of hydrocarbons in the soil air

2.1.3. Study of the gas concentrations dynamics in the well 1010 annulus

The nature of gassing at the mouth of the well 1010 is shown in figure (Figure 4).

From July to August, there is an abrupt increase in methane concentration from 0.6 to 7.1 mol/m^3. The same is observed at the wells 1053, 1361 and 1315. From August to September, the methane concentration in soil air reduces by a value of 6.33 mol/m^3. In the range from 0.001 to 0.011 mol/m^3 there is a change in the concentration of carbon monoxide (II). From May to July, hydrogen was recorded, a change of which correlates with such gases as carbon dioxide and hydrogen sulphide.

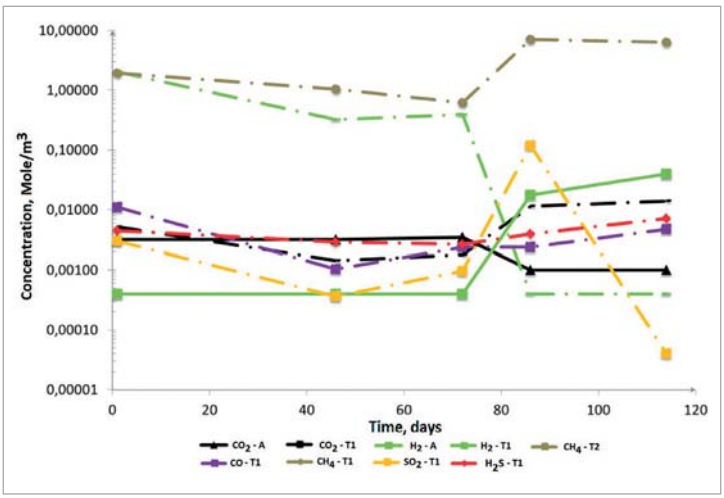

Figure 4. Analysis of gas released from the well head 1010
(solid line – atmospheric air; dash-dotted with a single dot - T1)

The concentration of hydrocarbons varies from $2.9 \cdot 10^3$ to 200 mg/m^3 with a peak in May (Figure 5). From May to June, there is a sharp decrease in concentration by 2,671 mg/m^3. From August to September, the content of hydrocarbons in the soil air is stable at level of 1,100 mg/m^3.

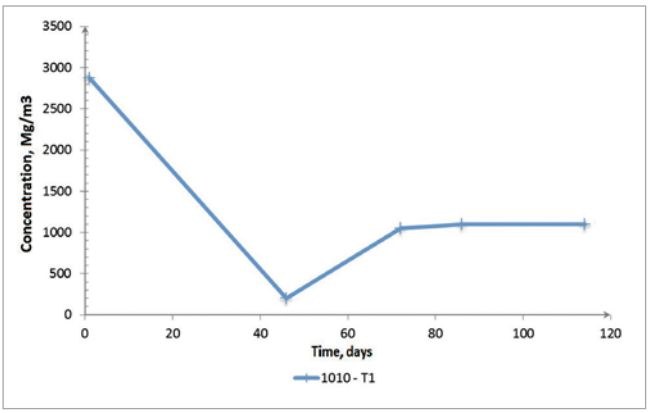

Figure 5. Concentration of hydrocarbons

In general, based on the gas monitoring one may note that the concentration of carbon dioxide, sulphur dioxide and hydrogen in the soil air of the wells varied within three orders of magnitude, methane and carbon monoxide - within two orders of magnitude, and sulphur dioxide - within four. Such a change in concentration is like a salvo emission, at that the dynamics of the gas concentration at the mouth of the well 1010 is more stable. Thus, we can make an assumption about the existence of "gassing" wells in estuarine areas, peculiar intermediate buffer zone in the rock mass where gas accumulates. Presumably, as gas is accumulated in them, pressure grows to a certain threshold above which "discharge" – happens, i.e. release of gas, and this explains the sharp increase/decrease in the concentration of gases in the above charts.

2.2. Areal gas survey

The results of the gas surveys in the estuarine areas of the wells 1355 and "Glubokaya", 1236, 1361 for methane in soil air are shown in Figure 7, for carbon dioxide for the wells 1355. "Glubokaya", 1315 and 1317 - in Figure 7. At wells 1315, 1317 and 1053 no significant concentrations of methane were found at the survey points; at the wells 1236, 1361 and 1053 – no carbon dioxide was found.

Methane

At the estuarine sites of the wells "Glubokaya", 1361 and 1236 section with elevated concentrations of methane were found, the area which in some cases exceed the area of research. It may be noted that the gas-permeable structures are located not only near the mouth of the wells, but at a distance of more than 350 meters, more importantly, the points with maximal concentration of methane, as a rule, are not in close proximity to "warfare" borehole, but at a distance of 200 m. Area of the elevated concentrations at the well "Glubokaya" is 450 x 500 m$^{2.}$ while in the north-eastern part of the site the concentration of methane reaches 0.8%

(Figure 6a). The methane in soil air of wells 1361 and 1236 covers an area of 500x500 m^2. There are a few points with the methane concentration <0.02% (Figure 6. c, d).

At the well 1355, methane was revealed only at 7 points, while the concentration on its north-eastern section was twice as much than at the well "Glubokaya" and comprised 2.0%. Maximal concentrations are observed at the points of T30 and T31 (see Figure 1 and 6b).

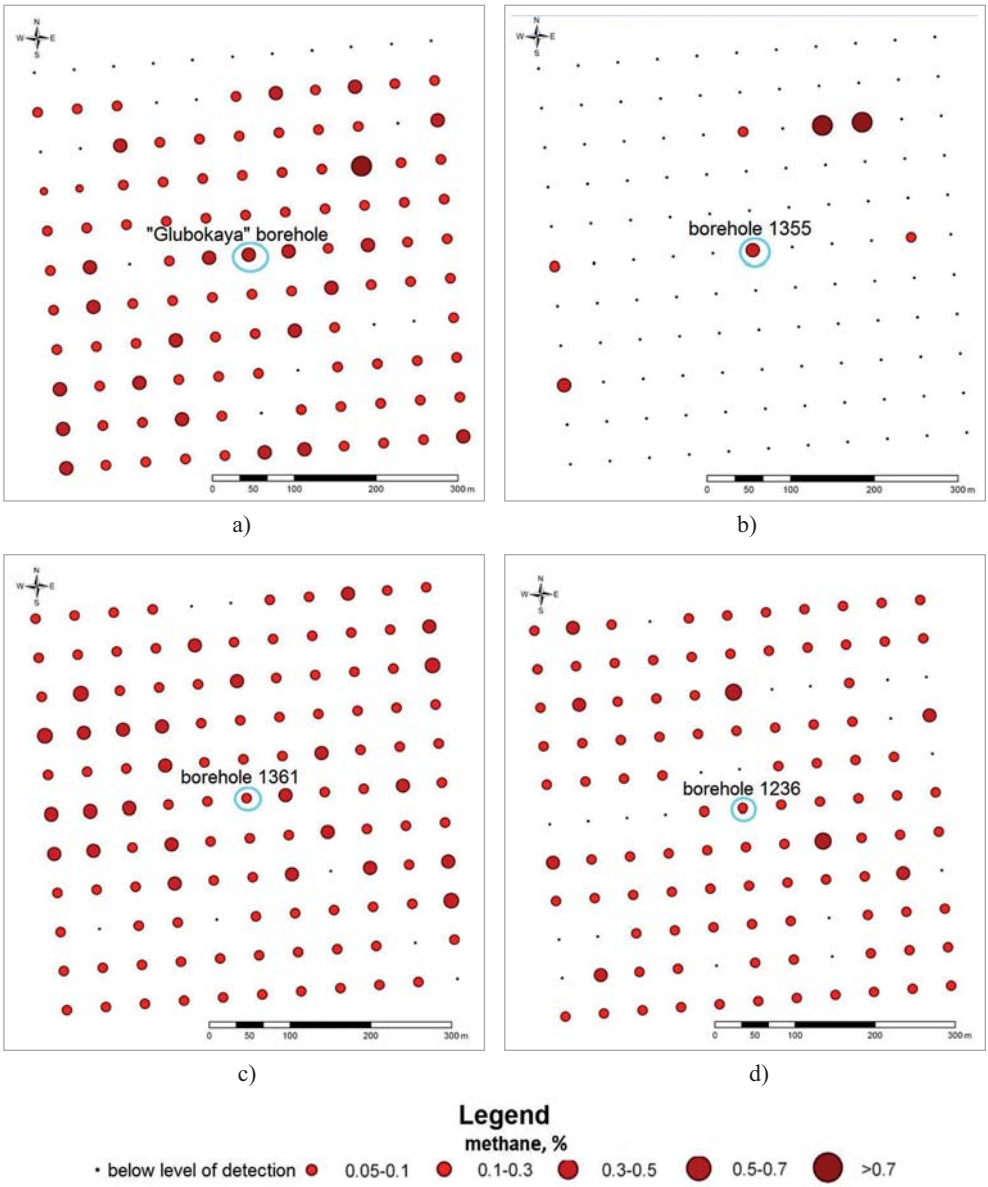

Figure 6. Areal distribution of methane in the wells: a) "Glubokaya"; b) 1355; c) 1361; d) 1236

Carbon dioxide

Of the surveyed wells, zones with relatively high contents of carbon dioxide were found at the sites of the wells 1355 and 1315 (Figure 7). The areas of maximal concentrations cover the northern part of the investigated area with a width of 150-200 meters. Upon that the points with maximal values reaching 0.13% (0.05 mol/m^3) are also located at the extreme profiles of the survey grid.

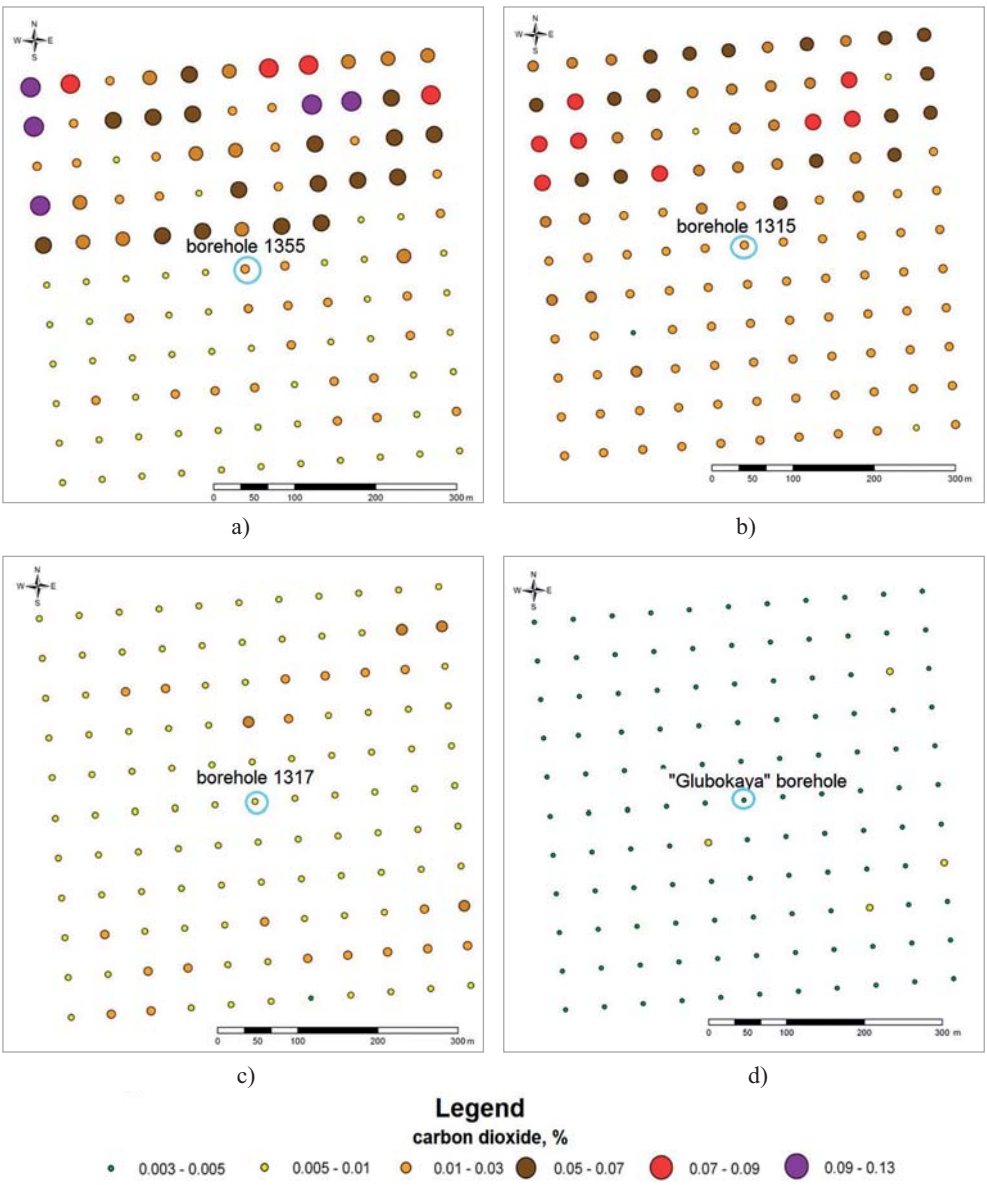

Figure 7. Areal distribution of carbon dioxide in the wells a) 1355; b) 1315; c) 1317; d) "Glubokaya"

At the well "Glubokaya" no areas with a high content of carbon dioxide in the soil air were revealed, but some points had significant concentrations of carbon dioxide in the soil air. The three points located within a radius of about 150 m from the well head (T28, T74 and T58) had concentrations of carbon dioxide in excess of the background value 0.003% (0.0012 mol/m^3).

3. RESULTS AND DISCUSSION

3.1. Gas monitoring

According to the results of gas monitoring, it is possible to say (see Figure 2) that almost all the wells had no significant concentrations for the majority of the determined gases. Even at the well 1010, where we observed the most intense release of gases, only carbon dioxide was detected in the atmosphere, and the ratio of average concentrations in the soil and the air is 1.4 (Table 2). The totality of these facts leads to the conclusion that monitoring of gases in the atmosphere in terms of assessing the process of underground gasification is unpromising.

The well 1010 provided data on the concentrations of gases in soil air, and the gases sampled directly from the well head. Below is a comparison of the data (Table 2).

Table 2.

Comparative table of the averaged data for the well 1010

##	Gas	Sampling spot			ratio $C_o/C_п$	ratio $C_п/C_a$
		Well casing (o)	Soil air (п)	Atmospheric air (a)		
1	CO_2, %	0.0046	0.0034	0.0024	1.35	1.42
2	CO, %	0.003	<0.000009 (<0.1 mg/m^3)	-	-	-
3	SO_2, %	0.0014	<0.000004 (<0.1 mg/m^3)	-	-	-
4	H_2S, %	0.004	<0.000007 (<0.1 mg/m^3)	-	-	-
5	CH_4, %	2.250	0.072	-	31	-
6	H_2, %	0.640	0.038	-	17	-

According to the many years of gas surveys [2, 4, 8] at the point located directly in the head of the well 1010, all the determined gases are recorded; upon that the concentration of gases is maximal compared to all other wells at the sites "Balapan" and "Sary-Uzen". It should be noted that sometimes decapsulation of the sealing plug (made of, as a rule, concrete and gravel fillings) took place during the nuclear tests, which later resulted in noble gas seepage. Thus, the "warfare" boreholes might have gas-permeable zones. Based on the above facts, we can conclude that the monitoring of gas concentrations in the head of the well 1010 maximally reflects the gas generation processes occurring at depth. It follows thence that all heads of the wells need to be surveyed for gases released from them, because exactly such a point may be most informative in terms of underground gasification monitoring.

Comparison of gases concentrations measured in an emanating flow directly from the head of the well 1010 and the soil air at the mouth of the well shows that the difference in the concentrations of methane and hydrogen is almost two orders of magnitude (Table 4) with such gases as carbon monoxide, hydrogen sulphide, sulphur dioxide in the soil air are observed at all. This phenomenon can be attributed to the interaction of these gases with groundwater:

$$SO_2 + H_2O \rightarrow 2H^+ + SO_3^{2-} \quad (1)$$

$$H_2S + 2H_2O \rightarrow 2H_3O^+ + S^{2-} \quad (2)$$

$$CO + OH^- \rightarrow HCOO^- \quad (3)$$

Thus, the effect of the "secondary" factors defining the process of passing the gases through the thickness of rocks for these gases is complicated by the fact of a possible interaction with groundwater, so that these gases may be the least informative indices. So, monitoring of methane and hydrogen in the soil air is the most informative method.

Based on gas monitoring, there were analysed the data that considered the relations and their indices between the two points of the same well site, and thus indirectly the effect of the "secondary" factor was measured. Data reflecting the similarity of the gas concentration dynamics in the soil air between the sampling points for each well are presented in Table 3 below.

Table 3.

Correlation coefficients, reflecting the similarity in the gas release dynamics at various points of soil air sampling

Gas/well	H_2	CO_2	CH_4	SO_2	Gas/well	H_2	CO_2	CH_4	SO_2
1355	0.61	-0.14	0.50	-	**1315**	0.51	-0.04	0.89	-
1317	0.78	0.99	0.08	-0.25	**1053**	0.83	0.46	0.53	-
1010	-0.43	-0.34	-0.34	-	**"Glubokaya"**	0.87	0.94	0.89	0.99
1236	-0.44	-0.26	0.04	-	**1361**	-0.31	0.13	0.95	-0.11

A good correlation for 4 gases is therefore established for the well "Glubokaya". This may be explained by the fact that the entire well head section represents an area of gas permeable structure. According to the results of the gas survey, this area is not less than 450x500 m^2. It is likely that the formation of large gas discharge zone at this well is associated with the proliferation of gases and explosion that occurred in 1992 [1]. It is assumed that at the present time there is no gas accumulation in the subsurface at the well "Glubokaya".

Further, an analysis was carried out for concentrations values obtained in paired sampling points. Appropriate number of significant values was obtained for carbon dioxide and hydrogen. The graph (Figure 10a) shows that the majority of hydrogen concentrations in the soil air for the point T1 are similar in value to the data for the point T2. This means that the selected distance between the gas sampling points is not significant in terms of variation of the "secondary" factors effect.

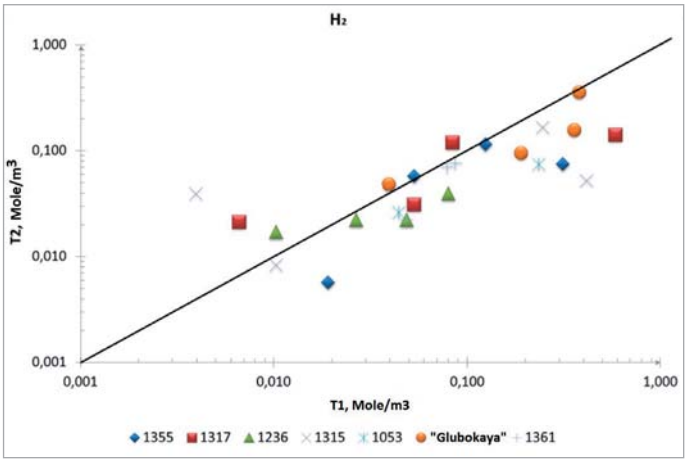

a) hydrogen

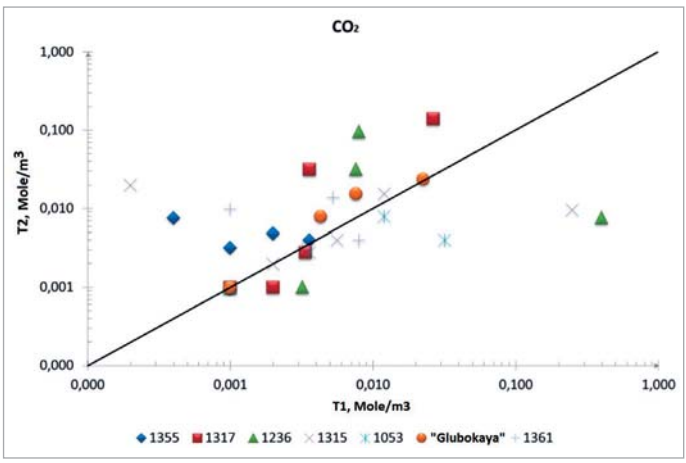

b) carbon dioxide

Figure 10. Results convergence assessment for the points: a) hydrogen b) carbon dioxide

It should be kept in mind that the soil air initially contains greater amount of carbon dioxide than the atmospheric air, and the value of its concentration is affected by a number of factors. Therefore, the dynamics of carbon dioxide may not adequately reflect the nature of the underground gasification process.

3.2. Areal gas survey

At the wells "Glubokaya", 1236 and 1361 the surveys show that most (80%) of the site is a gas-permeable zone for methane. Probably, the resulting gas penetrates through these porous structures to the atmosphere without being accumulated in the intermediate areas and thus there less likelihood gas salvo emission, as it was at the well "Glubokaya". However, the burn-out of the rocks may form place of low coherence with high porosity, in case of col-

lapses/crumples there may happen collapses and subsidence of the surface. Consequently, the wells where gas fields have been recorded, must be classified as potentially dangerous. As the areal survey showed, areas with gas anomalies at the wells may not be limited to the size of 500x500 m^2 and go beyond the boundaries of the selected survey area. In order to establish the boundaries of gas anomalies, additional gas surveying is needed in larger scale to be performed at estuarine areas of the wells "Glubokaya", 1361, 1236, 1355, 1315 and 1317.

Attention should be drawn to the results of areal gas survey at estuarine area 1355. Relatively high concentrations of methane were revealed there in several points. It is possible that there are processes of underground gasification, and methane generated from these processes reaches the surface at low concentrations, which may lead to an accumulation of methane in underground cavities, which can then lead to emissions of gas and subsidence of the surface. Thus, it is still impossible to make an unambiguous conclusion about the hazards of "gassing" and "non-gassing" wells.

In addition, it should be noted that it is appropriate to set up special observation wells to study the underground gasification at UNEs venues. Gas sampling from these wells, measuring temperature of groundwater, as well as water analysis will provide new data on the process of gassing. Currently we are able to start works using the existing hydrogeological wells. In close proximity to some of the "warfare" boreholes are the hydrogeological wells (110/14, 1010/1, 125/1 and 110/14, etc.) [2] that can be used for research. It is likely that additional deeper wells (up to 200 meters or more) would be needed for the fractured waters for a detailed study of each gassing well.

CONCLUSION

The gas monitoring revealed that further monitoring of gas concentrations in the atmospheric air at the wells is unpromising in terms of assessment of underground gasification processes.

The long-term studies of gas effects at the head of the well 1010 found that it is expedient to carry out additional investigations of all the well heads for the presence of gas releases, since such particular points may be most informative in terms of underground gasification monitoring.

Since the effect of the "secondary" factors which define the process of gases proliferation through the rocks are not severely complicated by possible interactions of methane and hydrogen with groundwater, monitoring of these gases in the soil air is the most informative, and studying the dynamics of carbon dioxide, due to the influence of quite large number of factors, will not allow gaining adequate information about the gasification processes.

As it was mentioned above, burn-out of the rocks during gasification may cause subsidences and collapse of the surface. To monitor such changes it is appropriate to maintain geomorphological monitoring employing long-term benchmarks to be arranged in the locations of gas anomalies in the estuarine areas of the wells, as well as in those spots near the wells that have high concentrations of gases in soil air.

According to the areal survey of estuarine parts of the wells "Glubokaya", 1361, 1236, 1355, 1315 and 1317, the boundaries of the gas anomalies to be re-surveyed at a large scale are needed to be defined. It should be noted that at the present time we cannot make any un-

ambiguous conclusion about the hazards imposed by "gassing" and "non-gassing" wells, but the "gassing" wells clearly should be classified as potentially hazardous objects.

REFERENCES

1. Subbotin S.B. Assessment of possibilities for catastrophic events at Balapan site / Subbotin S.B., Lukashenko S.N. // Topical Issues in Radioecology of Kazakhstan [Proceedings of the Institute of Radiation Safety and Ecology for 2007-2009] [in Russian]
   Субботин С.Б. Оценка возможностей протекания процессов катастрофического характера на площадке "Балапан" / Субботин С.Б., Лукашенко С.Н. // Актуальные вопросы радиоэкологии Казахстана [Сборник трудов Института радиационной безопасности и экологии за 2007 – 2009гг.]. – Вып. 2. – Павлодар: Дом печати, 2010. – С. 401-448. : ил. - Библиогр.: с. 54. - ISBN 978-601-7112-32-5.
2. Safety Assurance at the former Semipalatinsk Test Site. State Budgetary Program 011 "Radiation Safety Assurance": R&D Report (Final), Kurchatov: IRSE NNC RK, 2008. [in Russian]
   Обеспечение Безопасности Бывшего Семипалатинского Испытательного Полигона Республиканская Бюджетная программа 011 "Обеспечение радиационной безопасности" : отчет о НИР (итоговый) по договору № 36-2008/1 от 10.10.2008г. / ИРБЭ НЯЦ РК; рук. Лукашенко С.Н.; исполн.: Демин В.Н. – Курчатов: ИРБЭ НЯЦ РК, 2008. -121 с.
3. Aspirator for sampling and storage of gas samples. Technical specification. [in Russian]
   Аспиратор для отбора и хранения проб газа Техническое описание. - В/О: Машприбор,1979. - 4с.
4. Safety Assurance at the former Semipalatinsk Test Site. State Budgetary Program 011 "Radiation Safety Assurance": R&D Report (Informational), Kurchatov: IRSE NNC RK, 2010. [in Russian]
   Обеспечение Безопасности Бывшего Семипалатинского Испытательного Полигона Республиканская Бюджетная программа 038 "Обеспечение радиационной безопасности" : отчет о НИР (информационный) по договору № 4-20103 от 19.02.2010 /ИРБЭ НЯЦ РК; рук. Лукашенко С.Н. – Курчатов: ИРБЭ НЯЦ РК, 2010. -128с.
5. Handbook of Geochemistry / G.V. Voitkevich, A.V. Kokin, A.E. Miroshnikov, V.G. Prokhorov. – Moscow, 1990. [in Russian]
   Справочник по геохимии / Г.В. Войткевич, А.В. Кокин, А.Е. Мирошников, В.Г. Прохоров. – М.: Недра, 1990. - 480 с.: ил.
6. A.A. Beus. Environmental geochemistry / A.A. Beus, L. I. Grabovskaya, N. V. Tikhonov. - Moscow: 1976 [in Russian]
   Беус А.А. Геохимия окружающей среды / А.А. Беус, Л.И. Грабовская, Н.В. Тихонова. - М.: Недра, 1976. - 248 с.
7. Internet resource http://ru.wikipedia.org/wiki/Оксид_углерода (IV) [in Russian]

Интернет ресурс, режим доступа на http://ru.wikipedia.org/wiki/Оксид_углерода(IV)..

8. Safety Assurance at the former Semipalatinsk Test Site. State Budgetary Program 011 "Radiation Safety Assurance": R&D Report (Informational), Kurchatov: IRSE NNC RK, 2009. [in Russian]
Обеспечение Безопасности Бывшего Семипалатинского Испытательного Полигона Республиканская Бюджетная программа 011 "Обеспечение радиационной безопасности" : отчет о НИР (информационный) по договору № 17-2009 от 26.06.2009г. /ИРБЭ НЯЦ РК; рук. Лукашенко С.Н. – Курчатов: ИРБЭ НЯЦ РК, 2009. - 164 с.

"БАЛАПАН" АЛАҢЫНДАҒЫ ГАЗ ШЫҒАРУДЫҢ СИПАТЫН ЗЕРТТЕУ

[1]Романенко В.В., [1]Субботин С.Б., [1]Лукашенко С.Н., [2]Чернова Л.В.

[1]ҚР ҰЯО Радиациялық қауіпсіздік және экология институты
[2]ҚР ҰЯО Атом энергиясы институты

Мақалада 2010 жылы алынған, "Балапан" алаңындағы жерасты ядролық жарылыстардың эпиорталық аймақтарындағы газ шығару процестерінің нәтижелері ұсынылған. Газ мониторинг нәтижелері "қатерлі" ұңғымалардағы газ шығару процесінің көп жағдайда жеке сипатқа ие екендігін көрсетті. Бақылау кезеңінің ағымында бір ғана нүктедегі газдардың шоғырлануы 4 реттік көлемге дейінгі аралықта өзгеруі мүмкін. Сутегі мен метан шоғырлануының мониторингі "газ шығаратын" ұңғымалардың мониторингінің аса дәлме-дәл әдісі болып табылады. Құбыр артындағы кеңістік бойынша шығатын газдар мониторингі газ пайда болу процестерінің өзін – "алғашқы" факторлар кешенін өте шынайы бейнелейді. Алаңдық газдық зерттеу нәтижелері бойынша бірқатар ұңғымалар ауызалды алаңдардағы газдық ауытқулардың шекаралары 350 метрден көп арақашықтықта орналасуы мүмкін екендігі анықталды. ЖЯЖ жүргізу орындарындағы газ шығару процестерін ары қарайғы зерттеу үшін ұсыныстар келтірілген.

Түйін сөздер: Семей сынақ полигоны, көмірқышқыл диоксиды, метан, күкіртті сутек, аялық шоғырланулар, жерасты газдану, газ шығару, алаңдық газдық түсіру, газ шығару мониторингі, түзету.

ИССЛЕДОВАНИЕ ХАРАКТЕРА ГАЗОНОСНОСТИ НА ПЛОЩАДКЕ "БАЛАПАН"

[1]Романенко В.В., [1]Субботин С.Б., [1]Лукашенко С.Н., [2]Чернова Л.В.

[1]Институт Радиационной Безопасности и Экологии НЯЦ РК, Курчатов, Казахстан
[2]Институт Атомной Энергии НЯЦ РК, Курчатов, Казахстан

В статье представлены результаты исследования процессов газоносности в эпицентральных зонах подземных ядерных взрывов (ПЯВ) на площадке "Балапан", полученные в 2010 г. Результаты газового мониторинга показали, что в большинстве случаев характер процесса газовыделения на "критических" скважинах носит индивидуальный характер. Концентрация газов на одной и той же точке в течение наблюдаемого периода может изменяться в диапазоне до 4 порядков величины. Установлено, что мониторинг концентрации водорода и метана является наиболее адекватным методом мониторинга "газящих" скважин. Выявлено, что мониторинг газов выходящих по затрубному пространству наиболее объективно отображает собственно процессы газообразования – комплекс "первичных" факторов. По результатам площадного газового обследования выявлено, что границы газовых аномалий на приустьевых площадках ряда скважин могут располагаться на расстоянии более 350 метров. Приведены рекомендации для дальнейшего изучения процессов газификации в местах проведения ПЯВ.

Ключевые слова: Семипалатинский испытательный полигон, диоксид углерода, метан, сероводород, фоновые концентрации, подземная газификация, газовыделение, площадная газовая съемка, мониторинг газовыделения, корреляция.

УДК504.4.054:669.3/.6:622.258.4:577.4

FACTORS FORMING CONTAMINATION WITH HEAVY METALS AT NEAR-PORTAL AREAS OF DEGELEN SITE

Lukashenko S. N., Amirov A. A.

Institute of Radiation Safety and Ecology NNC RK, Kurchatov, Kazakhstan

The paper presents data on heavy metals in water and soil of watercourses of Degelen site. Contents of 45 chemical elements has been studied. The studies found abnormally high levels of some elements in water, relative to their average amount in natural water for this climatic zone. Abnormal excess concentration is the case for molybdenum, beryllium, uranium in the water of 8 watercourses and rare earth elements in the water in the adit #504, spatial characteristics of heavy metals in soils were identified. A conclusion has been made that the main factor for soil contamination at near-portal area is associated with the transfer of heavy metals with adit waters. Also the paper notes the need for continuous monitoring of the content of natural uranium in water as a factor of radiation risk.

Keywords: uranium, heavy metals, adit, portal, water, clark, lanthanides, contamination, watercourse, STS.

INTRODUCTION

Semipalatinsk Test Site is traditionally only referred to as a source of radiological hazards and any phenomena discovered there are explained by radiation, which is not quite correct. The influence of other factors, in particular, heavy metals (HM), the existence of which is confirmed by the available experimental data and by the deposits of mineral resources on the STS territory is not taken into account.

This research continues investigations carried out in the three areas adjacent to the mountain range Degelen in the previous years [1]. The investigations discovered anomalously high concentration of some elements in soil relative to their clarks. The highest excess was detected for molybdenum, arsenic and cadmium. The areal element distribution by concentrations has differentiated structure with local spots of irregular form in all three areas.

The necessity to continue the investigations was caused by the lack of the data on chemical composition of natural waters of the mountain range Degelen, as one of the ways of transfer of chemical elements is aqueous environment, and absence of qualitative information about soil contamination with heavy metals at the near-portal areas.

1. EXPERIMENTAL PART

Based on the above information we studied water routes from adits of the Degelen TEST SITE, took samples of natural water and soil, carried out laboratory analyses to determine concentrations of heavy metals and toxic elements using methods of mass-spectroscopy with inductively-coupled plasma as a source of ions excitation.

During operation of the Degelen test ground, the water outflow was registered in 50 adits. In 2010 continuous water inflow was observed in 8 adits: # 104, 165, 176, 177, 504, 506, 511, and 609 chosen as objects for investigations. (see Figure 1).

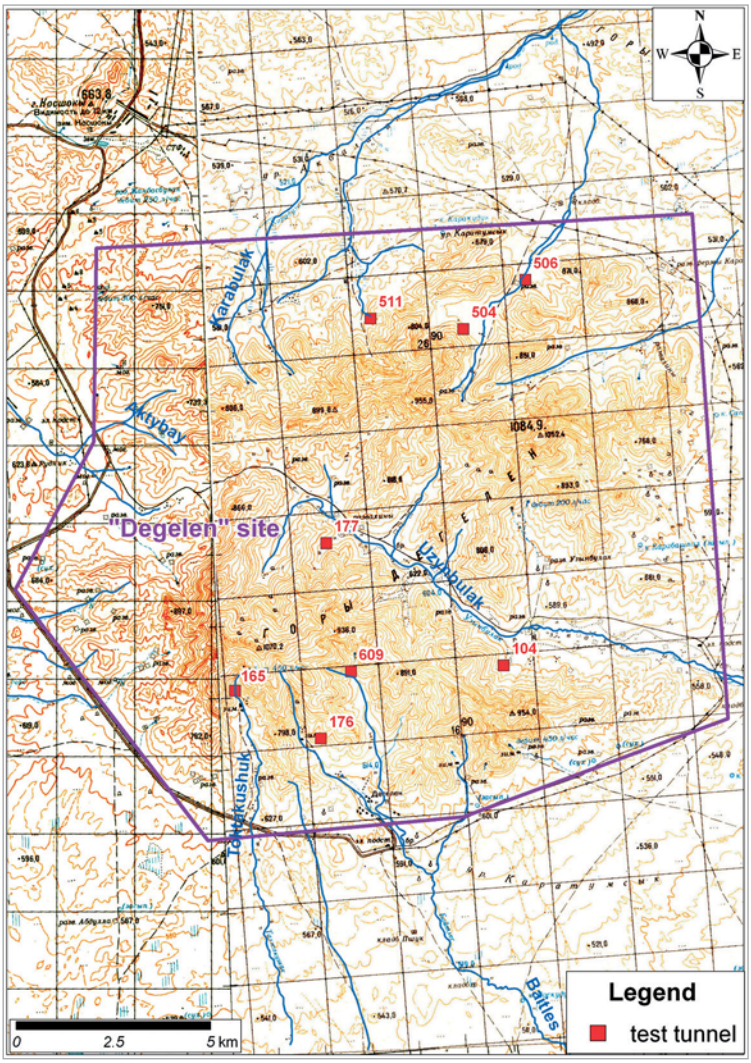

Figure 1. Adits with water effects

1.1. Water sampling

In order to estimate HM concentrations in water along the watercourse in the period 23–28 August, the samples were taken in the place where the watercourse rises to the day surface and every 50m along the watercourse till the mark of 300m.

To estimate variations in the HM concentrations in water in time water samples were taken in the place where the watercourse rises to the day surface in the periods: July 1-3, August 23–28 and September10-14. The number of water samples differed from month to month, which was caused by changes in water discharge from the adits.

Water samples were taken according to the State Standard GOST – 17.1.5.05-85 "General requirements to sampling of surface and sea waters, ice and atmospheric precipitations". The main procedures in water sampling included water filtration through a paper filter "white band" to remove mechanical admixtures, sample conservations by addition of concentrated nitric acid (HNO_3, "extra pure" quality), 3ml of HNO_3 per 1 liter of water sample. The water was sampled into clean 1l polypropylene bottles with screwed cap. The samples were conserved and filtered in the place where they were taken. Prior the analysis the conserved samples were stored in the dark cool place for 2–7 days.

1.2. Soil sampling

To determine the level of soil contamination at the near-portal areas of the Degelen adits, we took soil samples in adits # 177 and # 504. Soil sampling was made according to the following procedure: samples were taken along the profile (7 profiles in each adit, 5 points in each profile) perpendicular to the riverbed, the distance between the profiles was 50 m and the sampling interval was 10m. The central sampling point was directly in the riverbed. The samples were taken by pricks with a metal soil sampler. The depth of sampling was 0–5 cm, the area –100 cm^2.

1.3. Preparation of soil samples for analysis

Preparation of soil samples included soil drying, grinding and acid leaching. The samples were dried in the drying box at a temperature of 70° C for 5 hours. Then form the dry sample by quartering 100 g of weighed mass was taken. The sample was grinded manually by rubbing in the porcelain mortar to a particle size ≤ 250 mesh.

Leaching was carried out according to "Technique of sample preparation in the analytical autoclave NPVF "Ankon-AT-2. Soils. Biological objects for analysis" (MI 2339-95, VNIIMS, Moscow).

200 mg of weighed sample were placed in the Teflon gasket and small portions 10 cm^3 7M of nitric acid were added. Then the Teflon gasket was inserted into the Teflon "bomb", and the sample was decomposed in the autoclave at 150°C for 2 hours. After decomposition in the autoclave the precipitated sample was placed in the centrifuge vessel and centrifuged for 10min at the revolution frequency of 4,000 rev/min, then the sample was placed in the volumetric vessel of volume of 15 cm^3, and the sediment was washed in 5 cm^3 of 7M nitric acid and again subjected to centrifugation. After centrifugation the sample and the washing solution were united, and by adding 7M nitric acid their volume was brought to 15 cm^3. The initial and 1:10 diluted solutions were analyzed for the concentration of chemical elements.

1.4. Analysis procedure

The concentration of heavy metals and toxic elements was determined by ISP-MS with mass-spectrometer Elan 9000, firm PerkinElmerSCIEX, provided with a computer and specialized software. The device had a standard transverse-flowing system for insertion of liquid samples (Meynard-type pulverizer) and a single-collector two-segment ion detector.

To draw calibration plots we used multi-element standard samples registered in the RK GSI Register No. KZ.03.02.00902-2010, KZ. 03.02.00901-2010. Measurements quality was controlled by testing calibration solution after every 15 samples. In case of unsat-

isfactory result of calibration (10% deviation from the calibration curve) the device was re-calibrated.

This method was used to analyze water samples and soil leaches, it enabled to determine the presence of the following elements: Na, Mg, K, Ca, Al, Li, Be, Sc, Cr, Mn, Fe, Co, Ni, Cu, Zn, Ga, As, Se, Rb, Sr, Y, Mo, Ag, Cd, Cs, Ba, La, Ce, Pr, Nd, Sm, Eu, Gd, Tb, Dy, Ho, Er, Tm, Yb, Lu, Re, Tl, Bi, U. The analysis was carried out according to ISO 17294-2:2003 (E) (the number of state registration 022/10505 of 27.12.05г.). Macro-components (Na, K,Mg, Ca) were analyzed in solutions obtained by 10-fold and 100-fold dilution of the initial solutions.

2. RESULTS AND DISCUSSION

2.1. Identification of the main components in contamination of adit water

Table 1 gives mean arithmetical values of element concentrations in water samples taken during investigations in the points of water rising to the day surface compared to the average water composition for arid climatic zone [2] and maximum permissible elements concentrations in drinking water [3].

As the criterion in assessment of the level of water contamination with heavy metals we chose the method of comparing of the obtained data with the average water chemical composition in the arid climatic zone. The element concentrations in water corresponding to the average chemical composition or below it were not considered as potential contamination parameters.

The data presented in Table 1 show that in some points such elements as Al, Li, Be, Mn, Zn, Y, Mo, Cd, Cs, U and elements of lanthanum group were detected, and their concentrations many times exceeded the average concentrations in the waters in arid climatic zone. It should be noted that waters also have high concentration of natural uranium (the sum of isotopes ^{235}U and ^{238}U) 25 – 1,500 times exceeding in all adits the average concentration 2.8 μg/l [2] for the areas with arid climate.

Table 1.

Concentrations of elements in water of the mountain range Degelen

Adit	104	165	176	177	504	506	511	609	Average composition of subterranean waters [2]	Maximal allowable concentration for drinking water [3]
mg/l										
Na	20±2	11±1	18±2	20±2	27±3	14.5±1.5	14.0±1.5	25±2	392	200
Mg	15±1	10±1	6.0±0.5	11±1	23±2	14±1	19±2	9±1	67.5	
K	1.0±0.1	1.5±0.1	0.60±0.06	1.5±0.1	2.5±0.2	0.25±0.02	1.5±0.1	1.0±0.1	17.3	
Ca	130±13	106±10	46±4	75±7	185±18	140±14	110±10	60±6	111	
µg/l										
Al	200±15	<0.5	<0.5	<0.5	17600±1700	15±1	925±90	12±1	280	500
Li	67±6	64±6	34±3	54±5	125±120	10±1	70±7	51±5	33.5	30
Be	5.7±0.5	0.56±0.05	0.52±0.05	1.3±0.1	270±25	0.75±0.07	87±8	3.0±0.3	0.33	0.2
Sc	<0.5	<0.5	<0.5	<0.5	62±6	<0.5	<0.5	<0.5	0.03	
V	<0.20	<0.20	<0.20	<0.20	<0.20	0.77±0.07	<0.20	<0.20	2.6	
Cr	1.8±0.2	2.8±0.3	2.0±0.2	2.0±0.2	0.45±0.04	2.4±0.2	<0.20	3.0±0.3	4	500
Mn	41±4	1.2±0.1	1.5±0.1	<0.2	109000±10000	182±15	10180±1000	146±15	88	500
Fe	<0.5	<0.5	<0.5	<0.5	<0.5	<0.5	<0.5	<0.5	0.93	1000
Co	<0.2	<0.2	<0.2	<0.2	12±1	0.35±0.03	0.60±0.06	<0.2	0.6	
Ni	<0.5	<0.5	<0.5	<0.5	6.0±0.5	0.52±0.05	1.5±0.1	<0.5	5.5	100
Cu	<0.3	<0.3	<0.3	<0.3	18±1	<0.3	<0.3	10±1	10	1000
Zn	40±4	32±3	30±3	49±5	11000±1000	11±1	3770±370	7.0±0.7	45.2	5000
Ga	<0.1	<0.1	<0.1	<0.1	<0.1	<0.1	<0.1	<0.1	0.6	
As	<0.6	<0.6	<0.6	<0.6	<0.6	<0.6	<0.6	<0.6	1.9	50
Se	<1	<1	<1	<1	<1	<1	<1	<1	1.8	10
Rb	3.0±0.3	4.3±0.4	1.4±0.1	1.7±0.1	11±1	<0.02	5.0±0.5	3.0±0.3	2	

Adit	104	165	176	177	504	506	511	609	Average composition of subterranean waters [2]	Maximal allowable concentration for drinking water [3]
Sr	480±45	317±30	156±15	380±35	760±75	690±65	385±35	170±15	700	7000
Y	<0.01	<0.01	<0.01	<0.01	385±35	<0.01	<0.01	<0.01	0.15	
Mo	550±50	65±6	175±17	660±60	<0.3	10±1	0.82±0.08	165±15	4.1	250
Ag	<0.05	<0.05	<0.05	<0.05	<0.05	<0.05	<0.05	<0.05	0.44	
Cd	1.25±0.15	<0.3	1.0±0.1	<0.3	34±3	<0.3	9.0±1.0	<0.3	0.42	
Cs	1.4±0.1	1.4±0.1	1.0±0.1	0.15±0.01	6.5±0.5	<0.05	3.5±0.3	1.2±0.1	0.6	
Ba	10±1	10±1	3.0±0.3	13±1	8.0±0.6	20±2	5.5±0.5	1.0±0.1	33.6	100
La	<0.05	<0.05	<0.05	<0.05	455±40	<0.05	<0.05	<0.05	0.3	
Ce	<0.05	<0.05	<0.05	<0.05	890±85	<0.05	<0.05	<0.05	1	
Pr	<0.05	<0.05	<0.05	<0.05	85±8	<0.05	<0.05	<0.05		
Nd	<0.05	<0.05	<0.05	<0.05	280±25	<0.05	<0.05	<0.05		
Sm	<0.05	<0.05	<0.05	<0.05	65±6	<0.05	<0.05	<0.05		
Gd	<0.05	<0.05	<0.05	<0.05	100±10	<0.05	<0.05	<0.05		
Tb	<0.05	<0.05	<0.05	<0.05	16±1	<0.05	<0.05	<0.05		
Dy	<0.05	<0.05	<0.05	<0.05	95±10	<0.05	<0.05	<0.05		
Ho	<0.05	<0.05	<0.05	<0.05	19±2	<0.05	<0.05	<0.05		
Er	<0.05	<0.05	<0.05	<0.05	56±5	<0.05	<0.05	<0.05		
Tm	<0.05	<0.05	<0.05	<0.05	8.0±0.8	<0.05	<0.05	<0.05		
Yb	<0.05	<0.05	<0.05	<0.05	53±5	<0.05	<0.05	<0.05		
Lu	<0.05	<0.05	<0.05	<0.05	8.0±0.8	<0.05	<0.05	<0.05		
Re	<0.06	<0.06	<0.06	<0.05	2.0±0.2	<0.06	<0.06	<0.06		
Tl	<0.03	<0.03	<0.03	<0.03	<0.03	<0.03	<0.03	<0.03		
Pb	<0.01	<0.01	<0.01	<0.01	<0.01	<0.01	<0.01	<0.01	3.6	30
Bi	<0.05	<0.05	<0.05	<0.05	<0.05	<0.05	<0.05	<0.05	0.06	
U	2025±200	2565±250	1075±100	1960±200	4535±450	76±5	555±50	1040±100	2.8	

As in these adits nuclear tests were made, it was supposed that the uranium may come from nuclear charge material (uranium with different degrees of enrichment). Based on this assumption ratios of uranium isotopes ^{235}U and ^{238}U were measured by ISP-MS device. It was found that concentration of ^{235}U in natural waters of the Degelen ground corresponded to the natural isotope composition and was equal to 0.72% (Table 2).

For comparison Table 2 also contains data on concentration of plutonium and uranium isotopes in the natural water of the Degelen site. The concentration of uranium isotope ^{238}U in Bq/l 10 times exceeds the intervention level by NRB-99, which confirms the necessity of control over uranium isotopes concentration in natural waters; it must be included in the continuous monitoring of this parameter in all STS water objects.

Table 2.

Concentration of uranium isotope (^{238}U) in natural waters at Degelen, Bq/l

Adits	Concentration, $C^{238}U$, Bq/l	^{235}U concentration, %	$C^{238}U$/ A.U.	Concentration $C^{239+240}Pu$, Bq/l	$C^{239+240}Pu$/ A.U.	$\frac{(C^{238}U/\text{A.U.})}{(C^{239+240}Pu/\text{A.U.})}$
104	25	0.7245	8.0	0.080	0.025	**320**
165	32	0.7240	10.3	0.009	0.003	**3400**
176	9	0.7241	2.9	0.030	0.009	**32**
177	8	0.7243	2.6	0.110	0.035	**74**
504	21	0.7239	6.8	0.240	0.077	**88**
506	0.5	0.7240	0.16	0.020	0.006	**26**
511	4	0.7245	1.3	0.130	0.042	**31**
609	13	0.7241	4.2	0.185	0.059	**71**
Intervention level NRB-99	3.1			0.56		

Special attention is to be paid to the adit # 504, which has high concentration of the elements of lanthanum group. Such anomalous concentration may be caused by the fact that before rising to the surface the water passes through the rocks with high concentrations of lanthanum group elements. This fact requires more detailed examination. It was also found that waters of adit #504 have anomalous concentration of aluminum, manganese and zinc, which are close to the concentrations of macro-components (Na, K, Ca, Mg). Beryllium concentration in the waters from adit #504 is 800 times higher than the average concentration in the water in arid climatic zone.

Most adit waters have high concentration of molybdenum, for example, molybdenum concentration in waters in adit #104 is 200 times higher than the average concentration in the water in arid climatic zone. Adits #104, 176, 504, 511 have high cadmium concentrations, 2-20 times exceeding average concentrations in water.

2.2. Assessment of changes in HM concentrations with time

To get more detailed information about HM concentration in adit waters we present the data on variations in HM concentrations as a function of the period of water sampling and distance from the point of water rising to the day surface. Figure 2 gives data for each adit, which show changes in element concentrations in the period of water sampling in the points of water rising to the day surface.

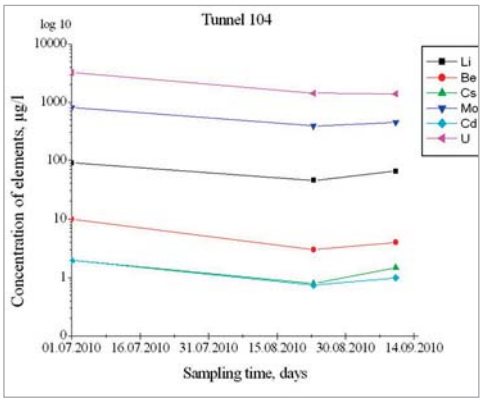

a) adit #104

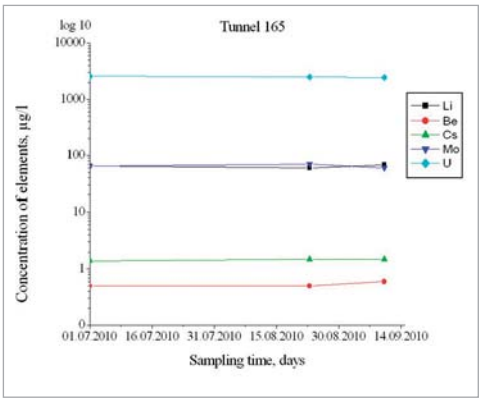

b) adit #165

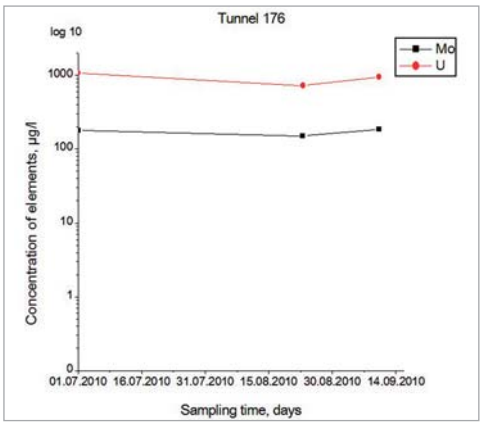

c) adit #176

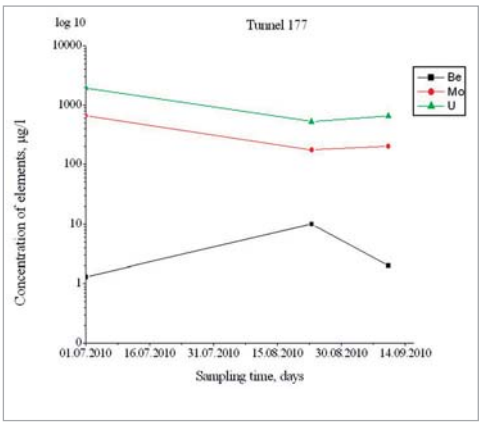

d) adit #177

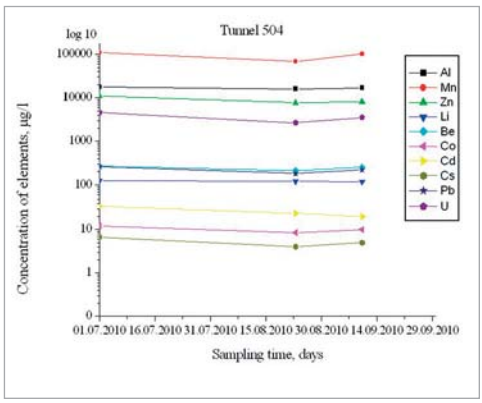

e) adit #504

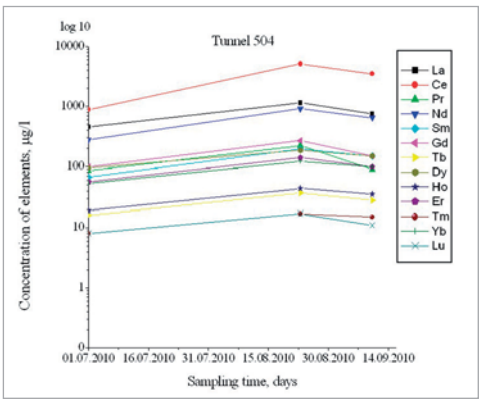

f) adit #504

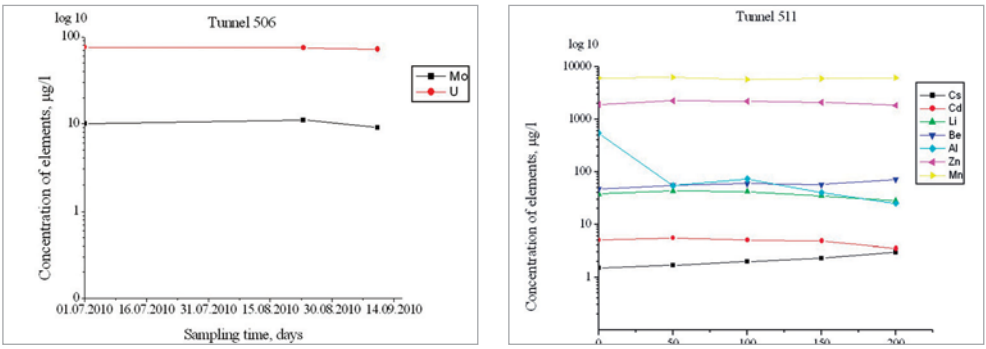

g) adit #506 i) adit #511

Figure 2. Changes in element concentrations in the period of water sampling in the point of water rising to the day surface

These results enable to make a conclusion that changes in concentrations in the period of observations were insignificant, from 5 to 15%. In most watercourses the decrease in element concentrations in water in August was registered, which could be caused by seasonal changes in water discharge.

However, in adit #165 no changes in concentrations of heavy elements in the period of water sampling were detected. It should be also noted that maximal lanthanides concentration in water from adit #504 was registered in August, the same picture was observed for beryllium in water from adit #177.

2.3. Investigations of changes in HM concentrations along the riverbed

Figure 3 shows changes in concentrations of the most important elements in water as a function of the distance from the point of water rising to the day surface.

The obtained results enable to make the following conclusions:

1. concentrations of lanthanides in water of adit #504 decreases almost to zero (limit of measuring devices) at a distance of 200m;
2. changes in other detected elements U, Mo, Cd, Pb, etc. do not follow the same dependence, which may be caused by the limited area of investigations and high migration abilities of these elements;
3. beryllium in water of all watercourses except adits #177 and 506 is detected at a maximal distance from the point of water rising to the day surface, which is also caused by migration ability of this element.

To estimate mechanisms a soil cover contamination we analyzed soils sampled on the banks of watercourses from adits #504 and # №177.

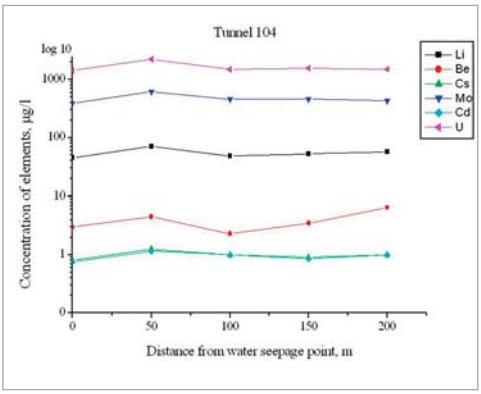

a) adit #104

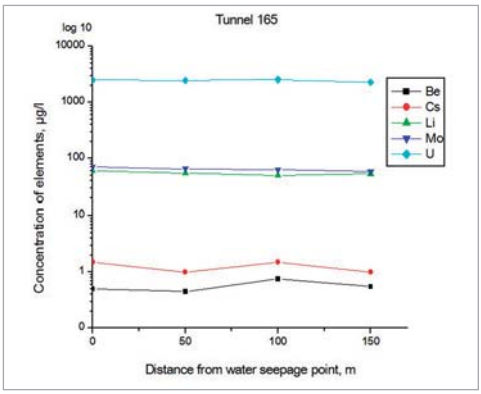

b) adit #165

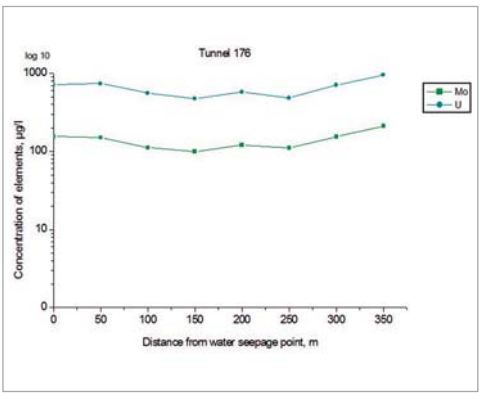

c) adit #176

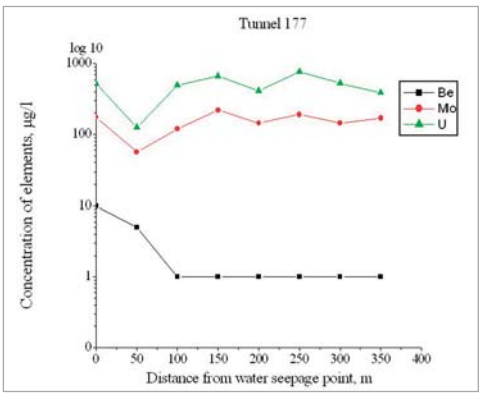

d) adit #177

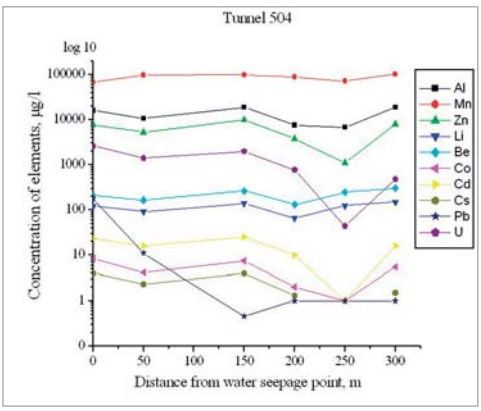

e) adit #504

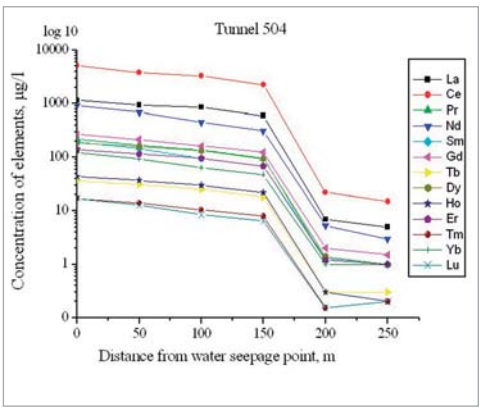

f) adit #504

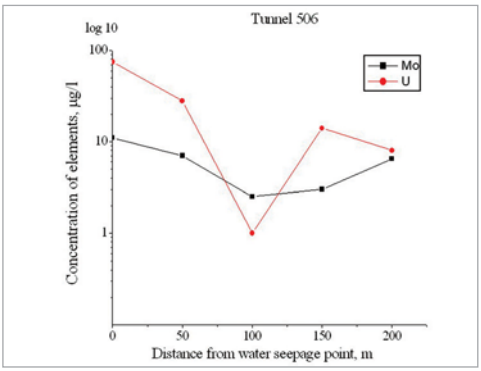

g) adit #506

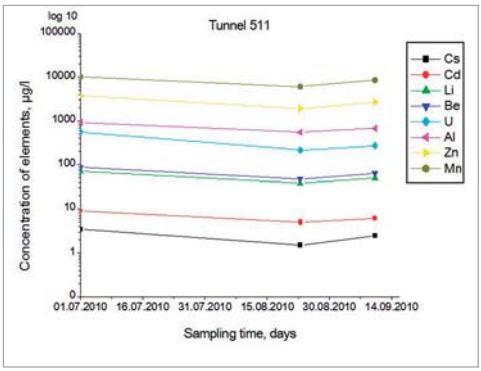

i) adit #511

Figure 3. Changes in element concentrations in water as a function of the distance from the point of water rising to the day surface

2.4. HM concentrations in soils at the near-portal areas of adits #504 and #177

Table 3 gives average arithmetic concentrations of chemical elements along the sampling profiles in acid extracts of soil samples gathered along the watercourse from adit # 504.

Table 3.

Average concentrations of the element in leached soil samples from adit # 504

Profile No.	1	2	3	4	5	6	7	Clarke number as by Vinogradov
mg/g								
Mn	4.0±0.4	3.9±0.4	12.0±1.0	5.1±0.5	14.0±1.0	17.6±1.5	13.7±1.3	1.0
La	1.0±0.1	1.3±0.1	2.2±0.2	2.3±0.2	5.2±0.5	6.3±0.6	2.1±0.2	0.049
Ce	5.8±0.5	6.9±0.7	11.5±1.0	10.0±1.0	19.8±2.0	19.7±2.0	5.0±0.5	0.070
U	2.2±0.2	2.8±0.2	6.2±0.6	3.8±0.3	4.7±0.4	4.5±0.4	1.0±0.1	0.4
Y	2.5±0.2	3.0±0.3	5.5±0.5	5.2±0.5	11.7±1.0	12.5±1.0	4.3±0.4	0.029
Nd	1.3±0.1	1.3±0.1	2.3±0.2	2.0±0.2	3.5±0.3	3.1±0.3	0.75±0.01	0.037
µg/g								
Be	20±2	32±3	76±7	63±6	141±14	134±13	90±9	3.8
Sc	835±85	680±70	1230±125	800±80	950±95	1000±100	420±45	10
Li	35±3	28±2	15±1	30±3	17±1	20±2	32±3	32
V	33±3	21±2	12±1	27±2	10±1	13±1	19±2	90

Profile No.	1	2	3	4	5	6	7	Clarke number as by Vinogradov
Cr	23±2	15±1	9±1	19±2	8.0±0.7	7.0±0.6	10±1	83
Co	8.0±0.7	6.0±0.6	5.0±0.4	7.0±0.6	6.0±0.5	13.0±1.0	18.0±1.5	18
Ni	35±3	32±3	18±1	18±1	17±1	23±2	50±4	58
Cu	1200±100	66±6	180±15	140±10	160±15	115±10	45±4	47
Zn	720±70	530±50	1000±80	980±80	2350±230	3120±300	2360±230	83
As	7.0±0.7	5.5±0.5	4.5±0.4	6.0±0.6	5.0±0.5	5.5±0.5	8.0±0.8	1.7
Sr	37±3	46±4	135±15	85±8	94±9	82±8	135±15	340
Cd	2.0±0.2	2.0±0.2	2.0±0.2	3.0±0.3	5.0±0.5	9.0±1.0	6.0±0.5	0.13
Cs	5.0±0.5	5.0±0.5	8.0±0.7	3.0±0.3	6.0±0.5	5.0±0.4	3.0±0.2	3.7
Ba	140±10	120±10	120±10	114±10	118±10	200±15	230±15	650
Pr	320±30	370±35	660±65	580±60	1150±100	1000±100	240±25	9
Sm	360±35	380±35	680±65	430±45	820±80	580±55	150±15	
Gd	360±35	400±40	765±75	600±60	1200±100	1000±100	280±25	
Tb	56±5	63±6	130±15	93±8	180±15	160±15	44±4	
Dy	245±25	285±25	560±55	440±40	880±85	780±75	217±20	5
Ho	60±6	65±6	130±10	110±10	220±20	200±20	49±5	1.7
Er	174±15	200±20	390±40	324±35	620±60	578±55	160±15	3.3
Tm	24±2	31±3	55±5	41±4	78±7	77±7	21±2	
Yb	180±15	200±20	370±35	250±25	490±50	370±35	100±10	3.3
Lu	27±2	30±3	55±5	36±4	70±7	50±5	12±1	0.8
Pb	765±75	320±30	100±10	40±4	53±5	29±3	32±3	16

To identify the most important elements – the main contaminants – we used the method of comparison of obtained results with the average elements concentration in soil (clark), though it is not quite correct with respect to acid extracts as clark implies bulk elements content in soil. As a result of comparison, it was found that the main soil contaminants in adit #504 were Be, U and rare-earth elements.

For the elements present in anomalous amounts, we made schematic maps of spatial elements distribution (Figure 4).

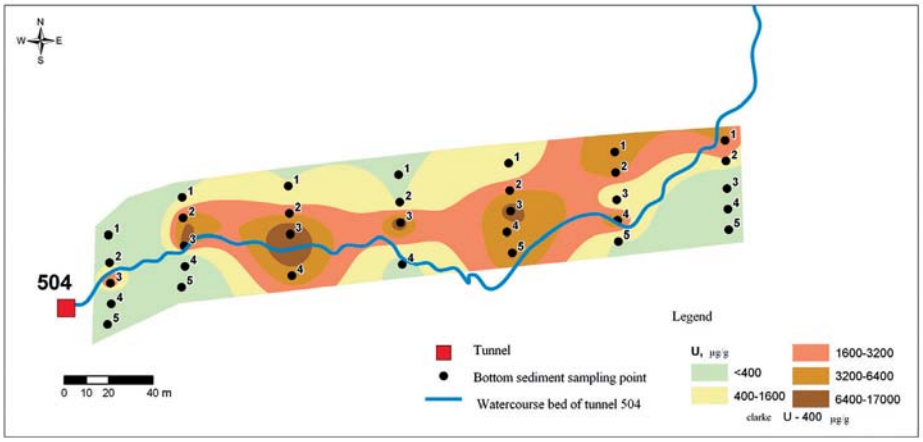
N
W
E
S
504
0 10 20 40 m
Legend
Tunnel
Bottom sediment sampling point
Watercourse bed of tunnel 504
U, μg/g
<400
400-1600
1600-3200
3200-6400
6400-17000
clarke U - 400 μg/g

a)

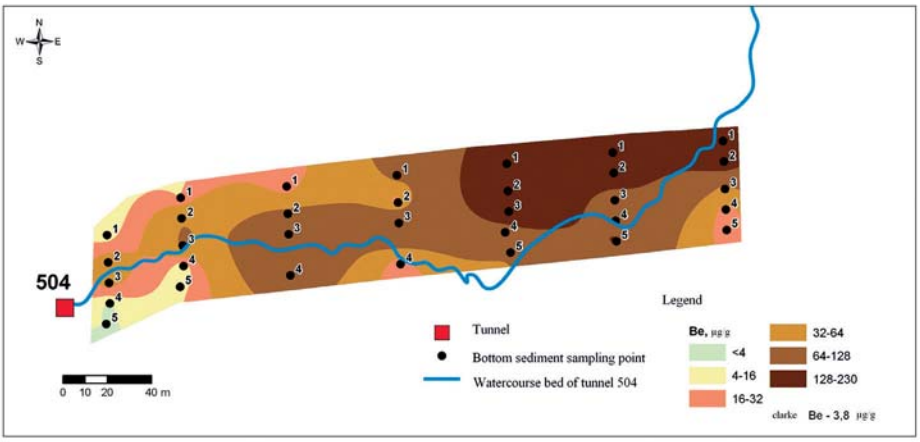
N
W
E
S
504
0 10 20 40 m
Legend
Tunnel
Bottom sediment sampling point
Watercourse bed of tunnel 504
Be, μg/g
<4
4-16
16-32
32-64
64-128
128-230
clarke Be - 3,8 μg/g

b)

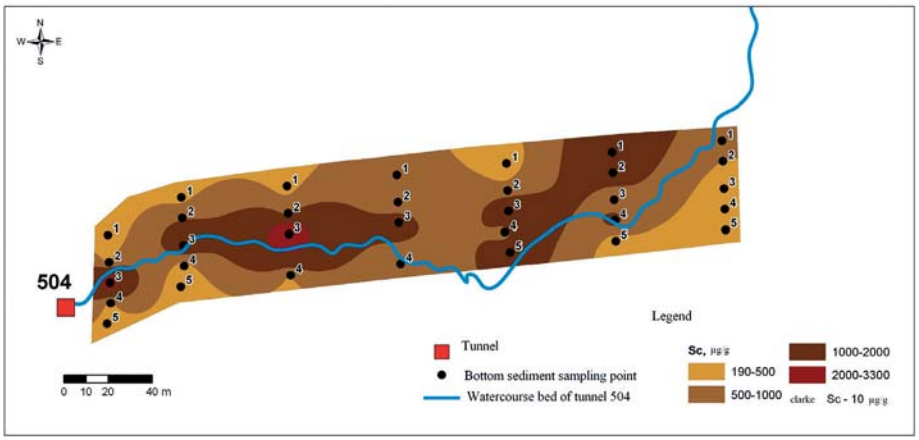
N
W
E
S
504
0 10 20 40 m
Legend
Tunnel
Bottom sediment sampling point
Watercourse bed of tunnel 504
Sc, μg/g
190-500
500-1000
1000-2000
2000-3300
clarke Sc - 10 μg/g

c)

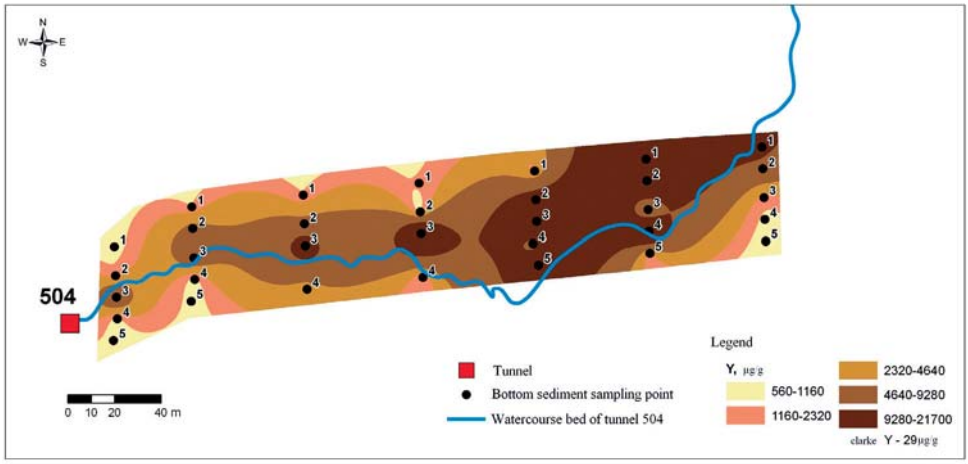

d)

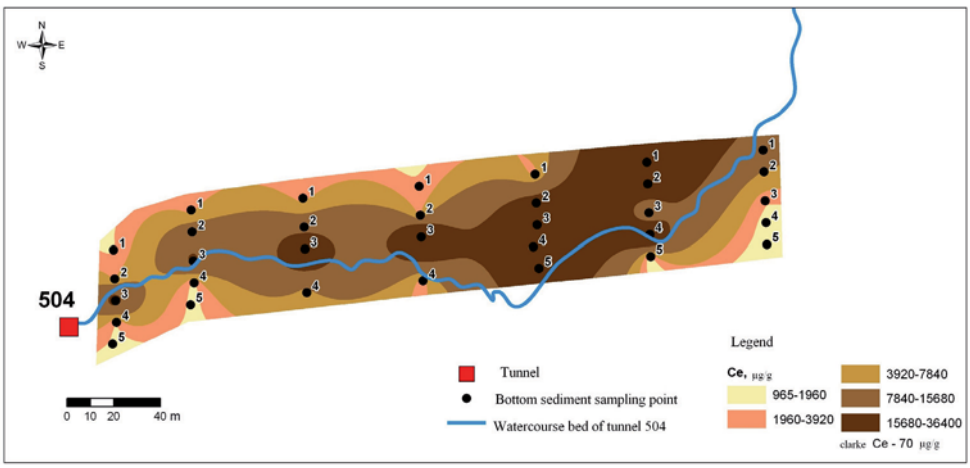

e)

Figure 4. Spatial layout for distribution of some elements in soil at the near-portal area of adit #504: a) uranium, b) beryllium, c) scandium, d) yttrium, e) cerium

An analysis of the spatial distribution showed that such elements as uranium, beryllium and lanthanides were concentrated very close to the watercourse, and points with maximal concentration were located in the riverbed.

To make the picture more demonstrative, in Figure 5 we give transverse profiles of the typical distribution of concentration for the elements of lanthanum and yttrium subgroups.

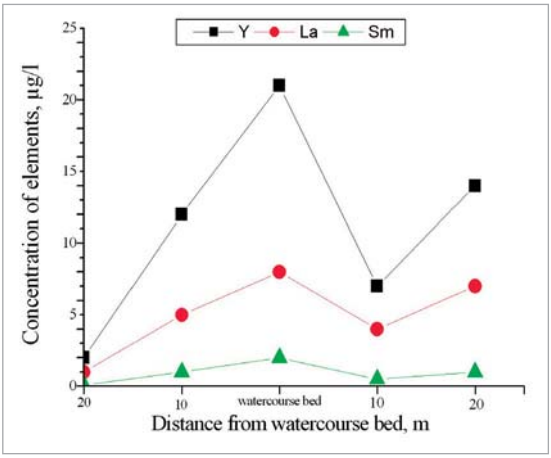

Figure 5. Typical elements distribution in leached soil samples from adit #504 along the sampling profile

An analysis of obtained results enables to make a conclusion that points with maximal concentration of elements are located in the riverbed, and the HM concentration in soil at a distance of 20m decreases by a factor of 10.

It enables to make a conclusion that contamination of the near-portal area is caused by transfer of lanthanides by adit waters and is not connected with their presence in the soil of the near-portal area.

Table 4 presents similar data for adit #177.

Table 4.

Average elements concentration in leached soil samples from adit #177

Profile No.	1	2	3	4	5	6	7	Clarke number as by Vinogradov
				µg/g				
Li	25±2	20±2	21±2	20±2	26±2	23±2	25±2	32
Be	14±1	7.0±0.7	4.0±0.4	10±1	3.0±0.3	5.0±0.5	3.0±0.3	3.8
Sc	260±25	170±15	180±15	200±20	270±25	230±20	230±20	10
V	35±3	28±2	30±3	34±3	44±4	39±4	40±4	90
Cr	31±3	22±2	21±2	25±2	30±3	27±2	27±2	83
Mn	450±45	650±60	710±70	920±90	970±90	1280±120	800±80	1000
Co	5.0±0.4	5.0±0.4	5.0±0.4	5.0±0.4	7.0±0.6	7.0±0.6	7.0±0.6	18
Ni	<0.5	6.0±0.5	23±2	<0.5	14±1	<0.5	<0.5	58
Cu	53±4	54±4	33±3	40±4	29±3	28±3	24±2	47
Zn	210±20	160±15	145±15	220±20	105±10	156±14	100±8	83
Sr	127±10	127±10	78±7	79±7	100±8	63±5	55±4	340
Y	1400±140	720±70	670±65	750±70	830±80	780±75	700±65	29

Profile No.	1	2	3	4	5	6	7	Clarke number as by Vinogradov
Cd	2.0±0.2	<0.6	<0.6	2.0±0.2	1.0±0.1	1.0±0.1	<0.6	0.13
Cs	4.0±0.3	3.0±0.2	2.0±0.2	2.0±0.2	3.0±0.3	3.0±0.3	3.0±0.3	3.7
Ba	165±15	150±15	130±10	140±10	260±20	220±20	170±15	650
La	510±50	390±35	420±40	440±40	550±50	530±50	510±50	49
Ce	2000±200	1700±150	2200±200	2100±200	3200±300	3100±300	2800±250	70
Pr	120±10	90±9	100±10	100±10	135±12	130±12	120±10	9
Nd	510±50	370±35	400±40	400±40	470±45	460±45	450±45	37
Sm	100±10	70±7	71±7	74±7	96±8	91±8	87±8	
Gd	120±10	76±7	73±7	78±7	106±10	99±10	97±9	
Tb	13.0±1.0	6.5±0.6	6.0±0.6	6.5±0.6	9.0±0.8	7.5±0.7	8.5±0.8	
Dy	72±7	40±4	39±4	43±4	56±5	53±5	50±5	5
Ho	16.0±1.5	8.0±0.8	7.5±0.7	8.5±0.8	10.0±1.0	10.0±1.0	9.0±0.8	1.7
Er	55±5	28±2	27±2	29±2	39±3	35±3	32±3	3.3
Tm	5.0±0.5	2.0±0.2	1.0±0.1	1.0±0.1	2.0±0.2	1.0±0.1	1.0±0.1	
Yb	50±5	25±2	24±2	27±2	33±3	30±3	26±2	3.3
Lu	5.0±0.5	3.0±0.3	1.0±0.1	1.0±0.1	2.0±0.2	2.0±0.2	1.0±0.1	0.8
Pb	25±2	33±3	22±2	29±3	33±3	39±3	27±3	16
U	271±25	48±4	132±15	106±10	42±4	70±7	47±4	

Applying the above-used method of comparison with clark, we detected the elements that are considered as the main contaminating components: Be, Y, U, Ce, Pr, Cd.

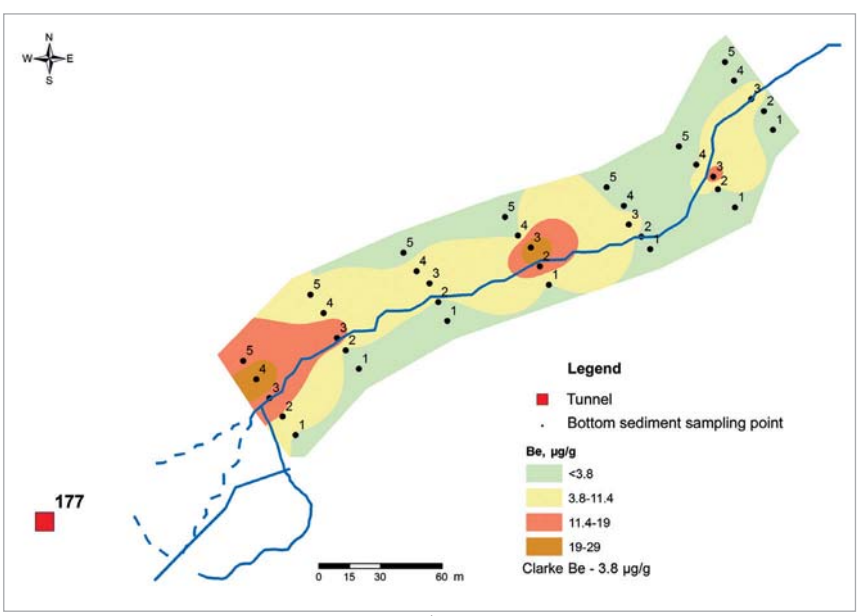

a)

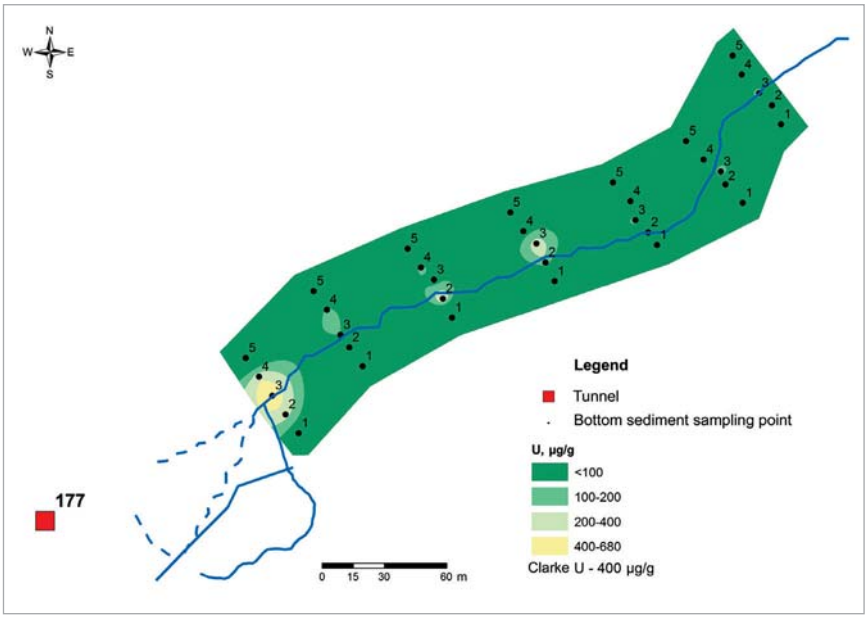
N
W
E
S
177
0 15 30 60 m
Legend
Tunnel
Bottom sediment sampling point
U, μg/g
<100
100-200
200-400
400-680
Clarke U - 400 μg/g

b)

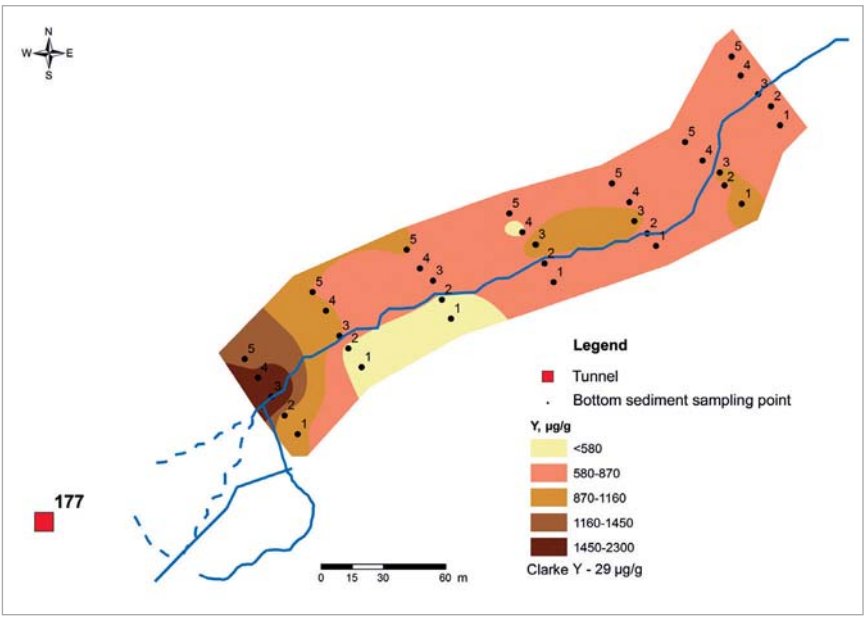
N
W
E
S
177
0 15 30 60 m
Legend
Tunnel
Bottom sediment sampling point
Y, μg/g
<580
580-870
870-1160
1160-1450
1450-2300
Clarke Y - 29 μg/g

c)

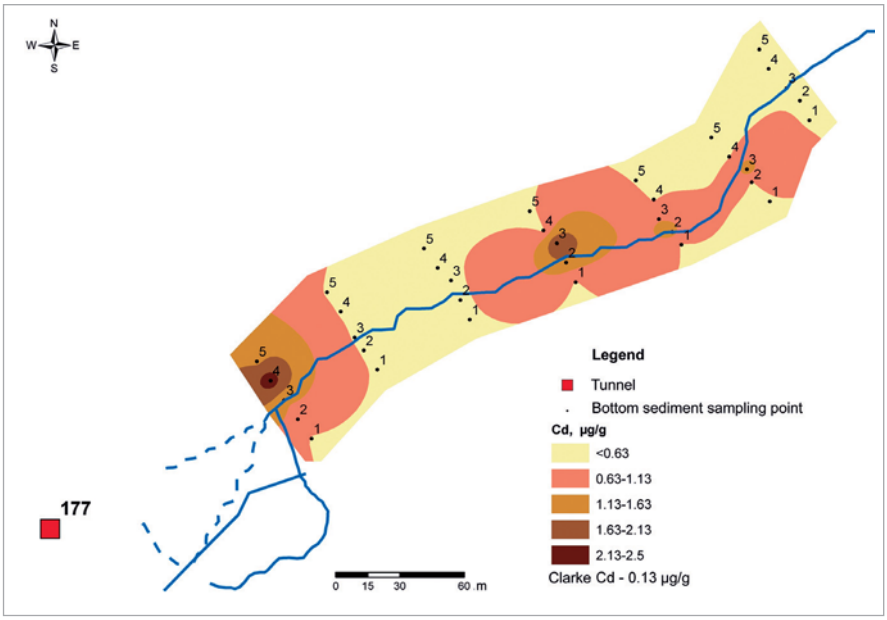
N
W
E
S
177
0 15 30 60 m
Legend
Tunnel
Bottom sediment sampling point
Cd, μg/g
<0.63
0.63-1.13
1.13-1.63
1.63-2.13
2.13-2.5
Clarke Cd - 0.13 μg/g

d)

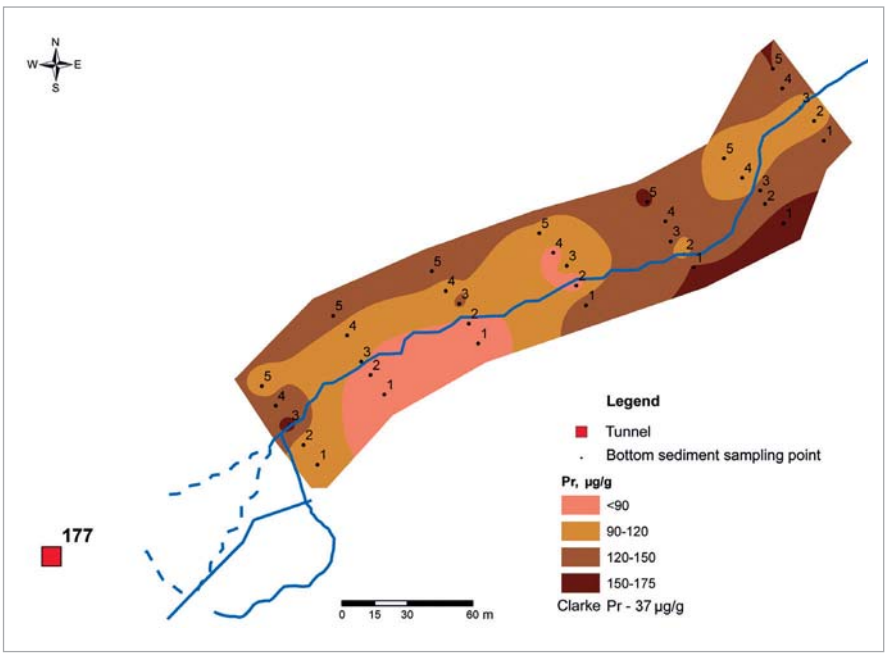
N
W
E
S
177
0 15 30 60 m
Legend
Tunnel
Bottom sediment sampling point
Pr, μg/g
<90
90-120
120-150
150-175
Clarke Pr - 37 μg/g

e)

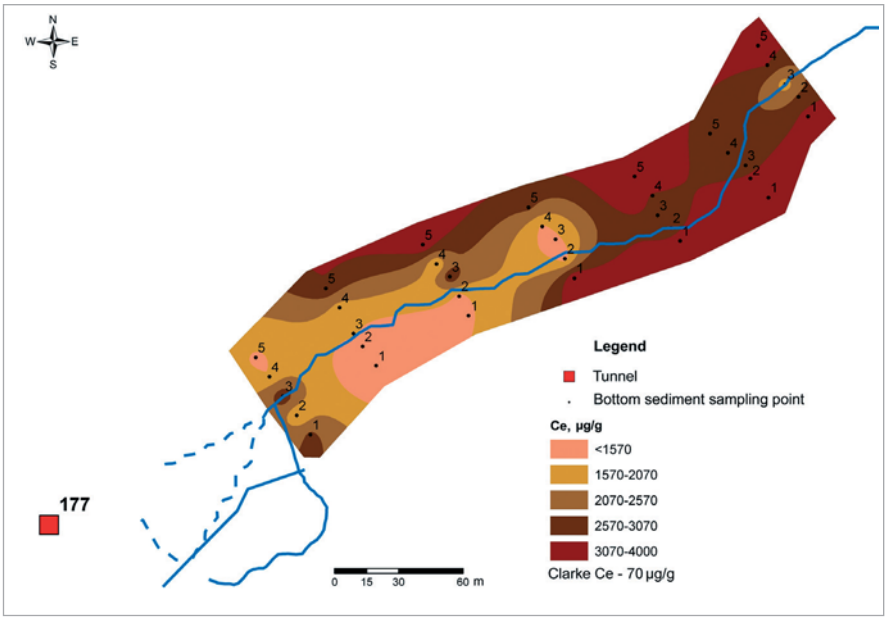

f)

Figure 6. Spatial layout for distribution of some elements in soil at the near-portal area of adit #504: a) beryllium, b) uranium, c) yttrium, d) cadmium, e) praseodymium, f) cerium

In the soil of this adit we also detected elements of lanthanide subgroup, but they were not detected in water of the watercourse. It shows that high concentrations of these elements are not the result of their transfer by adit waters but are caused by geochemical structure of the area. This fact is confirmed by spatial distribution of detected elements as their maximal concentration is not located in the riverbed (Figure 7).

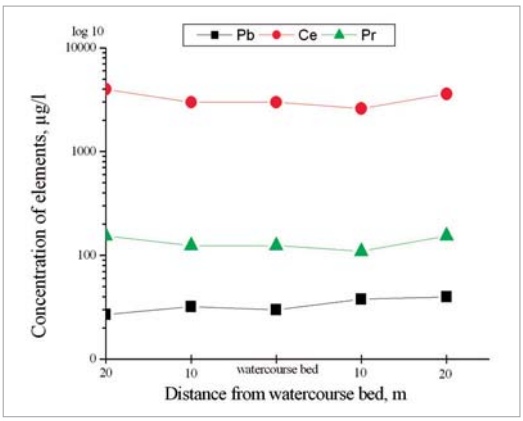

Figure 7. Typical distribution of the elements in leached soil samples from adit #177 along the sampling profile

CONCLUSION

The experimental results presented in this paper enable to consider the ecological situation at the STS, in particular, on the Degelen site, as a complex system of radiation and non-radiation factors. The main conclusions of this research:

- all examined adits have increased concentration of uranium, beryllium and molybdenum, in water of some adits (adit #104) the molybdenum concentration is 800 times higher than its typical concentration in water for this climatic zone;
- the water in adit #504 has a unique elemental composition, in particular, it has high concentration of lanthanides (the sum of all rare-earth elements is about 4 mg/l) and concentrations of aluminum, manganese and zinc, which are comparable with concentrations a macro-components;
- an analysis of concentration of comparable in toxicity α-nuclides – natural isotope ^{238}U and plutonium isotopes $^{239+240}Pu$ showed an important role of natural uranium in composition of studied waters in terms of radiation safety and potential radiation dose rates. Therefore it is necessary to take into account this factor in estimating radiation safety of the STS objects;
- high concentration of rare-earth metals in soil at the near-portal area of adit #504 is mainly caused by heavy metals transfer with waters of the adit water stream. The soil in adit #177 also has increased concentration of rare-earth metals, but it is caused by geochemical structure of the area.

The authors express their gratitude to all the staff of the Institute of Radiation Safety and Ecology, NNC RK, for help in organization of field works and data processing.

REFERENCES

1. Актуальные вопросы радиоэкологии Казахстана [Сборник трудов Института радиационной безопасности и экологии за 2007 – 2009 гг.] / под рук. Лукашенко С.Н. – Вып. 2. – Павлодар: Дом печати, 2010. – 527с.: ил.- Библиогр.: С.518. - ISBN 978-601-7112-32-5.
   Current issues in radiology of Kazakhstan [Proceedings of the Institute of Radiation Safety and Ecology for 2007-2009] / Sup. by Lukashenko S.N. – V.2. – Pavlodar: Printing House, 2010. – 527 pp.: illustration.- appendix.: p. 518. - ISBN 978-601-7112-32-5. – [in Russian]
2. Шварцев С.Л. Гидрогеохимия зоны гипергенеза /С.Л. Шварцев. - М.: НЕДРА, 1998.
   Shvartsev S.L. Hydrogeochemistry in hypergenesis zone / Shvartsev S.L. – M.: NEDRA, 1998. – [in Russian]
3. СанПиН 2.1.4.1074-01.
   Sanitary Norms SanPiN 2.1.4.1074-01. – [in Russian]
4. Isotopic Compositions of the Elements 1989, Pure Appl.,Chem. - Vol.63. - No.7
5. Виноградов А.П. Среднее содержание химических элементов в главных типах изверженных горных пород земной коры / А.П. Виноградов // Геохимия. – 1962. - №7.

Vinogradov A.P. Average concentration of the chemical elements in the basic types of igneous mountain crustal rocks // Geochemistry. – 1962. Vol.7. – [in Russian]

6. Шоу Д.М. Геохимия микроэлементов кристаллических пород / Д.М. Шоу. - Л: НЕДРА, 1969.
   Shou D.M. Geochemistry of mickroelements in canks / Shou D.M. – L: NEDRA, 1969. – [in Russian]
7. Беус А.А. Геохимия окружающей среды /А.А. Беус, Л.И. Грабовская, Н.В. Тихонова // Геохимия. - М.: НЕДРА, 1976.
   Beus A.A. Geochemistry of the environment / Beus A.A., Grabovskaya L.I., Tikhonova N.V. // Geochemictry. – M.: NEDRA, 1976. – [in Russian]
8. Войткевич Г.В. Справочник по геохимии / Г.В. Войткевич, А.В. Кокин, А.Е. Мирошников, В.Г. Прохоров. - М.: НЕДРА, 1990.
   Voitkevich G.V. Reference book on geochemistry / Voitkevich G.V., Kokin A.V., Miroshnikov A.Ye., Prokhorov V.G. – M.: NEDRA, 1990. – [in Russian]
9. Энерглин У. Аналитическая геохимия / У. Энерглин, Л. Брили. - Л.: НЕДРА, 1975.
   Energlin U. Analytical geochemistry / Energlin U., Brili L. – L.: NEDRA, 1975. – [in Russian]

ДЕГЕЛЕҢ АЛАҢЫНЫҢ ПОРТАЛАЛДЫ ТЕЛІМДЕРІНДЕ АУЫР МЕТАЛЛДАРМЕН ЛАСТАНУДЫҢ ҚАЛЫПТАСУ ФАКТОРЫ

Лукашенко С.Н., Амиров А.А.

ҚР ҰЯО Радиациялық қауіпсіздік және экология институты, Қазақстан, Курчатов қ.

Бұл мақалада, Дегелең алаңының штольнясынан шыққан ағын сулардың суында және топырақта ауыр металлдардың орын алған құрамы жайлы деректер келтірілген. Химиялық 45 элементтің құрамы зерттелді. Зерттеулердің деректерге сәйкес, аталған климаттық белдеу үшін табиғи судағы орташа мәніне қатыстылығы бойынша, судағы бірқатар элементтердің құрамы ауытқымалы жоғары екені анықталды. №504 штольняның суында сирек кездесетін элементтер мен 8 ағын судың суында молибден, берилий, уранның шоғырлануының ауытқымалы жоғарылауы орын алған, топырақтағы ауыр металлдардың кеңістіктік сипаты анықталды. Порталалды телімдердің топырағының ластануының негізгі факторы, штольня суларымен ауыр металлдардың шығуына байланысты деген тұжырым жасалды. Сонымен қатар, радиациялық қатер факторы ретінде, судағы табиғи уранның құрамын тұрақты түрде бақылау қажеттілігі байқалды.

Түйін сөздер: уран, ауыр металлдар, штольня, портал, су, кларк, лантаноидтар, ластану, ағын су, ССП.

ФАКТОРЫ ФОРМИРОВАНИЯ ЗАГРЯЗНЕНИЯ ТЯЖЕЛЫМИ МЕТАЛЛАМИ ПРИПОРТАЛЬНЫХ УЧАСТКОВ ПЛОЩАДКИ ДЕГЕЛЕН

Лукашенко С.Н., Амиров А.А.

Институт радиационной безопасности и экологии НЯЦ РК, Курчатов, Казахстан

В статье представлены данные о содержании тяжелых металлов в воде и почвеводото ковштоленплощадкиДегелен.Исследовано содержание 45 химических элементов. По данным исследований было установлено аномально высокое содержание ряда элементов в воде по отношению к их среднему значению в природной воде для данного климатического пояса. Аномальное превышение концентрации имеет место для молибдена, бериллия,урана в воде 8 водотоков и редкоземельных элементов в воде штольни №504, определены пространственные характеристики тяжелых металлов в почвах. Сделаны выводы о том, что основной фактор загрязнения почв припортальных участков связан с выносом тяжёлых металлов штольневыми водами.Такжеотмечается необходимостьпостоянного контроля содержания природного урана в воде как фактора радиационного риска.

Ключевые слова: уран, тяжелые металлы,штольня, портал, вода, кларк, лантаноиды, загрязнение, водоток, СИП.

PART: GENERAL ISSUES OF RADIATION SAFETY

УДК 577.4:504.064:614.876:539.16

ASSESSMENT OF THE IMPACT FROM "FUKUSHIMA-1" NPP ACCIDENT ON THE RADIOLOGICAL SITUATION IN THE REPUBLIC OF KAZAKHSTAN

[1] Lukashenko S.N., [1] Aidarkhanov A.O., [1] Timonova L.V., [2] Silachyov I.Yu., [2] Milts O.S., [3] Rsymbetova R.S.

[1]Institute of Radiation Safety and Ecology NNC RK, Kurchatov, Kazakhstan
[2]Institute of Nuclear Physics NNC RK, Almaty, Kazakhstan
[3]Mangystau Regional Centre for Sanitary-Epidemiological Expertise, Aktau, Kazakhstan

This paper presents the results of air monitoring in the Republic of Kazakhstan. An accident at the "Fukushima-1" NPP resulted in radioactive contamination of water and air with artificial radionuclides. Radioactive contamination has been observed in Japan and neighbouring states and on territories located at a considerable distance. Specialists of the National Nuclear Centre of Kazakhstan (NNC RK) assessed the accident aftermath impact on the radiation situation in Kazakhstan. Concentrations of artificial radionuclides in air of Kazakhstan did not exceed those established by the Radiation Safety Standards of Kazakhstan (NRB-99).

Keywords: radiation monitoring, gamma-spectrometric measurements, radionuclides ^{131}I, ^{134}Cs, ^{137}Cs, air samplers, collective dose

INTRODUCTION

On March 11, 2011 the devastating earthquake and ensuing tsunami resulted in an accident at the nuclear power plant Fukushima-1 in Japan. Within three days a radiation leakage from 4 nuclear power units occurred. These events led to the release of huge quantities of radioactive substances into the environment. Water and air medium of Japan and other countries got radioactively contaminated [1, 2].

To assess the impact of the accident on the territory of the Republic of Kazakhstan, the specialists from NNC RK have launched environmental radiation monitoring from March 15, 2011. The radiation monitoring included sampling of air aerosols and their laboratory analyses to determine concentrations of artificial radionuclides.

The monitoring stations were established at the Institute of Radiation Safety and Ecology NNC RK in Kurchatov, at the Institute of Nuclear Physics in Almaty, and at the Mangystau Regional Centre for Sanitary-Epidemiological Expertise in Aktau. There were also used data from stations located within 120 km from the town of Kurchatov, at "Karadzhal" fluorite deposit and "Degelen" testing site (Figure 1).

Figure 1. Layout of monitoring posts

1. EXPERIMENT

Air aerosols to determine the extent of air contamination with radionuclides were sampled by aspiration method, taking into account the basic principles for sampling of radioactive substances from the air [3]. The method consists in pumping a certain volume of air through the filter, and then the filter is analysed in the laboratory to determine the radionuclide content in accordance with certain procedures. A required volume of air pumped is calculated based on the technical characteristics of the spectrometric equipment used for laboratory measurements, and considering standard levels for radionuclides to be determined.

Based on the specification of the spectrometric equipment, it was determined that one air sample pumped through should be $n \cdot 10^3$ m^3.

The gamma-spectrometric measurements of the samples prepared from the environment were carried out in compliance with the method for measurements at the gamma-spectrometer MI 2143-91 RK [4]. Measurement time for one sample comprised at least 8 hours.

In all points for sampling of aerosols we used 0.2 mm thick Petryanov's synthetic filtering chlorvinyl fabric (FPP-15-1.5) as a filter. The Petryanov's fabric is a layer of ultrathin fibers with an average size of 1.5 microns, deposited over a gauze substrate. Penetration coefficient for oil fog is 0.1.

1.1. Sampling of aerosols

Town of Kurchatov

A device "EPRAM-01-SOLO" was used for air aerosols sampling. This device is an automatic, stationary unit for sampling of air that is highly contaminated with gas-aerosol

mixtures of hazardous substances. Pumping rate is 2,000 l/min, relative error in volumetric air flow rate is ±5%, filter area is 4,400 cm2. Filtration rate is 4.6 m/sec.

The filters were replaced once a day, the equivalent volume of each sample was about 2,800 m3.

City of Almaty

The aerosols were sampled in the territory of the Institute of Nuclear Physics NNC RK. A stationary unit was used as a sampler device; the init has been designed and manufactured in the Institute. The unit pumping rate is 70 m^3/h. The aerosols were sampled on the filter with an area of 225 cm^3. Filtration rate was 3,100 m/s 1,700 m^3.

It took 24 hours to take one sample; volume of the air pumped is 1,700 m^3.

City of Aktau

In the city of Aktau, a device "EPRAM-01-SOLO" was used to sample the aerosols. The sampler operated only during daytime (working hours) for 6-8 hours. The first sample of aerosols in the city of Aktau was taken during 42 days. The total volume of pumped air was about 22,500 m^3. The second sample was collected during 10 days and amounted to 7,900 m^3.

Territory of Karadzhal fluorite deposit

A device used for sampling of air aerosols at Karadzhal fluorite deposit was AKL-4 with pumping rate 346 m^3/h. The device operated continuously for 15 days. The filter area was 1,660 cm^2. Filtration rate of the device was 34 m/sec.

Volume of the air pumped through was 130,000 m^3.

Degelen testing site

Typhoon-4 device was used at Degelen testing site, pumping rate - 650 m^3/h. The device operated about 8-10 hours per day. Total time of sampling is 27 hours. Filtration rate was 0.5 m/sec.

Volume of pumped through air was 16,000 m^3.

1.2. Gama-spectrometric analysis

Preparation of air aerosol samples for the gamma-spectrometric analysis implied pressing of the filter through which air was pumped in a special pressing device to shape it as a cylinder with diameter less than the diameter of the detector used in measurements of artificial radionuclides content in the air.

The prepared filters were measured at "ORTEC" gamma-ray spectrometer which has the following configuration:

- coaxial semiconductor detector "ORTEC" with a beryllium window GMX20-P4; resolution of 1.33 MeV ^{60}Co – 1.9 keV, on the basis of pure germanium crystal with a cryostat CFG-PV4. Dewar DRW-30;
- digital multichannel analyzer DSPEC-jr-2.0-NEGGE with high-voltage power supply NEGGE;
- PC I/O device with software "MAESTRO-32";
- protective lead housing.

Qualitative analysis of the sample gamma-ray spectrum was carried out using "MAESTRO-32" software package; quantitative analysis of the identified radionuclides was performed using "AnalGamma" software.

2. RESULTS

2.1. Monitoring in Kurchatov

Results of laboratory research are graphically presented in Figures 2 and 3.

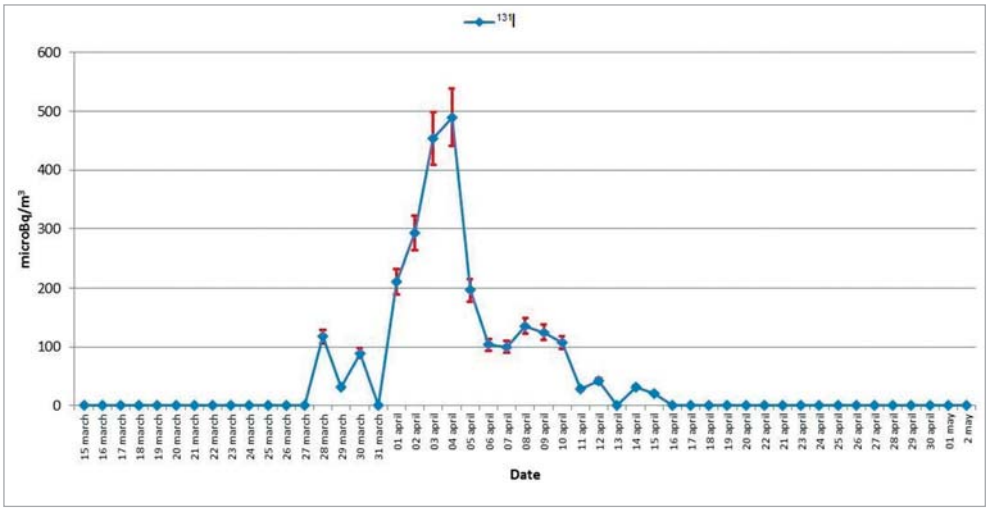

Figure 2. Distribution of ^{131}I in the air of Kurchatov

Data in figure 2 show that the first emergence of ^{131}I was registered on the 28th of March. Maximal concentration was registered on the 4th of April (500 μBq/m^3).

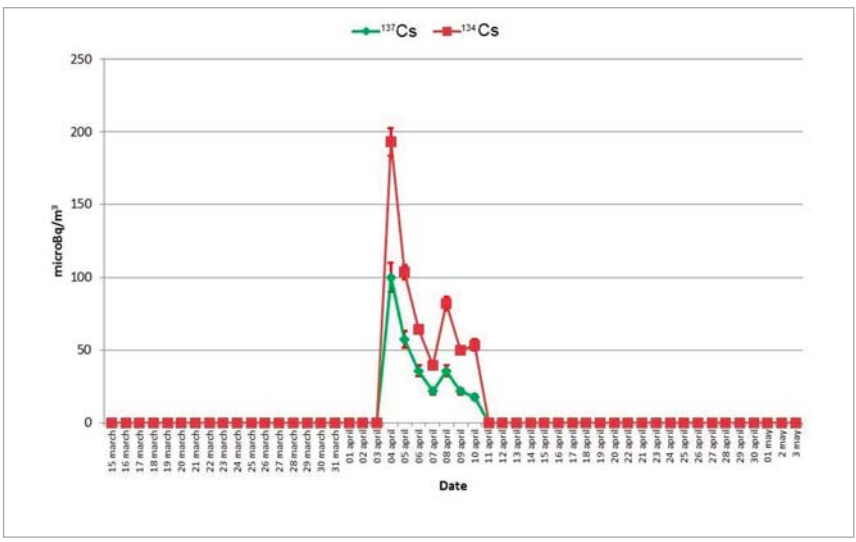

Figure 3. Distribution of ^{134}Cs and ^{137}Cs in the air of Kurchatov

A somewhat different pattern is observed with artificial radionuclides ^{134}Cs and ^{137}Cs. Their maximal concentration was recorded on the first day of their emergence - April 4 (30-50 μBq/m^3).

2.2. Monitoring in Almaty

Similar results were obtained from monitoring observations in Almaty performed in INP NNC RK.

Results of air monitoring in Almaty are shown in figures 4 and 5.

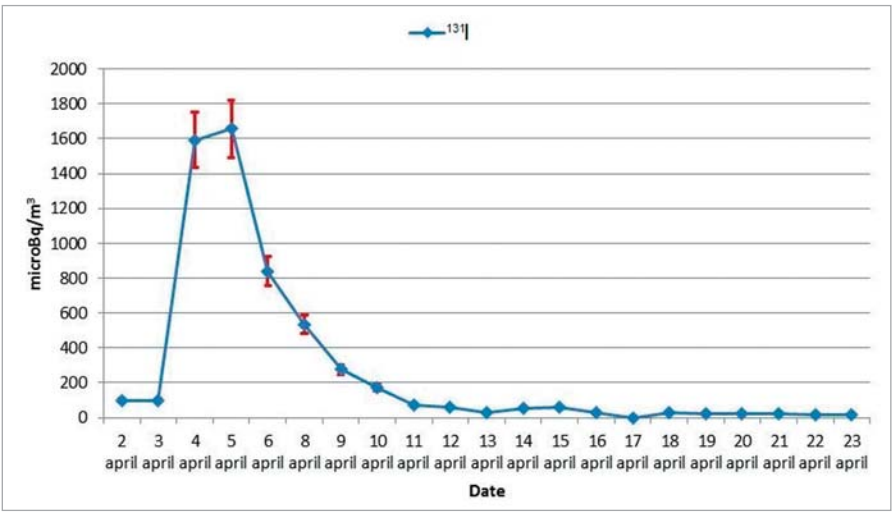

Figure 4. Distribution of ^{131}I in the air of Almaty

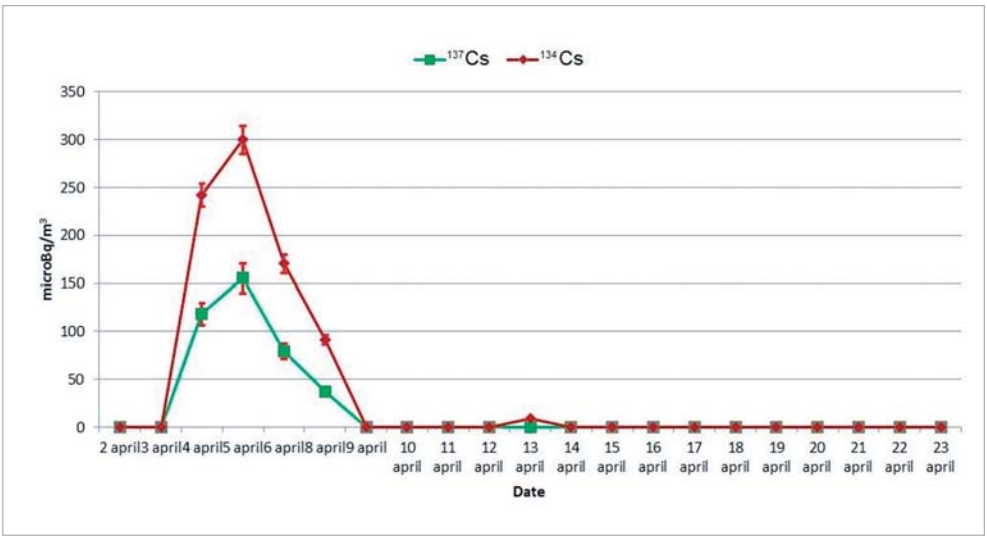

Figure 5. Distribution of ^{134}Cs and ^{137}Cs in the air of Almaty

2.3. Monitoring in Aktau

Radionuclides ^{131}I, ^{134}Cs, ^{137}Cs were also found in the air of Aktau.
Laboratory report is presented in Table 1.

Table 1.

Lab report on research of aerosols in Aktau

Sampling date	^{131}I, µBq/m^3	^{134}Cs, µBq/m^3	^{137}Cs, µBq/m^3
16.02.11 - 29.03.11	2.0 ± 0.2	< 20	3.0
30.03.11 - 08.04.11	50.0 ± 0.5	100 ± 10	100 ± 10

2.4. Monitoring at "Karadzhal" deposit and "Degelen" testing site

In addition, artificial radionuclides were detected at a distance of 120 km from Kurchatov at Karadzhal fluorite deposit and at Degelen testing site. Radionuclides ^{131}I, ^{134}Cs, ^{137}Cs were also detected there.

Laboratory report is presented in Table 2.

Table 2.

Lab report on determination of aerosols at "Karadzhal" deposit and "Degelen" testing site

Point and date of sampling	^{131}I, µBq/m^3	^{134}Cs, µBq/m^3	^{137}Cs, µBq/m^3
Degelen testing site 11.04.11	50.0 ± 5	30.0 ± 0.3	50.0 ± 0.5
Karadzhal fluorite deposit 01.04.11-15.04.11	1.0 ± 0.1	< 0.8	2.0 ± 0.2

3. RESULTS AND DISCUSSION

The monitoring of ambient air found that artificial radionuclides ^{131}I, ^{134}Cs, ^{137}Cs were registered by different laboratories throughout the territory of Kazakhstan during the period from March 28 to April 14.

Maximal concentrations of artificial radionuclides registered in the air basin of the different regions of Kazakhstan are presented in Table 3.

Table 3.

Maximal concentrations of artificial radionuclides in the air of Kazakhstan

Sampling point	^{131}I, µBq/m^3	^{134}Cs, µBq/m^3	^{137}Cs, µBq/m^3
Kurchatov	500	100	90
Almaty	1,700	140	150
Aktau	50	100	90
AVA_{pop}, µBq/m^3 (NRB-99)	7,300,000	19,000,000	27,000,000

In order to confirm the assumption that the emergence of artificial radionuclides in the air is directly related to the accident at Fukushima-1 NPP, isotopic ratios $^{134}Cs/^{137}Cs$ were

analyzed. In case there is one source of radionuclides emissions into the air, the ratio of these isotopes should remain the same. Data on the United States were taken from [5] (Table 4).

Table 4.

$^{134}Cs/^{137}Cs$ ratios

№	USA	$^{134}Cs/^{137}Cs$	Kazakhstan	$^{134}Cs/^{137}Cs$
1	Dutch Harbor	0.87	Aktau	0.90
2	Juneau	0.84	Kurchatov	0.7
3	Nome	0.88	Almaty	1.2
4	Anaheim	0.82		
5	San Bernardino	0.70		
6	Kauai	0.81		
7	Oahu	0.91		
Average in the USA		**0.83**	**Average in Kazakhstan**	**0.92**

Fukushima origin of the radionuclides ^{134}Cs and ^{137}Cs is proved by the fact that the ratio $^{134}Cs/^{137}Cs$ in all cases is equal to ≈ 0.88.

Taking into account the fact that the first emergence of ^{131}I in the air basin of Kazakhstan was recorded on March 28, 2011, and inflow of artificial radionuclides ^{134}Cs, ^{137}Cs was recorded on April 4, 2011, one can make an assumption that there are at least two ways for radionuclides to inflow. Perhaps the inflow of ^{131}I is associated with the first vapour emissions. The sources of ^{134}Cs, ^{137}Cs are the following explosions at the plant when fuel rods were melting.

To assess the possible damage to health of Kazakhstani population, collective dose from exposure to artificial radionuclides was determined. According to NRB-99, 1 manSv collective effective dose leads to potential damage, equal to the loss of one person from population a year. Money equivalent of loss of 1 man-year is established with guidance in the amount of not less than 1 annual per capita national income. Average per capita national income was taken as 265.4 U.S. dollars per month (about 39,000 tenge per month) for a citizen of Kazakhstan [5].

The calculation was performed on the basis of 15 million people of the Republic of Kazakhstan. It was believed that the intake of radionuclides into organism occurs through inhalation during the day continuously. The dose coefficients, limits of annual intake with air and food, allowable volumetric activity in the inhaled air were taken from Annex P-2 of NRB-99.

CONCLUSION

It is well established that the accident at "Fukushima-1" nuclear power plant has had an impact on radionuclide contamination of the air basin in the Republic of Kazakhstan. The studies found that the maximal concentrations of ^{131}I are 14 500 times below the allowable volumetric activity in the air for population, which is 7.3 Bq/m^3 as per NRB-99.

The values obtained for ^{134}Cs are 210 000 times, for ^{137}Cs - 300 000 times below the allowable volumetric activity in the air for the population, which is $1.9 \cdot 10^{1}$ Bq/m^3 and $2.7 \cdot 10^{1}$ Bq/m^3, respectively, as per NRB-99.

The value of collective dose to the population of Kazakhstan did not exceed $1.5 \cdot 10^{-2}$ manSv. Thus, the monetary damage from the accident at "Fukushima-1" was $48.

REFERENCES

1. www.kp.ru/daily/25651/815413/
2. http://ru.wikipedia.org/wiki/Авария_на_АЭС_Фукусима_I
3. ISO 2889-75: General principles for sampling airborne radioactive materials
4. Activity of radionuclides in bulk samples. Technique for measuring on gamma-spectrometer MI 2143-91. [in Russian]
   Активность радионуклидов в объемных образцах. Методика выполнения измерений на гамма - спектрометре: МИ 2143-91. - Введ. 1998-06-02. - Рег. № 5.06.001.98. – М.: НПО ВНИИФТРИ, 1991. - 17 с.
5. http://www.undp.kz/pages/30.jsp

"ФУКУСИМА-1" АЭС АПАТТЫҢ ҚАЗАҚСТАН РЕСПУБЛИКАСЫНДАҒЫ РАДИАЦИЯЛЫҚ ХАЛ-АХУАЛЫНА ӘСЕРІН БАҒАЛАУ

[1]Лукашенко С.Н., [1]Айдарханов А.О., [1]Тимонова Л.В., [2]Силачев И.Ю., [2]Мильц О.С., [3]Рсымбетова Р.С.

[1]ҚР ҰЯО Радиациялық қауіпсіздік және экология институты
[2]ҚР ҰЯО Ядролық физика институты
[3]Санитарлық-эпидемиологиялық сараптамалаудың Маңғыстаулық облыстық орталығы

Бұл мақалада, Қазақстан Республикасының аумағындағы ауа ортасын мониторингілеу нәтижесі келтірілген. "Фукусима-1" АЭС апаттық жағдай ауа және су ортасының техногенді радионуклидтермен радиоактивті ластануына алып келді. Жапония аумағы және едәуір арақашықтықта орналасқан, оған көршілес мемлекеттердің аумағы радиоактиві ластануға ұшырады. Қазақстан Республикасының Ұлттық Ядролық Орталығының мамандары ҚР радиациялық хал-ахуалына апаттың әсер ету салдарын бағалау жұмыстарын жүргізді. ҚР ауа ортасында техногенді радионуклидтердің орын алғаны анықталды, алайда оның мөлшері ҚР Радиациялық қауіпсіздік нормаларымен бекітілген мәннен аспайды (РҚН-99).

Түйін сөздер: Радиациялық мониторинг, гамма-спектрометриялық өлшеулер, ^{131}I, ^{134}Cs, ^{137}Cs техногенді радионуклидтері, атмосфералық ауаның сынамаалғыштары, ұжымдық доза.

ОЦЕНКА ВЛИЯНИЯ АВАРИИ НА АЭС "ФУКУСИМА-1" НА РАДИАЦИОННУЮ СИТУАЦИЮ В РЕСПУБЛИКЕ КАЗАХСТАН

[1]Лукашенко С.Н., [1]Айдарханов А.О., [1]Тимонова Л.В., [2]Силачев И.Ю., [2]Мильц О.С., [3]Рсымбетова Р.С.

[1]Институт радиационной безопасности и экологии НЯЦ РК, Курчатов, Казахстан
[2]Институт ядерной физики НЯЦ РК, Алматы, Казахстан
[3]Мангистауский областной центр санитарно-эпидемиологической экспертизы, Актау, Казахстан

В данной статье представлены результаты мониторинга воздушной среды на территории Республики Казахстан. Аварийная ситуация на АЭС "Фукусима-1" привела к радиоактивному загрязнению водной и воздушной среды техногенными радионуклидами. Радиоактивному загрязнению подверглись территории Японии и сопредельных с ней государств, а также территории государств, расположенных на значительном удалении. Специалистами Национального ядерного центра Республики Казахстан (НЯЦ РК) проведена оценка влияния последствий аварии на радиационную ситуацию в РК. Зафиксировано присутствие техногенных радионуклидов в воздушной среде РК в количествах, не превышающих значения, установленных Нормами радиационной безопасности РК (НРБ-99).

Ключевые слова: Радиационный мониторинг, гамма-спектрометрические измерения, техногенные радионуклиды ^{131}I, ^{134}Cs, ^{137}Cs, пробоотборники атмосферного воздуха, коллективная доза.

УДК 504.75.05:615.849:539.16

DEVELOPMENT OF THE METHOD FOR DIRECT DETERMINATION OF ^{210}PB AND ^{214}BI ACTIVITY IN HUMAN BODY

Zhadyranova A.A., Kashirsky V.V., Shatrov A.N.

Institute of Radiation Safety and Ecology, NNC RK, Kurchatov, Kazakhstan

The paper discusses the development of the method for direct activity determination of incorporated ^{210}Pb and ^{214}Bi radionuclides in the human body. Knee joint which together with the shin bone is approximated as a cylinder has been chosen as an object for the measurements. A mathematical algorithm has been developed in this geometry to calculate the detection efficiency. The detection threshold comprised 120 Bq for ^{210}Pb and 270 Bq for ^{214}Bi.

Keywords: natural radionuclides, whole-body counter, internal irradiation, radionuclide distribution in organism, ^{214}Bi, ^{210}Pb, minimum detectable activity.

INTRODUCTION

Presence of the radionuclides ^{210}Pb, ^{214}Bi, ^{222}Rn, ^{226}Ra in the environment and their migration with food chains results in their intake by humans and subsequent internal irradiation of all human organs and tissues. The State Rules on control and assessment of radiation dozes for citizens of Kazakhstan require assessing the doze loads on population; this can be done by two methods: direct and indirect.

The direct method is the measurement of irradiation count rate in a specific organ or in a whole body; it implies detection of gamma-irradiation emitted by incorporated radionuclides by whole body counter (WBC) [1].

Spectrometry of body radiation makes it possible to identify in the human organism both the natural radionuclides (^{226}Ra, ^{232}Th, ^{210,212}Pb, ^{212,214}Bi, ^{40}K, ^{235,238}U) and γ-emitting radionuclides generated by the technology (^{60}Co, ^{134,137}Cs, ^{241}Am).

Isotopes ^{210}Pb and ^{214}Bi are members of ^{238}U natural series. Their basic intake pathways are the gastrointestinal tract via the alimentation chain and the respiratory tract via ^{222}Rn inhalation. According to the literature data [2-8], the average content of ^{226}Ra in the human body varies from one to dozens of Bq per body. In accordance with the radioactive equilibrium law, all radionuclides in the ^{226}Ra decay series, being in a closed system, have similar activity. In other words, the minimum activity of ^{214}Bi and ^{210}Pb in the human body would also be within the same range, from one to dozens Bq for each radionuclide. However, such level of radionuclides under study is caused by only ^{226}Ra intake by a human body. The real level of radionuclides under study in a human body would be higher due to the radon inhalation [9-12].

According to the biokinetic models, lead and bismuth isotopes from the lungs and gastrointestinal tract quite quickly migrate to the bone tissues. The ratio of the activity of lead and bismuth isotopes in the bone tissues to their activity in the soft tissues is 10. Hence, it is reasonable to measure ^{210}Pb and ^{214}Bi activity in the skeleton parts converting it to the whole body.

1. LITERATURE REVIEW

Currently in Kazakhstan there are no methods approved for determining ^{210}Pb and ^{214}Bi in human body using WBC; therefore, no institution has been carrying out such measurements.

The review of literature on the nature of radionuclides and their distribution in the human body has been carried out to choose basic elements of the procedure. Reference [13] presents the results of ^{210}Pb measurements in the human skeleton in a shielded chamber. According to the data, approximately 2 % of ^{210}Pb in the skeleton is due to the inhalation of radon, 86 % due to meal and approximately 12 % due to the direct inhalation of lead from air. Ref. [14] describes ^{210}Pb measurements in the bone tissues using NaI (Tl)-based scintillation detectors. The examinees were the miners at a uranium plant. It is also known about ^{210}Pb measurements in the brainpan. The measurements were carried out in a special shielded chamber at 8 m depth and under the ground [15]. From the literature review is follows that the bone tissues is the most promising organ for the measurements.

From Ref. [16] on the seasonal change of ^{214}Bi in the human body it can be inferred that radon passes quite quickly to the adipose tissues. In this paper it is also shown that radon is not fully exhaled during breathing; ^{214}Bi is found in high-fat tissues, primarily, in the cerebrum and abdominal cavity. The same paper presents the results of measuring ^{214}Bi in men and women bodies. The results show that the content of ^{214}Bi in the women body is higher than that in the men. Hence, it is advisable to carry out the measurements also for the adipose tissues.

Despite a diversity of papers on this subject, the obtained sources have not provided the specific description of measurement methods.

2. EXPERIMENT

2.1. Selection of basic elements for the method

The shin bone has been chosen as an object for the measurements because it has the highest volume and the lowest thickness of muscular-dermic tissue (in the knee joint). In the process of measurements, patella is regarded as an irradiator, and the distance between the patella and the bone is ignored.

^{214}Bi isotope has three basic γ–lines: 609.3 keV, 1120 keV and 1764 keV with 46.3 %, 15.1% and 15.4 % quantum yields, respectively. The line 609.3 keV has been chosen for the analysis because its quantum yield is three times higher than that of 1120 keV and 1764 keV lines. Hence, the statistical error in the total-absorption peak of 609.3 keV must be three times less compared to other emission lines.

^{210}Pb isotope is determined by the only γ– line of 46.5 keV with 4% quantum yield.

The coaxial arrangement of the shin bone and detector is most preferable for the measurements. In this case, the mathematical modeling of detection efficiency becomes simpler. The distance between the detector and the body, as regards its minimization on the one hand and safety of measurements on the other, is taken as 10 mm. An additional feature is that the shin bone is simulated well enough as a cylinder the geometry of which can be computed using medicine manuals for each examinee individually [17].

A semiconductor detector has been chosen as a gamma-radiation receiver because the resolution of scintillation detector does not make it possible to separate lines in the soft spectral region. The measurement geometry is illustrated in Figure 1.

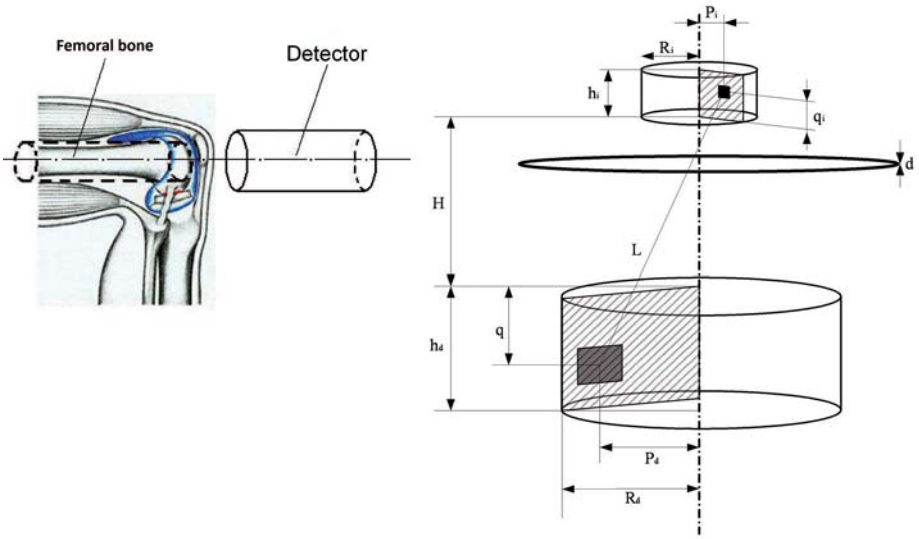

a) b)

Figure 1. Proposed measurement geometry (a) and "source-detector" arrangement (b)

2.2. Development of efficiency calibration mathematical algorithm

As the length of shin bone depends on the height, age, weight and sex, it is difficult to create a phantom that would imitate the human shin bone with different anthropometric parameters. It was, therefore, decided to develop a mathematical algorithm for the calculation of detection efficiency as a function of man's height.

2.2.1. Calculation of the efficiency calibration mathematical algorithm

For the calculation it is assumed that the detector and the source have regular cylindrical shape, consist of homogeneous materials, are collimated, and arranged as shown in the figure (Figure 1).

Here:

L - distance between the elementary volume of the detector and elementary volume of the source;

H - distance between the upper plane of the detector and the lower plane of the source;

h_i - height of the source;

h_d - height of the detector;

q_i - distance between the elementary volume of the source and the lower plane of the source;

q_d - distance between the elementary volume of the detector and the upper plane of the source;

P_i - distance between the elementary volume of the source and the source axis;

P_d - distance between the elementary volume of the detector and the detector axis;

R_i - radius of the source;

R_d - radius of the detector;

d - thickness of the detector window.

To account changes in the detection efficiency, we need to know the distance passed by gamma-ray quantum in the source, detector window and detector body from the elementary volume of the source (point of γ–ray quantum escape) to the elementary volume of the detector (point of γ–ray detection).

These distances are as follows:

the distance covered by γ-ray quantum in the detector window, L_o

$$L_0 = \frac{d \times L}{H + q_i + q_d} \tag{1}$$

the distance covered by γ-ray quantum in the source, L_i

$$L_i = \frac{q_i \times L}{H + q_i + q_d} \tag{2}$$

the distance covered by γ-ray quantum in the detector L_d:

$$L_d = \frac{q_d \times L}{H + q_i + q_d} \tag{3}$$

Then, attenuation of γ-ray quantum on its way from the elementary volume of the source to the elementary volume of the detector is

$$D = \exp\left\{-\frac{L \times (\mu_0 d + \mu_d q_d + \mu_i q_i)}{H + q_i + q_d}\right\}, \tag{4}$$

where: μ_0 - linear attenuation coefficient of the detector window material;

μ_d - linear attenuation coefficient of the detector material;

μ_i - linear attenuation coefficient of the source material;

Transferring to the mass attenuation coefficient, we have

$$D_m = \exp\left\{-\frac{L \times (\overline{\mu_0} d \rho_0 + \overline{\mu_d} q_d \rho_d + \overline{\mu_i} q_i \rho_i)}{H + q_i + q_d}\right\}, \tag{5}$$

where: $\overline{\mu_0}$ - mass attenuation coefficient of the detector window;
ρ_0 - density of the detector window material;
μ_d - mass attenuation coefficient of the detector material;
ρ_d - density of the detector material;
μ_i - mass attenuation coefficient of the source material;
ρ_i - density of the source material;
Then the activity due to elementary volume of the source detected in the elementary volume of the detector is:

$$dA_V = \frac{A_0 \times D_m \times L}{4\pi \times L^2 \times (H + q_i + q_d)} \times \rho_d \times \tau_d \times dq_i \times dq_d \times dp_i \times dp_d \times d\alpha \qquad (6)$$

where τ_d is the photo-ionization cross-section of the detector material.

Formula 6 should be integrated to calculate the activity of total volume of the source registered in the total volume of the detector.

$$A_V = \frac{A_0}{4\pi} \int\int\int\int\int \frac{D_m \times L}{L^2 \times (H + q_i + q_d)} \times \rho_d \times \tau_d \times dq_i \times dq_d \times dp_i \times dp_d \times d\alpha \,, \qquad (7)$$

A_0 is calculated using the formula

$$A_0 = \frac{N}{\varepsilon(E) \times I} \,, \qquad (8)$$

where N - registered count rate;
I - relative line intensity;
$\varepsilon(E)$ - detector recording efficiency.

$\varepsilon(E)$ - detection efficiency of the detector, equal to the ratio of the registered number of gamma-ray quantum to the number of gamma-ray quantum that hit the detector volume. This value depends on the radiation energy only, i.e. photoeffect cross section of the detector material, in this case germanium.

We write formula 7 as

$$A_V = \frac{N}{\varepsilon(E) \times I} \times K \qquad (9)$$

where K is the correction factor as a function of the geometry and density of the test sample:

$$K = \frac{1}{4\pi} \int\int\int\int\int \frac{D_m \times L}{L^2 \times (H + q_i + q_d)} \times \rho_d \times \tau_d \times dq_i \times dq_d \times dp_i \times dp_d \times d\alpha \qquad (10)$$

Formula (9) the change in the sample geometry takes into account the correction factor, so no need to be calibrated for each measurement geometry separately. To calculate the correction factor, a computational procedure in DELPHI software environment has been written using the numerical integration method.

2.2.2. Verification of the efficiency calibration mathematical algorithm

Three cylindrical test specimens with the validated ^{214}Bi activity have been prepared to verify the mathematical algorithm derived for accounting the geometrical factor influence on the measurements of cylindrical sources of γ–emission. The source geometry, averaged results of measurements and their deviation from the validated value are presented in the table (Table 1).

Table 1.

Dimensions of test specimens and results of ^{214}Bi activity tests

Sample No.	Mass, g	Diameter, mm	Height, mm	Average ^{214}Bi activity throughout tree parallel measurements, Bq/kg	Deviation from certified value, %
1	127	75.2	20.5	17.1 ± 0.3	0.6
2	79	61.4	19.1	17.4 ± 0.1	2.4
3	22	31.9	20	16.8 ± 0.6	- 1.2

Based on the performed experiments, a conclusion can be made that the mathematical algorithm developed for the calculation of correction factor makes it possible to carry out measurements with the cylindrical test specimens irrespective of their dimensions and density.

A change in the human shin bone length depending on the man's height may affect the measurements. Since the direct measurement of human shin bone length is rather difficult, the estimated values of shin bone length as a function of the man's height have been obtained from Ref. [18].

The algorithm enabled us to have calculated change in the detection efficiency as a function of human height. The calculations are shown in the table (Table 2).

Table 2.

Calculation data on ^{214}Bi and ^{210}Pb detection efficiency depending upon man's height

Human height, cm	Shin bone length, cm	Registration effectiveness, %	
		^{214}Bi	^{210}Pb
140	37.8	0.401	1.825
150	40.5	0.382	1.805
160	43.2	0.365	1.790
170	45.9	0.353	1.782
180	48.6	0.342	1.775
190	51.3	0.331	1.769
200	54.0	0.323	1.765
210	56.7	0.316	1.763

Figure 2 presents the dependencies diagrams.

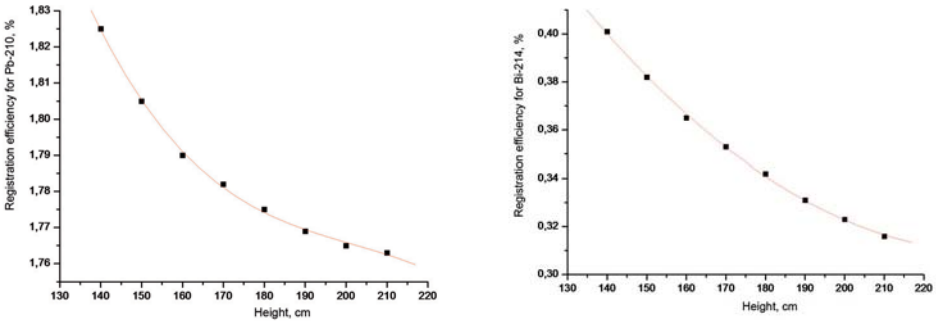

a b

Figure 2. Dependence diagram for the change in (a) ^{210}Pb and (b) ^{214}Bi detection efficiency depending upon the man's height

The presented dependencies are approximated well enough by a polynomial of the degree 2 for ^{214}Bi and a polynomial of the degree 3 for ^{210}Pb:

$$\varepsilon_{^{214}Bi} = 0,84904 - 0,00455 \times H + 9,58 \cdot 10^{-6} \times H^2 \quad (13)$$

$$\varepsilon_{^{210}Pb} = 3,1985 - 0,02066 \times H + 1,01 \times 10^{-4} \times H^2 - 1,67 \times 10^{-7} \times H^3 \quad (12)$$

where H is the man's height.

We also performed verification of the accuracy of accounting the difference in density and linear attenuation coefficients of the calibration source and bone tissue for soft energies. Table 3 lists mass fractions of chemical elements composing the sand and the bone tissue of shin bone and their corresponding linear attenuation coefficients for 46.5 keV line.

Table 3

Linear attenuation coefficients of shin bone sand and bone tissue for 46.5 keV gamma-emission

Substance	Element	Percentage	Linear attenuation factor μ_i, cm^{-1}
Sand	Si	0.33	0.5476
	O	0.49	
	Al	0.071	
	Fe	0.037	
Shin bone tissue	H	0.05	0.4475

As it is seen from the table, the difference between the linear coefficients μ_i for the two materials is up to 20 %. For the computations given in this paper, a linear attenuation coefficient of sand is used which, according to the preliminary estimations, may cause 10–15 %

overestimation in the measured values. However, subsequently we intend to introduce a correction factor for such effect.

2.4. Determination of the background characteristics and the detection limit.

To reduce the background in ^{210}Pb and ^{214}Bi detection region, the detector is placed in a lead shield with 8-cm walls. The lead shield already includes lead isotopes and its inner surface is, therefore, covered by a cadmium sheet serving as a filter for the soft gamma-emission. As the camera walls contain natural radionuclides, the detector shield has been tested by moving it off from the camera walls. The test has been performed in the presence of lead shield and without it.

The data on the background rate of count in ^{210}Pb detection windows with a cadmium filter and without it and the data on the background rate in ^{210}Pb and ^{214}Bi detection windows depending on the distance from the camera cells are listed in Table 4.

Table 4.

Background count rates for ^{210}Pb and ^{214}Bi at different detection conditions

Nuclide	Background, count per second					
	With cadmium	Without cadmium	Detector-to-camera wall distance			
			70 cm		180 cm	
			Shielded	No shield	Shielded	No shield
^{210}Pb	0.012	0.018	0.012	0.044	0.012	0.028
^{214}Bi	-	-	0.370	0.622	0.356	0.518

As it is seen from the Table, the optimal is the combination of lead shield and cadmium filter and remoteness from the detector and the camera walls.

A series of MDA computations has been carried out at different exposure times to choose the exposure time (Table 5).

The experimental data show that an increase in the time for more than 3 hours does not increase greatly the sensibility. Hence, the most optimal exposure time is 3 hours, which is conditioned by a necessity to minimize the statistical error taking into account a possibility of a man to stand motionless in the same position.

Table 5

Dependence of MDA on measurement time

Measurement time, h	MDA ^{210}Pb, Bq	MDA ^{214}Bi, Bq
1	260	610
2	185	430
3	140	330
4	130	305
5	120	270

A series of phantom measurements of human shin bone filled with distilled water has been carried out to assess HCS in ^{210}Pb and ^{214}Bi detection windows. The background in the region of total absorption peak of the nuclide is 0.012±0.002 counts per second for ^{210}Pb and 0.36±0.01 counts per second for ^{214}Bi. To determine the minimum detectable activity, we used the 3σ criterion:

$$MDA = 3 \cdot \frac{\sqrt{S_\Phi}}{\varepsilon(\mathrm{E}) \cdot I \cdot t} \tag{13}$$

where S_F is the total number of background pulses in the ^{214}Bi and ^{210}Pb detection windows, t stands for exposure time, $\varepsilon(\mathrm{E})$ is the detection efficiency of the detector for the principal emission line of ^{214}Bi and ^{210}Pb, and I is the quantum yield of principal emission lines for ^{214}Bi and ^{210}Pb.

At 180 min time of spectrum registration and 70 kg weight of an examinee, the detection limit for ^{214}Bi is 35 Bq/kg-bone and for ^{210}Pb - 15 Bq/kg-bone.

3. DESCRIPTION OF ^{210}PB AND ^{214}BI DIRECT DETERMINATION METHOD

3.1. General description of the method

In accordance with the developed method of ^{210}Pb and ^{214}Bi detection in the human body, the measurement procedure is as follows.

- Prior to the measurements, the examinee takes a shower to wash off the daughter products of radon's radioactive decay from the skin and changes into special working clothes.
- The examinee's anthropometric parameters: height, average diameter of distal parts of shoulder, forearm, lower leg and shin are measured. The measurement of distal parts of shoulder, forearm, thigh and shin is performed using the anthropometric points in accordance with the medical rules of their measurement.
- The examinee is placed in an armchair in a sitting position. The detector is taken to the knee joint and fixed. The detector-to-knee joint distance is 1 cm.
- After fixing the measurement geometry, the spectrum collection is started. The exposure time is 3 h.
- Based on the spectrum collection, the ^{210}Pb and ^{214}Bi activities for the whole body of examinee and the corresponding errors are computed.

3.2. Hardware

The following equipment is used for the measurements:

- Semiconductor detector BE3830 based on high-purity germanium, Canberra. The energy resolution is 376 eV for 5.9 keV line, 641 eV for 122 keV line, and 1694 eV for 1332 keV line.
- Lead collimator covered inside with a 2 mm-thick cadmium sheet. Thickness of the lead collimator walls is 8 cm.
- Multichannel analyzer of pulses, DSA2000 with 1024 number of channels;
- Caliper, height meter to measure anthropometric parameters of a man.

3.3. Calculation of specific activity and its errors

After processing and identification of spectra, the background in the total-absorption peak areas of ^{210}Pb and ^{214}Bi principal emission lines is taken into consideration:

$$S = S_{Полная} - \frac{t}{t_Ф} \cdot S_Ф \,, \tag{14}$$

where S is the total-absorption peak areas of ^{210}Pb and ^{214}Bi principal emission lines minus the background, $S_{Полная}$ is the total-absorption peak areas of ^{210}Pb and ^{214}Bi principal lines in examinee's spectrum, and t is the time of spectrum collection.

The absolute error of S value is determined by the following expression

$$dS = \sqrt{\left(dS_{Полная}\right)^2 + \left(\frac{t}{t_Ф}\right)^2 (dS_Ф)^2} \tag{15}$$

where $dS_{Полная}$ and dS_F are the statistical errors of total absorption peak areas and background in ^{210}Pb and ^{214}Bi detection windows in the examinee's spectrum.

Specific activities of ^{210}Pb and ^{214}Bi in the shin bone surveyed are

$$A_{^{214}Bi} = \frac{S}{(0{,}84904 - 0{,}00455 \times H + 9{,}58 \cdot 10^{-6} \times H^2) \cdot t \cdot I \cdot m_{б.к.}} \times K \tag{16}$$

$$A_{^{210}Pb} = \frac{S}{(3{,}1985 - 0{,}02066 \times H + 1{,}01 \times 10^{-4} \times H^2 - 1{,}67 \times 10^{-7} \times H^3) \cdot t \cdot I \cdot m_{б.к.}} \times K \tag{17}$$

where $m_{б.к.}$ is the calculated weight of examinee's shin bone.

The error of ^{210}Pb and ^{214}Bi specific activity without considering the errors due to the dependence of shin both length on the man's height and the ratio of activity of lead and bismuth isotopes in the bone tissues to their activity in the soft tissues at 95% confidence probability is

$$dA_m = 2 \cdot \sqrt{\left(\frac{dS}{\varepsilon(E) \cdot t \cdot I \cdot m_{б.к.}}\right)^2 + \left(\frac{S \cdot d\varepsilon(E)}{\varepsilon(E)^2 \cdot t \cdot I \cdot m_{б.к.}}\right)^2} \tag{18}$$

The measured result is written as: $A_m \pm dA_m$.

3.4. Calculation of activity per human body

Based on the results of measuring the anthropometric parameters, the surveyed skeleton weight is calculated using the formula [19]:

$$m = 1.2 \times Q^2 \times H \,, \tag{19}$$

where m i is the weight of skeleton surveyed, Q is the average diameter of distal parts of shoulder, forearm, hip and lower leg of examinee, and H is the height of examinee.

When the specific activities of ^{210}Pb and ^{214}Bi in the human shin bone are equal to $A_{б.к}$ (^{210}Pb) and $A_{б.к.}$ (^{214}Bi) Bq/kg, the absolute activities of these radionuclides per skeleton are accordingly equal to $A(^{210}Pb)_{б.к.} \times m$ and $A(^{214}Bi)_{б.к.} \times m$.

According to the literature data, the ratio of activity of lead and bismuth isotopes in bone tissues to their activity in soft tissues is taken as 10.

Making a proportion, we convert the activity of ^{210}Pb and ^{214}Bi in a skeleton to the whole body.

$$A_{мягкиеткани,^{214}Bi} = \frac{A(^{214}Bi)_{б.к.} \times m}{10} (Бк) \quad (20)$$

$$A_{тело,^{214}Bi} = A(^{214}Bi)_{б.к.} \times m + \frac{A(^{214}Bi)_{б.к.} \times m}{10} (Бк) \quad (21)$$

$$A_{мягкиеткани,^{210}Pb} = \frac{A(^{210}Pb)_{б.к.} \times m}{10} (Бк) \quad (22)$$

$$A_{тело,^{210}Pb} = A(^{210}Pb)_{б.к.} \times m + \frac{A(^{210}Pb)_{б.к.} \times m}{10} (Бк) \quad (23)$$

CONCLUSION

The method for direct assessment of ^{210}Pb and ^{214}Bi activity in the human body has been developed. The detection limits are 120 Bq for ^{210}Pb and 270 Bq for ^{214}Bi.

Taking into consideration that the content of ^{226}Ra in the human body varies within 10 Bq per body, sensibility of the developed procedure is definitely not sufficient to carry out the public examination. However, the achieved detection limit can be quite sufficient for examination of personnel in case of emergencies at uranium mining enterprises.

For qualitative public examination it is necessary to reduce the detection limit of this procedure by one or two orders. It can be achieved by decreasing the general WBC background by its installation in a more perfect shield against background radiation and increasing the number of detectors.

REFRENCES

1. Оценка профессионального облучения вследствие поступления радионуклидов Серия норм МАГАТЭ по безопасности № RS – G – 1.2. - Вена, Австрия: МАГАТЭ, 1999. - С. 21 -31.
   Assessment of Occupational Exposure due to intakes of radionuclides. IAEA Safety Standards Series No. RS-G-1.2. – Vienna, Austria: IAEA, 1999.
2. Internet resource: http://www.proatom.ru/modules.php?name=News&file=article&sid=129
3. Учебно-методическое руководство по радиоэкологии и обращению с радиоактивными отходами для условий Казахстана. – Алматы: ОАО «Волковгеология», 2002. - С. 139 - 142.
   Methodological guide on radioecology and handling the radioactive wastes in Kazakhstan. – Almaty: Public Corporation "VolkovGeologiya", 2000. – pp. 139-142. – [in Russian].
4. Голутвина М.М. Контроль за содержанием радиоактивных веществ в организме человека / М.М. Голутвина, Н.М. Садикова. – М.: Атомиздат, 1979. – С. 34 – 36.
   Golutvina M.M. Contol for content of radioactive substances in human organisms / Golutvina M.M., Sadikova N.M. – M.: Atomizdat, 1979. – pp. 34-36. – [in Russian].
5. Пивоваров Ю.П. Радиационная экология /Ю.П.Пивоваров, В.П.Михалев. – Москва: Издательский центр «Академия», 2004. – С. 10.
   Pivovarov Yu.P. Radiation ecology / Pivovarov Yu.P., Mikhalev V.P. – Moscow: Printing Center "Akademiya", 2004. – p. 10. – [in Russian].
6. Радиационная защита Рекомендации Международной комиссии по радиологической защите (вторая публикация) Государственное издательство литературы в области атомной науки и техники. – Москва, 1961. - с. 75.
   Radiation Safety. Recommendations of the International Committee on Radiological Safety (second edition). State publishing house for literature on nuclear science and techniques. – Moscow, 1961, p. 75. – [in Russian].
7. Голутвина М.М. Контроль за поступлением радиоактивных веществ в организм человека и их содержанием / М.М.Голутвина, Ю.В.Абрамов. – Москва: Энергоатомиздат, 1989. - С. 89.
   Golutvina M.M. Contol for intake of radioactive substances into human organisms and content of them. / Golutvina M.M., Abramov Yu.V.. – Moscow: Energoatomizdat, 1989. – p.89. – [in Russian].
8. Моисеев А.А. Справочник по дозиметрии и радиационной гигиене / А.А. Моисеев, В.И. Иванов. - Москва: Энергеатомиздат, 1984. - С. 91.
   Moiseyev A.A. Reference book on dosimetry and radiation hygiene / Moiseyev A.A, Ivanov V.I. – Moscow: Energoatomizdat, 1084. – p. 91. – [in Russian].
9. Internet resource: http://narod.yandex.ru/100.xhtml?profbeckman.narod.ru/Uran.files/Glava10.pdf

10. Internet resource: http.www.IATP.BY.mht
11. Internet resource: http.www.Радионуклиды_1.mht
12. Internet resource: http.www.ОМЗ-Естественный(природный)радиационный-фон.mht
13. Internet resource: http://www.inive.org/members_area/medias/pdf/Inive%5CRadon1999%5C165.pdf
14. Internet resource: https://www.osti.gov/opennet/servlets/purl/16289240-4kKkUJ/16289240.pdf
15. Internet resource: http://www.helmholtz-muenchen.de/iss/personendosimetrie/projects/partial-body-counter-towards-personalised-dosimetry/index.html
16. Internet resource: http://healthandenergy.com/images/HPMay0736.pdf
17. Internet resource: http://www.skeletos.zharko.ru/main/G131
18. Internet resource: http://forens.ru/index.php?showtopic=2386
19. Осанов Д.П. Дозиметрия и радиационная биофизика. - М.: Энергоатомиздат, 1983.-230с.
    Osanov D.P. Dosimetry and radiation biophysics. – M: Energoatomizdat, 1983. – 230 pp. – [in Russian].
20. Internet resource: http://www.forens-med.ru/book.php?id=272Ресурс
21. Мартиросов Э.Г. Технологии и методы определения состава тела человека / Э. Г. Мартиросов, Д.В. Николаев, С.Г. Руднев. – Москва: Наука, 2006. – С. 32 -50.
    Martirosov E.G. Technologies and methods of determination of human body contents / Martirosov E.G., Nikolayev D.V., Rudnev S.G. – Moscow: Nauka, 2006. – pp. 32-50. – [in Russian].

АДАМНЫҢ ДЕНЕСІНДЕГІ ^{210}Pb ЖӘНЕ ^{214}Bi БЕЛСЕНДІЛІГІН ТУРА АНЫҚТАУДЫҢ ӘДІСТЕМЕСІН ӘЗІРЛЕУ

Жадыранова А.А., Каширский В.В., Шатров А.Н.

ҚР ҰЯО Радиациялық қауіпсіздік және экология институты, Курчатов, Қазақстан

Бұл мақалада, адамның денесіндегі ^{210}Pb және ^{214}Bi радионуклидтерінің бір құрамға біріктірілген белсенділігін тура анықтаудың әзірленген әдістемесі мен оны апробациялаудың нәтижелері келтірілген. Өлшеу нысаны ретінде тізе буындары алынды, ол ортанжілік сүйекпен цилиндр ретінде жуықтайды. Аталған геометрияда тіркеу тиімділігін есептеу үшін математикалық алгоритм әзірленді. Бір топ тұлғаларды өлшеу нәтижелері бойынша, адамның денесіндегі ^{214}Bi және ^{210}Pb белсенділігінің мәні, сыртқы аяның жоғары деңгейімен шартталған айтарлықтай жоғары шаманың шегі түрінде алынды.

Түйін сөздер: табиғи радионуклидытер, адамның сәулеленуін есептегіш, ішкі сәулелену, ағзада радионуклидтердің таралуы.

РАЗРАБОТКА МЕТОДИКИ ПРЯМОГО ОПРЕДЕЛЕНИЯ АКТИВНОСТИ ^{210}Pb И ^{214}Bi В ТЕЛЕ ЧЕЛОВЕКА

Жадыранова А.А., Каширский В.В., Шатров А.Н.

Институт радиационной безопасности и экологии НЯЦ РК, Курчатов, Казахстан

В данной статье представлена разработка методики прямого определения активности инкорпорированных радионуклидов ^{210}Pb и ^{214}Bi в теле человека. В качестве объекта измерения выбран коленный сустав, который вместе с бедренной костью апроксимируется как цилиндр. Для расчета эффективности регистрации в данной геометрии разработан математический алгоритм. Предел обнаружения для ^{210}Pb составил 120 Бк, для ^{214}Bi – 270 Бк.

Ключевые слова: естественные радионуклиды, счётчик излучения человека, внутреннее облучение, распределение радионуклидов в организме, ^{214}Bi, ^{210}Pb, минимально детектируемая активность.

УДК:577.4:621.039.58:541.28

DEVELOPMENT OF CORE STAGES FOR INORGANIC LIQUID RADIOACTIVE WASTE REPROCESSING TECHNOLOGY FROM REACTOR PLANT BN-350

Korovina O. Yu., Lukashenko S.N., Kashirsky V.V., Zvereva I.O.

Institute of Radiation Safety and Ecology NNC RK, Kurchatov, Kazakhstan

This paper is devoted to the research aimed at the development of an efficient technology for reprocessing of liquid radioactive waste (LRW), formed as a result of operations of the fast neutron reactor (BN-350) located in Aktau (Kazakhstan). In our experiments we used model solutions simulating the chemical composition of the liquid radioactive waste from BN-350, determined as a result of theoretical and practical estimations.

The technology suggested for reprocessing of liquid radioactive waste is based on the successive destruction of the LRW organic component and the deposition of radionuclides with special reagents, selected taking into account chemical properties of radionuclides in the BN-350 liquid radioactive waste and economic costs of waste reprocessing.

Based on the experimental studies we suggested the main stages of the technology to be used for reprocessing of the LRW from BN-350 and determined their optimal conditions. It was found out that the most appropriate method to be used to oxidize the LRW organic component is the permanganate oxidation, and to cleanup the LRW from Cs isotope it was proposed to use a cheaper sorbent – a freshly prepared suspension of copper ferrocyanide.

Keywords: reprocessing of liquid radioactive waste, fast neutron reactor, radionuclide composition of LRW from BN-350, efficiency estimate of LRW purification, permanganate oxidation of LRW, sorption purification of LRW, copper ferrocyanide, the degree of purification of radionuclides, Trilon B, oxalic acid, ^{241}Am, ^{154}Eu, isotopes of Pu, ^{90}Sr, ^{134,137}Cs, ^{60}Co, ^{54}Mn, ^{90}Sr.

INTRODUCTION

By the present time almost 5,000 m^3 of liquid radioactive wastes of total activity of 10^7-10^8 Bq/l have been accumulated in the storage facilities of the Mangustau Nuclear Power Plant in Aktau. The radioactivity of the LRW is mainly due to the radionuclides ^{134,137}Cs, ^{60}Co, ^{54}Mn, ^{90}Sr, ^{241}Am, and plutonium isotopes. A long-term storage of the LRW of various chemical composition with high salt concentration causes corrosion of construction materials of the reservoir. Therefore, long-term storage of large LRW volumes is a source of radiation and ecological hazard to the region. It is necessary to solve this problem, and its solution requires large capital investments.

A project of a complex for reprocessing of the LRW from the reactor plant BN-350 has been developed [1]. According to various estimates, the total cost of construction of the technological complex and its further implementation for LRW processing amounts to several tens of billions of tenge. These facts formed the basis for the tests aimed at search for a more efficient and economically acceptable technology.

In order to process the LRW accumulated in the reactor facility BN-350, the Russian specialists from RAOTEKH offered to use a technology including the following stages: preliminary filtration and preparation of the initial solution, oxidation of the LRW organic

component with the usage of ozone, filtration and selective cesium sorption by the sorbent Termoksid-35.

It was offered to use ozone as an oxidizer in order to decompose the organic component. Ozone has high oxidation ability, and it efficiently oxidizes organic compounds, even in solutions with high salt concentration [2]., Ozonation, however, has some disadvantages: an explosion risk in the process, high cost because of high power consumption, and the necessity to mount the ozonation station. This makes it necessary to carry out investigations aimed at the development of an economically attractive technology, providing higher safety. It is known that the oxidizing ability of potassium permanganate is not lower than that of ozone, and its application in technological processes meets the requirements of safety and economic efficiency.

After decomposition of the LRW organic component and cleaning wastes from $^{6^{\circ}}$Co and ^{54}Mn, the project envisages sorption cleaning of the BN-350 LRW from the major radioactive contaminant – cesium isotopes. At this stage it was proposed to use Termoksid-35: a spherical-granulated sorbent consisting of nickel ferrocyanide on the inorganic carrier – zirconium hydroxide. However, in this case the usage of the commercial product Termoksid-35 is not unambiguous. According to the results of laboratory analyses [3], in 90%-100% of cases the above sorbent was used to clean LRW from cesium isotopes. However, to clean highly mineralized LRW solutions from Cs isotopes, a large amount of Termoksid-35 is needed. As a result of this technology a large amount of solid radioactive wastes (SRW) will be formed, which will hamper the technological process and require additional economic expenses. Of greater interest is the other, a simpler method of LRW cleaning from Cs isotopes, i.e. sorption on ferrocyanide of transition metals (copper, nickel). The study of the properties of this sorbent and Termoksid-35 in model solutions as well as the determination of optimal conditions of their application will enable us to choose the most efficient and economically profitable method of LRW cleaning from Cs isotopes.

Based on the experimental studies and literature sources we chose the main stages of the reprocessing technology for the BN-350 liquid radioactive wastes, which included destruction of the organic component of liquid radioactive wastes by permanganate oxidation with the intermediate stage – filtration, and LRW cleaning from Cs isotopes by the sorbent. After experimental studies, the necessity of additional stages of cleaning for specific radionuclides will be determined.

1. EXPERIMENTAL PART

The object of investigations was model solutions of liquid radioactive wastes prepared on the base of:

- organic compounds (sodium ethylene diamine tertaacetate (EDTA) – trilon B, oxalic acid);
- organic compounds (sodium ethylene diamine tertaacetate (EDTA) – trilon B, oxalic acid, mineral salts and radioactive indicators (tracers) used to model the chemical composition of the BN-350 LRW).

As salts, the salts of stable isotopes (Co, Mn, Sr, Cs, Ca, Fe, K, Mg, Na) in the form of metal nitrates, chlorides and sulfides were used. As isotope markers, we used the solutions

containing a certified amount of radionuclides ^{241}Am, ^{154}Eu, and ^{242}Pu. The amount of Trilon B in 1 liter of the model solution was 30g, the amount of oxalic acid was 8.5 g/l.

The composition of the model solution, maximally close to the LRW solution from BN-350, is presented in Table 1.

Table 1.

Composition of the model solution

Organic compound	Element composition, μg/l									Volume activity, Bq/l		
	Cs	Sr	Mn	Co	Na	Mg	Ca	Fe	K	^{241}Am	^{154}Eu	^{242}Pu
Trilon B + oxalic acid	16	7	31	47	19 000	11 400	4 000	750	470	20	1	0.5

1.1. Investigation of the method of permanganate oxidation of the LRW organic compound with subsequent separation of precipitations by filtration

The following three-stage procedure was used to determine the destruction efficiency of the LRW organic component by permanganate oxidation:

1. Determination of optimal parameters of Trilon B oxidation;
2. Determination of optimal parameters of oxalic acid oxidation;
3. Determination of optimal parameters of oxidation of the organic component of the model solution, whose chemical and radionuclide composition is as much as possible close to that of the BN-350 LRW.

The choice of optimal oxidation conditions for the LRW organic component implied the choice of the amount of potassium permanganate needed for oxidation in various media (acid, neutral and alkaline). The experiments were carried out in normal conditions (t=20±2 °C). In order to determine the degree of decomposition of the organic component in permanganate oxidation, the concentrations of Trilon B and oxalic acid were determined by the titrimetric method. To determine the Trilon B concentration in the solution, the method of titration of the 0.1H model calcium chloride solution in the presence of indicator – murexide (color transfer from violet to rose-red) was used. To determine the concentration oxalic acid in model solutions, the model solution was titrated by the 0.1H solution of potassium permanganate in the presence of sulphuric acid (till a rose color appeared).

To estimate the efficiency of the method suggested for cleaning of BN-350 liquid radioactive wastes from radionuclides, the concentration of radionuclides in the model solution after oxidation and filtration was determined. The precipitations formed in the process of permanganate oxidation were separated from the model solution by two types of filtration: rough filtration (on the paper filter "blue ribbon") and fine filtration (on the membrane filter with a pore diameter less than 0.2 μm).

To determine the concentration of radionuclides in the model solution after oxidation and filtration, gamma-spectrometric (determination of concentration of ^{241}Am and ^{154}Eu), alpha-spectrometric (determination of ^{242}Pu concentration) and mass-spectrometric (Co, Mn,

Sr, Cs, Ca, Fe, K, Mg, Na) analyses were used. The gamma- spectrometric analysis was made by direct measurements of filtered solutions on the gamma-spectrometer with a semiconductor detector from a super-pure germanium (BE3830, Canberra). The sediment formed after oxidation and filtration was dissolved in a small amount of hydrochloric acid and was subjected to preliminary radiochemical cleaning according to the standard method used to determine the concentration of plutonium isotopes with ion-exchange resin AB-17. The alpha-source obtained in the analysis was measured on the alpha-spectrometer (AlphaAnalyst, Canberra). The element composition of the samples was determined on the mass-spectrometer with inductively coupled plasma (Elan9000, PerkinElmer). The model solutions after oxidation and filtration were studied.

In the investigations special attention was paid to the control of the medium pH, which was made using a pH-meter (SevenEasy, MettlerToledo).

Determination of optimal parameters for Trilon B oxidation

To choose optimal parameters for trilon B oxidation by potassium permanganate, the experimental studies of oxidation of the model solution with trilon B concentration of 0.58 N. (97.4g) were carried out. As the trilon B concentration in the solution increases, its solubility decreases, and the salt precipitates [4].

Using the data from [5], the oxidation was made with a 5% solution of potassium permanganate in standard conditions (t=20±2 °C) in various media (acid, neutral and alkaline). The solution of potassium permanganate was added to the model solution of trilon B drop-by-drop with constant mixing. If sediment was formed, the oxidation was stopped, the solution was kept for 15-20 minutes, filtered and trilon B concentration in the solution was determined.

The pH of the medium was regulated by adding ammonium hydroxide (to get an alkaline medium) or concentrated sulfuric acid (to get an acid medium) to the model solution.

When sulfuric acid was added to the model solution, white sediment was formed. According to literature data [6] a clear dependence of complexon (including trilon B) solubility on medium pH with maximum for pH=0-3 is observed at room temperature. In this case, under the acid action the protonated salts of EDTA, which have lower solubility than ordinary salts such as Me-EDTA, are formed.

In order to determine the amount of trilon B in the solution after adding sulfuric acid and precipitation, the solution was filtered through a paper filter, after which the trilon B concentration in the solution was redetermined.

In all cases, the sediment was filtered through the paper filter "blue ribbon". The amount of trilon B remained in the solution was determined with a titrimeter.

In the experiments 100ml model solutions were used.

Experimental results and discussion

In the process of permanganate oxidation of trilon B in the alkaline medium a sediment was formed, whose color varied from green to dark brown. In the oxidation in the acid or neutral medium, the color of the solution varied from dark red to brown, with formation of a small amount of sediment.

The results of permanganate oxidation of model solutions with different pH of the medium are presented in Figure 1.

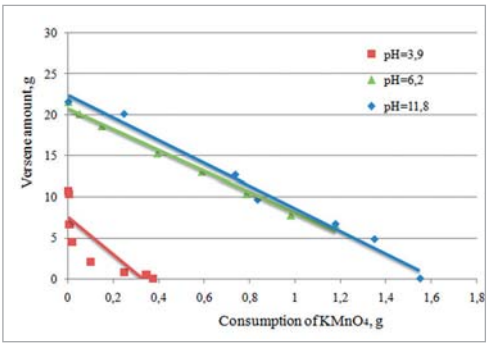

Figure 1. Trilon B concentration in the solution vs the amount of potassium permanganate consumed

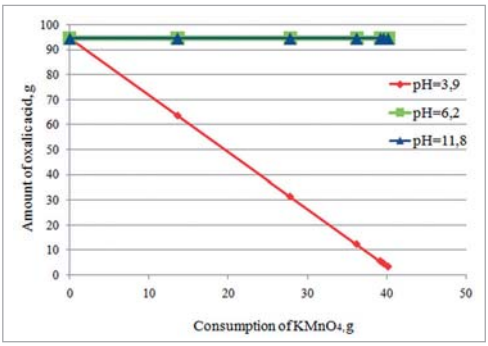

Figure 2. Oxalic acid concentration in the solution vs the amount of potassium permanganate consumed

The obtained results show that the processes of trilon B oxidation in all three media (acid, neutral and alkaline) do not differ considerably, which is demonstrated by almost the same slope of lines at different pH values. One can suppose that it is preferable to carry out oxidation in the acid medium as the amount of consumed potassium permanganate can be reduced even at required pH values due to formation of indissoluble protonated EDTA salts.

The investigations showed that about 0.8g of potassium permanganate is needed to decompose 1g of trilon B.

Determination of optimal parameters for oxalic acid oxidation

In order to determine the amount of potassium permanganate needed to decompose the oxalic acid, theoretical calculations and experimental studies of the oxidation of model solutions with various concentrations of oxalic acid and various pH values were carried out.

To determine the solubility of oxalic acid a saturated acid solution was prepared. The sediment formed in the oversaturated solution was filtered. The acid concentration was determined by titration with a standard solution of potassium permanganate. For titration the aliquot parts (~30 ml) of the oxalic acid solution were taken, which were acidified by the concentrated HNO_3 solution and filtered by potassium permanganate during heating in the water bath (t= 70-80 °C). The solution was titrated till the appearance of the pale-rose color, not disappearing for 2-3 minutes.

To determine the amount of potassium permanganate needed to oxidize the oxalic acid, the solutions with concentrated oxalic acid: 95, 64, 31, 12, 6, 5 and 3 g/l were prepared. The model solutions were oxidized by a 5% solution of potassium permanganate under normal conditions (t=20±2 °C) in acid, neutral and alkaline media. The pH of the medium was regulated by adding either ammonium hydroxide (to obtain an alkaline medium) or concentrated HNO_3 solution (to obtain an acid medium) to the model solution. We used 100ml of model solutions in the investigations.

Experimental results and discussion

In the experiments on the oxalic acid oxidation in the acid medium, the color of the solution changed to rose, and after a few minutes of sedimentation some dark-brown sediment was formed. It is important to note that in the alkaline medium the potassium permanganate does not oxidize oxalates [7].

The results of permanganate oxidation of model solutions are presented in Figure 2.

According to the literature data [7], the oxalic acid oxidation in the alkaline medium proceeds according to the reaction stochiometry:

$$5C_2O_4^{2-} + 2MnO_4^- + 16H^+ \rightarrow 10CO_2 + 2Mn^{2+} H_2O$$

In this case the theoretical calculation shows that to decompose 1g of oxalic acid in the alkaline medium 0.68g of potassium permanganate is needed. In our experimental studies about 0.71g of potassium permanganate was used to decompose 1g of oxalic acid.

Based on the fact that the decomposition of trilon B requires 0.08g of potassium permanganate, and the decomposition of 1g of oxalic acid requires 0.71 g of the oxidizer, we calculated the amount of potassium permanganate needed to decompose the complex-forming component in model solutions imitating the composition of BN-350 LRW. According to the calculation, to decompose 1 liter of LRW solution (containing 30g of trilon B and 8.5g of oxalic acid) it is necessary to spent about 8.4g of potassium permanganate.

Testing of the technology chosen for oxidation of the organic component using a model solution, the chemical and radionuclide composition of which is very close to that of BN-350 LRW

In order to test efficiency of the suggested oxidation technology on the LRW organic component by potassium permanganate, the model solution, whose chemical composition is given in Table 1, was oxidized. The oxidation was carried out under standard conditions in acid, neutral and alkaline media. The pH of the medium was regulated by adding either ammonium hydroxide (to get an alkaline medium) or concentrated sulfuric acid (to get an acid medium) to the model solution.

The volume of model solutions was 100ml, and the amount of added potassium permanganate was 0.7g. The potassium permanganate was added in small amounts; the solution was mixed, and left for sedimentation for 5-15 minutes depending on the speed of sedimentation of the formed sediment. When all calculated amount of potassium permanganate was added, the solution was filtered through a paper filter. To determine the concentration of ^{242}Pu in the solution, it was first measured on the gamma-spectrometer (to determine ^{241}Am concentration), and then on the mass-spectrometer with inductively-coupled plasma (to determine concentration of Co, Sr, Cs and Fe). The results of experiments were used to estimate the degree of cleaning of model solutions from radionuclides at the stage of oxidation of LRW organic compound at various pH values.

Experimental results and discussion

The results of different levels of cleaning of the LRW model solutions from radionuclides after oxidation and separation of formed sediments by filtration are presented in Figure 3.

The obtained data show that the efficiency of isotope extraction in the alkaline medium is higher except for iron, which is better extracted from the solution in the acid medium and could act as a co-precipitator of plutonium isotopes. However, in the process of permanganate oxidation, no co-oxidation of plutonium and iron was observed. Rather high values were obtained in cleaning of Cs, Sr, Co and Am isotopes. After testing the main stages of the LRW cleaning, the additional studies of waste cleaning from specific radionuclides, in particular, plutonium isotopes will be carried out. The data on cleaning in the neutral medium

are not presented, as after adding of the calculated amount of potassium permanganate to the medium, even after a long time period, no sediment was formed. It enables us to make an assumption that cleaning at the given pH values will not proceed.

Obviously, it is necessary to introduce additional stages for additional cleaning from transuranium radionuclides and ^{90}Sr.

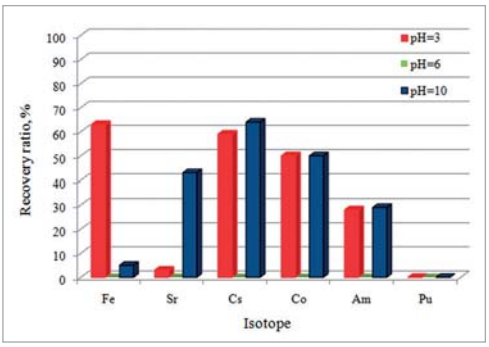

Figure 3. The efficiency of cleaning of the LRW model solution from radionuclides for various pH values

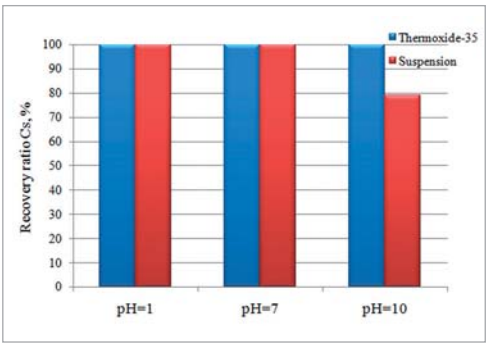

Figure 4. The efficiency of cesium extraction from model solutions for various pH values

Choice of the method for LRW cleaning from cesium isotopes

In order to choose the most efficient method of LRW cleaning from Cs isotopes, the model solutions were cleaned with the industrial sorbent – Termoksid-35 and fresh suspension of copper ferrocyanide.

The efficiency of cleaning of model solutions from cesium isotopes was studied in acid, neutral and alkaline media at normal conditions (t=20±2 °C). The pH of the medium was regulated by adding either ammonium hydroxide (to get an alkaline medium) or concentrated sulfuric acid (to get an acid medium) to the model solution. In the experiments we used the model solutions, whose composition is shown in table 1. The volume of each sample was 100ml. The experiments were repeated three times.

The sorption ability of Termoksid-35 was studied by filtering a model solution through a stationary sorbent layer in the chromatographic column at a constant speed (1 column volume (40ml) per hour). The experiment was made on a glass column with an internal diameter of 7.9mm. The sorbent mass (Termoksid-35) in the column was 5g. After filtering solution through the sorbent, it was analyzed on the mass-spectrometer in order to determine Cs amount.

The suspension was prepared in the laboratory by mixing equal volumes of 0.25M $K_4[Fe(CN_6)]$ and 0.5M $CuSO_4$. The required pH value of the suspension (pH=2) was obtained by adding nitric acid to the solution. After adding of 50ml of the suspension to the model solution (which is equivalent to 1g of copper ferrocyanide), the solution was mixed for 30 minutes. After 15-hour sedimentation, the solution was filtered through a paper filter "blue ribbon", and was analyzed on the mass-spectrometer to determine the Cs amount.

In order to choose the most economically profitable method of precipitation of Cs isotopes from LRW solutions, sorption capacities of the two sorbents – Termoksid-35 and copper ferrocyanide suspension – were compared.

According to the project data [8], the sorption capacity of 1kg of Termoksid-35 for Cs isotopes is about $3.4 \cdot 10^{10}$ Bq.

In order to determine sorption capacity of copper ferrocyanide, prepared in laboratory conditions, two 100ml model solutions prepared in the base of distilled water and stable Cs in a form of its salt $CsNO_3$ (2 and 20mg/l) were used. Using the above-described method, the copper ferrocyanide suspension was prepared and added to model solutions. After sedimentation, the solutions were filtered through a paper filter. The Cs amount in the solution after cleaning was determined using the mass-spectrometric analysis. The experiment was repeated two times.

Experimental results and discussion

Comparative efficiency analysis of two sorbents Termoksid-35 and copper ferrocyanide suspension are presented in Figure 4.

According to the obtained data, the LRW can be cleaned up to 99.9% from Cs employing these sorbents. The copper ferrocyanide gives maximal efficiency in the acid and neutral medium, its usage in the alkaline medium is less efficient (79% of Cs extraction from LRW solutions).

The values on sorption capacity of copper ferrocyanide are presented in table 2.

Table 2.

Results of mass-spectrometric analysis

Number of model solution	Cs amount in the initial solution, mg/l	Cs amount in the solution after sorption, mg/l	Efficiency of Cs extraction from the solution, %
1	2	0.001	99.95
2	2	0.001	99.95
3	20	0.01	99.5
4	20	0.01	99.95

In these experiments the sorbent was not saturated. The experimental data show that the sorption capacity of the suspension is not less than 20mg of Cs per 1g of sorbent, which in the units of ^{137}Cs activity is not less than $6.6 \cdot 10^{13}$ Bq per 1kg of sorbent. However, it is necessary to take into consideration that this value of sorption capacity of copper ferrocyanide does not take into account the presence of other elements (stable and radioactive isotopes) in the LRW solution, which can also be sorbed by the sorbent.

The results of studying of extraction of Cs isotopes from the LRW by sorption show that the sorption capacity of the copper ferrocyanide suspension is not less than 3 orders of magnitude higher than that of Termoksid-35. Therefore the amount of solid radioactive wastes formed in case of suspension usage will be smaller. However, it is necessary to keep in mind that the sorption capacity of the copper ferrocyanide decreases as the pH of the solution increases.

1.2. Economic evaluation of the proposed technology

In order to justify the choice of the proposed technology, a larger-scale economic analysis of the two variants of cleaning of the LRW containing $4.8 \cdot 10^{11}$ Bq/m^3 of ^{137}Cs activity and the expenditures on disposal of solid radioactive wastes formed after sorption was carried out. The calculation was made in order to compare economic characteristics of the main technological stages of the two most perspective variants of LRW cleaning without account for man-hours, depreciation, obligatory payments, public utilities and services of third parties, which are supposed to be practically the same in both cases.

The first variant described in [3] includes LRW ozonation with further filtration and ion-exchange cleaning from cesium isotopes with Termoksid-35. In calculations of the expenditures for this method of LRW cleaning it was accepted that to clean all volume of the BN-350 LRW (about 5 000m^3 according to the experimental data presented in [1]), it is necessary to use at least 10 ozonizing facilities of rated capacity of 2.5kg/h for ozone. The cost of one facility is about 31 000 000 tenge. Therefore the cost of equipment for processing 1 m^3 of LRW will amount to 31 000 000 / 5 000 * 10= 62 000 tenge/m^3.

The cost of reagents includes the cost of sorbent Termoksid-35 (5 300 tenge/kg), taking into account that 14kg of the sorbent are needed to clean 1m^3 of LRW. The productivity of a commercial ozonizer is 2.5kg of ozone per hour [9]. According to the laboratory experiments described in [3], the minimal ozone consumption for processing of 1m^3 of LRW will be not less than 171kg. Taking into account that power consumption of the ozonizer is 37 kWt/h, the time needed to clean 1m^3 of LRW is 68.4 hours, hence, the cost of electric energy will be 37*68.4*8.01=20 272 tenge.

The second technology is based on permanganate oxidation of the LRW organic compound with further filtering of solutions and extraction of cesium isotopes by copper ferrocyanide. The main expenses of the technology are the cost of reagents: potassium permanganate, sulfuric acid, copper ferrocyanide, copper sulfide and nitric acid.

In calculations of expenditures on disposal of solid radioactive wastes (SRW) produced after processing of 1m^3 of LRW we used the experimental data according to which the amount of solid wastes in the first technology will be 16kg and 8kg in the second technology.

Kazakhstan has only one complex for long-term SRW disposal, Baikal, located in Kurchatov-city. According to the official data, the cost of disposal of 1kg of SRW is about 500 tenge. All calculations for LRW processing were made in the same monetary unit – tenge.

The results of comparative analysis of the two technologies are presented in Table 3.

Table 3.

A larger-scale economic calculation of two technologies of LRW processing

Technology	Cost of electric energy for oxidation of 1m^3 of LRW, tenge	Cost of special equipment for oxidation of 1m^3 of LRW, tenge	Cost of chemical reagents for processing of 1m^3 of LRW, tenge	Cost of disposal of SRW produced in processing of 1m^3 of LRW, tenge	Total cost of processing of 1m^3 of LRW, tenge
1	20 000	62 000	74 000	8 000	164 000
2	-	-	17 000	4	17 004

Based on the experimental and calculation data, it was determined that the cost of disposal is three times lower in the copper ferrocyanide technology than in the Termoksid-35 technology, the cost of chemical reagents is 4 times cheaper in the second technology than in the first one, what is more, in the second technology it is not necessary to buy an expensive equipment, the cost of which for processing of $1m^3$ of LRW may be as high as 62 000 tenge. The safety of the process and the efficiency of the second technology enable us to suppose that the suggested method of LRW processing may be economically profitable for processing BN-350 liquid radioactive wastes.

CONCLUSION

As a result of experimental assessment of the main stages of technologies suggested for processing of BN-350 LRW, a technology which is more efficient, safer and more economically profitable than the other technology was chosen. The main stages of the technological process of inorganic LRW processing include:

- The stage of oxidation of the complex-forming component, in which potassium permanganate can be used as a rather efficient oxidizer of the LRW organic component;
- The stage of sorption cleaning, in which it is suggested to use copper ferrocyanide as a sorbent.

After oxidative decomposition of the LRW organic component and separation of formed slurry, it is necessary to envisage the usage of additional stages of cleaning from transuranium elements and ^{90}Sr. In particular, it is necessary to envisage the stage of LRW cleaning from plutonium isotopes. The usage of sedimentation, co-sedimentation and sorption procedures for LRW cleaning several times may considerably decrease the total activity of liquid radioactive wastes and concentrate the main radioactive contaminants in a small volume of radioactive wastes.

After technology testing on real LRWs from BN-350 and confirmation of the efficiency of the proposed method, it will be possible to discuss application of described technological operations on an industrial scale for utilization of liquid radioactive wastes.

REFERENCES

1. Комплекс по переработке жидких неорганических радиоактивных отходов РУ БН-350. Здания 157, 157А, 155. Проект. Технологические решения. Том 4. Часть 1. Книга 1. ЗАО "МЭТР", Москва, 2004. С.13
   A Complex for Processing of BN-350 Inorganic Liquid Radioactive Wastes. Buildings 157, 157A, 155. Project. Technological Solutions. V. 4. Part 1. Book 1. METR, CJSC, Moscow, 2004. p.13. – [in Russian]
2. Рабинович В.А. Краткий химический справочник /В.А. Рабинович, Хавин З.Я. - М.: Химия, 1977. - С.376.
   Rabinovich V.A. Abridged Chemical Reference Book. /V.A. Rabinovich, Z.Ya. Khavin – M. Chemistry, 1977. – p.376. – [in Russian]

3. Актуальные вопросы радиоэкологии Казахстана. Выпуск 2. Труды Института радиационной безопасности и экологии за 2007-2009 гг.: сб.ст. / под.рук. С. Н Лукашенко.- Павлодар: Дом печати, 2010. – С.528.
Topical Issues in Radioecology of Kazakhstan. Issue 2. Proceedings of the Institute of Radiation Safety and Ecology for 2007-2009, col./ edited by S.N. Lukashenko- Pavlodar, Dom Pechati, 2010. – p.528.
4. Пршибил Р. Аналитические применения этилендиаминтетрауксусной кислоты и родственных соединений / Р.Пршибил. – Москва: "Мир", 1975. – С.40.
Prshibil R. Analytical Applications of Ethylene Diamine Tetraacetic Acid and Related Compounds / R. Prshibil. – Moscow, Mir, 1975. – p.40. – [in Russian]
5. Кобелев П. Технология переработки плавов, накопленных на АЭС / П.Кобелев, А.Е.Савкин, О.Г.Синякин, Е.А.Качалова, А.Н.Сороколетова, В.Р.Нечаев.П.Кобелев, А.Е.Савкин, О.Г.Синякин, Е.А.Качалова, А.Н.Сороколетова, В.Р.Нечаев // Безопасность и экология. - 2007. - №3. - С. 91-98.
Kobelev P. Technology of Procesessing of Fusion Cakes Stored at NPPs / P. Kobelev, A.E. Savkin, O.G. Sinyakin, E.A. Kachalova, A.N. Sorokoletova, V.P. Nechayev. // Safety and Ecology. - 2007. – No.3. – pp. 91-98. – [in Russian]
6. Дятлова Н.М. Комплексоны и комплексонаты металлов / Н.М.Дятлова, В.Я. Темкина, К.И. Попов. – Москва: "Химия", 1988. – С.390-395.
Dyatlova N.M. Complexons and Complexonates of Metals. / N.A. Dyatlova, V.Ya. Tyemkina, K.I. Popov. – Moscow, "Khimiya", 1988. – pp.390-395. – [in Russian]
7. Крешков А.П. Основы аналитической химии. Теоретические основы. Количественный анализ, книга вторая / А.П. Крешков .– М. Химия, 1976.- 480 с.
A.P. Kreshkov. Fundamentals of Analytical Chemistry. Theoretical Basis. Quantitative Analysis, book 2. / A.P. Kreshkov .– M. "Khimiya", 1976.- p. 480. – [in Russian]
8. Исследования режимов переработки жидких радиоактивных отходов реактора БН-350: отчет о НИР.– Москва: МосНПО "Радон", 2001. - С.11-28.
Investigations of Regimes of Reprocessing of BN-350 Liquid Radioactive Wastes: NIR report.– Moscow: MosNPO "Radon", 2001. – pp.11-28. – [in Russian]
9. Комплекс по переработке жидких неорганических радиоактивных отходов РУ БН-350. Здания 157, 157А, 155. Проект. Технологические решения. Том 4. Часть 1. Книга 1. ЗАО "МЭТР", Москва, 2004. С.13.
A Complex for Processing of BN-350 Inorganic Liquid Radioactive Wastes. Buildings 157, 157A, 155. Project. Technological Solutions. V. 4. Part 1. Book 1. METR, CJSC, Moscow, 2004. p.13– [in Russian]

ОРГАНИКАЛЫҚ ЕМЕС СРҚ РҚ ЖН-350 ҚАЙТА ӨҢДЕУ ТЕХНОЛОГИЯСЫНЫҢ НЕГІЗГІ КЕЗЕҢДЕРІН ӨҢДЕУ

Коровина О.Ю., Лукашенко С.Н., Каширский В.В., Зверева И.О.

ҚР ҰЯО Радиациялық қауіпсіздік және экология институты, Курчатов, Қазақстан

Бұл мақала, Ақтау қ. (Қазақстан) орналасқан, жылдам нейтрондағы реакторлық қондырғылардың (РҚ ЖН) қызметі нәтижесінде пайда болған сұйық радиоактивті қалдықтарды (СРҚ) қайта өңдеу технологиясын әзірлеу мақсатында өткізілген зерттеулерге арналған. Зерттеулер үшін, теоретикалық және іс-тәжірибелік түрде бағалау нәтижесінде анықталған, СРҚ РҚ ЖН-350 химиялық құрамын ұқсататын үлгідегі ерітінділер қолданылды.

СРҚ қайта өңдеудің ұсынылған технологиясы, СРҚ органикалық құрамын біртіндеп бұзуға негізделген және СРҚ РҚ ЖН-350 орын алған химиялық қасиеттерді ескере отырып тиісті реагенттердің көмегімен радионуклидтердің тұнуына негізделген, сонымен қатар аталған қалдықтарды қайта өңдеуге экономикалық шығындарын ескере отырып іріктеп алынған.

Тәжірибелік зерттеулер нәтижесінде, СРҚ РҚ ЖН-350 қайта өңдеу технологиясының негізгі кезеңдері ұсынылды, олардың оңтайлы шарттары таңдап алынды. Осының барысында анықталғаны, СРҚ оңтайлы тәсілмен органикалық құрамының тотығуы үшін перманганатты тотығу оңтайлы тәсіл болып табылады, ал СРҚ Cs изотоптарынын тазалау үшін одан да арзан сорбент – мыс ферроцианидінің жаңадан дайындалған суспензиясын қолдану ұсынылды.

Түйін сөздер: сұйық радиоактивті қалдықтарды қайта өңдеу, жылдам нейтрондағы реактор, СРҚ РҚ ЖН-350 , радионуклидтіқұрамы, СРҚ тазалау тиімділігін бағалау, СРҚ перманганатты тотығуы, СРҚ сіңіргіштік тазалау, мыс ферроцианиді, радионуклидтерден тазалау дәрежесі, трилон Б, қымыздық қышқылы, ^{241}Am, ^{154}Eu,Pu изотоптары, ^{90}Sr, ^{134,137}Cs, ^{60}Co, ^{54}Mn, ^{90}Sr.

ОТРАБОТКА ОСНОВНЫХ ЭТАПОВ ТЕХНОЛОГИИ ПЕРЕРАБОТКИ НЕОРГАНИЧЕСКИХ ЖРО РУ БН-350

Коровина О.Ю., Лукашенко С.Н., Каширский В.В., Зверева И.О.

Институт радиационной безопасности и экологии НЯЦ РК, Курчатов, Казахстан

Данная статья посвящена исследованиям, проведенным с целью разработки эффективной технологии переработки жидких радиоактивных отходов (ЖРО), образовавшихся в результате деятельности реакторной установки на быстрых нейтронах (РУ БН-350), расположенной в г. Актау (Казахстан). Для исследований использовались модельные растворы, имитирующие химический состав ЖРО РУ БН-350, определенный в результате теоретической и практической оценки.

Предлагаемая технология переработки ЖРО основана на последовательном разрушении органической составляющей ЖРО и осаждении радионуклидов с помощью соответствующих реагентов, подобранных с учетом химических свойств присутствующих в ЖРО РУ БН-350 радионуклидов, а также экономических затрат на переработкуданных отходов.

В результате экспериментальных исследований предложены основные этапы технологии переработки ЖРО РУ БН-350, выбраны их оптимальные условия. При этом определено, что для окисления органической составляющей ЖРО наиболее приемлемым способом является

перманганатное окисление, для очистки ЖРО от изотопов Cs предложено использовать более дешевый сорбент – свежеприготовленную суспензию ферроцианида меди.

Ключевые слова: переработка жидких радиоактивных отходов, реактор на быстрых нейтронах, радионуклидный состав ЖРО РУ БН-350, оценка эффективности очистки ЖРО, перманганатное окисление ЖРО, сорбционная очистка ЖРО, ферроцианид меди, степень очистки от радионуклидов, трилон Б, щавелевая кислота, ^{241}Am, ^{154}Eu, изотопы Pu, ^{90}Sr, ^{134,137}Cs, ^{60}Co, ^{54}Mn, ^{90}Sr.

УДК 621.386.12:616-07:615.849

QUALITY ASSESSMENT FOR OPERATIONAL PARAMETERS OF X-RAY DIAGNOSTICS EQUIPMENT IN KAZAKHSTAN

Bozhko V.V., Mustafina E.V., Ossintsev A. Yu.

Institute of Radiation Safety and Ecology NNC RK, Kurchatov, Kazakhstan

In this work we reviewed the quality of operational parameters of X-ray diagnostic equipment at the example of East-Kazakhstan oblast. The paper describes the main inspected operational parameters, their significance in respect to the absorbed dose gained by a patient and the form of their assessment. It has been revealed that in the East Kazakhstan oblast, out of the 32 surveyed X-ray machines, 50% did not meet the requirements for controlled settings.

Keywords: X-ray diagnostics, X-ray diagnostic machines, medical exposure, dose, monitoring of operational parameters.

INTRODUCTION

Use of ionizing radiation sources in medicine contributes significantly to the irradiation exposure of the population; a major doze is gained by the patients during X-ray preventive and X-ray diagnostic procedures.

At present, the state control over the observance of radiation safety requirements for the X-ray radiology examination has become tougher to reduce the irradiation exposure of population and personnel. Thus, from 2008 the Republic of Kazakhstan has introduced the sanitary and epidemiologic rules and norms "The Sanitary and Epidemiologic Requirements for Design, Maintenance and Operation of X-Ray Diagnostics and Therapy Rooms" (so called SanPiN doc) the second edition of which was issued in 2010.

Technical state and accuracy of the use of X-ray diagnostic equipment contribute significantly to the dose load on patients. Scheduled inspection of operational parameters of medical X-ray equipment should be periodically to reveal technical failures. The introduced sanitary and epidemiologic rules and norms have established inspection intervals to be not less than once in two years.

Institute of Radiation Safety and Ecology (IRSE) has been inspecting the operational parameters of medical X-ray equipment since 2009.

The objective of this work is to assess the operational quality of X-ray diagnostic equipment in the Republic of Kazakhstan.

1. EXPERIMENT

1.1. Research objects

Research in seven medical institutions of East Kazakhstan Region has been carried out to assess the operational quality of X-ray diagnostic units. Total 32 X-ray machines have been surveyed. The inspection covered practically all types of X-ray diagnostic equipment (Table 1).

1.2. Research methodology

The list of controlled operational parameters has been taken as specified in Appendix 15 of the Sanitary and Epidemiologic Rules and Norms [1]:

1) net filtration of X-ray beams;
2) accuracy of anodic voltage setting, half-value layer;
3) control of curve shape and anodic voltage ripple;
4) accuracy of anode current setting;
5) accuracy of electric current quantity setting (mA·s);
6) accuracy of exposure time setting;
7) repeatability of radiation dose in snap shot mode in manual and automatic modes;
8) linearity of irradiation at preset voltages;
9) radiological protection check for X-ray-emitter at the plug on;
10) measurement of radiation yield;
11) availability of alarm signaling at exposure time exceeding 5 min;
12) overlapping of optical (light) and X-ray radiation fields;
13) control of central X-ray beam drift at change in position of the support and focal distance;
14) propel effort of moving members of spot film device;
15) angle and depth of images for the tomography.

Each of the above parameters affects the operational performance of a machine and directly or indirectly contributes to the change in radiation dose gained by patients or personnel. Moreover, many of the parameters are mutually related to each other (for instance, the electric quantity is calculated as a product of current strength and exposure time). With the accurately adjusted machine, a good-quality picture requires a correct balance between the voltage and electric current quantity settings.

To realize a necessity of control of exactly these parameters, it is necessary to analyze their significance and assessment procedure.

Parameter 1 – a range of total filtration values is available for this parameter, expressed as Al equivalent typical for various-type machines. An increase in the filtration leads to the absorption of low-energy X-ray radiation that, in its turn, reduces the absorbed dose.

Parameter 2 is assessed as a ratio of specified settings to the measured ones that should not exceed 10 %. This parameter is directly related to the dose: at higher voltage the average energy of X-ray radiation increases and absorbed dose, therefore, decreases.

Parameter 3 is assessed as a ratio of the voltage drop on the tube during exposure to the specified voltage value. This Parameter mainly characterizes the quality of feeder performance and the power supply. Deviations of this parameter result in unstable operation of a machine.

Parameter 4 is assessed as a ratio of the specified settings to the measured ones that should not exceed 10 %. This parameter is directly related to the dose: at higher currents the absorbed dose increases.

Parameter 5 is assessed as a ratio of the specified settings to the measured ones that should not exceed 10 %. The absorbed dose increases at higher electric quantity like in the case of current.

Parameter 6 is assessed as a ratio of the specified settings to the measured ones that should not exceed 10 %. The parameter is directly related to the dose: at higher exposure time the absorbed dose proportionally increases.

Parameter 7 determines the mean deviation of dose that should not exceed 20 %. The parameter characterizes mainly the quality of machine operation. Deviations in this parameter result in unstable operation of a machine and incorrect analysis of gained dose.

Parameter 8 determines the relationship between the dose and the electric quantity at constant anode voltage. The relationship must have linear character.

Parameter 9 determines the correctness of operation of the emitter protection system. Incorrect operation of the protection system may cause uncontrolled irradiation of both the patients and the personnel.

Parameter 10 determines the dose load on the personnel for each particular machine under basic operating conditions; subsequently this value is used in the clinical practice. The parameter is needed for calculation of dose absorbed by patients during examination.

Parameter 11 determines the operability of signaling in a "scopy" mode. Absence or disoperation of signaling causes overexposure of patients and personnel.

Parameter 12 determines overlapping of optical (light) and X-ray radiation spots which should not be more than 2 %. The parameter is directly related to the dose: when the size of X-ray spot exceeds that of optical field, the absorbed dose will be higher than that expected by the medical personnel.

Parameter 13 determines the drift of the central ray of the X-ray beam from the geometrical perpendicular to the focal spot that should not be more than 2 %. The parameter affects the X-ray image quality.

Parameter 14 determines the propel effort of moving parts of the spot film device. The parameter characterizes the operation efficiency of moving parts of the spot film device (jamming or failure of movable pivot points that makes it impossible to fix the spot film device in the required position). The parameter does not affect the dose.

Parameter 15 determines the deviation from the specified angle settings and cutting depth against the measured ones that should not be more than 1 mm for the cut depth and 1º for the cut angle. The parameter is related to the quality and accuracy of information obtained from the image.

One should note that measuring of all required parameters for all types of machines is not always possible. Hence, this list of inspected parameters should be modified for each type of machine (optical field, etc. is absent in dental and photofluorographic machines).

Moreover, no research on some parameters has been carried out due to impossibility to make measurements employing noninvasive methods (lack of special electric contacts to check the accuracy of anode current strength and electrical quantity settings). No research has been carried out on point 9 during execution of these works due to absence of a plug on these machines to shut the emitter window.

After considering each parameter separately, all parameters have been subdivided into 2 groups: parameters directly affecting the absorbed dose and parameters indirectly affecting the dose. The first group includes the parameters 1, 2, 4, 5, 6, 8, 9, 10, 11 and 12, the second group - the parameters 3, 7, 13, 14, 15.

With established relevant requirements, only four documents on the measurements included in the State Register of the Republic of Kazakhstan are available in the sphere of services on monitoring of operational parameters. The documents cover a minor part of the required controlled parameters and types of X-ray diagnostics equipment available in the Republic of Kazakhstan. Due to lack of sufficient regulatory and legal documentation, all investigations have been carried out according to the Russian and international standards.

The following measuring means, phantoms and test tools have been used during the investigations:

- universal dosimeter for monitoring of the characteristics of X-ray machines (Unfors Xi type);
- beam alignment test tool 162A;
- collimator alignment test tool Ref.161;
- set of test tools for linear tomography, ТКЛ-1 and ТКЛ-2;
- contrast sensitivity test tool, ТКЧ-11/21;
- special mammographic phantom Ref: 011A Tissue-Equivalent Mammography Phantom;
- dental phantom Ref.VD0903150 Digident U Dental Phantom.

2. RESULTS

2.1. Inspection Results in East-Kazakhstan Region

The results obtained during the inspections are presented in Table 1.

Table 1.

Inspection of operational parameters

Machine Type, quantity	Compliance with the requirements	Number of machines inspected for specific parameter, items													
		Parameter 1	Parameter 2	Parameter 3	Parameter 4	Parameter 5	Parameter 6	Parameter 7	Parameter 8	Parameter 10	Parameter 11	Parameter 12	Parameter 13	Parameter 14	Parameter 15
X-ray diagnostic machines (XDM), 5 items	Meets the requirements	5	4	4			3	5	5	5	2	4	4	5	2
	Fails to meet the requirements		1	1	1	1						1	1		
	Cannot be assessed				4	4	2				3				3
Ward apparatus, 12 items	Meets the requirements	12	11	12			5	12	12	12		9	8	12	
	Fails to meet the requirements		1				3					3	4		
	Cannot be assessed				12	12	4				12				12
Fluorographic machines 4 items	Fails to meet the requirements	4	1	3				4	3	4					
	Fails to meet the requirements		3	1					1						
	Cannot be assessed				4	4	4				4	4	4	4	4
Dental machines, 4 items	Meets the requirements	4	3	4			1	4	4	4			2	4	
	Fails to meet the requirements		1										2		
	Cannot be assessed				4	4	3				4	4			4
Mammographic machines, 4 items	Meets the requirements	4	3	4				4	4	4		3	4	4	
	Fails to meet the requirements		1												
	Cannot be assessed				4	4	4				4	1			4
X-ray machines, 3 items	Meets the requirements	3	2	3			2	3	3	3		3	3	3	
	Fails to meet the requirements		1												
	Fails to meet the requirements				3	3	1				3				3

Analyzing the obtained data (Table 1), two and more cases of non-conformance with specification parameters in the same machine have been revealed.

The non-compliance identified by the inspections was mainly related to the high-voltage systems and the X-ray beam forming systems (misalignment of radiation and light fields). At that, both the malfunctions relate to the parameters directly affecting the dose. An example of such misalignment of radiation and light fields (more than 5 %) is shown in Figure 1.

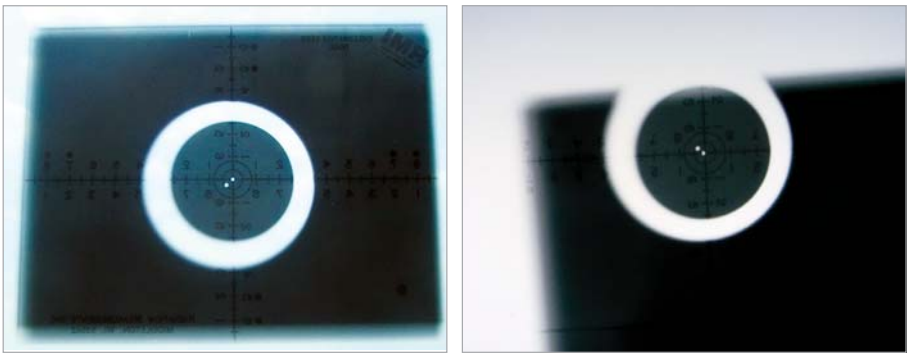

Figure 1. X-ray films obtained by measurement of the parameters 12 and 13

Total 50 % of the surveyed X-ray diagnostic machines do not meet the requirements for the parameters specified in Appendix 15 of Sanitary and Epidemiologic Rules and Norms [1].

According to the chosen classification, 44 % of the surveyed X-ray diagnostic machines do not meet the requirements for the parameters directly affecting the absorbed dose and 6% – those indirectly affecting the dose.

Analysis of the quality of operational parameters versus the date of the machine manufacturing (Figure 2) has shown that 42% of the <20years old machines do not meet the requirements, and in some cases this category includes the machines manufactured in 2008–2009.

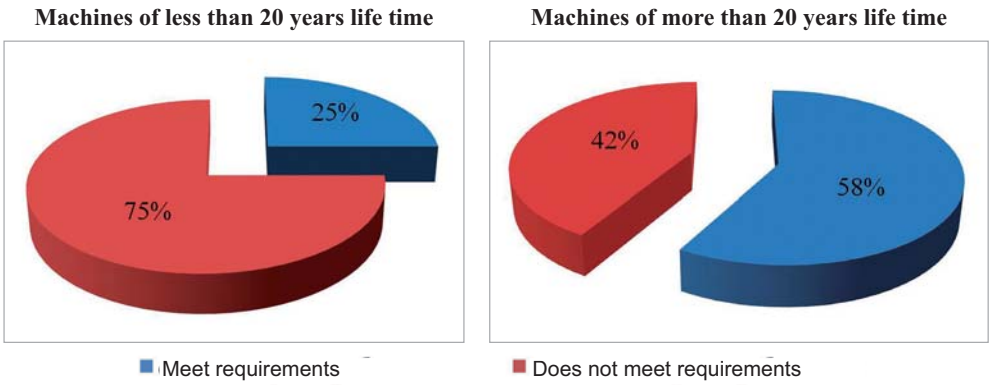

Figure 2. Inspection of operational parameters versus the machine service life

The situation with the machines of more than 20 years life time is much worse (Figure 2, second chart): ¾ of the surveyed machines have shown non-conformance.

2.2. State of Control in the Republic of Kazakhstan

According to the official data provided by the Republic of Kazakhstan Sanitary and Epidemiologic Station, by 2008, the Republic of Kazakhstan had 1814 X-ray diagnostic machines (Table 2).

Table 2.

Amount of X-ray machines in medical institutions of Kazakhstan

No	Function	Quantity
1	Radiography	726
2	Radiography, radioscopy	264
3	Radiography, radioscopy, tomography	15
4	Radiography, tomography	1
5	Radioscopy	9
6	X-ray therapy	22
7	X-ray fluorescence analysis	47
8	Angiograph	3
9	Dental	206
10	Cardiology	1
11	Lithotriptor	1
12	Mammography	85
13	Bone density analysis	1
14	Tomography	30
15	Urology	4
16	Fluorography	385
17	Other	14
TOTAL		1 814

At present, 4 organizations have licenses for inspections of operational parameters in X-ray diagnostic equipment (official information provided by the State Atomic Energy Committee):

1. LLP "SPC Gamma", Almaty;
2. LLP "EKOSERVIS-C", Almaty;
3. LLP "Alia&Co.", Aktobe;
4. SE Institute of Radiation Safety and Ecology RGP NNC RK, Kurchatov.

Inquiries have been made to all organizations as to the total quantity of machines surveyed by them and the number of machines not meeting the requirements. The following data on the whole country have been obtained as of the end of February 2011 (Table 3, Figure 3) according to the statistics based on the data provided by the organizations licensed to inspect operational parameters of X-ray diagnostic equipment.

Table 3.

Inspections of operational parameters in Kazakhstan as of the end of February 2011

Monitoring organization	Quantity of devices monitored		
	Total, item	Non-conforming	
		item	%
LLP "EKOSERVIS-C"	48	10	21
LLP "SPC Gamma"	62	12	19
LLO "Alia & Co."	3	0	0
Institute of Radiation Safety and Ecology	32	16	50
Total	145	38	26

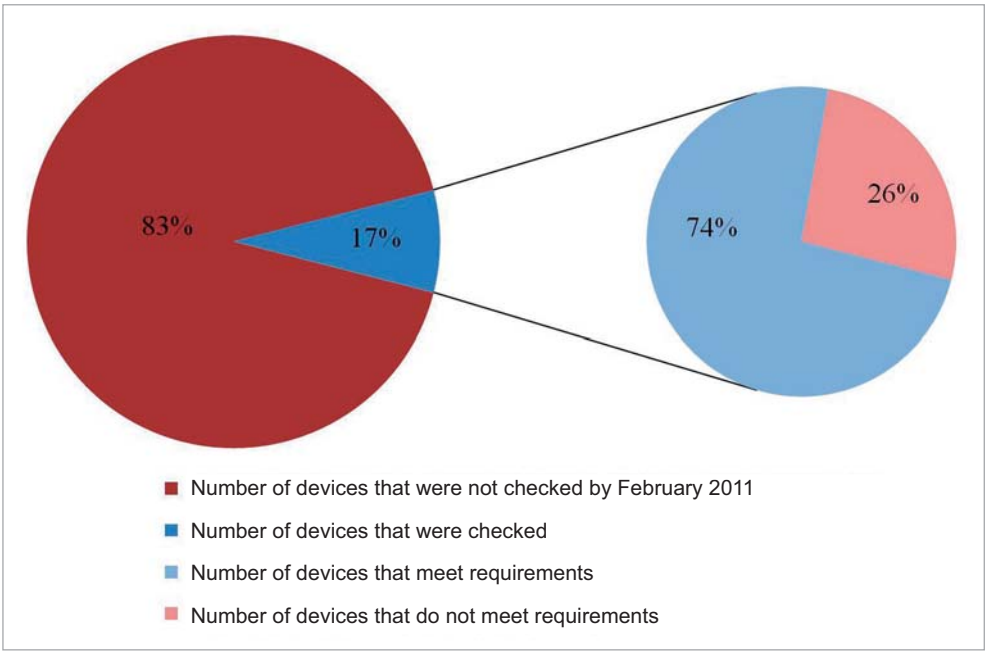

Figure 3. Inspection of operational parameters in Kazakhstan as of the end of February 2011.

By the end of February 2011, in the Republic of Kazakhstan, about 83% of X-ray diagnostic machines had not been inspected.

CONCLUSION

Since 2008, the requirements for design, maintenance and operation of radiology rooms in the Republic of Kazakhstan include inspection of operational parameters to reduce the radiation exposure during medical examinations.

To date, under a pressure of the supervisory bodies, medical institutions equipped with X-ray diagnostic installations have been increasingly requesting relevant organizations to perform such inspections. Whereas by the end of 2010 in East Kazakhstan oblast less than 10 machines had been surveyed, in the first quarter of 2011 this quantity had increased to32.

The survey carried out in East Kazakhstan oblast has shown that 50% of X-ray diagnostic machines used for medical examination does not to meet the requirements. In the Republic of Kazakhstan, minimum 26% of the X-ray diagnostic machines do not meet the requirements.

The authors would like to express their gratitude to the staff of LLP Ekoservis-C Akhmetov M.A., Tumanbayev T.V.; LLP Alia&Co. Baudiyarova G.K., Baudiyarov A., Vasina M.I.; LLP SPC Gamma Aimanov M.S., Loktina N.A, Vermenichev R.; Institute of Radiation Safety and Ecology Dementiev A.V for the data provided.

REFERENCES

1. Санитарно-эпидемиологические правила и нормы «Санитарно-эпидемиологические требования к проектированию, содержанию и эксплуатации кабинетов лучевой диагностики и терапии», 12.08.2010, № 633.
   Sanitary and epidemiologic rules and standards "Sanitary and Epidemiologic Requirements for Design, Maintenance and Operation of Radiodiagnostics and Radiation Therapy Rooms", 12 August, 2010, No 633.

ҚАЗАҚСТАН РЕСПУБЛИКАСЫНДАҒЫ РЕНТГЕНДИАГНОСТИКАЛЫҚ ЖАБДЫҚТАРДЫҢ ЭКСПЛУАТАЦИЯЛЫҚ ПАРАМЕТРЛЕРІНІҢ САПАСЫН БАҒАЛАУ

Божко В.В., Мустафина Е.В., Осинцев А.Ю.

ҚР ҰЯО Радиациялық қауіпсіздік және экология институты, Қазақстан, Курчатов қ.

Аталған жұмыс, Шығыс-Қазақстан облысының үлгісінде рентгендиагностикалық жабдықтардың эксплуатациялық параметрлерінің сапасын қарастыру үшін жасалған. Бұл мақалада, негізгі бақыланатын эксплуатациялық параметрлер, пациент алатын сіңірілген дозасына қатыстылығы бойынша маңыздылығы мен оларды бағалау формасы қарастырылды. Өткізілген жұмыстардың нәтижесі бойынша, Шығыс-Қазақстан облысында зерттелген 32 рентгендиагностикалық аппараттың 50 % бақыланатын параметрлер бойынша талаптарға сәйкес келмейтіні анықталды.

Түйін сөздер: рентгендиагностика, рентгендиагностикалық аппараттар, медициналық сәулелену, дозалар, эксплуатациялық параметрлерді бақылау.

ОЦЕНКА КАЧЕСТВА ЭКСПЛУАТАЦИОННЫХ ПАРАМЕТРОВ РЕНТГЕНОДИАГНОСТИЧЕСКОГО ОБОРУДОВАНИЯ В РЕСПУБЛИКЕ КАЗАХСТАН

Божко В.В., Мустафина Е.В., Осинцев А.Ю.

Институт радиационной безопасности и экологии НЯЦ РК, Курчатов, Казахстан

Данная работа проведена для рассмотрения качества эксплуатационных параметров рентгенодиагностического оборудования на примере Восточно-Казахстанской области. В статье рассмотрены основные контролируемые эксплуатационные параметры, их значимость по отношению к поглощенной дозе, получаемой пациентом, и форма их оценки. По результатам проведенных работ было установлено, что в Восточно-Казахстанской области из 32 обследованных рентгенодиагностических аппаратов 50 % не соответствуют требованиям по контролируемым параметрам.

Ключевые слова: рентгенодиагностика, рентгенодиагностические аппараты, медицинское облучение, дозы, контроль эксплуатационных параметров.

УДК 615.849.12:504.75.05

THE DATABASE FOR STORAGE AND PROCESSING OF INFORMATION ON DOSE LOADS TO PERSONNEL

Semenin M.S., Ossintsev A.Yu., and Mustafina E.V.

Institute of Radiation Safety and Ecology NNC RK, Kurchatov, Kazakhstan

The paper describes the database developed for storing and processing of information on the dose loads to personnel. Objectives and basic functions of the database are defined. Detailed structure of storing and processing of data obtained at personal radiation monitoring is described. Basic capabilities of the database and prospects for its further development are also described.

Keywords: personal radiation monitoring, database.

INTRODUCTION

One of the basic principles in utilization of atomic energy is prohibition of any practices involving exposure of people to radiation at which the benefits derived for the people and the society do not exceed the risk of possible detriment caused by additional radiation. This can be monitored only subject to the availability of a functioning system of recording and accounting of radiation exposure to personnel and population.

At present, in Kazakhstan, there are several legislative acts regulating the accounting and control of individual radiation doses gained by people during handling ionizing radiation sources, medical and radiological examination and due to technogenic background radiation.

Pursuant to the Government Decree of the Republic of Kazakhstan dated 19 December, No 1277 "On Approval of Rules for Accounting and Control of Individual Radiation Doses Gained by Individuals during Work with Ionizing Radiation Sources, Medical and Radiological Examination and due to Technogenic Background Radiation", in the Republic of Kazakhstan there shall be established and implemented "the State System of Accounting and Control of Individual Exposure Doses to Population". Such system must collect and keep records on individual radiation control of personnel and general population, and keep record of annual effective dose during the whole job performance period.

The objective of the database is to increase the capabilities and to provide relevant data to the decision makers.

The database functions are:

- collection and storage of information;
- provision of data for the analysis of doses gained by personnel;
- accounting of individuals exposed to radiation above the specified limits;
- provision of a possibility for the general population, enterprises, institutions and organizations to obtain unbiased and credible information on exposure doses to the citizens; and
- report generation, review and visualization of accumulated statistics.

DESCRIPTION OF THE DATABASE

A database platform has been chosen. The chosen work platform is a free database management system (FDMS) MySQL.

Web-interface has been chosen to provide client-server technology that makes it possible to create multi-platform software. This is a free-software. Thus, the following programming languages and markup languages are used: PHP, HTML, JavaScript.

By now, the Institute of Radiation Safety and Ecology has developed the database structure (Figure 1) and design.

The centre of the database structure is the table of data about an individual. The table stores basic data on the personnel: full name, data about organization, occupation, date of birth, etc. In case a person changes his job, the database keeps tracking this. When necessary, it can be found out at which place of employment and in which position a person has received maximal radiation dose.

The database design is structured so that the data on individual radiation control are grouped according to organizations and cities of their location. On choosing a city, the whole list of organizations in this city the workers of which are subject to individual dose control is displayed.

Accordingly, on choosing an organization, a list of its employees under control opens. The system provides control over the compliance with the normative base requirements of the Republic of Kazakhstan. Thus, for instance, the system keeps track of age and informs of women under 45 for which there exist separate requirements for the exposure doses.

The database design, software and hardware have been developed to provide maximum information and convenience in the work, facilitate, and speed up processing of information obtained during individual radiation control.

DATABASE CAPABILITIES

The developed database takes two types of data similar to the Russian Federation forms of data collection No 1-DOZ "Data on Radiation Exposure on Personnel under Conditions of Normal Operation of Artificial Sources of Ionizing Radiation" and No 2-DOZ "Data on Radiation Exposure of Personnel under Conditions of Radiation Accidents or Planned Elevated Radiation and Residents Exposed to Emergency Irradiation".

The database can store a great number of records limited only by the dimensions of hand-end equipment hardware.

The basic performance capabilities of the database are as follows:

- automation of information collection, processing and output;
- automation of accounting of individual dosimeters storage;
- graphical display of data on doses gained by personnel and their distribution both throughout the country and within one organization; and
- automation in generation of protocols and reports to be submitted to the controlled organizations.

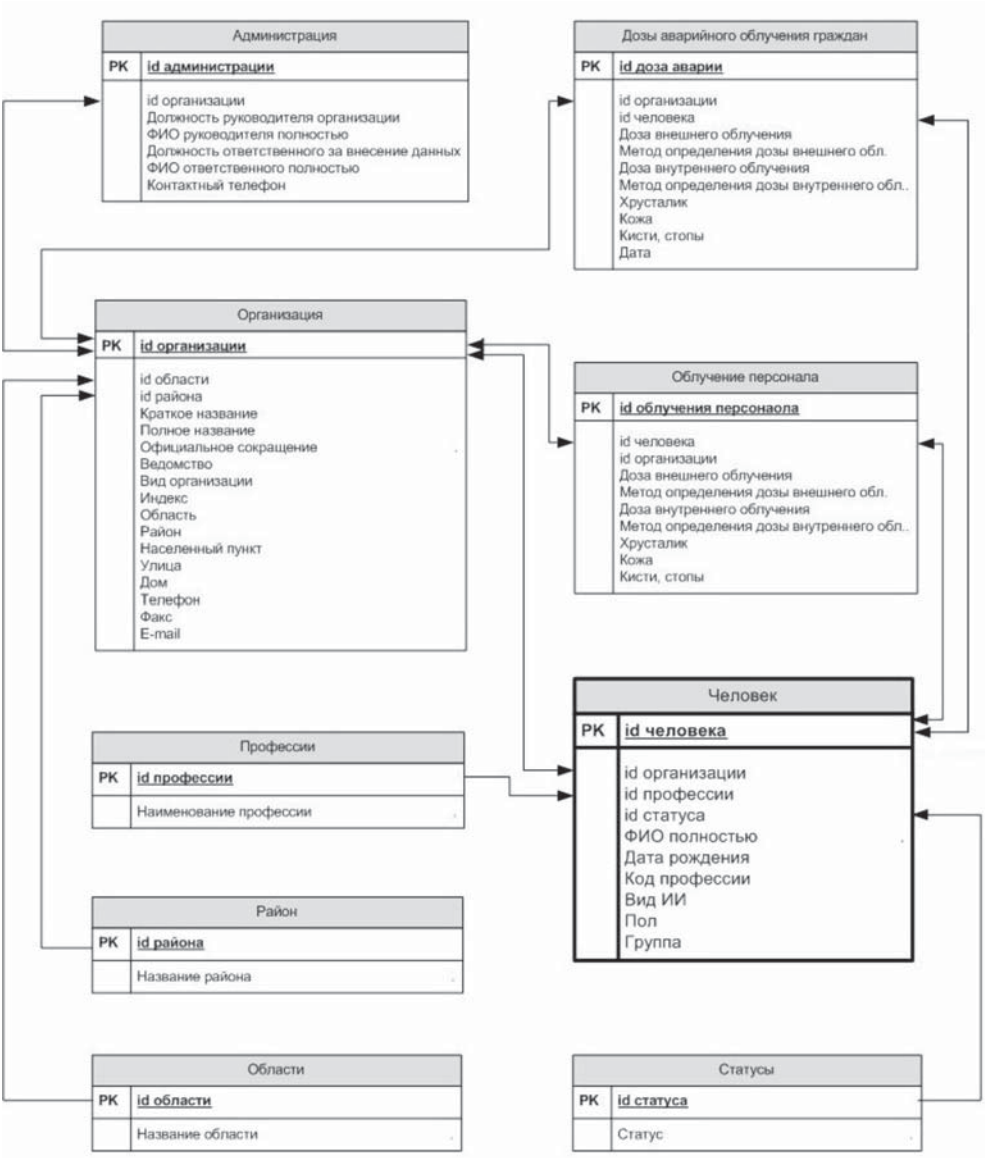

Figure 1. The database structure

At this stage, the database can display the following data in graphical form according to the Form of Request (Figure 2) and data on the distribution of doses rained by the personnel quarter-by-quarter (Figure 3).

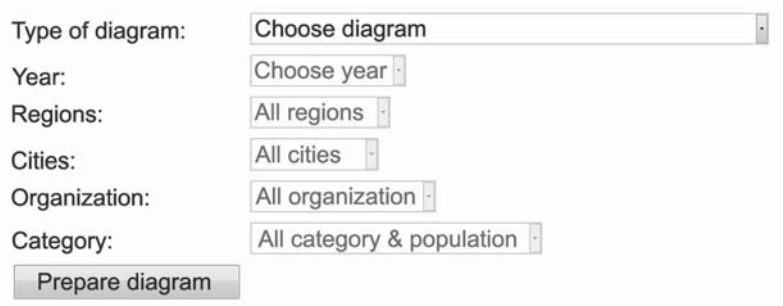

Figure 2. Form of Request

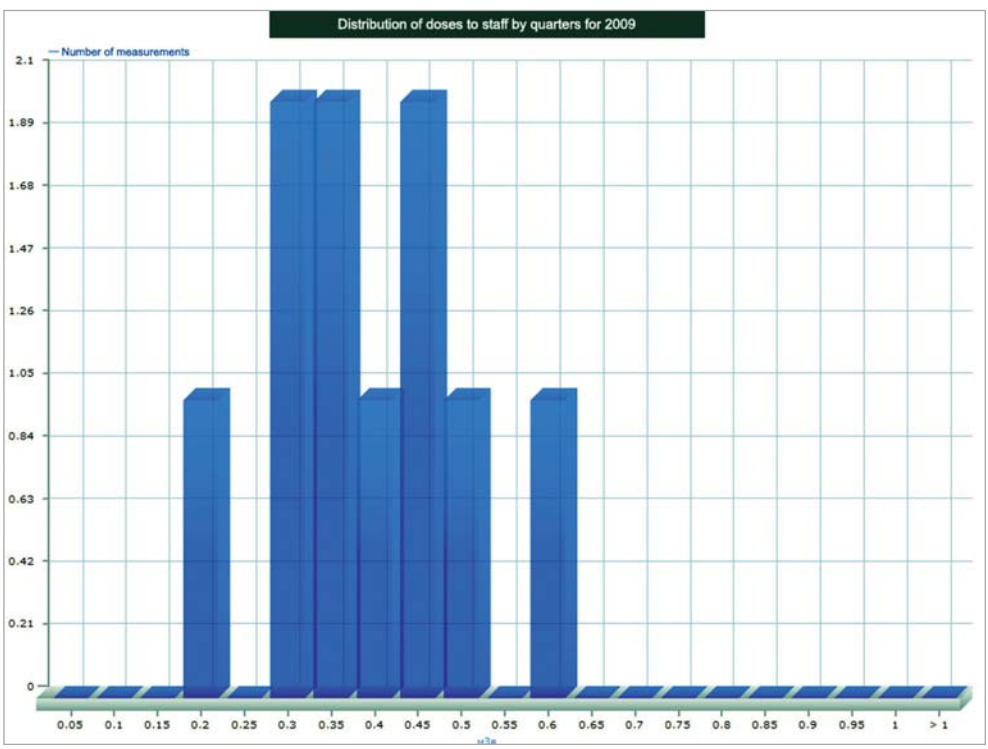

Figure 3. Distribution of exposure doses to the personnel by the quarters

Interactive maps displaying in graphical form the maximum, medium and minimal doses gained by the personnel in oblasts of the Republic of Kazakhstan (Figure 4) have also been developed.

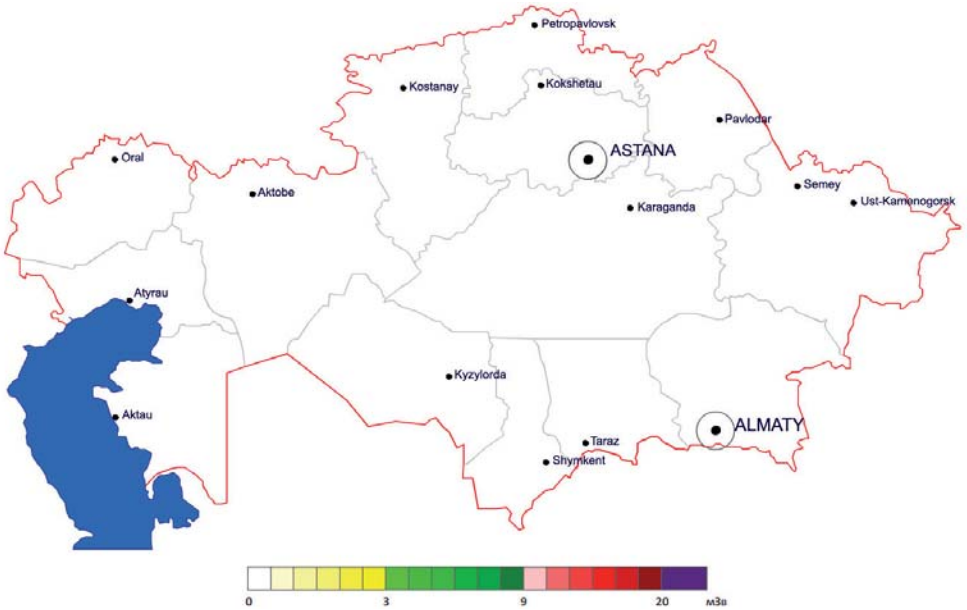

Figure 4. Map with distribution of doses

A quite important feature is the support of multiuser operation with the database by local network and through the Internet. This makes it possible to work simultaneously with many distant operators and users.

User-friendly interface assures comfortable operation even in feeble data transmission networks such as GPRS, telephone connection (dial-up), etc.

The developed database has been launched for the test operation in the Radiological Research Laboratory. In the course of operation, data on individual radiation control of personnel obtained during the Laboratory work have been entered. Errors are revealed and corrected, and the database is permanently improved.

On the whole, the database is operational and, subject to implementation of protective measures and provision of hardware, can be launched for the work in the Internet.

CONCLUSION

On the long-term, for the database development it is planned to implement an on-line possibility to review, analyze and assess the data stored in the database. A module for the document preparation based on the obtained data and display of statistical, tabular and visual data (tables, charts) is developed to deliver report documentation to supervisory bodies.

The development of similar database at the national level will make it possible to speed up the collection of data necessary for making an informed decision on the reduction of radiation exposure to citizens of the Republic of Kazakhstan based on the actual data. Availability of the system would consistently contribute to the reduction of dose exposure to citizens of the Republic of Kazakhstan.

ҚЫЗМЕТКЕРЛЕРДІҢ ДОЗАЛЫҚ ЖҮКТЕМЕЛЕРІ БОЙЫНША АҚПАРАТТЫ ӨҢДЕУ ЖӘНЕ САҚТАУҒА АРНАЛҒАН ДЕРЕКТЕР БАЗАСЫ

Семенин М.С., Осинцев А.Ю., Мустафина Е.В.

ҚР ҰЯО Радиациялық қауіпсіздік және экология институты, Курчатов, Қазақстан

Мақалада, қызметкерлерге арналған дозалық жүктемелер бойынша ақпараттарды өңдеу және сақтау үшін жасалып жатқан деректер базасы суреттелген. Деректер базасының негізгі әзірлемелері мен қызметтерінің мақсаты анықталды. Қызметкерлерге жеке дозиметрлік бақылау өткізу барысында алынған деректерді өңдеу және сақтауға қатысты құрылым толық суреттелген. Сонымен қатар, деректер базасын әзірлеудегі негізгі мүмкіндіктер мен оны келешекте жетілдіру жағы суреттелген.

Түйін сөздер: жеке дозиметрлік бақылау, деректер базасы.

БАЗА ДАННЫХ ДЛЯ ХРАНЕНИЯ И ОБРАБОТКИ ИНФОРМАЦИИ ПО ДОЗОВЫМ НАГРУЗКАМ НА ПЕРСОНАЛ

Семенин М.С., Осинцев А.Ю., Мустафина Е.В.

Институт радиационной безопасности и экологии НЯЦ РК, Курчатов, Казахстан

В статье описана разрабатываемая база данных для хранения и обработки информации по дозовым нагрузкам на персонал. Определены цели разработки и основные функции базы данных. Описана подробная структура хранения и обработки данных, полученных при проведении индивидуального дозиметрического контроля персонала. Также описаны основные возможности разрабатываемой базы данных и перспективы развития.

Ключевые слова: индивидуальный дозиметрический контроль, база данных.

УДК 528:577.4:504.064

DEVELOPMENT OF GIS-PROJECT "STS"

Yakovenko Yu.Yu., Lukashenko S.N., Subbotin S.B.

Institute of Radiation Safety and Ecology NNC RK, Kurchatov, Kazakhstan

The paper presents the results of the design and creation of GIS-project "STS", as well as examples of its use for organization of research and data analyses to assess the state of territories and ecosystems.

A large scope of diverse information on the territory of the former Semipalatinsk Test Site (STS) have been accumulated what finally brought us to the problems with its storage, timely access and effective data processing. To solve these problems and implement comprehensive research at STS, a GIS-technologies-based GIS project "STS" is being designed and developed.

This development allowed systematizing a large amount of stored information, including data on radioactive contamination of STS and certain TEST SITEs as well as providing ongoing informational and analytical services to a large amount of users.

Keywords: GIS project, layer, database, initial data, data analysis.

INTRODUCTION

By now, large scope of diverse information on the territory of the former Semipalatinsk Test Site (STS) has been accumulated: this included the outcomes of research programs and commercial projects carried out by different organizations. Due to the large amounts of data, we encounter problems related to storage, timely access and effective data processing. To solve these problems and carry out comprehensive research at the STS, application of geographic information systems (GIS) is particularly effective.

The main objective of the GIS project "STS" is to create an information module based on GIS technology in order to/for:

- collection and systematization of information to carry out filed works at STS;
- preparation of initial data for field works;
- analyze the data obtained during research for decision-making;
- determine the nature and mechanisms for contamination of the territory.

1. GENERAL DESCRIPTION OF THE WORKS

1.1. Approaches to the GIS-project

The model of GIS project was based on three main components: initial data, software unit and analysis. The fourth component, the block of decision-making, is the resultant component of the system [1].

A tool (software package) to create the GIS-project was software ArcGIS 9.x with optional modules for analysis (Spatial Analyst, Geostatistical Analyst). The GIS project is executed in a coordinate system WGS-1984_UTM_Zone_43N (Universal Transverse Mer-

cator Zone 43, Spheroid WGS 84) – a global rectangular coordinate system, which is used at present in Kazakhstan and other countries to bring the data to a single standard.

Initial data for the GIS-project were various reports, remote sensing data, topographic and thematic paper maps, and data from field and laboratory studies. A core of initial data was geo-database and database "Radioecology". The databases are interacted using the built-in function OLE DB Connection.

A special analytical database "Radioecology" represents a structured enormous amount of factual material accumulated in the course of radio-ecological studies at STS (more than 40 000 samples with the results of various analyses), and it keeps growing. The base is implemented in the DBMS Access, because its interface is simple and provides convenient features for data manipulation.

Processing of initial data included the sequence presented in Figure 1.

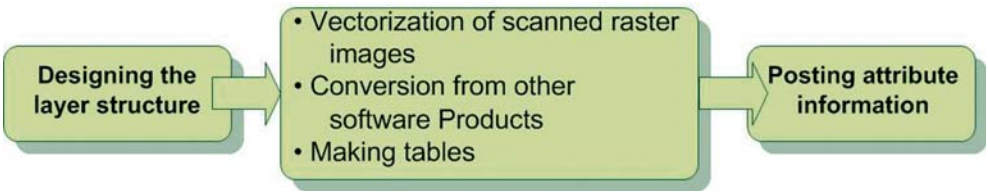

Figure 1. Processing of initial data

The data processing included making the structure of each layer, i.e. it is to be determined what information a layer should contain in order to obtain sufficient data for analysis.

The next step, depending on the type of initial data, was entering initial data into the geo-database.

The topographic and thematic maps were scanned to obtain bitmap data. If necessary, the bitmaps were processed (joined) employing software Easy Trace, which also allows vectoring an image. This was followed by vectorization of scanned (raster) images – digitization of maps. In order to work with geometric objects (dots, lines, testing sites), they initially are tied-in to maps and define the projection, and then bitmap is vectorized [2]. To prepare thematic maps on some remote sensing data (RSD) on an area of interest, multispectral medium-resolution satellite images are used. Shots were classified in the automatic mode; selected outlines were authenticated in field conditions.

The layers made using such software as AutoCAD, MapInfo and received in electronic form were converted to a GIS project in required projection. The data collected in the reports were converted into structured tables and, based on them, the layers were made.

Analysis of spatial and semantic data usually includes information processing, particularly through various queries: spatial (including geostatistical), statistical analysis. One of the main types of spatial analysis that we use is mapping the areal contamination – charting the processes of mapping and prediction of their dynamics in space and time [3]. The studies examined a number of principles that allow aiming the program sequence to solve the objectives set:

- development of classification system for mapping of contamination processes (we use 255-level three-color scale for making the color scale);
- development of symbols for different types of environmental sampling;
- selection of methods for map construction.

The mapping was carried out using standard modules Spatial Analyst, Geostatistical Analyst. These modules require a lot of ways to create maps, therefore the methods were analyzed and the optimal method of mapping - kriging - was selected [4].

Statistical analysis involves processing of information through the module Geostatistical Analyst and the results are different charts and graphs.

1.2. STRUCTURE OF THE GIS PROJECT "STS"

Data generalization and analysis brought us to the structure of the GIS-project "STS": it consists of ten blocks (sets of layers), which all together give a complete picture of the Test Site:

1. Boundaries of STS and its TEST SITEs
2. Topography (topographic base, raster images)
3. Locations of nuclear and other tests
4. Economic activities at the STS
5. Water bodies
6. Vegetation
7. Soils
8. Geology
9. Radiation characteristics of the environment
10. Other features of the environment

Each block (set) includes layers that are logically grouped for the users' convenience and analysis of the data. The layers can be turned on or off as needed in order to avoid map overloading with information (Figure 2).

The blocks must contain information required to conduct research and monitoring at the Test Site.

Boundaries of the STS and its TEST SITEs. This is the fundamental block that must contain information on the geographical location of the territory: the boundary of the Test Site and TEST SITEs (used and unused), boundaries of the oblasts, administrative regions (and adjacent ones), etc.

Topography. It should represent topographic base of scale from 1:500 000 to 1:100 000, including terrain relief, hydrography, road networks, and bitmap images in the form of satellite shots, various schemes.

Locations of nuclear and other tests. This historic block should include the venues where earlier nuclear tests, etc. (adits, wells) were carried out and their consequences in the form of radioactive fallout traces.

Economic activities at the STS. This block should provide information relating to venues of commercial activities in the test site territory: populated settlements (villages, wintering sites at STS as well as outside it), deposits, reactor facilities being developed.

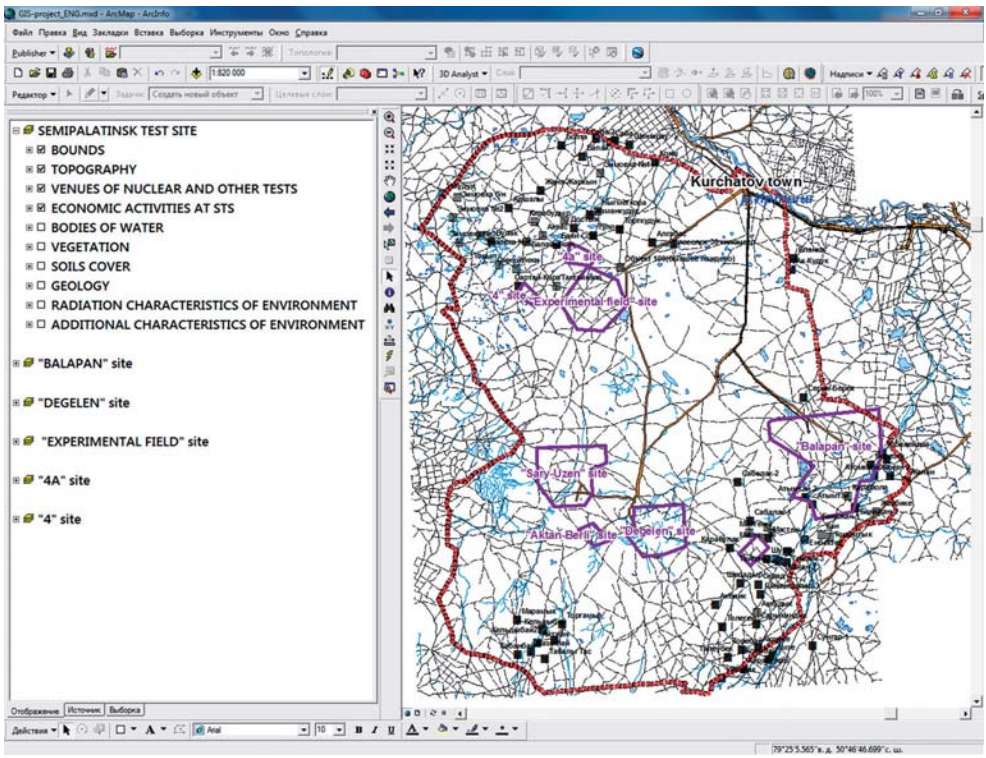

Figure 2. Primary window the GIS-project

Water bodies. This block should include potential water consumption bodies - wells, springs, etc.

Vegetation. This should represent different scale vegetation cover maps and diagrams of major ecosystems.

Soil. This block shall include a different scale soil map, as well as maps of the actual material.

Geology. This block should provide information regarding the geological structure of the area: geological and hydrogeological maps with application of specific information, mineral deposits.

Radiation characteristics of the environment. The block should include results of all survey works on all environmental objects (soil, air, etc.) of both regional (in the entire territory of the former STS) and the local level (certain areas, objects).

Other features of the environment. The block contains data on chemical composition of an object, etc.

The composition and structure of GIS data have become formed by the environmental objects (soil, air, plants, etc.), as well as processes (environmental contamination, migration processes).

2. RESULTS

2.1. Initial data preparation

As a part of the GIS project "STS", a wealth of information has been processed, systematized and converted into electronic format as a bitmap images:

- reports on the State Budgetary Programs and international projects over the past 10 years. Processed all the information that has gridded: results of field studies (e.g., pedestrian gamma-survey), economic monitoring, drilling, etc.;
- topographic maps with scale of 1:500 000. 1:200 000 and 1:100 000. Maps: 20 sheets with scale of 1:100 000, 8 sheets with scale of 1:200 000, 4 sheets with scale of 1:500 000 have been scanned and attached in accordance with the nomenclature. Maps that had been built by the State Institute of Agricultural Aero-photo-geodesic survey (GISHAGI, 2003) were purchased to update the topographic maps with scale of 1:100 000;
- to build such thematic maps as soil, geological, hydrogeological maps, requests were made to the public funds to obtain map sheets for the territory. We received 6 sheets of geological maps, 5 sheets of hydrogeological maps with scale of 1:200 000, 4 sheets of soil maps with scale of 1:300 000;
- to build maps of actual data, there have been collected materials in the form of data sheets on such objects as soil cross sections, boreholes, wintering sites, etc.;
- to build maps of soil and vegetation, there have been acquired multispectral medium-resolution satellite images from spacecraft ALOS, obtained in 2007 and 2009, on the 60% of the STS lands.

2.2. Loading the GIS - project

Boundaries of STS and its TEST SITEs. The boundaries of the Test Site and TEST SITEs have been obtained in the form of shape-files (*.shp) and exported to the geodatabase (provided by the NNC RK). The administrative boundaries of the regions and areas were digitized from the Atlas of Kazakhstan. The coordinates of marking poles were taken from the published information.

Also, this block contains a set of layers "Perspective map", which includes the proposed boundaries of the region, which would include the territory of the Test Site, and the contours of the detailed examination of the territory until 2020.

This block contains a total of 12 layers.

Topography. This block includes the following subsets of layers: surface topography (contour line) with elevations, drainage system (rivers, lakes, etc.), roads and power lines.

The layers are based on the topographic map sheets with scale of 1:100 000. The required attributive information has been recorded: names of rivers, lakes, road types (main, ground), etc. The relief with scale of 1:500 000 was obtained in the form of shape-files and exported to the geodatabase (provided by NNC RK). Also in this block includes layers of nomenclatorial sheets with different scales.

This block contains currently 14 layers. In 2011 it is planned to complete the layer "Relief" with scale of 1:100 000 using of which a 3D-terrain model will be built.

Venues of nuclear and other tests. These data were earlier plotted on a variety of maps, but with the advent of a new technical basis for obtaining the coordinates these layers have been updated. On all objects - tunnels, boreholes - attributive information were entered (object number, date of test) and data sheets on the objects were attached, which if necessary can be seen when point to the object. Also, when zooming in about 1:3 000, one can see the situation at the object (survey areas near boreholes, tunnels). Technical grounds at "Experimental Field" site and silos (launchers) are plotted on separate layers.

Also in this block is a set of layers "Traces", since they are digitized from various sources which must be indicated. A layer has been built based on tabulated data presented in the literature. We took into account the venue of testing and magnetic azimuth of the radioactive cloud movement direction. This layer is used for detailed examination of the territory where the traces pass.

This block contains a total of 19 layers.

Economic activities in the STS. The block includes a layer "Human settlements", which is digitized from map sheets with scale of 1:100 000. According to the results of the economic monitoring (field studies) and based on the created layer there were plotted wintering sites (summer pastures), the following attributive information were recorded: name, coordinates, state of the object (abandoned or residential), cattle head. Also according to the field studies and on the basis of formal requests there were plotted land allotments of business entities with the following information: owner, name of the entity, type of works and area of land allotments. To date there are in total 52 business entities, including 7 – being developed minefields and 45 – agricultural ones. These layers are constantly replenished with attributive information based on the results of annual monitoring. Also this block has a layer "Reactor facilities", which are industrial facilities and are marked with special symbols.

In accordance with the results of agricultural mapping and aerial photography in 2001, a map of agricultural land, with contours of 70% of the entire territory of the STS, was built.

This block currently consists of 7 layers.

Water bodies. The block includes wells and springs, which are digitized from the map sheets with scale of 1:100 000. Then, based on the data about the layers and field studies, layers were created with the specified coordinates. The layer "Wells" was provided with data sheets of the wells, which contain a picture of the object, the tabular results of chemical and radionuclide composition of the water in the well (Figure 3).

The block contains 5 layers total.

Vegetation. At the moment there has been built geobotanical contours map at 30% of the STS territory with a scale of 1:100 000. Multispectral medium resolution images were used to create a layer based on remote sensing (RS). Classification of contours was carried out by the NNC RK. Then, points for the field validation were chosen, after description of the contours and matching with the topographic base, a map of geobotanical contours was constructed followed by loading corresponding attributive information. On this basis a map of major ecosystems has been built. Total the block contains two layers.

Soils. Two ways were used to make the block: digitizing the map sheets with scale of 1:300 000 based on remote sensing and field validations (scale 1:100 000). A layer "soil profiles" includes all the factual materials, collected over many years, each profile is assigned a detailing passport.

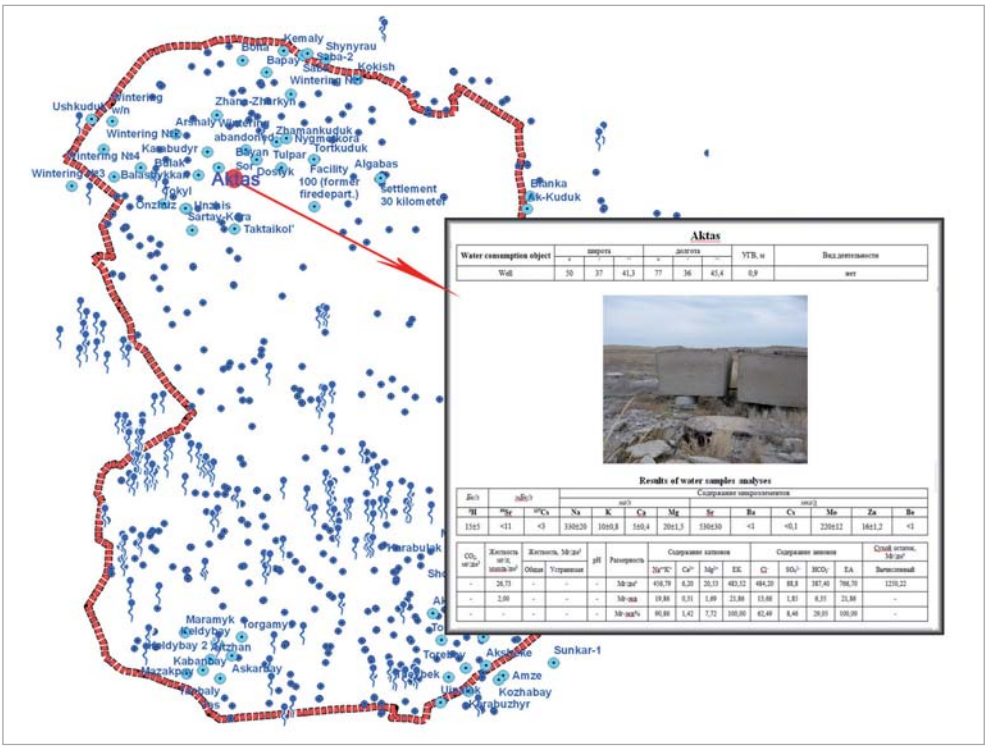

Figure 3. Data sheet of water consumption objects

Total the block contains 3 layers.

Geology. The block includes a set of layers "Geology" and "Hydrogeology". Created layers are direction of water flows, the contours of the catchment basins, mineral deposits, hydrogeological and structural wells.

Set of the layers "Hydrogeology" and "Mineral deposits" is scheduled to be updated in 2011. There will also be built geomorphological map at the scale 1:200 000.

The block currently consists of 11 layers.

Radiation characteristics of the environmental objects. This block is a dynamic one since constantly new objects of research emerge, both spot and large-area sites. The block has its own structure; information is broken down by years and objects of the environment (soil, water, air, plants). Coordinates of environmental sampling points together with the results of field and laboratory investigations are displayed as dots on a map through a database connection "Radioecology" with the GIS - project.

Then we build maps of areal soil contamination of the territory with different natural and artificial radionuclides, such as ^{137}Cs, ^{241}Am, etc. Or, if the sampling points are not enough to build an areal distribution in a given area, they are drawn in colour gradation. Also we process data for other objects of the environment in the form of spot colour gradations.

This block currently consists of 10 layers on the entire territory and more than 500 layers in the local areas.

Other features of the environment. The block currently has only one layer - the "wells" with the attributive information on the chemical composition of water.

So, for now the GIS project "STS" contains more than 80 layers with the required attributive information to describe the object, which in turn contain more than 20 000 objects. The names of various objects in attribute-value table are listed in three languages: Kazakh, Russian and English. The alias of each layer contains a summary info: source of information (for instance, the atlas of Kazakhstan or a report on the Republican budget program 011. 2008), date of creation.

Currently, there is an opportunity to use this GIS-project with the application's viewer ArcReader, which opens the GIS-project at the server in IRSE NNC RK. A user will have such features as to disable or enable the layers: he or she can open the data sheets of the objects directly by pointing to the object, determine the location of the point (object), if the coordinates are known, view attributive information on each layer. When working with the tools, we use standard features of the program, also an enhancement of the user interface is being considered.

3. EXAMPLES OF GIS-PROJECT USAGE

The basic function of the GIS project is data analysis. For the tasks of spatial and statistical analysis, the GIS has a rich set of tools. They allow building buffer zones and coverage areas, determining distances, obtaining geometric characteristics of objects (length, area), perform different spatial and attribute access (based on SQL-queries), perform overlaying operations (layup), etc. These are important functions of the GIS, and the effectiveness and usefulness of the GIS itself depends on their efficiency.

As a result of GIS-analysis, the territories are shown with high-quality thematic maps, graphs and tables that are intelligible and provide answers to research questions. Much attention has been paid to visualization.

An analysis of data using the GIS is implemented both at the stage of initial data preparation for research, and at the final stage of processing the information obtained during the field and laboratory works.

3.1. Arrangement of field works

To organize and conduct field works it is needed to perform integrated assessment of the studied area using GIS-project: determination of the radiation situation in the planned area based on the data obtained earlier in the research, revealing local areas with high level of contamination with artificial radionuclides, provision of various thematic maps (topographic, soil, etc.), satellite images to the area in question. The information is analyzed in aggregate with other natural features (climate, soils, vegetation, etc.). After analyzing the initial data, we determine the spacing of sampling network and radiological surveys.

For example, in order to carry out radiological examinations at near-portal areas of the adits, a grid of 5x10 m is overlapped, in the nodes of which radiometric measurements are carried out (gamma-, beta-surveys) (Figure 4). The calculated coordinates of the grid nodes are passed over for further surveys.

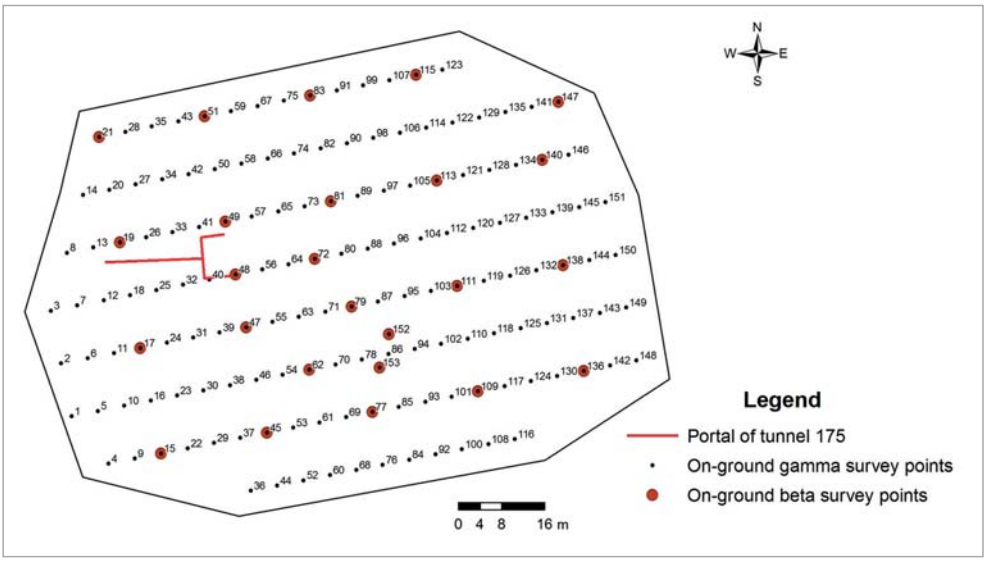

Figure 4. Grid of 5x10 m at near-portal area of the Adit 175

3.2. Use of geostatistical and statistical analysis

In order to interpret the obtained data, geostatistical and statistical analysis of the information is needed. Using the method of geostatistical discrete kriging based on the results of field studies, maps of gamma-, beta-, alpha-flows distribution are built; from laboratory studies - maps of areal contamination with radionuclides of natural and artificial nature. Statistical data processing techniques allow formulating firm conclusions regarding the distributions obtained.

For instance, in the "northern" part of STS based on the results of laboratory analyses there was built a map of areal contamination with ^{241}Am employing Geostatistical Analyst module with a colour gradation from light, less polluted, to the dark colour, in the form of contour lines as a result of interpolation of data for any point on the surveyed area [5]. Based on spatial analysis and charting the specific activity of ^{241}Am, 6 areas with high concentrations were revealed in the ^{241}Am distribution. The statistical analysis allowed calculating the average ^{241}Am concentrations on each contour and identified the most pronounced – the maximal value (Figure 5).

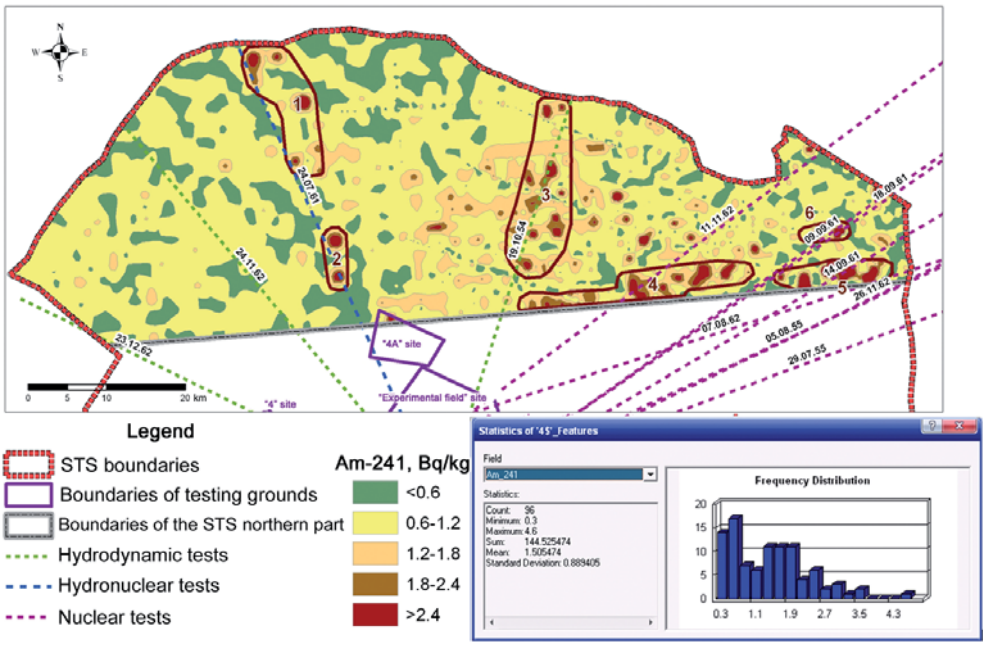

Figure 5. Interpretation of data for the radionuclide ^{241}Am

3.3. Determination of the nature and mechanisms of contamination

One of the typical problems in analysing the results of research is identifying the nature of and mechanisms for contamination of an object, site, area.

For example, when conducting the research in the area of "Baitemir" the nature and mechanisms of contamination in its territory were determined. According to the results of laboratory tests, a map of areal contamination with ^{137}Cs was built. The main contaminated area clearly stands out. Layup - a trace of contour lines 0.3 Ci/km^2 ^{137}Cs as per the results of aero-gamma survey with a map of areal distribution of the radionuclide ^{137}Cs in the area, clearly shows that the ^{137}Cs contamination is confined to passing, on this section, the trace of radioactive fallout in 1953 (Figure 6).

The zones with high concentrations in the "northern" part of STS can also be demonstrated in imposing the traces of radioactive fallouts after the hydronuclear, hydrodynamic and nuclear tests.

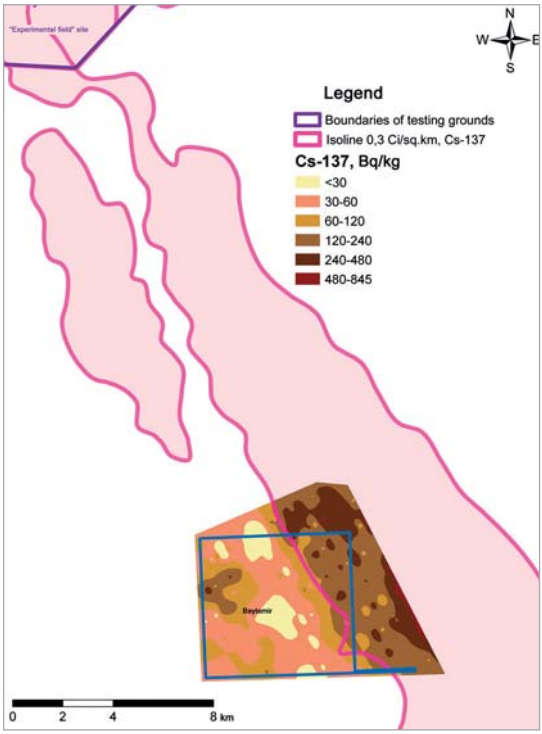

Figure 6. Layup - map of areal contamination and radioactive fallout trace

CONCLUSION

This development has made it possible to synergize a large scope of accumulated information on such things as radioactive contamination at STS and certain TEST SITEs; it also assures information and analytical services for a large number of end users – experts in various fields of science and technology.

This work continued for several years. At present, the GIS project "STS" contains more than 80 layers, which in turn contain more than 20 000 objects. It should be noted that at present all the data currently available with spatial references undergo processing and incorporation into the GIS project "STS".

Further development of the GIS project will expand the scope of the GIS allowing it predicting the changes in the state of the radiation environment, assessing collective and individual doses on the population engaged in economic activities at the STS, modeling radioactive contamination of the atmospheric air and groundwaters in the STS territory.

REFERENCES

1. *Yu. K. Korolev.* The geoinformatics. Part 1 [Theoretical geoinformatics.]. Issue 1 [in Russian]
   Королев Ю. К. Общая геоинформатика. Ч.1 [Теоретическая геоинформатика.]. Вып.1 / Ю. К. Королев. – М: ООО СП Дата, 1998. – 118 с.
2. Geoinformatics / A.D. Ivannikov, V.P. Kulagin, A.N. Tikhonov [et al] [in Russian]
   Геоинформатика / под.ред. А. Д. Иванников, В.П. Кулагин, А.Н. Тихонов [и др.] – М: МАКС Пресс, 2001. – 349 с.
3. *I. G. Zhurkin.* The geoinformation systems. [Russian]
   Журкин И. Г. Геоинформационные системы / И.Г. Журкин, С.В. Шайтура. – М.: КУДИЦ-ПРЕСС, 2009. – 272 с.
4. *E. Mitchell.* Guide to GIS Analysis [Spatial patterns and relationships.]. P.1. / E. Mitchell. - Copyright: ESRI, 1999] [in Russian]
   Митчелл Э. Руководство по ГИС анализу [Пространственные модели и взаимосвязи.]. Ч.1. / Э. Митчелл.
5. *V.I. Laykin.* Geoinformatics: Tutorial / V.I. Laykin, G.A. Uporov. - Komsomolsk-on-Amur: AmGPGU, 2010 [in Russian]
   Лайкин В. И. Геоинформатика: учебное пособие / В. И. Лайкин, Г. А. Упоров. – Комсомольск-на-Амуре: АмГПГУ, 2010. – 162 с.

"ССП" ГАЖ-ЖОБАСЫН ӘЗІРЛЕУ

Яковенко Ю.Ю., Лукашенко С.Н., Субботин С.Б.

ҚР ҰЯО Радиациялық қауіпсіздік және экология институты, Курчатов, Қазақстан

Бұл мақалада, "ССП" ГАЖ-жобасын өңдеу және әзірлеу бойынша жұмыстардың нәтижелері келтірілген, сонымен қатар зерттеулерді ұйымдастыруға арналған оның үлгілері мен аумақтың және экожүйенің хал-ахуалын бағалауға арналған деректердің талдамасы келтірілген.

Бұрыңғы Семей сынақ полигонының (ССП) аумағына қатысты ақпараттардың үлкен көлемі жинақталды, осыған байланысты деректерді сақтауға, уақытылы енуге және тиімді өңдеуге қатысты мәселелер туындайды. ССП-ғы кешенді зерттеулерді іске асыруда және осы мәселелерді шешу үшін ГАЖ технологиясы негізінде "ССП" ГАЖ-жобасы өңделді және әзірленіп жатыр.

Аталған өңдеулер жинақталған ақпараттардың, сонымен қатар ССП мен жеке бір сынақ алаңдарының радиациялық ластануы бойынша үлкен көлемін жүйеге келтіруге, сонымен қатар мамандардың көпшілігін ақпараттық және аналитикалық қамтамасыз етуге мүмкіндік берді.

Түйін сөздер: ГАЖ-жобасы, қабат, деректер базасы, алғашқы деректер, деректер талдамасы.

РАЗРАБОТКА ГИС-ПРОЕКТА "СИП"

Яковенко Ю.Ю., Лукашенко С.Н., Субботин С.Б.

Институт радиационной безопасности и экологии НЯЦ РК, Курчатов, Казахстан

В статье представлены результаты работы по разработке и созданию ГИС-проекта "СИП", а также примеры его использования для организации исследований и анализа данных для оценки состояния территории и экосистем.

Накоплен огромный объем информации, касающийся территории бывшего Семипалатинского испытательного полигона (СИП), в связи с чем возникают проблемы хранения, своевременного доступа и эффективной обработки данных. Для решения этих задач и осуществления комплексных исследований на СИП на основе технологий ГИС разработан и создается ГИС-проект "СИП".

Данная разработка позволила систематизировать большой объем накопленной информации, в том числе по радиационному загрязнению СИП и отдельных испытательных площадок, а также обеспечить постоянное информационное и аналитическое обслуживание большого числа специалистов.

Ключевые слова: ГИС-проект, слой, база данных, исходные данные, анализ данных.

AUTHOR INDEX

ABOUT THE PRINCIPAL AUTHORS

Lukashenko S.N. graduated from Leningrad Institute named after Lensovet majoring in radiation chemistry in 1986 and worked for the Institute of Nuclear Physics under Kazakh Academy of Sciences until 2006. In 2006 he was appointed Deputy Director General for Radioecology in NNC RK and Director of the Institute of Radiation Safety and Ecology NNC RK. His main scientific interests lied in different years in the following areas: development of methods for elemental and radionuclide analysis, development of methods for radiochemical separation of radioactive isotopes, research/determination of conditions and states of various radiation-hazardous facilities including former nuclear test sites Semipalatinsk and Azgir, places of peaceful nuclear tests (LIRA site, Batolit, Region, and other), nuclear reactor facilities (reactor plant BN-350 in Aktau, research reactor WWR-K in Almaty), sites of uranium mining and uranium processing facilities (tailings Koshkar-Ata, waste repository from UMP, etc.), facilities and areas with high natural radiological characteristics.

He has a long record as a manager/supervisor in major national and international projects. In 2006 he became a member of the Consultative Group on Nuclear Applications under the Director General of the International Atomic Energy Agency. He is a co-author in over 110 scientific publications.

Aidarkhanov A.O. graduated from East Kazakhstan State University in 2001 majoring in physics. He started his career at INP NNC RK. In 2008 he was appointed Head of Department for Development of Environmental Monitoring Systems at the Institute of Radiation Safety and Ecology. The main areas of research are: study of radioecological situation in places of nuclear explosions (Semipalatinsk Test Site); radiation monitoring of economic activities at STS (Karazhyra coal strip mine, Karadzhal fluorite minefield); study of artificial radionuclides migration with groundwater (sites "Degelen", "Balapan" and Shagan River); development of methods for isotopic hydrogeology.

Glushchenko V.N. graduated from S.M. Kirov Kazakh State University in 1988 with a degree in physics, participated in development and adoption of nuclear-physical methods of analysis in geophysics. Since 2001 he has been working for the Institute of Nuclear Physics NNC RK, currently heads the Center for Complex Environmental Research. His main activities are in comprehensive study of states of various radiation-hazardous objects including the former test sites Azgir and Semipalatinsk, places of peaceful nuclear tests – LIRA facilities, Mangyshlak, Meridian and others, nuclear research and power plants - reactor BN-350 in Aktau, water-moderated water-cooled reactor in Almaty, facilities of uranium industry - tailing Koshkar-Ata, facilities of uranium mining and processing industry in Northern Kazakhstan, radiation-hazardous facilities and oil industry areas. Co-author in more than 40 scientific papers.

Gorlachev I.D. graduated from the Novosibirsk Electrical Engineering Institute in 1985 majoring in engineering electrophysics. Since 1987 he has been working for the INP NNC RK; currently – Head of Analytical Group. The main areas of research are: physics of charged particle beams, development and application of analytical methods employing accelerated beams of charged particles, use of nuclear-physical methods of analysis in geology and ecology.

Kashirsky V.V. graduated from East Kazakhstan State University in 1998 majoring in physics and earned his MS in physics (spectroscopy) there in 2000. He started in 1999 as an engineer in the laboratory for low-background studies of the INP NNC RK. Since 2008 he became a team leader for spectrometric studies at IRSE NNC RK. The main areas of research are development of methods for determination of alpha-, beta-, gamma-emitting radionuclides in various environmental media, study of radioecological situation at nuclear explosion sites, study of isotopic ratios of transuranic elements at nuclear explosion sites, assessment of dose loads on personnel and public from external and internal exposure. Co-author in 16 scientific papers.

Korovina O. Yu. graduated in 1998 from the faculty of natural sciences of Shakarim Semipalatinsk State University with a degree in chemistry and ecology. That year her career began as an engineer-chemist at the Institute of Atomic Energy NNC RK. In 2009 she successfully completed Master's programme in ecology in Semipalatinsk State Pedagogical Institute and got her MS in natural sciences. The main areas of research are study of composition of liquid radioactive wastes and development of efficient methods for their re-processing, development of indirect methods for determination of radionuclides in human body to assess dose loads, creation of hardware and methodological framework for operation of the Republic of Kazakhstan Center for Complex Dosimetry.

Kunduzbaeva A.E. graduated in 2002 from Shakarim Semipalatinsk State University majoring in chemistry; got her MS degree in macromolecular chemistry in 2004. Since 2004 she has been working at the Institute of Radiation Safety and Ecology. Currently she is an engineer in the Department of Integrated Ecosystem Studies. One of the main activities is investigation of behaviour of artificial radionuclides in soils. Co-author in 10 scientific publications.

Lyakhova O. N. graduated in 2000 from East Kazakhstan State University majoring in physics, specialization in "spectroscopy." After graduation she went to work at the IAE NNC RK as an engineer-physicist in the laboratory for Radiation studies and migration of fission products. Since 2006 she has been working at the IRSE NNC in the department for Development of environmental monitoring systems. Currently she is a Head of the laboratory "Experimental studies of transport mechanisms". The main area of activity is study of contents and distribution of tritium in atmospheric air at nuclear testing sites, distribution of tritium in various systems of the environment "water-atmosphere", "soil-atmosphere", "groundwater-atmosphere", "plant- atmosphere". Co-author in 10 scientific papers.

Magasheva R. Yu. graduated from the Kazakh Polytechnic Institute in 1961 majoring in hydrogeology and engineering geology, Alma-Ata. From 1961 to 1997 she worked at the Institute of Soil Sciences of Science Academy of Kazakh SSR (Almaty) first as a research assistant, and after successful defense of doctoral dissertation in 1978 in the position of Senior Scientific Officer. The scientific career was spent in the departments and laboratories of the Institute and was related with problems of improvement of soils in Kazakhstan, ameliorative forecast in substantiation of hydro-economic activities in the country. From 1998 to 2000 she worked under INTAS International Grant Project "Intas-Kz" *"Formation of vegetation and Radioecology of Semipalatinsk Test Site"*. Since February 2003 she has been working for the Institute of Radiation Safety and Ecology under National Nuclear Center of RK. Her research activities are related to the problems of radioecology of soil and vegetation in the former Semipalatinsk Nuclear Test Site and surrounding lands. Author of 40 scientific papers.

Strilchuk Yu. G. graduated from the Leningrad Higher Military-Topographic Command School named after Army General A.I. Antonov in 1990 majoring in command tactical geodesy. After graduation, he served at the Semipalatinsk Test Site in a military unit 52605B. Since 1996 he has been working for the Institute of Radiation Safety and Ecology. Currently holds the position of Head of Training and Information Center of IRSE NNC RK. Scientific interests lie in study of radiation situation at the STS and surrounding regions, in areas of nuclear testing in Kazakhstan, study of distribution of radionuclides in the environment resulted from nuclear testing, assessment of dose loads to personnel and population. He is currently a supervisor in the IRSE of the Republican Budgetary Program 038 "Radiation safety in the territory of the RK" for the section "Safety Assurance of the former STS" He has more than 40 scientific articles.

Subbotin S.B. began his career as a dosimetrist at a uranium mine after graduation in 1975 from Central Asian Polytechnic Institute with a degree in mineral deposits exploration geology. Since 1979 he worked at the Semipalatinsk Test Site and was engaged in engineering and geological provisions for nuclear explosions. In 1988 he graduated from Tomsk Polytechnic Institute where he majored in hydrogeology and engineering geology. Since 1995 he has been working for the IRSE NNC RK. He was actively involved in the Institute's radioecological studies at nuclear testing sites both in the former Semipalatinsk Test Site and in other regions of Kazakhstan. His great contribution as a developer and manager of scientific and technical sections and issues related to contaminated groundwater was made to the state programs, which are of great importance for assessment and development of modern radiological situation at the former Semipalatinsk Test Site. In co-authorship with IRSE researchers he published over 20 scientific articles.

Yakovenko Yu.Yu. graduated in 2002 from East-Kazakhstan State University (EKSU), Ust-Kamenogorsk, majoring in applied mathematics. In 2004 she earned MS in mathematics from EKSU, specialization mathematical/numerical simulations.

She works for IRSE NNC since 2008 as a Group Leader of Geo-Information Systems at the Department of GIS Technologies. Job Profile: systematization and structuring of information on the STS using GIS technologies; preparation of cartographic materials of radiometric surveys, surface contamination of STS; statistical and geo-statistical analysis of radioecological studies. She is responsible for maintaining the analytical data base of the Institute on radioecological situation at STS and leads the GIS project "STS".

Ministry of Industry and New Technologies

The Republican State Enterprise
"The National Nuclear Center of Kazakhstan"

Affiliated State Enterprise
"Institute of Radiation Safety and Ecology"

TOPICAL ISSUES IN RADIOECOLOGY OF KAZAKHSTAN

Issue 3
Volume 2

Proceedings
of the National Nuclear Center
of Kazakhstan
for 2010

Under general editorship of the Deputy Director General
for Radioecology RSE NNC RK and Director of the IRSE Lukashenko S.N.

Technical Editor: G. Trubitskaya
Computer-aided makeup: A. Vus

Approved for printing
Format 70x100/16. Offset paper. Conv. Print. P. 24.5
500 copies. Order № 518 ц.
Printed in "Dom Pechati" LLP
140000, Pavlodar, 143 Lenina St.